Environmental Assessment of the Alaskan Continental Shelf

Annual Reports of Principal Investigators for the year ending March 1979

Volume IX. Hazards

U.S. DEPARTMENT OF COMMERCE
National Oceanic and Atmospheric Administration

U.S. DEPARTMENT OF INTERIOR
Bureau of Land Management

VOLUME I	RECEPTORS -- MAMMALS
	BIRDS
VOLUME II	RECEPTORS -- BIRDS
VOLUME III	RECEPTORS -- FISH, LITTORAL, BENTHOS
VOLUME IV	RECEPTORS -- FISH, LITTORAL, BENTHOS
VOLUME V	RECEPTORS -- MICROBIOLOGY
	CONTAMINANT BASELINES
VOLUME VI	EFFECTS
VOLUME VII	TRANSPORT
VOLUME VIII	TRANSPORT
VOLUME IX	HAZARDS
VOLUME X	HAZARDS
	DATA MANAGEMENT

Environmental Assessment of the Alaskan Continental Shelf

Annual Reports of Principal Investigators for the year ending March 1979

Volume IX. Hazards

Outer Continental Shelf Environmental Assessment Program
Boulder, Colorado

October 1979

U.S. DEPARTMENT OF COMMERCE
National Oceanic and Atmospheric Administration

U.S. DEPARTMENT OF INTERIOR
Bureau of Land Management

DISCLAIMER

Mention of a commercial company or product does not constitute an endorsement by National Oceanic and Atmospheric Administration. Use for publicity or advertising purposes of information from this publication concerning proprietary products or the tests of such products is not authorized.

ACKNOWLEDGMENT

These annual reports were submitted as part of contracts with the Outer Continental Shelf Environmental Assessment Program under major funding from the Bureau of Land Management.

HAZARDS

CONTENTS

UNITED STATES
DEPARTMENT OF THE INTERIOR
GEOLOGICAL SURVEY
Conservation Division
800 A Street
Anchorage, AK 99501

TECHNICAL ANNOUNCEMENT
U.S. GEOLOGICAL SURVEY

April 16, 1979
Further information:
R.H. McMullin 907-271-4361

BATHYMETRIC MAPS OF KODIAK OUTER CONTINENTAL SHELF WESTERN PACIFIC, ALASKA RELEASED BY USGS

Thirteen bathymetric maps of the Kodiak outer continental shelf area, Alaska, where an oil and gas lease sale is scheduled for 1980, were released on February 28, 1979, as U.S. Geological Survey Open-File Report 79-263.

These 1:250,000-scale bathymetric maps were constructed using high-resolution seismic data from two surveys and accurately show topographic features of the sea bottom that may be of concern to future oil and gas exploration and development. The shapes of outcropping bedrock and/or fault scarps show up as linear features on bathymetric highs, and lower amplitude sand waves occasionally show as tortuous contour lines. The seismic lines were intentionally oriented so as to be approximately orthogonal to the major structure trends.

U.S. Geological Survey Open-File Report 79-263, "Bathymetric Maps of the Kodiak Outer Continental Shelf, Western Gulf of Alaska," by B.W. Turner, G.P. Thrasher, G.B. Shearer, and K.D. Holden, may be inspected at the following offices: U.S. Geological Survey libraries at Denver, CO, Reston, VA, and Menlo Park, CA; and U.S. Geological Survey Public Inquiries Offices at Anchorage, AK, Los Angeles, CA, San Francisco, CA, and Denver, CO.

Papercopy or microfiche may be purchased from the Open-File Services Section, Branch of Distribution, U.S. Geological Survey, Box 25425, Federal Center, Denver, CO 80225. Prices: papercopy, $45.50; microfiche, $6.50.

Annual Report

A SEISMOTECTONIC ANALYSIS OF THE SEISMIC AND VOLCANIC HAZARDS IN THE PRIBILOF ISLANDS-EASTERN ALEUTIAN ISLANDS REGION OF THE BERING SEA

Contract: NOAA 03-5-022-70

Research Unit: 16

1 April 1978 through 31 March 1979

Principal Investigators

Dr. John N. Davies
Dr. Klaus H. Jacob

Lamont-Doherty Geological Observatory

of Columbia University in the City of New York

TABLE OF CONTENTS

I. SUMMARY

Objectives. Through work carried out under this project we attempt to assess the volcanic and earthquake hazards that exist in the Eastern Aleutian Islands and Pribilof Islands of the southeast Bering Sea and the western Gulf of Alaska. This assessment is made in the context of exploration and possible future development of petroleum resources on the continental shelves which constitute most of the region. The present work focuses on the collection and analysis of new seismic data obtained from a seismic network jointly funded under this NOAA project and a larger companion project supported by D.O.E.; however, through the companion DOE and several smaller projects other geophysical, geodetic, and geologic and seismic engineering data are available to this study and the results relevant to hazards assessment are reported here to NOAA.

The Specific Objectives of the Current Work are: (1) to monitor seismic activity in the Shumagin Islands and Dutch Harbor regions of the Eastern Aleutian Island Arc and western Alaska Peninsula regions, and of the Pribilof Islands region of the southeast Bering Sea; (2) to relate this seismic activity to particular faults or fault zones, where possible; (3) to monitor seismically the eruptive activity of three volcanoes: Pavlof, Akutan and Makushin; (4) to evaluate these seismic and volcanic activities for their potential hazards to exploration for and development of petroleum resources on the continental shelves within the study area. An important aspect of seismic hazard assessments is that they require a long-term continuous and reliable data base.

Major Conclusions and Implications: The Aleutian arc segment near the Shumagin Islands and the tip of the Alaska Peninsula is found to be the likely site of one or more great ($M \geq 7.75$) or large ($M \geq 7$) earthquakes and related aftershock sequences within the next several years or a few decades. Such events have a high potential for producing destructive tsunamis and inducing hazardous submarine mudflows. At the present time this "seismic gap" is relatively quiescent, and we note occasional, moderate-sized earthquakes (m_b 5 to 6.5) associated with unusually high stress drops (600 to 800 bars) and above-average levels of groundmotion. These events occur near the down-dip end (depths of about 40 km) of the inferred zone of contact between the North American and Pacific plates. They are located directly beneath fore-arc basins which have potential for petroleum exploration. Minor, probably shallow crustal activity appears to be associated with the Sanak Basin on the Pacific Side, and the southwesternmost portions of Bristol Bay, near the Black Hills (Alaska Peninsula) on the Bering-Sea side of the studied arc segment. These areas are of interest because of their potential for bearing petroleum. Other minor, shallow crustal seismicity in the overriding (North American) plate is apparently related to volcanic or magmatic activity. The Dutch Harbor region appears to be characterized by moderate seismicity typical of most portions of the former 1957 rupture zone, although data coverage was incomplete during this reporting period. Some events were recorded in the southeast Bering Sea with a single seismic station located on St. Paul, in the Pribilof Islands. The distance range inferred from seismic travel times would indicate that some of these events are associated with the St. George Basin. The single-station limitation does not, however, allow any definite correlation with specific tectonic structures.

Progress has been made to develop computer methods for analyzing previously collected broad-band seismic data in an attempt to develop a data set which would

be important for seismic engineering purposes on Alaskan continental shelves. Results from closely coordinated tilt, geodetic and geologic (terrace) studies are reported and are consistent with the conclusion that the Shumagin Islands region has in the Recent experienced significant vertical movements and, hence, can expect to do so in the future. The regional coherence, rates, and causes of these vertical motions is still an unresolved subject of investigation. If this problem can be resolved, it could bring about an important refinement in the assessment of both local and regional seismic hazards, which have so far been evaluated mostly on the basis of a limited set of seismic data. We have not yet attempted to quantify volcanic hazards in the study region, although first results indicate that forecasting of volcanic events both in time and space, may be technically possible. The most difficult, as-yet-unresolved task is finding a basis for estimates of recurrence times of major volcanic activity.

II. INTRODUCTION

General Nature and Scope of Study. The present NOAA funded study, "A Seismotectonic Analysis of the Seismic and Volcanic Hazards in the Pribilof Islands - Eastern Aleutian Islands Region of the Bering Sea" is an amplification of the hazards aspects of a previously existing and concurrent seismotectonic study of the Aleutian arc, funded by D.O.E. The D.O.E. study is very broad in scope and as such includes hazards analysis, but at a low level of priority. NOAA funds are used to accelerate hazards analysis by providing (1) additional staff, (2) equipment for data collection for projects specifically or primarily directed toward hazards analysis, and (3) logistic support to maintain the extensive network of seismic stations and fieldwork required by the combined studies. The general goal of the present study is to monitor seismic and volcanic activity over a long time span and to evaluate this activity in terms of the hazard it implies for the exploration for and possible development of petroleum resources within the study area. The evaluation of this seismic and volcanic data requires a broad seismotectonic framework. This broad framework is provided by the D.O.E. study and by occasional special projects like the geologic investigation described in this report.

Specific Objectives. The specific objectives of the past year have been (1) to continue to monitor the seismic activity in the Sand Point, Dutch Harbor and St. Paul areas, (2) to attempt to relate this activity to specific faults, including a geologic investigation of the Shumagin Islands region for this purpose, (3) to monitor the activity of Pavlof, Akutan and Makushin Volcanoes, and (4) to begin to evaluate the data (where it is sufficient) in terms of its hazards implications.

Relevance to Problems of Petroleum Development. The relevance of this work to petroleum development is straightforward: The basic problem is to design structures that will withstand expected earthquakes, associated tsunamis, and volcanic activity within an acceptable level of risk. This design problem requires, as inputs, knowledge of the probable space-time distribution of large earthquakes, the acceleration vs. distances relations for those earthquakes and the distance to which various volcanic eruptions can be expected to be destructive. Prediction of the space-time distribution of large earthquakes requires a comprehensive understanding of the seismotectonic setting, knowledge of the distribution of pre-existing faults and the longest possible record of previous seismic activity. Determination of acceleration vs. distance relations requires actual measurements of accelerations within the region over as broad a range of distance and magnitude as possible. Specification of the minimum safe distance from a given volcano requires knowledge of the type of eruption to be expected and the frequency of eruption. The data being collected are essential to each of the above prerequisites to the inputs for the problem of designing safe and economical structures.

III. CURRENT STATE OF KNOWLEDGE

Shumagin Islands Seismic Gap. Our present understanding of the seismic regime in the Shumagin Islands region is based on the concepts of plate tectonics (Isacks et al., 1968) and seismic gaps (Kelleher, 1970; Sykes, 1971; McCann et al., 1978). The Aleutian Island arc, of which the Shumagin Islands region is a part, is a convergent plate boundary between the Pacific and North American (Alaskan) plates. Along this plate boundary most of the seismic energy is released during great earthquakes ($M \geq 7.8$) (Kanamori, 1977). The aftershock zones of these great earthquakes do not overlap, which suggests that the area left between recent aftershock zones, the seismic gaps, are the most likely sites of the next great earthquake. Other things being equal, the longer the time since the occurrence of a great earthquake in a given gap, the higher is the probability that the gap will be the site of the next great earthquake.

Davies et al. (1976) discussed the historic record of earthquakes in the Shumagin Gap and assessed various methods for estimating the occurrence time of the next great earthquake there. Unfortunately, the error limits on all such estimates are so large as to make them impractical as predictions. We report below the results of the D.O.E. funded geodetic tilt measurements. While still preliminary, they suggest that the Shumagin Islands region is tilting trenchward at .4 to 4 microradians per year. This tilt rate, if substantiated, would be consistent with that observed in Japan for interseismic periods (Scholz, 1974); i.e. the period between great earthquakes during which strain energy is accumulating. This suggests that such an earthquake was not imminent (due within a few months) at the time of the last measurement (June, 1978).

Davies and House (1978) have compared the Benioff zone seismicity beneath the Shumagin Islands with that beneath other regions of the Aleutian arc and with some other subduction zones. This comparison suggests that the future fault plane of a great earthquake in the Shumagin Gap will be in the main thrust zone (MTZ), the shallowly dipping portion of the Benioff zone above 40 km depth. Below, we interpret most of the shallow seismicity (less than 25 km depth) as being the result of an edge effect of stress accumulation around this future fault plane. This is consistent with Mogi's (1969) observations of a "doughnut" pattern of seismicity around future fault planes in Japan. It may be that the relatively high level of activity that we observe in the Dutch Harbor region and that the University of Alaska seismologists observe (Gedney, 1978) along the SW end of Kodiak Island also reflect this "doughnut" pattern.

The high stress levels implied by this "edge effect" interpretation have been observed in two studies. Archambeau (1977) computed the stress drop for several earthquakes in the Shumagin Islands region using Ms/Mb ratios. The high, kilobar stress drops that he obtained have been questioned by some seismologists. House and Boatwright (1978) obtained a maximum stress drop of 600-900 bars for the April 1974 Shumagin Islands earthquake. Additionally, we have recorded two more earthquakes (M_b = 5.5 and 6.5) near the Shumagin Islands. Both of these events were located at the lower edge of the MTZ and triggered the strong-motion instrument at Sand Point. Unfortunately, these records are not suitable to the stress-drop analysis of House and Boatwright (1978). It is possible that such a record was obtained by the strong motion accelerograph at Simeonof Island, though this will not be known

until that station is serviced during June 1979. In any case the occurrence of these events is consistent with the Mogi "doughnut" pattern described above and strengthens our conclusion that high stresses are accumulating in this region.

The high stress level observed in the main thrust zone probably implies relatively high stress in the upper crust. This stress will most likely be relieved along pre-existing faults. We are only just now beginning to acquire enough shallow seismicity data to identify active surface faults. Similarly we may be on the verge of being able to detect secondary features in the Benioff zone seismicity that would allow us to identify possible segmentation of the downgoing slab. If this segmentation exists, there would be linear zones transverse to the arc that would have a high risk for large strike-slip or normal faulting earthquakes. We have also observed terraces (see the geologic results below) that are evidence for episodic uplift. It may be that a study of uplifted terraces would allow us to define boundaries for crustal blocks. These boundaries, too, would be zones of high risk for fault motion during large earthquakes.

Pribilof Islands Region. We continue to record earthquakes at the St. Paul seismic station whose hypocenters are probably located in the St. George Basin. This basin is fault bounded (Marlow et al., 1977) and these faults may extend northwesterly between St. George and St. Paul Island (Hopkins, 1976). We cannot determine the association, if any, of the earthquakes to these or other faults until we have more than one seismic station in the Pribilof Islands.

IV. STUDY AREA

In the combined D.O.E. - NOAA program, by far the strongest concentration of effort has been in the Shumagin Islands region. Within the OCSEAP program this region is classified as part of the western Gulf of Alaska. The specific area referred to as the Shumagin Islands region extends from the SW end of Kodiak Island to Sanak Island. Within this area is the 12 station network of seismic stations on Pavlof Volcano which is supported primarily by D.O.E. This area is also the same as the Shumagin Islands seismic gap in its broadest application; although there are some reasons to restrict the definition of the seismic gap to the western half of this area.

The Dutch Harbor area, also within the western Gulf of Alaska, receives the second highest level of effort. This area includes the NOAA funded stations on Akutan and Makushin Volcanoes.

Lastly we operate a single station on St. Paul Island, one of the Pribilof Islands. This station is in the Bering Sea region according to the OCSEAP classifications.

V. SOURCES, METHODS, AND RATIONALE OF DATA COLLECTION

Seismic Data. Our primary emphasis in data collection is the operation of local, high gain, telemetered networks of short period seismic stations. These local networks allow the precise location of smaller magnitude earthquakes that is necessary for the timely and accurate delineation of tectonic features such as active faults, segmentation of the subducted slab and patterns of volcanic activity. The principal regional network is located in the Shumagin Islands (see Figure 1). It consists of 15 remote (single component, vertical) stations and one 3-component station at the recording center, Sand Point (SAN). The stations on the perimeter of this network are (clockwise from the upper left in Figure 1): False Pass (FPS), Black Hill (BLH), Ivanof Bay (IVF), Chernabura Island (CNB) and Sanak Island (SNK).

Within this network we also operate a dense, 12 station network around Pavlof Volcano (near PVV). The main purpose of this D.O.E. funded network is to provide data with which to study the geothermal potential of Pavlof Volcano. This network, in conjunction with the regional Shumagin Islands network, may also provide data that would allow us to study the relationship between variations in local volcanic activity and changes in the regional stress field as inferred from seismic activity. Several studies have suggested that such volcanic activity may be useful in predicting great earthquakes (Kimura, 1976; Nakamura et al., 1977; McCann and Kimura, 1978).

At Dutch Harbor we record two local components (one vertical and one horizontal) and two remote stations (Akutan and Makushin Volcanoes). This three station "network" is very poorly distributed (geographically) and consists of the minimum number of stations to locate earthquake hypocenters. The local components are intended to complement the long period seismograph there and the remote stations are primarily intended to monitor volcanic activity on Akutan and Makushin volcanoes. In this year's renewal proposal, we request funds to add a remote repeater station and to relocate the Makushin station closer to the volcano to better monitor it and to slightly improve the geographical distribution of the network. It is possible that we will be forced to move the recording station if the present building is torn down in connection with planned modernization of the airport. The installation of the repeater station will allow for this eventuality and will permit future expansion of the Dutch Harbor network. The purpose of such a network would be threefold: (1) to locate local earthquakes to better define the seismotectonic regime (relate activity to faults, block boundaries, and the Benioff zone), (2) to locate accurately hypocenters of events that trigger strong motion accelerographs so that useful acceleration vs. distance relations can be constructed, and (3) to monitor the activity on the western edge of the Shumagin Seismic Gap that may be a key to predicting the time of the next great earthquake there.

At St. Paul, in the Pribilof Islands, we operate a single, short period, vertical seismometer. This instrument monitors local activity levels as a function of distance and also complements the long period seismograph there.

Other sources of seismic data are the long period seismographs that we operate under D.O.E. funding at Sand Point, Dutch Harbor, and St. Paul, the broad band data that we discuss below in the hazard analysis section under "Results", and the World Wide Standard Seismograph Network.

Strong Motion Accelerographs. For the past few years (primarily under D.O.E. funding) L-DGO has operated Kinemetrics SMA-1 accelerographs at Dutch Harbor, Cape Sarichef, Sand Point and Port Moller. The USGS has maintained one at Cold Bay. Because the RCA communications site at Port Moller was closed this year, we relocated the SMA from there to Simeonof Island. In our current proposal we are funded to install one additional strong-motion instrument near Dutch Harbor. See Figure 16 for these SMA sites. The purpose of these instruments is to collect acceleration data with which to construct acceleration vs. distance relations that are essential to the safe engineering design of large structures such as drilling rigs, pipelines, and holding tanks.

Tilt Measurements. Under D.O.E. and U.S.G.S. funding we annually reoccupy 1 km level lines at Sand Point (2 lines), Squaw Harbor (1 line) and Simeonof Island (1 line). We also continue to operate the tide gauges installed under NOAA funding. For the past two years these tide gauges have been supported by DOE. Beginning last October their operation is supported by the USGS. These tilt measurements provide important data regarding the accumulation of stress in the Shumagin Seismic Gap.

Geologic Investigations. During June 1978 we employed two geologists in a reconnaissance of faults and terraces in the Shumagin Islands region. They mapped several minor new faults and tentatively identified several terraces. The identification and evaluation of faults is essential to the assessment of the activity level of faults within the study area. The ages, heights and distribution of terraces can provide extremely important data regarding past episodes of rapid uplift, perhaps during previous great earthquakes. These terraces may help to define block boundaries that may be particularly prone to relative motion during future earthquakes.

Because these investigations are not seismologic in nature and because the proposal for the present seismic network is considerably above the guideline figure, we have submitted a separate proposal to NSF for the geologic investigations. This work has been approved by NSF for two years. (This and the tide gauges are examples of NOAA funding working as seed money to start relevant research that is eventually carried on by other agencies: USGS and NSF). These geologic investigations are potentially extremely valuable to the pruposes of seismic hazards evaluation.

VI. RESULTS, VII. DISCUSSION, IX. NEED FOR FURTHER STUDY

A. Shumagin Islands Seismicity

Introduction. The main conclusions outlined in last year's Annual Report regarding the seismicity of the Shumagin Islands region remain in force. It is a seismic gap in which high stresses are accumulating along the main thrust zone (MTZ: that portion of the Benioff zone between depths of 10 and 50 km). Most of the seismic activity occurs along the Benioff zone between the depths of 20 and 100 km. The largest events ($4.5 \leq M_b \leq 6.5$) occur along the deep edge of the MTZ. Stress drops (600-900 bars) have been calculated for two of these events that indicate high stress levels for the MTZ. Most of the crustal seismicity occurs in a diffuse zone of hypocenters that trends upward from the lower edge of the MTZ; roughly at right angles to it. Some shallow hypocenters ($h \leq 10$ km) appear to be related to the boundary faults of the graben-like Sanak Basin.

New results described below strengthen the interpretation given above and suggest some new possibilities. Two moderate sized earthquakes occurred along the lower edge of the MTZ: an $M_b = 5.5$ on 28 January 1979 and an $M_b = 6.5$ on 13 February 1979. The locations of these events are consistent with a "Mogi (1969) donut" interpretation for the Shumagin gap that ascribes them to high stress levels around the edge of a future fault plane. Some of the shallow focus ($h \leq 20$ km) earthquakes on the Alaska Peninsula appear to be related to volcanic activity near Stepovak Bay; others to structures north of Black Hill. An attempt to look for segmentation of the Benioff zone failed because of a lack of resolution near the edges of the network. A preliminary study of seismicity as a function of time and space suggests that there may be periods of 3/4 and 2 1/2 years in the seismicity rate and that the occurrence of moderate-sized ($4.5 \leq M_b \leq 6.5$) earthquakes may be related to the phase of the seismicity rate.

Seismicity Maps. Figures 1 and 2 are seismicity maps that show epicenters for all of the earthquakes that are well-located by the Shumagin Seismic Network. The epicenters are marked by numerals giving the focal depth in kilometers. Figure 1 covers the period July 1973 through 10 July 1978, from inception of the network through the most recent events that have been located. Figure 2 covers the period April 1978 through 10 July 1978, the most recent quarterly data set processed.

The most obvious feature seen on the map in Figure 1 is the linear grouping of three clusters of epicenters that trends southwest from a point at about 55°N and 160°W, near the southwest end of Nagai Island. The central cluster began as the aftershock zone of the 4 April 1974 Shumagin Islands Earthquakes ($M_b = 5.7$, 6.0, 4.2); the adjacent ones formed subsequently. The general area of these clusters continues to be active through the spring of 1978, as can be seen in Figure 2.

On 27 January 1979 a magnitude (M_b 5.4 earthquake occurred in the vicinity of the southwesternmost of these clusters. On 13 February 1979 a magnitude (M_S) 6.5 earthquake occurred to the east of the network. A joint location, using data from the Shumagin Network and the University of Alaska's Kodiak Island-Alaska Peninsula Network, places this event at 50 km depth and about 55.2°N and 157.0°W. Thus,

since April of 1974, four events in the magnitude range 5.4 to 6.5 have occurred within 225 km of one another along the lower edge of the MTZ.

The allignment of these events along the lower edge of the MTZ may be understood as part of a "Mogi donut". Mogi (1969) suggested that as a region (seismic gap) prepares to release a major earthquake, the focal plane becomes quiescent while the edges become active. The resultant pattern of seismicity resembles a torrus or "donut". The lack of seismicity along the MTZ toward the trench (Figures 1 and 9) is also consistent with this "donut" pattern. The high stress drops (Archambeau, 1977; House and Boatwright, 1978) for the April 1974 events confirm the high stress levels implied by the "Mogi-donut" interpretation.

The seismicity maps shown in Figures 3 and 4 show only those epicenters for events with depths less than 25 km. Almost all crustal events are shown on these maps; if there are allignments that correlate with crustal faults they should be apparent on maps such as these.

The vast majority of the shallow events are limited to the outer half of the continental shelf, in a band subparallel to the trend of the arc, that includes Sanak and Nagai Islands and is bounded on the seaward side by the trench-slope break. Note that it is exactly this band in which the Sanak and Shumagin Basins are located. This circumstance is probably genetic rather than coincidental: The tectonic forces that created the basins are still at work continuing to form them and causing the earthquakes presently recorded. These events are part of the concentrated zone of crustal earthquakes that trends upward from the lower edge of the MTZ. Therefore, it should not be surprising to find active tectonic features here.

In last year's Annual Report we noted the allignment of epicenters of shallow earthquakes along the boundary faults of the Sanak Basin, suggesting that these faults are seismically active. The most recent quarterly data set, shown in Figure 4, shows 7 more epicenters that lie along strike of the Sanak Basin.

There are several other apparently linear clusters of epicenters east of Sanak Basin. More data and an assessment of the accuracy of these locations are needed before associations between these clusters of epicenters and geological features can be made.

While the crust of the Alaska Peninsula is seismically relatively inactive there are two areas of activity worth noting: They are NW of stations IVF and BLH, respectively.

The cluster of epicenters NW of IVF is plotted on a topographic map in Figure 5 and can be seen in cross-section in Figure 10, below and right of the arrow labeled "V". In cross-section, the slight inclination trenchward of this cluster is similar to that of clusters of hypocenters beneath volcanoes within the Amchitka and Adak networks in the central Aleutians (Engdahl, 1977). On the map (Figure 5) the large solid circles mark the epicenters and the small ones indicate the locations of fumerolic vents. The locations of these vents and the outline of the flows on Kupreanof and the "New" volcano were provided by Tom Miller (USGS Anchorage, unpublished map, 1978). These vents have probably been more or less active since at least 1944 (T. Miller, personal communication, 1978; Capt. E. Skinner, flight logs of Reeve Aleutian Airways 1958-1961; the author, personal observations, 1976). The seismic events are sporadically distributed in time and are probably part of a

long-term (decades) sequence of activity at depths from 5 to 15 km beneath the volcano. These depths are not well-constrained because they have been determined from arrival times at stations of the regional Shumagin Network; the third closest effective station being some 80 km distant. To pin down these depths and to obtain a better idea of the spatial and temporal pattern of the seismic activity it would be necessary to establish one or two stations within 5 km of the volcano.

The last area of special note is that about 30 km NW of the station BLH, Black Hill. On the map in Figure 3 there is only one event plotted in this area. Several more have occurred in this vicinity but were not locatable with sufficient accuracy to plot on this map. These events are notable in that they are the only ones detected by the Shumagin Network that are north of the Alaska Peninsula. They also happen to be located at the place where the Jurrasic sediments trend offshore. Burk (1965) notes that the source plutons for these sediments are missing. It is possible that the seismic events are related to a possible faulted northern boundary of these beheaded sediments.

Hypocentral Cross-sections. The hypocentral cross-sections shown in Figures 6-10 were plotted in an attempt to locate a suspected offset or segmentation of the Benioff zone between sections C-C' and D-D'. The resolution of the Benioff zone in the outer sections (A-A', B-B', E-E' and F-F') was so poor that no conclusion could be drawn regarding the segmentation question. We suspect that refraction along the dipping slab is causing an additional difficulty in locating events just outside of the network. This problem will be investigated in the next few months using a ray-tracing program now being revised by Jacob and Krause (Jacob, 1970).

In section C-C', Figure 8, there is a remarkable vertical allignment of hypocenters, suggestive of an active fault plane breaking toward the surface. The hypocenters less than 25 km in depth form the cluster of epicenters seen in Figure 3, about 30 km SW of Nagai Island in the reentrant of the 50 fm isobath.

Section D-D' is located through the middle of the Shumagin Islands and is therefore the best constrained by the geographic distribution of the seismic network. This section best defines several features of the Benioff zone and related crustal seismicity. These features are depicted in Figure 12 in a cartoon based on section D-D'. The seismicity has been assigned to one of several zones. This zonation will be important when computing the seismic hazard/risk of the region. The zones and their characteristic seismicity are described below:

MAIN THRUST ZONE - This zone lies along the interface between the underthrusting Pacific plate and the overriding wedge of the island arc crust. It extends from about 10 to about 50 km depth. The great thrust-type earthquakes occur in this zone; these can have the largest possible magnitude: in the range 8-9. When the great earthquake occurs that "fills" the Shumagin gap, its fault plane will lie along the MTZ. We have described above the magnitude 5.5-6.5 events that are occurring along the lower edge of the MTZ and their implications for high stress there. That there are few events located here (Figures 6-11) is consistent with the hypothesis that this zone is "locked" and hence accumulating strain energy to be released in a great earthquake.

NORMAL ZONE - This is a zone of generally shallow earthquakes that lies under or just seaward of the trench. The focal mechanisms of these events indicate normal faulting (Stauder, 1968; House, 1977). Extremely rare, great normal-

faulting earthquakes have occurred in this zone, but for practical purposes an upper limit of 7.5 or 8 can probably be placed on the magnitude of events to be expected here.

COMPRESSION ZONE -
TENSION ZONE - These zones have only recently been identified as being separate and characterized by opposite focal mechanisms: down-dip compression and tension, respectively for the upper and lower zones (Umino, 1976; Engdahl and Scholz, 1978). The existence of these zones has not been established for the Shumagin Island region, hence the question marks in the cartoon. The earthquakes in these zones are the result of body or bending forces; their maximum magnitude is probably on the order of 8.

CRUSTAL CONCENTRATION ZONE - This is a zone of persistent, low-magnitude earthquake activity, probably in response to the highly stressed region at the base of the MTZ. Maximum magnitudes here and in the Diffuse zone will probably be about 7.5 and result from strike slip faults.

VOLCANIC ZONE - Associated with several Aleutian volcanoes there is a small inclined zone of low magnitude earthquakes. The cause and maximum magnitude of these events are not clear.

DIFUSE ZONE - The remaining crust of the island arc, outside of the Volcanic and Concentrated Zones, is called the Difuse Zone because only a few events are recorded here. These events are probably caused by a variety of stress conditions and may include some large magnitude earthquakes of the order 7.5.

ASEISMIC ZONE - Below the Difuse and Concentrated Zones and above the Compression Zone there is an aseismic region that has been observed to be a universal feature of island arc subduction zones. Yoshii (1975) characterized this zone in Japan by its trenchward extent at about 40 km depth: he called this the aseismic front. The aseismic front is indicated in the cartoon in Figure 12 by the arrow marked "AF".

These and possibly other zones should be studied by the OCSEAP seismic investigators. Characteristic mechanisms, maximum magnitudes and recurrence intervals should be specified for inputs to seismic hazard/risk calculations.

Seismicity Rates. A preliminary study of the temporal and spacial patterns of the seismicity detected by the Shumagin Islands seismic network is summarized by the plots shown in Figures 13 and 14.

Monthly totals of the events detected at and within 250 km of the seismic station, SQH, near Squaw Harbor are plotted in Figure 13. When this station was only recorded for part of a month the count for that part is indicated by the solid bar top; the extrapolated count for the month is indicated by the dashed bar top. If no count was made for a given month, this is denoted by an "X" in the column for that month. A "detected event" is any event for which an S-P time could be measured for SQH.

This plot shows that the seismic rate thus measured for SQH ranges between about 10 and 131 events per month. Averaged over 9-month intervals the monthly rate ranges between 20 and 70 events per month. The period July 1973-April 1974

averaged between 60 and 70 events per month, culminating in the 131 events, most of which were aftershocks of the 6 April 1974 earthquake sequence. During the following 16 months the rate dropped sharply to an average 26 events per month, less than half the previous rate. In September 1975 the rate returned close the previous high average, at about 50 events per month. If this long term change in rate from high to low to high were indicative of some periodic phenomena it would have a period of some 2 1/2 years.

Also plotted in Figure 13 are the times of the largest magnitude events. A very tentative suggestion of this data is that the larger magnitude events appear to correllate with high or increasing seismic rate, when that rate is averaged over about 9 months.

In Figure 14, a time-space plot of the seismicity shown in Figure 1 is given. The region covered by this plot is approximately that between the center lines of the sections A-A' and F-F' shown in Figure 1.

The most striking feature of this plot is an apparent 9-month periodicity in the seismic activity. This must be viewed cautiously because several of the data gaps that result from partial or total network failure enhance this apparent periodicity. Nevertheless there are several instances of an increase or decrease in seismic activity that are regional. That is, the activity increases or decreases across the entire region, as if in response to a regional change in stress. This periodicity or quasi-periodicity, if real, might be very useful in making intermediate-term earthquake predictions.

Summary. The seismic activity in the Shumagin Islands region is consistent with that expected for a seismic gap. Most of the seismicity occurs along the lower edge of the MTZ with two M $\sim$ 6 events indicating high stress levels there. In the crust there are three regions of special activity: (1) along the boundary faults of the Sanak Basin; (2) beneath Kupreanof Volcano; and (3) along the edge of the Jurrassic structures north of Black Hill.

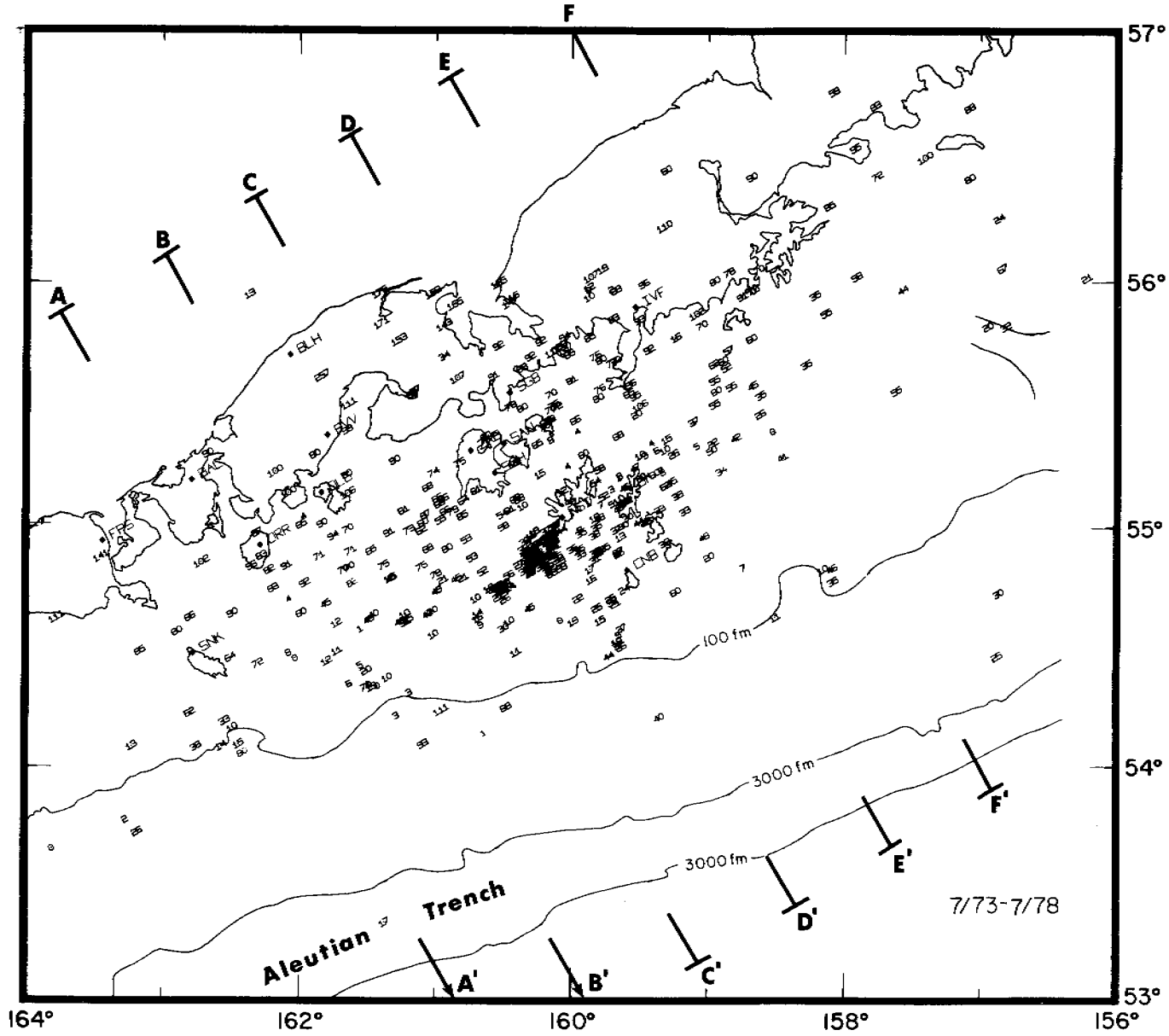

Figure 1. Seismicity map. All highest quality events are plotted for the period July 1973 - 10 July 1978. Epicenters are marked by numerals that give the depth in km. Seismic stations are marked with a solid square and labeled by their 3-letter designator code. The lines A-A', B-B', ... F-F' locate the central plane of the volume within which hypocenters were projected onto the cross-sections shown in Figures 6, 7, ... 11, respectively.

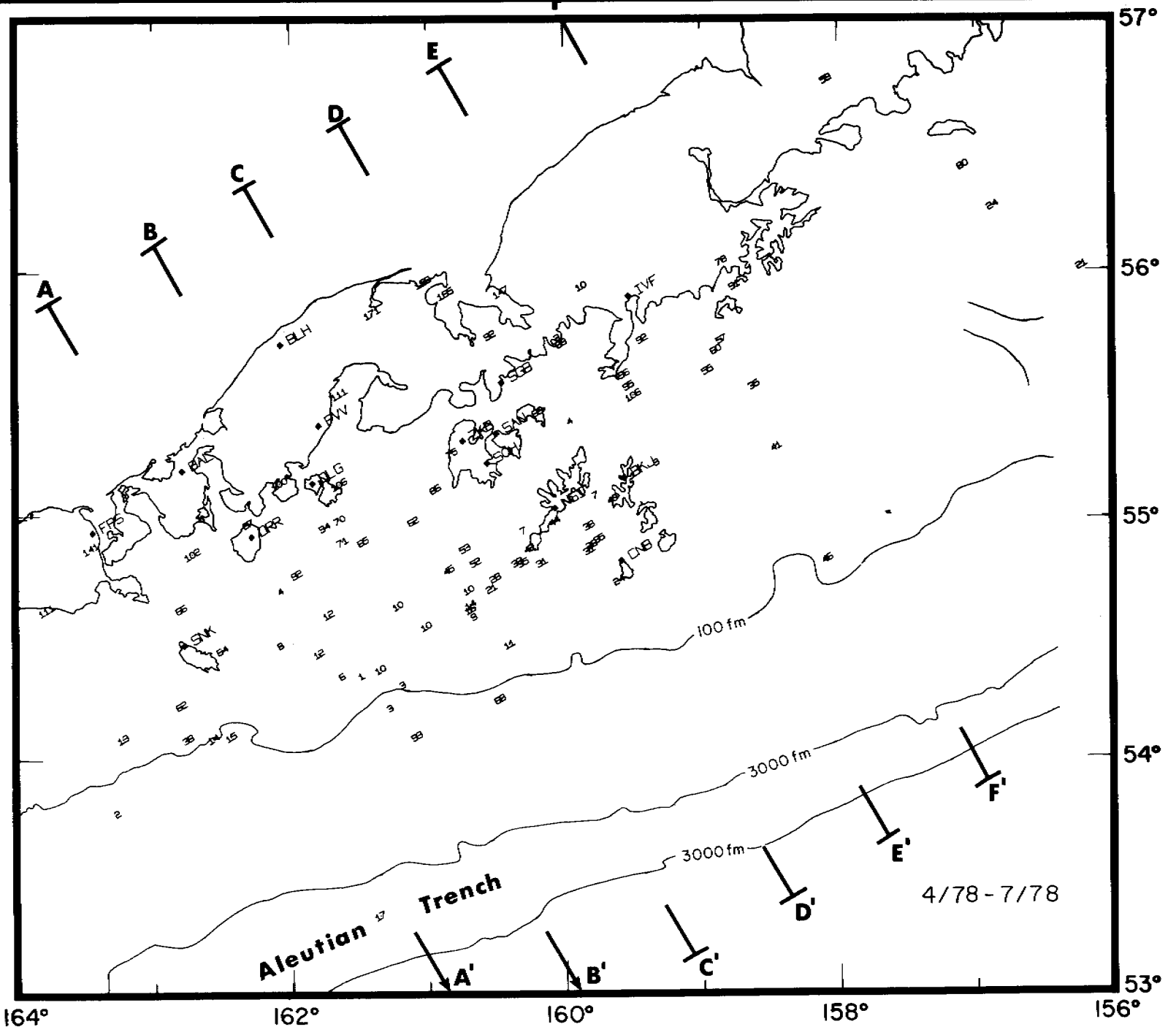

Figure 2. Seismicity map. Same as Figure 1, except that the period is April, 1978 - July 1978.

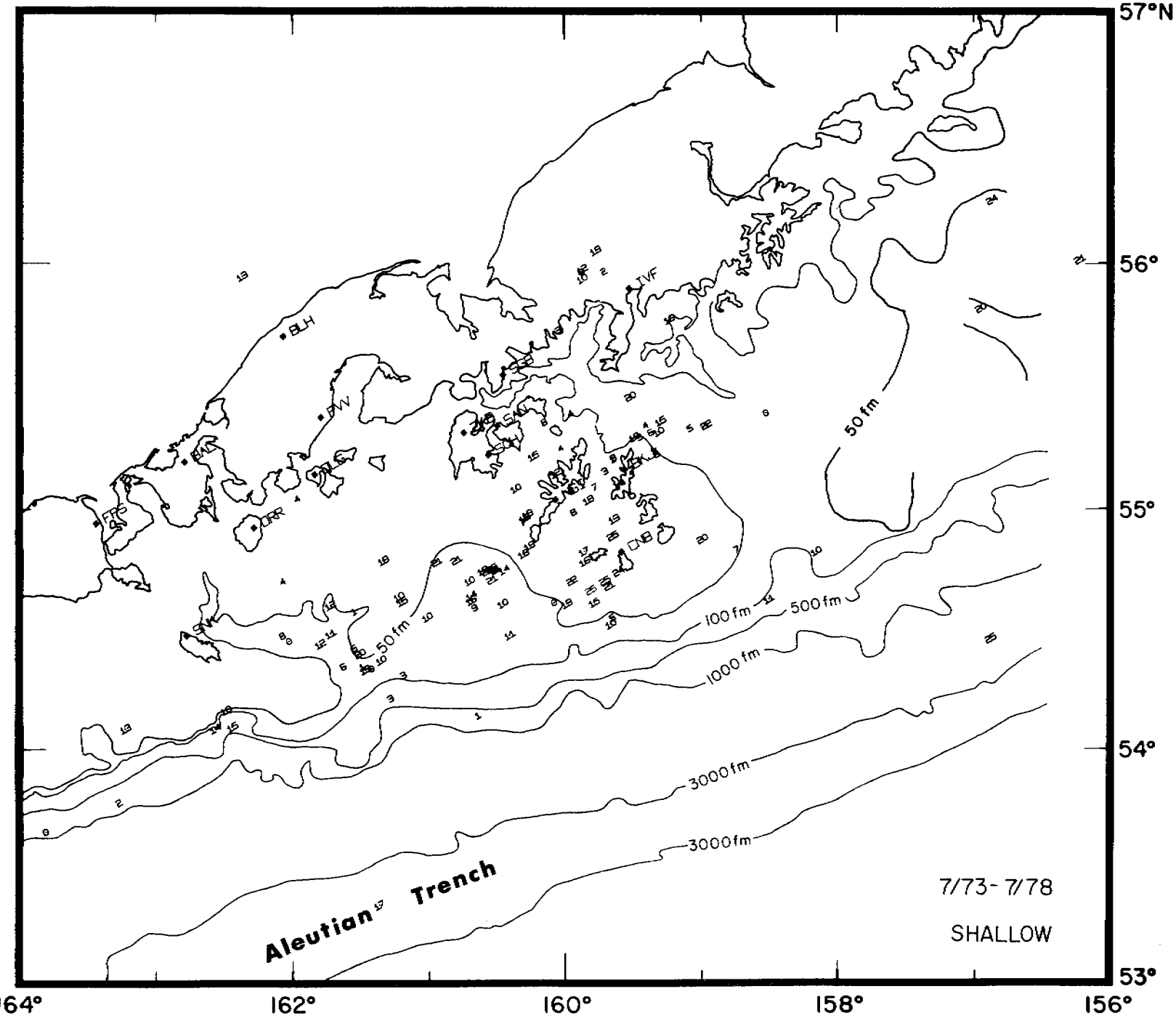

Figure 3. Shallow seismicity map. Same as Figure 1 except only those events shallower than 25 km depth are

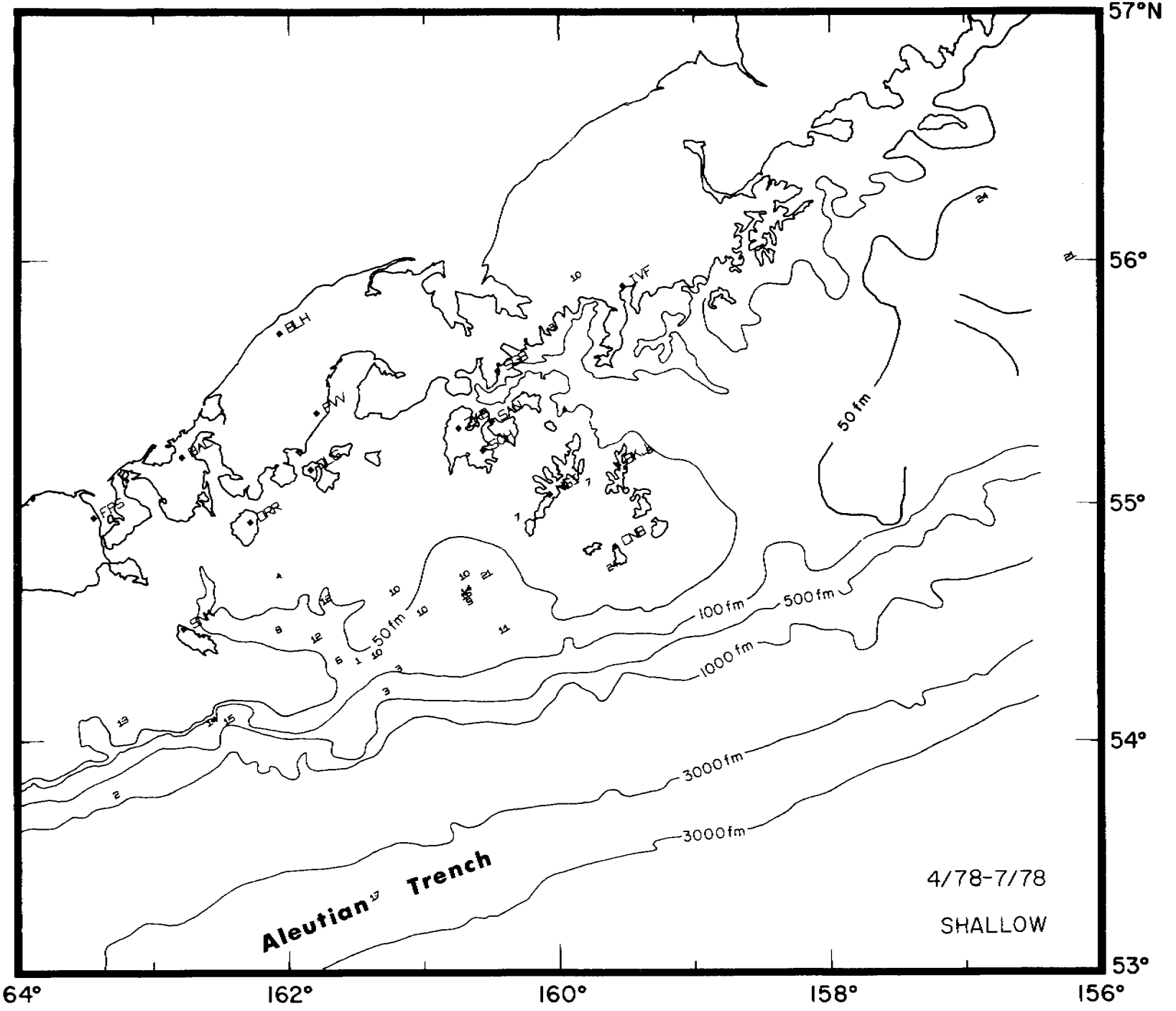

Figure 4. Shallow seismicity map. Same as Figure 3 except events are shown only for the period April - 10 July 1978.

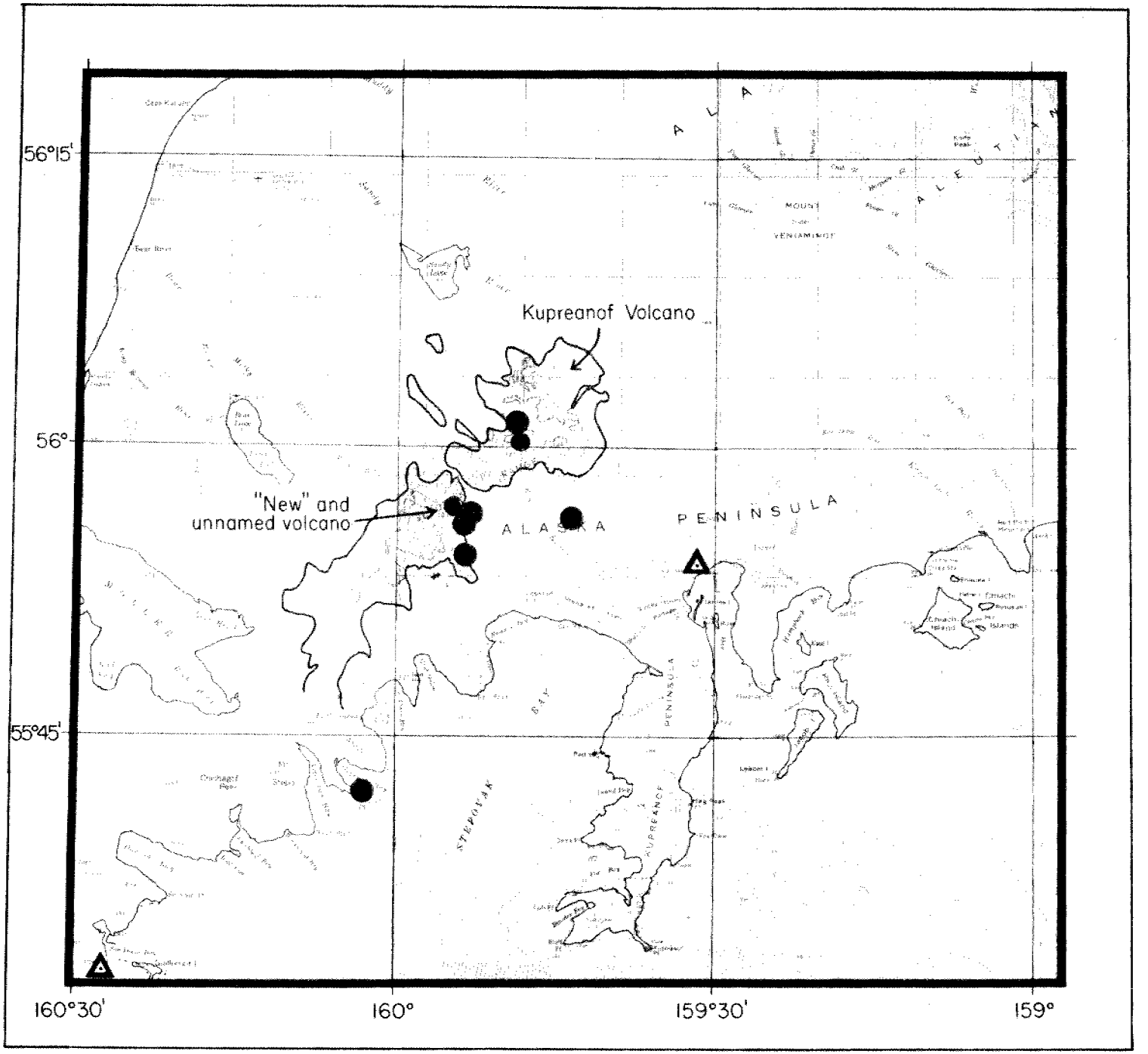

Figure 5. Volcanic seismicity map. Epicenters shown by larger solid circles. Fumerolic vents shown by smaller solid circles. Locations of vents and recent flows, shaded areas, provided by Tom Miller, USGS Anchorage. Nearest seismic stations shown by open triangles.

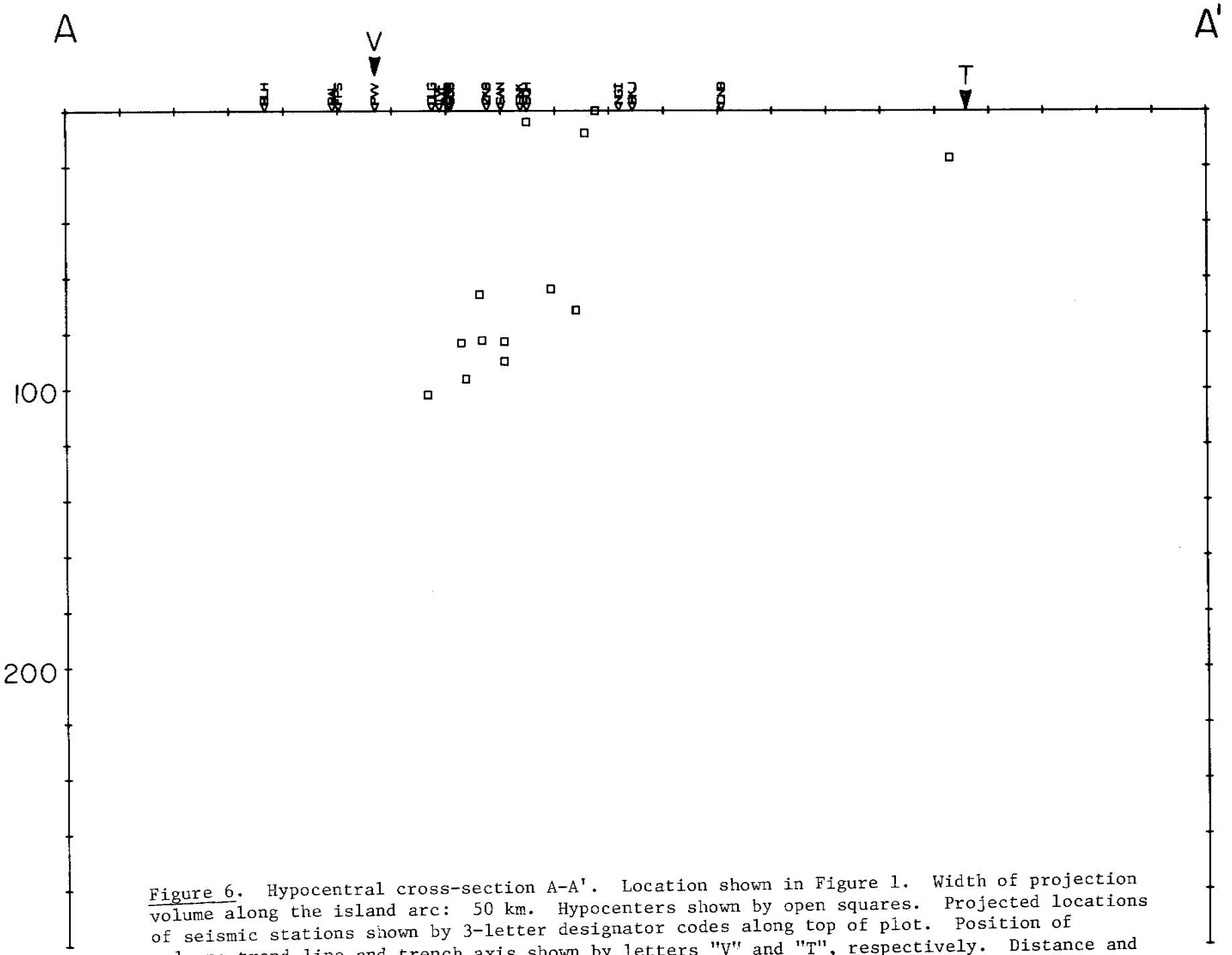

Figure 6. Hypocentral cross-section A-A'. Location shown in Figure 1. Width of projection volume along the island arc: 50 km. Hypocenters shown by open squares. Projected locations of seismic stations shown by 3-letter designator codes along top of plot. Position of volcano trend line and trench axis shown by letters "V" and "T", respectively. Distance and depth indicated by 20 km tic-marks; no vertical exaggeration.

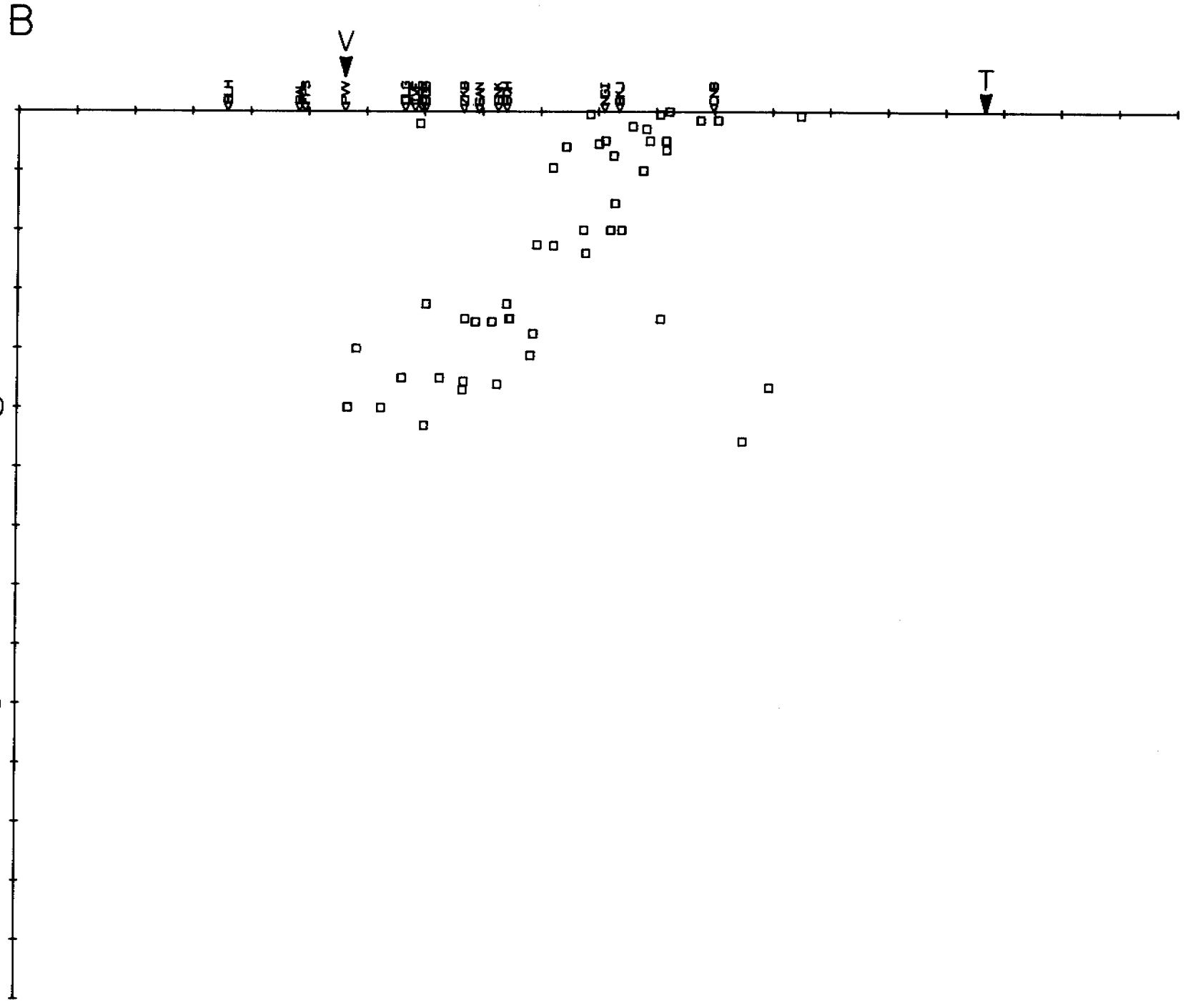

Figure 7. Hypocentral cross-section B-B'. Details same as Figure 6.

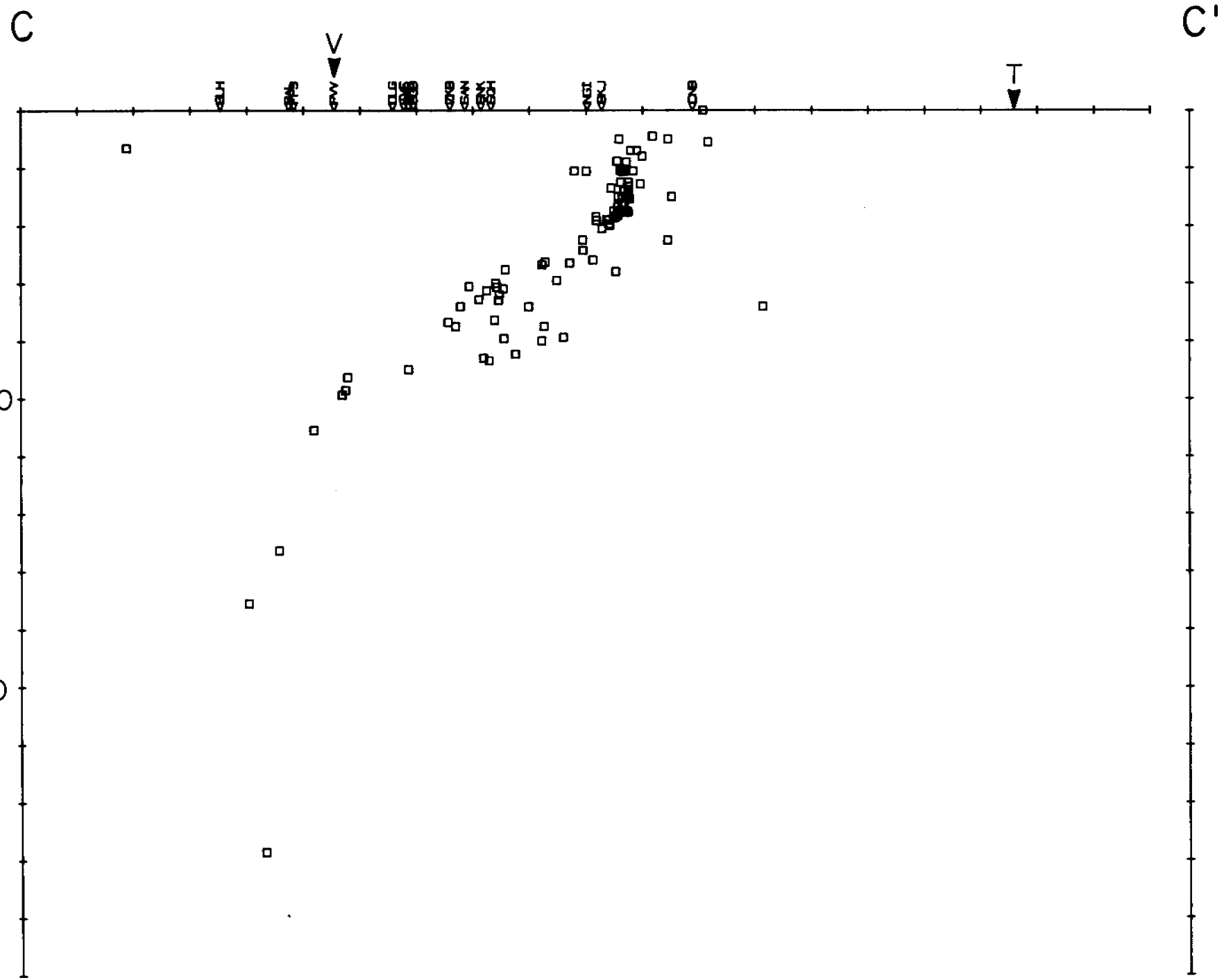

Figure 8. Hypocentral cross-section C-C'. Details same as Figure 6.

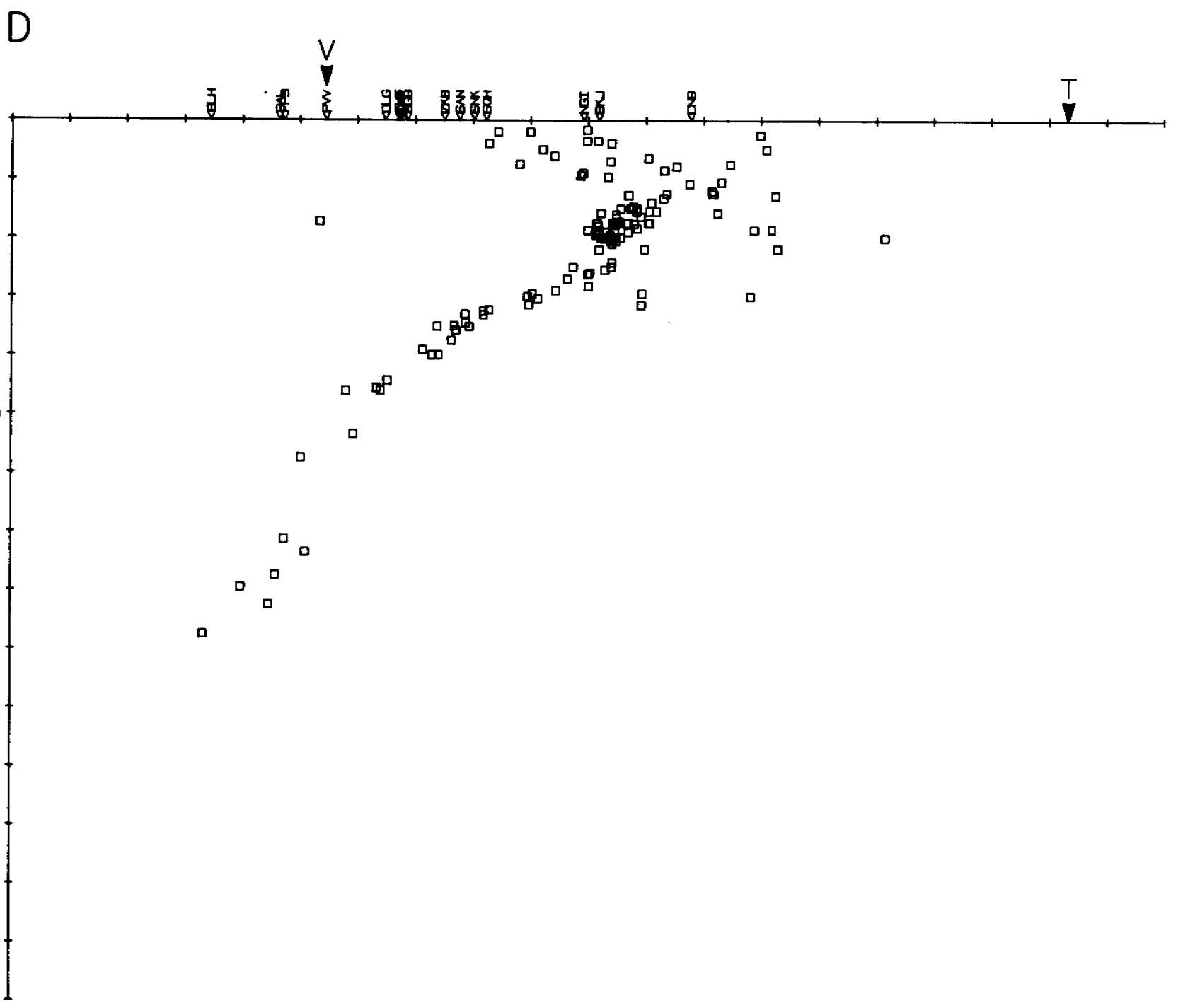

Figure 9 Hypocentral cross-section D-D'. Details same as Figure 6.

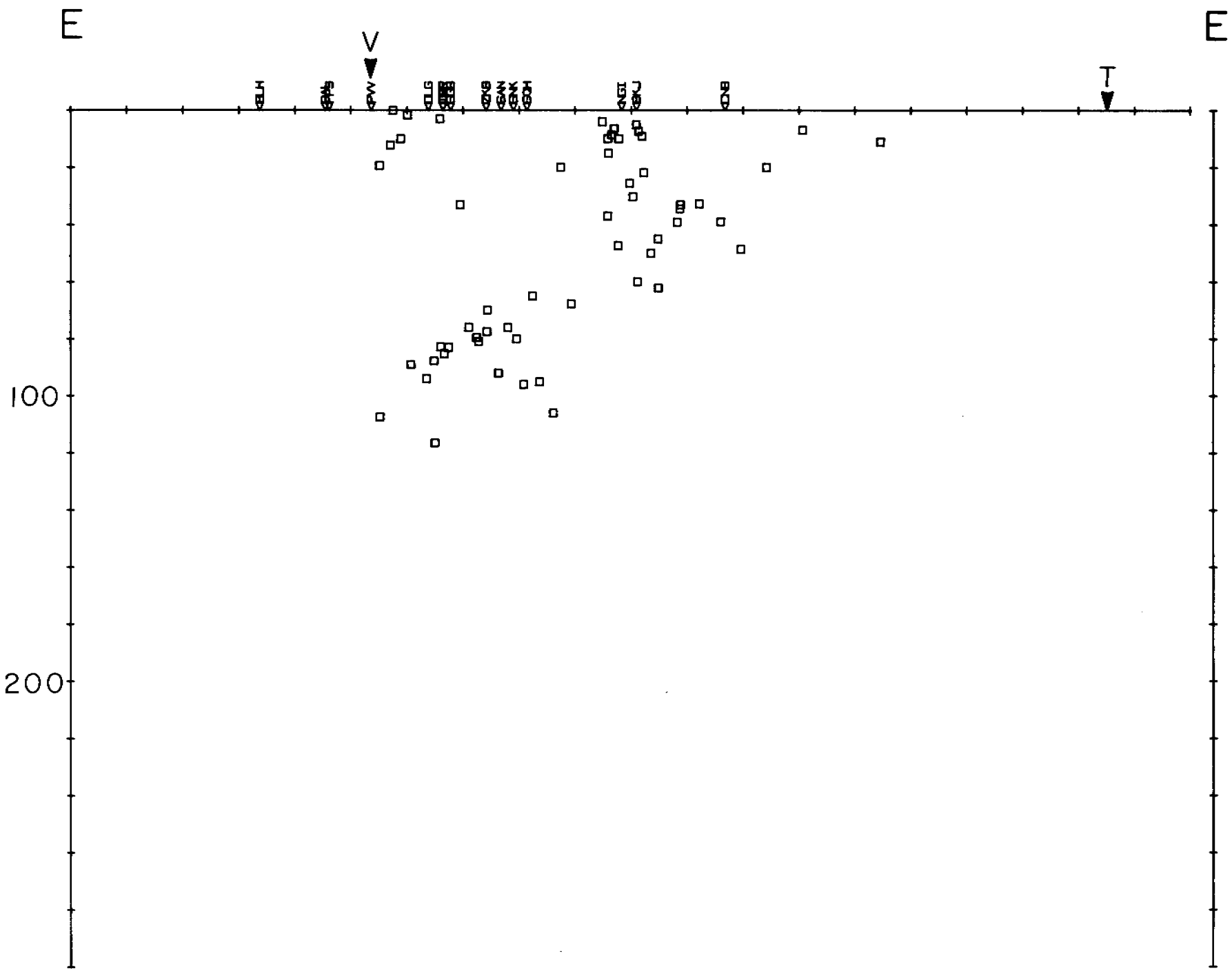

Figure 10. Hypocentral cross-section E-E'. Details same as Figure 6.

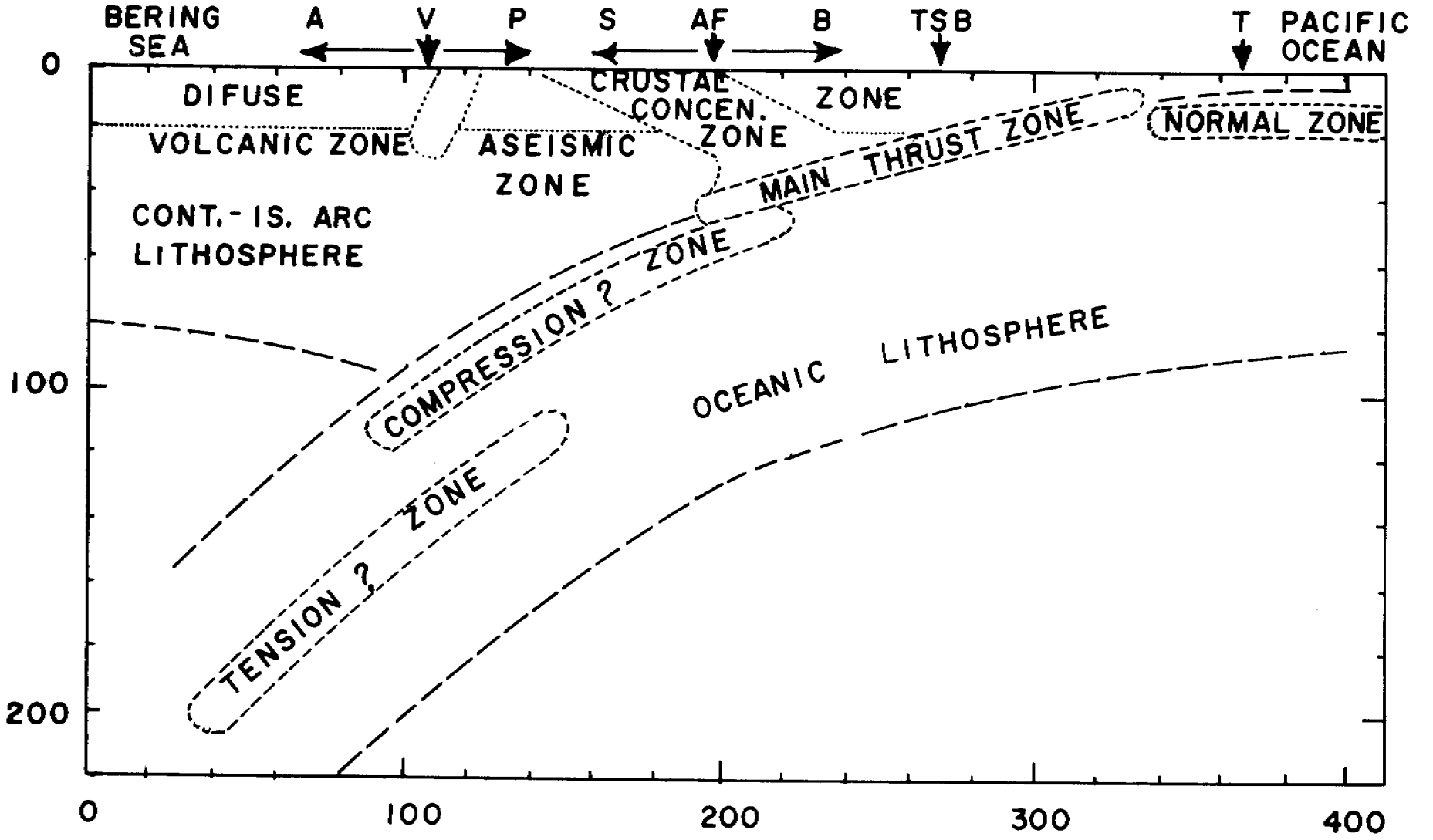

Figure 12. Cartoon cross-section of subduction zone. Based on section D-D', Figure 9. Width of Alaska Peninsula indicated by horizontal arrows labeled "A" and "P". Width of "continental" shelf occupied by sedimentary basins indicated by horizontal arrows labeled "S" and "B". Locations of volcanic trend line, aseismic front, trench-slope break, and the trench axis marked by letters "V", "AF", "TSB" and "T", respectively. Boundaries of lithospheric plates are largely hypothetical; principal assumptions: (1) trench and dip-slip events at bottom of MTZ mark upper surface of the Pacific plate, (2) this surface curves downward rather smoothly, remaining above compression zone, and (3) lithosphere is about 80 km thick. Seismic zones are described in the text.

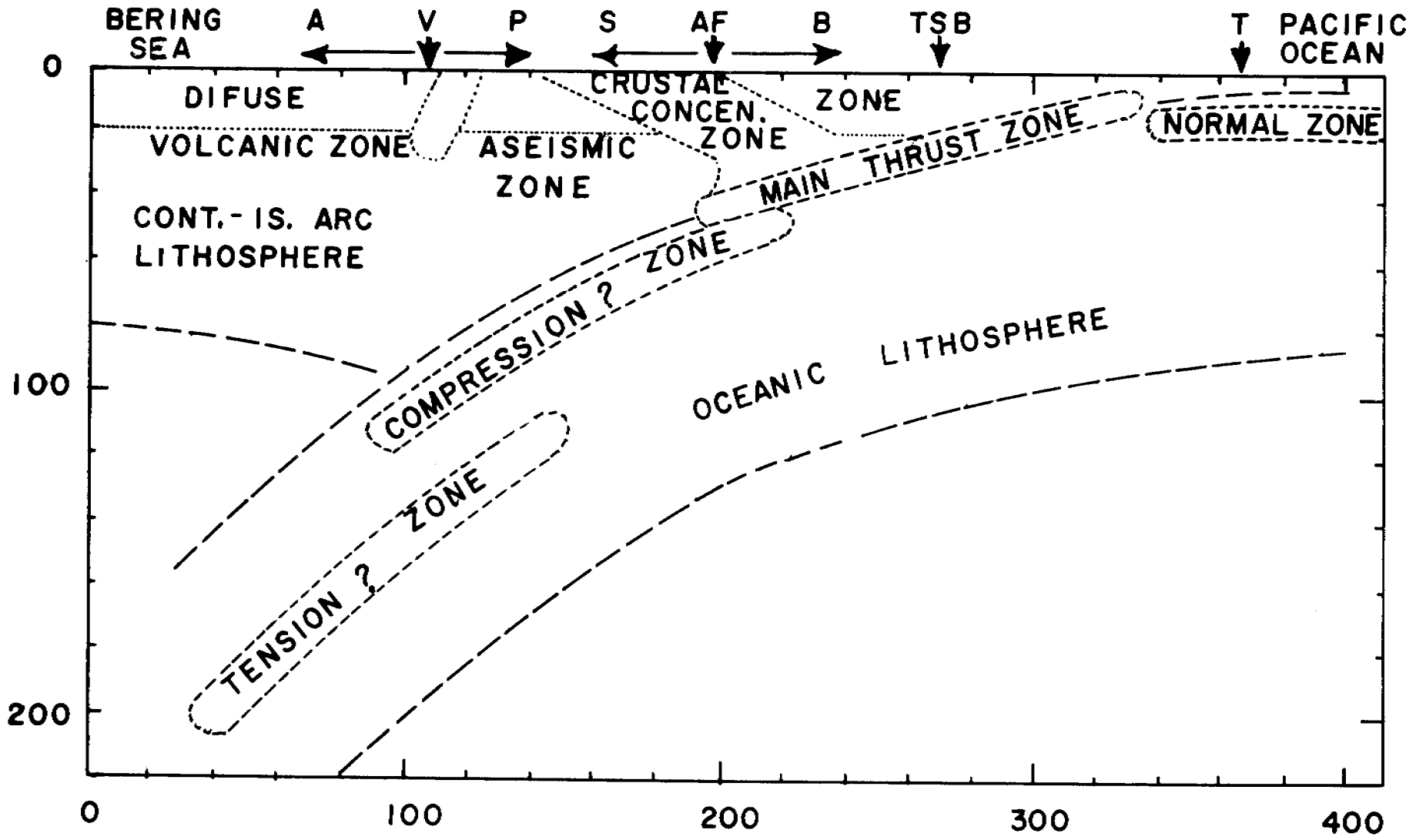

Figure 12. Cartoon cross-section of subduction zone. Based on section D-D', Figure 9. Width of Alaska Peninsula indicated by horizontal arrows labeled "A" and "P". Width of "continental" shelf occupied by sedimentary basins indicated by horizontal arrows labeled "S" and "B". Locations of volcanic trend line, aseismic front, trench-slope break, and the trench axis marked by letters "V", "AF", "TSB" and "T", respectively. Boundaries of lithospheric plates are largely hypothetical; principal assumptions: (1) trench and dip-slip events at bottom of MTZ mark upper surface of the Pacific plate, (2) this surface curves downward rather smoothly, remaining above compression zone, and (3) lithosphere is about 80 km thick. Seismic zones are described in the text.

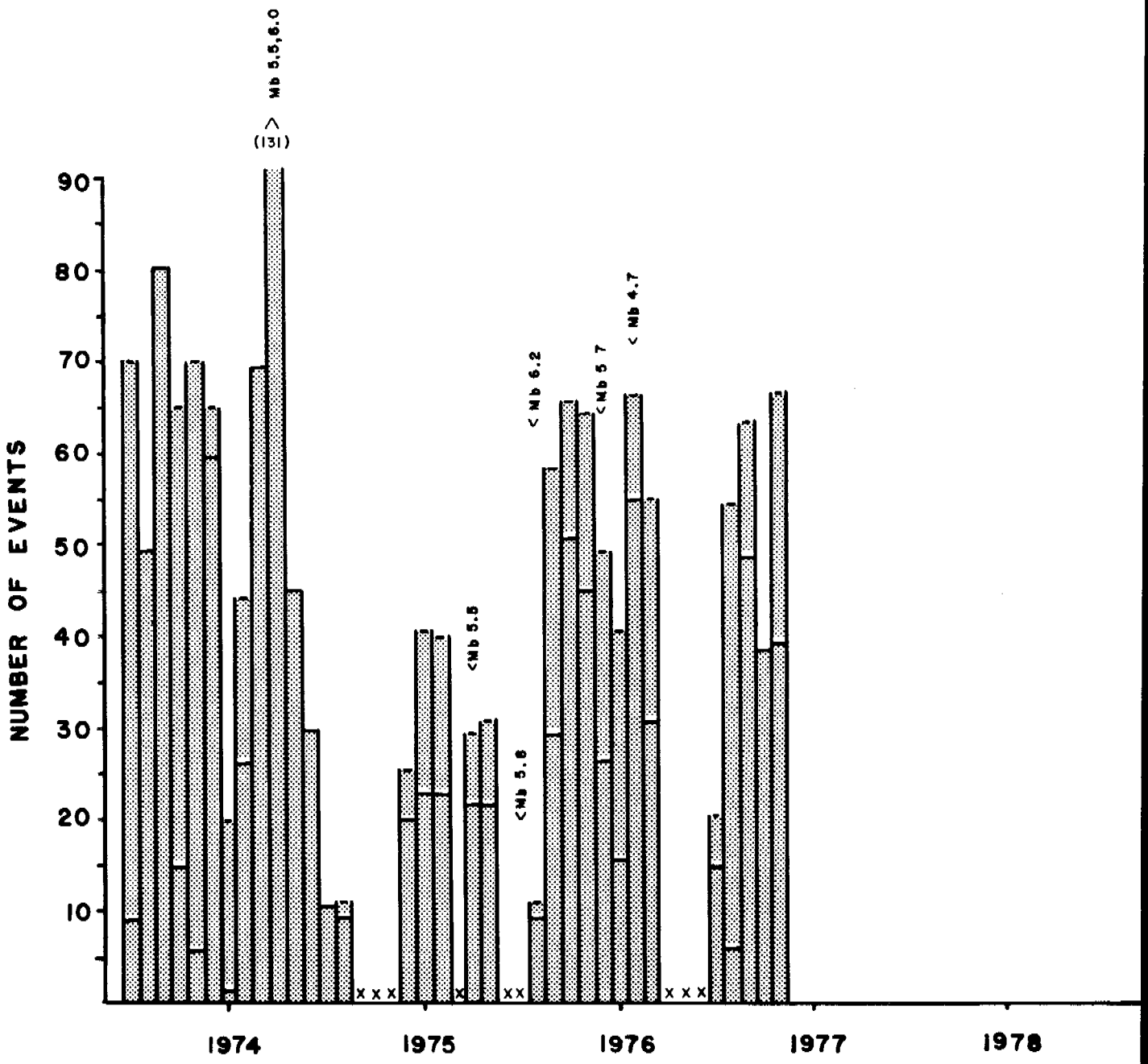

Figure 13. Monthly count of events within 250 km of Squaw Harbor, recorded by station SQH since installation. The solid bar tops represent the actual count of events; the dashed bar tops are the counts corrected for recorder down time. Counts in months for which large corrections are necessary are, therefore less reliable counts. For several months, the recorder was not operating for the whole month, counts for these months are marked as 'X'. Occurrence times of teleseismically located events with $m_b \geq 5.5$ and epicenters within 250 km of SQH are plotted, also, as well as that of a smaller earthquake, $m_b = 4.7$, which was part of a sequence located by the network.

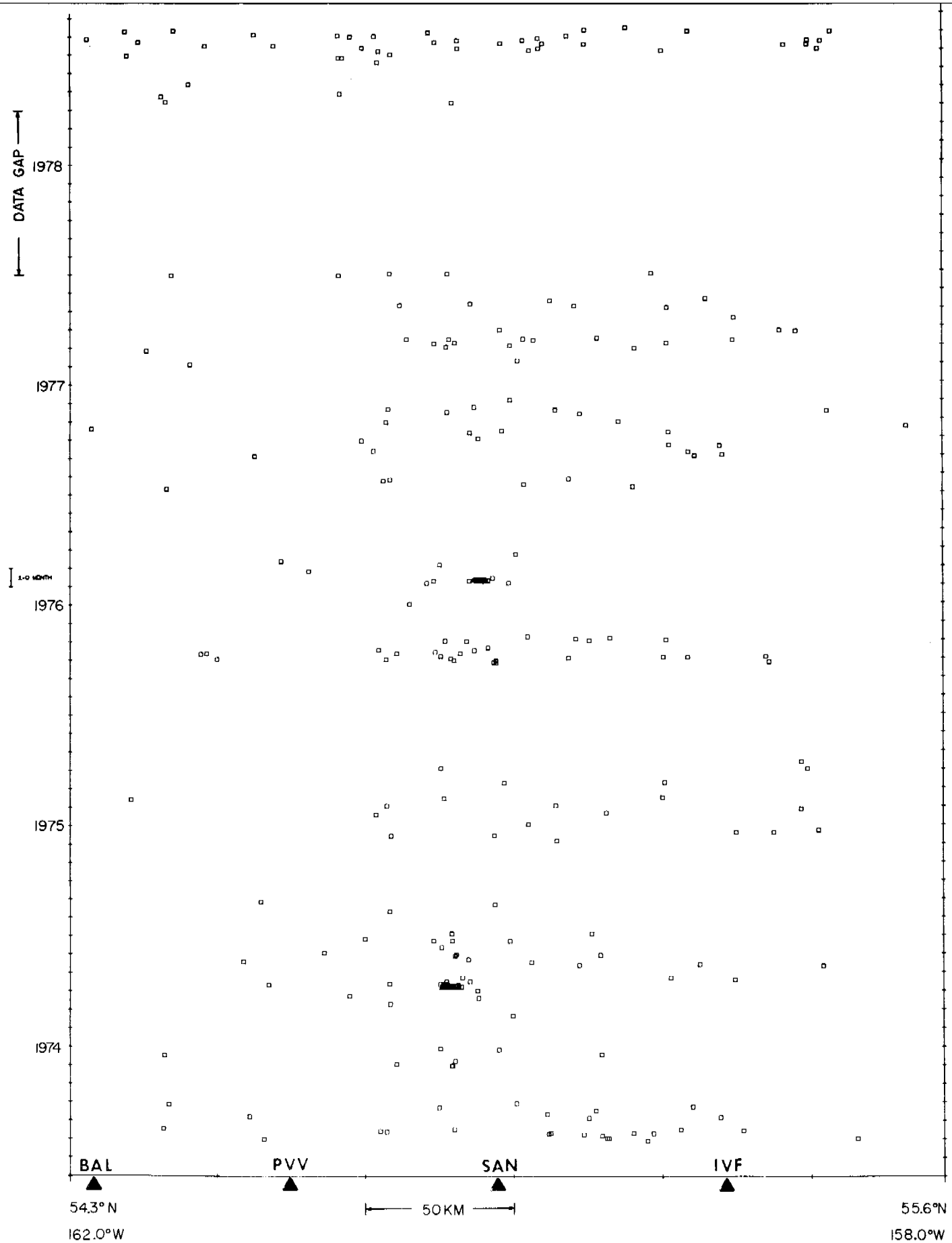

Figure 14. Time-space seismicity plot. The seismicity shown on the map in Figure 1 (between lines A-A' and F-F') is projected onto a line subparallel to the island arc; this line is the horizontal axis of the plot. The vertical axis is time, in months. The events are marked by the open squares. Time intervals marked "data gap" refer to times when no data is available because the network was not operational. The locations of selected seismic stations are projected onto the space-axis and labeled with their 3-letter designators.

B. Seismicity in the SE-Bering Sea

Lamont operates a seismic station on St. Paul Island, in the Pribilofs, consisting of one long period and one short period vertical seismometer. With this limited set of instruments it is not possible to locate earthquakes, or correlate earthquakes with any known tectonic features. However, it is possible to determine approximate radii to epicenters which fall within the Bering Sea, by using the difference in arrival times of S and P phases, and to determine whether the loci of possible epicenters intersect any known faults.

The Saint George Basin, southeast of Saint George Island, has been mapped as a long (> 300 km), narrow (30-50 km) graben with more than 10 km of upper Mesozoic and Cenozoic sedimentary deposits (Marlow et al., 1977). Using single and multichannel marine seismic data, Marlow et al. (1977) have mapped normal faults which rupture the sedimentary rocks and correlate with offsets in the basement surface. These faults are thought to possibly be active features. Because of the possibility of petroleum exploration in this basin, it is important to determine the level of seismic activity in that area. Although the activity recorded by the Saint Paul station is low, there were a number of events detected within the past year which would fall within the proper distance range for a source in the Saint George Basin.

Table 1 shows all the events recorded by the Saint Paul instruments, excluding the very distant teleseisms recorded by the long period seismometer. (There were no records for the months of May and June, as the local operator was away). The low rate of recorded activity may also be due to the extremely low gain at which this station must be operated in order to minimize surf noise (the station is near the shore), and because the station is located on unconsolidated volcaniclastic sediments. It is estimated that the magnitudes of the events are approximately 4 or less. Five events have S-P times between 14 and 31.5 seconds which, assuming near-surface foci, puts them at distances between approximately 112 and 250 km from St. Paul Island. This distance range would be consistent with the St. George Basin as a source area. Two events had S-P times of 7.9 and 11 seconds, which would put them closer to Saint Paul, at distances of approximately 63 and 88 km. The remaining events recorded by the short period isntrument fall within approximate radii of 376 to 584 km, and may be associated with the Aleutian island arc seismicity.

Figure 15 shows an example of an event which was recorded by the short- and long-period vertical instruments on July 13, 1978 at 13:26:29 GMT. It was located in the Fox Islands and assigned a surface wave magnitude of 5.7 by the P.D.E. This event was also recorded by the Shumagin/Cold Bay array and by the Dutch Harbor station. For local events of sufficient magnitude which are recorded by all of the Lamont instruments in the Aleutian-Bering Sea region, it is possible to obtain better epicentral locations. Information regarding crustal structure, lateral inhomogeneities in seismic velocity, and other path-dependent effects can be gained by studying the surface wave dispersion and other features of the seismograms recorded by the entire network at different azimuths.

Precise location of earthquakes and their correlation with known tectonic features is not possible with the existing instruments on St. Paul. In order to understand the distribution of seismicity in the southeast Bering Sea, it would be necessary to install more instruments in the Pribilofs - perhaps on St. Paul and

St. George Islands. With the existing data set, it is difficult to accurately assess the seismic hazards - with respect to petroleum exploration or other activities - in the southeast Bering Sea. The most we can say at present is that there is a moderately low level of activity which falls within distance ranges consistent with possibly-active features, such as the St. George Basin. We have no estimates of the expected ground accelerations for determining construction designs. Based on new methods presently being developed for analyzing broad-band seismic data recorded by an instrument at Sand Point, and extrapolating the results to regular long- and short-period records, it may be possible to estimate a range of expected ground motions at Saint Paul from existing seismic records and from intensities listed in historical felt reports for the Pribilof Islands.

TABLE 1

EVENTS RECORDED BY THE SEISMIC STATION AT SAINT PAUL

SHORT-PERIOD VERTICAL

Date*	Time (GMT)	Max. Amplitude (mm,p-p)	Period (sec.)	S-P (sec.)	Approximate Δ (km)
4/25/78	04:30:20.9	∿ 7 mm	∿ .5	73.1	584.8
7/07/78	∿ 04:27	Questionable event of very small magnitude			
7/13/78	13:26:29.0	∿ 9.5 mm	∿ .8-.9	28	224
7/19/78	9:34:36	≤ 1	∿ 1	not clear	
7/24/78	14:52:34.1	∿ 2 mm	∿ 1	7.9	63.2
8/02/78	10:14:40.0	∿ 2	∿ .6	∿ 72	576
8/05/78	17:45:19.5	∿ 2	∿ .6	∿ 63.5	189
8/09/78	01:51:00	2	.5	47	376
8/09/78	04:36:26	2	.5	52	416
8/15/78	12:49:48.5	2	1	not clear	
8/24/78	9:01:20.5	4.5	.5	31.5	252
8/26/78	2:54:30.5	2	.5	51	408
8/26/78	5:57:51.0	4.5	.5	53(?)	424
9/24/78	16:43:15	3	.75	11	88
9/25/78	9:41:58	∿ 5	∿ .8	?	
11/03/78	5:23:32	2.5	.5	53.5	428
11/29/78	17:42:25	2.5	.6	14	112

*Date as noted on top of record. Actual date is one day later.

TABLE 1 (con't.)

LONG PERIOD VERTICAL

Date	P-Time (GMT)	Amplitude	Period	S-P	Comments
6/13/78	08:21:19			5 min 41 sec	Clipping surface waves $\Delta \sim 24.5°$
7/10/78	00:16:57				Probable local event, but small and unclear
*7/13/78	13:26:28	$\sim$ 23 mm	18 sec (surface)	28	$\Delta \sim 2°$
7/24/78	14:52:32			8 min 28 sec	$\Delta \sim 36.5°$
9/15/79	11:46:24			5 min 16 sec	$\Delta \sim 22.7°$

*PDE (weekly) 7/13/78 13:25:20.5 52.56N 168.95W Fox Islands
MSZ = 5.7 h = 51 km

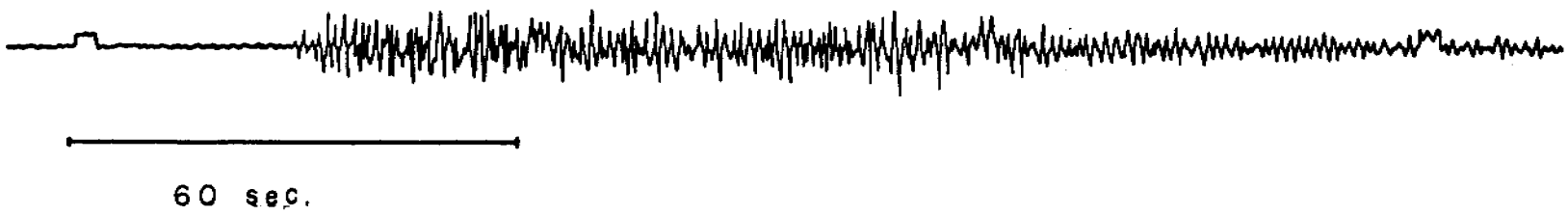

Figure 15a. Saint Paul short period vertical record from July 12, 1978. First minute mark shown in 13:26 GMT. The event occurred in the Fox Islands, with surface wave magnitude of 5.7 (P.D.E.).

Figure 15b. Saint Paul long period vertical record for the same event as that shown in Figure a. The minute mark immediately before the first arrival is 13:26.

C. Strong Ground Motions and Quantitative Hazards Analysis

During this reporting period three major advancements towards assessment of hazards from seismic strong ground motions were made: (1) The number of strong-motion accelerometer records was doubled (from 3 to at least 6); (2) Interpretation of some of the earlier strong motion records yielded unusual seismic source properties (i.e. high stress drops ranging from 600 to 900 bar) for some of the moderate-size earthquakes (m_b 5 to 6) within the Shumagin Islands seismic gap; and (3) Computer software was developed to process some 30 broad-band records obtained during 1972/1973 from earthquakes (with magnitudes m_b = 3 to 6) which generated ground motions of a slightly lower level than usually are recorded by standard strong-motion accelerometers; this data set, when properly scaled, will be an important complementary data base to standard accelerograms that can be used to arrive at realistic forecasts for ground motions from future great, gap-filling earthquakes in the Shumagin Islands segment of the Alaskan outer continental shelf.

(1) New Strong-Motion Records. Figure shows the present distribution of 4 Lamont- and 1 USGS-operated strong-motion accelerometers in the wider Shumagin Islands region. Two earthquakes (January 27, 1979, m_b = 5.4; and February 13, 1979, m_b = 6.5) occurring at a distance of 58 km and 225 km, respectively from the Sand Point (SDP) site triggered the SDP accelerometer and produced useful strong-motion records (Figure 16). We anticipate that the larger shock may have triggered also the accelerometer at Simeonof Island (SIM, see Figure 16) installed there during 1978. Since this site cannot be visited by us until the field-season in June/July 1979, we cannot yet ascertain whether a useful record was obtained.

A strong-motion accelerogram from a Lamont-installed instrument was also obtained outside the Shumagin area from a magnitude Ms 7 3/4 to 8 earthquake (near St. Elias mountain) in the northeastern Gulf of Alaska on February 28, 1979. This event triggered the strong-motion instrument at Yakutat at an epicentral distance of about 155 km and showed a peak horizontal acceleration of about 0.07 g (Lahr et al., 1979). The record was retrieved by the U.S. Geological Survey and is presently processed there for inclusion into the strong motion central data file. For more information on the February 28 St. Elias earthquake see note appended to this annual report. The peak horizontal accelerations (1.0% g and 6.1% g, respectively) from the two Sand Point records are plotted on Figure 18, as a function of distance to the causative fault together with earlier peak acceleration values obtained in the Shumagin Islands, and are compared with similar data collected by Page et al. (1972) for the western U.S. The new data confirm the trend suggested by the earlier Shumagin data; i.e., that for a given magnitude and distance from the source, peak horizontal accelerations in the Eastern Aleutian arc are generally a factor of 2 to 4 higher than in the western U.S. This higher level of shaking can be caused by the difference in source properties or by the differences in attenuation and propagation properties of the two tectonically distinct regions. In the next paragraph we suggest that the higher stress drops observed in the Shumagin Islands region are at least in part responsible for these higher levels of shaking.

(2) Investigation of Two High-Stress Drop Earthquakes in the Shumagin Seismic Gap, Alaska. Two moderate size (m_b = 5.7, 6.0) earthquakes occurred within the local network of short-period seismograph stations in the Shumagin Islands, Alaska, on April 6, 1974. They were followed by 69 aftershocks recorded over the next two

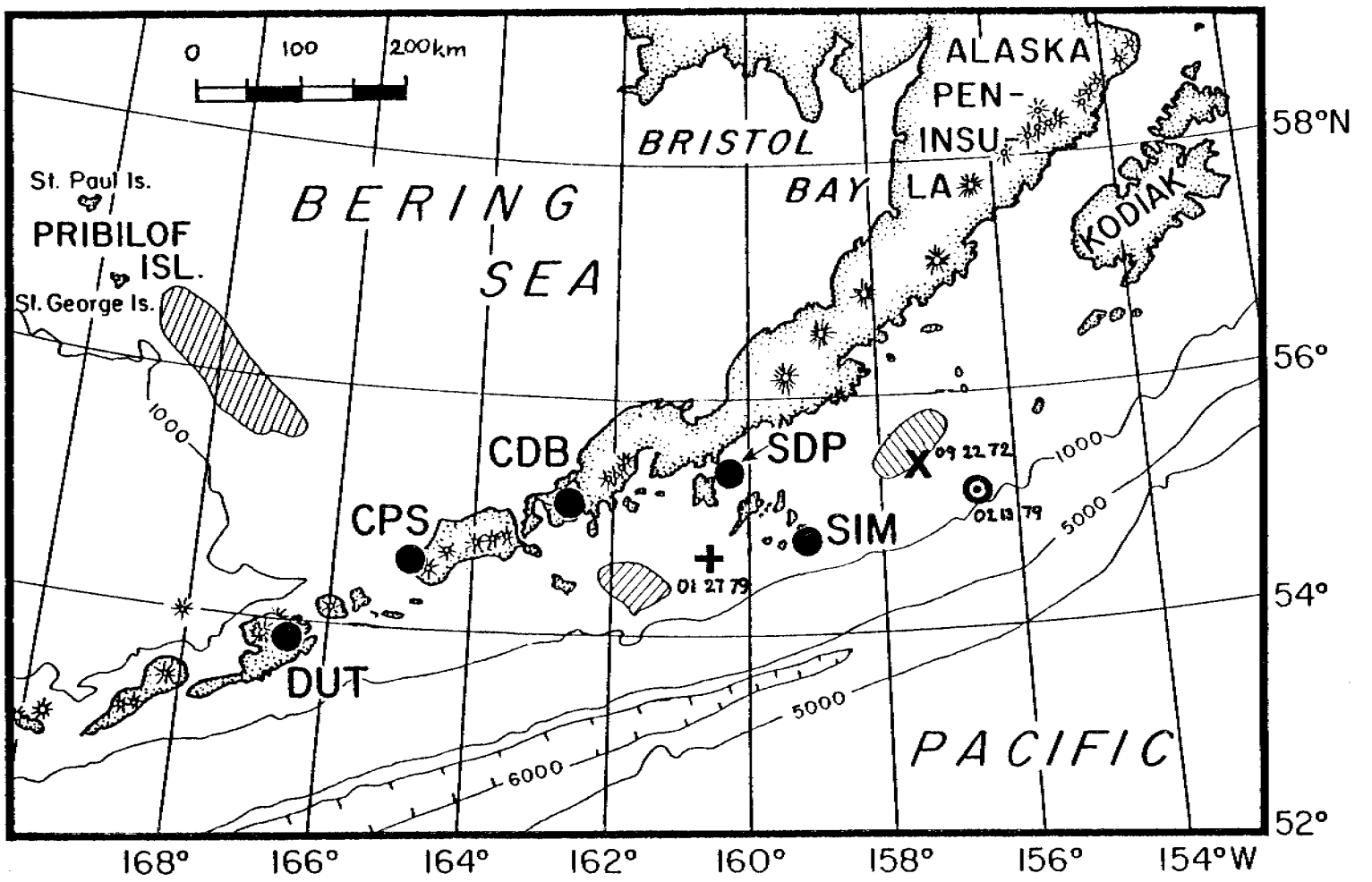

Figure 16. Location map of presently operated strong-motion instruments (solid circles; CDB is operated by USGS, others by Lamont-Doherty). Two events (+, M = 5.4 and 0, M = 6.5) triggered strong motion instruments at Sand Point (SDP). The event indicated by x is discussed in the text for digital data processing for broad-band records (see also Figure).

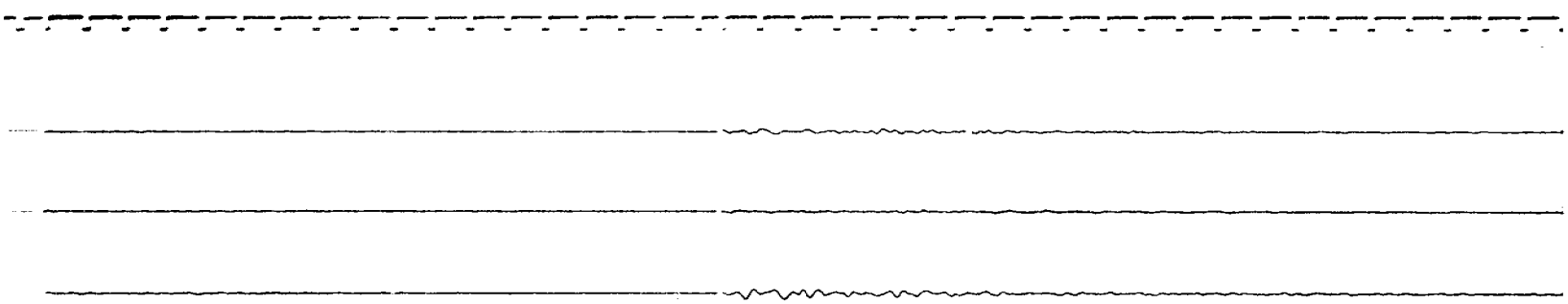

27 January 1979

M_b = 5.4, a_p = 1%g, Δ = 58 km

13 February 1979

M_b = 6.5, a_p = 6.1%g, Δ = 226 km

Figure 17. Strong Motion Accelerograph records from the Kinemetrics SMA-1 located at Sand Point.

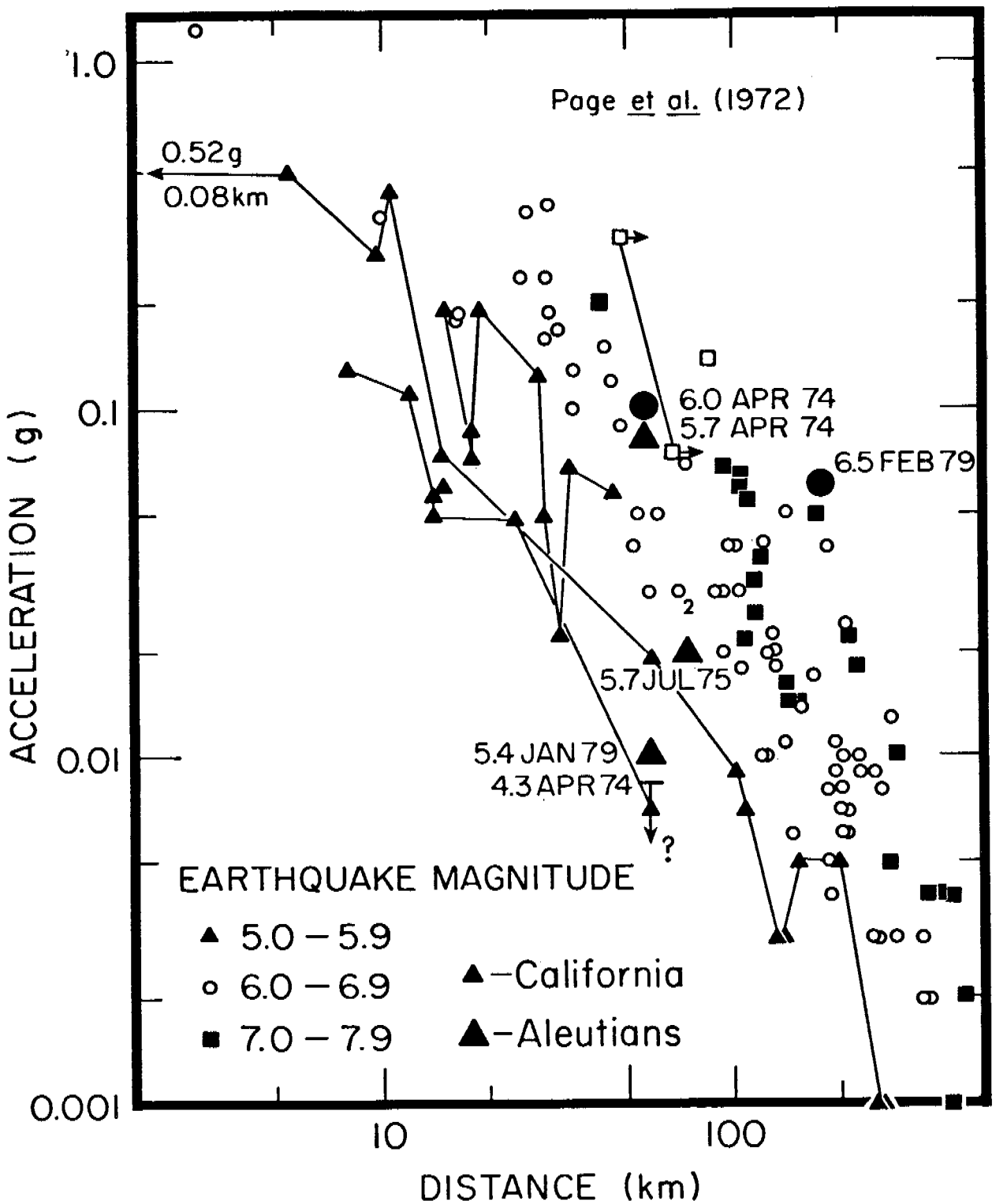

Figure 18. Comparison of peak-horizotnal accelerations (larger symbols) measured for 6 easte Aleutian earthquakes at Sand Point (SDP), Alaska, with those compiled by Page et al. (1972) f the western United States (smaller symbols). The magnitudes and dates of the 6 events are in cated. Note that for the Aleutians most of the peak horizontal accelerations are slightly higher than those from the western U.S. for the equivalent magnitudes and distances.

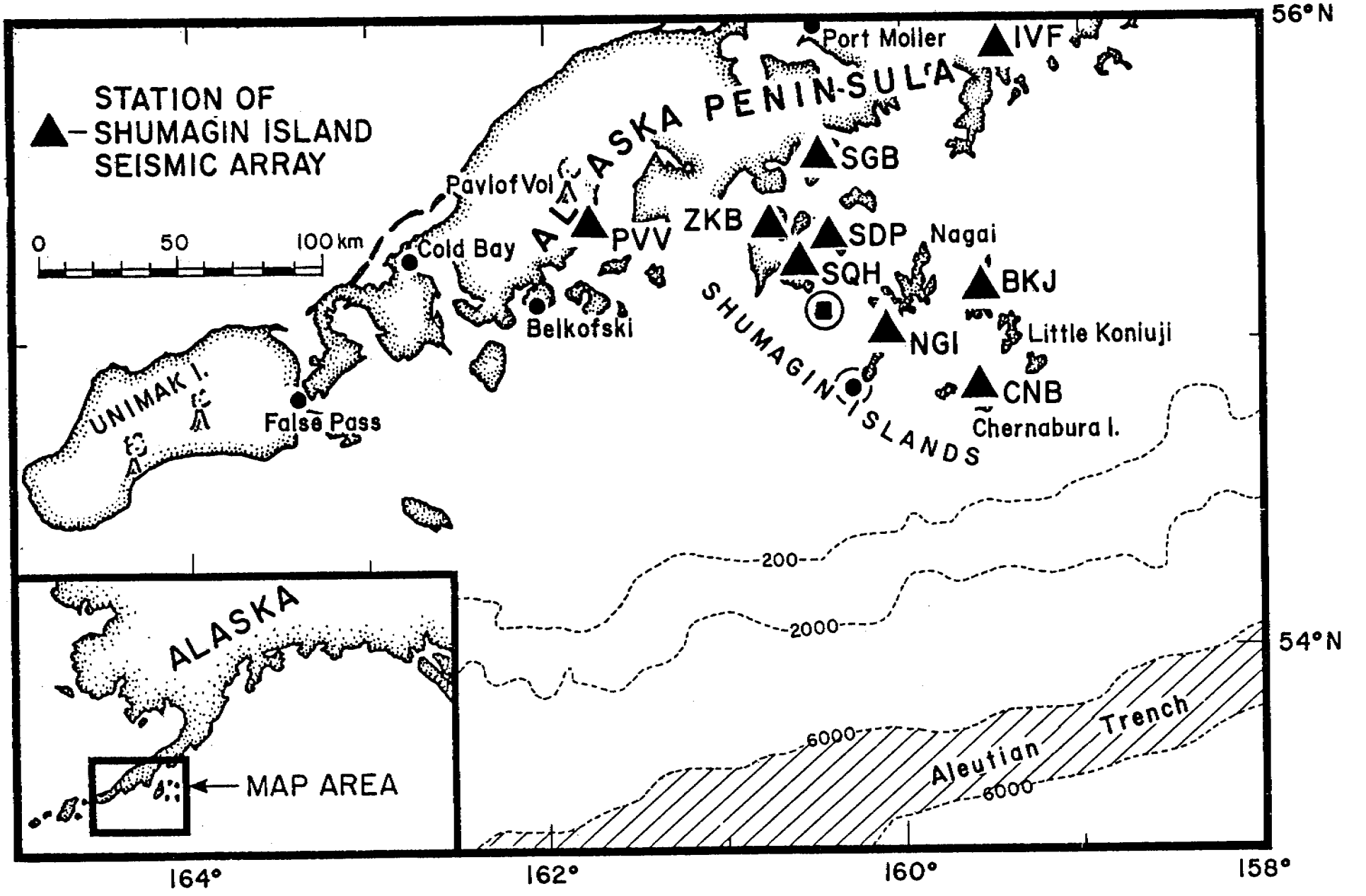

Figure 19. Location map of the Shumagin Islands and April 6, 1974 earthquakes (solid dot in circle). Shumagin network seismic stations are indicated by triangles and three letter station circles. For comparison the (mislocated) PDE epicenter is also shown (solid square in circle).

Figure 20. Cross section views of hypocenters of the main shocks and well located aftershocks. Symbol size is scaled to magnitude; full symbols are "A" quality locations; 1/2 full are "B" quality; empty are "C" quality. Tick marks are at 5 km intervals, both horizontally and vertically. Approximate rupture zone dimensions of the main shocks, as obtained from analysis of the SMA records, are dashed.

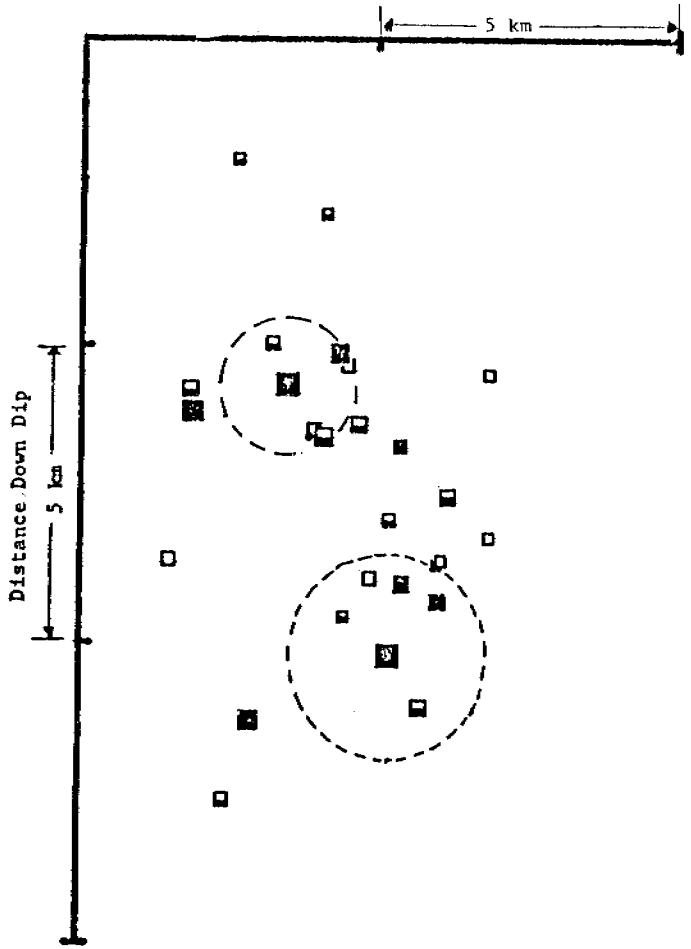

Figure 20a. Vertical cross section oriented normal to the arc. "View" is N60°E. The 0153 main shock is the shallower of the two. Note the distribution of events (espécially the A and B quality) about a plane with a clip of approximately 30° northwest (left in the figure).

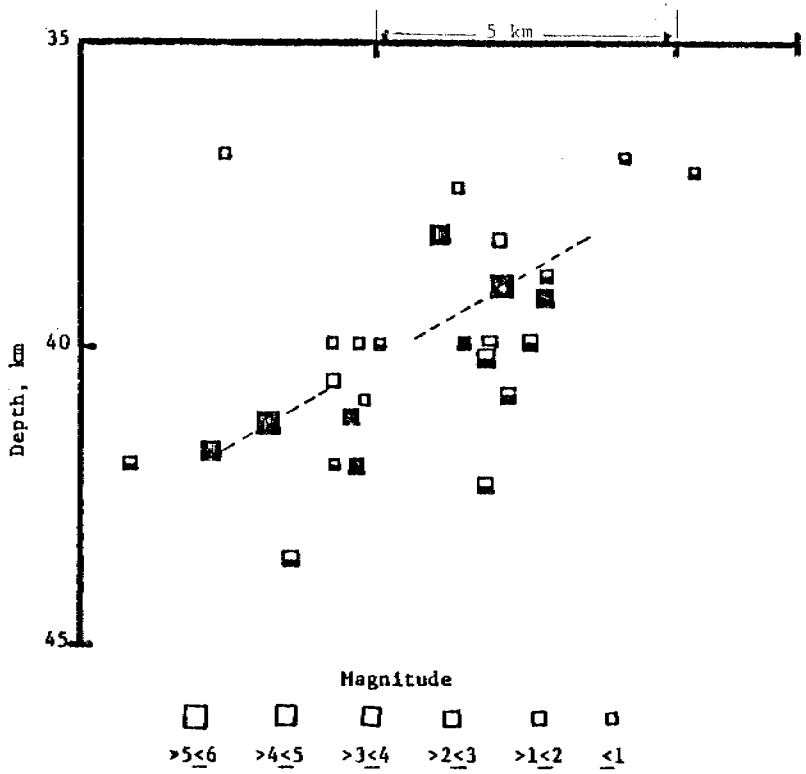

Figure 20b. Inclined cross section oriented parallel to the 30° dipping plane from (a). "View" is upward at the plane of the Benioff zone, with northeast to the right of the figure and down dip of the Benioff zone down in the figure. Note the separation of aftershocks of the two events.

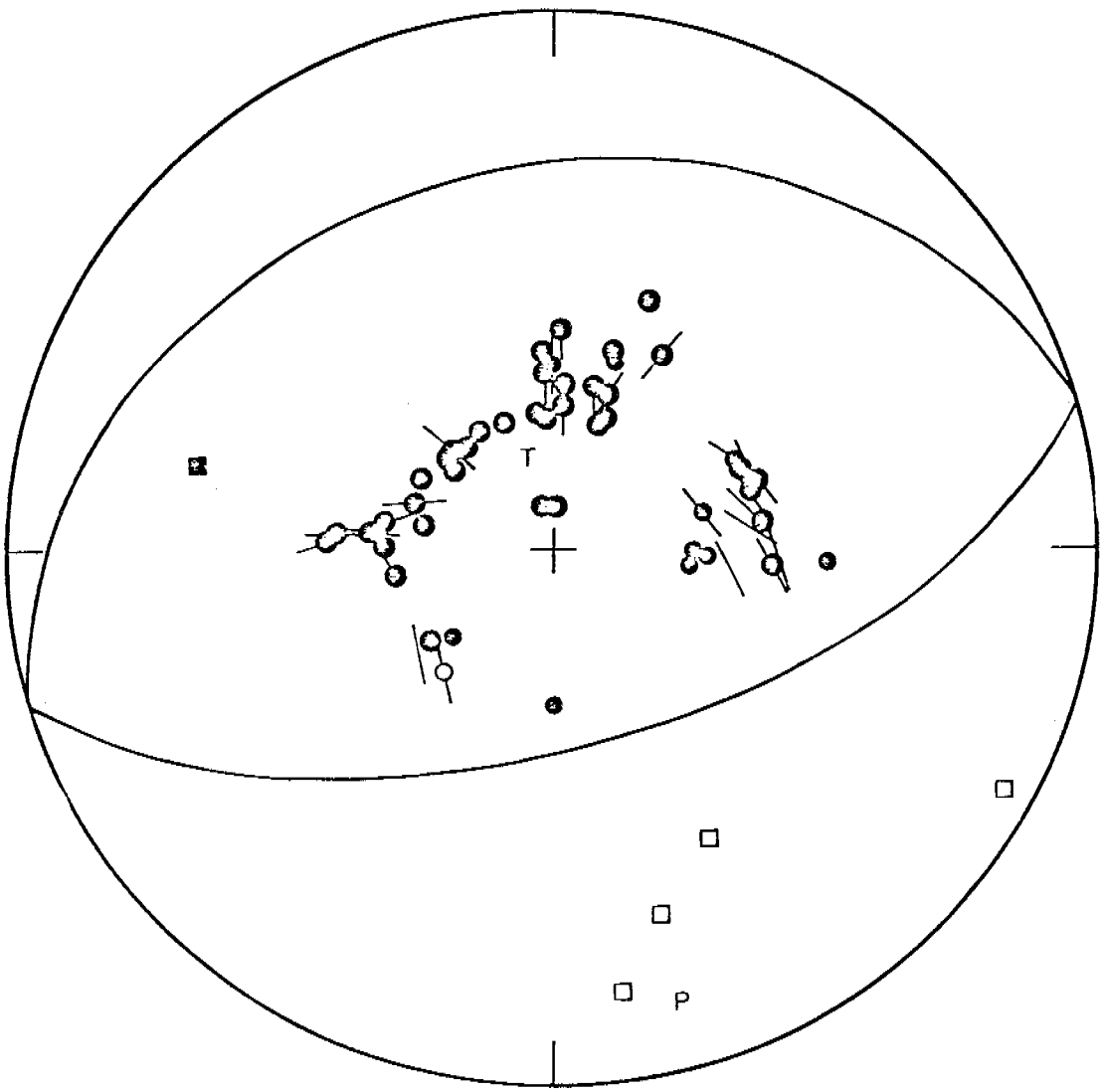

Figure 21. Focal mechanism of the 0356 hrs event on April 5, 1974. First motions and S-wave polarizations are projected onto a lower hemisphere, equal area net. WWSSN long period first motions are circles, filled are compressions, empty dilatations; smaller symbols are less reliable data. Local network short period first motions are squares; filled are compressions; empty, dilatations. S-wave polarizations are lines on figure, less reliable determinations are only half the length.

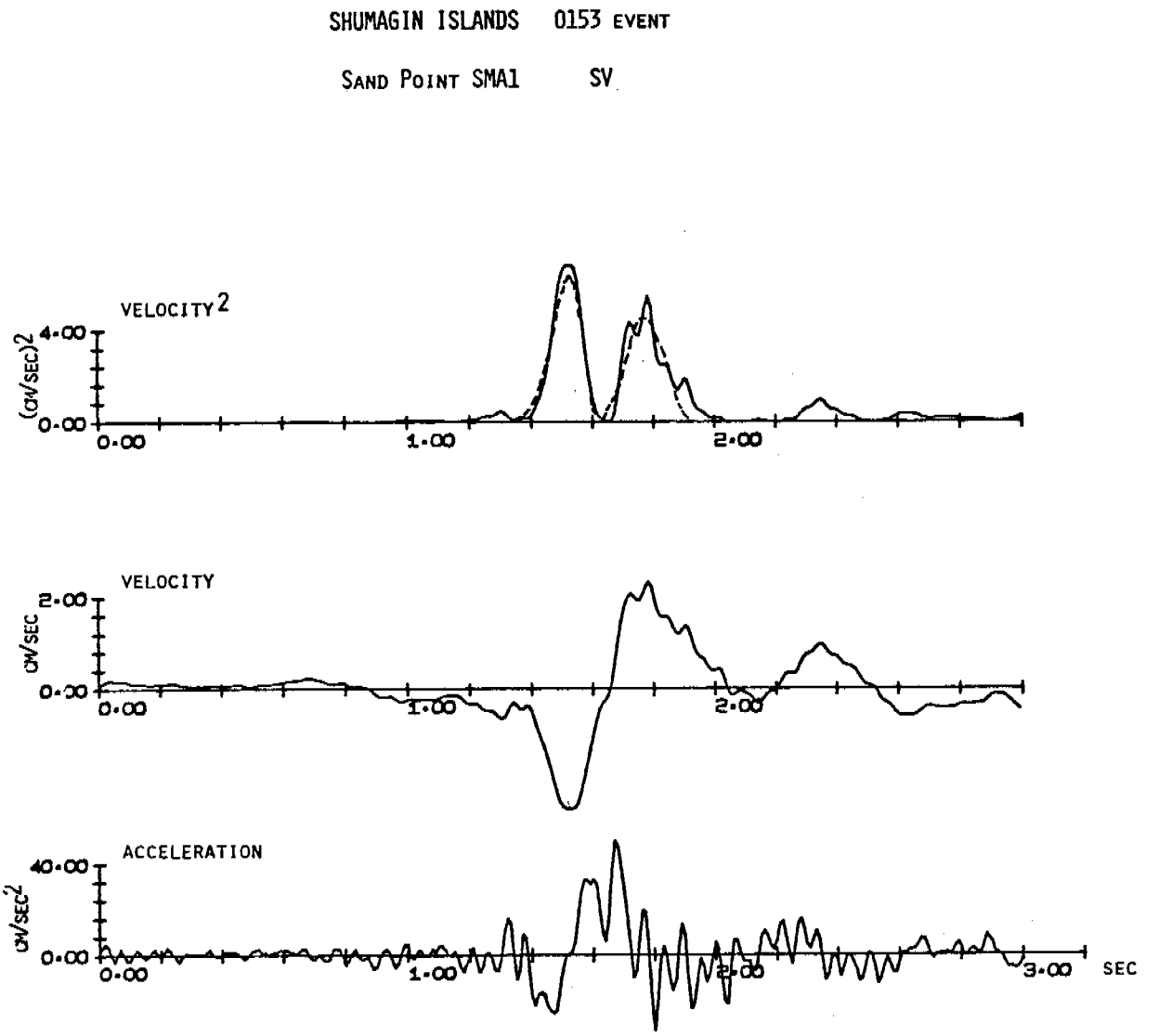

Figure 22. S_V component of S wave for 0153 event, April 6, 1974. Bottom: instrument and free surface corrected acceleration. Center: Velocity trace obtained from integrating baseline corrected acceleration. Top: Velocity-squared trace; dashed line is velocity-squared trace of final model.

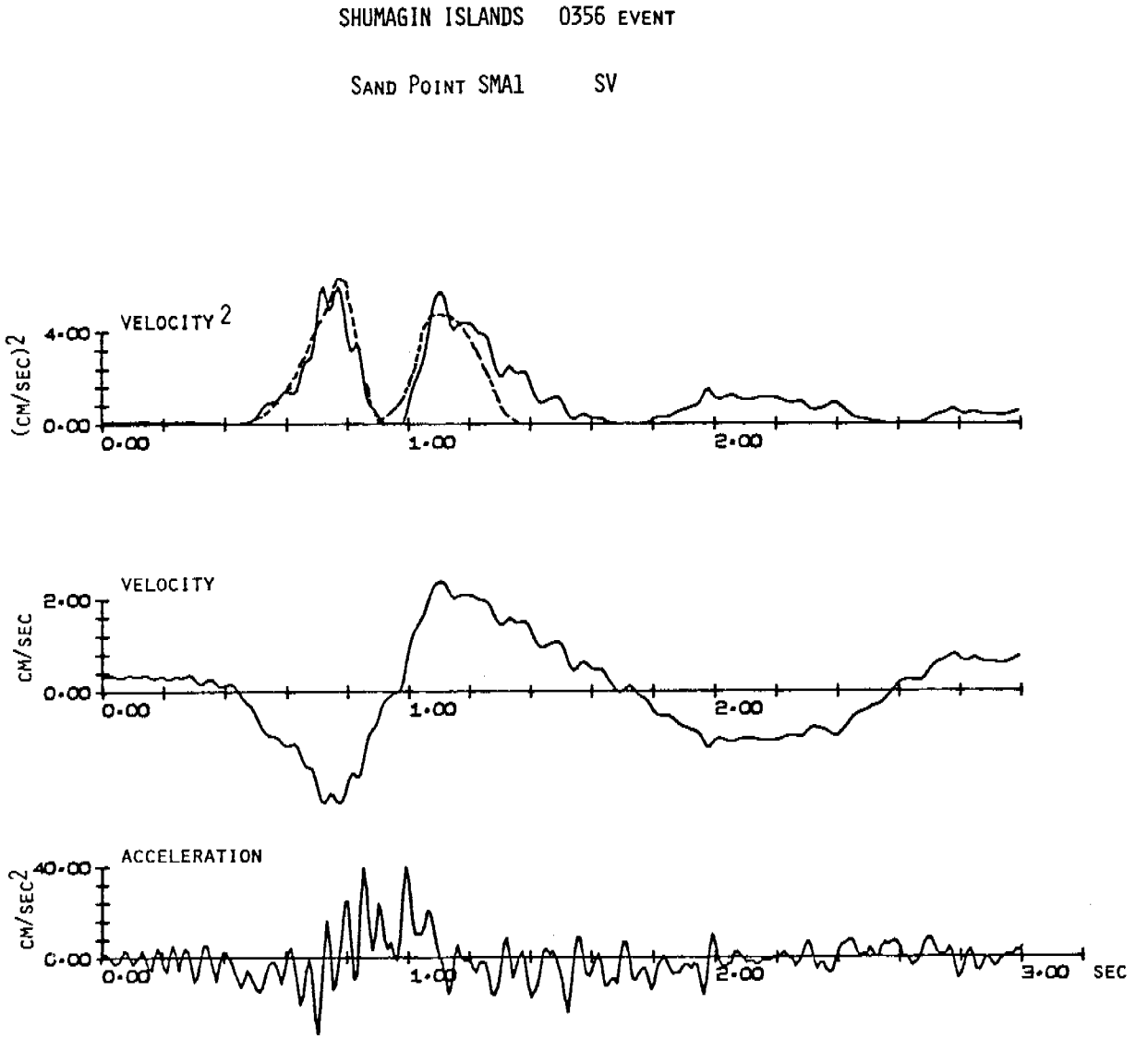

Figure 23. S_V component of S wave for 0356 event, April 6, 1974. Description similar to that of Figure 12.

weeks. Both main shocks triggered a strong motion accelerograph (SMA) located at Sand Point, 50 km NNW of their epicenters.

Location of the earthquake sequence in relation to the stations of the Shumagin Islands seismic network is shown in Figure 19. Five stations (SDP, SQH, SGB, CNB, and PVV) recorded the arrivals from the main shocks and 29 of the aftershocks. The station NGI unfortunately was not operational at the time. BKJ operated only intermittantly during this time period. P arrivals were picked to within 0.05 sec accuracy for all the 31 events studied. Making consistently reliable S-picks proved to be impossible except at SDP, where an E-W short period component was operated. Computed standard horizontal errors for the best (A) quality locations were approximately 1 km (vertical slightly larger), errors for the B- and C-quality locations were about 2 and 3 km, respectively. Figure 20a and 20b show the earthquake locations in cross sections. As can be seen in Figure 20a the hypocenters define a plane with a dip of about 30° to the NW. Figure 20b is a view normal to the plane of the Benioff zone and shows that aftershock zones for the two mainshocks are adjacent, but relatively distinct. Aftershock zone dimensions (diameters) are about 3-4 km for the 0153 event and about 4-5 km for the 0356 event.

Long period data from WWNSS stations were used to determine the focal mechanism of the 0356, m_b = 6.0 earthquake. The mechanism is shown in Figure 21. Data for the 0153 event are fewer, but identical to those of this earthquake. P wave first motions were not sufficient to constrain either of the two nodal planes. Consequently it was important to use S-wave polarizations. Also, the fact that the S wave motion from the Sand Point SMA is nearly entirely SV provided important constraints on the mechanism. S wave polarization angles from 9 of the WWNSS stations with the large S arrivals, and from the SMA were used in an attempt to refine the mechanism determination and quantify the uncertainty in it. Focal parameters resulting from this refinement were strike of nodal plane chosen as the fault plane 254° $\pm$ 15°, dip 30° $\pm$ 5° rake (of slip vector) 90° $\pm$ 15°. The error limits presented are one standard deviation. The tight constraint on dip was important for estimation of the source parameter.

This focal mechanism represents nearly pure thrusting. The choice of the gently NW dipping nodal plane as the fault plane is suggested by the tectonic setting of these earthquakes. Equally important, however, is the parallelism between the trend of the aftershocks as shown in Figure 20a and the NW dipping nodal plane. We therefore interpret these earthquakes as underthrusts which resulted from differential motion between lithosphere of the Pacific and North American plates.

Analysis of the Strong Motion Accelerograph (SMA) records was carried out using techniques described by Boatwright (1978 and 1979). The S wave arrivals from the SMA records were digitized, instrument-corrected, and rotated to S_V and S_H components. Since the S_H amplitudes were less than 10% of those for S_V, the subsequent analysis was restricted to the S_V component only. The free-surface corrected accelerograms are shown in Figures 22 and 23, as well as respective velocity and V^2 traces. Note the remarkable similarity of V^2 plots in pulse shapes and amplitudes for the two events. This probably indicates the events share a similar rupture geometry and velocity, since they have the same focal mechanism. The nearly equal amplitudes of the rupturing and healing phases suggest either down-dip propagation of rupture (towards the Sand Point SMA) or a slow rupture velocity, approximating 0.6 shear wave velocity, if the rupture was circular. The V^2-plots from the final modelling are shown also (dotted lines, Figures 22 and 23).

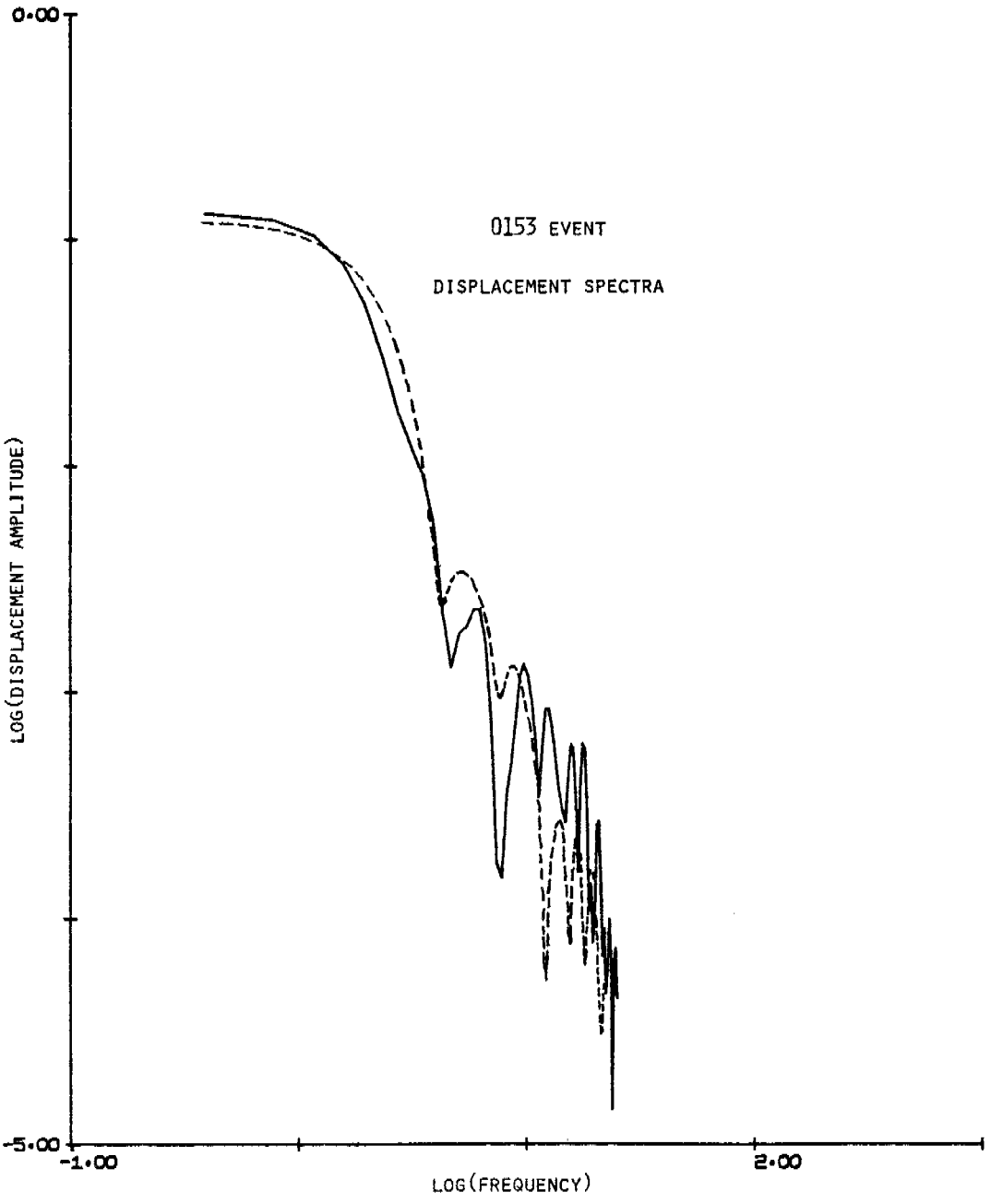

Figure 24 . Displacement spectra of S_V component of S wave for 0153 event, dashed line is displacement spectra of final model.

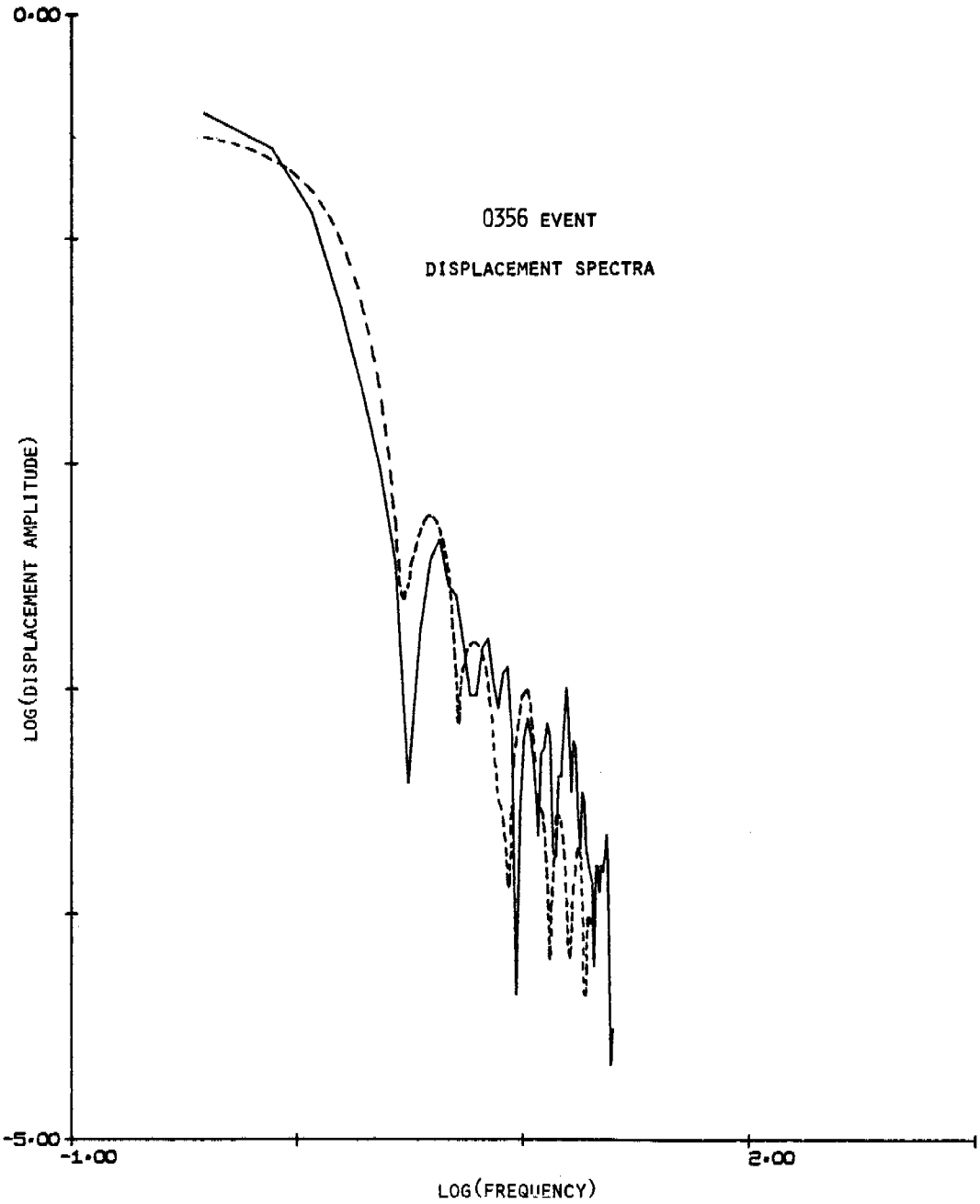

Figure 25. Displacement spectra of S_V component of S wave for 0153 event, dashed line is displacement spectra of final model.

TABLE 2

Characteristic Rupture Times

Method	0153-event	0356-event
Corner Frequency	.41 $\pm$ .1 secs.	.62 $\pm$ .2 secs.
Characteristic Frequency	.37 $\pm$ .1 secs.	.53 $\pm$ .15 secs.
Rise Time	.39 $\pm$ .08 secs.	.60 $\pm$ .1 secs.
Average	.34 $\pm$ .05 secs.	.59 $\pm$ .1 secs.

TABLE 3

Derived Source Parameters

0153-event

Radius - $a = 1.2$ km

Moment - $M_o = 3.5 \pm .8 \times 10^{24}$ dyne·cm

Stress drop - $\Delta\sigma = 890$ bars Range 600-1100 bars

Effective Stress - $\tau_e = 1040 \pm 350$ bars

Radiated Energy - $E_s = 8.7 \pm 3.0 \times 10^{20}$ dyne·cm

Apparent Stress - $\tau_a = 160 \pm 60$ bars

0356-event

Radius - $a = 1.65$ km

Moment - $M_o = 6.7 \pm 1.5 \times 10^{24}$ dyne·cm

Stress Drop - $\Delta\sigma = 650$ bars Range 350-800 bars

Effective Stress - $\tau_e = 780 \pm 250$ bars

Radiated Energy - $E_s = 12.4 \pm 4.0 \times 10^{20}$ dyne·cm

Apparent Stress - $\tau_a = 120 \pm 50$ bars

Figures 24 and 25 show displacement spectra for the two events, as well as the final model spectra (dotted lines). A Q of 400 was assumed in correcting the spectra for attenuation.

Source dimensions were estimated by several different techniques, including corner frequency, characteristic frequency (Boatwright, 1978a) and width of the first pulse (rupture phase) of the V^2 plot. Estimates from these techniques (assuming a circular rupture) are summarized in Table 2. Using rupture velocities, V as $.55\beta < V < .8\beta$, the source radii are 1.0 km $< a <$ 1.4 km for the 0153 event, and 1.4 km $< a <$ 2.0 km for the 0356 event.

An analysis of the short period P-wave pulse shapes at 6 WWSSN stations, all of which have a similar ($\sim$ 30°) take off angle from the hypocenter (relative to the fault plane) suggests that rupturing was nearly symmetric (circular).

Detailed source modelling was carried out using a circular version of the quasi-dynamic models discussed in Boatwright (1979) and Boatwright (1978b). These models have an "elliptical" or self-similar slip distribution and causal healing. Since the displacement spectra for these events falls off more steeply than ω^{-2}, we presume that the ruptures stopped gradually, rather than abruptly (Madariaga, 1978), and this gradual stopping was incorporated into the model.

Final modelling was done by filtering the data by circular ruptures. The V^2 pulse shapes and displacement spectra for the models are shown in Figures 22 to 25. Rupture velocities for the two models were $v = 0.6\beta$ and $v = 0.55\beta$ for the 0153 and 0356 events, respectively. Final model parameters are listed in Table 3.

The high stress drops for these two events may indicate either a regional stress build-up prior to a major earthquake or the release of a localized high strength region (asperity) which was unbroken by the most recent (1938) major earthquake.

Since these earthquakes are located near the deepest part of the rupture zone of the 1938 earthquake (Davies and House, 1978), and since major earthquake ruptures often initiate at depth and propagate up-dip, the location and character of high stress-drop events are important results for an evaluation of seismic hazards in the Shumagin Islands area. The importance of these results lies in the fact that this type of strong-motion study will eventually allow separation of the contributions of source and of propagation-path to the level of ground motion. The two key numbers which represent this approach in a nutshell are: (1) the source region for the two earthquakes studied appears to be characterized by high ambient stresses as indicated by high stress drops (600 to 900 bars), and (2) the attenuation along the propagation path is characterized by an effective quality factor Q of about 400. If many more source regions and propagation paths can be studied in the near future it will be possible to map out stress distribution and attenuation properties. Both types of information are basic elements in any seismic hazards evaluation and are essential for forecasting of severity of shaking during future large earthquakes.

(3) Processing of Broad-Band Seismic Records. This data set contains 30 earthquakes recorded at Sand Point during 1972/1973 with magnitudes ranging from m_b 3.0 to 6.0 at distances 30 to 250 km from the recording site. Only a vertical component was recorded. The basic data set and the instrumental characteristics were discussed in our last Annual Progress Report (April 1977-March 1978). Since then we have developed

the software to carry out routine processing of these broad-band records to obtain acceleration, velocity and displacement time histories from these records in a limited pass-band for frequencies from 2.5 to 0.04 cps. Figure 26 shows an example demonstrating the major steps of processing these broad-band records. The sample event occurred on September 22, 1972, had a magnitude $m_b = 4.6$ and was located at shallow depth about 125 km east of Sand Point (Figure 19). The major processing steps are:

1) The original seismogram (Figure 26a) is digitized into approximately 1500 points. The digitization is fed into a program which corrects for the curvilinear nature of the recording pen. In addition to translating the curvilinear deflection into rectlinear displacement, a correction has to be made for a constant pen deflection (i.e. the pen is at a small angle from the horizontal trace). It turns out that the frequency characteristics, and hence the velocity plot, is rather sensitive to this angle. Accuracies of better than 0.5° are necessary for good velocity resolution.

The effect of minute marks within the seismogram was compensated for by subtracting our synthesized minute marks at the appropriate places. The minute marks are not simple step functions because they were sent through the instrument's low-pass filter.

Figure 26b is a digitized version of the seismogram with the curvilinear to rectilinear corrections and the minute marks taken out.

2) This corrected digitization is then processed by another program which interpolates the digitization to a standard time interval of 0.1 second. The signal is then band-pass filtered from 0.04 to 2.5 cps using a Butterworth filter run forward and backward across the data.

A deconvolution operator for the frequency response (see Figure 27; frequency response curve) is constructed and convolved with the data to obtain a velocity plot (Figure 26c). Note that in the frequency range of 0.1 to 1.0 cps the displacement response rises at 6 db per octave. So the displacement magnification is basically a linear function of frequency. Hence the output is roughly proportional to velocity. This can be seen in the similarities between the corrected seismogram (Figure 26b) and the deconvolved velocity plot (Figure 26c).

3) The velocity plot is then integrated to obtain a ground displacement plot. The integral was computed by approximating the area under the velocity curve with rectangles of width 0.1 seconds. The resulting time histories of the remaining 30 events still to be processed will allow us to derive response spectra for acceleration, velocity, and displacement such as are commonly used for engineering purposes. Another attempt will be made to obtain V^2-plots and interpret them in terms of source parameters and stress-level at the source region. Most of this analysis is expected to be carried out with NSF support, but we will continue to report to NOAA/OCSEAP any results with direct application to hazards evaluation in the Alaska-Shumagin Islands region.

In summary, except for interpretation of two strong-motion records in terms of stresses at the source region, our main progress during this year lies in increasing our data base for strong-motion records and in processing of broad-band data. All strong-motion records either have been, or (for the most recent ones) will be for-

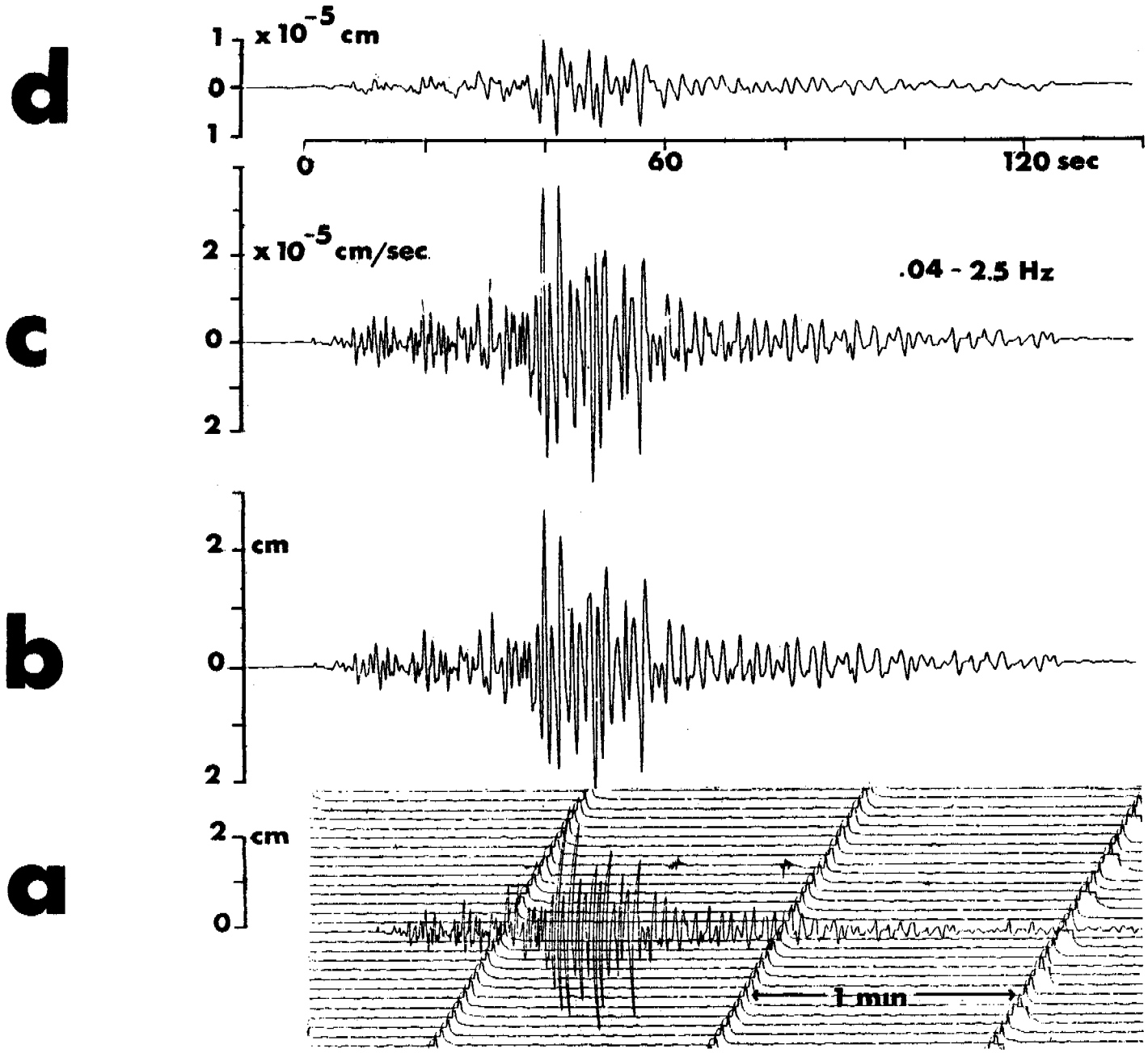

Figure 26 Example for digital processing steps of Sand Point Broad-Band records.

a) Original seismogram (vertical component) from Sand Point Broad-Band instrument for a magnitude m_b = 4.6 event at an epicentral distance of about 125 km.

b) Digitized version with curvilinear to rectilinear correction, and minute marks taken out.

c) Deconvolved plot of vertical ground velocity, band-pass filtered from 0.04 to 2.5 Hz, interpolated at constant time intervals of 0.1 sec.

d) Ground displacement obtained from integration of velocity plot.

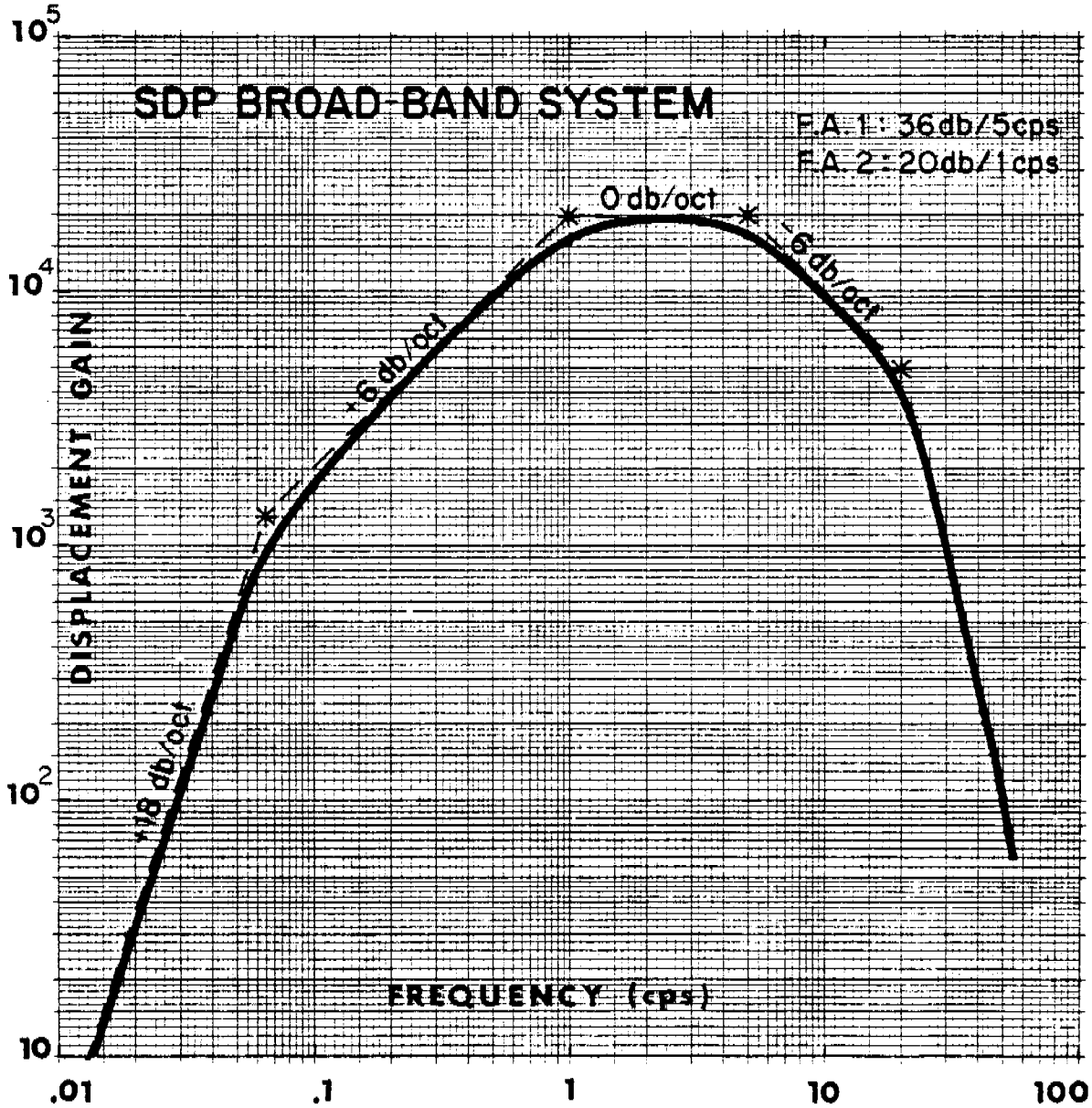

Figure 27 Frequency Response for ground displacement of Sand Point broad-band instrument.

warded to the U.S. Geological Survey's strong motion group for routine processing and for incorporation into the U.S. strong motion central data file. This will allow for any interested user to request from the U.S. Geological Survey the standard processed data derived from the Lamont-collected original data.

A synthesis of all Lamont-collected strong-motion data over and above the results presented here seems at this time premature in light of the few records obtained. We also feel that with a future increase in strong- and medium-range ground motion instrumentation along the Alaska-OCSEAP area such a more thorough analysis and synthesis should be postponed until a statistically significant number of records (e.g. more than 50) will become available. However, our recent studies have shown that strong-motion and seismic source characteristics in the Shumagin Islands seismic gap differ sufficiently from those in the western U.S. that any seismic engineering decisions for this part of Alaska cannot be based on strong-motion characteristics from the better studied regions in California and adjacent states. Strong motion levels measured at Sand Point were in general higher. This emphasizes the need for intensified strong-motion and medium-gain seismic instrumentation in this poorly studied subduction-zone seismic regime.

D. Record of Volcanic Activities

General Comments. Physical volcanology in general and volcano-seismology in particular are in their early stages of development compared to some other well advanced disciplines in seismology or in the Earth Sciences in general. The reasons for this deficiency are obvious: Volcanic processes are physically very complex; they occur only intermittently or in a rapidly changing form and often in hostile, inaccessible environments where reliable monitoring is difficult or impossible. Even on a world-wide basis, very few coordinated attempts have been made to collect sufficient data over sufficiently long periods in the vicinity of active volcanic features (e.g., Hawaii, Sicily, Japan, Kamchatka, New Zealand). The necessity of evaluating volcanic hazards in areas of future petroleum exploration and development demands a far greater understanding of eruption dynamics and periodicity than currently exists. Our study of Pavlof, Akutan, and Makushin volcanoes in the Eastern Aleutian arc is an attempt to collect seismic, historic, and geologic data and develop a paradigm whereby volcanic eruptions may be predicted both in space and time. In particular we are studying the specific properties of explosive island-arc volcanism at an actively convergent plate boundary, which differ in many respects from the more thoroughly studied volcanic processes in non-convergent tectonic settings (i.e., those in Hawaii or in the western U.S.). One or more of the following aspects are known or suspected to be highly variable with the tectonic setting: Chemistry and rheology or eruptiva; Regional tectonic stress system (including the temporal variations in this stress system); Explosiveness; Residence time of magma in magma "chambers" and the size and shape of these chambers.

In the absence of both a sufficiently long and complete record of volcanicity and of a good understanding of the basic volcanic processes in the study regions (Pribilofs and Eastern Aleutian Arc/Alaska Peninsula) it is at present very difficult to assess volcanic hazards in a more quantitative way than to say that in both regions volcanic activity has occurred during the last few million years at a number of well defined volcanic centers (Kennedy and Waldron, 1955; Coats, 1950; Cox et al., 1966; Burckle, L., personal communication; Smith and Soule, 1973). Therefore it can be expected that such volcanic activity will continue in the future. Our efforts subsequently described cannot be directly used at this time to quantify the volcanic hazards in the subject region. But they lay the groundwork for making such an assessment a meaningful undertaking. Our approach is twofold: (1) To obtain a data base to establish the frequency of occurrence and "magnitudes" of volcanic eruptions for a future statistical, rather than deterministic analysis of volcanic hazards; and (2) to try to understand the physical processes associated with island arc volcanic eruptions (funded by D.O.E., not by this OCSEAP study) in the hope that individual volcanic eruptions can in the future be predicted from seismic or other geophysical monitoring in a deterministic fashion. The subsequent paragraphs describe some of the problems addressed.

We have focussed during the present reporting period on screening the large amount of seismic data already collected from our network on Pavlof volcano to search systematically for different types of seismic signals and their occurrence patterns in time related to visually observable (eruptive) patterns. In addition we have been extending our chronology of volcanic activity for all Eastern Aleu-

tian and Western Alaska Peninsula volcanoes backwards in time (through the middle of the 18th century) using published reports and personal communications relating the visual observations of explorers, historians, geologists, and local residents.

Before we illustrate this approach in more detail, we briefly outline the two basic classes of phenomena that determine the seismic signals: (1) sources of volcano-seismic excitation and (2) propagational effects. Either of these two factors are likely to be more variable and complex, than in ordinary tectonic seismological environments. Tectonic earthquakes stem from brittle shear failures on more or less planar faults. The sources for volcanic events are thought to consist of either (1) oscillations of a (more or less) spherical magma chamber (Shima, 1958; Kubotera, 1974), (2) organ-pipe-like oscillations in a (more or less) cylindrical central vent of a strato volcano (Steinberg, 1965); (3) jerky motion associated with the growing of magma-filled cracks (radial dykes) driven by the over-pressure of the magma (Aki, Fehler and Das, 1977); (4) partly seismic, partly acoustic radiation from steam or gas explosions near the top of the central vent; or (5) tectonic (dry brittle) events near the volcano; or (6) any combinations thereof with variable weight of source strength as the eruption progresses.

The distinction of these different possible volcano-seismic sources by analyzing the volcano-seismic signals radiated and their variation in time is impeded by the wave-propagational effects in the laterally very complex and heterogeneous volcano structures. The heterogeneities have often dimensions similar to those of the wavelength of excited signals. Hence refraction, scattering and attenuation effects may mask the source-related wave shapes to a degree where extraction of the source function may be difficult or impossible except in special circumstances. Nevertheless, volcano seismology is one of the few means to "X-ray" and monitor the emplacement of magma bodies, and to study the physical processes in the island-arc environment associated with magma emplacement and eruption. Without this knowledge it will be difficult to develop models for the forecasting of volcanic activity in this tectonic regime. Keeping the before mentioned complexities in mind we now discuss some of the observational data and our attempts to classify them.

Pavlof Network and Data. In the summer of 1976 an array of 12 seismometers was set up on the flanks of Pavlof volcano to locate and investigate associated magma reservoirs and processes of magma transport and eruption. Figure 28 shows the locations of the seismometer sites together with those of two other stations (PVV and Black Hills) from the Shumagin network. Enough data has now been collected to warrant a first major analysis effort. We discuss here those results and aspects of the Pavlof investigation which emerged from our recent screening of data and will again received the most attention during the upcoming year: harmonic tremors, explosive events, impulsive events of presumed non-explosive origin, attenuation of signals from local tectonic events, long-perm variations in volcanic activity, and short-term variations in volcanic and volcano-seismic activity.

Harmonic tremors. Figure 29 shows a typical volcanic tremor (Event 1) recorded on 20 September 1976 during a period of time when the Center for Short-Lived Phenomena and local sources in the Shumagin Islands reported intense emissions of smoke, steam, and ash from Pavlof[1]. These tremors, which are predomi-

[1]Only four out of the twelve seismic channels have been played-back for presentation in this report. Of these four channels PS3 was inoperative during this eruptive episode.

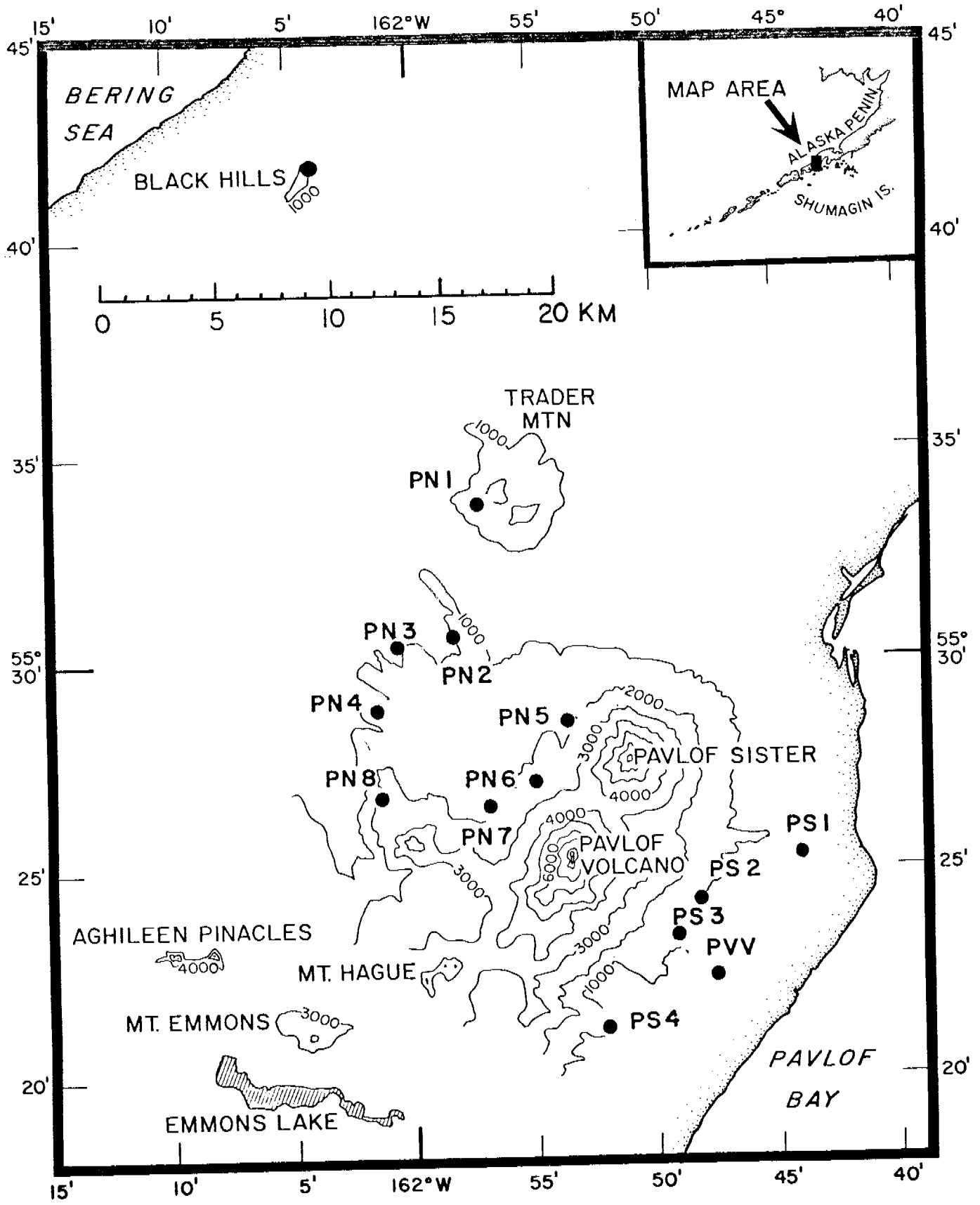

Figure 28. Locations of stations of the Pavlof seismograph array-

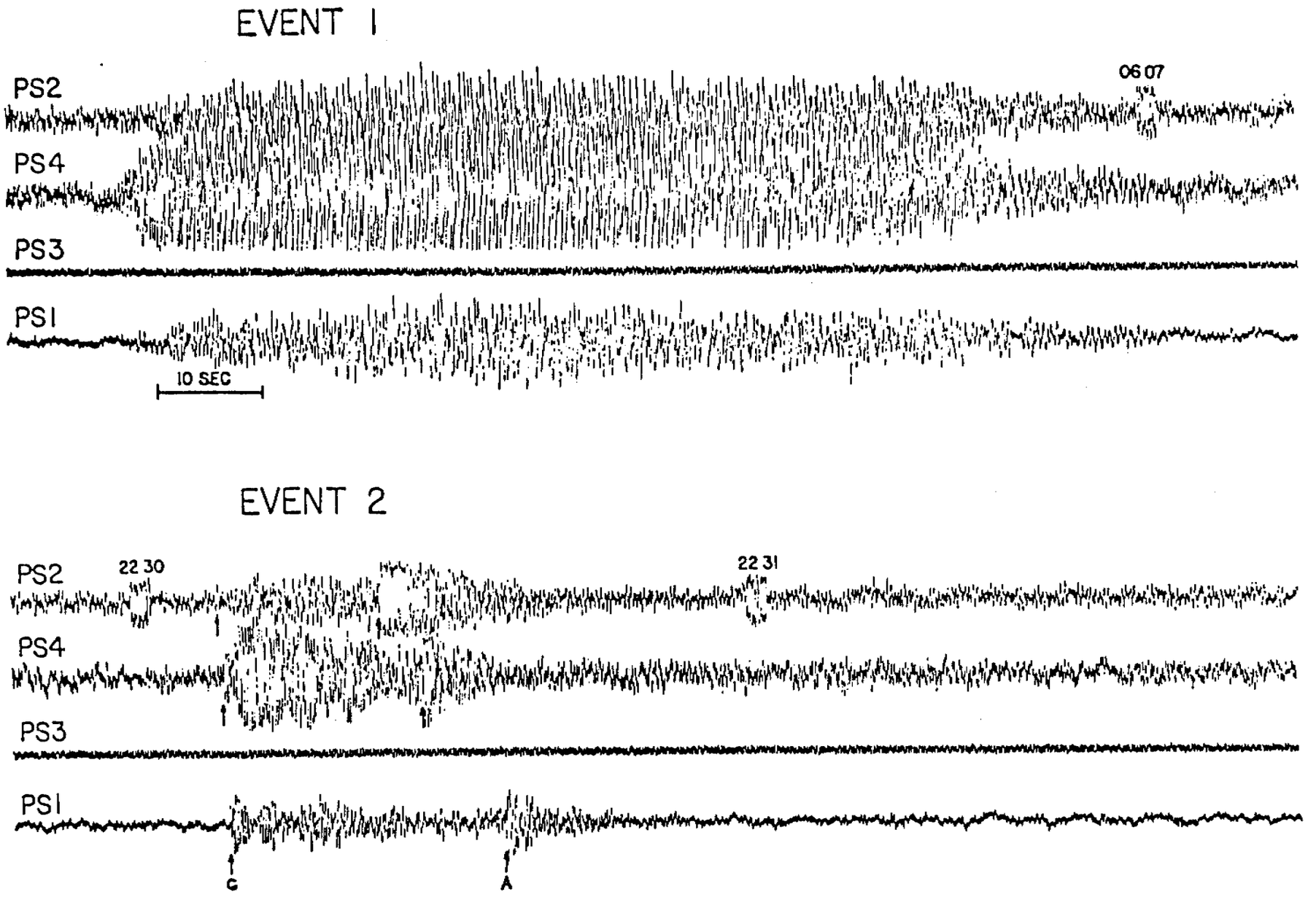

Figure 29. Examples of volcanic events recorded at the Pavlof array during an eruptive episode late in 1976. Event 1 is a harmonic tremor from 20 September 1976. Event 2 is an explosive event showing an impulsive ground phase (G) followed by a much slower air phase (A) from 22 September 1976. For both events the PS3 station was inoperative.

nantly harmonic in character, are presumed due to either the actual eruption of material, the propagation of magma-filled cracks, or the oscillations of magma "chambers" or columns (organ pipe effect). We are presently preparing an analysis scheme involving a moving-window spectral analysis of these tremor signals to study their source- and path-dependent characteristics.

We hope to differentiate between source effects and path effects through study of the distance and azimuthal variations in frequency spectra. Wave-form characteristics produced by behavior of the source would be in a different way dependent on distance and azimuth (via the radiation pattern and directivity, if any) than those produced by purely propagational effects, such as layering, attenuation and scattering. If the frequency of harmonic tremors can be related to source size and growth of magma filled cracks (Aki et al., 1977), then spectral analysis of source related portions of the signals should define such parameters as magma pressure, orientation and depth of magma filled cracks or pipes. Using much simpler models than Aki et al.'s (1977), Kubotera (1974), for example, through comparison of observed and predicted frequency spectra for tremors from Aso volcano, Japan, determined the radius of its assumed magma chamber to be between 2 and 4 km. Path effects, however, would presumably be in the form of dominant modes produced by the propagation of shear waves through layered media of contrasting velocities. They should have dispersive character and, hence, could be recognized by the moving-window analysis as a function of distance. Analysis of the characteristics of such guided waves may shed some light on the velocity structure of the volcanic cone and underlying crust.

If tremors can be found whose onsets are impulsive enough to allow for source locations, then phenomena such as upward and/or outward migrations of the source along presumed magma pipes or dikes could be studied. Provided the tremors contain a sufficiently broad frequency band, but do not show impulsive onsets, another analysis technique can be developed: The cross correlation technique, which uses a delay-and-sum process on the signals to obtain a best fit correlation between recordings at different stations of the same event, would be an alternative method by which "travel times" of tremors could be determined and used for source locations. If it can be shown that certain types of volcanic tremors originate from the growth of magma filled cracks (as proposed by Aki et al., 1977) then the source location of these tremors becomes crucial as a means by which we can "follow" an actively extending magma conduit to the surface and predict both the time and location of a future volcanic outbreak.

Directions of preferred azimuthal migration could be compared with those predicted from a simple model of magma-fracturing operating within a uniform principal tectonic stress field. This would provide a "real-time" test of the proposal by Nakamura et al. (1977) that tectonic stress orientation in the Aleutian Island arc determines the preferred orientation of radial and parallel dike swarms.

Explosive Events. Explosive blasts from Pavlof have been reported during a previous eruptive episode in 1975 where air shocks were strong enough to "rock boats in Pavlof Bay" (R. Motyka, personal communication). A sample of an event (Event 2) of probable explosive origin from 22 September 1976 is shown in Figure 29. Arrows indicate the first impulsive arrivals of ground phase (G) pre-

sumed to be a P-wave and an air phase (A). We assume the focus of these events to be located at the apex of the Pavlof cone - a reasonable assumption based on reports we received from visual observations of Pavlof eruptions by local people. Figure 30 shows a plot of arrival times for each phase against slope distance from the apex of Pavlof to the recording station. A theoretical value of 0.331 km/sec for the velocity of sound air (STP) shows a good fit to the observed arrivals for the air phase. The value of 3.70 km/sec for the ground phase was obtained as a best fit to the observed first arrivals. The failure of these two velocity lines to converge on the same origin time could be due to an increase in seismic velocity with depth below the surface of the volcanic cone. If this explanation were valid, the ground phase line would be expected to resemble that for a refraction study in which points closer to the origin correspond to successively lower velocities. The mismatch of intercept times could also be due to different "origin" times resulting from slow propagation to the vent of a pressure pulse inside the magma column.

Using characteristics such as air phases to indicate explosive events, we may be able to correlate specific types of seismic phenomena (e.g., air shocks) with certain types of volcanic activity (e.g., explosive ejection of material) to give us much more precise knowledge of when Pavlof is actually erupting, and the mode of eruption (i.e. Strombolian type, phreatic mode). This is especially important in working with Aleutian volcanoes because persistent cloud cover and remoteness from population centers make visual reports very unreliable. This information would make more meaningful any attempts to correlate specific aspects of Pavlof's seismicity with its pre-eruptive, eruptive, and post-eruptive stages.

Impulsive Events. Events with impulsive arrivals but without air shocks have also been recorded on the Pavlof array. If these events can be accurately located, then we can study changes in hypocentral depth with time with regular earthquake relocation procedures. We then will search for upward or other spatial migrations of events preceding a period of high volcanic activity. In addition, if certain types of events are found to correlate with probable emplacement of dikes and dike swarms then this would be another method for investigating the validity of using dike orientation as an indicator of tectonic stress.

Tectonic Events. Events of tectonic origin, located using the Shumagin Array, have already been used to study P- and S-wave attenuation and travel time delays for ray paths passing beneath Pavlof volcano (Davies, unpublished data, 1977). The initial results of this preliminary study suggest that this technique will allow us to define a magma "chamber" (region concentration of magma) beneath Pavlof volcano. More work along this line will soon be undertaken by graduate student S. Hickman in cooperation with J.N. Davies.

Note Regarding Recent Activity near Kupreanof Volcano. During the period 1973-1978, six shallow (0-20 km) earthquakes have been located by the Shumagin array in the vicinity of Kupreanof volcano and a "new" and unnamed volcano northwest of Ivanof Bay (Figure 5). These two volcanoes, which have shown no eruptions in historic times (Coats, 1950; Smith and Soule, 1973), are currently experiencing mild fumerolic activity (T. Miller, J.N. Davies, and E. Skinner, personal communications).

Long-Term Variations in Volcanic Activity. We are presently conducting an extensive literature search with the purpose of establishing an eruption history for Pavlof, Akutan, Makushin, and eight other volcanoes in the Shumagin Islands

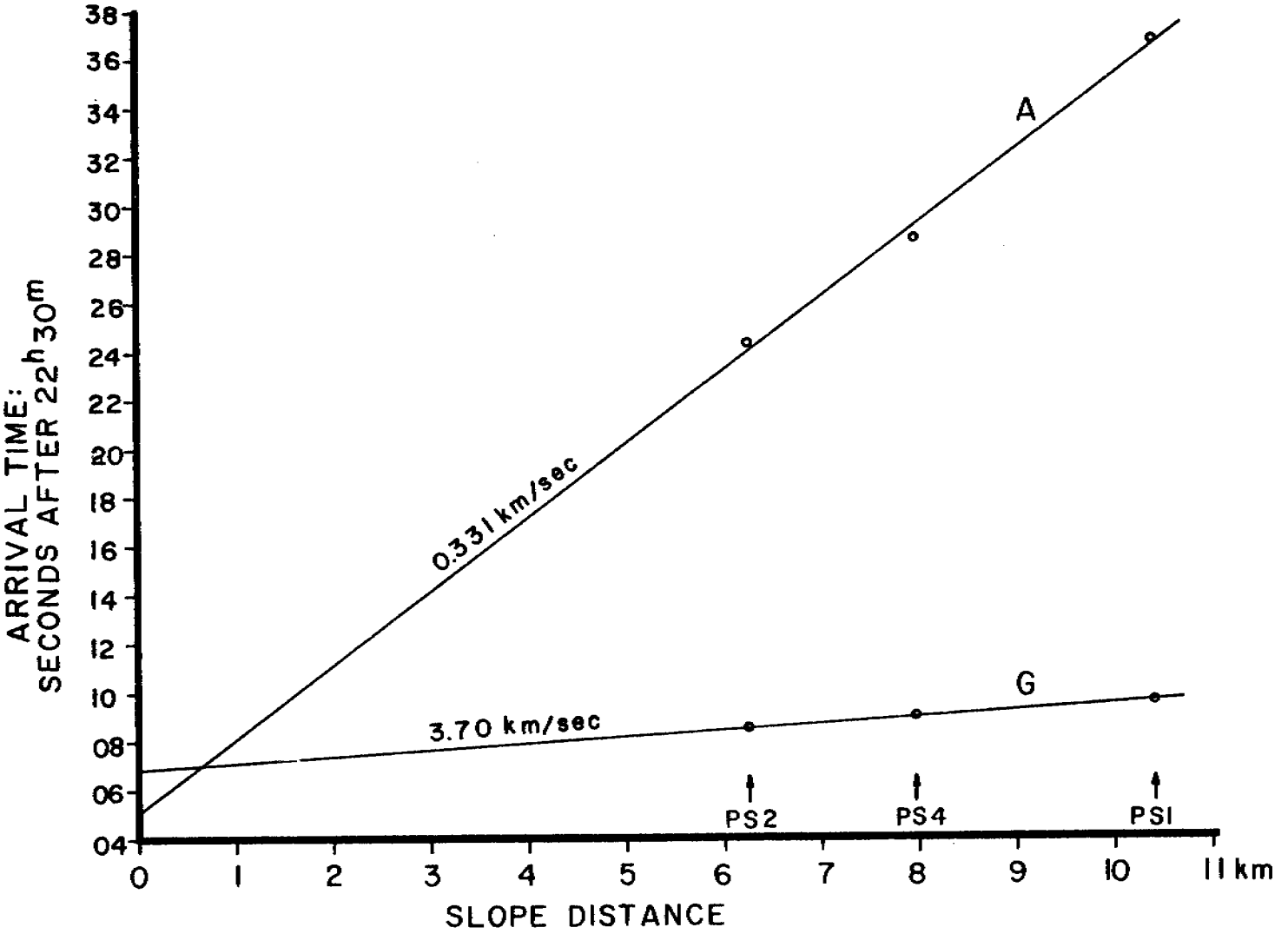

Figure 30. Graph of arrival times of the ground (G) and air (A) phases recorded from Event 2 against slope distance of each station from the apex of Pavlof volcano. The first arrivals of the air phase are compared with a line giving the theoretical value for the velocity of sound in air (o.331 km/sec at STP). The value of 3.70 km/sec for the ground phase was obtained as the best fit to the data. The failure of these two lines to converge on the same arrival time may be due to a layered velocity structure where velocity increases with depth. The actual velocity value therefore, may be expected to decrease with decrease in slope distance.

area. Our data base for this history extends from 1760 (e.g., Coats, 1950; Petroff, 1880; Dall, 1870) to the present (e.g., Scientific Event Alert Network Bulletin; personal communications from local residents, pilots, and geologists). From this information we will make estimates of eruption recurrence times for these volcanoes so that we can then assess more accurately the long-term volcanic risks that exist for specific sites on the adjacent continental shelf. Obviously, because of low population density, persistent cloud cover, and the relatively short history of written records in this region one must consider any attempt at establishing a long-term chronology of volcanic eruptions in the Aleutians Islands to be incomplete at best. An eruption chronology based on visual reports can only be a "lower bound" for the frequency of volcanic eruption which, in reality, is almost certainly higher than that which is observed and reported.

Volcanic Seismicity Plots for Pavlof Volcano. Records from the PVV station are nearly continuous from October 1973 to the present. These data were collected in cooperation with Jurgen Kienle of the University of Alaska. At Lamont-Doherty we have made a summary of the number of volcanic earthquakes per day for the first seven month's of the station's operation (15 October 1973 - 15 April 1974) and for the six month period 1 September 1974 - 28 February 1975 (Figure 31). We are continuing this count up to the present.

To investigate the time distribution of volcanic earthquakes in more detail, histograms showing the number of events occurring during each 2 hour interval are now being routinely prepared for Pavlof Volcano. To date, helicorder records for the time period 1 November 1974 through 28 February 1975 have been systematically reduced. Number and size of volanic earthquakes, occurrence of air shocks, incidence and duration of harmonic tremor, and occurrence of local tectonic earthquakes have been catalogued for each 2 hour interval for the 4 month period.

Figure 32 shows examples of each of these types of earthquakes as they appear on the PVV helicorder records. Plots have been prepared (Figure 33) and the information has also been computerized so that statistical tests (such as moving averages, time series analyses, etc.) can be routinely made to examine short term variations in activity. This information, together with visual eruption reports from local sources and others such as the Smithsonian Institution's Center for Short-Lived Phenomena, provide us with solid data base to overview Pavlof's activity during the past five years.

B-Values. Seismic b-values are higher in general for volcanic earthquakes than for tectonic earthquakes (Minikami, 1960; Utsu, 1971). A seismic b-value was calculated for Pavlof Volcano using 1316 volcanic earthquakes which took place during the time period 1-8 December 1974. Magnitudes were calculated according to the following formula, modified from Richter (1958):

$$M = \log A_{zp} + \omega(f) + R(D)$$

where ω and R are constants, f is the observed frequency of 1.5 Hz, and D is the distance from the summit of the volcano to the seismometer, 7.5 km. Because of the close similarities in coda length, coda shape, and frequency between volcanic earthquakes with and without air shocks, we assume that most of the volcanic earthquakes take place at or just below the summit of the volcano. Events with magnitudes in the range from -.23 to .88 were observed.

The seismic b-value was calculated by the linear regression method according to Richter's (1958) formula (Figure 34):

$$\text{Log } N = A + bM$$

where N = number of earthquake of magnitude M or greater, and A and b are constants. Our calculated value of 2.6 is consistent with values reported for other volcanoes (Minikami, 1960). Using the same data set, the b-value was recalculated using the maximum likelihood estimate (Utsu, 1971) and found to be 3.2.

The analyzed time period corresponds to a period of mild eruptive activity at the volcano, as indicated by a moderately high number of volcanic earthquakes per

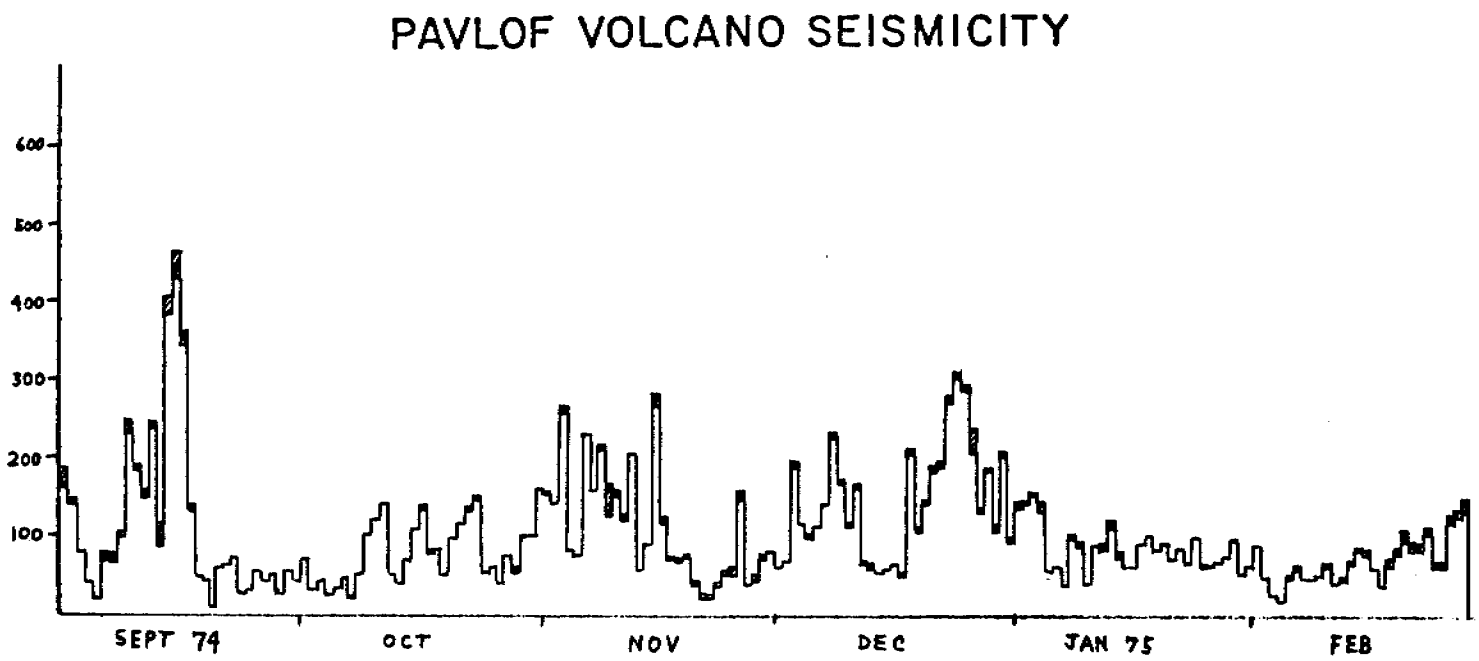

Figure 31. Histogram of Pavlof Volcano daily seismicity, from PVV helicorder records, September 1974 to February 1975. Daily seismicity is normalized to a 24-hour period, and to helicorder attenuation of -30 db.

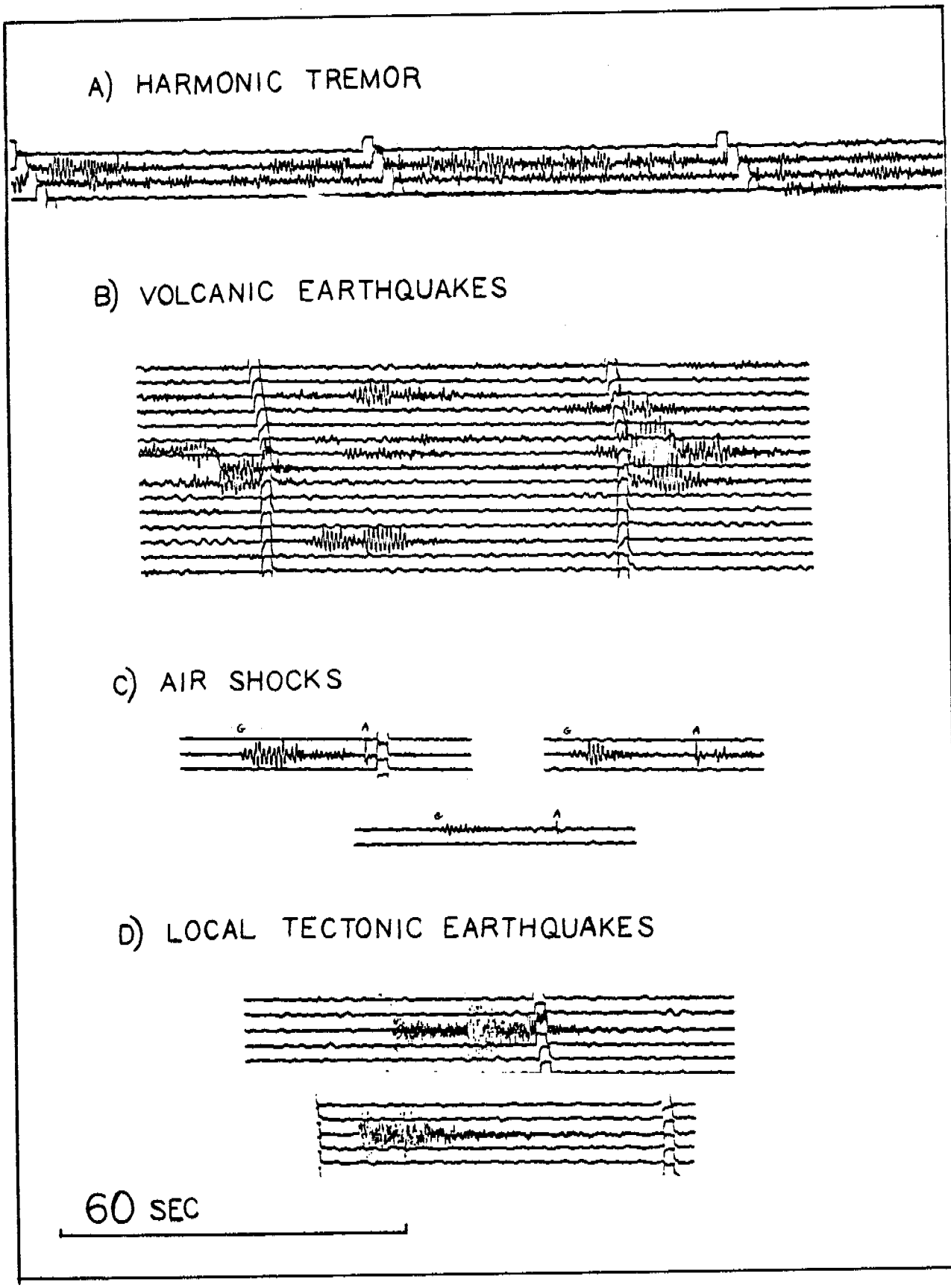

Figure 32. Volcanic earthquakes as recorded on the PVV short period helicorder. (a) Harmonic tremor; (b) Volcanic earthquakes without airshocks; (c) Volcanic earthquakes with air shocks. A = Air phase, G = Ground phase; (d) Local tectonic earthquakes.

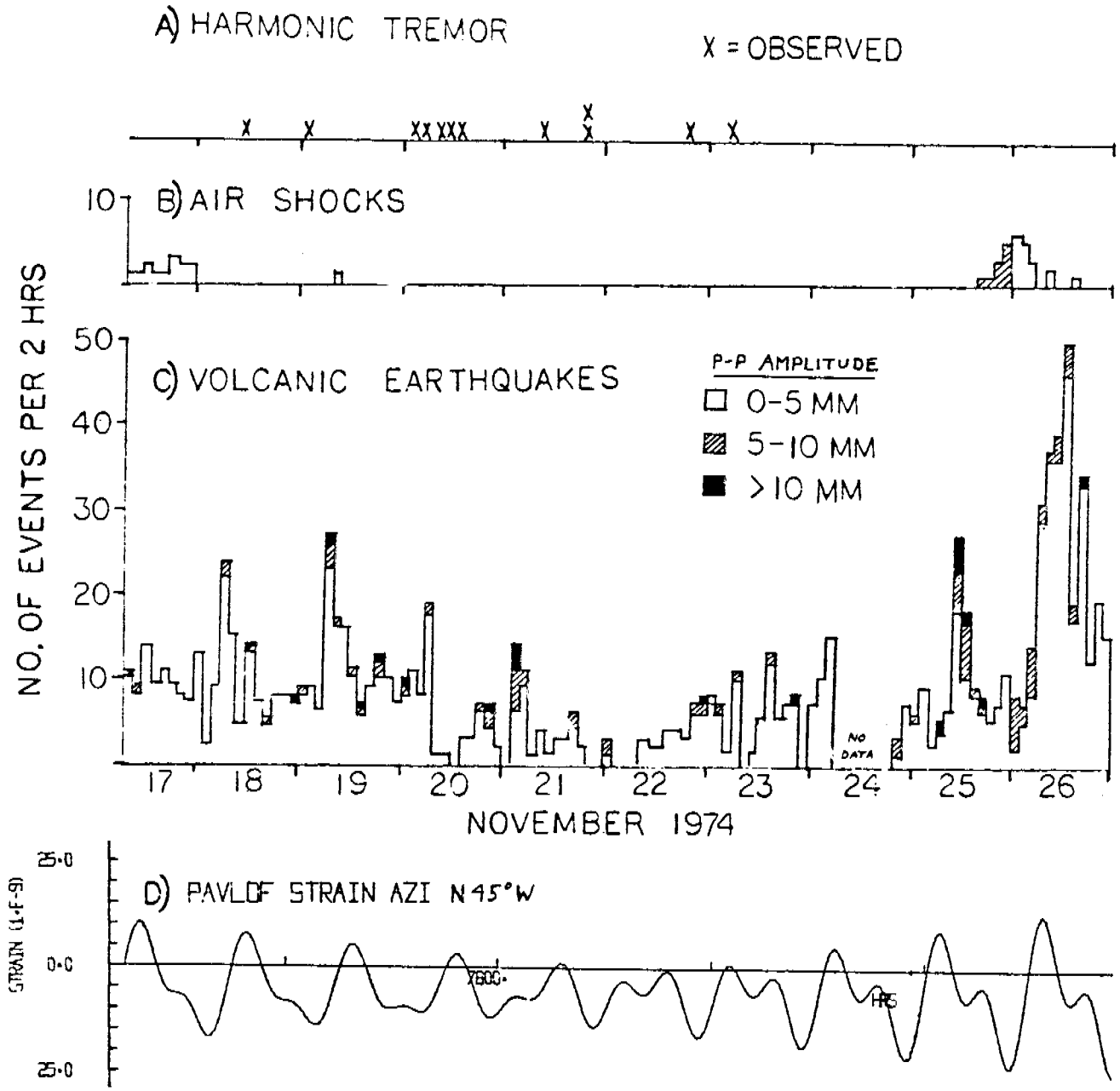

Figure 33. Pavlof Volcano seismicity, from PVV helicorder records, November 17-26, 1974.

a) Shows whether or not harmonic tremor was observed during each two hour period;

b) Histogram of the number of volcanic earthquakes with air shocks per two hour interval;

c) Histogram of the total number of volcanic earthquakes per two hour interval;

d) Theoretical horizontal strain tide for Pavlof. Azimuth is N45°W.

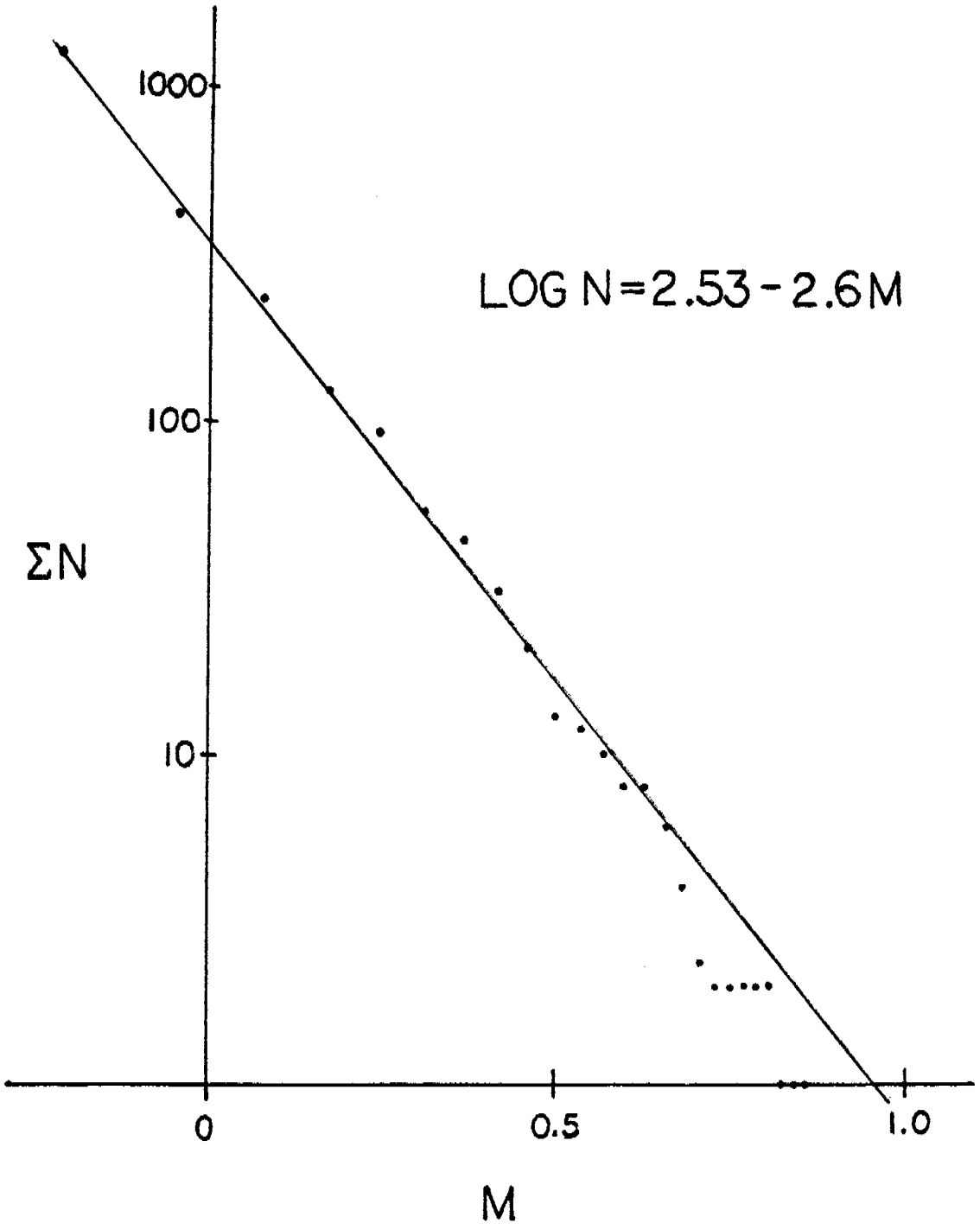

Figure 34. Plot used to calculate seismic b-value for Pavlof Volcano. Data plotted represents 1316 volcanic earthquakes which took place from 1-8 December 1974. Amplitudes were measured to the nearest .5 mm for all 1316 events. Magnitudes were then calculated according to the formula given in the text.

2 hour time interval, intermediate air shock activity, and low incidence of harmonic tremor. A b-value of 4.78 was reported for Pavlof for the period 11-22 November 1973, during which time the volcano was actively erupting (DOE Annual Progress Report for 1977-1978). Short term temporal variations in b-value may indicate changes in activity or eruptivity which may be of predictive value. For this reason we are developing computer software to systematically evaluate temporal changes in b-value.

Air Shocks. Air shocks as described earlier in this report are observed on many of our PVV (Pavlof station) helicorder records. These events are quite similar to other volcanic earthquakes in their frequency, coda shape, and coda length. However, a distinct explosion phase occurs as a sharp spike on the helicorder records approximately 21 seconds after the onset of the ground (assumed P) phase (see Figure 32).

Results to date show that volcanic events tend to occur in swarms of several hours duration. Swarms of air shocks begin 2-6 hours after swarms of volcanic earthquakes. We interpret this sequence of earthquakes followed by air shocks as indicating shallow migration of magma and subsequent degassing and eruption. The four months of data analyzed thus far show cyclic variation with five episodes of increased activity of variable duration (2-17 days), separated by periods of quiescence of from 5 to 11 days. Frequency of air shocks varies from 0 over a period of 3 weeks 30 January 1975 - 20 February 1975, to 26 in a single 2 hour interval on 25 December 1974. The former situation corresponds to a period of virtual inactivity, the latter to a period of mild eruptivity. The information obtained in these studies will be useful in determining rates of magma migration and periodicities in eruption cycles.

Earth Tides. Other workers (for example Mauk and Kienle, 1973) have shown that swarms of volcanic earthquakes tend to be triggered by the solid earth tide. Certain episodes of volcanic earthquake activity at Pavlof show a positive correlation with both the fortnightly and semidiurnal components of the theoretical solid earth strain tide. In particular, swarms occurring 3-4 days before and 3-4 days after periods of mild eruptive activity correlate well with the horizontal component of the strain tide (Figure 33).

For comparative purposes, three tidal time series were generated: the vertical gravity tide, the horizontal strain tide parallel with the volcanic arc axis (azimuth 45°), and the horizontal strain tide perpendicular to the axis (azimuth 135°). The tide is calculated as a time series by Longman's (1959) method using the astronomy given by Munk and Cartwright (1966) and Cartwright (1968). There is no correction for height above sea level or for the ellipticity of the Earth (see Broucke et al., 1972). The Love and Shida numbers used are those of Longman (1966): h_2 = .612, k_2 = .302, l_2 = .083, h_3 = .290, k_3 = .093 and l_3 = .014. The lunar tides are calculated for spherical harmonic orders 2 and 3, the solar tides for order 2 only. The lunar and solar tides are then added together (Beavan, personal communication).

We are presently undertaking a computer time series analysis of earth tides and volcanic earthquake activity. Existing software is being modified and some new software is being developed. Preliminary results indicate that earthquake swarms at Pavlof occur with a phase delay of approximately 4 hours after the maximum compression (low tide) for the 135° azimuth (Figure 33). This azimuth corresponds to the direction of plate motion or the slip vector between the North American and Pacific plates. The observations are consistent with the hypothesis that the regional stress field is locally altered on a short term basis by the earth tides.

The relationship between tidal peaks and earthquake swarms then provides important clues about near surface magma transport. This information is being used in conjunction with information about air shock and harmonic tremor activity to quantitatively evaluate short term periodicities in eruptivity.

These factors have a direct bearing on the timing and intensity of eruptive activity, and are hence of predictive value.

E. Tilt and Sea-Level Meter Results

RESULTS 1978. The work described in this section has not been directly funded by NOAA since 1976. The NOAA helicopter pilots have, however, provided invaluable logistic support during the 1977 and 1978 field seasons by flying personnel to sea-level and geodetic sites at times when this does not interfere too seriously with the seismic work. We hope that such support can continue in the future.

Sea Level. A network of mean sea-level gauges is being tested in the Shumagin Islands with a view to detecting anomalous land deformation prior to a major earthquake. We hope ultimately to be able to reliably monitor mean sea level to 1 mm precision with instruments spaced at 20 to 30 km intervals and to examine the data for anomalies in near real time. Then a real possibility would exist to utilize the data for earthquake prediction.

We have made progress on three fronts during 1978: (1) modifications to the sea-level gauge to improve performance; (2) installation of additional instruments; (3) installation of satellite telemetry at most sites.

(1) Experiments elsewhere led us to hope that the water-level in a stilling well just above the high water mark might accurately follow mean sea level. If this were true it would obviate the need for the complicated entry tube arrangement in the "sea level" type gauge (see Annual Report 1977/1978). We installed three of the stilling well or "pore pressure" type gauges during 1978, two of them (at PRC and EBT; see Figure 35) in parallel with regular sea-level gauges to evaluate relative performance. Initial results from the pore pressure gauges are not encouraging; the sites we were able to instrument were either poorly coupled to the sea or were strongly affected by rain and run-off water.

(2) A new installation containing both sea-level and pore pressure gauges was made at EBT on the south shore of Nagai Island. A pore pressure gauge was added at PRC. The gauge at SDP was converted to pore-pressure type. Continued bad weather prevented the planned installation of gauges on the mainland. Figure 35 shows the present status of the array.

(3) LaBarge satellite transmitters (DCP's) were installed at four sites (SDP, PRC, EBT and SMH) to relay sea-level data to Lamont in near real time via the ERTS (LANDSAT) satellite, the Goldstone or Gilmore tracking stations and Goddard Space Flight Centre. The delay in receiving the data is presently about four weeks but this will be shortened in the future. The data received by satellite between July and December 1978 are shown in Figure 36.

Geodetic Leveling. Levelling measurements are not immediately applicable to an earthquake prediction situation as they are repeated too infrequently, but they give accurately the rate of tilt at specific locations and may be used in conjunction with sea-level measurements to define crustal blocks (Bilham and Beavan, (1979) They are subject to less noise than sea-level measurements and are therefore more readily interpretable. It is also important that levelling can be done at very little cost once the personnel are already in the field for other work.

With one exception, all the existing level lines and dry tilt figures were remeasured during June 1978. The SQH level line continues to show a tilt down towards the

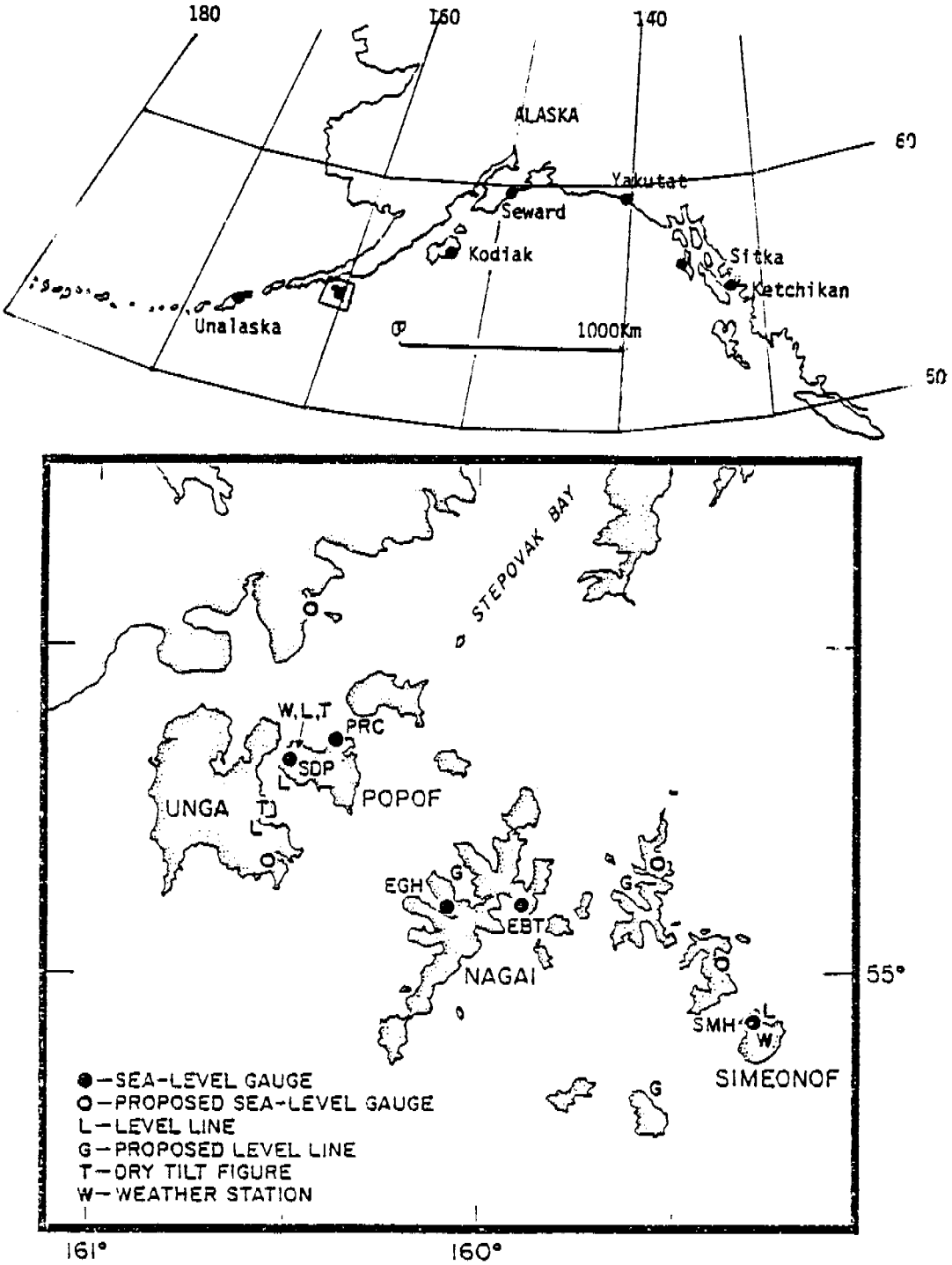

Figure 35. Location of tide gauges and mean sea-level monitors in the Gulf of Alaska and the Shumagin Islands. The region to the west of 163°W experienced a major earthquake in 1957 and the region between 155°W and 145°W broke in 1964. A major earthquake may have partly released strain energy in the eastern Shumagin Islands in 1938 (McCann et al. [3]).

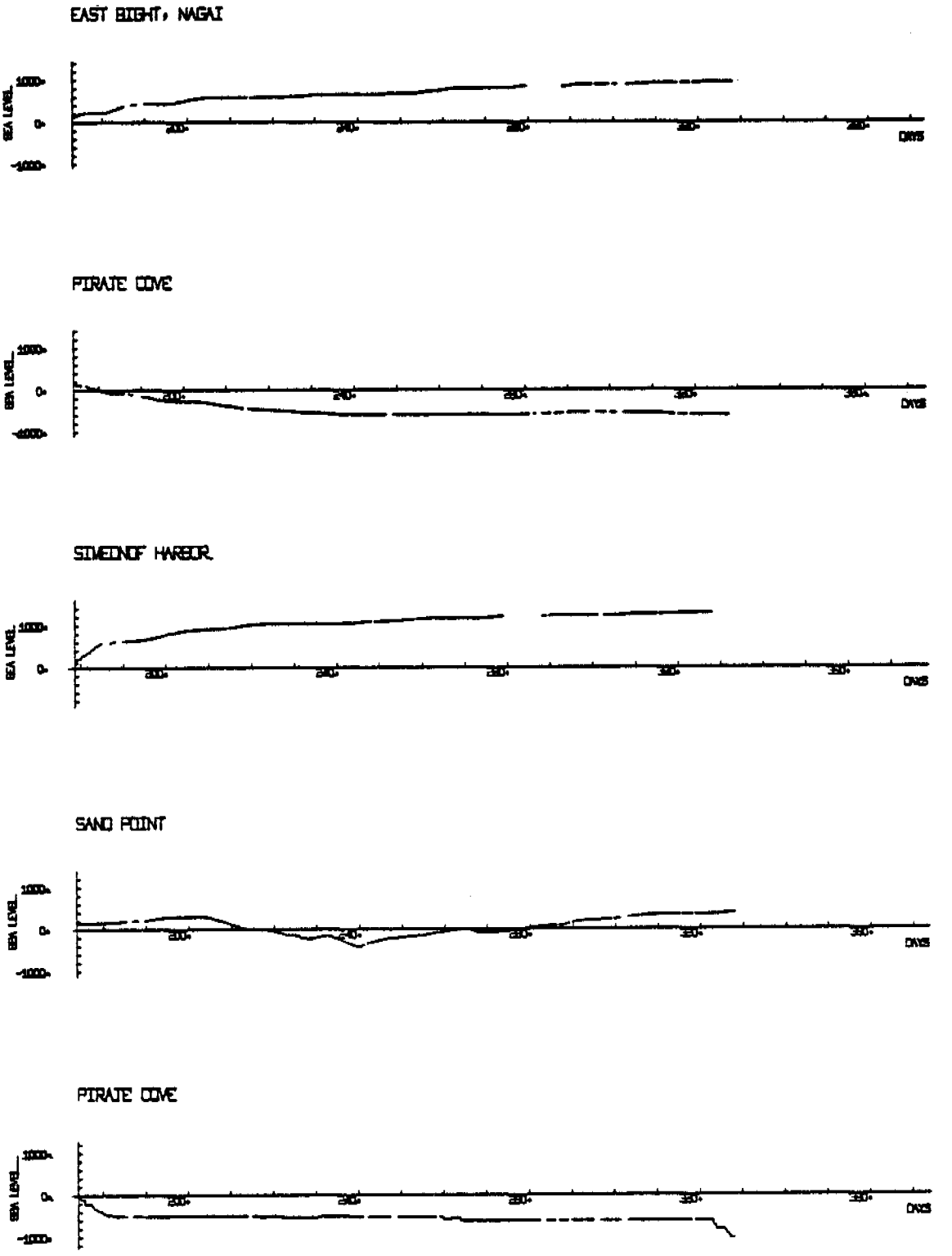

Figure 36. Sea-level data received via satellite from four locations in the Shumagin Islands between July and December 1978. The instruments have hydraulic time-constants of approximately 200 hours. The lower two records are from piezometric monitors. On the lowest record the gauge was malfunctioning from soon after installation until day 322 when it was visited. The vertical scale on these plots is 1000 units equals 40 cm.

trench of about 8×10^{-7} radians/year (Figure 37). All the levelling data to date have recently been uniformly re-analyzed and the SDP data are now reasonably consistent with SQH, though they are too noisy to draw any conclusions from them alone.

DISCUSSION. Sea Level. The sea-level measurement program has not yet been as successful as we had hoped due to the poor reliability of the gauges over long periods of time and the difficulty of servicing them over the Alaskan winter. Since the 1978 field season a USGS contract has allowed us to re-design the sea-level monitor in a form that should be more reliable. The new instrument uses as the working fluid a silicone fluid in a closed system rather than sea water in an open system, and all parts above the low water mark are constructed of stainless steel rather than plastic. The new features should immediately prevent the problems of dirt clogging the filters, and of air locks due to air exsolved from the sea water or sucked through the plastic tubing. A further feature is the reduction in the hydraulic filter time constant from 80 to 4 hours. This was done for several reasons: 1) the large time constant was originally chosen to reduce the tidal range to less than a few cm so that the gauge standpipe could be buried a few inches (rather than several feet) below mean sea level; in the new gauge the tidal range is reduced by backing off the silicone fluid column against a mercury column and measuring the position of the mercury, rather than the silicone fluid, surface. This also reduces the long period signals we are interested in so that a higher resolution transducer is required; 2) the shorter time constant makes the setting up and checking of the gauges much easier; 3) using clean fluids the filters will retain their time constant rather than changing with time as at present; 4) silicone fluid is slightly less dense than sea water so the gauge need not be buried to attain immunity from freezing conditions making it suitable for a much wider variety of coastline

NEED FOR FURTHER STUDY. Sea Level. The sea level program is still in its infancy and several years more study will be required to determine its usefulness as a tool in earthquake prediction. It is important to continue working in areas where we expect earthquake activity in the near future as the only true test of the instrumentation is to actually observe an earthquake. Such an area is the Shumagin seismic gap. We also hope to instrument an area near Yakutat Bay/Icy Bay, Alaska where the February 28, 1979 earthquake broke only part of that seismic gap, suggesting that the other part may break in the near future.

Geodetic Levelling. Levelling remains by far the most accurate means of measuring vertical deformation and will remain so for the foreseeable future. Level lines are inherently stable so that their usefulness increases with time after installation. It is therefore important to install lines at as early a date as possible, and we hope to be able to put in one or two new 1 km lines this summer.

24 Mar 79

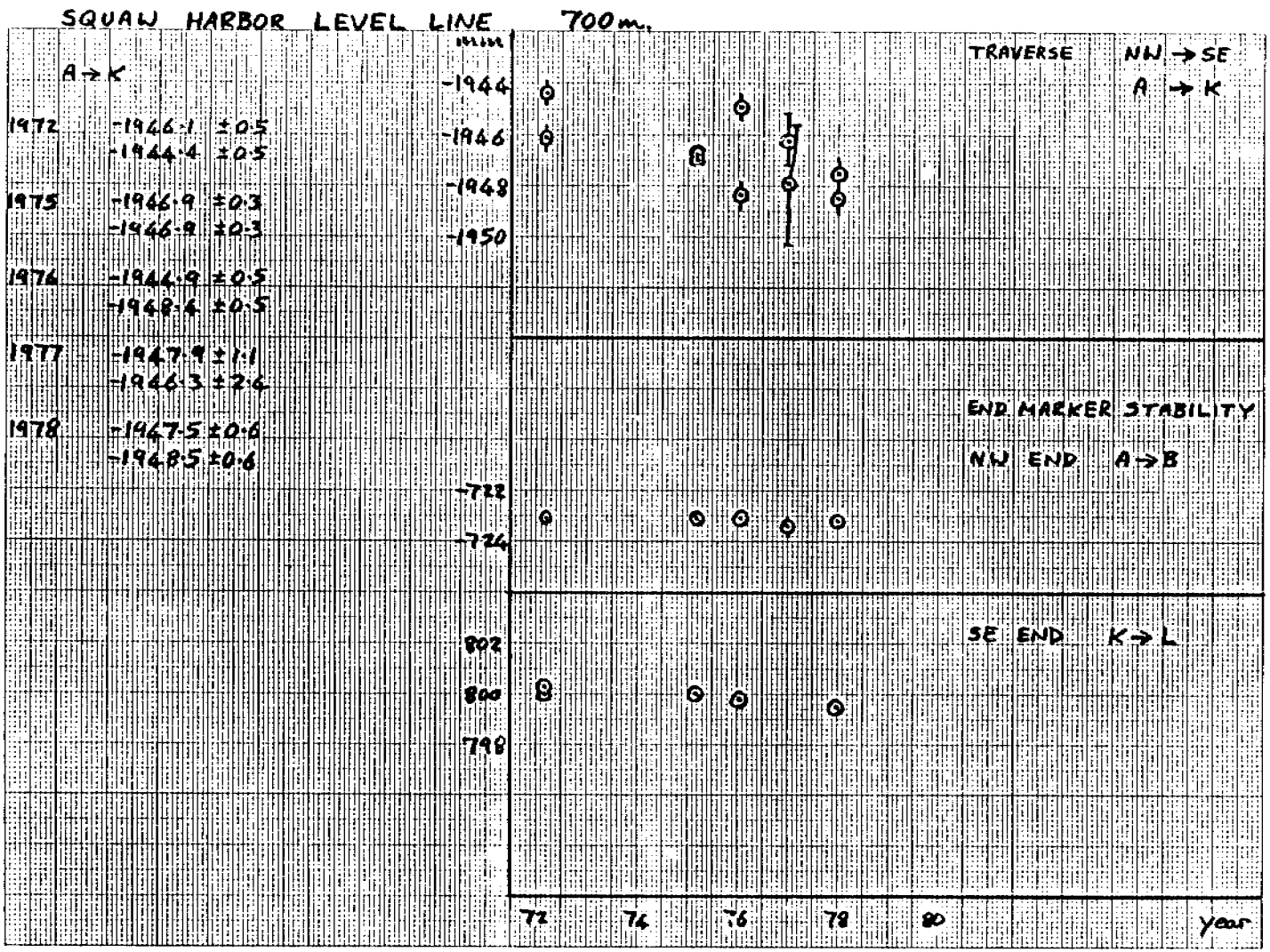

Figure 37. Results from Squaw Harbor level line. The top figure shows the height of the SE end of the line relative to the NW end. Error bars are one standard deviation; where they are not shown they are within the symbol size. The lower figures show the relative height between markers at each end, and demonstrate that the ends are much more stable than the observed tilt.

F. Geologic Inyestigation

An aerial reconnaissance was begun in 1978 by M. Winslow in the area of the Shumagin Islands and adjacent Alaska Peninsula in order to pinpoint areas of greatest potential for post-glacial uplift, tilting and active faulting. Six areas were chosen for an isobase survey based on obvious terrace development and suitable geological structures. Terrace development was most clear in the tightly folded Upper Cretaceous rocks, where the eroded surfaces cut across all lithologic boundaries. In areas of flat-lying strata, planar surfaces of erosional origin obscured any potential terraces, and were thus avoided, except where surfaces crossed lithologic boundaries. The intrusive rocks show the least evidence for terrace formation. However, terrace surfaces can be traced into the igneous terrain by a slope break. In certain localities, wind gaps aligned with surveyed terraces and were surveyed as well.

An isobase survey was conducted for each sub-area using an aledade to triangulate and locate separate terrace levels as shown by sea cliffs, wave-cut platforms, former dunes, and slope breaks. Due to the inaccuracies of the topographic maps and paucity of geodetic bench marks, it was determined that an isobase study, semi-independent of the topographic maps, would be preferable to plotting the terraces directly onto the available maps (Figure 38).

Aerial reconnaissance indicated the presence of several post-Pleistocene faults which were recognizable as distinct, linear valleys, coast lines, and linear changes in vegetation. Only those lineaments which cut across lithologies and form scarps were recorded. Three of these were examined in the field. The azimuth, height, and dip of the scarps were measured, and field relationships were noted. Small-scale fracture sets and tension displacements have not yet been determined. The inland faults do not appear to affect local terrace heights, nor do they appear to control major block boundaries.

Specifically, uplifted marine and river terraces are found on Nagai, Korovin, Dolgoi, Popof, and Simeonof Islands. The terraces are recognized by major sea cliffs, which can be followed inland as slope breaks and river terraces. The relief on these surfaces varies somewhat, but sub-planar surfaces are present regardless of lithologic changes. The most pronounced uplifted marine and river terraces are found in the poorly indurated Tertiary-age rocks and tightly folded upper Cretaceous sedimentary rocks. Cretaceous intrusives show slope breaks that can be followed along strike toward marine terraces. Soft sediments form the lowest level marine and river terrace levels. On Nagai Island, wind gaps (of similar elevation regardless of lithology) were included in the survey if they could be traced along strike to major slope breaks and sea cliffs. Preliminary terrace levels are plotted on Figure 39. Relative heights are compared from one locality to another. The terrace widths qualitatively indicate the persistence of certain terraces relative to others. However, correlation of these terraces with data from adjacent regions awaits age data by radiometric and paleontologic methods.

Evidence for Holocene faulting was seen on Nagai, Korovin, and Unga Islands. Fault traces are visible from the air as 1-3 km scarps, fissures, and as linear valleys and coasts. Although fault displacement were not determined due to poor exposures, the fault scarps and fissures cut across structures and lithologies obliquely, and are visible in unconsolidated alluvium. Steep scarps on three of

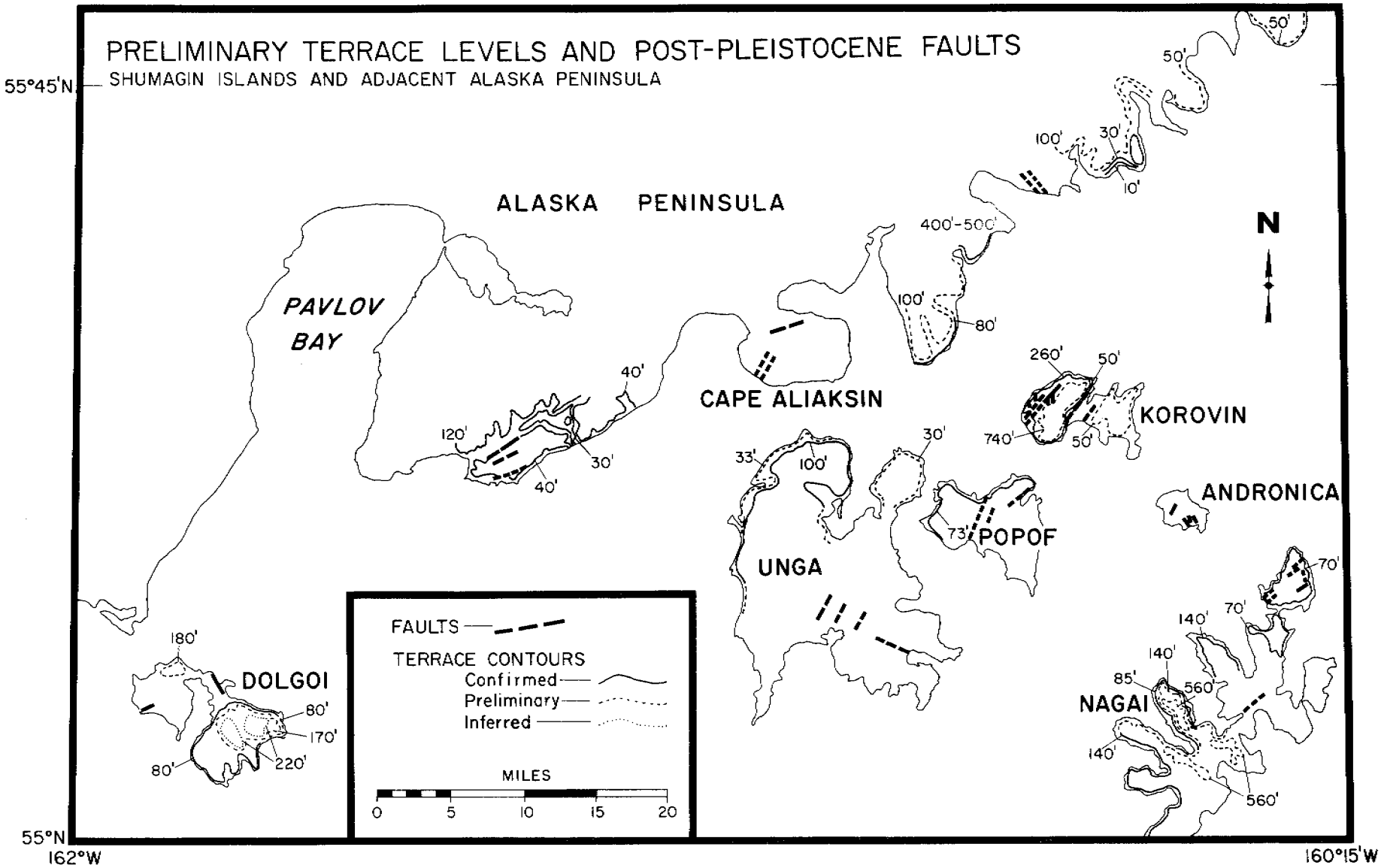
PRELIMINARY TERRACE LEVELS AND POST-PLEISTOCENE FAULTS
SHUMAGIN ISLANDS AND ADJACENT ALASKA PENINSULA
55°45'N
55°N
162°W
160°15'W
ALASKA PENINSULA
PAVLOV BAY
CAPE ALIAKSIN
KOROVIN
ANDRONICA
POPOF
UNGA
DOLGOI
NAGAI
N
FAULTS
TERRACE CONTOURS
Confirmed
Preliminary
Inferred
MILES
0 5 10 15 20
50'
100'
30'
10'
400'-500'
80'
260'
740'
120'
40'
33'
73'
180'
170'
220'
70'
140'
85'
560'

Figure 38

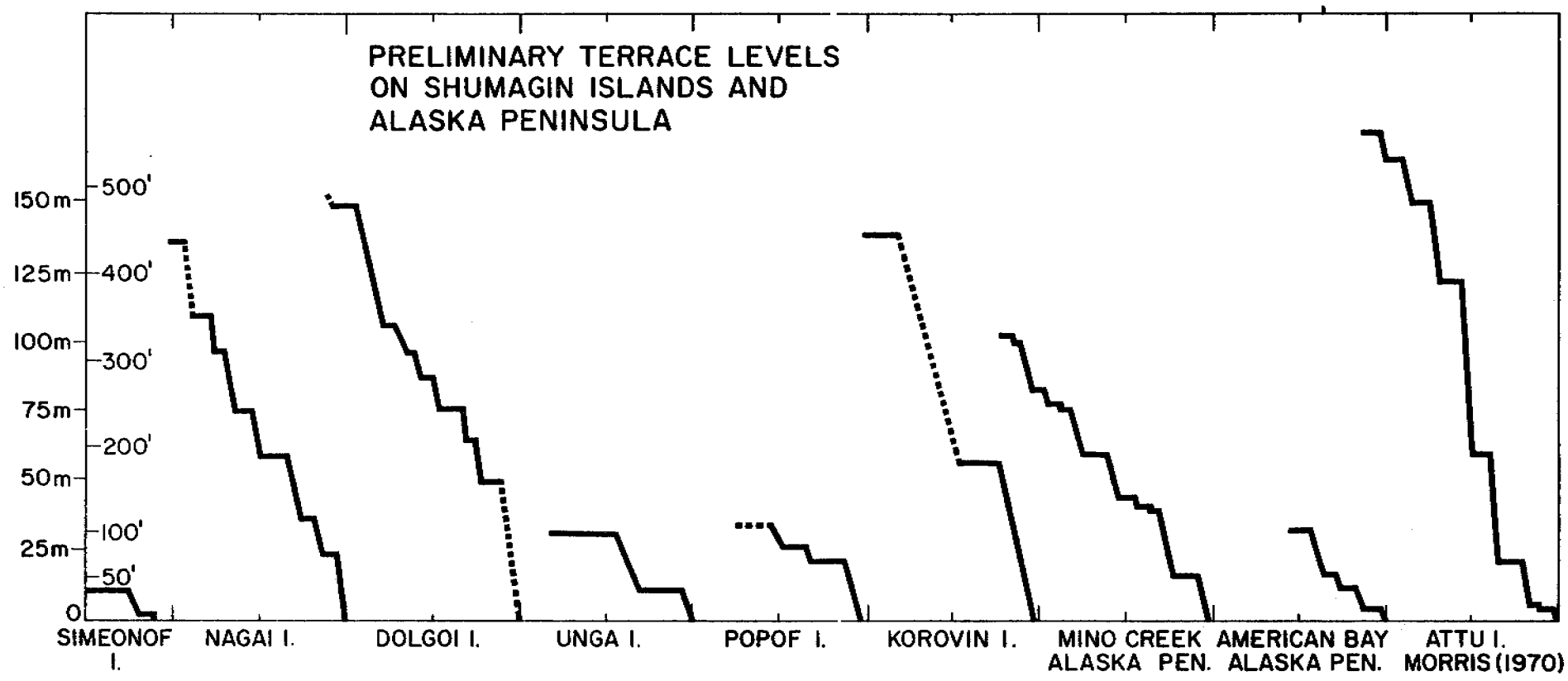
PRELIMINARY TERRACE LEVELS
ON SHUMAGIN ISLANDS AND
ALASKA PENINSULA
150m
125m
100m
75m
50m
25m
0
500'
400'
300'
200'
100'
50'
SIMEONOF I.
NAGAI I.
DOLGOI I.
UNGA I.
POPOF I.
KOROVIN I.
MINO CREEK ALASKA PEN.
AMERICAN BAY ALASKA PEN.
ATTU I. MORRIS (1970)

Figure 39

these faults strike at high angles to the trench and generally face east of southeast. Fracture sets and tension gashes were measured across one of these faults, but did not reveal a unique displacement direction, except to suggest a right-lateral component to an apparent high-angle thrust.

The importance of continued and additional geodetic releveling in this seismic gap includes the following factors:

1. A major earthquake may be imminent in the area and preseismic processes may be revealed during regular geodetic re-measurements. Should a major event occur it is vital that a baseline of measurements be available for subsequent study of the physical processes involved.

2. Crustal strain buildup in this area as the Pacific plate underthrusts Alaska (6 cm/yr) should generate tilts on the order of 1 microradian/yr (i.e. 1 mm/yr/km). The Shumagin Islands is one of the few locations where a two dimensional profile (transverse to the trench) of downwarping can be studied since the islands extend more than 100 km from the mainland toward the trench. The most southerly islands lie approximately 100 km from the trench and only 30 km above the Benioff zone (Davies and House, 1978).

3. Recent tilts have been observed along leveling lines at one site in the area (other sites show tilts that are within the error of the measurements).

4. The leveling measurements provide an independent measure of tilts to compare with that obtained from a dense array of sea level monitors operating in the region.

Significance. The assessment of uplift periodicities is a critical problem in earthquake hazards studies. Evidence for episodic versus steady state uplift must be studied in order to evaluate relative rates of vertical displacements along faults and the potential for producing tsunamis (Plafker and Rubin, in press, 1978). Dating of older terraces will contribute to the understanding of total uplift rates, and periodicities, and would set a maximum limit to long term uplift rates in the arc-trench gap associated with Pacific underthrusting during the Quaternary.

Crustal deformation in arc-trench gaps does not occur in a linear manner due to the existence of fragmented crustal blocks of 5 to 50 km dimensions. Such large-scale blocks appear to be common in regions of intense tectonic activity. The boundaries are weaker than the internal parts of the block, which results in strain concentration at block boundaries, with abrupt diminution of strain within the blocks. The boundaries may respond visco-elastically or exhibit strain dependent elastic properties as in Japan (cf. Scholz and Kato, (1978). Hence, nonlinear behavior may be a characteristic of regions of fragmented crustal blocks, which introduces complications to the observations of surface strain and tilt.

Geodetic survey data has been obtained in many parts of the world, especially in Japan, where large numbers of strainmeters and tilt meters have been operated simultaneously (e.g. Harada, 1976; Hosoyama, 1976). The data from Japan confirmed the presence of semi-independent blocks (Yamasaki, 1928; Tsuboi, 1933) and introduced compelling evidence for recent activity mainly confined to block boundaries. Geodetic releveling is systematically more precise than triangulation or trilateration particularly since fixed benchmarks for the former method can be much more closely spaced.

Block activity is most pronounced at times of seismic energy release or volcanic activity. Coseismic block motion forms the bulk of the observed phenomena but post-seismic activity on block boundaries has been documented (Scholz, 1972). Studies in Japan indicate post-seismic activity up to 15 years after a seismic event (Scholz and Kato, 1978). Miyabe (1933) noted several examples of adjoining blocks moving semi-independently for a certain period, but behaving as if locked at other times. Long leveling lines indicate the existence of semi-independent blocks, tilts, and hinge lines or flexures. These short term data combined with long term net uplift history from terrace studies are essential to an understanding of the uplift and overall crustal behavior at the Aleutian convergent plate boundary.

VIII. CONCLUSIONS

The Shumagin Islands region of the eastern Aleutian Island Arc has been identified as a seismic gap. Through support from DOE, USGS and NSF as well as the present contract with NOAA/OCSEAP, investigators at Lamont-Doherty Geological Observatory are engaged in a broad, multi-disciplinary study of the seismotectonic setting of this seismic gap. Disciplines directly involved in this study are seismology, volcanology, geodesy and geology. Specific conclusions from investigations in these various disciplines follow.

Shumagin Islands Seismicity. In general the broad pattern of seismicity in the Shumagin Islands region is similar to that expected for a seismic gap: relatively little or no activity along the main thrust zone with increased activity both down-dip and along strike from the quiescent region or gap. This pattern was first described (for Japan) by Mogi (1969) and is often referred to as a "Mogi donut". Two recent, moderate-sized earthquakes (M_b = 5.4 and 6.0) occurred along the lower edge of the main thrust zone. This location for these events is consistent with the Mogi-donut pattern and adds weight to the interpretation (given below) that the lower edge of the main thrust zone is highly stressed.

Crustal seismicity is generally concentrated in an inclined zone that extends at approximately right angles to the main thrust zone. This crustal concentration zone originates in the highly stressed region at the lower end of the main thrust zone and "outcrops" at the surface along a band subparallel to the island arc that essentially occupies the outer (seaward) half of the Pacific continental shelf. It is within this portion of the continental shelf that the Sanak and Shumagin sedimentary basins are forming. The same tectonic process is probably responsible for the formation of these basins and the shallow (depth less than 25 km) earthquakes of the crustal concentration zone.

A preliminary study of the hypocenters in the Sanak basin area shows that they are very shallow (depth generally less than 10 km) and probably associated with the boundary faults of the grabel-like Sanak basin. Other clusters of crustal earthquakes of special interest are: (1) SW of Nagai Island above the aftershock zones of the April 1964 earthquakes, (2) NW of Black Hill on the Bering Sea side of the Alaska Peninsula, and (3) north of Stepovak Bay under Kupreanof Volcano.

SE-Bering Sea Seismicity. In ten months of recording the single station on St. Paul Island, in the Pribilofs, recorded 5 events in a distance range consistent with a probable location in the St. George Basin. This station operates at very low gain so the number of events is low compared to what would have been recorded by an average seismic station.

Strong Ground Motion in the Shumagin Island Region. In April 1974 two moderate (M_b = 5.7, 6.0) earthquakes occurred SW of Nagai Island and were recorded on a Kinemetrics SMA-1 at Sand Point, Popof Island. These recordings have been extensively studied (House and Boatwright, in preparation) in a comparison with synthetic records based on a quasi-dynamic model of a rupture process thought to well represent that which caused these earthquakes. An important result of this study is that the stress-drops for these earthquakes were very high; in the range 600-900 bars, compared to normal values of 10-100 bars. The high stress level implied

for the lower edge of the main thrust zone (where these earthquakes were located) is consistent with the identification of the Shumagin Islands region as a seismic gap in which strain energy is accumulating in preparation for a great ($M \geq 7.8$) earthquake.

Also consistent with the above interpretation, are the locations and generally high accelerations observed for five of the largest earthquakes that have occurred since the network has been in place and that were recorded on the Sand Point SMA-1 accelerograph. All of these events were located along the lower edge of the main thrust zone, a region of high stress in which one might expect the larger of the moderate-sized earthquakes to occur. The peak-horizontal accelerations for 4 of these 5 events are 2-4 times higher than those for events of comparable magnitude and distance to the causitive fault that have been recorded in California and adjacent states. This difference between the Californian and Alaskan data may be due in part to a path-dependent transmission effect. In any case, the Alaskan data are significant because they are among the first strong-motion data recorded in the Aleutian arc.

Because these data are scarce and there is a need to evaluate accelerations-vs.-distance relations for the Aleutians in a timely manner we have begun a study to evaluate the feasibility of using broad-band recordings of smaller, more frequent events to simulate those from the less frequent, larger events necessary to trigger a strong-motion recorder. Several of the computer programs necessary to this study have been written and the remainder are being worked upon now. This study is supported by NSF.

Volcanic Studies. Characterization of the hazard posed by the Aleutian volcanoes depends upon knowledge of the long-term patterns of eruptive activity for one or more types of volcanoes and upon specification of the type and state of specific volcanoes. Presently, none of this knowledge is adequate. Therefore we are undertaking volcanic studies aimed at these two general problems. Firstly, we are attempting to amass as complete a record as possible of the eruptive history of Aleutian volcanoes. Sources for this study range from logs of DSDP cores and Russian exploration histories to present day eye-witness accounts and our own (and others) seismic monitoring of specific volcanoes. Secondly, through the monitoring of specific volcanoes - Pavlof, Akutan and Makushin - we are attempting to characterize the type and state of these specific eruptive centers. This study focuses most strongly on Pavlof volcano where we also attempt to understand the physical mechanisms involved in the eruption process. Additional support for the Pavlof study is provided by DOE for an evaluation of the geothermal potential of Pavlof.

Geodetic Studies: Level-Lines and Sealevel Meters. Results from the 600 m level line at Squaw Harbor indicate a 0.8 microradian per year tilt, down to the SSE. This is consistent with measurements made in the interseismic period in Japan prior to a large earthquake.

Other level lines and the sealevel meters yield results consistent with the Squaw Harbor results, but too noisy to be definitive as yet.

Major support for these geodetic studies is now provided by the USGS, except for certain critical logistic support provided by NOAA/OCSEAP in cooperation with the servicing of seismic stations.

Geologic Investigations of Faults and Terraces. A preliminary field study of faults and terraces in the Shumagin Islands region was carried out during the month of June, 1978. Several minor faults and a number of terraces were mapped. Knowledge of the heights, geographical extents of the terraces and their ages would be very important in understanding the rate and pattern of past tectonic deformation. For example, one could obtain some constraints on the long term rate of uplift and of the recurrence times for great earthquakes. We now have NSF support to continue this work during the next two field seasons. We will attempt to date and more accurately map some of the better defined terraces.

X. SUMMARY OF FOURTH QUARTER OPERATIONS

(January-March 1979)

Data Reduction. A major part of our routine effort is devoted to the analysis of the data collected from the seismic networks. The primary, immediate result of this analysis is the cataloging of hypocentral coordinates, origin time and magnitude for earthquakes in the Shumagin Islands region. During the fourth quarter we submitted to the NOAA/OCSEAP archive this earthquake catalog information for the period 1 July through 30 September, 1978. This submission contained the above parameters for 200 events.

Fieldwork. A maintenance trip, planned for early March was extended to include an attempted visit to the epicentral region of the 28 February 1979 St. Elias earthquake. Due to poor weather Yakutat was as close as we could get to the epicenter, approximately 155 km away. More than 50 felt reports were collected (and sent to the USGS) from Ketchican, Juneau, Douglas, Yakutat, Cordova and Anchorage. We set up a Sprengnether digital event recorder in Yakutat, but no large aftershocks were recorded. Several smaller events were, but the background noise was too high to allow spectral analysis of the data. For more on this earthquake see item XI.C.

Routine maintenance work was carried out at the Sand Point and Dutch Harbor recording centers. In the course of this work two new SMA-1 records were collected at Sand Point. See section VIC for more on the records.

Meeting. Two P.I.'s, John Davies and Klaus Jacob, and two graduate students, Leigh House and Janet Krause, attended the NOAA/OCSEAP meeting on Alaskan Outer Continental Shelf Seismology in Boulder, Colorado, 26-29 March 1979.

XI.A. REFERENCES

Aki, K., M. Fehler, and S. Das (1977). Source mechanism of volcanic tremor: Fluid-driven crack models and their application to the 1963 Kilauea eruption, Jour. Vol. Geothermal Res., 2, 259-287.

Archambeau, C.B. (1977). Earthquake predictions based on tectonic stress determinations, EOS, 57 (4), p. 290, abstract.

Bilham, R., and J. Beavan (1979). Tilts and strains on crustal blocks, Tectonophysics, in press.

Boatwright, J. (1978a). Radiated seismic energy and the implications of energy flux measurements for strong motion seismology, Proceedings at a seminar-workshop on strong ground motion; Cal Tech (in press).

Boatwright, J. (1978b). Pseudo-dynamic models of simple earthquakes and the implications of energy flux pulse shapes as modelling constraints, Abstract for XII symposium on Mathematical Geophysics, Caracas, Venezuela.

Boatwright, J. (1979). A spectral theory for circular seismic sources; simple estimates of source dimension, effective stress and radiated energy, submitted to BSSA.

Broucke, R.A., W.E. Zürn, and L.B. Slichter (1972). Lunar tidal acceleration on a rigid earth, in Geophys. Mono. Series 16, Flow and Fracture of Rocks, H.C. Heard, I.Y. Borg, N.L. Carter, and C.B. Raleigh, eds., American Geophysical Union.

Burk, C.A. (1965). Geology of the Alaska Peninsula - island arc and continental margin, GSA Mem. 99, part 1, 250 p.

Cartwright, D.E. (1968). A unified analysis of tides and surges round north and east Britain, Phil. Trans. R. Soc. Lond., A-263, 1-55.

Coats, R. (1950). Volcanic activity in the Aleutian Arc, USGS Bull. 974-B, 35-47.

Cox, A., D. Hopkins, and G.B. Dalrymple (1966). Geomagnetic polarity epochs: Pribilof Islands, Alaska, GSA Bull. v. 77, 883-910.

Dall, W.H. (1870). Alaska and Its Resources, Boston, Lee and Shepard, 627 p.

Davies, J.N., L. House, K.H. Jacob, R. Bilham, V.F. Cormier, and J. Kienle (1976). A seismotectonic study of the seismic and volcanic hazards in the Pribilof Islands - Eastern Aleutian Islands region of the Bering Sea, Annual Report to NOAA, April 1, 1975 - March 31, 1976.

Davies, J.N., and L. House (1978). Aleutian subduction zone seismicity, volcano-trench separation and their relation to great thrust-type earthquakes, Accepted for publication in the Jour. Geophys. Res., JGR MS# 4847.

Davies, J.N., K.H. Jacob, J. Beavan, R. Bilham, L. House, J. Krause, M. Hamburger, and P. Beck (1978). A comprehensive study of the seismotectonics of the Eastern Aleutian arc and associated volcanic systems, Annual Progress Report to U.S. Department of Energy, March 1, 1977 - February 28, 1978.

Engdahl, E.R. (1977). Seismicity and plate subduction in the central Aleutians, In: Island Arcs, Deep Sea Trenches and Back-Arc Basins, Maurice Ewing Ser., vol. 1, edited by M. Talwani and W.C. Pitman III, 259-272, AGU, Washington, D.C.

Engdahl, E.R., and C.H. Scholz (1977). A double Benioff zone beneath the central Aleutians: An unbending of the lithosphere, Geophys. Res. Lett., 4 (10), 473-476.

Gedney, L. (1978). Summary of Alaskan Earthquakes/April, May, June 1978, Seismological Bulletin No. 4, Alaska Earthquake Analysis Center, Geophysical Institute, University of Alaska, Fairbanks, Alaska.

Harada, T. (1976). Accumulation of data by the geographical survey institute, Jour. Geol. Soc. Jap., 22, 228-234.

Hopkins, D.M. (1976). Fault history of the Pribilof Islands and its relevance to bottom stability in the St. George Basin, In: Environmental Assessment of the Alaska Continental Shelf, Principal Investigators Annual Reports April 1975 - March 1976, NOAA/BLM OCSEAP, Geology Volume 13, 41-68.

Hosoyama, K. (1976). Observational accuracy of crustal movements, Jour. Geod. Soc. Jap., 22, 235-241.

House, L.S. (1977). Stress orientations inferred from focal mechanisms in the Aleutians, Trans. Amer. Geophys. Union, 58 (10), 992.

House, L.S., and J. Boatwright (1978). Manuscript in progress.

Isacks, B., J. Oliver, and L.R. Sykes (1968). Seismology and the new global tectonics, JGR, 73, no. 18, September 15, 5855-5899.

Jacob, K.H. (1970). Three-dimensional seismic ray tracing in a laterally heterogeneous spherical earth, Jour. Geophys. Res., 75, no. 32, 6675-6689.

Kanamori, H. (1977). The energy release in great earthquakes, Jour. Geophys. Res., 82 (20), 2981-2988.

Kelleher, J.A. (1970). Space-time seismicity of the Alaska-Aleutian Seismic Zone, Jour. Geophys. Res., 75 (29), 5745-5756.

Kennedy, G., and H. Waldron (1955). Geology of Pavlof Volcano and vicinity, Alaska, USGS Bull. 1028-A.

Kimura, M. (1976). Major magnetic activity as a key to predicting large earthquakes along the sagams trough, Japan, Nature, 260, 5547, 131-133.

Kubotera, A. (1974). Volcanic tremors at Aso Volcano, In: L. Civetta, P. Gasparini, G. Luongo, and A Rapolla (eds.), Physical Volcanology, Elsevier, Amsterdam, 29-48.

Lahr, J.C., G. Plafker, C.D. Stephens, K.A. Fogleman, and M.E. Blackford (1979). Interim report on the St. Elias earthquake of 28 February 1979, preprint.

Longman, I.M. (1959). Formulas for computing the tidal accelerations due to the sun and moon, J. Geophys. Res., 64, 2351-2355.

Longman, I.M. (1966). Computation of Lov numbers and load deformation coeefficients for a model earth, Geophys. J. R. astr. Soc., 11, 133-137.

Madariaga, R. (1977). Implications of stress drop models of earthquakes for the inversion of stress drop from seismic observations, Pure and Appl. Geophy., in press.

Marlow, M.S., D.W. Scholl, and A. Cooper (1977). St. George Basin, Bering Sea Shelf: A Collapsed Mesozoic Margin, In: Island Arcs, Deep Sea Trenches and Back-Arc Basins, Talwani and Pitman, eds., Maurice Ewing Series I, Amer. Geophys. Union, 211-220.

Mauk, F.J., and J. Kienle (1973). Microearthquakes at St. Augustine Volcano, Alaska, Triggered by earth tides, Science, 182, no. 4110, 386-389.

McCann, W.R., and M. Kimura (1978). Unpublished manuscript.

McCann, W.R., S.P. Nishenko, L.R. Sykes, and J. Krause (1978). Seismic gaps and plate tectonics: Seismic potential for major plate boundaries, Manuscript submitted for publication.

McCann, W.R., O.J. Perez, and L.R. Sykes (1979). Yakataga seismic gap, southern Alaska: Seismic history and earthquake potential, submitted to Science.

Minikami, T. (1960). Fundamental research for predicting volcanic eruptions (Part I), Earthquakes and crustal deformations originating from volcanic activities, Bulletin of the Earthquake Research Institute, 38, 497-544.

Miyabe, N. (1933). Block movements of the Earth's crust in the Kwanto district, Bull. Earthq. Res. Inst., 11.

Mogi, K. (1969). Some features of recent seismic activity in and near Japan, 2, Activity before and after great earthquakes, Bull. Earthquake Res., Inst. Tokyo University, 47, 395-417.

Munk, W.H., and D.E. Cartwright (1966). Tidal spectroscopy and prediction, Phil Trans. R. Soc. Lond., A-259, 533-581.

Nakamura, K., K.H. Jacob, and J.N. Davies (1977). Volcanoes as possible indicators of tectonic stress orientation - Aleutians and Alaska, In: Stress in the Earth, Max Wyss (ed.), PAGEOPH, 115, 87-112.

Page, R.A., D.M. Boore, W.B. Joyner, and H.W. Coultner (1972). Ground motion values for use in the seismic design of the Trans-Alaska Pipeline System, United States Geological Survey Circular No. 672.

Perez, O., and K.H. Jacob (1979). Fault plane solutions of earthquakes in the eastern Gulf of Alaska: Implications for tectonic models and seismic hazards, To be submitted to Journ. Geophys. Res.

Petroff, I. (1880). Alaska: Its population, industries, and resources, In: Report on the Population, Industries, and Resources of Alaska, 10th U.S. Census, v. 8, 87-96.

Plafker, G., and M. Rubin (1978). Uplift history and earthquake recurrence as deduced from marine terraces on Middleton Island, Alaska, preprint, paper presented at the Conference on seismic gaps and earthquake recurrence, May 25-27, 1978.

Richter, C.F. (1958). Elementary Seismology, W.H. Freeman and Company, San Francisco.

Scholz, C.H. (1972). Crustal movements in tectonic areas, Tectonophysics, 14, 201-217.

Scholz, C.H. (1974). Postearthquake dilatancy recovery, Geology, 2, 551-554.

Scholz, C.H., and T. Kato (1978). The behavior of a convergent plate boundary: Crust deformation in the South Kanto District, Japan, Jour. Geophys. Res., 83 (B2), 783-797.

Shima, M. (1958). On the second volcanic micro-tremor at volcano Aso, Bull. Disaster Prevent Inst., Kyoto University, 22, 1-6.

Smith, R.L., and C.E. Soule (1973). Western Alaska and Bering Sea Islands: Alaska Peninsula and the Aleutian Islands and Range, In: Data Sheets of the Post-Miocene volcanoes of the world with index maps (IAVCEI, Rome, 1973).

Stauder, W. (1968). Tensional character of earthquake foci beneath the Aleutian trench with relation to sea-floor spreading, Jour. Geophys. Res., 73 (24).

Steinberg, G.S. (1965). Genesis of volcanic tremors and the long-range forecasting of eruptions, Dokl. Akad. Nauk, 165, 1294-1297.

Sykes, L.R. (1971). Aftershock zones of great earthquakes, seismicity gaps, earthquake prediction for Alaska and the Aleutians, Jour. Geophys. Res., 76, 36, 8021-8041.

Tsuboi, C. (1933). Investigation on the deformation of the Earth's crust by precise geodetic means, Jap. J. astr. Geophys., 10, 98-248.

Umino, N., A. Hasagawa, and A. Tokagi (1976). Fine structure of deep seismic zone uncer N.E. Japan, abstract, Fall Annual Meeting, Seismo. Soc. Japan, 112, 1976.

Utsu, T. (1971). Aftershocks and earthquake statistics (III) - Analysis of the distribution of earthquakes in magnitude, time, and space with special consideration to clustering characteristics of earthquake occurrence (I) - Journal of the Faculty of Science, Hokkaido University, Ser. VII, Geophysics, vol. III, no. 5, 379-441.

Yamasaki, N. (1928). Report on the precise levellings in the Mezoseismal area of the Tango earthquake, Proc. Imp. Acad. Japan, 4, 60.

Yoshii, T. (1975). Proposal of the "Aseismic Front", Zishin, 20, 365-367.

XI.B. ORAL PRESENTATIONS

SEISMIC GAPS AND PLATE TECTONICS: SEISMIC POTENTIAL FOR MAJOR PLATE BOUNDARIES

W. R. McCann
S. P. Nishenko
L. R. Sykes
J. Krause (all at: Lamont-Doherty Geological Observatory and Department of Geological Sciences of Columbia University, Palisades, New York 10964)

The theory of plate tectonics provides a framework for evaluating the potential for future great earthquakes along major plate boundaries. The identification of specific tectonic regimes, as defined by dip of the inclined seismic zone, the presence or absence of aseismic ridges and seamounts on the downgoing slab, the age contrast between the overthrust and underthrust plates, and the presence or absence of back-arc spreading, have led to a refinement in the application of plate tectonic theory to the evaluation of seismic potential.

The term seismic gap refers to any region along an active plate boundary that has not experienced a large thrust or strike-slip earthquake for more than 30 years. A region of high seismic potential is a gap that, for historic or tectonic reasons, is considered likely to produce a large shock during the next few decades. The seismic gap technique provides estimates of the location, size of future events and origin time to within a few tens of years at best; these should not be considered to be predictions in which a precise estimate of time of occurrence is specified.

A map is presented showing the seismic potential of the major plate boundaries in and around the margins of the Pacific. Six categories that represent the range from high to low seismic potential for the next few decades are indicated on the map. Three categories define a time-dependent potential based on the amount of time elapsed since the last large earthquake. The other categories are used for areas that have ambiguous seismic histories, their potential is inferred from various tectonic criteria.

1. 033692McCANN
2. 1978 Fall Meeting (AGU)
3. Seismology
4. Premonitory Seismicity and Seismic Gaps
5. No
6. No to poster presentation only. Must be done in both talk and poster presentation format.
7. 50%
8. Bill to: (Mrs. Alma Kesner) Purchasing Department, Lamont-Doherty Geological Observatory Palisades, New York 10964

A MULTI-DISCIPLINE STUDY OF THE TECTONICS AND HAZARDS IN THE SHUMAGIN ISLANDS SEISMIC GAP, ALASKA

K.H. Jacob
J. Beavan
J.N. Davies (all at: Lamont-Doherty Geological Observatory of Columbia University, Palisades, New York 10964)
L. House (Lamont-Doherty Geological Observatory of Columbia University and Dept. of Geological Sciences, Palisades, New York 10964)

Results from a multi-discipline long-term study of the tectonics and seismic hazards in this seismic gap of the Aleutian arc are summarized: (1) Data from a telemetered seismic network accurately define the dipping seismic zone to depths of at least 150 km. Seismicity is of low level at present, but is sufficient to delineate the probable fault geometry of a future great shallow earthquake. (2) Few strong-motion and several broad-band records from some 20 regional events (m_b = 3.8 to 6.0) were collected since 1971 and are used together with a scaling assumption to estimate the ground motions for the maximum credible event in this gap. (3) Precision leveling for a six-year period indicates on Unga Island a secular, pre-seismic tilt rate of 1 microradian/year with downward motion towards the trench. At other sites tilts only within the observational errors were measured. Data from new sea-level meters cover too short a period to be conclusive but are not inconsistent with the geodetically measured tilt rates. (4) Other results include identification of uplifted and tilted marine terraces and of high ambient stress levels from seismic source studies. Volcanic activity is monitored seismically at several volcanoes. At least 3 eruptions of Pavlof volcano since 1975 could be confirmed.

These different kinds of long-term data indicate a "pre-seismic" stage of the region containing the gap. No anomalies which might indicate a great earthquake in the immediate future are apparent.

1. 021138JACOB
2. 1978 Fall Annual Meeting (AG
3. Seismology
4. Premonitory Seismicity and Seismic Gaps
5. No
6. No
7. 10%, AGU 77.
8. Alma Kesner
   Purchasing Department
   Lamont-Doherty Geological Observatory
   Palisades, New York 10964
9. None

INVESTIGATION OF TWO HIGH STRESS-DROP EARTHQUAKES IN THE SHUMAGIN SEISMIC GAP, ALASKA

L. House
J. Boatwright (both at: Lamont-Doherty Geological Observatory and Dept. of Geolog. Sci., Columbia University, Palisades, N.Y. 10964)

Two moderate size (m_b=5.8, 6.0) earthquakes occurred within a local network of short-period seismograph stations in the Shumagin Islands, Alaska, on April 6, 1974. They were followed by 69 aftershocks recorded over the next two weeks. Both mainshocks triggered a strong-motion accelerograph (SMA) at Sand Point, 50 km NNW of their epicenters.

High quality locations obtained from local network arrivals for the mainshocks and 29 aftershocks plot at depths between 35km and 45km and define a plane dipping about 30° to the NW. A nearly pure-thrust focal mechanism for the larger (m_b=6.0) earthquake was obtained from long-period data. The fault plane dips 30° in the direction N 16°W. This sequence was located along the dipping seismic zone beneath the Aleutians and was presumably related to underthrusting of the Pacific plate beneath North America.

Analysis of the SMA data by modelling of the energy flux (Richards and Boatwright, 1977) yields the following estimates of source parameters for the m_b=5.8 and 6.0 earthquakes, respectively: moment, M_o=3.6 x 10^{24} dyne-cm, and 6.6 x 10^{24} dyne-cm; stress drop, 650 bars and 540 bars. A high frequency spectral fall-off of ω^{-3} suggests that the ruptures stopped gradually.

The Shumagin Islands region is believed to have a high potential for a future large earthquake (Kelleher, 1970; Sykes, 1971; Kelleher, et al., 1973). The location of this earthquake sequence at the deepest part of the rupture zone of the 1938 earthquake (M_S=8.7) (major earthquake ruptures often initiate at depth and propagate up dip) and the high stress-drops of the shocks in 1974 may indicate considerable accumulation of stress prior to a major earthquake in the Shumagin Islands region.

1. 026666 HOUSE
2. 1978 Fall Meeting (AGU)
3. Seismology
4. Premonitory Seismicity and Seismic Gaps
5. No
6. No
7. 0
8. Alma Kesner
   Lamont-Doherty Geological Observatory
   Palisades, New York 10964

EVIDENCE FOR QUATERNARY UPLIFTED TERRACES AND TILTING IN A SEISMIC GAP: THE SHUMAGIN ISLANDS, SOUTHWEST ALASKA

M. A. Winslow
S. H. Hickman (both at: Lamont-Doherty Geological Observatory of Columbia University, Palisades, New York 10964)

During reconnaissance surveys in the Shumagin Islands and the adjacent Alaska Peninsula, a region identified as a seismic gap, uplifted marine and river terraces of regional significance were found. Isobase surveys on the peninsula and Nagai, Korovin, Unga, Dolgoi, Popov, and Simeonof islands revealed one to three Quaternary terraces per island, with elevations that vary from a few to 170 m among islands. There is a suggestion of higher terrace levels and additional terraces away from the trench, with a gentle trench-ward tilt on the lowest terrace. (The study area does not include the Pavlov volcano which intrusive component has resulted in significant uplift in the surrounding region). Evidence for Holocene faulting was seen on Korovin, Unga, and Nagai islands. Faults of yet unknown displacement histories generally have steep east- or southeast-facing scarps striking at high angles to the trench. Correlation of the most recent terrace development following systematic mapping with the results from ongoing seismicity and tilt studies depend on the availability of absolute dates for the terraces. If these can be obtained, they will help to quantitatively assess the long term tectonic activity and seismic hazards in this present seismic gap.

1. 047656 HICKMAN
2. 1978 Fall Annu Meeting (AGU)
3. Seismology
4. Premonitory Seismicity and Seismic Gaps
5. No
6. Yes, acceptabl
7. 0%

XI.C. NOTE ON THE 28 FEBRUARY 1979 ST. ELIAS EARTHQUAKE, EASTERN GULF OF ALASKA

A large earthquake (M_S = 7.7) occurred on February 28, 1979 in the Chugach-St. Elias mountains in the eastern Gulf of Alaska. This earthquake filled only a portion of a formerly identified seismic gap (Sykes, 1971) to which a high seismic potential had been assigned (McCann et al., 1978). This earthquake is important in two aspects: (1) the earthquake occurred within an identified seismic gap and thus confirms the strength of the seismic gap hypothesis to forecast successfully the approximate location of large earthquakes along major plate boundaries and within a certain time frame. (2) The earthquake was not that large, however, to fill the entire gap. Thus, one or two large or even great earthquakes are still required, possibly in the not too distant future, to "fill in" this seismic gap. A paper by McCann et al. (1979) is in preparation which describes some of the teleseismically observable space-time patterns of seismicity for the region of this remaining 'Yakataga seismic gap'. These patterns are consistent with the notion that a gap exists, with a ring of recent seismicity surrounding that region that is expected to rupture in the future.

Just prior to the February 28 St. Elias earthquake a study was completed of all earthquakes in the eastern Gulf of Alaska for which teleseismic data yielded reliable fault-plane solutions (Perez and Jacob, 1979 in prep.). Figure 40 shows the lower hemisphere projections of the solutions obtained. Preliminary data for the St. Elias earthquake indicate a solution almost identical to that of solution 8 and 9 of Figure 40. This implies shallow angle thrusting on a very shallow northeasterly dipping fault; the slip vector strikes N18°W which is in almost perfect agreement with the local slip vector for the relative motion of the Pacific with respect to the North American plate as derived from inversion of global plate motion data. The study by Perez and Jacob (1979) also concludes that the off-shore Tertiary province, the Yakutat wedge (YW), south of Yakutat Bay (YB in Figure 40) overthrusts the Pacific plate in a southwesterly direction along a fault that outcrops along the northwesterly striking base of the shelf edge. This motion is represented by fault plane solutions 5, 6, 7 and 12 (Figure 40). Since this motion is at a high angle to the regional slip vector which represents motion of the Pacific plate versus the North American plate (at a rate of about 5.5 cm/yr) it may occur only at a small rate amounting to about 1 cm/yr. Hence, in addition to earthquakes filling the Yakataga gap, there is a small but finite probability for a future large, shallow thrust earthquake to occur directly beneath the Yakutat-wedge portion of the off-shore Tertiary province.

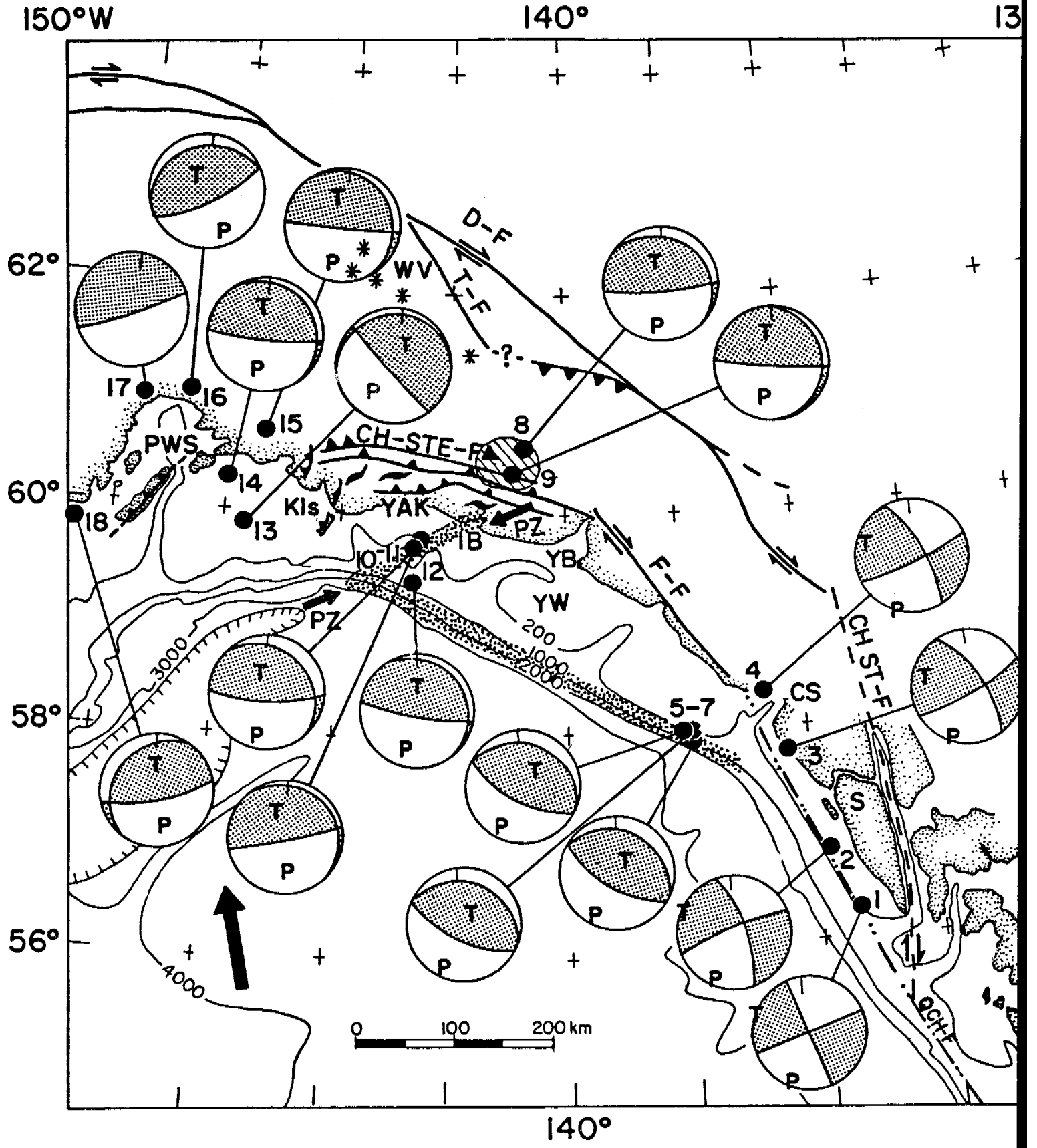

Figure 40 . Fault plane solutions (lower hemisphere projections) for earthquakes in the eastern Gulf of Alaska. Shaded areas are quadrants with P-wave compressions at receiving stations. T and P represent the inferred axes of deviatoric maximum tension and pressure, respectively. The triangle and the diagonally hatched area indicate the epicenter and approximate after shock zone of the St. Elias earthquake (M_S = 7.7) of February 28, 1979. Except for the strike slip solutions (#1 through 4) always the shallow dipping nodal plane is assumed to represent the plane of faulting.

XI.D. SUMMARY OF OPERATIONS AT DUTCH HARBOR

Dutch Harbor Recording System. In November, 1978 the Dutch Harbor recording site was upgraded to include an event detecting system, with data recorded on two four-channel TEAC tape recorders. A TS-250 clock with IRIG B time code output was installed in place of the TS-100.

Figure 41 is a schematic diagram of the Dutch Harbor stations as of March, 1979. The frequency-modulated signals are mixed and recorded on a delay loop on the first tape recorder, as well as the IRIG B time code and a 4080-Hz reference tone. The event detectors (ED1-5) monitor the seismic signals from the discriminators for stations AKV and MKV, and the audio tones from the amplifiers for the three DUT instruments. The event detection is based on a comparison of a short term average (STA) and a long term average (LTA) of each signal. When the (STA-LTA) exceeds a selectable level, a signal is sent to the control unit. Whenever an event is detected, the contents of the tape loop are recorded on the second tape recorder with a delay of twenty seconds. The algorithm which determines whether an event is to be recorded is that the (STA-LTA) of the long-period or any 2 short-period seismometers exceed a specified value. The intervals of data recorded before and after the event can be selected, and are set at 20 seconds of pre-event memory and 60 seconds of post-event memory at present. The loops and reels of tape are changed weekly and shipped to Lamont, where the tapes are played back on existing facilities. At the end of each recorded event, a DC offset is put on both helicorders.

Data Analysis. For the period July through November, 1978 the outputs from the short-period and long-period vertical seismometers were being recorded on the long-period helicorder. The short-period helicorder has been recording the output of the short-period horizontal seismometer at Dutch Harbor since July 1978. Beginning in March, 1979 the telemetered signals from SKV and MKV have alternated with DUT-SPH in being recorded on the short-period helicorder.

For the months July through September the data set is complete, and consists of two helicorder paper records per day: the short-period horizontal (SPH) on one record, and the long-period and short-period verticals (LPZ and SPZ) on the other. The data set for October is incomplete, as we were without a station operator for part of the time. In mid-November tape coverage of the data began, but there were problems with the system, and the data set is not complete. Due to failures of the equipment at Lamont, all of the tapes have not been played back as yet, so a complete assessment of the seismicity recorded by the Dutch Harbor system is not possible at this time. For the data recorded by the DUT seismometers during July, August, and September it is only possible to establish radii to epicenters, and not to obtain locations, because stations AKV and MKV, which would provide some azimuthal control, were not being recorded. The quality of all the records is poor because the station is presently located in the Reeve terminal at the airstrip, and there is interference from radio transmissions and airplane noise. The "pickable" local events recorded by the DUT short-period instruments for the months July through September include 8 events with (S-P) times of less than 25 seconds, and lie within radii up to $\sim$ 80 km (assuming surface focus) and 3 events with (S-P) times of 25 to 75 seconds, lying within radii up to $\sim$ 590 km.

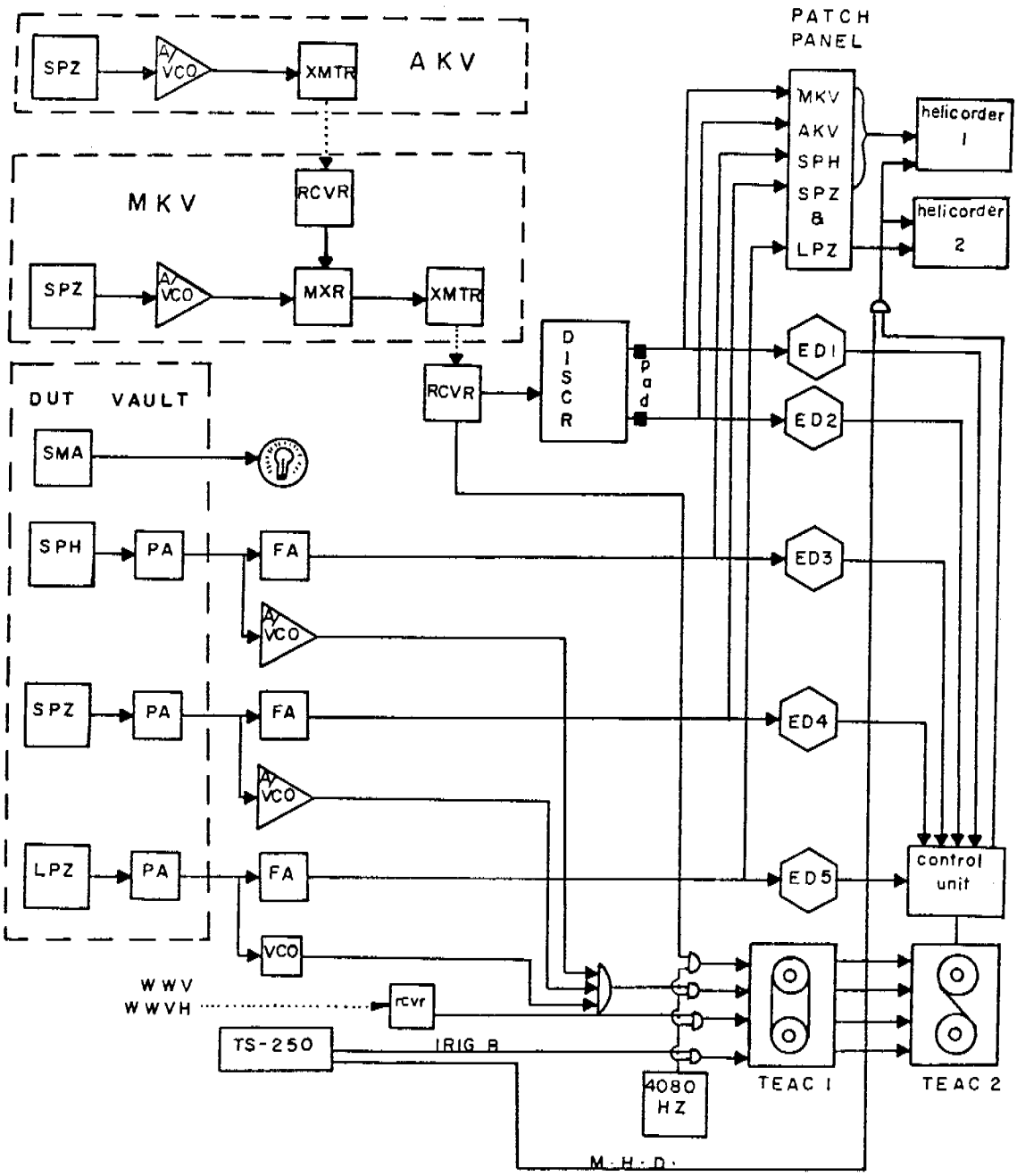

Figure 41. This diagram shows schematically the recording system at Dutch Harbor. This configuration is current as of March, 1979, when the station was most recently visited. The signal from AKV (Akutan Volcano) is telemetered to MKV (Makushin Valley) where it is mixed with the MKV signal and telemetered to DUT (Dutch Harbor). There the mixed signal is fed into a discriminator, the output of which is fed into two event detectors (ED1 and ED2). Voltage dividers ("pad") at the outputs of the discriminator provide an additional 31.5 db attenuation to bring the signal levels from AKV and MKV within the half-volt limit detectable by the event detectors. The outputs from the short-period horizontal (SPH), short-period vertical (SPZ) and long-period vertical seismometers are fed into pre-amplifiers (PA) in the vault at Dutch Harbor. Inside the recording room each signal is fed into a filter amplifier (FA) and an amplifier and/or voltage-controlled oscillator (A/VCO or VCO). The outputs of the filter amplifiers go to ED 3-5. The signals from the VCO's go to the continuous-loop tape recorder (TEAC 1), along with a 4080-Hz reference tone, IRIG B time code from the TS-250 clock, and (optionally) the WV time signal. When the (STA-LTA) of any two of ED 1-4 or ED 5 exceeds a certain pre-determined value, the control unit causes the reel-to-reel tape recorder (TEAC 2) to begin recording the data from TEAC 1 which is, by that time, 20 seconds old. At present, the time intervals during which data are recorded are set at 20 seconds before and 60 seconds after the event. After the event (when the (STA-LTA) falls below a specified value), an offset is put onto the two helicorders. When the strong motion accelerometer (SMA) in the vault is triggered, a light goes on in the recording room. The TS-250 clock puts out an IRIG B time code as well as minutes, hours, and days (M.H.D.) in binary-coded decimal.

Contract No. - 01-5-022-2313
Research Unit No. - RU105
Reporting Period - 1 April 1978-
31 March 1979
Number of Pages - 22

ANNUAL REPORT

DELINEATION AND ENGINEERING CHARACTERISTICS OF PERMAFROST BENEATH THE BEAUFORT SEA

Principal Investigators:

P.V. Sellmann
E. Chamberlain

Associate Investigators

S. Arcone
S. Blouin
A. Delaney
K.G. Neave

1 April 1979

UNITED STATES ARMY
CORPS OF ENGINEERS
COLD REGIONS RESEARCH AND ENGINEERING LABORATORY
HANOVER, NEW HAMPSHIRE, U.S.A.

I. Summary

The objective of CRREL's subsea permafrost program is to obtain information on the distribution and properties of permafrost beneath the Beaufort Sea. We are currently acquiring information on the distribution of ice-bonded permafrost from analysis of the velocity structure of commercial seismic records. This report summarizes the results of all studies to date, including engineering property analysis and preliminary interpretation of seismic data. Emphasis is placed on results that are relevant to offshore development of this region. Discussion of the CRREL drilling and laboratory program represents the most current interpretation of these data.

After the 1976 field season we concluded that the fine-grained sediments were overconsolidated only at one of the three drill sites occupied. However, after analysis of the 1977 field engineering property data and further analysis of the 1976 data, we have concluded that overconsolidated sediments occur in the upper fine-grained section at all the drill sites occupied (Fig. 1a). The densest, most uniform, most highly overconsolidated clays occur seaward of Reindeer Island at site PB-2.

Seasonal freezing of the bed sediments is common for the range of water depths investigated. The strength of these frozen sediments is greatest in shallow water (<2 m). In deeper water only partial freezing of the interstitial water is suggested by the penetrometer observations, which may not significantly increase the strength of the sediments. Therefore the properties of the surface fine-grained section, which ranged from 3 to 10 m in thickness at the sites investigated, can vary greatly as a result of overconsolidation and seasonal freezing. In general they vary from soft, weak sediments in the center of Prudhoe Bay to stiff, highly overconsolidated sediments north of Reindeer Island. Seasonally, well-bonded sediments occurred along the shore and in shoal areas.

The depth to ice-bonded permafrost is also extremely variable, since ice-bonded permafrost can occur within 30 m of the seabed as far as 17 km from the mainland. These sediments could contain excess ground ice since ice was reported in the log of the Humble Reindeer Island Hole.

Preliminary interpretation of seismic records based on eight near-shore lines also indicates extensive distribution of ice-bonded permafrost. This near-shore data indicates that a high velocity band parallels the coast and probably represents bonded permafrost. The data analyzed provide information from Prudhoe Bay to approximately 55 km to the east. Information on the offshore extent of this high velocity zone is limited by the length of the near-shore seismic lines, some of which extent only 15 km offshore. However, preliminary examination of four marine seismic lines from farther offshore (> 15 m water depth) indicates velocities of less than 2.0 km/s, values not normally associated with ice-bonded sediment.

The variability of the offshore permafrost, and uncertainties concerning some of its critical properties, such as ice volume, will require future development activities to be accompanied by detailed site-specific investigations. This is particularly true since there has been little experience with a thermal and physical setting such as this.

II. Introduction

The first two years of the CRREL subsea permafrost program centered on detailed investigation of the properties and distribution of permafrost beneath the Beaufort Sea in the Prudhoe Bay area of Alaska. This was based on a joint effort with the USGS, the University of Alaska and Robert Lewellen. Data were acquired from two seasons of drilling, sampling and penetrometer investigations. This year's efforts provided a transition from the field studies and permitted the completion of all laboratory studies on engineering properties and preparation of results for technical reports and presentations.

In addition, the emphasis of this program has been shifted to the study of commercial seismic records to obtain more regional information on permafrost distribution. Reprocessed upper portions of seismic records have been acquired for the lines shown in Fig. 1b. They are currently being interpreted by K.G. Neave, who participated in the analysis of the industry seismic data from the Canadian Beaufort Sea studied by the Geological Survey of Canada.

Efforts have also been made during the year to acquire samples from the current USGS Conservation Division program for additional chemical and engineering properties analysis.

III. Current State of Knowledge

To date, information on subsea permafrost in the U.S. Beaufort Sea is still extremely limited. The available information is primarily based on observations acquired as part of the OCSEAP program, and other non-industry studies such as Lewellen's conducted near Barrow, Alaska. The results of the current USGS Conservation Division program should help to improve this situation.

The acquisition of the current data has helped to illustrate the complexity of this permafrost environment, and difficulties associated with generalizing about properties and distribution.

The most significant gaps in information include details on bonded permafrost properties such as ice content, strength and thaw settlement data. This type of data will obviously vary greatly, depending on local geology and the thermal and sea level history of a region. We also have little information on gas hydrates.

We now know the permafrost is very extensive and that bonded sediments can occur many kilometers from shore. This report provides summary

illustrations of the engineering property data from our studies as well as discussing the preliminary interpretation of some of the seismic data.

IV. Study Area

The locations of the drill and probe sites for the joint USGS-CRREL study conducted in the Prudhoe Bay area are shown in Fig. 1a. Details concerning these sites and the rationale for their selection have been discussed in previous OCSEAP literature. Their location is shown to provide a reference for discussion of new data and current conclusions.

A map is also provided to show the general location of seismic data being interpreted (Fig. 1b). Lines situated far offshore are from marine surveys, while the near-shore data were acquired over the sea ice. The upper two seconds of these records were purchased from Geophysical Service Incorporated.

V. Sources, Methods and Rationale of Data Collection

Sample handling and drilling techniques used in the earlier studies have been discussed in previous annual reports and in CRREL Special Reports 76-12 and 77-41.

Considerable discussion and preparation has taken place in order to obtain samples from the current USGS drilling program. Sample-storage containers have been shipped to Anchorage so that we can take the opportunity to subsample the new cores when they are released. This effort is being coordinated with Dave Hopkins of the USGS, Menlo Park, Calif.

Selection of seismic data has been to a great extent controlled by the location of available lines. Line selection was aimed at obtaining information from the shore to water depths as great as 90 m. The near-shore data provide the transition from land. Data were also selected from the immediate Prudhoe Bay area for comparison with information obtained as part of the OCSEAP studies. The upper two seconds of the records selected along the lines shown were reprocessed from the field tapes with increased gain. The resulting plots were then interpreted to determine variations in velocity with depth that might indicate high velocity layers that could be interpreted as bonded permafrost.

The high velocity first arrival data were interpreted by K.G. Neave using both reflection and refraction procedures in an attempt to determine which was appropriate. This was done because the receiver array is usually designed to favor the reflected signals and because refracted energy is expected to be less, relative to some reflections. Therefore in some cases the first arrivals may be reflected energy. The results of this dual approach suggest that the refraction interpretation provides a velocity structure that appears logical and can be correlated with limited control.

VI and VII. Results and Discussion

The results of all aspects of the drilling and sampling program have been covered in several reports. In addition to those mentioned in the previous annual report, several papers were prepared for journals, conference proceedings, and CRREL publication:

1. Engineering Properties of Subsea Permafrost in the Prudhoe Bay Region of the Beaufort Sea, E.J. Chamberlain et al. (1978). In: Proceedings of the Third International Conference on Permafrost, Vol. 1, p. 629-635.

2. Chemistry of Interstitial Water from the Subsea Permafrost, Prudhoe Bay, Alaska, I.K. Iskandar et al. (1978). In: Proceedings of the Third International Conference on Permafrost, Vol. 1, p. 93-98.

3. Geochemistry of Subsea Permafrost at Prudhoe Bay, Alaska, F.W. Page and I.K. Iskandar (1978). CRREL Special Report 78-14.

4. Determining Subsea Permafrost Characteristics with a Cone Penetrometer - Prudhoe Bay, Alaska, S.E. Blouin et al. (1979). Cold Regions Science and Technology (Elsevier Scientific Publishing Company), Vol. 1, No. 1.

5. Penetration Tests in Subsea Permafrost, Prudhoe Bay, Alaska, S.E. Blouin et al. (in press). CRREL Report.

6. Permafrost Beneath the Beaufort Sea Near Prudhoe Bay, Alaska, P.V. Sellmann and E.J. Chamberlain (1979). In: Proceedings of the Eleventh Offshore Technology Conference, Vol. 3.

The following discussion summarizes the results to date, including data from the interpretation of the commercially obtained seismic records. Copies of the reports mentioned above and those referenced last year are available upon request.

Emphasis will be placed on updating previously reported results, particularly information that may tend to change earlier conclusions or assumptions.

Seismic Data. Interpretation of the velocity structure of eight lines spaced along the coast from Prudhoe Bay to a point approximately 55 km to the east was completed. Four of the more offshore marine lines were also analyzed. Most of these lines are marked with a dot in Fig. 1b. Two of the near-shore lines are not shown but parallel the coastline between Prudhoe and the most eastern line. Most of the lines shown in Fig. 1b were only recently received and will be interpreted in the near future. Therefore, since only a small part of the data has been analyzed, comments concerning data interpretation must be considered preliminary. The transition from the land to the marine environment seen in the near-shore data is fortunate since it provides some control, allowing changes from high permafrost velocities on land to lower velocities offshore to be seen.

The surface velocities observed on land are approximately 4.0 km/s or greater. In the marine environment, adjacent to the land, a band of varying width consisting of two high velocity layers parallels the coastline. Near Prudhoe Bay this band is approximately 9 km wide and it appears to narrow in the two easternmost lines examined. The upper layer has velocities in the 2.5 km/s range and appears to be approximately 300 m thick. The lower layer has higher velocities, in the 3.1 to 4.5 km/s range. Seaward of this high velocity zone there is a single high velocity layer with velocities around 2.5 km/s. The seaward limit of this layer has not been established since it extends at least as far offshore as the survey lines, a minimum of approximately 16 km near Prudhoe Bay and 12 km at the easternmost line studied.

Farther offshore the refraction analysis of the limited amount of marine data available for analysis indicated that no velocities were greater than 2.0 km/s. The lines examined were all seaward of the 15-m water depth and in two cases extended beyond the 90-m water depth. The large quantity of marine data recently recieved may alter this observation. When all of these data have been examined, a contour map of the velocities will be constructed.

The possibility of the high velocity subsea material being bonded permafrost is great, particularly since bedrock or other materials with velocities as high as those observed do not appear to occur in this depth range.[1,2] The velocities can also be observed decreasing from the high land values to lower values progressively offshore in a region where no unique geology would be expected to be associated with this part of the coastline, except difference in permafrost properties. The low velocities (less than 2.0 km/s) observed in the far offshore marine data are more typical of those expected for unbonded sediments.

Material Properties. A summary of the index properties and hole lithology is given in Fig. 2-8. The properties of the fine-grained sediments are quite variable, both with depth and from site to site.

At site PB-1, which is located near the middle of Prudhoe Bay along line 1 (see Fig. 1a), soft organic silts dominate the 4.5-m-thick fine-grained section. In the upper three-quarters of this section, water content (Fig. 2) exceeds or nearly exceeds the liquid limits (41 to 43%). Near the boundary between the fine-grained sediments and the underlying sands and gravels, the water content falls markedly to below 20% in non-plastic silty sediments.

At site PB-5, which is also along line 1 but seaward of the shoal separating Prudhoe Bay from the Beaufort Sea, the water content (Fig. 5) ranges from 24 to 37%, also exceeding the liquid limits. Thicker (7.1 m) non-plastic inorganic sands and silts dominate this site.

At site PB-6, the drill site nearest the shore along line 2, the water content is below 20% in principally non-plastic interbedded sands and silts 3 m thick (Fig. 6). Further seaward along this line at site PB-7 in thicker (4.5 m) but similar sediments, water content ranges from 26 to 38%, with one value as low as 9% just above the sands and gravels (Fig. 7).

Continuing further seaward along line 2 to site PB-3, which was located approximately midway between the shore and Reindeer Island, the fine-grained sediments are dominated by silts of low plasticity. These sediments are approximately 5 m thick. Water content (Fig. 4) ranges from 20 to 42%, increasing with depth. In the shallow part of these silts the water content is near the plastic limit, but it increases steadily to the liquid limit with increasing depth.

Just shoreward of Reindeer Island at site PB-8 the fine-grained section is 12 m thick and is dominated by the clay sizes. Water content (Fig. 8) ranges from 20% in the upper half of this section to 40% in the lower half. In the upper half the water content falls near the plastic limit. In the lower half it ranges between the liquid and plastic limits.

The most uniform fine-grained section was observed at site PB-2, which is located seaward of Reindeer Island. The sediments are approximately 7.5 m thick, with water content ranging between 20 and 22% (Fig. 3). In all cases the water content was at or below the plastic limit.

The implication of the relationship between the misture content and Atterberg limit data is that much of the fine-grained marine sediments are overconsolidated, and those at PB-2 and certainly some of those at site PB-8 are highly overconsolidated.

Strength Tests. The strength determinations discussed in this section are for the fine-grained sections from which good "undisturbed" cores could be obtained.

The shear strength profile for site PB-1 is shown in Fig. 2. These sediments are soft and weak to a depth of 2.5 m below seabed, with a maximum shear strength of 45 kPa. At 4.1 m the shear strength increases to 135 kPa near the transition between the shallow silt and clay and the deeper sands and gravels.

Just seaward of the shoal that separates Prudhoe Bay from the Beaufort Sea at site PB-5, the maximum shear strength ranged between 35 and 63 kPa to a depth of 7.1 m below the seabed (Fig. 5). Non-plastic inorganic sands and silts dominated this site.

The five sites along line 2 (Fig. 1a) provide considerable information on the variability of the sediments in this region. For the two sites nearest shore (PB-6 and PB-7) only one sample from a silty sand layer 1.4 m below the seabed was tested. The shear strength S_u of this material was 76 kPa, which is probably representative of the unfrozen sandy sediments found in this region.

Further seaward, at PB-3, the shear strength ranges from 25 to 120 kPa (Fig. 4), the weaker samples coming from the high moisture content sediments in the lower portion of the fine-grained section. Just shoreward of Reindeer Island at PB-8, S_u ranges from 25 to 100 kPa, with considerable variation occurring over the entire 12-m-thick section (Fig. 8).

At the most seaward site, PB-2, considerably higher S_u values were observed (Fig. 3). Shear strength values ranged from 85 kPa at shallow depths to more than 260 kPa 8 m below the seabed.

Consolidation Properties. The high shear strengths of the fine-grained sediments that constitute the upper part of the sections indicate that these sediments are overconsolidated, which, of course, supports the earlier observations made from the Atterberg limit, water content, and consolidation test results. But the magnitudes of the overconsolidation pressures are uncertain in many cases because of difficulties in interpreting the consolidation test results.

Following the suggestions of Berre[3] we used a modified version of Skempton's[4] relationship between the ratio S_u/p_c and the plasticity index I_p to estimate p_c from the strength data.

There is generally good agreement with one exception between these p_c values and those obtained from the consolidation tests at PB-2 (Fig. 3). However at the other site (PB-8) where there are sufficient data to make this comparison (Fig. 8) the estimated values are considerably less.

Berre[3] believes that S_u for overconsolidated clays is influenced less by disturbance during sampling than the p_c values obtained from the consolidation test, and therefore that his method is preferable for obtaining p_c. For the purpose of our discussion, we have assumed that he is correct.

We have established, then, that most of the fine-grained sediments studied are overconsolidated. The degree of overconsolidation and the magnitude of the preconsolidation pressures, however, are quite variable. Preconsolidation pressures estimated from the strength data range from a low of 90 kPa at site PB-3 to a high of 1850 kPa at PB-2. Overconsolidation ratios vary from 2.2 at PB-8 to 1090 at PB-5.

The preconsolidation pressures are nearly constant with depth at PB-2 and PB-5, the average values being much greater at PB-2 (1635 kPa versus 475 kPa), and the preconsolidation pressure increases with depth at PB-1 (300 to 1800 kPa) and decreases with depth at PB-3 (1000 to 90 kPa) and PB-8 (1000 to 100 kPa).

The range and variability of p_c and p_c/p_o' from site to site and at different depths are difficult to explain. In an earlier paper[5] we dismissed the traditional overconsolidation mechanisms such as: 1) accumulation and subsequent erosion of overburden, 2) desiccation, and 3) glaciation. We also rejected the possibility that the forces of drifting ice caused the overconsolidation, and came to the conclusion that freezing and thawing was most likely the mechanism. We supported this theory with laboratory freeze-thaw consolidation test results.

At that time we had p_c data for site PB-2 only and assumed that the other two sites (PB-1 and PB-3) were normally consolidated. We also had concluded that the sediments at PB-2 were no more than 10,000 years old, and thus had always been submerged and had frozen and thawed during the passage of the transient barrier island, Reindeer Island. More recent

dating of these sediments[6] suggests that their age is much greater than 10,000 years and that they may have been exposed to freezing temperatures during a period of low sea level that followed their deposition.[7]

We believe, now, that the overconsolidation is the result of complex geological, chemical and thermal processes. As we are uncertain in most cases precisely what happened, we will defer speculating on the processes other than to say that: 1) Brown and Rashid[8] suggest that changes in chemistry can cause a low degree of overconsolidation, and 2) it appears that a few meters of sediments have been eroded locally,[9] which could also have caused a low degree of overconsolidation. It is also probable that Reindeer Island passed over site PB-2 and that it induced freezing as it is doing today.[10,11] And the large differences between the overconsolidation pressures and ratios at sites PB-2 and PB-8 are probably due to the more recent freezing and thawing of sediments at PB-2.

The highly overconsolidated clays play an important role in the degradation of ice-bonded permafrost in this region of the Beaufort Sea. According to Hopkins,[9] wherever the highly overconsolidated silt or clay is preserved on the sea bottom, ice-bonded permafrost lies close to the sea floor, the dense sediments inhibiting the infiltration of more saline waters into the deeper sands and gravels.

Penetrometer Observations. In general, penetration resistance values were low in the upper few meters and approached refusal (40 MPa) at depths between 10 and 14 m below the seabed. The spread between maximum and minimum penetration values was narrow in the upper 4 m, compared with the wider range of values observed in the material below. However, in shallow water, where seasonally frozen sediments were encountered, very high penetration resistance was observed. We found that variations in the resistance data could be readily correlated with geologic features and the occurrence of frozen material. Extremely high penetration resistance in coarse-grained sediments caused termination of probing at all sites.

Blouin et al.[12] give a detailed discussion of all penetrometer records. A summary of these data obtained along line 1 is shown in Fig. 9.

Unique penetration characteristics were identified with sediment types and frozen sediment by comparing penetration resistance curves with drill hole logs and temperature profiles. Subtle variations in grain size as well as depositional patterns and frozen zones were apparent.

The resulting correlations allowed us to establish stratigraphic cross sections along each of the study lines. These sections show the distribution of sediments and zones where they may be frozen.

For instance, the stratigraphic section along line 1 (Fig. 10) shows a distinct difference between the sediments seaward and shoreward of the shoal separating Prudhoe Bay from the Beaufort Sea. A weak fine-grained section occurs from the surface down to stronger coarser-grained sediments at PH-6, PH-7 and PH-8. A similar section occurs under the shoal at PH-5 and PH-9, but is capped with sandy sediment. Seaward of the shoal the surface sand and silt unit increases in thickness and caps a weaker fine clayey silt section.

Furthermore, from the penetration resistance and temperature profiles, we determined that the shallow sediments in the shoal region (PH-4, PH-5 and PH-9) were seasonally frozen. Similarly, the sediments near the bottom of PH-5 were found to be frozen (possibly perennially frozen).

A discussion of the stratigraphic sections along the other study lines can be found in Blouin et al.[12]

Temperature Profiles. Temperature profiles were obtained at 18 of the 27 probe sites. Subsea sediment temperatures were below $0^{o}C$ at all sites.

The temperature profiles obtained with the penetrometer differ considerably from site to site. In areas where the sea ice was near or in contact with the seabed (water depth less than 2 m) the temperature at the seabed ranged from -2.2 to $-11.4^{o}C$, with the temperatures apparently being controlled by the length of time the sea ice was in contact with the bed.

In water depths greater than 2 m, where sea water circulation was possible beneath the ice, the variation was much less, -1.7 to $-2.3^{o}C$. In the center of Prudhoe Bay (PH-6), which is apparently a closed basin because of the sea ice freezing to the shoal separating it from the Beaufort Sea, the seabed temperature was $-3.4^{o}C$ in 2.93 m of water. Extremely cold saline brines approaching 60 ppt were also observed in this region, indicating that little or no circulation occurs to flush the salts excluded during the freezing of the sea ice.

The highest temperature measured at the bottom of a probe hole was $-0.8^{o}C$, which was at PH-2 approximately 6 m below the seabed. This site was located in an open marine environment along line 1 with a water depth of 3.2 m.

The lowest temperature measured at depth in a probe hole was $-3.4^{o}C$ 12.7 m below the seabed at PH-27, which is on line 3 off the Sagavanirktok River delta in 1.89 m of water. Profiles along all the study lines are provided in Blouin et al.[12]

The temperature profiles in the deeper drill holes also differed considerably, depending on depth and site location. The temperatures at the bottom of the drill holes ranged from -1.7 to $-2.5^{o}C$. The lowest bottom hole temperature was obtained almost a kilometer from shore at site PB-6, 28 m below the seabed.[13,14]

The sediment temperatures at all the probe and drill sites increase with depth to depths ranging from 4 to 10 m, and then, with the exception of PH-5 and PH-9, decrease with depth, indicating that perennially frozen sediments occur at all sites. The temperature profiles at PH-5 and PH-9 do not show this trend, simply because the probe did not reach beyond the depth of seasonal cooling.

The relative accuracy of the thermal data is best demonstrated by comparing the probe results with those taken in the drill holes. In Fig. 11 the probe temperature profiles are superimposed on the drill hole profiles.

Fig. 11 shows that there is good agreement between the probe and drill hole data. The small differences can be attributed to thermal disturbances induced during the drilling activity, to seasonal cooling, and to local

temperature variations. (The probe observations were not made at precisely the same locations as the drill hole observations.)

Chemistry. Another means of establishing he position of seasonally and perennially frozen sediments was through comparison of pore water freezing point profiles calculated by Page and Iskandar[15] from the salinity data with the thermal profiles obtained from the drill holes. We show these profiles for all the drill holes in Fig. 12.

One can see that the temperature near the seabed is below the freezing point of the interstitial water in all cases, which indicates that the bed sediments are seasonally frozen. Although we did not observe ice during drilling, it is quite possible that ice and water are in equilibrium in these sediments, with little bonding of sediments occurring. The decrease in freezing temperatures below this zone, which is the result of increases in salinity, probably reflects brine exclusion from above during freezing.

The freezing point and temperature data also suggest that perennially frozen sediments occur near the bottoms of all the drill holes except PB-1 and PB-5. With the exception of PB-8 this observation agrees extremely well with observations made during the drilling program. At PB-8 it appears that we stopped short of perennially frozen sediments.

Depth to Perennially Frozen Sediments. Although perennially frozen sediments appear to occur at all of the sites investigated, the depths are extremely variable and currently unpredictable.

Fig. 13 shows a composite of data for the location of the top of ice-bonded permafrost along line 2. Our data and that of our colleagues at the U.S. Geological Survey and the University of Alaska are included in this figure.[7,10,11,16,17,18] Superimposed on these data is our estimate of the depth to perennially ice-bonded sediments. One can see that there is good agreement between the drill and probing estimates and those obtained by seismic means.

We attribute the difference between the seismic data and the probe and drill hole data principally to differences in alignment of the study lines (see Fig. 1a).

Several distinct regions occur along this profile:

1) The near-shore shallow water (< 1 m) region where perennially frozen sediments lie close to the seabed.
2) The region seaward to PB-3 where the depth to ice-bonded permafrost falls to 50 or 60 m,
3) The 140-m-deep depression between PB-3 and PB-8,
4) The very shallow perennially frozen sediments in the region of Reindeer Island,
5) The shallow rising ice-bonded permafrost table beyond Reindeer Island.

VIII. Conclusions

In the Prudhoe Bay region of the Beaufort Sea fine-grained sediments cover coarser dense sands and gravels interspersed occasionally with finer grained sediments. The thickness of the fine-grained section ranges from 3 to 10 m at the sites investigated. The properties of these materials vary greatly from soft, weak sediments in the center of Prudhoe Bay to stiff, highly overconsolidated sediments north of Reindeer Island.

All of the fine-grained sediments appear to be overconsolidated, but the degree of overconsolidation varies widely. The densest, most uniform and most highly overconsolidated clays occur seaward of Reindeer Island. We believe that freezing and thawing has probably caused the overconsolidation of these fine-grained sediments.

The sands and gravels appear to be a good source of borrow material and good materials for some types of foundations. Access to them, however, may be restricted in shallow water locations where the fine-grained sediments freeze seasonally and in the regions of dense overconsolidated clays.

Although we did not observe segregated ice during our study, the occurrence of ice-rich sediments cannot be discounted. Ice-rich sediments are extremely likely to occur in shallow coastal sites, particularly to the west of Prudhoe Bay in areas where rapid coastal retreat is occurring. Ice has been seen in the Humble C-1 Reindeer Island hole[11] and in the Canadian Beaufort Sea.[19]

Permafrost properties and distribution are extremely variable in the marine environment as they are on land, with greater potential for variability because of saline waters and complex thermal histories imposed by varying coastal processes. Of particular concern and interest is the rising ice-bonded permafrost table seaward of Reindeer Island because of the high potential for segregated ground ice at shallow depths far out on the continental shelf. The seismic data appears to confirm the extensive distribution of bonded permafrost along the coast with high velocity material occurring many kilometers offshore along lines studied from Prudhoe to 55 km to the east. The high velocity material extends offshore along the entire length of the nearshore lines, for example at least 12 km along the most eastern study line.

References

1. Reimnitz, E., Wolf, S.C., and Rodeick, C.A.: "Preliminary Interpretation of Seismic Profiles in the Prudhoe Bay Area, Beaufort Sea, Alaska. U.S. Geological Survey, Open-file Report 548 (1972).
2. Howitt, F.: "Permafrost Geology at Prudhoe Bay," World Petroleum, Sept. (1971).
3. Berre, T.: Marine Geotechnique (1978).
4. Skempton, A.W.: "Discussion on the Planning and Design of the New Hong Kong Airport," Proc. Inst. Civ. Eng. (1957) 7, 305-310.
5. Chamberlain, E.J., Sellmann, P.V., Blouin, S.E., Hopkins, D.M., and Lewellen, R.I.: "Engineering Properties of Subsea Permafrost in the Prudhoe Bay Region of the Beaufort Sea," In: Proceedings of the Third International Conference on Permafrost (1978), Vol. 1, 629-635.

6. Hopkins, D.M.: "Offshore Permafrost Studies and Shoreline History of Chukchi and Beaufort Seas as an Aid to Predicting Offshore Permafrost Conditions," Quarterly Report, October-December 1978, to National Oceanic and Atmospheric Administration, Outer Continental Shelf Environmental Assessment Project (1978).
7. Barnes, P.W. and Hopkins, D.M., eds.: "Geological Sciences," In: Environmental Assessment of the Alaskan Continental Shelf, Interim Synthesis; Beaufort/Chukchi," U.S. National Oceanic and Atmospheric Administration and U.S. Bureau of Land Management, Boulder, Colorado (1978), 101-133.
8. Brown, J.D. and Rashid, M.A.: "Geotechnical Properties of Nearshore Sediments of Canso Strait, Nova Scotia," Can. Geotech. J. (1974) 12, 44-57.
9. Hopkins, D.M.: "Offshore Permafrost Studies, Beaufort Sea, Alaska," Quarterly Report, April-September 1978, to National Oceanic and Atmospheric Administration, Outer Continental Shelf Environmental Assessment Project (1978).
10. Osterkamp, T.E. and Harrison, W.D.: "Subsea Permafrost Probing, Thermal Regime and Data Analysis," Quarterly Report, October-December 1978, to National Oceanic and Atmospheric Administration, Outer Continental Shelf Environmental Assessment Project (1978).
11. Humble C-1: "Reindeer Island, Drill Log of Reindeer Island Hole," Drilled by Younger Brothers Drilling Co., Humble Oil Production Department Files, Los Angeles, California (unpublished).
12. Blouin, S.E., Chamberlain, E.J., Sellmann, P.V., and Garfield, D.E.: "Determining Sub-sea Permafrost Characteristics with a Cone Penetrometer - Prudhoe Bay, Alaska," Cold Regions Science and Technology (1979) 1, No. 1.
13. Marshall, B.V.: Personal Communication (1978).
14. Lachenbruch, A.H. and Marshall, B.V.: "Subsea Temperatures and a Single Tentative Model for Offshore Permafrost at Prudhoe Bay, Alaska," U.S. Geological Survey Open-File Rept. 77-395 (1977).
15. Page, F.W., and Iskandar, I.K., "Geochemistry of Subsea Permafrost at Prudhoe Bay, Alaska," U.S. Army Cold Regions Research and Engineering Laboratory Special Report 78-14 (1978).
16. Rogers, J.C. and Morack, J.L.: "Geophysical Investigation of Offshore Permafrost at Prudhoe Bay, Alaska," In: Proceedings of the Third International Conference on Permafrost (1978), Vol. 1, 560-566.
17. Osterkamp, T.E. and Harrison, W.D.: "Subsea Permafrost at Prudhoe Bay, Alaska: Drilling Report and Data Analysis," University of Alaska, Geophysical Institute Report UAG-R-245 (1976).
18. Osterkamp, T.E. and Harrison, W.D.: "Subsea Permafrost Probing, Thermal Regime and Data Analysis," Quarterly Report, April-June 1978 to National Oceanic and Atmospheric Administration, Outer Continental Shelf Environmental Assessment Project (1978).
19. MacKay, J.R.: "Offshore Permafrost and Ground Ice, Southern Beaufort Sea, Can. J. Earth Sci. (1972) 10, No. 6, 979.

IX. Summary of 4th Quarter Operations

A. Laboratory Activities. The quarter was spent preparing a paper for the Offshore Technology Conference which covered the final results of the subsea permafrost engineering property studies conducted as part of CRREL's contributions to the OCSEAP program. Data interpretation of the seismic records was also continued. Arrangements were also made to acquire samples

from the USGS Conservation Division drilling program, which included providing insulated sample containers. All of the seismic data that was ordered has now been received. The program is on schedule. The only modification in the plan is that some funds originally planned for acquiring additional seismic data are being held in anticipation of activities centered on analyses of samples we plan to receive from the current USGS program.

B. Significant Problems. None.

C. Estimate of Funds Obligated. As of 31 March a total of $30,000 of the total $65,000 FY78 funding has been obligated.

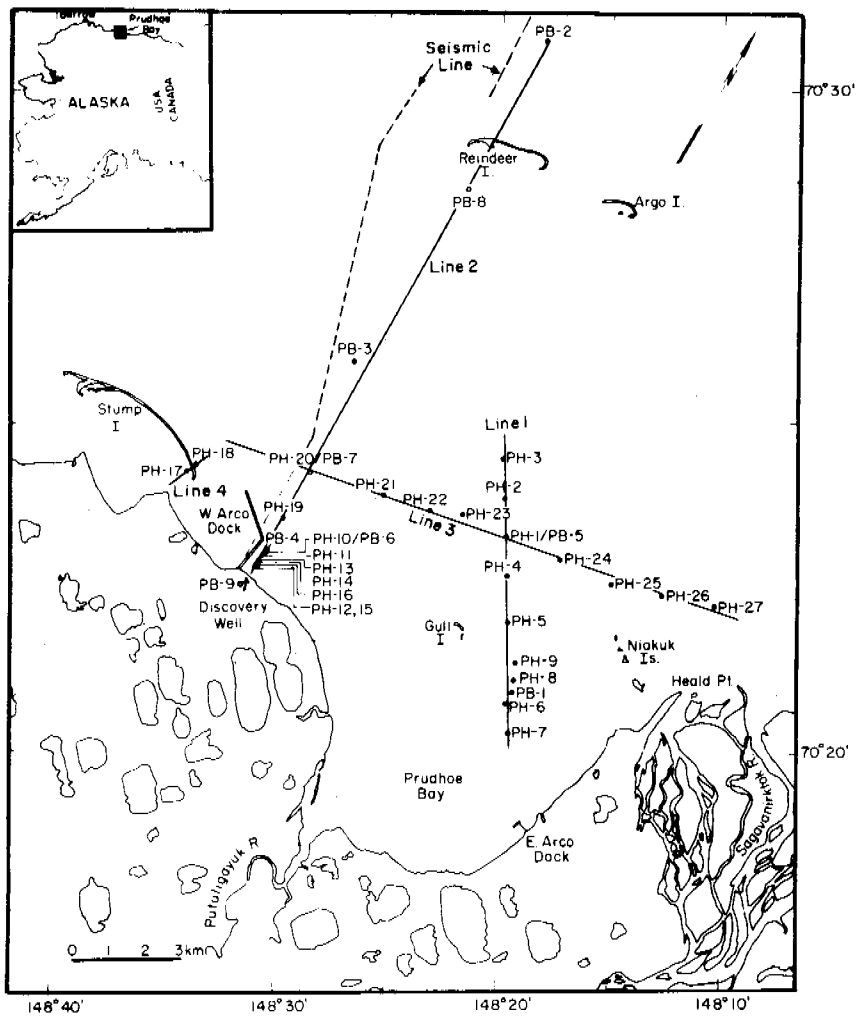

Fig. 1a - Site locations and major study lines (PB indicates drill hole, PH probe hole, except for PB-4 which is a 1976 probe hole location). The dashed line indicates the location of Rogers' seismic data shown in Figure 13.

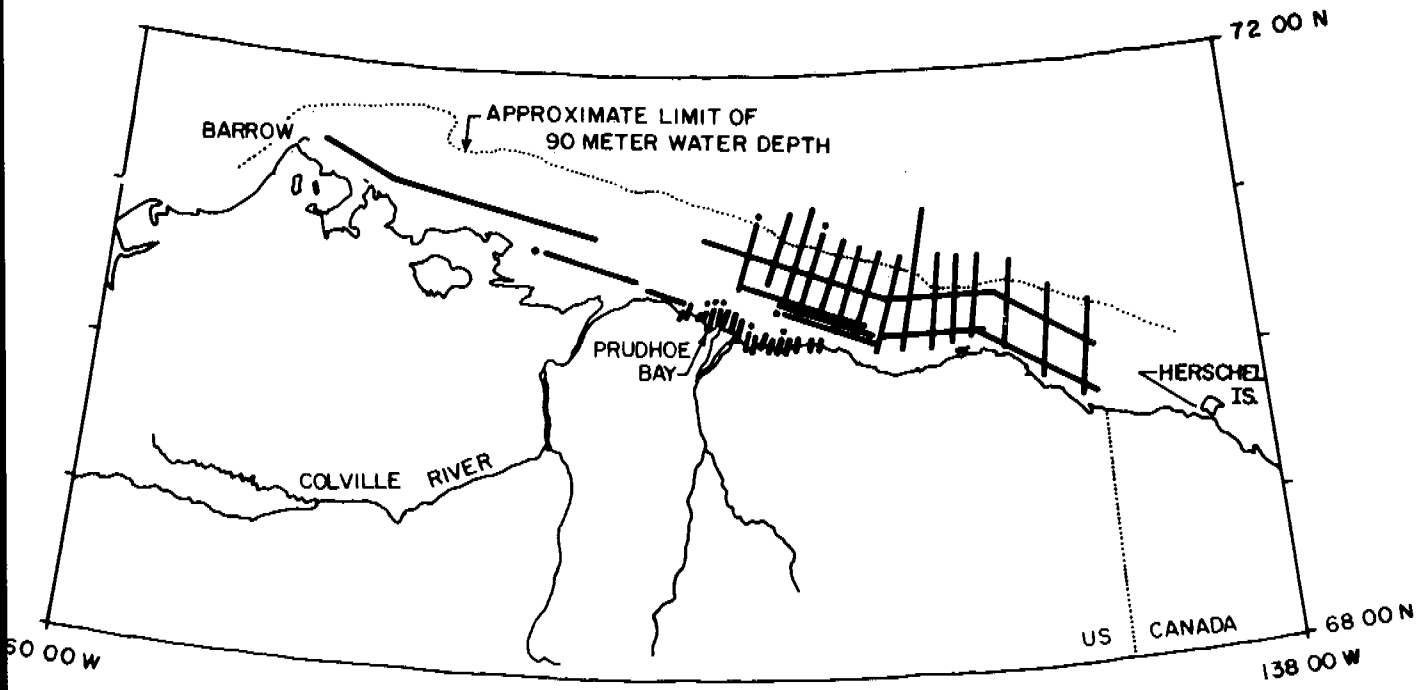

Fig. 1b - General location of seismic data acquired for analysis. Dots indicate lines discussed in this report. Nearshore lines that parallel the coast between Prudhoe Bay and the eastern limit of the nearshore data are not shown.

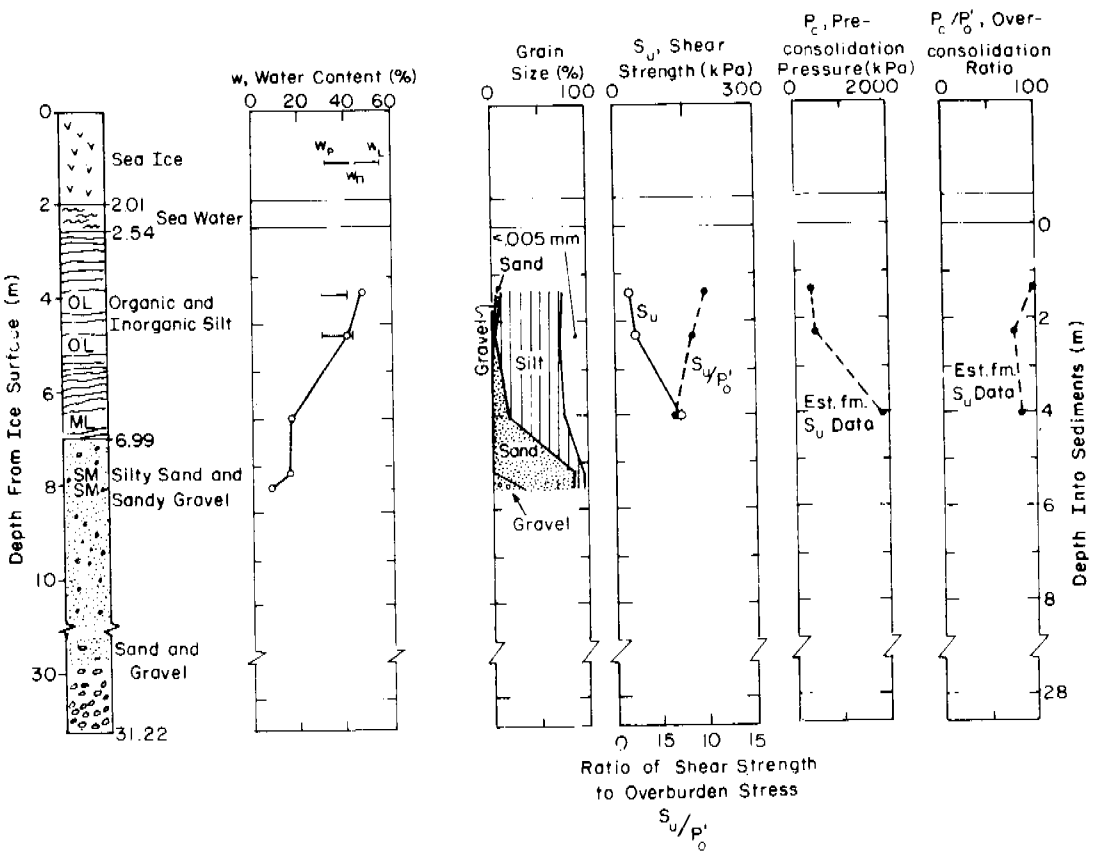

Fig. 2 - Drill hole log and engineering properties for site PB-1.

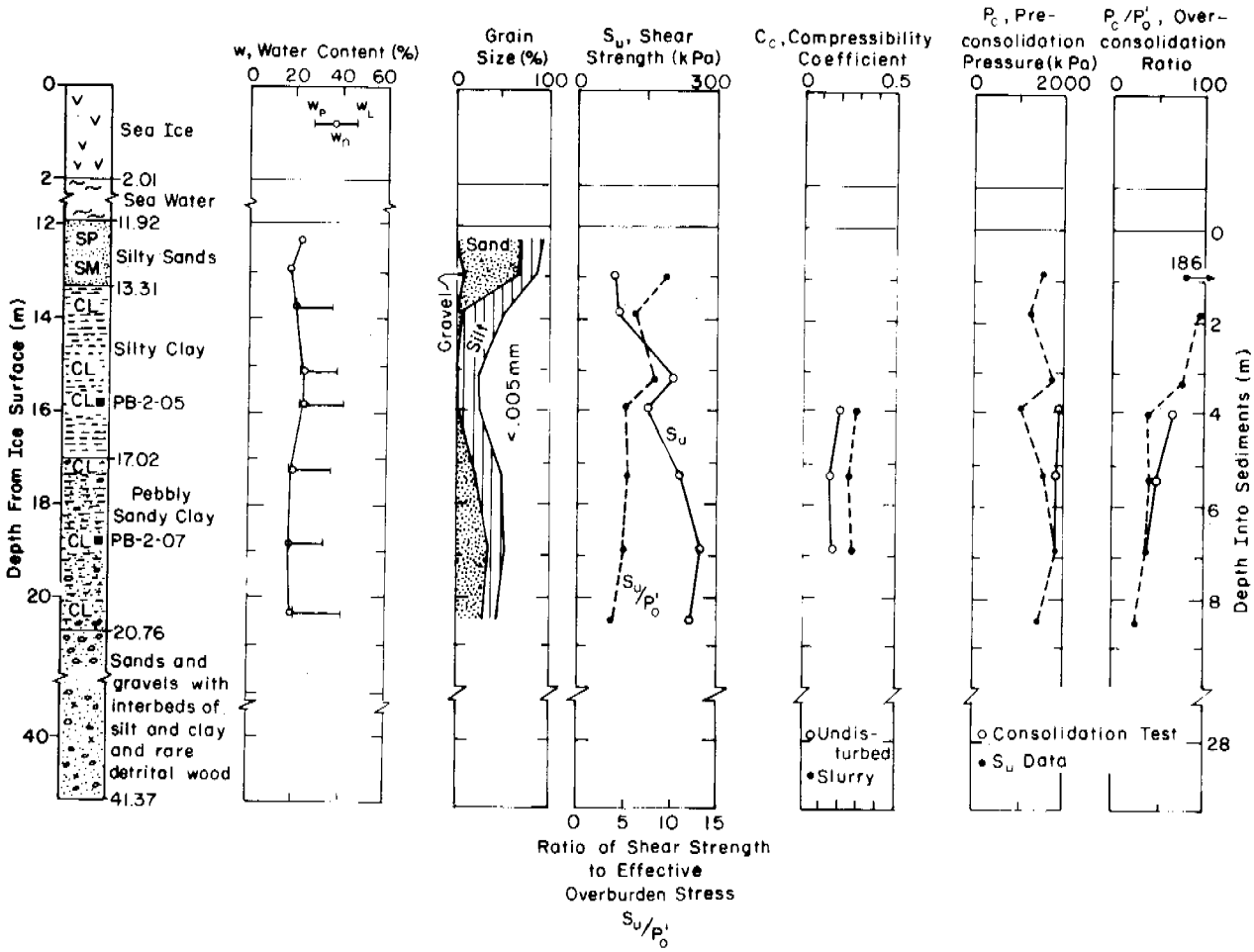

Fig. 3 - Drill hole log and engineering properties for site PB-2.

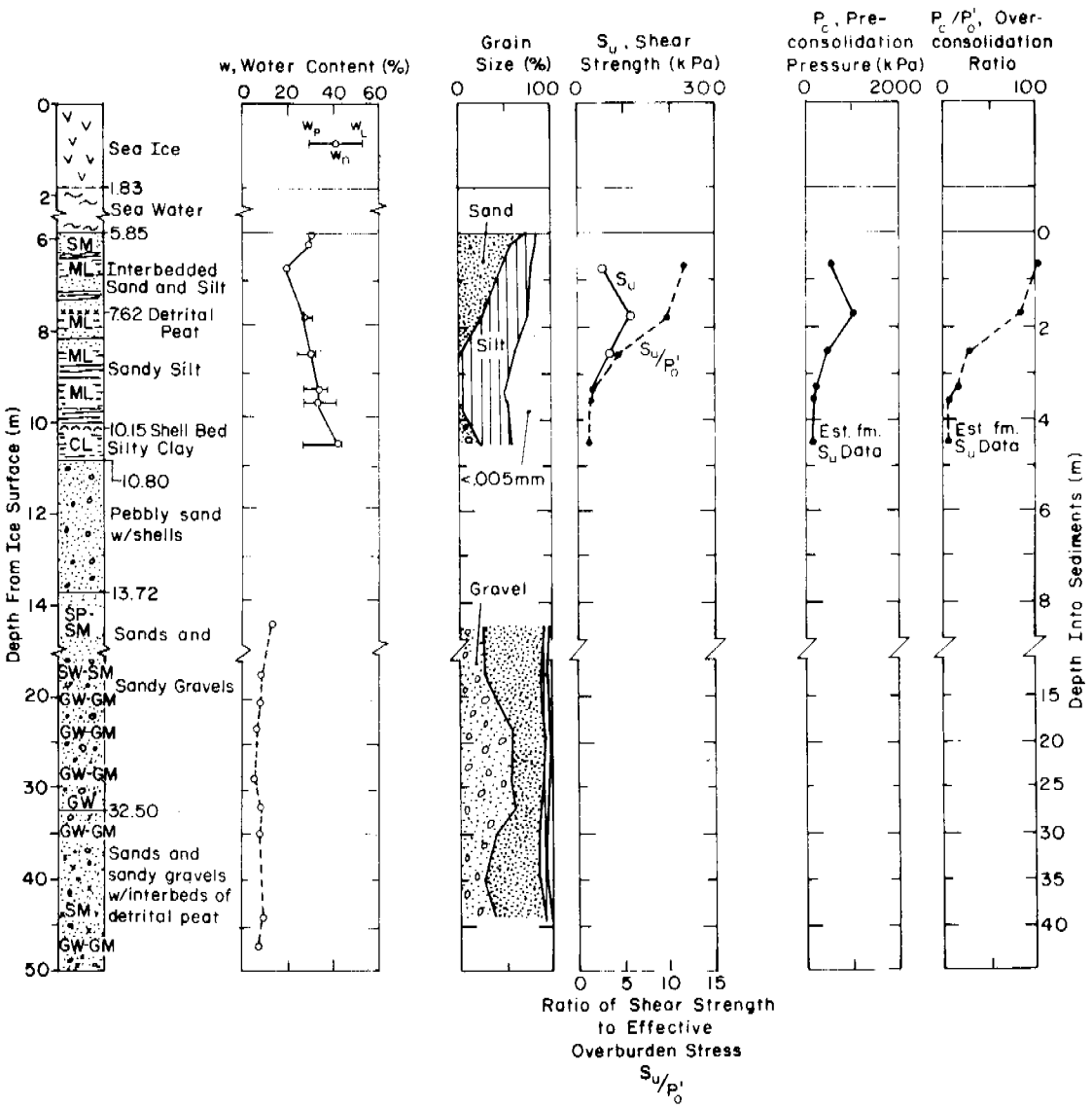

Fig. 4 - Drill hole log and engineering properties for site PB-3.

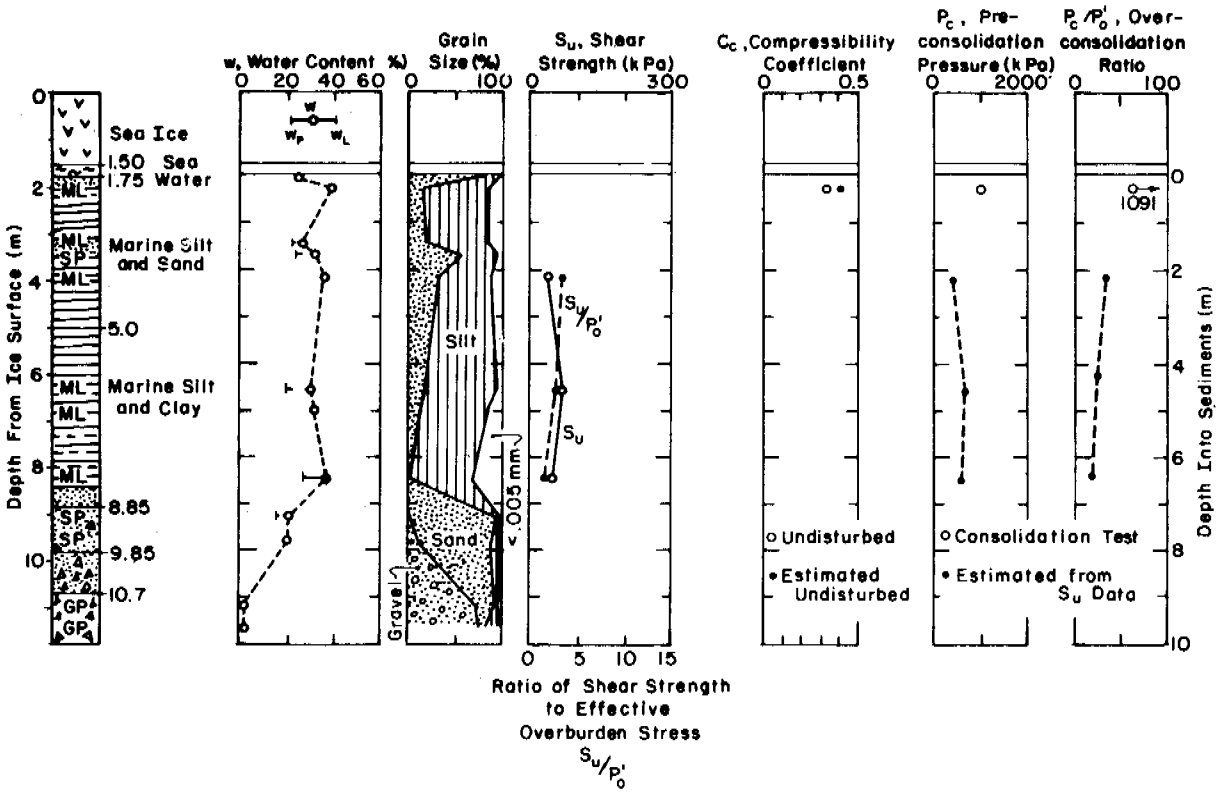

Fig. 5 - Drill hole log and engineering properties for site PB-5.

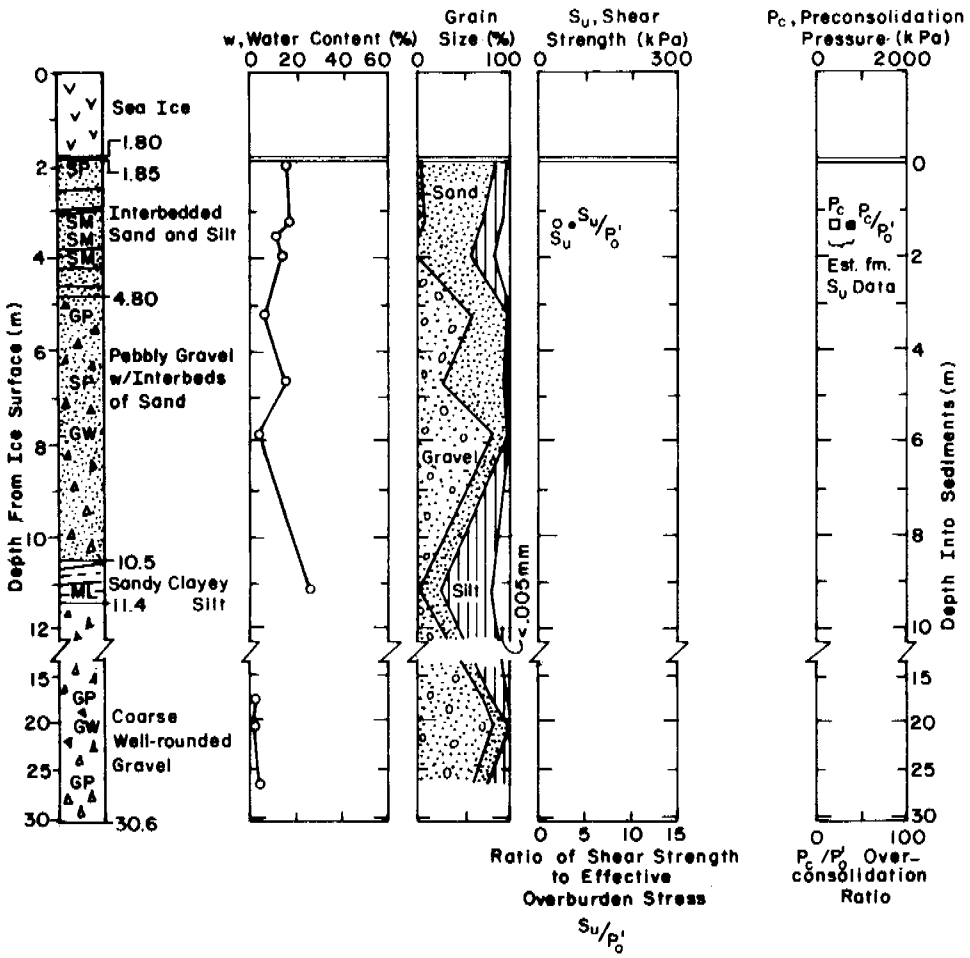

Fig. 6 - Drill hole log and engineering properties for site PB-6.

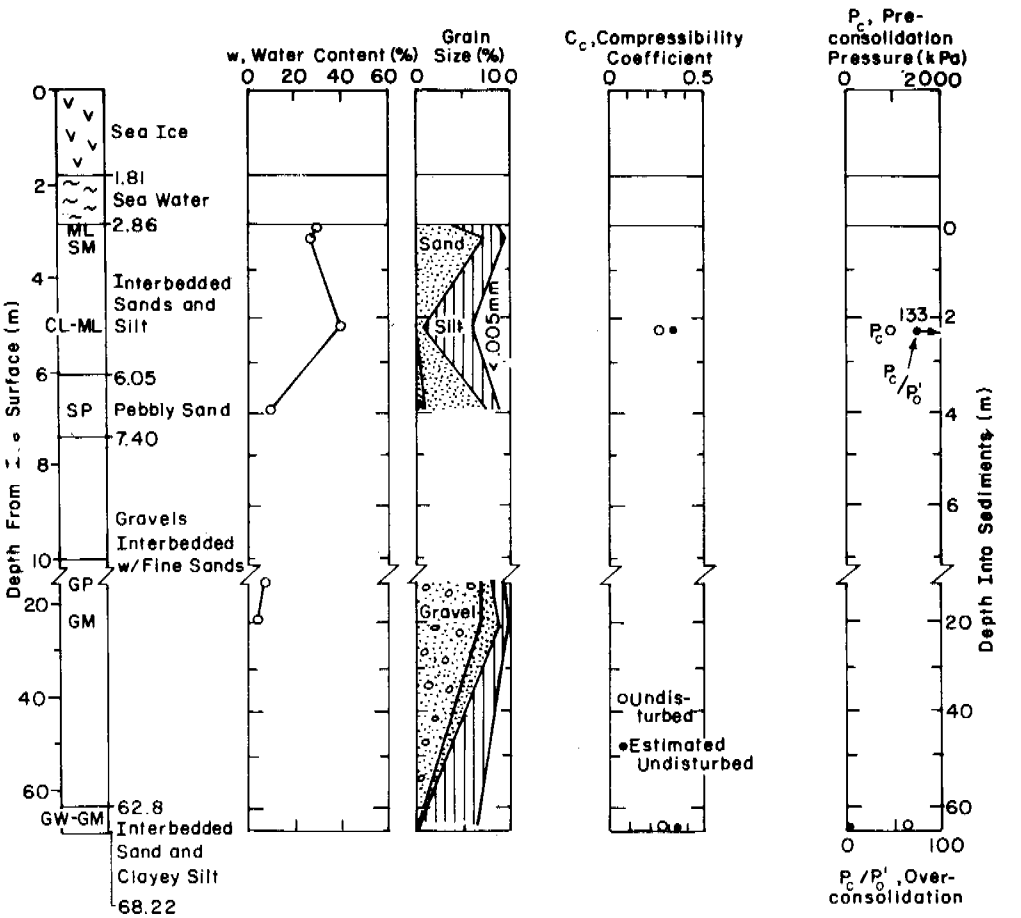

Fig. 7 - Drill hole log and engineering properties for site PB-7.

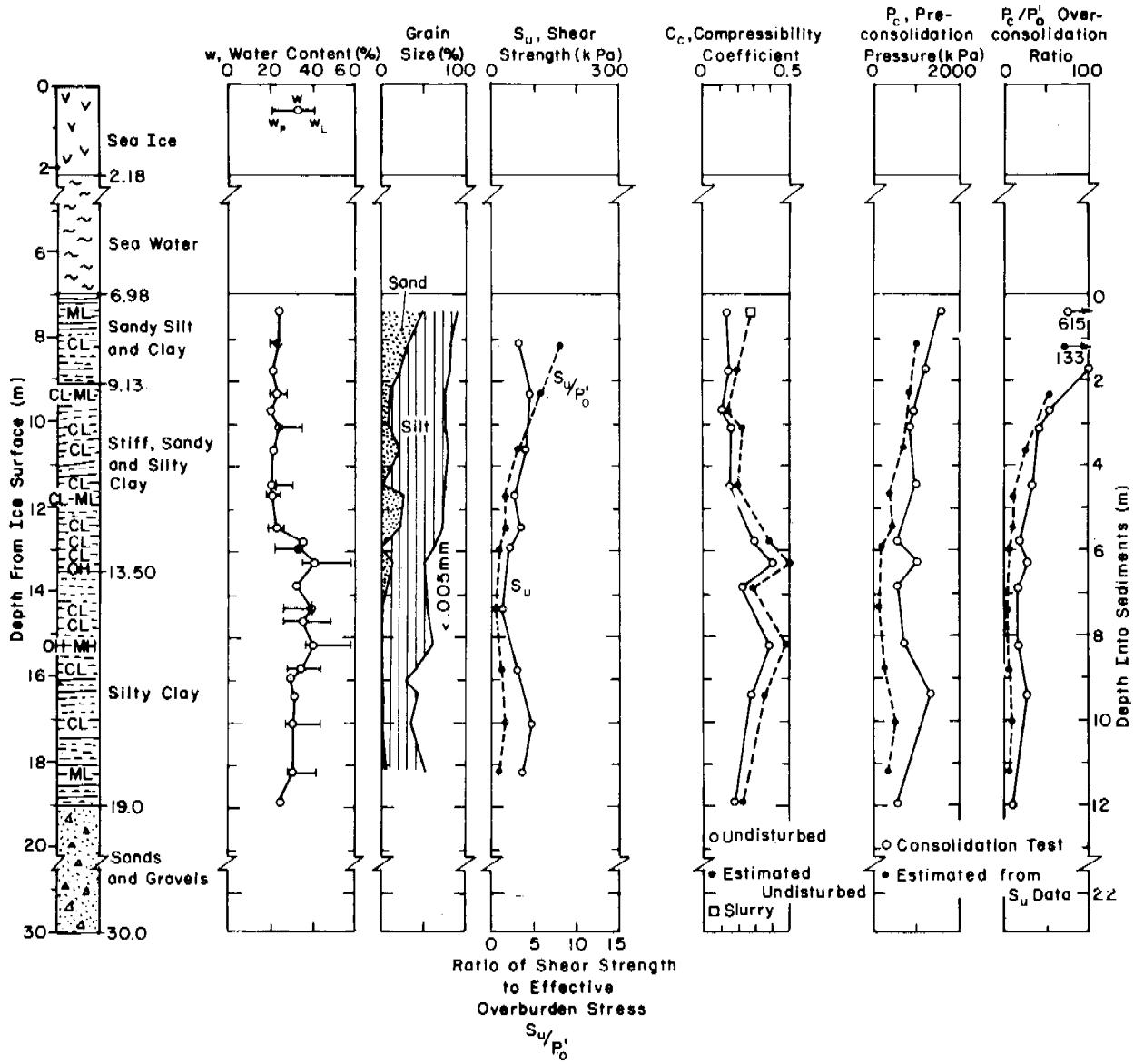

Fig. 8 - Drill hole log and engineering properties for site PB-8.

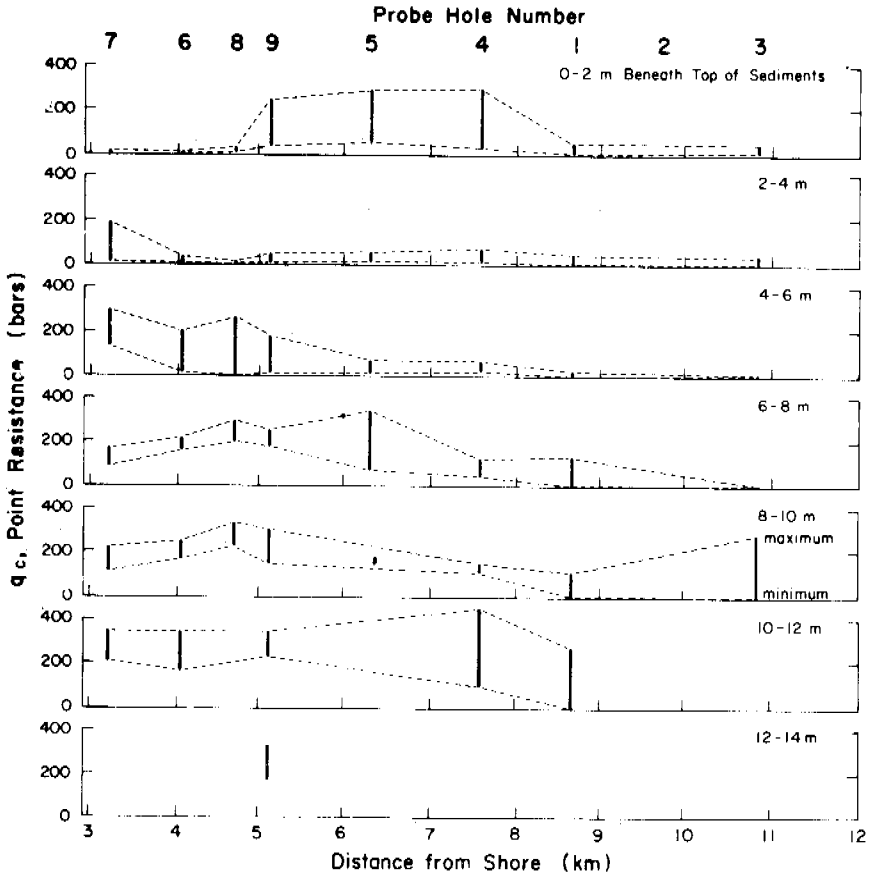

Fig. 9 - Summary of penetration resistances along line 1. (1 bar = 100 kPa.)

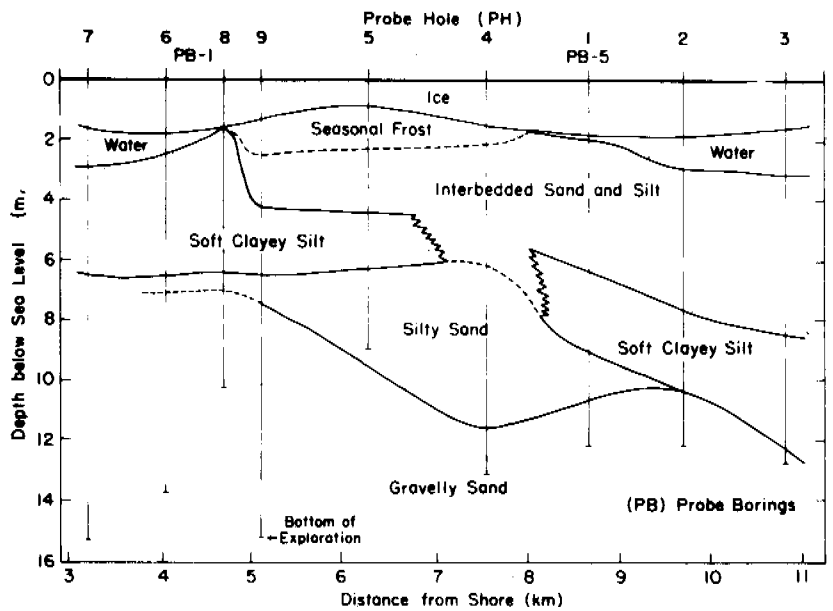

Fig. 10 - Stratigraphic section along line 1.

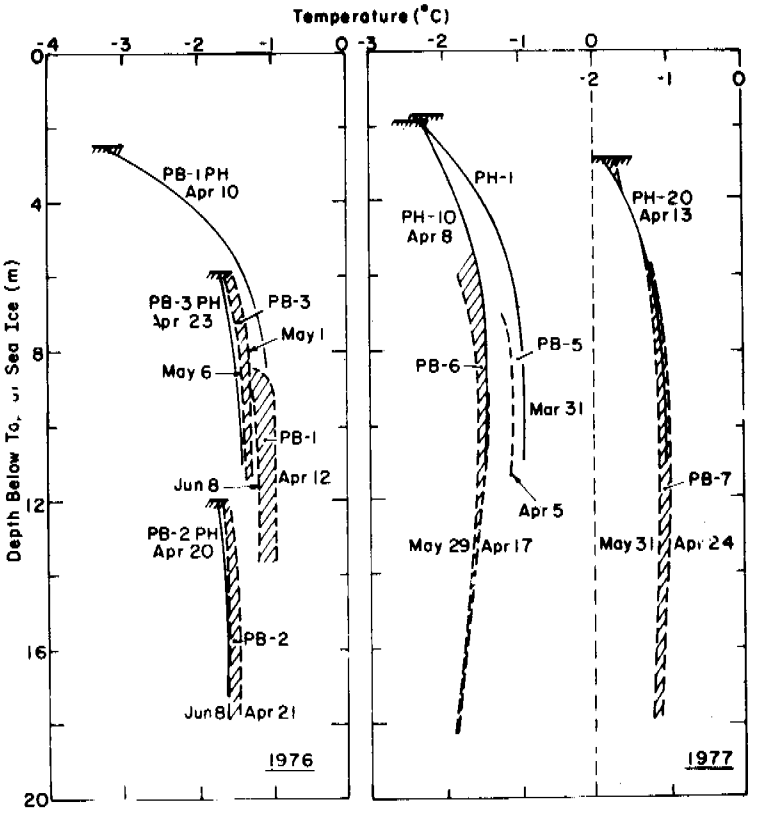

Fig. 11 - Comparison of drill hole and probe temperature profiles.

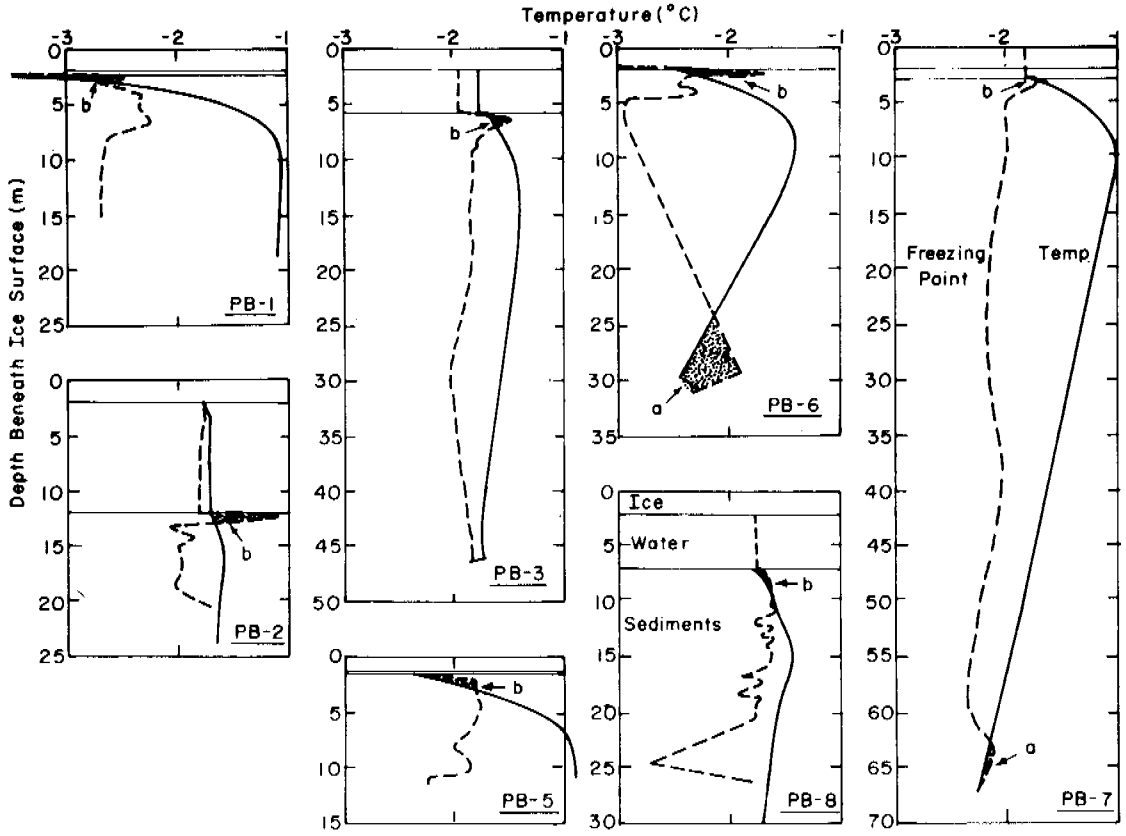

Fig. 12 - Comparison of the calculated freezing point and temperature profiles.

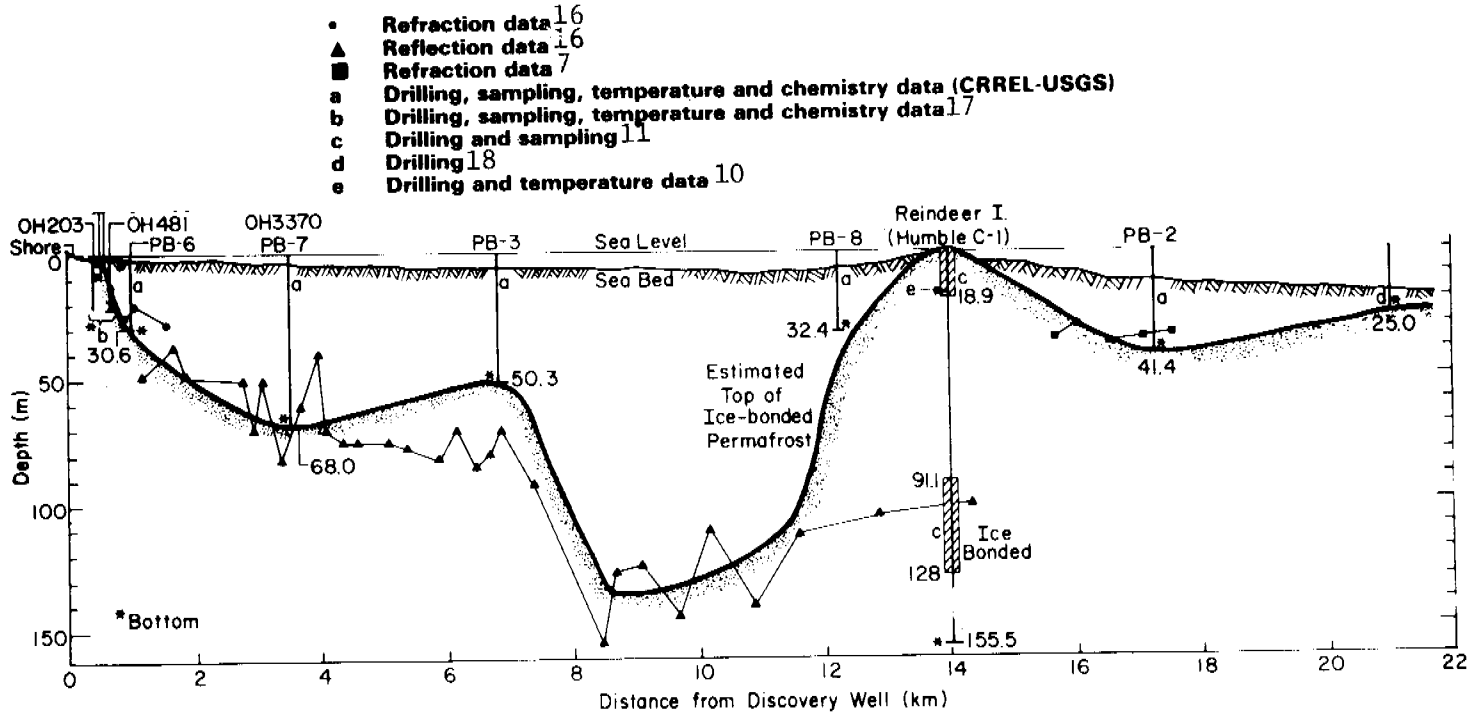

Fig. 13 - Summary of available data on depth to ice-bonded permafrost along line 2. Dark shaded line is our estimate of the position of the top of ice-bonded permafrost.

Annual Report
April 1978 to March 1979
Research Units 204 and 473
Task D-9

OFFSHORE PERMAFROST STUDIES AND SHORELINE HISTORY OF CHUKCHI AND BEAUFORT SEAS AS AN AID TO PREDICTING OFFSHORE PERMAFROST CONDITIONS

P. A. Smith and D. M. Hopkins
U.S. Geological Survey
345 Middlefield Road
Menlo Park, CA 94025

April 1979

Table of contents

Annual Report Task D-9
R.U. 204 and 473

OFFSHORE PERMAFROST STUDIES AND SHORELINE HISTORY OF CHUKCHI AND BEAUFORT SEAS AS AN AID TO PREDICTING OFFSHORE PERMAFROST CONDITIONS

P. A. Smith and D. M. Hopkins
U.S. Geological Survey
345 Middlefield Road
Menlo Park, CA 94025

I. SUMMARY

The main objectives of our studies are to determine the extent of offshore permafrost on the Beaufort Sea shelf and to explore the relationship of coastal geology and geomorphology to shoreline history and offshore permafrost. Toward this purpose, results from seven boreholes drilled in Prudhoe Bay during 1976 and 1977 have been analyzed and attempts to correlate lithologic, paleontologic and permafrost characteristics of borehole sediments have been made. Ice-bonded permafrost on the Beaufort Sea shelf in the Prudhoe Bay region is deeply thawed in what we interpret as paleovalleys excavated by the major rivers on the coast during the last low sea-level interval. It may be possible to predict the distribution of areas of deeply thawed ice-bonded permafrost elsewhere on the shelf by establishing the paleo-drainage pattern.

A report included in our 1978 Annual Report has been revised and published as "Coastal morphology, coastal erosion, and barrier islands of the Beaufort Sea", U.S. Geological Survey Open File Report 78-1063.

A tabulation of 22 radiocarbon dates provides information on stratigraphy of offshore boreholes, rates of peat and aeolian sand accumulation, rates of ice-wedge growth, sea-level history, the age of a volcanic ash layer found in Holocene sediments along the Beaufort Sea coast, and the age of an ancient storm surge event in the Kuk River estuary.

Continuing study of the ice-rafted boulders in the "Flaxman Formation" establishes that they were probably derived from northern Greenland and that the most recent episode of Flaxman deposition on the continental shelf and the coastal areas of the Beaufort Sea probably took place at some time between 60,000 and 30,000 years ago.

In February and March of 1979, D. M. Hopkins and R. W. Hartz participated as OCSEAP investigators in the permafrost and geotechnical drilling program in the Beaufort lease area, undertaken by the Conservation Division of the U.S. Geological Survey. No results are available from the program at this time, but will be included in later quarterly and annual reports.

II. INTRODUCTION

Exploration and production of offshore oil and gas reserves in the Beaufort Sea requires a thorough understanding of offshore permafrost distribution. The study of coastal processes operating today can provide insights into past events, and can help to predict possible problem areas. Thus, our projects strive to

apply studies of coastal geology and geomorphology to knowledge gained from offshore boreholes. Methods for predicting the depth and distribution of permafrost on the shelf is valuable in setting up guidelines for the siting of offshore oil and gas wells, while determination of shoreline history, storm-surge limits and coastal erosion rates on the Beaufort Sea shelf aid in planning the location of onshore support facilities necessary for oil and gas production.

III. CURRENT STATE OF KNOWLEDGE

Although the existence of permafrost on the continental shelf of the Arctic Coast has been known for some time, it has only been in recent years that its distribution, thickness, state, and temperature have begun to be studied in depth. Current annual reports by these and other investigators adequately sum up the results of research now being conducted.

IV. STUDY AREA

During the past year fieldwork took place along the Beaufort Sea coast from Barrow to the Colville River, concentrating primarily in Harrison Bay. In addition, paleontologic identifications and radiocarbon dates from other locations on the Beaufort and Chukchi coasts were analyzed.

V. SOURCES, METHODS, AND RATIONALE OF DATA COLLECTING

Natural and excavated sections of coastal bluffs were examined, and samples were taken from them for radiocarbon dating, pollen studies, and paleontologic identifications.

Observations of driftwood lines found along coastal bluffs were used to plot the extent of storm-surges along the Beaufort Sea.

An attempt was made to synthesize all the information available on the plant and animal remains present in our borehole samples, and to correlate this information with changes in lithology throughout the drill holes.

Radiocarbon dates received on borehole samples and on samples collected at onshore locations were tabulated.

Core samples from PB-3 and PB-8 were submitted for pollen studies. Moss polsters and algal muds were collected for use in determining the modern pollen rain on the Beaufort Sea coast.

VI. RESULTS

Diagrams showing the lithology and paleontology of the Prudhoe Bay boreholes have been drawn up and are presented as Appendix 1. For PB-1, -2, and -3 foraminifera and ostracode abundance and diversity, mollusk identifications, radiocarbon ages of organic material within sediment samples, and preliminary identification of seeds and other organic matter is recorded, along with general comments on the environment at the time of deposition. Information on PB-5, -6, -7, and -8 is not complete, and their diagrams will be updated in the future.

A correlation exists between the depth at which ice-bonded permafrost is found, and the presence or absence of an overconsolidated clay which is older than the last rise in sea level. In general, where this overconsolidated clay is present, ice-bonded permafrost is shallow, and where the clay is lacking the ice-bonded permafrost is deep. A more detailed account of this relation is presented in Appendix 2 of this report.

Pollen studies on selected core samples from PB-3 and PB-8 have been completed and are reported on separately in Appendix 3 b. The modern pollen rain on the Beaufort Sea coast is reported in Appendix 3a.

Twenty-two radiocarbon dates from the Chukchi and Beaufort Sea coasts have been tabulated. These dates and their implications are reported in Appendices 4 and 5 of this report. Appendix 4 contains the date list along with general comments on implications for coastal processes, while Appendix 5 details the evidence for a storm-surge event along the Kuk River on the Chukchi Sea coast.

"Coastal morphology, coastal erosion, and barrier islands of the Beaufort Sea" by D. M. Hopkins and R. W. Hartz has been published as U.S. Geological Survey Open File Report 78-1063. This report can be obtained from the authors or from U.S.G.S. Public Information offices. Material for the report was collected as part of our coastal studies in 1976 and 1977, and an earlier draft of the report appeared in our 1978 Annual Report for R.U. 473.

Discussions with Dr. R. L. Christie and other colleagues of the Geological Survey of Canada in Calgary and Ottawa indicates that the ice-rafted "Flaxman boulders" were most likely derived from northern Greenland, rather than from Ellesmere Island or the Amundsen Gulf region as had been previously assumed. The most recent episode of introduction of erratic boulders to the continental shelf took place at some time after the last interglacial interval and at a time when relative sea level was at least 3 or 4 m higher than at present along the Beaufort Sea coast. Oxygen isotope records suggest that world sea level fell to a low level about 70,000 years ago, then underwent a partial recovery between 60,000 and 30,000 years ago, and then finally fell to its late Wisconsinan minimum position about 18,000 years ago (Shackleton and Opdyke, 1973). Thus, it seems likely that the Flaxman boulders were deposited between 60,000 and 30,000 years ago. Beaches that may have represented the Flaxman shoreline have been dated as about 36,000 years old at Point Barrow (Sellmann and Brown, 1973). However, the Sagavanirktok River paleovalley delineated by our drill holes seems to have been excavated earlier than 42,000 years ago, yet after the time of deposition of the Flaxman boulders. The precise age of the most recent episode of deposition of ice-rafted Flaxman boulders remains uncertain.

VII & VIII. DISCUSSIONS AND CONCLUSIONS

Appendices 2 through 5 present further discussions of our results, along with conclusions which have been drawn from them.

IX. NEED FOR FURTHER STUDY

It has been suggested that a date on the granitic component of the "Flaxman boulders" would be helpful in pinpointing their original source

area. However, our samples have been too small to use for dating purposes. Also, the gneissose appearance of some of our samples suggests that any date received might be ambiguous. The need continues for further investigations into possible source areas for these rocks, both in Greenland and in Canada.

When paleontological information still missing from PB-5, -6, -7, and -8 is obtained, it should be added to the existing diagrams and used to further the paleo-environmental analyses.

Information on the paleontology and geotechnical properties of the 1979 boreholes will further our investigation into the distribution of permafrost on the Beaufort Sea shelf.

X. SUMMARY OF QUARTERLY ACTIVITIES, Jan-March 1979

A. Ship or Laboratory Activities

1. Field Activities

During February and March of 1979, D. M. Hopkins and R. W. Hartz took part in the offshore drilling program in the Beaufort Lease area.

2. Scientific Party

D. M. Hopkins, USGS, principal investigator
R. W. Hartz, USGS, granulometry, coastal studies
R. E. Nelson, USGS, palynology
P. A. Smith, USGS, preparation of samples, paleo-environmental studies

3. Methods

a. Field

Logging boreholes
Monitoring and collecting wash samples

b. Analysis
Correlation of microfossil, radiocarbon and sedimentological data
Identification of pollen
Radiocarbon dating

4. Sample Localities

20 holes in the Beaufort Lease area, detailed locations not yet available.

5. Data Collected or Analyzed

a. None available at this time.
b. 6 radiocarbon dates received, 8 more submitted.

XI. REFERENCES

Sellmann, P. V., and Brown, J., 1973, Stratigraphy and diagenesis of perennially frozen sediments in the Barrow, Alaska region, in Permafrost; the North American Contribution to the Second International Conference: National Academy of Sciences, p. 171-181.

Shackleton, N. J., and Opdyke, N. D., 1973, Oxygen isotope and paleomagnetic stratigraphy of equatorial Pacific core V28-238; oxygen isotope temperatures and ice volumes on a 10^5 year and 10^6 year scale: Quaternary Research, v. 3, p. 39-55.

Appendix 1

ORGANIC REMAINS AND DEPOSITION ENVIRONMENT IN UPPER PART OF BOREHOLES PB-1 THROUGH PB-8

The following seven diagrams are a compilation by P. A. Smith and D. M. Hopkins of information obtained on core samples from boreholes PB-1 through PB-8. Samples were submitted from marine muds overlying beach or outwash gravels. Samples from depths greater than those shown on the diagrams were barren of microfossils.

Identification of foraminifera in these samples was provided by Kris McDougall, of ostracodes by Ellen Compton, Tom Cronin, and Joe Hazel, and of mollusks by Louie Marincovich and Warren Addicott. Radiocarbon dates were provided by Steve Robinson.

The muds are all Holocene in age, except where noted as Flaxman Formation (Wisconsin) or as an unnamed formation of Sangamon age. The explanation of symbols given in Figure 1.1 applies to all seven diagrams.

Ostracode data for PB-5, -6, -7, and -8 is not complete, and their diagrams will be updated in the future.

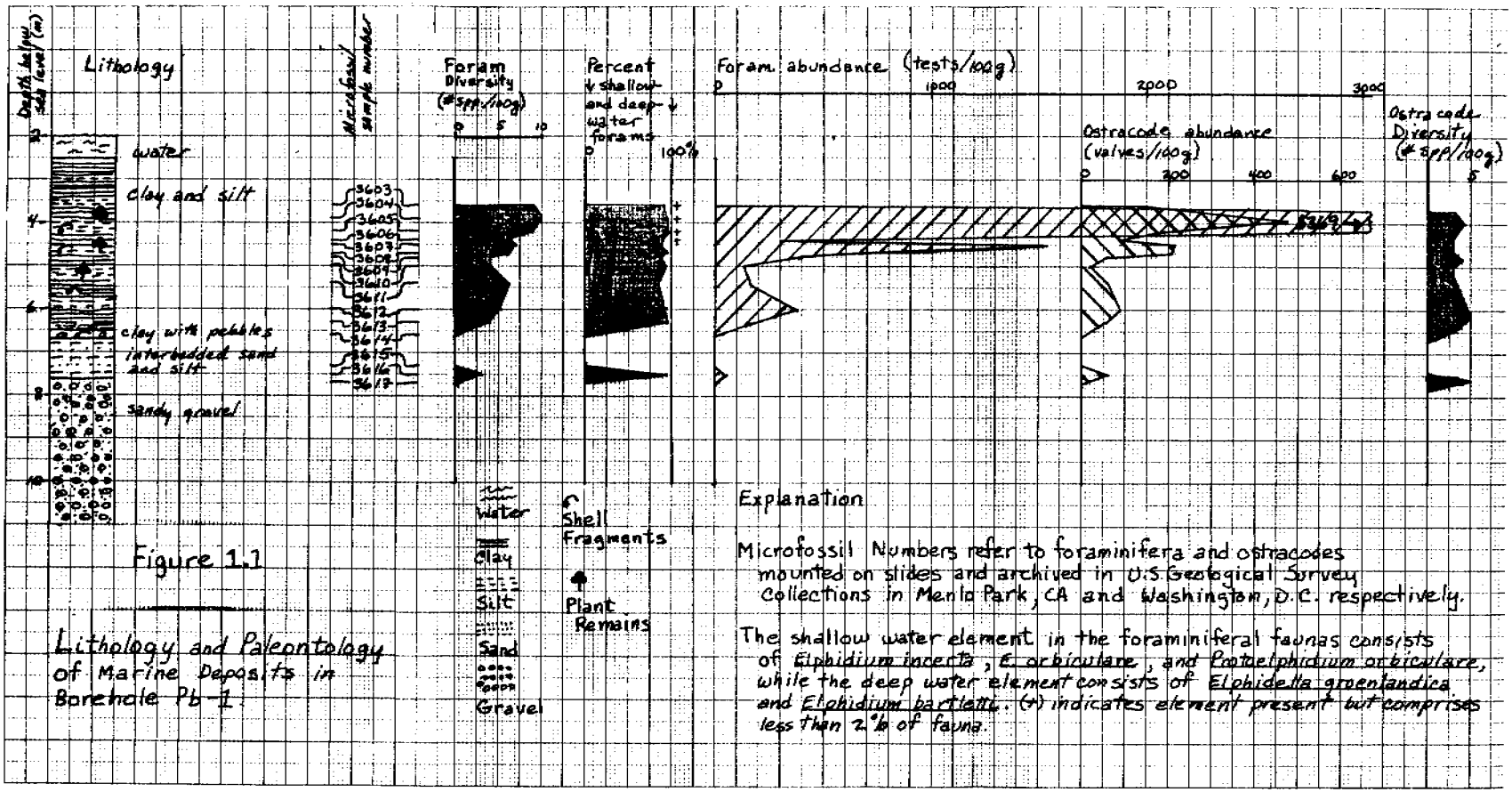

Figure 1.1

Lithology and Paleontology of Marine Deposits in Borehole Pb-1.

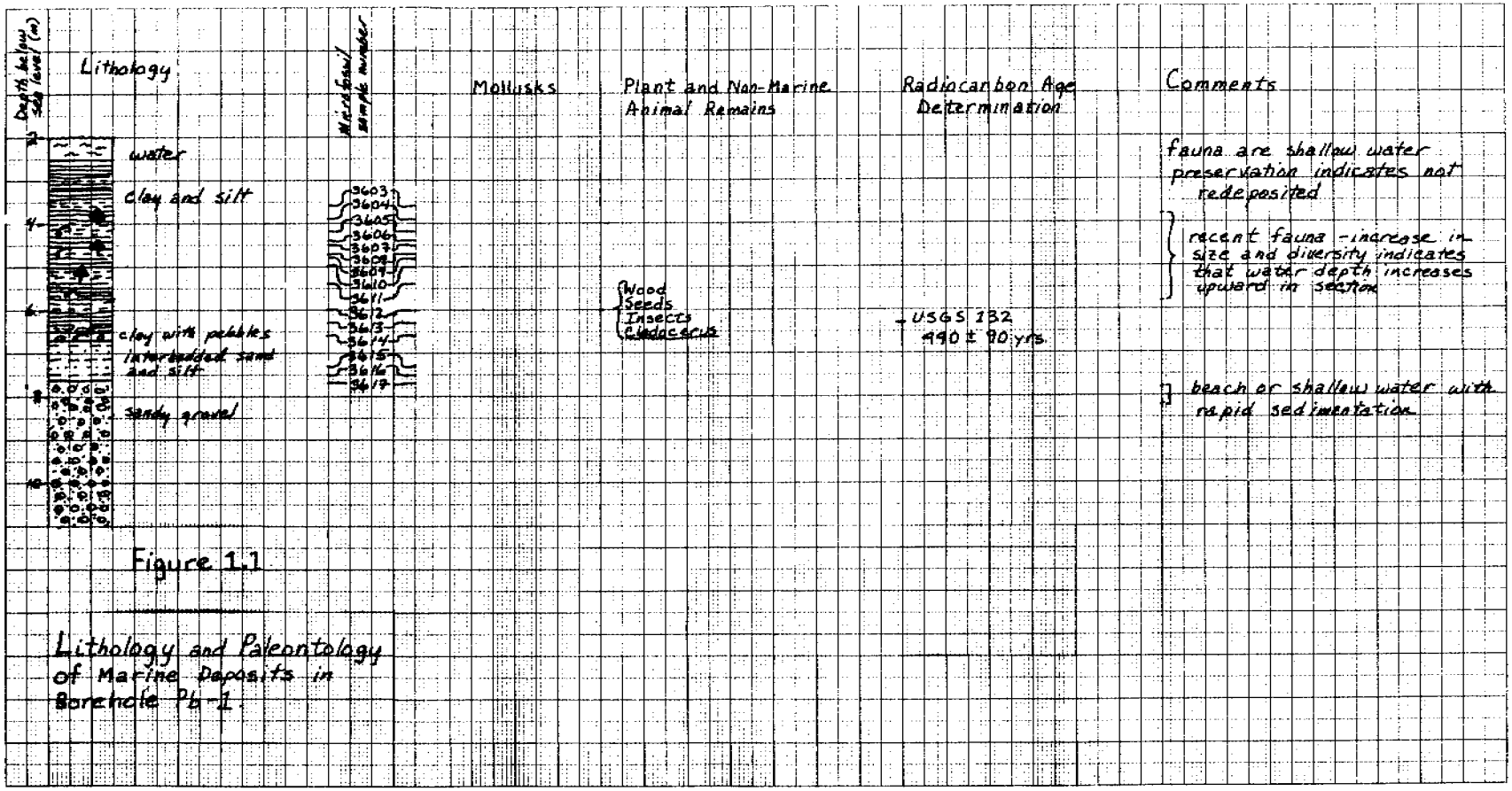

Figure 1.1

Lithology and Paleontology of Marine Deposits in Borehole Pb-1.

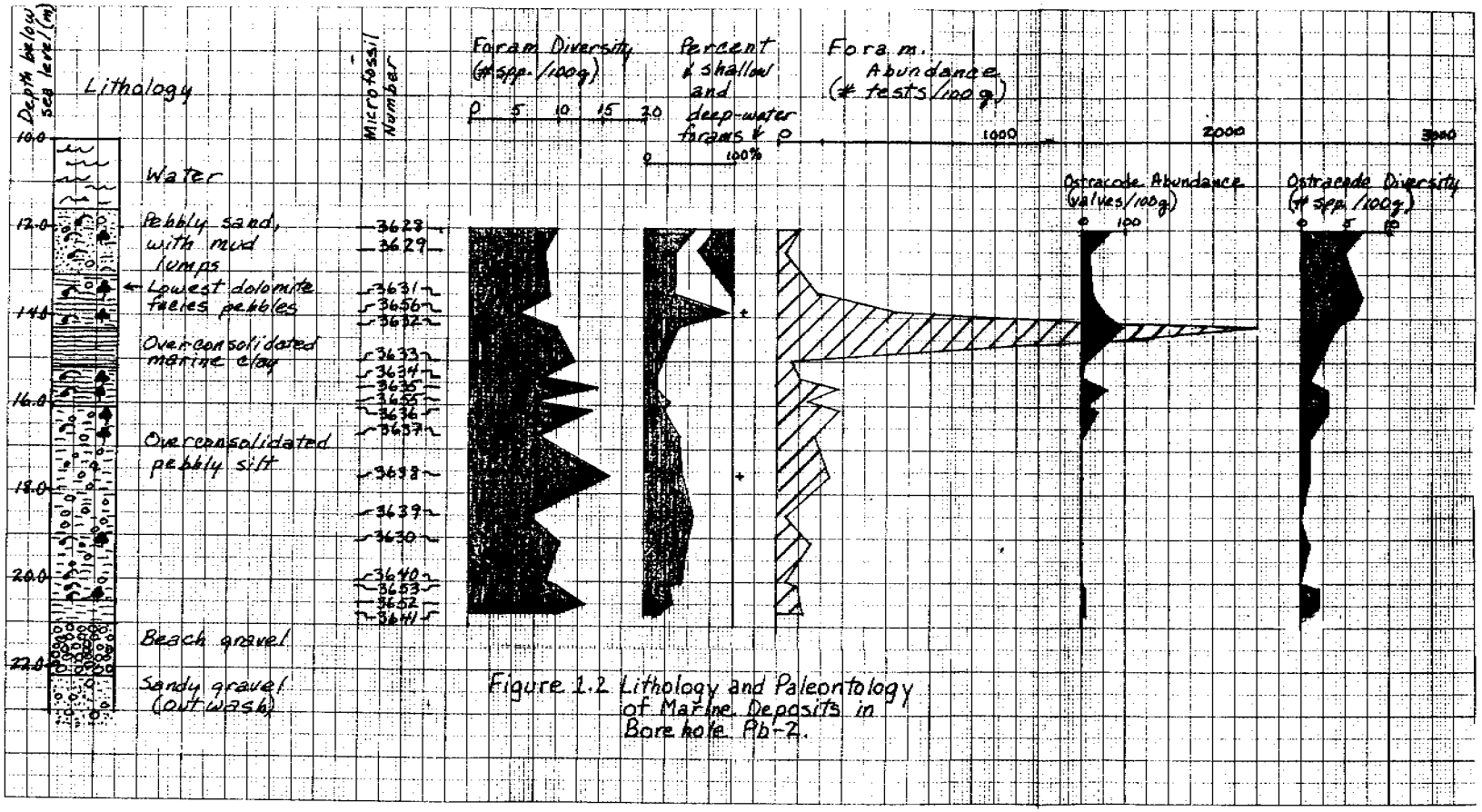

Figure 1.2 Lithology and Paleontology of Marine Deposits in Bore hole Pb-2.

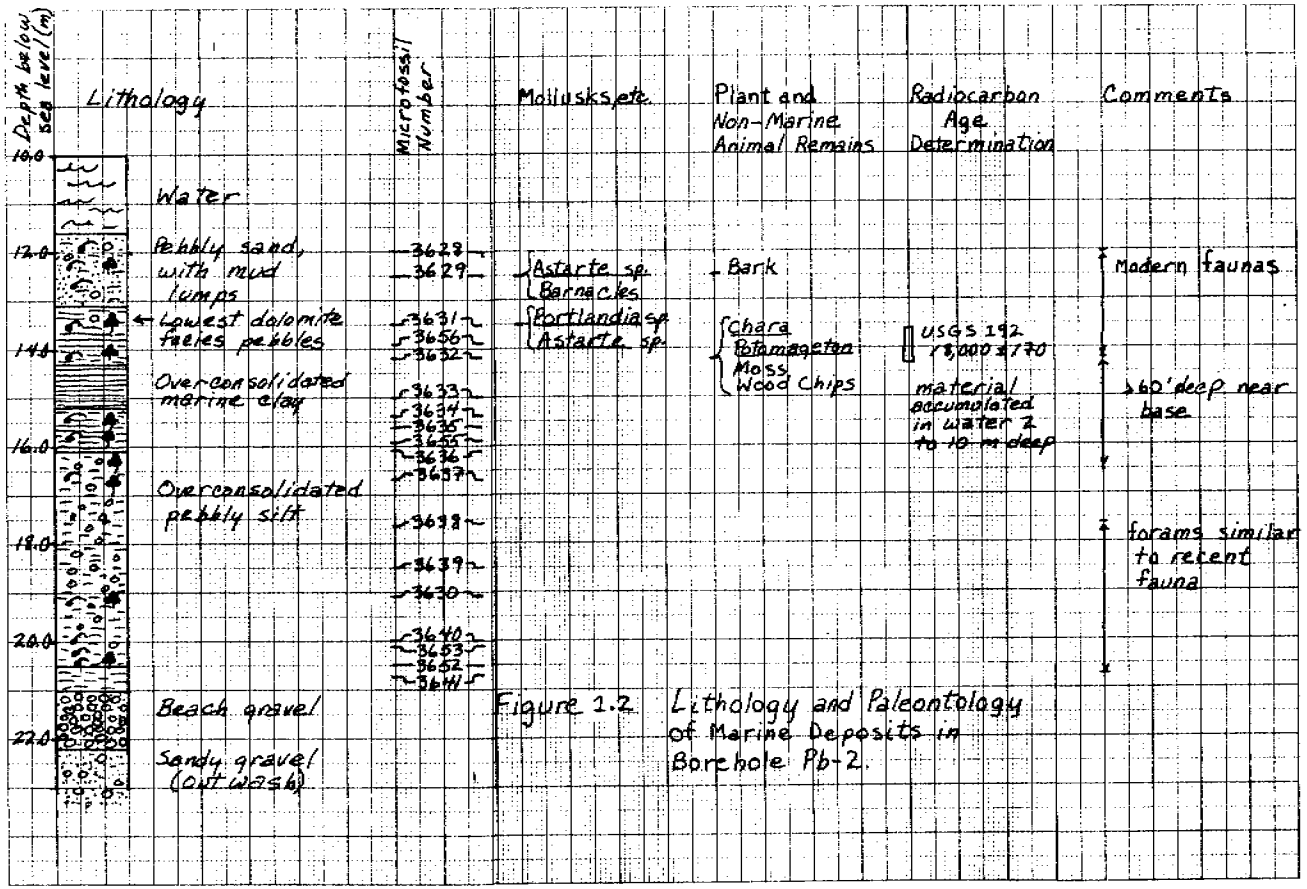

Figure 1.2. Lithology and Paleontology of Marine Deposits in Borehole Pb-2.

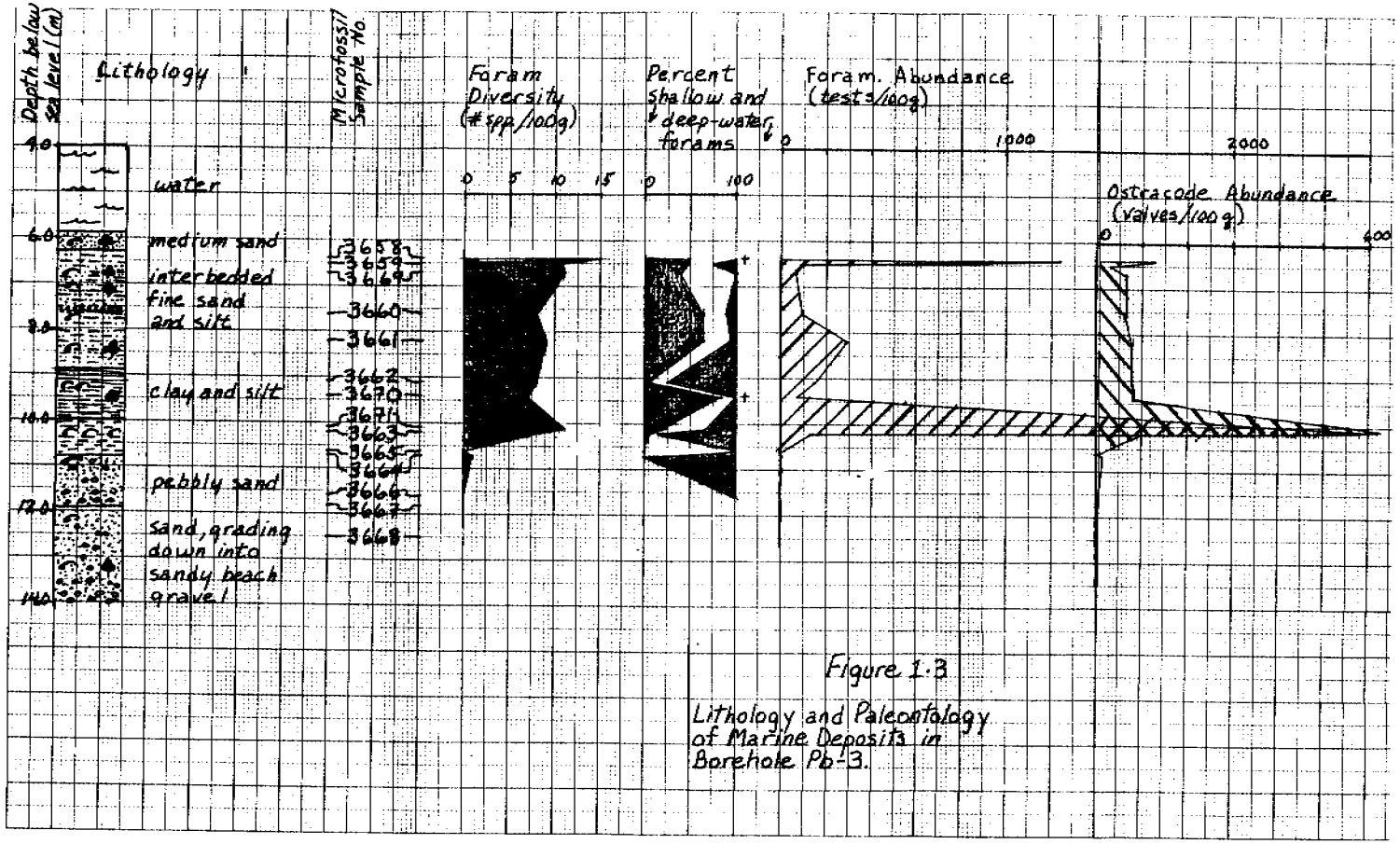

Figure 1.3

Lithology and Paleontology of Marine Deposits in Borehole Pb-3.

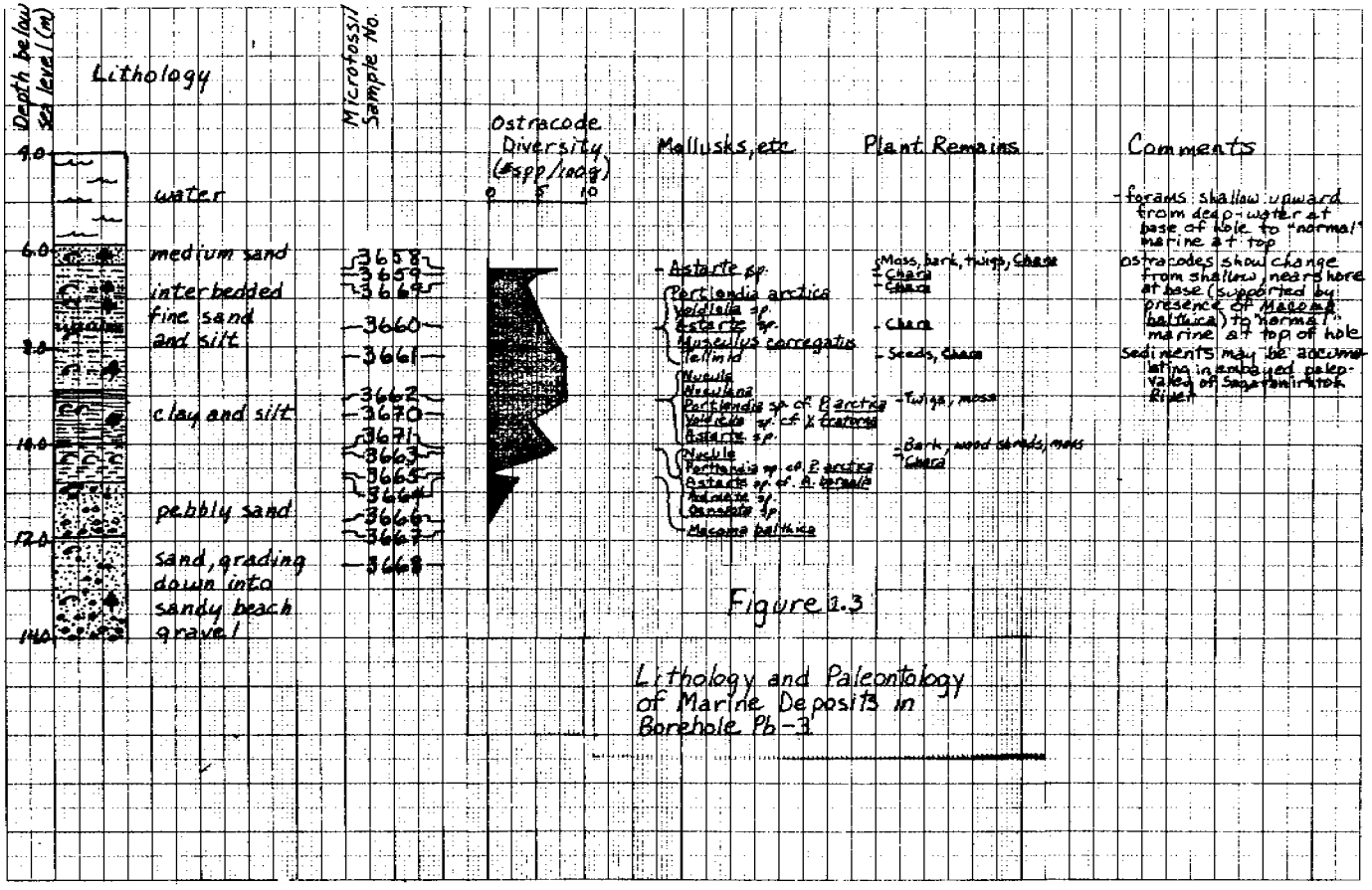

Figure 2.3

Lithology and Paleontology of Marine Deposits in Borehole Pb-3

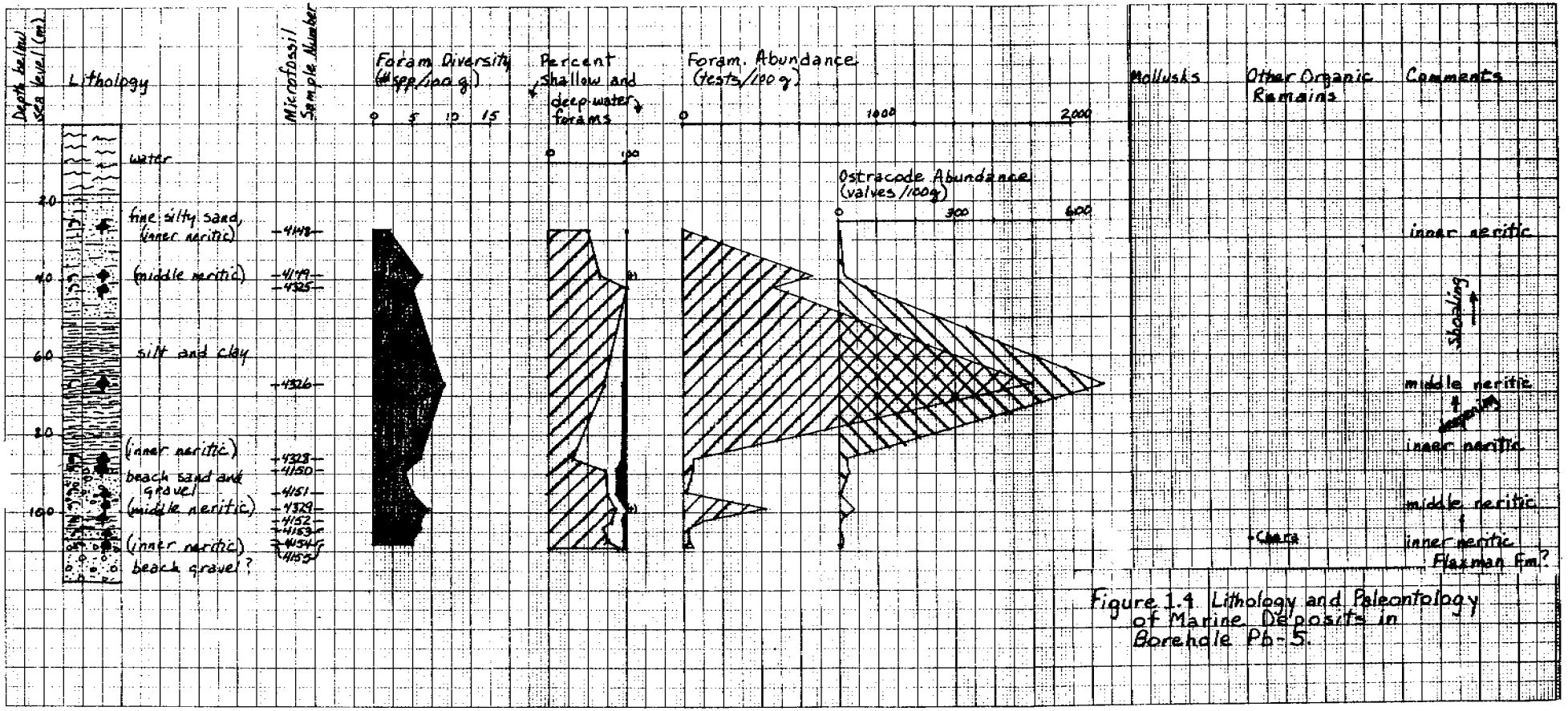

Figure 1.4 Lithology and Paleontology of Marine Deposits in Borehole Pb-5.

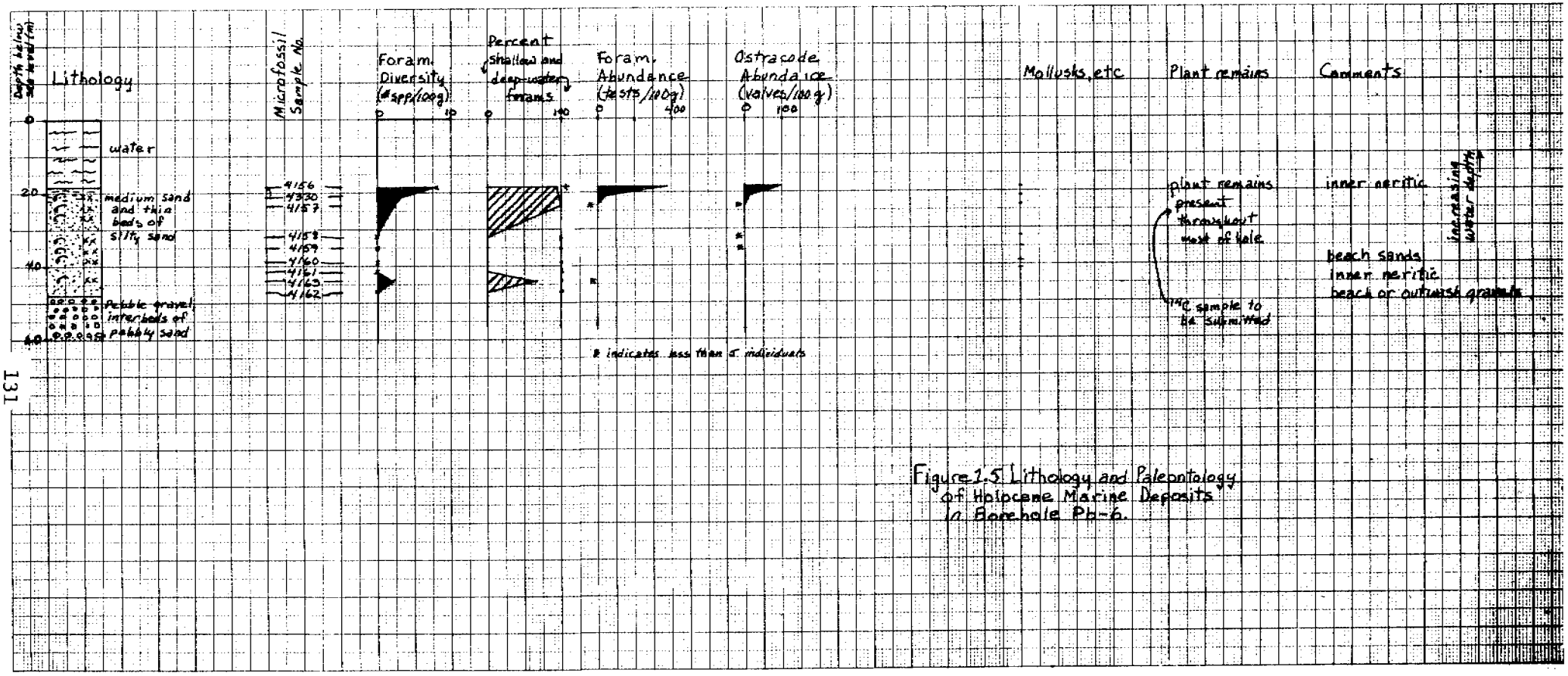

Figure 2.5 Lithology and Paleontology of Holocene Marine Deposits in Borehole Ph-6.

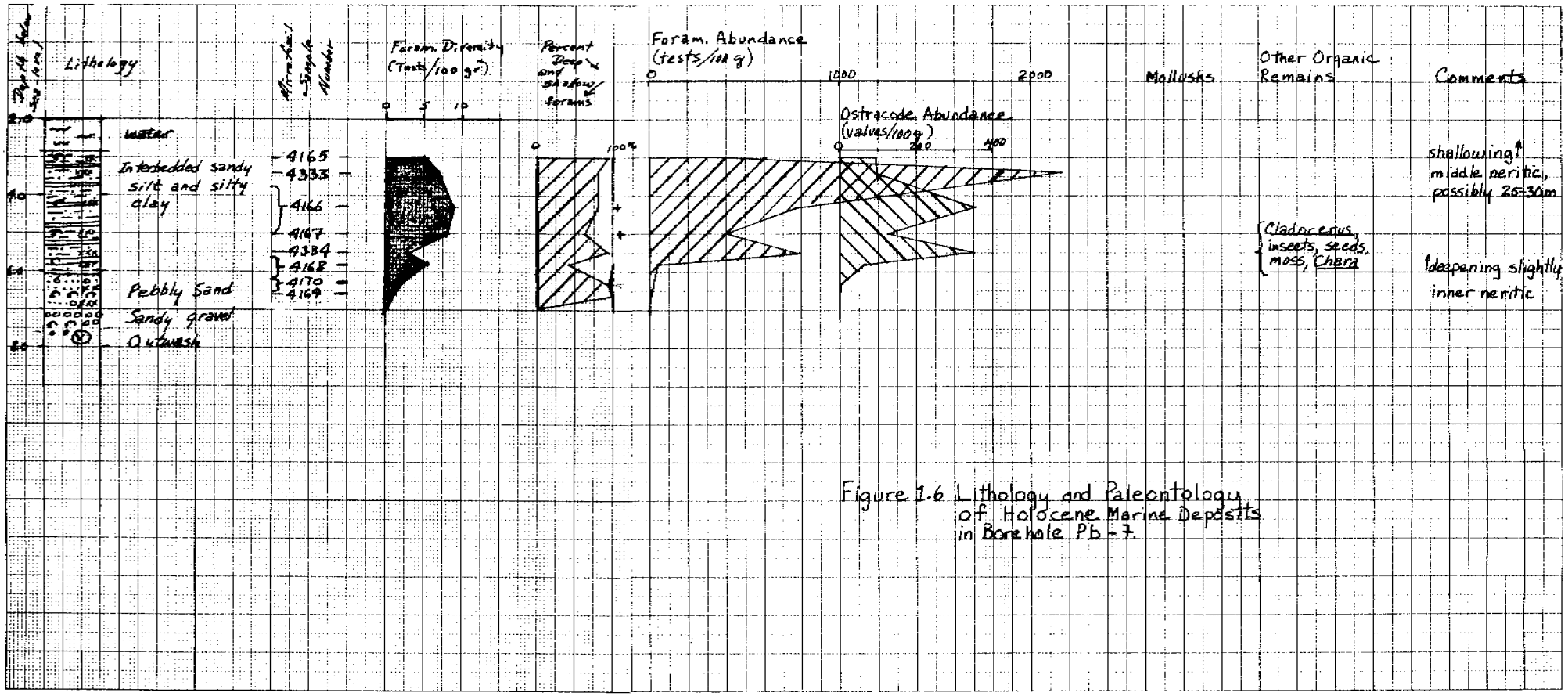

Figure 1.6 Lithology and Paleontology of Holocene Marine Deposits in Borehole Pb-7.

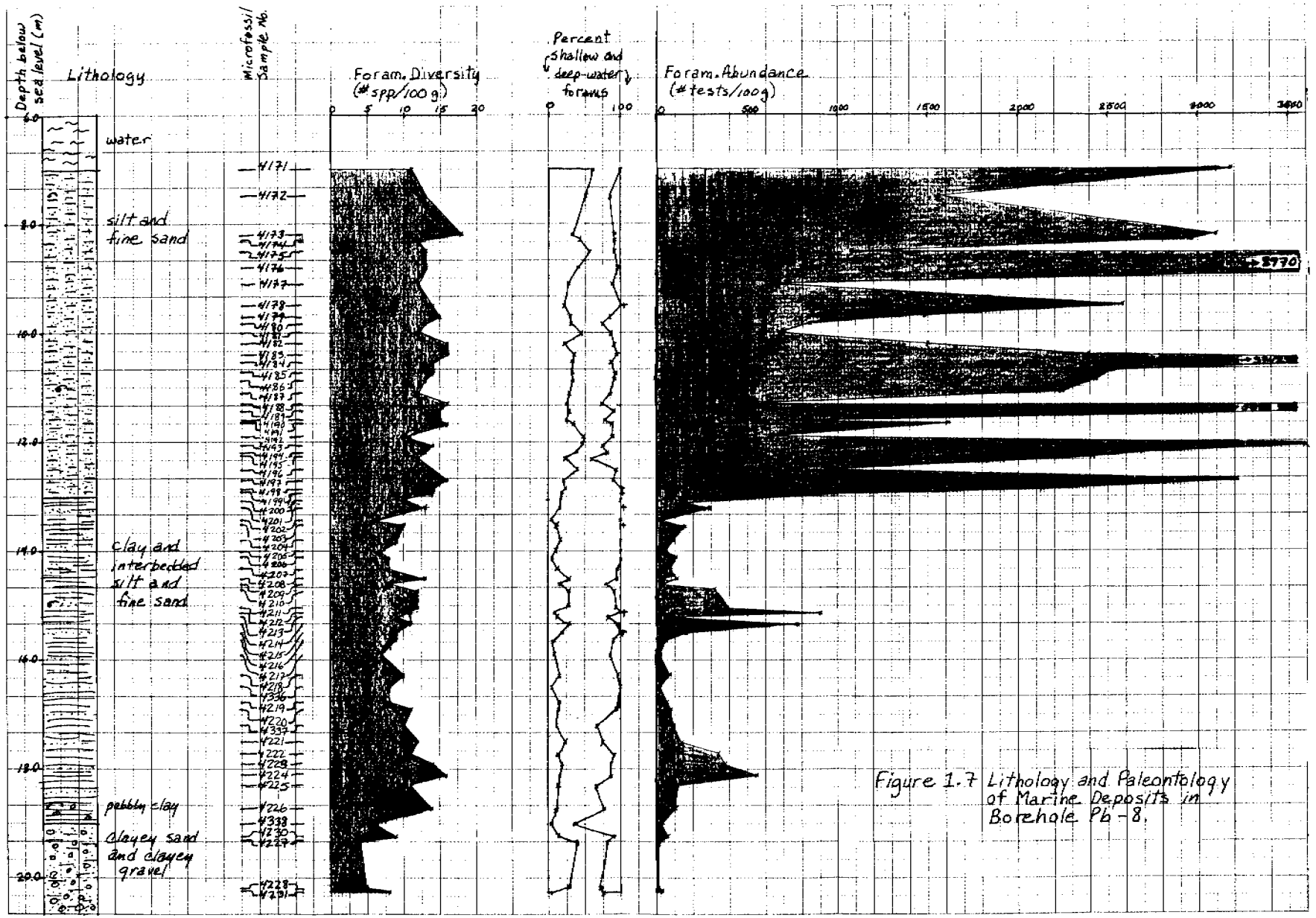

Figure 1.7 Lithology and Paleontology of Marine Deposits in Borehole Pb-8.

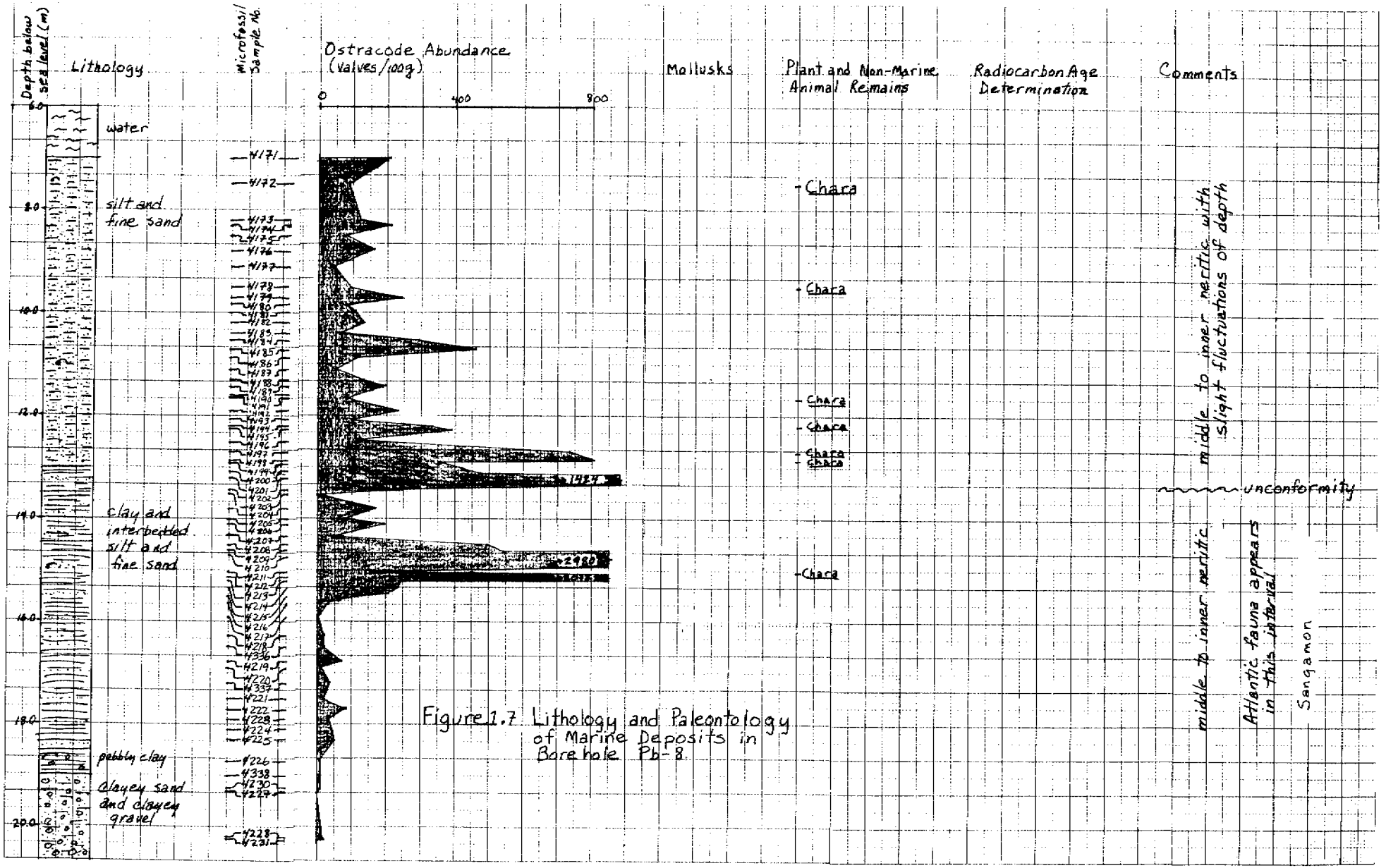

Figure 1.7 Lithology and Paleontology of Marine Deposits in Borehole Pb-8.

Appendix 2

BURIED VALLEYS AS A POSSIBLE DETERMINANT OF THE DISTRIBUTION OF DEEPLY BURIED PERMAFROST ON THE CONTINENTAL SHELF OF THE BEAUFORT SEA

D. M. Hopkins[1/], P. V. Sellmann[2/], E. Chamberlain[2/], R. E. Lewellen[3/], and S. W. Robinson[1/]

With colleagues in our own organizations and at the University of Alaska, we have conducted a study of the distribution of ice-bonded permafrost on the continental shelf of the Beaufort Sea (Barnes and Hopkins, 1978). The study has been conducted by means of thermal, geochemical, geotechnical, paleontological, and stratigraphic study of cores from offshore boreholes (Osterkamp and Harrison, 1976; Hopkins, 1977; Sellmann and others, 1977; Chamberlain and others, 1978; Harrison and Osterkamp, 1977; Hopkins and Hartz, 1978a; Iskandar and others, 1978; Page and Iskandar, 1978), thermally instrumented soil probes (Blouin and others, in press), analysis of seismic reflection and refraction lines (Rogers and Morack, 1977), and examination of natural exposures of Quaternary sediments in coastal bluffs, river banks, and gravel pits (Hopkins and Hartz, 1978b; Hopkins and Robinson, Appendix 4, this report). The study is a part of the Outer Continental Shelf Environmental Assessment Program, funded by the United States Bureau of Land Management and managed by the United States National Oceanographic and Atmospheric Administration.

Ice-bonded permafrost has been shown to be present on the continental shelf to a distance of at least 17 and probably 20 km from the present mainland coast of the Beaufort Sea, but its depth below sea level differs widely from place to place. The ice-bonded layer lies as little as 10 m below sea level, for example, in areas only a few kilometers off the present mouth of

1/ U.S. Geological Survey, Menlo Park, California

2/ U.S. Army Cold Regions Research and Engineering Laboratory, Hanover, NH

3/ Arctic Research, Inc., Littleton, Colorado

the Sagavanirktok River, but it also lies at shallow depths in some areas on the outer continental shelf seaward of the Midway Island (fig. 1). Areas of shallow ice-bonded permafrost coincide at least partly with areas where overconsolidated clay older than the last rise in sea level lies at or near the sea bottom. Areas where ice-bonded permafrost is overlain by a thick layer of sediment soaked in cold but unfrozen brine are generally areas where the overconsolidated clay is lacking and where alluvial or outwash gravel is mantled by a surficial deposit of Holocene marine silt and clay.

The permafrost on the continental shelf is relict, having formed during the last interval of glacio-eustatic lowering of sea level. Overconsolidation of older marine silt and clay probably resulted from dewatering and densification due to freezing while exposed above sea level (Chamberlain and others, 1978). Areas where permafrost is now deeply thawed seem to lie beneath drowned and partly buried valleys, areas in which the overconsolidated silt and clay was stripped away in the course of valley erosion during the low sea levels of late Wisconsin time. According to this hypothesis, the deep thawing of permafrost would have resulted from infiltration of salt water into alluvial or outwash gravel during the Holocene recovery of sea level. If this hypothesis is correct, it should be possible to predict the distribution of areas of shallow and deeply thawed ice-bonded permafrost by reconstructing the paleodrainage pattern across the continental shelf (fig. 2.1).

We interpret our borehole and outcrop data to indicate that the main stem of the Sagavanirktok River once flowed along the present course of the Putuligayuk River, extended through the present site of Prudhoe Bay, and then turned westward through a broad valley excavated to a depth of at least 50 m below present sea level. A zone of detrital peat about 43,000 years old,

now lying 50 m below sea level in borehole PB-7 may be traceable to a paleosol and detrital peat layer still undated, but separated by about 3 m of gravel from an overlying sand and detrital peat layer dated as 26,000 years old, exposed in a deep gravel pit along the lower Putuligayuk River (samples USGS-249 and USGS-505, table 1, Hopkins and Robinson, Appendix 4, this report). Our boreholes and Rogers and Morack's (1977) seismic data indicate that ice-bonded permafrost lies at depths of 50 to 80 m in the area of the inferred valley.

Little is known, thus far, about other elements in the paleo-drainage pattern on the Beaufort Sea shelf, but one can reasonably assume that most areas of thick Holocene sediment (Barnes and Hopkins, 1978, fig. 3.5) lie within the paleovalleys and that areas of overconsolidated silt and clay and areas in which the bottom is littered by erratic ice-rafted boulders (Rodeick, 1975; Reimnitz and Ross, 1979) lie between valleys. There are other clues: the Staines River is shown by Hopkins and Robinson (Appendix 4, this report) to have once flowed through Leffingwell Channel between Flaxman Island and Brownlow Point, and changes in beach-pebble lithology suggest that the major passes in the Plover Islands also developed on the sites of former river valleys (Hopkins and Hartz, 1978b). Given these observations, it is reasonable to assume that some of the other major passes between barrier islands may lie on the sites of former river valleys.

Based on these inferences, it seems probable that the Colville River cut a valley extending generally northward from the present river mouth and that the Sagavanirktok River flowed westward, a few kilometers north of the Return Islands to join the Colville paleovalley about 30 km northwest of Oliktok Point (fig. 2.1). The Kuparuk River paleovalley may have extended northward between Egg and Stump Islands, joining the Sagavanirktok River paleovalley just to the north. The paleovalley of the Shaviovik River has

not yet been defined, but the widespread distribution of Flaxman Boulders north and east of Point Brouwer indicates that it did not extend anywhere east of Newport Entrance between Karluk and Pole Islands. The Shaviovik paleovalley probably extends northward through Newport Entrance or northwestward through Challenge Entrance between Belvedere and Challenge Islands. As noted, the Staines River evidently flowed northward through Leffingwell Channel between Flaxman Island and Brownlow Point between 5,000 and 2,000 years ago and perhaps earlier. One cannot even guess the location of the Canning, Staines, and Shaviovik paleovalleys on the open continental shelf to the north.

Appendix 2

References cited

Barnes, P. W., and Hopkins, D. M., eds., 1978, Geological sciences, in Environmental Assessment of the Alaskan Continental Shelf, Interim Synthesis; Beaufort/Chukchi: National Oceanic and Atmospheric Administration and U.S. Bureau of Land Management, Boulder, CO, p. 101-133.

Blouin, S., Chamberlain, E., Sellmann, P., and Garfield, D., in press, Subsea penetrometer studies, Prudhoe Bay, Alaska: U.S. Army Cold Regions Research and Engineering Laboratory Report 98.

Chamberlain, E. J., Sellmann, P. V., Blouin, S. E., Hopkins, D. M., and Lewellen, R. I., 1978, Engineering properties of subsea permafrost in the Prudhoe Bay region of the Beaufort Sea: Proceedings of the Third International Conference on Permafrost, Edmonton, July 1978, p. 629-635.

Harrison, W. D., and Osterkamp, T. E., 1977, Subsea properties; probing thermal regime and data analysis; National Oceanic and Atmospheric Administration, Environmental Assessment of the Alaskan Continental Shelf: Annual reports of principal investigators for the year ending March, 1977, v. 17, Hazards, p. 424-466.

Hopkins, D. M., 1977, Offshore permafrost studies, Beaufort Sea; National Oceanic and Atmospheric Administration, Environmental Assessment of the Alaskan Continental Shelf: Annual reports of principal investigators for the year ending March, o977, v. 16, Hazards, p. 396-518.

Hopkins, D. M., and Hartz, R. W., 1978a, Shoreline history of Chukchi and Beaufort Seas as an aid to predicting offshore permafrost conditions: Annual reports of principal investigators for the year ending March, 1978, in press.

_____1978b, Coastal morphology, coastal erosion, and barrier islands along the Beaufort Sea coast: U.S. Geological Survey Open File Report 78-1063, 54 p.

Hopkins, D. M., and Robinson, S. W., 1979, Radiocarbon dates from the Chukchi and Beaufort Sea coasts, in Alaskan Accomplishments Circular, Part B., in press.

Iskander, I. K., Osterkamp, T. E., and Harrison, W. D., 1978, Chemistry of interstitial water fr-m the subsea permafrost, Prudhoe Bay, Alaska: Proceedings of the Third International Conference on Permafrost, Edmonton, July 1978, p. 92-98.

Osterkamp, T. E., and Harrison, W. D., 1976, Subsea permafrost at Prudhoe Bay, Alaska, drilling report and data analysis: University of Alaska Geophysical Institute, Report UAG-R-245.

Page, F. W., and Iskander, I. K., 1978, Geochemistry of subsea permafrost at Prudhoe Bay, Alaska: U.S. Army Cold Regions Research and Engineering Laboratory Report 78-14, 70 p.

Reimnitz, E., and Ross, R., 1979, The Flaxman boulders in Stefansson Sound; a survey of the boulder patch, in Barnes, P., and Reimnitz, E., eds., Geologic processes and hazards of the Beaufort Sea shelf and coastal regions: Quarterly report, October through December 1978 to National Oceanic and Atmospheric Administration, Outer Continental Shelf Environmental Assessment Project, 10 p.

Rodeick, C., 1975, The origin, distribution, and depositional history of gravel deposits on the Beaufort Sea continental shelf, Alaska: San Jose State University, M.S. thesis, 87 p.

Rogers, J., and Morack, J., 1977, Beaufort Sea coast permafrost studies; National Oceanic and Atmospheric Adminsitration, Environmental Assessment of the Alaskan Continental Shelf: Annual reports of principal investigators for the year ending March, 1977, v. 17, Hazards, p. 467-510.

Sellmann, P. V., Chamberlain, E., Ueda, H. T., Blouin, S. E., Garfield, D., and Lewellen, R. I., 1977, CRREL-USGS subsea permafrost program Beaufort Sea, Alaska: U.S. Army Cold Regions Research and Engineering Laboratory Special Report 77-41, 19 p.

Appendix 3A

MODERN POLLEN RAIN ON THE ARCTIC SLOPE OF ALASKA - SOME NEW DATA

by

Robert E. Nelson

Branch of Alaskan Geology
U. S. Geological Survey
Menlo Park, California 94025

and

Dept. of Geological Sciences *
University of Washington (AJ-20)
Seattle, Washington 98195

INTRODUCTION

In a previous report (Nelson, 1978), I presented modern pollen spectra for ten sites along the Beaufort and Chukchi Sea coasts. Data are presented here for an additional eight sites, three of which are coastal while the other five lie inland along the Colville River (Fig. 3A.1 and Table 3A). In addition, a correction to the initial report is made: the location of sample 77ANr31b on the eastern Beaufort Sea coast was incorrectly shown some 15 km east of its actual position in the initial report. The data for this sample are presented again here, with the correct sample location indicated.

Preparation and counting of the samples followed the same procedures outlined in the previous report (Nelson, 1978) and need not be discussed in detail here. The pollen percentages in the spectra are calculated from the total pollen present and identifiable, exclusive of pteridophyte spores.

RESULTS

Only one new sample is reported from the Chukchi Sea coast. The spectrum from sample 76ANr10c, from Nokotlek Point, east of Icy Cape, is similar to that from sample 76ANr5 from Icy Cape (Nelson, 1978), with regards to the principal woody taxa (Betula, Alnus, and Salix), although heaths (Ericales) are more important elements in the pollen rain at Nokotlek Point. The most significant difference between the samples is the decreased importance of sedges (Cyperaceae) at Nokotlek Point, accompanied by a relatively high

---

* Please use this address for any correspondence.

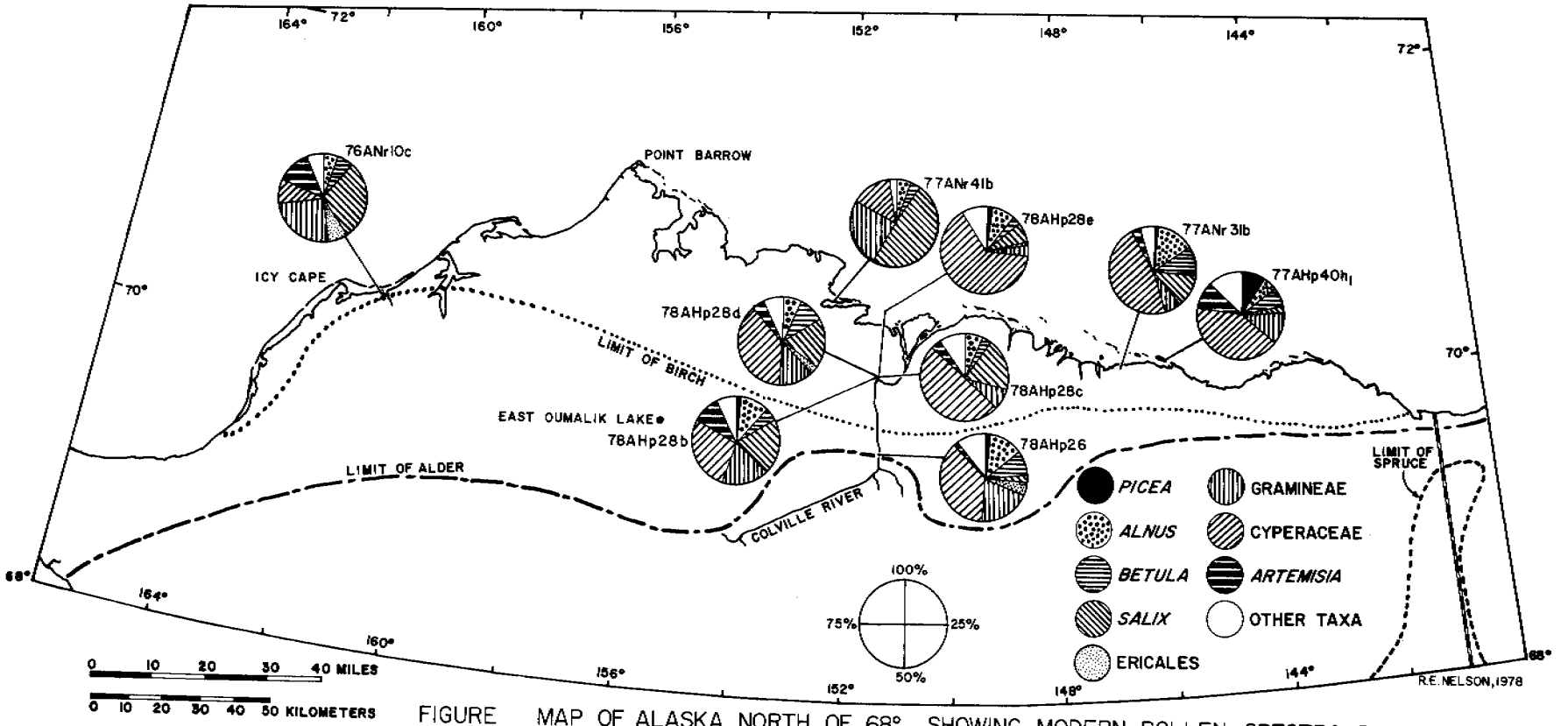

FIGURE 3A-1: MAP OF ALASKA NORTH OF 68°, SHOWING MODERN POLLEN SPECTRA REPORTED IN THIS STUDY. THE LOCATION OF SAMPLE 77ANr31b WAS INCORRECTLY INDICATED IN NELSON (1978); ITS CORRECT LOCATION IS SHOWN HERE. DISTRIBUTION LIMITS FOR SPRUCE, ALDER AND BIRCH FROM HULTÉN (1968) AND VIERECK AND LITTLE (1972), MODIFIED FOR BIRCH IN THE ICY CAPE REGION.

TABLE 3A.1.

SUPPLEMENTAL DATA FOR SAMPLES PRESENTED IN THIS REPORT

Sample number	Grains counted	Sample type	Local Environment and surrounding vegetation	Other taxa * >1% of Σ
76-ANr-10c	425	moss polster	Shallow swale below eroding sandy bluff; surrounded by Elymus arenarius, Carex, Salix, some Dryas, rare Ledum and Cassiope	Dryas - 1.2%
77-AHp-40h$_1$	243	surface mud, dry pond	Dry tundra, dominated by short Carex, Eriophorum, Gramineae and Cladonia; Cardamine, Papaver and Taraxacum on nearby bluff faces	Cruciferae - 9.9%
77-ANr-31b	245	surface mud, dry pond	Carex, Eriophorum and Gramineae dominant, with admixed Salix	none
77-ANr-41b	560	moss polster	Eriophorum-Carex-Salix marsh	none
78-AHp-26	466	moss polster	Moss bog with Eriophorum tussocks that are being colonized by a dry Carex. 10-cm high Salix shrubs and prostrate heaths nearby	Caryophyllaceae ..7%
78-AHp-28b	409	moss polster	Drained thaw lake; vegetation discontinuous. Salix reticulata, with scattered tufts of Carex and a grass, large patches of Dryas and some Potentilla.	Ranunculaceae - 1.0% Leguminosae - 2.2%
78-AHp-28c	439	moss polster	Sedge-moss marsh, with nearby low slopes covered with a Salix reticulata-sedge mat; upper slopes covered with Dryas, and top of slopes support 60-cm willows.	Chenopodiineae - 1.4% Dryas - 2.7%
78-AHp-28d	376	algal mud from puddles	same as sample 78-AHp-28c	Dryas - 1.6% Leguminosae - 1.3% unknown - 1.1%
78-AHp-28e	413	moss polster	Recently-drained thaw lake, presently dominated by Arctostaphylos and Cassiope, with scattered Salix, Dryas, grasses and sedges. Site was apparently a sedge	Dryas - 3.6% Saussurea - 6.1%

TABLE 3A.1.

SUPPLEMENTAL DATA FOR SAMPLES PRESENTED IN THIS REPORT

Sample number	Grains counted	Sample type	Local Environment and surrounding vegetation	Other taxa * >1% of Σ
76-ANr-10c	425	moss polster	Shallow swale below eroding sandy bluff; surrounded by *Elymus arenarius*, *Carex*, *Salix*, some *Dryas*, rare *Ledum* and *Cassiope*	*Dryas* - 1.2%
77-AHp-40h$_1$	243	surface mud, dry pond	Dry tundra, dominated by short *Carex*, *Eriophorum*, Gramineae and *Cladonia*; *Cardamine*, *Papaver* and *Taraxacum* on nearby bluff faces	Cruciferae - 9.9%
77-ANr-31b	245	surface mud, dry pond	*Carex*, *Eriophorum* and Gramineae dominant, with admixed *Salix*	none
77-ANr-41b	560	moss polster	*Eriophorum*-*Carex*-*Salix* marsh	none
78-AHp-26	466	moss polster	Moss bog with *Eriophorum* tussocks that are being colonized by a dry *Carex*. 10-cm high *Salix* shrubs and prostrate heaths nearby	Caryophyllaceae - 7.7%
78-AHp-28b	409	moss polster	Drained thaw lake; vegetation discontinuous. *Salix reticulata*, with scattered tufts of *Carex* and a grass, large patches of *Dryas* and some *Potentilla*.	Ranunculaceae - 1.0% Leguminosae - 2.2%
78-AHp-28c	439	moss polster	Sedge-moss marsh, with nearby low slopes covered with a *Salix reticulata*-sedge mat; upper slopes covered with *Dryas*, and top of slopes support 60-cm willows.	Chenopodiineae - 1.4% *Dryas* - 2.7%
78-AHp-28d	376	algal mud from puddles	same as sample 78-AHp-28c	*Dryas* - 1.6% Leguminosae - 1.3% unknown - 1.1%
78-AHp-28e	413	moss polster	Recently-drained thaw lake, presently dominated by *Arctostaphylos* and *Cassiope*, with scattered *Salix*, *Dryas*, grasses and sedges. Site was apparently a sedge marsh not long ago.	*Dryas* - 3.6% *Saussurea* - 6.1%

percentage of Artemisia (12.0%). Local topography at Nokotlek Point is considerably more irregular than at Icy Cape, and the resulting improvement in drainage is probably the main reason why Artemisia is more abundant at Nokotlek Point. Surprisingly, however, the nearby presence of dwarf birch (Betula nana), reflected in the abundance of Betula pollen (53.7%) in sample 76ANr15b (Nelson, 1978) from only two kilometers distant, is not strongly indicated in the pollen spectrum from sample 76ANr10c. This probably reflects a dominance of onshore winds in the area, which would tend to blow any pollen from the scattered birches farther inland rather than towards the more coastal sample site 76ANr10c.

The 44.7% Salix reported from the Kogru River area (Nelson, 1978, sample 77ANr43) was considered to be unusually high and possibly a spurious value, and so a second sample from a nearby site was analysed (this report, sample 77ANr41b). The spectrum from this second analysis, which includes 49.6% Salix, confirms that willows dominate the pollen rain in this area.

Sample 77AHp40h_1, from the eastern end of Flaxman Island, is a sample of surficial pond mud from the same site as moss polster 77AHp40h_2 (Nelson, 1978). The differences between the spectra deserve some comment. Spruce (Picea) pollen is much more abundant in the pond sediment (9.1%) than in the moss polster (2.2%), while sedges are only 42.0% in the pond mud, compared to 69.3% in the moss polster. Artemisia, which was only 1.7% of the moss polster spectrum, comprises 9.5% of the pond mud pollen, and Cruciferae, which were absent in the polster, account for 9.9% of the pollen in the pond mud. The differences between these samples, which were collected less than 25 m apart, illustrate how strongly local conditions can influence tundra pollen spectra, and why caution must be taken in interpreting them. The moss polster spectrum, in this instance, more closely approximates the

local flora than does that from the pond mud, although the pond mud pollen may be the better indicator of regional pollen rain.

Four samples from near Ocean Point, and one from further upstream on the Colville River, provide data for the interior coastal plain, a large region where the only published spectrum to date has been that of Livingstone (1955) from East Oumalik Lake (location shown in Fig. 3A.1). If one recalculates his data to exclude pteridophyte spores and grains "crushed beyond recognition" (i.e., to include only identifiable pollen grains in the basic pollen sum), his abundances for spruce, birch and alder are all higher than those found in the Colville River samples. However, since his spectrum was derived from surficial lake sediment and mine were from moss polsters, it is possible that these differences represent no more than a more accurate representation of local vegetation in moss polster spectra than in those from lake sediments, similar to the situation at Flaxman Island discussed above.

Sample 78AHp26, taken from along the Colville River very near the northern limit of alders, is surprisingly similar to sample 77ANr31b from near Bullen Point on the Beaufort Sea coast, considerably beyond the alder limit (Fig. 3A.1). Grass is less abundant, and willows more so, in the coastal sample than in the inland one. Ericales and Caryophyllaceae are insignificant (<1% of the basic pollen sum) in sample 77ANr31b, but comprise 5.2% and 7.7% of the pollen in sample 78AHp26, respectively. No climatic significance can be assigned to these differences, however, since the heaths and caryophylls are insect-pollinated and their presence in the pollen spectrum is most likely a local phenomenon. The differences in the percentages of grass and willow pollen between the samples could be merely a reflection of differences in drainage conditions at the two sites.

Four spectra from near Ocean Point on the Colville River show fairly wide variation in individual taxa, although all are unmistakeably tundra

assemblages. Spruce, alder and birch combined account for less than 20% of the total pollen present, while Salix comprises 17.6-19.6% of the spectra in three samples, but only 6.5% in the fourth. Cyperaceae range from 27.9-64.9%, and Artemisia from insignificant levels (less than 1%) to 9.3% of the total. Other herbs are present in wide variety, but only Dryas and Leguminosae comprise over 1% of the basic pollen sum in more than one sample.

Acknowledgments

I would like to thank D. M. Hopkins for providing me the samples from Flaxman Island and the Colville River, and for providing vegetational and geomorphic information pertinent to the Colville River samples. This work was carried out at the facilities of the Quaternary Research Center, University of Washington.

REFERENCES CITED

Hultén, E., 1968: Flora of Alaska and neighboring territories. Stanford University Press; 1008 p.

Livingstone, D. A., 1955: Some pollen profiles from Arctic Alaska. Ecology, v. 36, p. 587-600.

Nelson, R. E., 1978: Modern pollen rain on the Beaufort and Chukchi Sea coasts, Alaska, Appendix IVb to D. M. Hopkins and R. W. Hartz, Offshore permafrost studies, Beaufort Sea, in Environmental Assessment of the Alaskan continental shelf, Annual reports of principal investigators for the year ending March, 1978 (in press).

Viereck, L. A. and E. L. Little, Jr., 1972: Alaska trees and shrubs. U. S. Dept. of Agriculture, Handbook No. 410; 265 p.

Appendix 3B

REPORT ON POLLEN FROM BOREHOLES PB-3 AND PB-8

by

Robert E. Nelson

Branch of Alaskan Geology
U. S. Geological Survey
Menlo Park, California 94025

and

Dept. of Geological Sciences *
University of Washington (AJ-20)
Seattle, Washington 98195

INTRODUCTION

Boreholes PB-3 and PB-8 were drilled near Prudhoe Bay (Fig. 3B.1) in early 1976 and 1977, respectively. Complete, detailed stratigraphies of both boreholes are presented in Hopkins and Hartz (1978); generalized stratigraphic profiles of the upper parts of the boreholes are shown here in Figure 3B.2.

Samples from six horizons in Borehole PB-3, and nine levels in Borehole PB-8, were processed for pollen extraction in the laboratory of Thomas A. Ager (U. S. Geological Survey, Reston, Virginia, 22092). Prepared slides from each of these samples were then forwarded to me for study.

RESULTS AND DISCUSSION

Percentage pollen diagrams for the horizons studied in Boreholes PB-3 and PB-8 are presented in Figure 3B.3.

In Borehole PB-3, a single grain of *Abies*, most likely reworked from older strata, was encountered in sample 02 at a depth of slightly less than one meter in the sediment. Pine (*Pinus*) is represented by scattered grains, while spruce (*Picea*) is consistently present in amounts of 5-10% of the total pollen. Both alder (*Alnus*) and birch (*Betula*) pollen are present in amounts equalling or exceeding their abundance in the four modern marine spectra previously reported (Nelson, 1978), although alder declines from just over

---

* Please use this address for any correspondence.

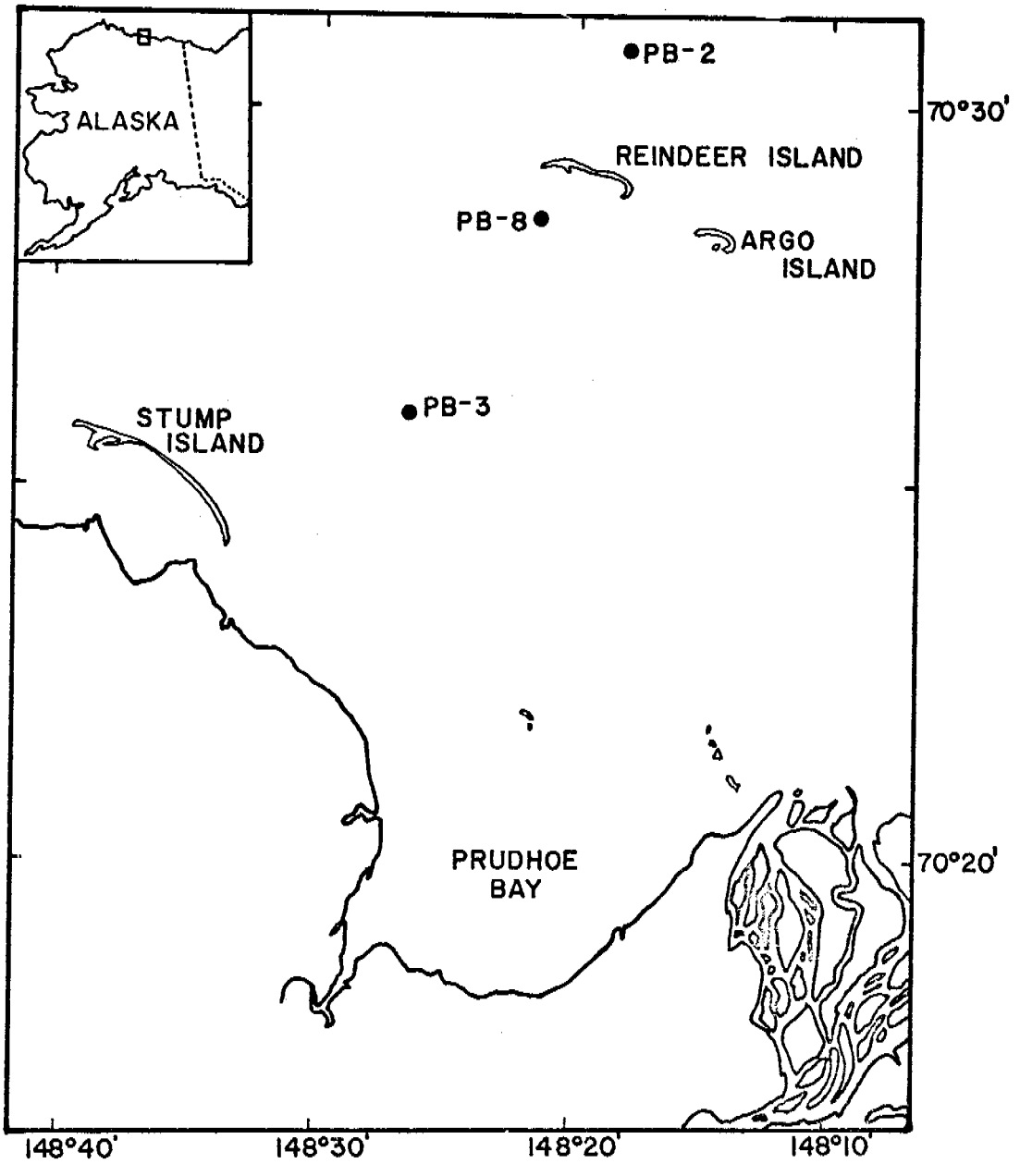

FIGURE 3B.1. INDEX MAP OF THE PRUDHOE BAY AREA, SHOWING LOCATIONS OF BOREHOLES STUDIED FOR POLLEN CONTENT. DATA FOR BOREHOLE PB-2 WERE REPORTED IN NELSON (1978).

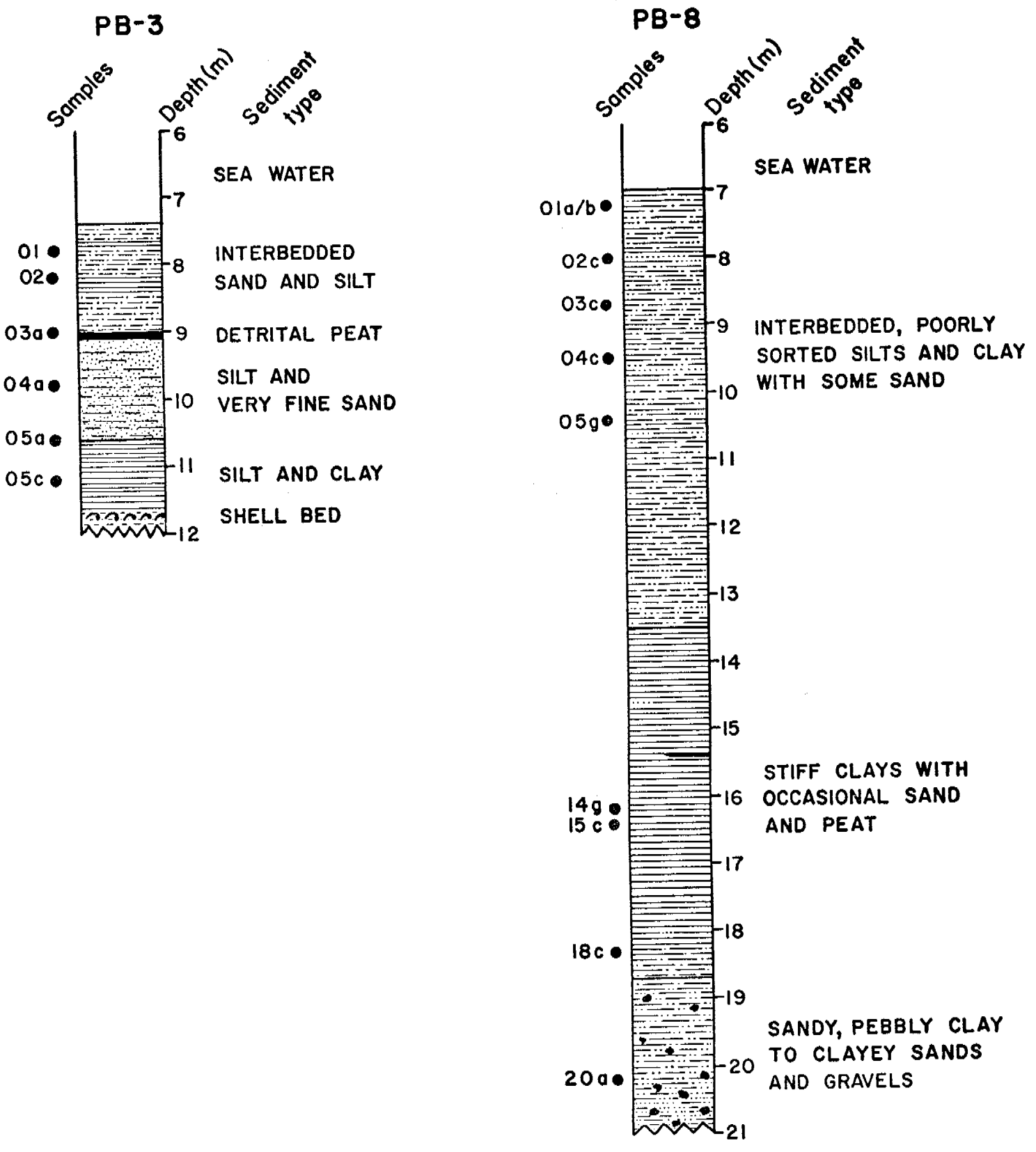

FIGURE 3B.2. STRATIGRAPHY OF THE UPPER PARTS OF BOREHOLES PB-3 AND PB-8, MODIFIED FROM HOPKINS AND HARTZ (1978). HORIZONS ANALYSED IN THIS STUDY ARE INDICATED TO THE LEFT OF EACH COLUMN.

FIGURE 3B-3

PERCENTAGE POLLEN DIAGRAMS FOR SELECTED SAMPLE HORIZONS IN BOREHOLES PB-3 AND PB-8.

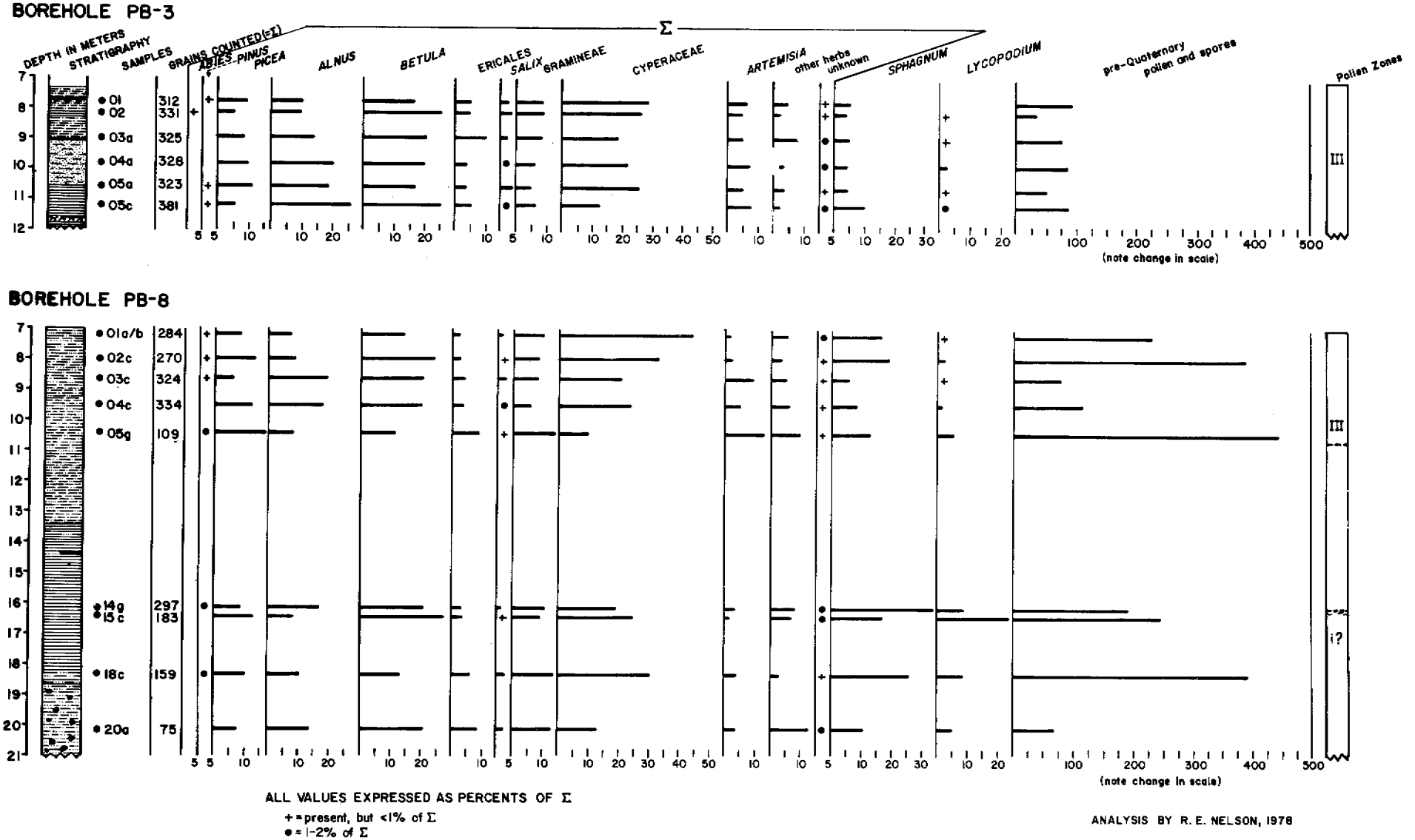

25% of the pollen sum at the base of the sampled section to less than 10% of the total at the uppermost sample horizon. Pollen of willows (Salix), grass (Gramineae), and heaths (Ericales) are present in abundances comparable to those seen in the modern spectra, but sedges (Cyperaceae) are consistently less important in the PB-3 spectra than in the modern ones. Spores of Sphagnum and Lycopodium, and reworked pre-Quaternary pollen and spores, are all about as abundant in the PB-3 spectra as in modern pollen spectra from Beaufort Sea shelf sediments.

The percentages of alder, birch, and sedge pollen in the PB-3 samples are comparable to those from all but the uppermost two samples from Borehole PB-2 (Nelson, 1978), but spruce pollen in PB-3 is only equalled in abundance by the bottom six PB-2 spectra. Grass pollen, however, is considerably more abundant in the PB-2 samples than in those from PB-3, and both Sphagnum and Lycopodium spores also are typically more abundant in the PB-2 spectra. Significantly, the sedge:grass ratios in the PB-3 spectra, while not as high as the 5:1 ratio characteristic of modern spectra, are still consistently higher than in those from almost every level sampled in Borehole PB-2.

The differences between the pollen spectra from Boreholes PB-2 and PB-3 indicate that it is unlikely the units studied are of the same age. Since the PB-3 spectra are clearly of nonglacial character, it seems likely that this portion of the core is of Holocene age. Since alder did not become abundant on the Arctic Slope until mid-Holocene time (Livingstone, 1957; Colinvaux, 1964a), this part of the core probably represents no more than the latter half of the Holocene, and is assigned to Livingstone's (1955) Zone III.

The pollen spectra from Borehole PB-8 are much more problematic than those from PB-3. An initial indication of this is the relatively high proportion of reworked, pre-Quaternary pollen and spores encountered in samples from this core (Fig. 3B.3). Pollen spectra from the upper four samples

are similar to those from Borehole PB-3, although Sphagnum tends to be more abundant in the PB-8 spore flora than in PB-3. The pollen spectrum from the fifth sample, number 05g, seems to be of questionable value. Quaternary pollen was very scarce in this sample, and the pollen present is almost evenly divided among all major taxa. Reworked pollen and spores were also more abundant in this sample than in any other so far studied, reaching almost 450% of the basic pollen sum (Σ).

The bottom four pollen spectra from Borehole PB-8 differ from the upper part of the core in that both Sphagnum and Lycopodium are more abundant in the spore flora than they are either higher in the core or in PB-3. Sedge:grass ratios in the upper four samples range from 2:1 to 4:1, similar to their range in samples from core PB-3, but in the bottom four samples from PB-8 they are 2:1 or less. Spruce, alder and birch are present in abundances similar to those in the upper part of the core, as well as in PB-3 and in PB-2.

The overall character of the bottom four spectra in PB-8, however, is very similar to spectra from the lower part of the pollen diagram from Borehole PB-2 (Nelson, 1978), of presumed Sangamon age. If this is indeed the case, then there exists an unconformity in the section, probably at the contact between the upper, poorly sorted unit and the lower stiff clays encountered in the drilling of PB-8 (Fig. 3B.2). The hiatus represented by this unconformity may well include all of Wisconsin time, as indicated by the absence of pollen spectra indicative of an herbaceous tundra lacking significant woody taxa, which is characteristic of Wisconsin environments of the Arctic Slope (Livingstone, 1955; Colinvaux, 1964a, 1965).

The similarities between the PB-2 pollen record (Nelson, 1978) and Colinvaux's (1964b) Zone i at Imuruk Lake on Seward Peninsula are considerable, and have been discussed in detail elsewhere (Nelson, 1979), where Colinvaux's (1964b) zone designation has been applied to all but the upper two samples in

Borehole PB-2. Since the lower part of the PB-8 pollen profile appears correlative to that of Borehole PB-2, this useage is retained and the lower part of Borehole PB-8 is tentatively assigned to Pollen Zone i. The upper portion of the PB-8 profile, which is more likely correlative to that of Borehole PB-3, is assigned to Livingstone's (1955) Pollen Zone III, representing the latter half of Holocene time. These conclusions support the stratigraphic interpretations for Beaufort Sea shelf sediments as presented in Hopkins and Hartz (1978, Appendix V).

ACKNOWLEDGMENTS

I would like to thank David M. Hopkins for providing the samples from Boreholes PB-3 and PB-8 for my study, and Thomas A. Ager for very kindly processing the samples for me. This work was carried out at the Quaternary Research Center, University of Washington.

REFERENCES CITED

Colinvaux, P. A., 1964a: Origin of ice ages: pollen evidence from Arctic Alaska. Science, 145:707-708.

-----, 1964b: The environment of the Bering Land Bridge. Ecol. Monogr., 34:297-329.

-----, 1965: Pollen from Alaska and the origin of ice ages - reply to W. L. Donn and M. Ewing. Science, 147:632-633.

Hopkins, D. M., and R. W. Hartz, 1978: Offshore permafrost studies, Beaufort Sea, in Environmental assessment of the Alaskan continental shelf, Annual reports of Principal Investigators for the year ending March, 1978 (in press).

Livingstone, D. A., 1955: Some pollen profiles from Arctic Alaska. Ecology, 36: 587-600.

-----, 1957: Pollen analysis of a valley fill near Umiat, Alaska. Am. Jour. Sci., 255:254-260.

Nelson, R. E., 1978: Final report on pollen from Borehole PB-2, Appendix IVa to D. M. Hopkins and R. W. Hartz, Offshore permafrost studies, Beaufort Sea, in Environmental assessment of the Alaskan continental shelf, Annual reports of Principal Investigators for the year ending March, 1978 (in press).

-----, 1979: Quaternary environments of the Arctic Slope of Alaska. University of Washington, M. S. thesis.

Appendix 4

RADIOCARBON DATES FROM THE CHUKCHI AND BEAUFORT SEA COASTS

D. M. Hopkins and S. W. Robinson

As a contribution to the Outer Continental Shelf Environmental Assessment Program, funded by the Bureau of Land Management and managed by the National Oceanic and Atmospheric Administration, we present here radiocarbon analyses for 22 samples from the coast and continental shelf of the Beaufort and Chukchi Seas (Table 4.1). They show that:

(a) Leeward accumulations of eolian sand on bluffs along the western sides of the Canning and Sagavanirktok Rivers (fig. 4.1a) accumulate in two places at rates of 0.9 and 1.25 mm/year. The active cliff-head dunes were initiated within the last 5,000 years in the three places where relevant samples have been dated;

(b) A leeward sand accumulation on the east end of Flaxman Island no longer has a source and is no longer active. Evidently the sand accumulated at a time when sea level was lower and the Staines River flowed through the present site of Leffingwell Channel between Flaxman Island and Brownlow Point. Dated samples indicate that the leeward sand accumulation on Flaxman Island began to develop a few centuries prior to 4,900 years ago and thus that the river was flowing through the area at that time. Deposition ceased shortly after 2,400 years ago, probably because rising sea level inundated Leffingwell Channel.

(c) A white or pink volcanic ash has been recognized in Holocene deposits near the east mouth of the Canning River, on Flaxman Island, and in the Putuligayuk River valley. When dated, this ash layer will be useful in making field estimates of the age of young aeolian, thaw lake, alluvial, or archaeological deposits along the

eastern Beaufort Sea coast. The ash layer is bracketed by samples dated as 3,300 and 3,950 years old at the mouth of the east branch of the Canning River, and the ashfall probably took place about 3,700 years ago. However, a sample which, according to our records, came from above the ash on Flaxman Island, yielded a radiocarbon age of 4,890 years. Other samples from the same section await radiocarbon analysis, and when complete these analyses will permit us to evaluate the significance of the seemingly anomalous Flaxman Island date. Radiocarbon samples bearing on the age of the ash were also collected in Holocene alluvium of the Putuligayuk River but have not yet been dated.

(d) Peat accumulates in low-center polygons at Nokotlek Point near Icy Cape (fig. 4.1b) at a rate of about 0.25 mm/year. Peat deposits there are about as thick as any seen along the Chukchi or Beaufort Sea coasts, so this may be fair approximation of the general rate of peat accumulation in marshes of the North Slope.

(e) A 1.5-m thick sequence of thaw-lake deposits near Cape Halkett accumulated within a 200-year interval, and a site south of Nokotlek Point has lain within the basin of two successive thaw lakes during the last 9,100 years. These observations are consistent with observations in the Old Crow Flats (W. W. Pettapiece, in Lowden and Blake, 1977, p. 17) and on the Seward Peninsula (D. M. Hopkins, unpublished data, 1978) that individual thaw lakes rarely persist on the landscape longer than 1,500 years.

(f) Active ice wedges near Cape Halkett have been growing at a rate of about 1 mm/year, but active ice wedges in the Wainwright-Nokotlek Point area are growing much less rapidly, at a rate of only about

0.2 mm/year (table 4.2 and fig. 4.2). This is consistent with experimental studies that indicate average growth rates of about 1 mm/year near Point Barrow and much less than 1 mm/year on Garry Island at the mouth of the MacKenzie River (MacKay and Black, 1973, p. 188).

(g) A prograded delta-like deposit at the mouth of the Kaolak River seems to provide the record of a late summer flood and storm surge about 1,000 years ago which raised water level at least 3 m in the Kuk River estuary system (Hopkins, Hartz, and Robinson, Appendix 5, this report).

References cited

Lowden, J. A. Robertson, I. M., and Blake, W., Jr., 1977, Radiocarbon dates XVII: Geological Survey of Canada Paper 77-7, 25 p.

MacKay, J. R., and Black, R. F., 1973, Origin, composition, and structure of perennially frozen ground and ground ice; a review, in Permafrost the North American Contribution to the Second International Conference: National Academy of Sciences, p. 185-192.

Table 4.2. Age of ice-wedge complexes in various places along the Chukchi and Beaufort Sea coasts.

LOCATION	AGE	RELEVANT RADIO-CARBON DATES	WIDTH OF ICE WEDGES IN M's			MEASUREMENTS[1]	
			Min.	Median	Max.	Number	Method
Chukchi Sea							
Nokotlek Point	<6235 ± 120	I-10329	.25	.40	.70	15	(1)
Nokotlek Point	<8275 ± 135 >9535 ± 150	I-10330 I-10331	1.3	1.75	3.0	4	(1)
Nokotlek Point	<8435 ± 160	I-10332	.35	.85	1.25	20	(1)
South of Wainwright Inlet	<9180 ± 150	I-10368	.70	1.37	2.50	8	(1)
Kaolak River	<1170 ± 45	USGS-500	"Less than 1 meter wide"			"A few"	(2)
Beaufort Sea							
Cape Halkett	<3130 ± 70 >2930 ± 50	USGS-501 USGS-502	2.0-	2.75	3.0+	Approx. 10	(3)

[1] Methods of Measurement

(1) Measured tops of wedges exposed in sea or lake bluff.

(2) Visual estimate.

(3) Measured width of sharply-defined polygon troughs in area of low-center ice-wedge polygons.

RECORD OF A PRE-HISTORIC STORM SURGE IN THE WAINWRIGHT INLET-KUK RIVER AREA

D. M. Hopkins, R. W. Hartz, and S. W. Robinson

Storm surges along the Beaufort and northern Chukchi Sea coasts have occasionally reached heights of 3 m above mean sea level during the present century (Aagard, 1978; Reimnitz and Maurer, 1978). The frequency of these events is not yet known, nor has there been evidence that surges of this height and intensity took place in earlier times. Evidence from the Wainwright Inlet-Kuk River area suggests, however, that storm surges of similar intensity took place in the pre-historic period. During field-work in 1977, we observed features along the Kaolak River which seem to record a storm surge that raised sea level about 3 m above the present level of the confluence of the Kuk and Kaolak Rivers during a late summer storm more than 1,000 years ago.

Kuk River is a tidal estuary connected to the Chukchi Sea by way of Wainwright Inlet, forming an estuary and tidal river system that extends some 60 km southward and inland from the Chukchi Sea coast (fig. 5-1). The lower 38 km of the system is brackish and lies at sea level. A confined delta 4.5 km long separates the estuarine lower Kuk River from the 18-km-long upper Kuk River, which is fresh and flowing but has current speeds and channel form strongly influenced by tides in the estuary. The tidal influence seems to end at the point where the Kaolak and Avalik Rivers join to form the Kuk River.

The Kaolak River, in its lower 5 km, flows in a narrow valley incised into the Cretaceous bedrock of the highest, innermost, and oldest of the three marine terraces comprising the Arctic coastal plain of Alaska (Williams and others, 1977). The meandering channel is confined between

banks consisting alternately of bedrock and the alluvium of a series of alluvial terraces which stood 3.5-4.5, 7, and 14 m above river level on July 22, 197[illegible] en stream discharge was low following about 10 days of dry weather.

The lowest of these terraces slopes more steeply than present-day river grade, standing 3.5 m above river level near the confluence with the Avalik River and 4.5 m above river level at a point 5 km upstream. Field observations indicate that the terrace must be relatively young. Ox-bow lakes and marshes unmodified by thermokarst processes can be observed on the terrace surface, and vertical exposures show that ice wedges are sparse and small. These observations suggest that the 3.5-4.5 m terrace is of Holocene age, and that it was formed at some time within the last 10,000 years.

The 3.5-4.5 m terrace consists in most places of horizontal beds of sandy alluvium 2 to 10 cm thick; concentrations of willow and other plant leaves and driftwood twigs delineate the bedding planes. The only vertebrate remains found consist of a fragment of reindeer antler. However, along the left bank of the Kaolak River at a point 250 m upstream from its confluence with the Avalik River, the flat-bedded alluvium of the 3.5-4.5 m terrace passes downstream into foreset-bedded medium sand with interbeds of twigs and leaves. The inclined beds extend from river level to a height of 3.0 m and are overlain by 0.5 m of flat-bedded peaty fine sand.

Radiocarbon analyses show that the 3.5-4.5 m terrace of the lower Kaolak River formed during a brief period of alluviation approximately 1,000 to 2,000 years ago. Twigs collected at a depth of 3.7 to 3.8 m below the surface of the 4.5 m terrace, 5 km upstream from the river mouth yielded a radiocarbon age of 1,730 $\pm$ 40 years (USGS-499), and twigs collected from

the foreset-bedded sand at the river mouth yielded a radiocarbon age of 1,170 ± 45 years (USGS-500). Although the two samples consist of wood of different ages, the older sample may consist of wood redeposited from slightly older floodplain sediments, and may have been deposited almost simultaneously with the younger sample. No unconformities, paleosols, or *in situ* peat were noted in a measured section at the upstream locality, and there is at least a possibility that the entire 4.5 m of sediment exposed above river level was deposited during a single flood episode, simultaneously with the foreset-bedded sediments at the river mouth.

The 3.5-4.5 m terrace of the lower Kuk River probably was formed during a brief period of high river discharge which coincided with a Chukchi Sea storm surge. The foreset bedding in the terrace deposits at the Kaolak River mouth reflects abrupt decrease in current discharge and seems to indicate that at the time of deposition, the upper Kuk River was ponded at a level 3 m above its level of July 22, 1978. The inclined surface of the Kaolak River terrace must reflect a temporarily steepened river gradient, probably resulting from the inability of the constricted lower Kaolak River valley to accommodate a greatly increased floodwater flow. Although storm surges can occur in the Beaufort and Chukchi Seas at any season, they are most frequent and most severe during September and October (Aagard, 1978; Reimnitz and Maurer, 1978). The rivers of Arctic Alaska experience their highest discharge and peak sediment load during spring snowmelt (Arnborg and others, 1967), but experience occasional floods during late summer and autumn storms, as well. K. Stefansson reports evidence of recent flood levels along the Kaolak and Ketik Rivers as high as 6 m during spring breakup in June 1948 (field notes in files of Branch of Alaskan Geology Technical Data Unit, U.S.G.S., Menlo Park, CA). The abundance of willow leaves in

peaty interbeds suggests that the 3.5-4.5 m terrace of the Kaolak River was deposited during late summer or autumn, rather than during spring.

Study of the terrace deposits along the Kaolak River confirms that flood levels along the Kaolak River may even now occasionally reach levels more than 4.5 m above normal stream grade and that these floods may coincide with intense storm surges.

References cited

Aagard, K., ed., 1978, Physical oceanography and meteorology, in Environmental Assessment of the Alaskan Continental Shelf; Interim Synthesis; Beaufort/Chukchi: National Oceanic and Atmospheric Administration, Boulder, CO, p. 56-100.

Arnborg, L., Walker, H. J., and Peipp, Johan, 1967, Suspended load in the Colville River, Alaska, 1962: Geografiska Annaler, v. 49A, p. 131-144.

Reimnitz, E., and Bruder, K. F., 1972, River discharge into an ice-covered ocean and related sediment dispersal, Beaufort Sea, coast of Alaska: Geological Society of America Bulletin, v. 83, p. 861-866.

Reimnitz, E., and Maurer, D., 1978, Storm surges in the Alaskan Beaufort Sea: U.S. Geological Survey Open File Report 78-593, 26 p.

Williams, J. R., Yeend, W. E., Carter, L. D., and Hamilton, T. D., 1977, Preliminary surficial deposits map of National Petroleum Reserve-Alaska: U.S. Geological Survey Open File Report 77-868, 2 sheets, scale 1:500,000.

ANNUAL REPORT

Contract: RK6-6074
Research Unit: 205
Reporting period: April, 1978-
March, 1979
Number of Pages:

Marine environmental problems in the ice covered Beaufort Sea shelf and coastal regions

Peter Barnes

Erk Reimnitz

Pacific-Arctic Branch of Marine Geology
345 Middlefield Road
Menlo Park, California 94025

April 1, 1979

TABLE OF CONTENTS

I. Summary of objectives, conclusions and implications with respect to OCS oil and gas development.

The present investigation is an expansion and intensification of our earlier studies on the marine geology and modern sedimentary environment off arctic Alaska with emphasis on rates and processes. In particular we have concentrated on phenomena involving ice and its unique influence on the shelf and inshore environment. The marine environment of the arctic shelf poses special problems to offshore development. Faulting, tectonic activity, and sea floor instability are environmentally of lower concern in the Beaufort Sea, when compared to processes and low temperatures involving sea ice. Seven years of study have provided a basic understanding of this unique marine geologic environment. However, many important aspects have yet to be addressed. For example, the major processes involved in ice gouging of the sea floor are reasonably understood, including distribution, densities, gouge trends, rates of gouging, depths of reworking and the variability of gouge formation from year to year. Critical questions remain regarding the interaction of the stamukhi with the continental margin, the distribution and character of gouging in this zone, rates of gouge infilling, and the time of formation of the stamukhi zone. Neither are the effects of the stamukhi zone on oceanographic circulation, sediment disruption and dispersal, and the shelf profile properly understood.

Another area where we have poor understanding involves coastal zone processes. The spring flooding of the sea ice with river water is reasonably well known as a phenomenon but the intensity of the associated processes of transport, scour and ice movement are only poorly understood. Rates of coastal erosion are known to be significant, but the fate of these erosional products, their relationship to river input, and the growth and maintenance of the barrier islands need to be assessed. Inside the 2-m bench where ice rests on the bottom at the end of the winter, a unique sedimentary environment exists where tides and surges set up significant currents. Furthermore, the ice canopy may interact with the seabed causing each to exhibit a unique character.

The past year of field work and subsequent laboratory and office work has resulted in the following observations regarding the arctic nearshore environment.

Preliminary analysis of a series of 60 vibracores taken in the nearshore area between the Sagavanirktok River and the Colville River shows five different environments. Lagoonal and bay sediments are indistinctly laminated sandy silts and clays. Cores in the vicinity of the barrier islands are sands and gravels with an abundance of depositional sedimentary structures. Offshore shoals are characterized by clean well-laminated sands underlain by finer material on the ridge flanks. Off the Colville delta layered sands, silts and peats are replaced seaward beyond 5 m by disrupted or poorly laminated muds, probably related to strudel and ice gouge reworking. The absence of gravels except in the immediate vicinity of the coastal bluffs and barrier islands is of significance to offshore development.

1. Investigations show snow depth and ice thickness correlate negatively, ice-bottom morphology correlates with a stable snow-ridge morphology, and loci of under-ice oil pockets are readily discernible from the surface. Both ice bottom and snow surface relief varied by about 30 cm on wave lengths of about 10 m. Seasonal variability in snow accumulation and wind patterns are expected to modify these observations.

2. A systematic grid of survey lines, coupled with bottom samples and diving observations, provides a detailed description of the size, configuration, surface characteristics, and geology of the boulder patch in Stefansson Sound and suggests the boulders originated as a shallow water lag deposit.

3. Sea floor morphology changed drastically between 1977 and 1978 from waves and currents associated with 1977 open season storms. The changes suggest a) erosion and deposition are episodic, b) maximum observed gouge incisions may be too shallow, and c) shelf sediments are predominantly deposited in gouge incisions.

4. Detailed observation on a recent ice gouge made after the large wave events of 1977 show extremely rapid rates of gouge infilling and reworking. These observations imply a) age of less than 10 to 20 years for gouges on the inner shelf, b) that acoustic measurements of older gouge incisions give values far below the true depth of incision, and c) that open excavations are likely to infill during a summer like that of 1977.

5. A bathymetric survey along the northeast side of Cross Island shows 7 m water depth where the island once was. This is coupled with diving observations which fail to show exposures of Quaternary Gubik Formation. This suggests that the island originated as a constructional form, similar to true barrier islands.

6. Eolian sand deposits are found on the fast ice downwind of gravelly barrier islands in the arctic. One small island exposure lost over 300 tons of sand in eight months, suggesting a deflation rate of 2 mm per winter. Wind winnowing of island surfaces is effective year round, while sediment supply by waves is effective for only two to three months in the arctic. This suggests wind removal of sand as a possible mechanism to explain their coarseness relative to those of lower latitudes, where sand dominates.

7. Vast quantities of sediment slush under-ice ice up to 5 m thick appear to be associated with the 'boulder patch'. The ice formed random-oriented plates and granules in early October 1978. Although of great significance to sediment transport and biological processes as well as to developmental activies, the mechanisms leading to ice growth, accumulation in observed formations, and the process of sediment inclusion remain unknown.

8. Ice cores obtained from the fast ice in the spring of 1978 show a widely distributed 'dirty' ice horizon up to 1 m thick. Sediment concentrations are an order of magnitude greater than would be expected from simple freezing of shelf sea water. Earlier observations show that 'dirty' ice is not present on the inner shelf every year. The accumulation has significant impact on light transmission and the growth of organisms as well as on the sediment transport regime and the thermal and structural character of the fast ice; yet these mechanisms are unknown.

9. The problem of how the shoals of the stamukhi zone interact with ice to control ice zonation is critical to ice management in the seaward part of the lease area. During the past winter there was no multiyear ice on the shelf during freeze-up. Our observations this spring showed massive ridges composed of first year ice clearly associated with shoals northwest of Prudhoe Bay. We also recovered sediments from the stamukhi ridges containing marine shells suggesting displacement from the nearby sea floor. An enigma exists where first year ice, not nearly thick enough to contact the crests of shoals, focused the major ridge building over these bathymetric features.

II. Introduction

A. General nature and scope of study

Arctic continental shelves, where ice is present seasonally for part of the year, comprise 25% of the total world shelf area. Yet the interaction of ice in the regime of sedimentary processes on North American arctic shelves is poorly understood. Investigation of the continental shelf and shores of the Chukchi and Beaufort Seas was initiated in 1970. The primary goal of this program has been to understand both the processes unique to arctic shelves and the role of more conventional processes in temperate latitudes.

B. Specific objectives

Many questions have been raised on the basis of our past investigations, which apparently hold the key to an understanding of the seasonal cycle in the marine environment. It is these tasks that we address in our current research.

1) Process of ice gouging - in particular the repetitive rates of gouging, rates of sediment infilling, seasonal distribution, and the extent to which it occurs outside the area of our past investigations. The ice bottom interactions in the stamukhi zone where the bulk of oceanic energy is expended on the continent needs special emphasis.

2) Shelf sediment transport regime - including ice rafting, anchor ice formation, river effluents, and reworking and resuspension of bottom materials by ice and benthos.

3) The fast-ice zone; its undersurface morphology and its influence on nearshore current circulation, bedforms, sediment transport, permafrost, and on river discharge.

4) An estimation of coastal erosion and its relationship to the formation of offshore islands, submerged shoals, and the stability of the coastal marine environment.

5) Inner shelf oceanography, and its relationship to the sedimentary environment. This includes upwelling in the coastal zone, the dispersal of highly saline (60 $^{o}/_{oo}$) and cold (-5°) water generated in the shallow embayments, lagoons, and river mouths during the winter, and the possibility of anchor ice formation and ice rafting as factors in the sedimentary environment.

6) Outlining the Pleistocene stratigraphy and geologic history of the shelf as an aid to determining a sea level curve for the Beaufort Sea.

7) Delineation of sediment character on the inner shelf from a correlation of available seismic reflection records, samples and drill hole data.

C. Relevance to problems of petroleum development

The character of the arctic continental shelf and coastal area, with year round and seasonal sea ice and with permafrost, faces the developer with many special problems. The interaction of the arctic shelf with the arctic pack ice takes the form of ice gouging and the formation of a large stamukhi zone each winter.

Oil drilling and production during the next several years will probably not extend into the stamukhi zone seaward of the seasonal fast-ice zone. Of critical concern are the ice gouge and strudel scour effects on structures and pipelines. A similar emphasis has been taken by the Canadian Beaufort Sea Project in their more advanced state of knowledge and readiness to lease their outer continental shelf lands (Milne and Smiley, 1976). Any structure which is to be mated with the ocan floor requires data concerning the strength and character of the ocean floor. Furthermore, foundation materials in the form of gravels will be needed for work pads offshore. In addition, the offshore drilling operation may encounter permafrost and associated gas hydrates which could be substantially altered during the process of pumping hot oil up to the sea floor or along the sea floor in gathering and transportation pipelines potentially causing structural failure and blowouts.

III. Current state of knowledge

The state of recent knowledge has been excellently summarized in the Arctic Institute of North America's 1974 publication: The Coast and Shelf of the Beaufort Sea. The bulk of background geologic material for the Alaskan Beaufort shelf has been summarized in articles by Reimnitz, Barnes, Naidu, Short, Walker and others, in this same volume. The OCSEAP Beaufort Sea synthesis volume contains a very useful summary of the current state of knowledge. References to more recent material may be found in the Results and Discussion sections below and in the appended reports. The interested reader is also directed to the comprehensive series of reports resulting from the Canadian Beaufort Sea Project.

Briefly, results to date have clearly established drifting ice as a major influence on the marine geologic and sedimentologic environment of arctic shelves (best summarized in Reimnitz and Barnes, 1974; Barnes and Reimnitz, 1974; and in the 1976 and 1977 Annual Reports).

Major boundaries exist which are related to inner shelf sea ice zonation (Fig. 1). Inside the 2 m contour, ice rests on the bottom at the end of the seasonal growth and generally remains stable and undisturbed through the winter. Seaward from this bottom fast ice, a zone of relatively undisturbed, floating fast ice as much as 2 m thick extends offshore to where it meets the moving ice of the polar pack. At this juncture, shear and pressure ridges develop which are grounded, forming the stamukhi zone. Each of these zones apparently has distinctive sedimentologic, permafrost, morphologic and ice gouge characteristics.

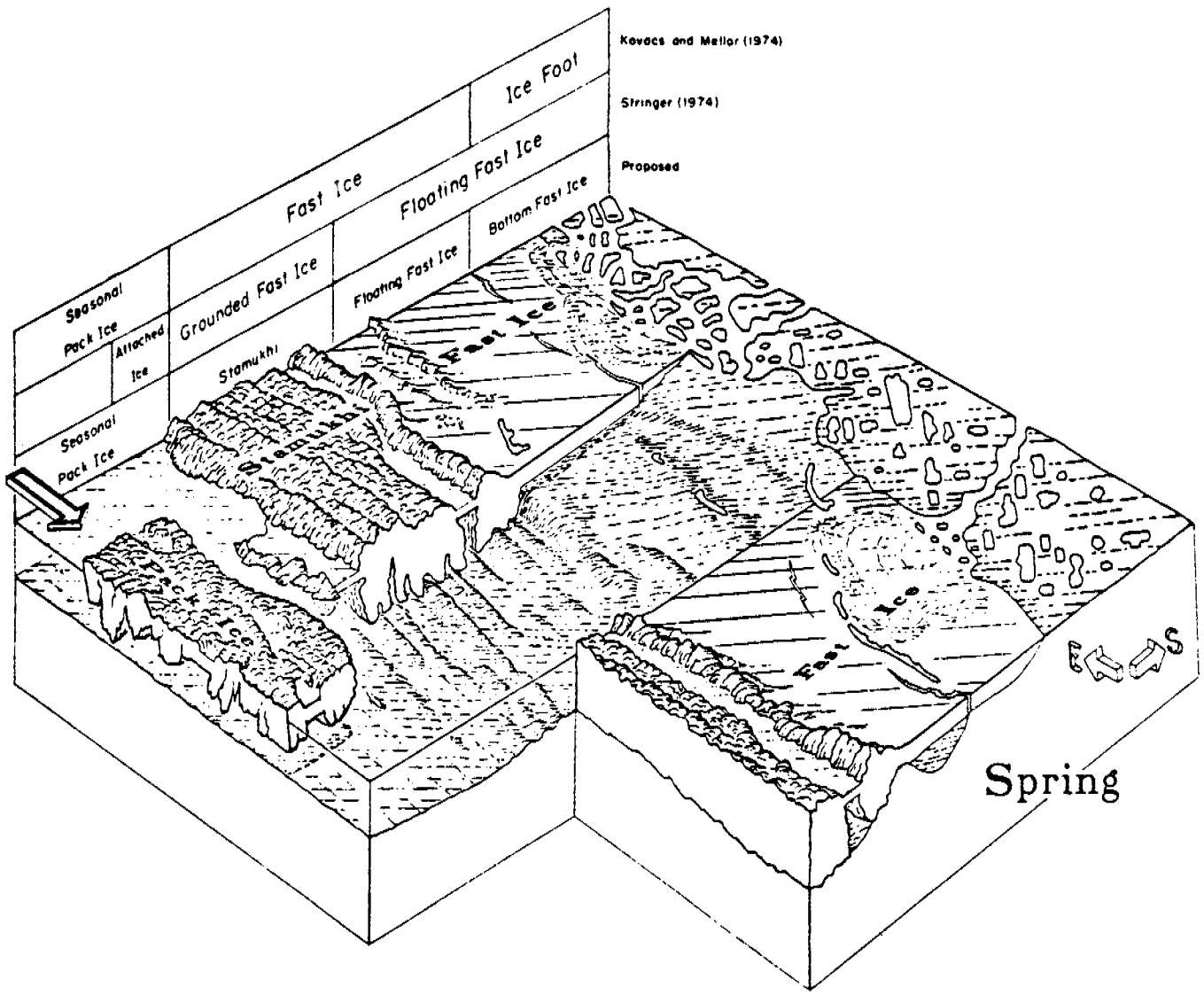

Figure 1. Diagram of an idealized cross-section of the fully developed ice zonation along the Alaskan Beaufort Sea coast at the time of maximum ice growth in spring. Drawing by Tau Rho Alpha.

A rudimentary framework for the processes and related sedimentologic record over the major ice zones can be established (Fig. 2) which relates the relative importance of ice and water as dynamic agents affecting the sea bottom. The major processes involved in each ice zone are:

Bottom fast ice zone:

1) River overflow onto the sea ice and subsequent drainage through strudle holes and cracks causes sea-floor scour depressions and initiates sub-ice sediment transport.

2) Sub-ice tidal and storm surge currents act to maintain and perhaps enlarge tidal channels in lagoons and bays.

3) Storm surges raise sea level as much as 3 m, erode beaches, coastal bluffs, and islands and inundate the coastal plains.

4) Wave action modifies beaches and coasts during the open water season.

5) Ice-push acts on exposed parts of coasts and offshore islands.

6) Ad-freezing of sediments and lowering of sediment temperatures occurs where sea ice is in contact with the bottom.

Floating fast ice zone:

1) Waves and currents result in moderate reworking of the bottom sediments.

2) Ice gouging occurs in exposed areas primarily in winter but to a lesser extent during summer. In years with exceptional storms, gouges on the inner shelf may be obliterated or vastly altered.

3) Bioturbation and sedimentation are most dominant in this zone throughout the year.

4) Fast ice thickness is inversely related to snow depth, forming elongate ice-bottom troughs parallel to the snow ridges formed on the surface by northeast winds (Fig. 3).

5) In some years phenomena apparently involving anchor ice formation concentrate sediments in and beneath the fast-ice canopy.

Stamukhi zone:

1) Ice gouging of bottom reworks sediments to depths in excess of 25 cm in less than 100 years, maximum gouge incisions are probably in excess of 2 m, obliterating sedimentary structures. Resulting sedimentary structures are a discontinuous series of shoestring deposits.

2) Current transport and scour are associated with grounded keels of ice.

3) Control of inner shelf ice character results from coastal configuration and distribution and orientation of submerged shoals. Creation or maintenance of these shoals is probably related to ice-related processes.

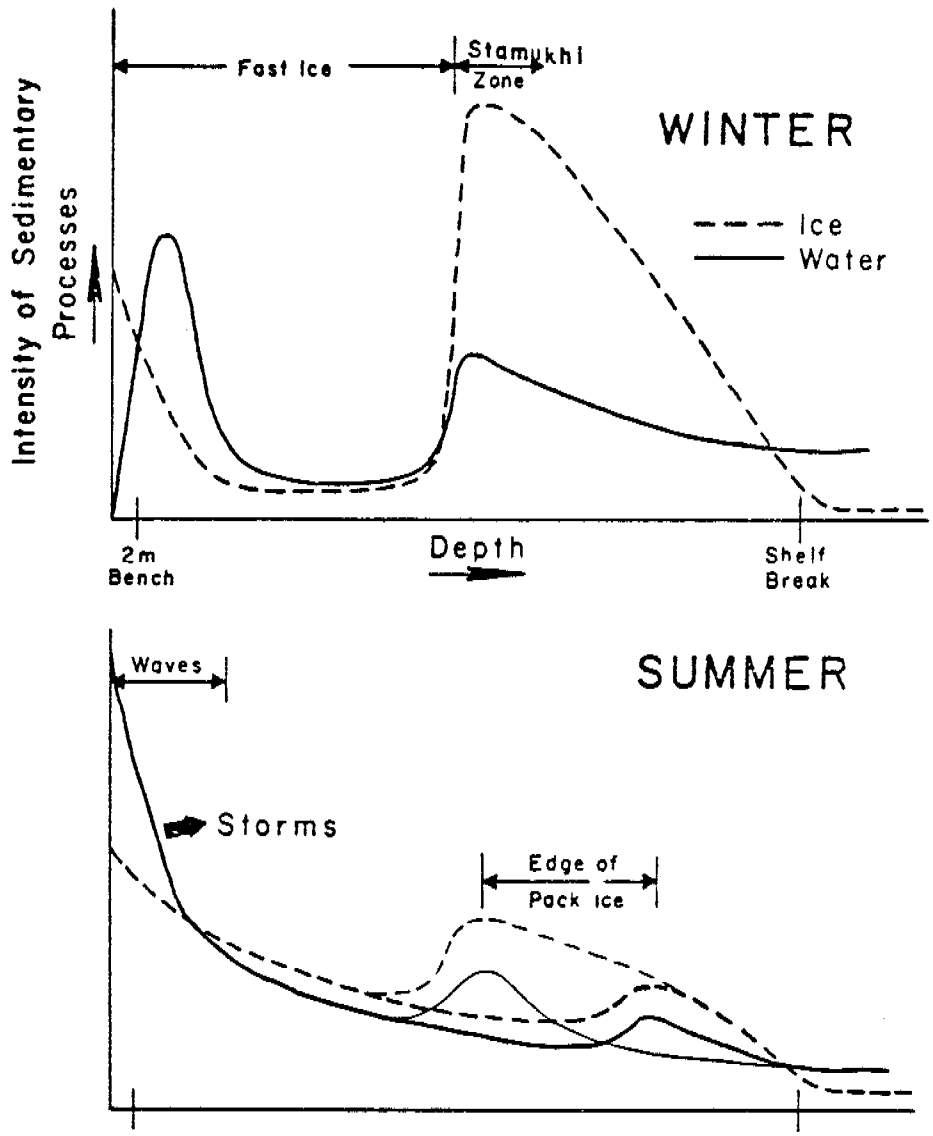

Figure 2. Conceptual model of the relative importance of ice and water as process agents on the bottom sediments of the arctic shelf off northern Alaska.

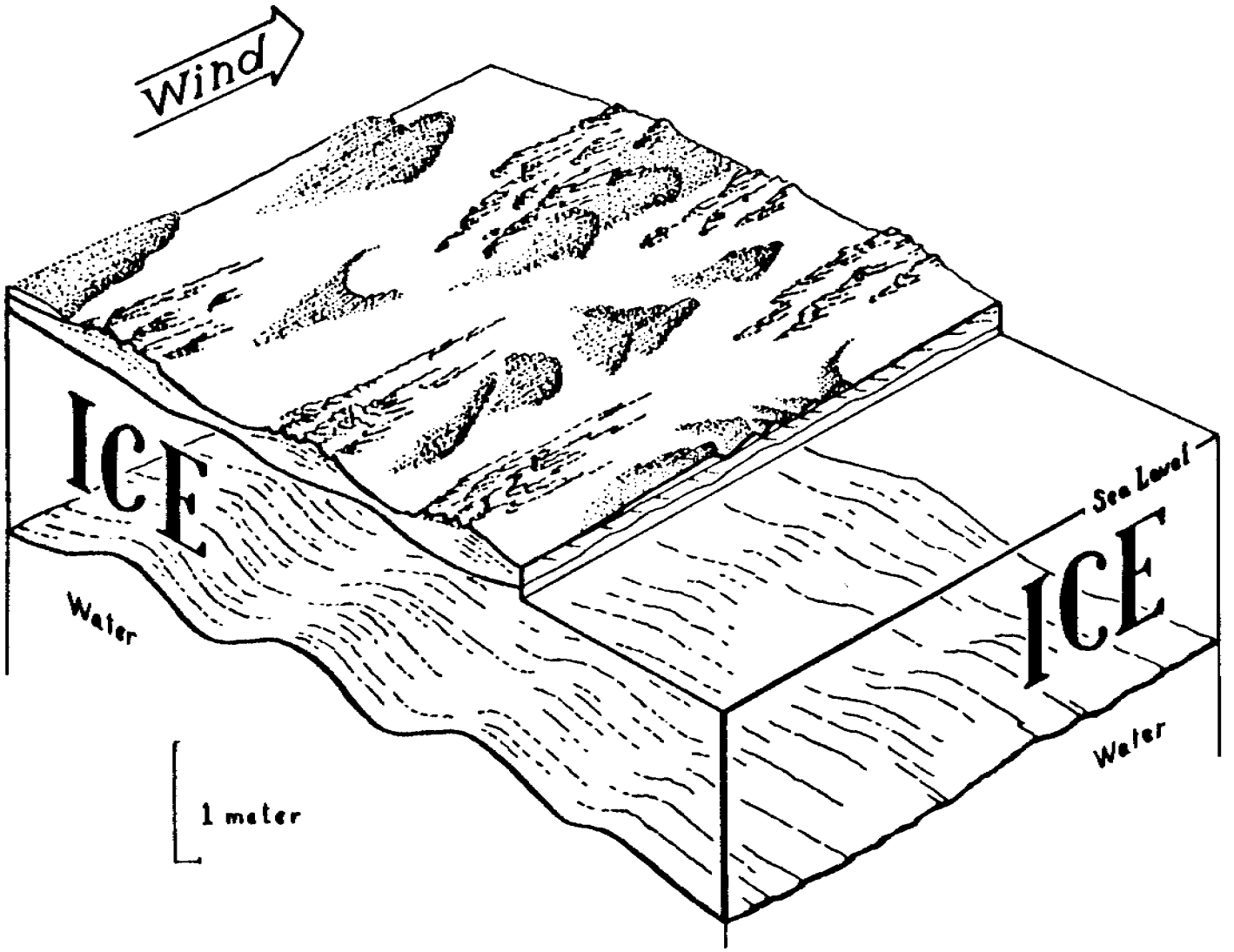

Figure 3. Block diagram by Tau Rho Alpha depicting the relationships between snow patterns and fast-ice morphology.

IV. Study Area

The primary study area includes the Beaufort Sea shelf between Barter Island on the east and Point Barrow on the west with emphasis on an inshore segment between Flaxman Island and Cape Halkett. The adjacent land is a broad, flat coastal plain composed mainly of Quaternary deposits of tundra-silts, sands, and gravels. In much of the area, the coast is being eroded by the sea at a rapid rate forming coastal bluffs as much as 6 m high. The line of bluffs is interrupted by low mud flats at the mouths of major rivers. Much of the coast is marked by islands at varying distances from the shore. Most of the islands are less than 3 m in elevation, narrow, and comprised of sand and gravel. Others are capped by tundra and are apparently erosional remnants of the inundated coastal plain. Coast-parallel shoals are also a feature of the inner shelf.

The shelf is generally rather flat and remains shallow for a considerable distance from shore. Off the Colville River the 2-m isobath is up to 12 km from shore. The width of the shelf is variable, ranging from 55 km in the east to 110 km in the west. The shelf break lies at depths of 50 to 70 m. The shallowness of the shelf break and the presence of elevated Pleistocene beach lines suggests a broad regional uplift. The Holocene marine sediments on the inner shelf are generally 5 to 10 m thick and composed of complex textural and compositional character. Ice and oceanographic factors interact to form a compound structural character of ice flow hetrogeneity or wave and current-bedded sequences.

The rivers flood in early June, delivering 50 to 80 percent of the yearly runoff in a 2-3 week period. The bulk of sediment input from rivers is associated with this flood. No river gravels presently reach the ocean. Initial flooding seaward of the river delta occurs on top of the unmelted sea ice, although the influx of warmer water eventually leads to ice-free areas off the deltas early in the sea-ice melt season. River drainage basins are located in the Brooks Range and the eastern rivers drain directly into the ocean while the western rivers meander across the broad coastal plain.

Sea ice is a ubiquitous feature in the study area. New ice starts to form in late September and grows to a thickness of 2 m through the winter, welding remnant older ice into more or less solid sheets. Where forces are sufficient, ice fractures and piles into hummocks and ridges. By June, sea-ice melting is well underway and usually sometime in July enough ice has melted so that the protected bays and lagoons are free of ice, and temperate latitude processes of waves and wind-driven currents are active. Ice remains on the shelf in the study area throughout the summer. Its location and concentration depend on the degree of melting and winds. The prevailing northeasterly wind tends to carry drifting summer ice away from the shore while the westerlies pile ice against the coast. Ice commonly remains grounded throughout the summer on many of the shoals on the inner shelf.

Currents and waves are a function of the winds during the open-water season. Waves are generally poorly developed due to the limited fetch which results from the presence of ice during most of the summer. Water circulation is dominated by the prevailing northeasterly winds which generate a westerly flow on the inner shelf. In winter currents under the ice are generally sluggish although restrictions of the tidal prism by ice at tidal inlets and on the broad, shallow, 2-m bench cause significantly higher velocities.

V. Sources, methods and rationale of data collection

A. Equipment operated routinely from the R/V KARLUK includes bottom sampling and coring gear, water salinity, -temperature, and -turbidity sensors, fathometers, a high and medium resolution seismic system, and a side-scan sonar. Precision navigation is maintained to 3 m accuracy with a range-range system.

Special techniques include (a) repetitive sonar and fathometer surveys of ice gouges, (b) diving observations and bottom photography, (c) measurements of sediment thicknesses within ice gouges by combined use of narrow beam echo sounder, and (d) a near-bottom tow package incorporating sub-bottom profiler and television, (4) nearsurface stratigraphic studies using a vibracorer capable of obtaining 2-m long cores and (f) detailed surveys of bathymetry in river and lagoonal channels and in the vicinity of manmade structures. Coastal observations of rates of bluff erosion and the distribution and elevation of storm surge strand lines was carried out by helicopter. Winter ice observations involve ice coring, diving observations along with modified system of upward-looking fathometer, and side-scan sonar.

B. The past and present status of data and product submission to NOAA-BLM-OCSEAP is given in the table on the following page.

VI, VII, VIII. Results, Discussion and Conclusions - (As attachments to report)

A. Gravel Deposition on Beaufort Sea Shelf

B. Eolian Sand Deflation: A Cause for Gravel Barrier Islands in the Arctic

C. Water Flow Patterns From Drifters on the Inner Shelf of the Beaufort Sea

D. Diving Observations on the Soft Ice Under the Fast Ice at DS-11 in Stefansson Sound Boulder Patch

E. Sediment Laden First Year Ice, Central Beaufort Coast, Alaska

RU-205, Barnes and Reimnitz

Product Submission Status

REPORTS TO NOAA-BLM

Data Products	Sept. 1975	Dec. 1975	March 1976	June 1976	Sept. 1976	Dec. 1976	Feb. 1977	March 1977	June 1977	Sept. 1977	Dec. 1977	March 1978	June 1978	Sept. 1978	Dec. 1978	March 1979	June 1979	Sept. 1979	Other Sources of Da (Numbers refer to references)
Non Digital																			
-core descriptions									x										
-acoustic profiles w/nav.			x		x			x							x				12,13,14
Digital																			
-water temp./sal.				x	x			x											
-current meter			x	x	x			x											Lost equipment
-nephelometer																			Lost equipment
Summary Products																			
1. Ice gouge maps							x						x				0	0	2,4,18,22,23,26,27
2. Evaluation of ice hazards	x	x	x		x		x	x	x				x		x		0	0	2,4,5,10,15,17,18,20,2
3. Offshore gravel resources					x		x						x		x	x		0	2,9,24
4. Holocene marine sediments		x				x	x	x	x					x	x	x	0		2,5,9,17,22,24
5. Bottom currents and processes	x	x	x	x		x	x	x			x					x	0		2,5
6. Sediment transport regime	x						x	x	x		x	x	x	x	x	x	0		2,5,6,8,9,17,22
7. Interpretation of stamukhi							x					x						0	2,3,4,5,9,15,17,20,21
8. Coastal erosion and delta progradation			x	x	x		x	x		x	x		x				0		2.6,11,16
9. Boulder patch								x							x	x		0	2
10. Ice thickness morphology													x		x	x			1
Additional Information																			
1. Sediment distribution and character			x				x	x	x				x		x	x	0	0	2,5,9,19,23-24,26
2. Charts			x	x									x						3,15,16
3. Oceanographic observations			x					x							x	x		0	1,5,8,16,25
4. Engineering properties						x		x								x			19
5. Chukchi Sea studies						x		x				x				x			26,27
6. Fresh water resources			x														0		7,11
7. Sediment interstitial salt, sea floor temperature												x						0	19
8. Diving observations									x						x	x			1,2,5,22
9. Barrier islands													x		x		0	0	2,5,6,17,22,24
10. River processes																x			7
11. Storm surges															x				16

x - data or information submitted

0 - work in progress or planned for this period

IX. Needs for further study

The primary emphasis of future work should include the following: recurrence rates and intensity of ice gouging in the stamukhi zone; rates of sediment reworking and sediment infilling; evaluation of the presence or absence of gas-charged sediments on the inner shelf and if present, their relationship to permafrost; determination of the rates of sediment migration along the mainland coast; assessing the character of ice sediment interaction in the vicinity of the 2-m bench, as related to sub-ice current scour, oil entrapment and sediment stability; an evaluation of the engineering character of surficial sediment units on the shelf; and an assessment of the Holocene stratigraphy for clues as to sea level history, gravel sources, and engineering character.

X. Summary of 4th Quarter Operations

A. Ship or Laboratory Activities

1) Ship or field trip schedule-Erk Reimnitz participated in the winter diving program in the boulder patch at DS-11, 1-10 March, 1979.

2) Personnel involved in project:

Peter Barnes	Project Chief - Geologist	U.S.G.S., Marine Geology
Erk Reimnitz	Principal Investigator-Geologist	" " "
Dennis Fox	Physical Science Technician	" " "
Ed Kempema	Physical Science Technician	" " "
Robin Ross	Physical Science Technician	" " "
Doug Rearic	Physical Science Technician	" " "

3) Methods

Efforts this quarter have been primarily aimed at data compilation, data reduction, and report writing. Significant project efforts during the quarter were:

a) description and characterization of old and new ice gouge records over large areas of the shelf
b) preparation of the annual report
c) preparation of manuscripts for internal and external publication
d) preparation and planning for summer field efforts
4) computer compilation of bathymetry and precision-navigation data of Reindeer and Cross Islands
f) compilation of ice gouge data from Barrow test site
g) compilation of sediment data for inner shelf

4) Data collected or analyzed:

DATA TYPE	Km of record or number of samples analyzed
Side-scan sonar	~100 km
Bathymetry profiles	~100 km

Published Reports

1 Barnes, P. W., Reimnitz, Erk, Toimil, L. J., and Hill, H. R., 1979, Fast-ice thickness and snow depth in relation to oil entrapment potential, Prudhoe Bay, Alaska, U.S. Geol. Survey open-file report 79-539, 28 p.

2 Barnes, P. W., and Hopkins, P. M., (Eds.), 1978, Geological Sciences, in: Interim Synthesis Report: Beaufort/Chukchi, Gunter Weller, David Norton, Toni Johnson, (Eds.), National Oceanic and Atmospheric Administration, Environmental Research Laboratories, Boulder, Colo., p. 101-131.

3 Barnes, P. W., and McDowell, David, 1978, Inner shelf morphology, Beaufort Sea, Alaska, U.S. Geol. Survey open-file report 78-785, 3 p.

4 Barnes, P. W., McDowell, David, and Reimnitz, Erk, 1978, Ice gouging characteristics: their changing patterns from 1975-1977, Beaufort Sea, Alaska, U.S. Geol. Survey open-file report 78-730, 40 p.

5 Barnes, P. W., Reimnitz, Erk, Drake, D. E., and Toimil, L. J., 1977, Miscellaneous hydrologic and geologic observations on the inner Beaufort Sea shelf, Alaska: U.S. Geol. Survey open-file report 77-477, 95 p.

6 Barnes, P. W., Reimnitz, Erk, Smith, Greg, and McDowell, David, 1977, Bathymetric and shoreline changes in northwestern Prudhoe Bay, Alaska, the Northern Engineer, v. 9, no. 2, p. 7-13.

7 Barnes, P. W., and Reimnitz, Erk, 1976, Flooding of sea ice by rivers of northern Alaska; in ERTS-1, A New Window on Our Planet, R. W. Williams, Jr., and W. D. Carter, eds., U.S. Geol. Survey Prof. Paper 929, p. 356-359.

8 Barnes, P. W., and Garlow, R., 1975, Surface Current Observations-Beaufort Sea, 1972, U.S. Geol. Survey open-file report 75-691, 3 p.

9 Barnes, P. W., and Reimnitz, Erk, 1974, Sedimentary processes on arctic shelves off the northern coast of Alaska, in Reed and Sater, eds.: The Coast and Shelf of the Beaufort Sea, The Arctic Inst. of N. Am., Arlington, Va., p. 439-576.

10 Grantz, Arthur, Barnes, P. W., Eittreim, S. L., Reimnitz, Erk, Scott, E. W., Smith, R. A., Stewart, George, and Toimil, L. J., 1976, Summary of sediments, structural framework, petroleum potential, environmental conditions, and operational considerations of the United States Beaufort Sea, Alaska area: U.S. Geol. Survey open-file report 76-830, 32 p.

11 Harden, Deborah, Barnes, P. W., and Reimnitz, Erk, 1977, Distribution and character of naleds in northeast Alaska: Arctic, v. 30, p. 28-40.

12 Maurer, D. K., Barnes, Peter, and Reimnitz, Erk, 1978, U.S. Geological Survey marine geologic studies in the Beaufort Sea, Alaska, 1977; data type, location, and records obtained, U.S. Geol. Survey open-file report 78-1066, 3 p

Published Reports (cont'd)

13 Reimnitz, Erk, Barnes, P. W., and Kempema, Ed, 1979, Marine geologic studies in the Beaufort Sea, Alaska, 1978; data type, location, records obtained, and their availability, U.S. Geol. Survey open-file report 79-384, 4 p.

14 Reimnitz, Erk, Barnes, P. W., and Maurer, Doug, 1979, U.S.G.S. Marine geologic studies in the Beaufort Sea, Alaska, 1976; data type, location, and records obtained, U.S. Geol. Survey open-file report (number pending) 3 p.

15 Reimnitz, Erk, and Maurer, D.K., 1978, Stamukhi shoals of the arctic-some observations from the Beaufort Sea, U.S. Geol. Survey open-file report 78-666, 17 p.

16 Reimnitz, Erk, and Maurer, D. K., 1978, Storm surges in the Alaskan Beaufort Sea, U.S. Geol. Survey open-file report 78-593, 26 p.

17 Reimnitz, Erk, Toimil, L. J., and Barnes, Peter, 1978, Arctic continental shelf morphology related to sea-ice zonation, Beaufort Sea, Alaska, Marine Geology, v. 28, p. 179-210.

18 Reimnitz, Erk, Barnes, P. W., Toimil, L. J., and Melchoir John, 1977, Ice gouge recurrence and rates of sediment reworking, Beaufort Sea, Alaska: Geology, v. 5, p. 405-408.

19 Reimnitz, Erk, Maurer, D. K., Barnes, P. W., and Toimil, L. J., 1977, Some physical properties of shelf surface sediments, Beaufort Sea, Alaska: U. S. Geological Survey oepn-file report 77-416, 8 p.

20 Reimnitz, Erk, Toimil, L. J., and Barnes, P. W., 1977, Stamukhi zone processes: Implication for developing the arctic offshore area: Offshore Technology Conference. Houston, Tex., Proceedings v. 3, p. 513-518.

21 Reimnitz, Erk, and Barnes, P. W., 1976, Influence of sea ice on sedimentary processes off northern Alaska: in ERTS-1, A new window on our planet, Williams, R. S., Jr., and Carter, W. D., eds., U.S. Geol. Survey Prof. Paper 929, p. 360-362.

22 Reimnitz, Erk, and Barnes, P. W., 1974, Sea ice as a geologic agent on the Beaufort Sea shelf of Alaska: in Reed, and Sater, eds., The coast and shelf of the Beaufort Sea, The Arctic Inst. of North America, Arlington, Virginia, p. 301-351.

23 Reimnitz, Erk, Barnes, P. W., and Alpha, T. R., 1973, Bottom features and processes related to drifting ice on the arctic shelf, Alaska: U.S. Geol. Survey Misc. Field Studies Map MF-532.

24 Rodeick, C. A., 1979, The origin, distribution, and depositional history of gravel deposits on the Beaufort Sea continental shelf, Alaska, U.S. Geol. Survey open-file report 79-234, 87 p.

25 Toimil, L. J., and Reimnitz, Erk, 1979, A herringbone bedform pattern of possible Taylor-Görtler type flow origin seen in sonographs, Sedimentary Geology, v. 22, p. 219-228.

Published Reports (cont'd)

26 Toimil, L. J., 1978, Ice-gouged microrelief on the floor of the eastern Chukchi Sea, Alaska: a reconnaissance survey, U.S. Geol. Survey open-file report 78-693, 102 p.

27 Toimil, L. J., and Grantz, Arthur, 1976, Origin of a bergfield at Hanna Shoal, northeastern Chukchi Sea and its influence on the sedimentary environment: AIDJEX Bull., no. 34, p. 1-42.

Published Reports included in 1979 Annual Report

Barnes, P. W., Reimnitz, Erk, Toimil, L. J., and Hill, H. R., 1979, Fast-ice thickness and snow depth in relation to oil entrapment potential, Prudhoe Bay, Alaska, U.S. Geol. Survey open-file report 79-539, 30 p.

Barnes, P. W., Reimnitz, Erk, Toimil, Larry, Maurer, Douglas, and David McDowell, 1979, Core descriptions and preliminary observations of vibracores from the Alaskan Beaufort Sea shelf, U.S. Geol. Survey open-file report 79-351, 71 p.

Maurer, D. K., Barnes, Peter, and Reimnitz, Erk, 1978, U.S. Geological Survey marine geologic studies in the Beaufort Sea, Alaska, 1977; data type, location, and records obtained, U.S. Geol. Survey open-file report 78-1066, 3 p

Reimnitz, Erk, Barnes, P. W., and Kempema, Ed, 1979, Marine geologic studies in the Beaufort Sea, Alaska, 1978; data type, location, records obtained, and their availability, U.S. Geol. Survey open-file report 79-384, 4 p.

Reimnitz, Erk, Barnes, P. W., and Maurer, Doug, 1979, U.S.G.S. Marine geologic studies in the Beaufort Sea, Alaska, 1976; data type, location, and records obtained, U.S. Geol. Survey open-file report 79-507, 3 p.

Attachment A

Rodeick, Craig A. (1979). The Origin, Distribution, and Depositional History of Gravel Deposits on the Beaufort Sea Continental Shelf, Alaska, U.S. Geological Survey Open File Report 79-234. 87 pp.

Attachment B

EOLIAN SAND DEFLATION: A CAUSE FOR GRAVEL BARRIER ISLANDS IN THE ARCTIC?

by

Erk Reimnitz and Douglas K. Maurer

U.S. Geological Survey, 345 Middlefield Road, Menlo Park, Ca 94025

ABSTRACT

Arctic barrier islands generally are composed of sandy gravel, whereas lower latitude barrier islands generally are composed of sandy material. This pronounced grain-size difference needs explanation. Because wind-winnowing of island surfaces is effective most of the yearly cycle, while sediment supply by waves is effective for approximately two months at most, eolian sand deflation might be a mechanism to explain the coarse sediments of arctic barrier islands. In the winter, plumes of windblown sand are found on the fast ice downwind of barrier islands. One small island exposure near Prudhoe Bay lost more than 300 tonnes of sand in one winter; this loss suggests a deflation rate of 2 mm for that period.

INTRODUCTION

The need for enormous amounts of sand and gravel to develop the petroleum resources on the arctic shelf has focused attention on the chains of sandy gravel barrier islands along the North Slope of Alaska. The coarseness of these barrier islands stands in strong contrast to the sandy composition of lower latitude barriers. This difference in particle size remains as a fundamental problem to our understanding of barrier islands, however, this problem has received little attention.

Glaeser (1978) takes a global view of the distribution of barrier islands in relationship to tectonic setting, availability of source materials, shelf physiography, and presence or absence of a flat coastal plain. However, he does not consider differences in physical environments and composition. Davies (1973), in his study of geographical variation in coastal development, considers the importance of pebbles as a beach constituent on a global perspective. He shows that pebbles are most abundant on high latitude beaches, and are generally absent on beaches in lower latitudes. The effects of glaciation in providing coarse source material is emphasized as a factor causing this relation. We briefly consider this and several other possible causes for differences in particle size between high latitude and low latitude barrier islands, and discuss our own observations,which indicate that sand deflation caused by winds without waves and littoral transport during winter may be be the most important mechanism responsible for the relative abundance of gravel.

REGIONAL SETTING

The barrier islands along the Beaufort Sea coast of Alaska are very low (1 to 2 m) and narrow (less than 100 m). They are composed of sandy gravel, lack dunes, and are generally devoid of vegetation. Much of the winter these islands barely protrude from a sea of ice and snow (Fig. 1). Morphological features related to ice push can generally be seen on any island. Ice push is mostly a fall phenomenon, involving ice less than 0.5 m thick. But overall arctic-beach morphology is primarily related to processes operating during the short open-water season (Wiseman et al. 1973) when limited ocean fetch owing to the presence of sea ice allows only small, short-period waves to develop. The seasonal fast ice forming around the islands reaches a thickness of 1.5 to 2 m by the end of the winter. The ice surface generally slopes up slightly onto the beach face and, where free-floating, has a freeboard of 10 cm and is covered by 10 to 20 cm of snow. In some years an ice foot develops on the foreshore, protecting it from winter processes. Even without an ice foot, however, only the crests of islands are exposed, as the more wind sheltered flanks are blanketed by snow.

POSSIBLE CAUSES OF THE GRAVELLY COMPOSITION OF ARCTIC BARRIER ISLANDS

Barrier islands and the beaches in the Alaskan Beaufort Sea are sandy gravel (Rex, 1964; Naidu and Sharma, 1971; LaBelle, 1973; Wiseman et al., 1973, Burrell et al., 1974, Short, 1979), and similar gravel barrier islands dominate south to the Arctic Circle. Possible explanations for the coarse nature of the islands are 1) a high level of wave energy, 2) ice rafting, 3) coarse source material, 4) effects of glaciations, and 5) a predominance of physical over chemical weathering in the drainage basins. All of these possible causes are discounted rather readily:

1) Wave Energy.-The energy level of waves in the high arctic is low and waves are active for only a short time during the year (Short, 1974; Wiseman et al., 1973).

2) Ice Rafting.-Ice Rafting is of very little importance in the modern sedimentary environment of the Beaufort Sea shelf (Barnes and Reimnitz, 1974). Observations on the gravel-free sand shoals of the stamukhi zone (Reimnitz et al., 1978), where the residence time of ice during the summer melt season is long and any sediment carried by ice should be offloaded preferentially (Reimnitz and Barnes, 1974; Reimnitz and Maurer, 1978), are also applicable to the question of ice rafting as a cause for gravel barrier islands. The sand shoals receive no gravel today, and therefore the barrier islands cannot receive a significant amount of gravel.

3) Source Material.-The rivers of the North Slope wind across a gently sloping tundra surface for a hundred kilometers and do not supply gravel to the marine environment; these rivers therefore carry no source material for the gravel islands (Rodeick, 1975). In extreme contrast to this condition is the Copper River draining into the Gulf of Alaska. This torrential alpine river carries a very large load of gravel to

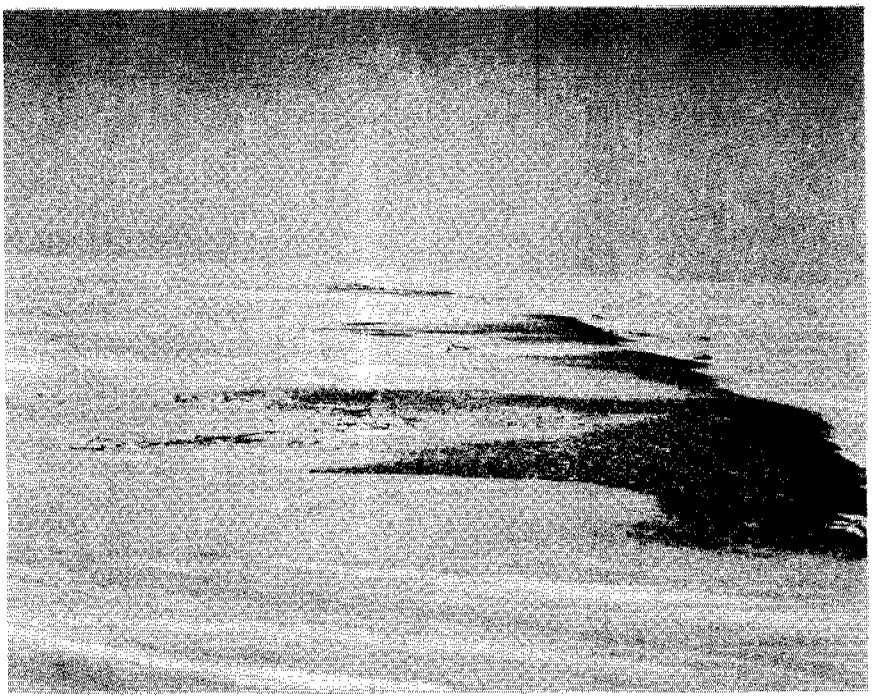

Figure 1. Early May photograph of an arctic barrier island with only crest exposed to wind winnowing, leaving a gravel pavement. Tongues of gravel trailing away from berm are alined parallel to sastrugi and dominant northeast wind. (Nearest tongue is about 2 meters long).

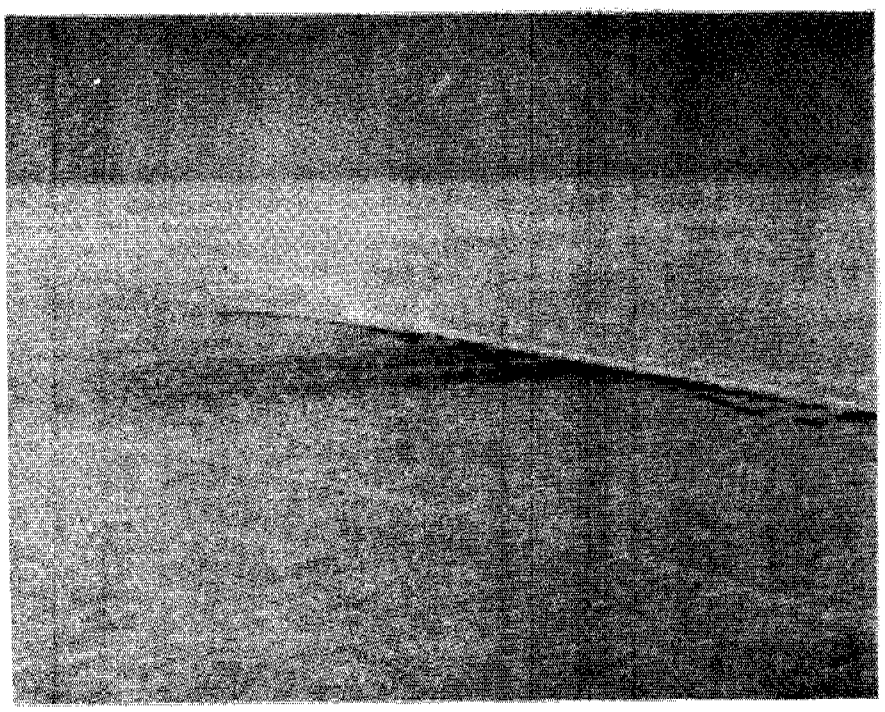

Figure 2. Aerial photograph of Long Island sand plume parallel to sastrugi, as seen under favorable light in late winter. Length of plume is about 1.4 km.

within a short distance of the sea, yet the barrier islands along the delta front are composed of sand (Reimnitz, 1966). Looking to the nearshore zone of the Beaufort Sea as a possible source of gravel, Barnes and Reimnitz (1974) report that only insignificant amounts are present. From numerous nearshore scuba diving traverses we know that, on a small scale, the sediment distribution is very patchy. Minor amounts of surficial gravel can be found in spots, but the bottom is covered mainly with muddy fine sand.

Many of the barrier islands in arctic Alaska are formed by rapid thermal erosion of the Gubik Formation, a process which often results in isolated remnants of this unit being surrounded by the sea and disappearing rapidly. Naidu and Mowatt (1976) contend that the gravelly nature of the mainland and barrier beach deposits is "predominantly attributable to a local unique provenance (e.g. the gravel-enriched Quaternary Gubik Formation underlying the tundra), rather than solely to depositional processes prevailing in the polar region." Table 1 presents percentages of the Gubic Formation's gravel, sand, and mud exposed either in coastal bluffs along the Alaskan sector of the Beaufort Sea, or in bluffs a short distance inland.

TABLE 1
SELECTED GRAVEL, SAND, AND MUD PERCENTAGES FOR THE GUBIC FORMATION

Location	Gravel	Sand	Mud	No. of Samples	
Christie Point	0	32	68	3	Black (1964)
Drew Point	0	8	92	7	" "
Teshekpuk Lake	0	42	58	3	" "
Atigaru Point	0	85	15	1	" "
Oliktok	0	69	31	5	Lewellen (unpub.)
Kavearak Point	0	70	30	2	" "
Tigvariak Island	3	63	34	1	U.S.G.S.

The gravel content of the coastal bluffs, when compared to that of other coastal bluffs where beaches and barrier islands are composed of sand, is not uniquely high.

4) Effects of Glaciation.-On a global scale, Davies (1973) found a correlation between areas with a history of glaciation and beaches containing significant amounts of gravel. A look at Alaska shows negative correlation. Along the Gulf of Alaska, where a number of tidal glaciers still supply coarse material to the sea and where very recent moraines are found on the inner shelf, barrier islands and beaches are

mainly composed of sand. Proceeding northward along the Alaskan coast to the arctic regions, where glaciers apparently did not reach the coast, the barrier islands become gravel rich.

5) Physical versus Chemical Weathering.-Moore (1968) stated that "an increase in the effectiveness of physical weathering over chemical weathering in cold climates makes gravel beaches more abundant there than elsewhere." As pointed out above, the potential sources for the construction of barrier islands provide plenty of sand and limited amounts of gravel.

Thus, the five most obvious explanations for the gravelly nature of barrier islands in the Arctic do not answer the question. Our observations suggest another possibility-- that removal of sand by wind is the mechanism by which barrier islands are enriched in gravel.

WIND WINNOWING OF BARRIER ISLAND SURFACES IN THE ARCTIC

crests of arctic barrier islands are exposed to wind winnowing most of the winter (Figs. 1 and 2), and wind-driven materials are commonly seen on the snow downdrift from the exposures. Leffingwell (1919, p. 176) reports that along this coast "Stones half an inch (1.25 cm) in greatest diameter have been observed on the sea ice a mile (1.6 km) from their probable source. They were scattered in a wide belt in the lee of a sand spit." We have seen only indirect evidence for eolian transport of such large clasts (Reimnitz and Barnes, 1974), but plumes of sand are a common sight. The dominant wind direction along the North Slope is from the northeast. This direction is indicated by sediment plumes observed in LANDSAT images trailing away from oilfield roads and camps (Barnes and Reimnitz, 1976), by the sastrugi pattern (wind-shaped snow relief), by wind-normal orientation of elongate lakes, and by dune alignment on river flood plains.

A sediment plume similar to the one shown in figure 2 was seen in early May 1978 trailing away from the western part of Egg Island. As sketched from the air, the visible plume was 0.7 km wide and 1.7 km long (Fig. 3). The exposed source area on Egg Island was about 0.1 km^2, but some of this surface was covered by active snow drifts. Several areas of the sediment plume on the lagoon ice were inspected. The snow thickness, measured at 35 points at 5 m intervals, ranged from 8 to 47 cm, with a mean of 17 cm. Sand was found in about the upper 8 cm of the snow canopy, while the lower part appeared free of sand. On the snow surface the sand distribution was patchy owing to highly active processes reshaping the snow surface every few days. A small area about 20 m downwind from the island outcrop was sampled and found to contain 421 g/m^2 of sand, all within the upper 8 cm. The snow surface in this area is shown in figure 4.

To estimate the amount of sand contained in the Egg Island plume, we assumed a linear decrease in sand concentration from the sample site value to zero at a point 300 m beyond the plume terminus visible from the air. Our sketchy data show that the plume contained about 309 tonnes or approximately 206 m^3 of sand, suggesting that the island was eroded about 2 mm during the winter.

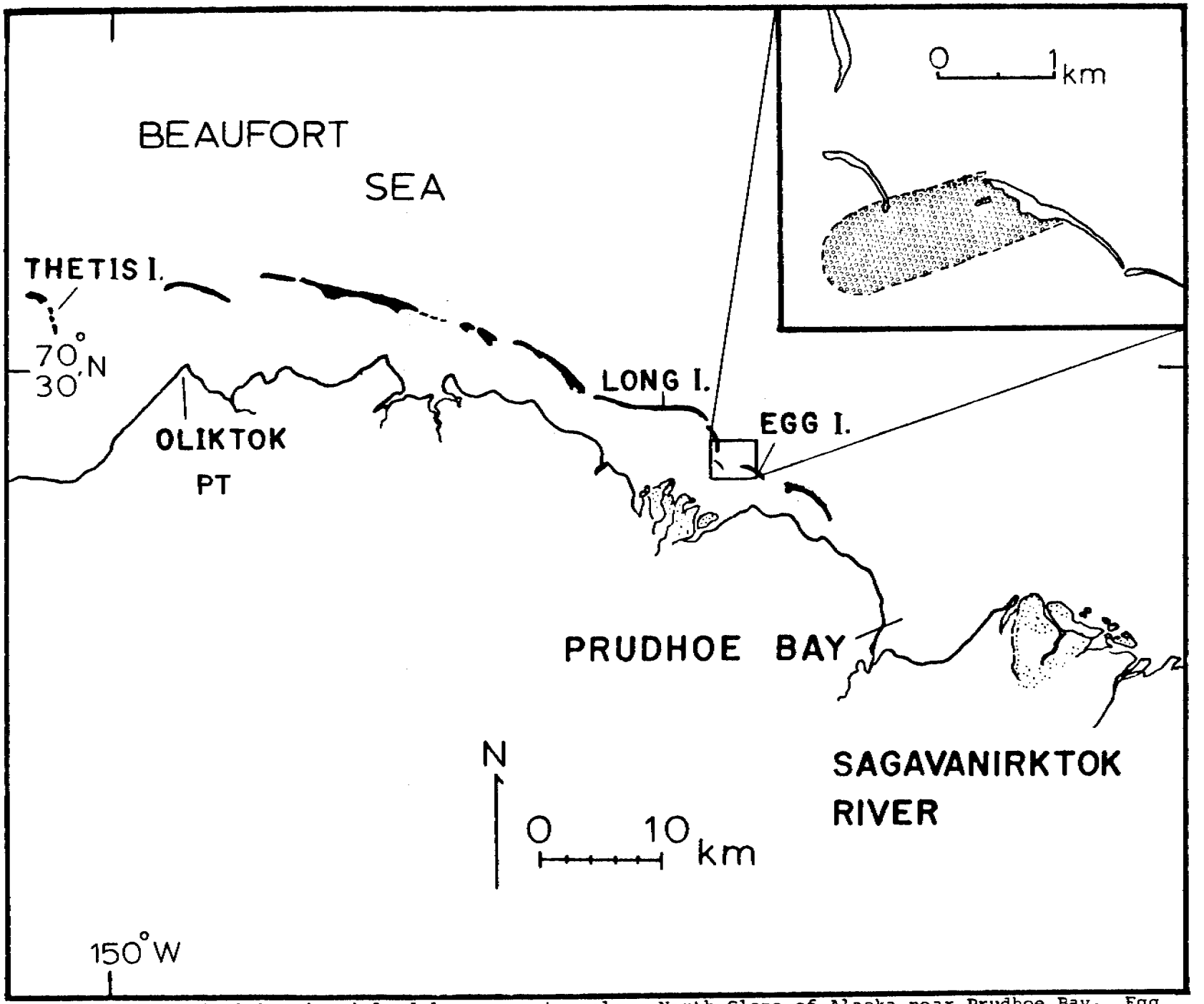

Figure 3. Typical barrier island-lagoon system along North Slope of Alaska near Prudhoe Bay. Egg Island sand plume (shaded) is sketched in inset.

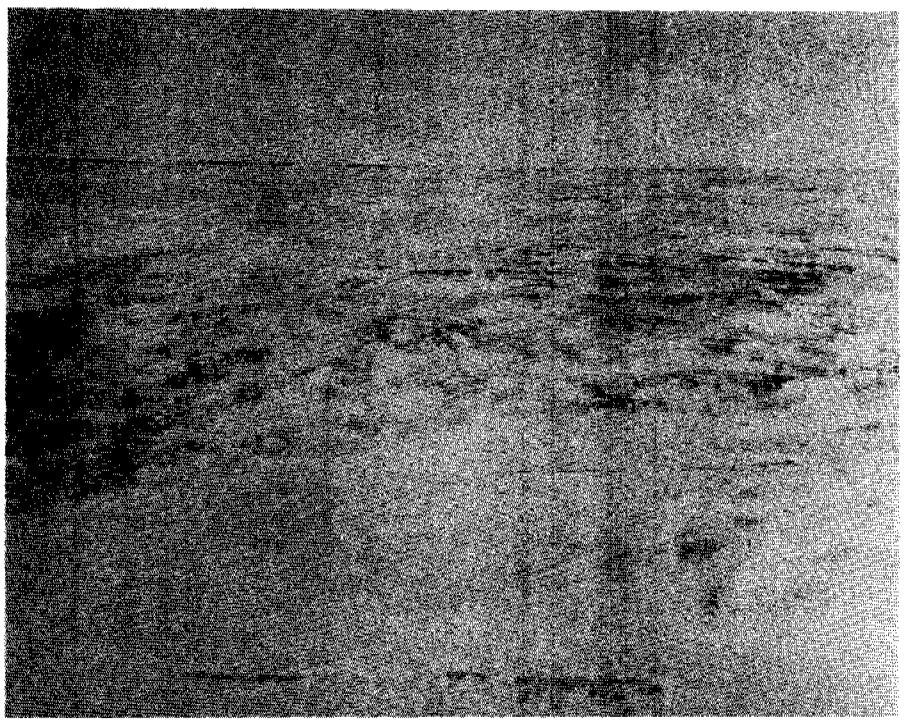

Figure 4. Close-up view of Egg Island sand plume, with Egg Island on horizon.

The grain-size distribution of the material sampled was determined by sieving, and the results are given as cumulative frequency percentages in figure 5. The curve shows that Egg Island is being depleted of very well sorted sand with a mean of 1.83 $\emptyset$ and nearly normal grain-size distribution (Folk, 1974).

DISCUSSION

We have not analyzed the grain-size distribution of the source area on Egg Island, but observed that the surface is paved by a veneer of pebbles similar to that shown in figure 1, underlain by gravel with a sand matrix. The environment around Oliktok (Fig. 3) is very similar to that at Egg Island and grain-size distribution curves representing berm material from Oliktok (Dygas et al., 1971) can therefore be related to the conditions at Egg Island (Fig. 5). The beach berms stand high on the islands and remain exposed during much of the winter. The berms are a bimodal distribution of sand and gravel from which the sand is being winnowed by wind. The significance of an estimated wind deflation rate of about 206 m^3 per winter to the sediment budget of Egg Island is not known, and can only be related to an estimated longshore transport rate of about 3,000 m^3/yr (Short, 1973). Most of the material moving from island to island by this process is sand.

A gravel pavement capping the barrier islands, if not disturbed, will eventually become thick enough to resist wind erosion. However, the gravel pavement is modified by ice push and reworked by waves and currents during storm surges (Reimnitz and Maurer, 1978), which brings some of the remaining sand to the surface. Still, the rate of deflation will decrease with time as the islands become more gravelly.

Some complications to this otherwise simple story should be mentioned. Sand plumes were not visible from the air adjacent to all the islands in the spring of 1978. The lack of plumes may be explained by poor lighting on the days of overflights or perhaps little sand is exposed on the surface on days following a period of drifting snow. We did note that on one of the barrier islands a rather sandy gravel surface was damp during sub-freezing temperatures and tasted salty. Thus the brine content of the sediment, which may be high due to salt spray from surf, may keep sand grains of the surface layer moist and cohesive. Summer surf action and salt spray are quite variable from island to island due to patchy ice distribution, and these variations might explain changes in wind erosion and sand plume development from one island to another. We were also puzzled by the lack of sand in the lower part of the snow blanket covering the sea ice. Snow ridges were measured to be migrating actively during an 18 day period in early May, and probably migrate all winter. Not knowing how a deposit consisting of a mixture of snow and sand moves during strong winds, one might assume that sand concentrates in a layer at the base of troughs between sastrugi. This was not the case. The position of the sandy unit in the snow section suggests that sand may only be a late winter contribution from the island. A late winter increase in dust transport by wind apparently occurs on the coastal plain (Benson et al., 1975). If so, the sand plume studied represents only a few months of winnowing. Since sand deflation is greater during the summer when all of the island

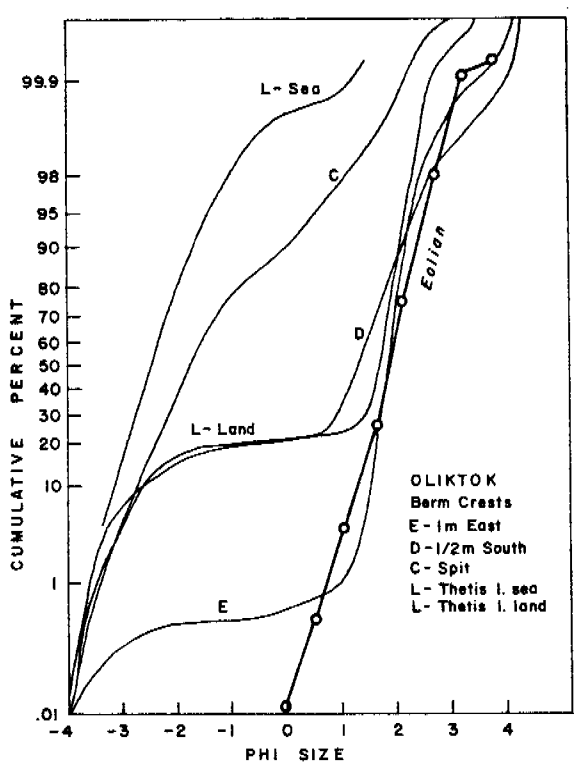

Figure 5. Grain-size distribution of eolian sediment of Egg Island plume, superimposed on curves representing berm-crest sediments from Oliktok area (Figure 3) with depositional environment similar to that of Egg Island. (Figure modified after Dygas et al., 1972).

surface is exposed rather than only the crests, the annual rate of removal would be accordingly higher.

Because of the dominant northeasterly wind on the North Slope, much of the sand eroded from barrier islands is deposited in lagoons behind islands. Along the Chukchi Sea coast much of the material is blown seaward. Small lakes on some of the islands catch eolian sand, as shown by the similarity between the grain size distribution of the Egg Island plume and lake sediments from Thetis Island (Dygas et al., 1971, Fig. E-9). Some barrier islands have small, rather deep lakes (4.5 m on Cross Island) that could be filled largely by eolian sand and could result in large lenses of clean sand in a sandy gravel deposit.

CONCLUSION

The barrier islands of the Arctic are exposed to reworking by wave action for only 2 to 3 months of the year, and during some summers not at all. Sand removal by wind is effective most of the year. In this environment, the balance of sand supply versus sand removal is tilted toward removal. The result is a gravelly composition for high latitude barrier islands, contrasting with a sandy composition for low latitude islands. The present gravelly composition may be the product of thousands of years of wind winnowing, suggesting that these features are very fragile and are sensitive to exploitation by industry.

ACKNOWLEDGMENTS

We are grateful to John Dingler, Bill Wiseman, and Andy Short for their review of this report. Critical comments by Robert Taylor also were very helpful.

REFERENCES CITED

Barnes, P.W., and Reimnitz, Erk, 1974, Sedimentary processes on arctic shelves off northern coast of Alaska, in The Coast and Shelf of the Beaufort Sea: Proceedings of the Arctic Institute of North American Symposium on Beaufort Sea Coast and Shelf Research, Arlington, VA., p. 439-476.

Barnes, P.W., and Reimnitz, Erk, 1976, Flooding of sea ice by the rivers of northern Alaska in ERTS-1 A New Window on Our Planet: U.S. Geological Survey Professional Paper 929, p. 356-359.

Benson, Carl, Holmgren, Bjorn, Timmer, Robert, Weller, Gunter, and Parish, Scott, 1975, Observations on the seasonal snow cover and radiation climate at Prudhoe Bay, Alaska during 1972 in Ecological Investigations of the Tundra Biome in the Prudhoe Bay Region, Alaska, Brown, Jerry, ed.: Biological Papers of the University of Alaska Special Report no. 2, p. 13-50.

Black, R.F., 1964, Gubik Formation of Quaternary age in northern Alaska: Geological Survey Professional Paper 302-C, Part 2, Regional Studies, p. 59-87.

Burrell, D.C., Dygas, J.A., and Tucker, R.W., 1973, Beach morphology and sedimentation of Simpson Lagoon in Environmental studies of an Arctic Estuarine System: Final Report no. R 74-1: Institute of Marine Science, University of Alaska, 539 p.

Davies, J.L., 1973, Geographical variation in coastal development, Clayton, K.M., ed.: Hafner Pub. Co., New York, 204 p.

Dygas, J.A., Tucker, R., Naidu, A.S., and Burrell, D.C., 1971, A preliminary sedimentological investigation of the Colville River and Oliktok Point coastal region in Baseline Study of the Alaskan Arctic Aquatic Environment: Institute of Marine Science, University of Alaska, Report no. R 71-4, p. 48-82.

Folk, R.L., 1974, Petrology of Sedimentary Rocks, Hemphill Pub. Co., Austin, TX, 182 p.

Glaeser, J.D., 1978, Global distribution of Barrier Islands in terms of tectonic setting: Journal of Geology, v. 86, no. 3, p. 283-297.

LaBelle, J.C., 1973, Fill materials and aggregate near Barrow Naval Petroleum Reserve No. 4, Alaska: Arctic Institute of North America, Washington, D.C., 143 p.

Leffingwell, E. de K., 1919, The Canning River region, northern Alaska: U.S. Geological Survey Professional Paper 109, 251 p.

Moore, G.W., 1968, Arctic beaches in The Encyclopedia of Geomorphology, Fairbridge, W., ed., Encyclopedia of Earth Sciences Series, Reinhold Book Corporation, New York, v. 3, p. 21-22.

Naidu, A.S., and Sharma, G.E., 1971, Texture, mineralogy and chemistry of Arctic Ocean sediments, Progress Report 1970-71 no. R 74-1: Institute of Marine Science, University of Alaska, 539 p.

Naidu, A.S. and Mowatt, T.C., 1976, Significance of textural criteria in the recognition of ancient polar deltaic sediments, in Recent and Ancient Sedimentary Environments of Alaska, Miller, T.P., ed., Alaska Geological Society, Anchorage, Alaska, p. D1-12.

Reimnitz, Erk, 1966, Late Quaternary history and sedimentation of the Copper River delta and vicinity, Alaska: Ph.D. Thesis, Univ. Calif., San Diego, 160 p.

Reimnitz, Erk, and Barnes, P.W., 1974, Sea ice as a geologic agent on the Beaufort Sea shelf of Alaska, in The coast and shelf of the Beaufort Sea: Proceedings of the Arctic Institute of North American Symposium on Beaufort Sea Coast and Shelf Research, Arlington, VA, p. 439-476.

Reimnitz, Erk, and Maurer, D.K., 1978, Stamukhi shoals of the arctic - Some observations from the Beaufort Sea: U.S.G.S. Open-File Report 58-666, 17 p.

Reimnitz, Erk, Toimil, L.T., and Barnes, P.W., 1978, Arctic continental shelf morphology related to sea ice zonation, Beaufort Sea, Alaska: Marine Geology, v. 28, p. 179-210.

Rex, R.W., 1964, Arctic beaches: Barrow, Alaska, in ed., Miller, R.L.: Papers in Marine Geology, p. 384-400.

Rodeick, C.A., 1979, The origin, distribution, and depositional history of gravel deposits on the Beaufort Sea continental shelf, Alaska: U.S. Geological Survey Open-File Report 79-234, 87 p.

Short, A.D., 1973, Beach dynamics and nearshore morphology of the Alaskan arctic coast, Unpublished Ph.D. dissertation: Louisiana State Unviersity, Baton Rouge, LA, 140 p.

Short, A.D., 1979, Barrier island development along the Alaskan-Yukon coastal plains, Geological Society of America Bulletin, v. 90, no. 1, p. 3-5.

Wiseman, W.J., Jr., Coleman, J.M., Gregory, A., Hsu, S.A., Short, A.D., Suhayda, J.N., Walters, D.C., Jr., and Wright, L.D., 1973, Alaskan arctic coastal processes and morphology: Technical Report #149: Louisiana State University, 171 p.

Attachment C

Water flow patterns from drifters on the inner shelf of the Beaufort Sea

by

Peter W. Barnes and Lawrence J. Toimil

U.S. Geological Survey,

345 Middlefield Road, Menlo Park, California 94025

ABSTRACT

During several summer open-water seasons the net flow patterns of surficial and near bottom waters of the Beaufort Sea inner shelf were studied using drifters and satellite imagery. West of the Prudhoe Bay area the net motion is to the west while east of the Prudhoe Bay area easterly motion of surface waters is common. Oceanographic and meteorologic studies suggest that coastal surface waters may exhibit a surface divergence to the east of Prudhoe Bay. Maps showing the drifter trajectories provide insight on the fate of floating pollutants released on the inner shelf.

INTRODUCTION

In terms of geologic processes, the long-term sediment transport vectors are significant. Sediment transport on the inner shelf of the Beaufort Sea is related to the movement of coastal waters which can be crudely observed using surface and bottom drifters returned by chance finders (Bumpus, 1965). Furthermore,as developmental activities accelerate along the Beaufort Coast of Alaska, a knowledge of drift trajectories of water, ice, sediment, and potential pollutants will be needed (Hufford and others, 1976). In this report we define the probable paths of transport of surface and nearbottom waters during the summer for segments of the central Beaufort Sea shelf.

Three sources of information are reported. During the 1972 U.S. Coast Guard WEBSEC Studies of August and September (Hufford and others, 1974), 4200 surface drift cards were released over much of the shelf between Barter Island

and Cape Simpson. Initial results from this study have been reported by Barnes and Garlow (1975). Another source was 1972 and 1973 LANDSAT 1 satellite imagery from Herschel Island to Barrow. Images free of clouds in the coastal zone were analyzed for the apparent displacement of coastal sediment plumes. The third source of data comes from the release of 500 bottom drifters off the Colville River in June of 1977.

The surface drifter used in this study consisted of a 10 by 15 cm printed orange card encased in a 6 mil clear plastic envelope (Fig. 1). A 2.5 cm steel washer was sealed in the bottom of the drifter as ballast. In order to reduce the direct effect of wind on the cards, the air trapped in the envelope was adjusted prior to sealing so that less than 2 cm of freeboard existed. Problems were encountered in achieving an adequate seal and an estimated 5 percent of the drifters sank when launched. Others have been quite sturdy; surviving several arctic winters. More than 20 percent of the cards returned were being found in 1975, when coastal visitation increased considerably due to a major Federal research effort. Cards continued to be returned through 1978.

LANDSAT transparencies of the coast waters were used to discern sediment plumes and their displacement along the coast. Observations were restrictd to the rare, fog-free summer days, when coastal waters could be clearly seen. The turbid water is most clearly shown on MSS bands 4 and 5 (green and blue) (Wright and others, 1973; Carlson, 1974). These bands were therefore used in our study. As the sediment plumes become elongate in the direction of flow, the directon of surface water flow can be readily ascertained.

A plastic seabed drifter (Lee and others, 1965) was used to measure the drift of water along the bottom in Harrison Bay. The drifter consists of a yellow perforated saucer; 18 cm in diameter, mounted on a red plastic stem 55

Sender LT. WILLIAM WADE

Address EPO BOX 33

SEATTLE, WASH 98790

Zip Code

POSTAGE AND FEES PAID
U.S. DEPARTMENT OF THE INTERIOR

INT 413

U.S.MAIL

POSTAGE WILL BE PAID BY —

OFFICE OF MARINE GEOLOGY

United States Geological Survey
345 Middlefield Road, Menlo Park,
California 94025

Attention: Dr. P. W. Barnes

4908

ТЕКУЩИЕ ИССЛЕДОВАНИЯ ОКЕАНА

OCEAN CURRENT SURVEY 4909

LOCATION WHERE CARD WAS FOUND: 70-10.4N 146-48W

DATE FOUND: JULY 17 1973
Month Day Year

CARD WAS FOUND: On Beach ☒ In Water ☐
In or On Ice ☐

Your assistance will help us determine the movement of ocean currents along the north coast of Alaska. Thank You

REMARKS: LOCATED WELL BELOW HIGH WATER LINE. ICE WAS APPROX 10 miles OFF SHORE

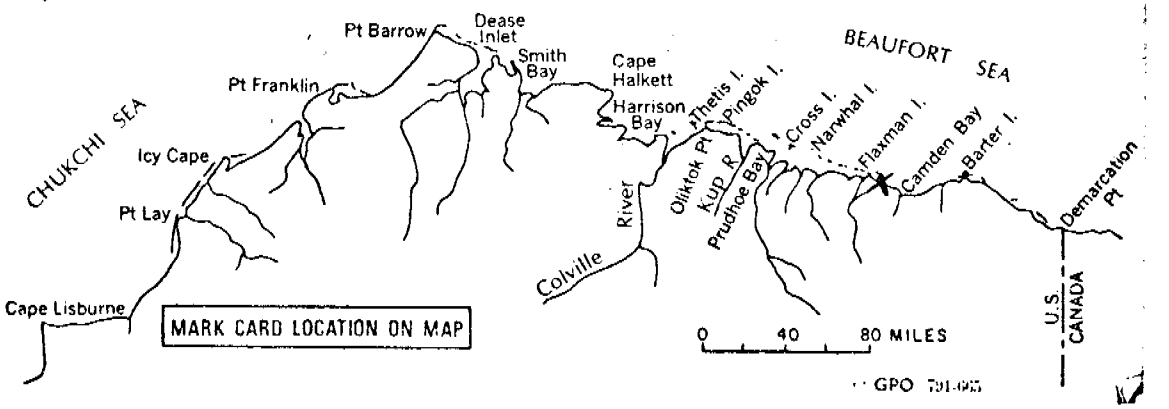

Figure 1. Reproduction of drift card used in this survey. Post Paid card was placed in 6 mil plastic envelope with a 2.5 cm washer and heat sealed.

cm long. Negative buoyancy for the drifter was assured by attaching a 5 gram brass collar to the lower end of the stem. Drifters were released from a low flying aircraft during a single 2-hour flight. The drifters were released in groups of 15 at each station while range-range navigation information was obtained simultaneously to locate the release points within 100 m. Water depths in the area of release were less than 10 m and little lateral movement occurred during the vertical transit of the drifters to the bottom.

OBSERVATIONS

Surface and Bottom Drifter Recovery

In view of the sparse population on the north slope of Alaska and the short season when beaches are not covered with ice and snow, the recovery rate is low compared to studies made elsewhere (Conomos and others, 1971). Recoveries have come predominately from the existing population centers: Barrow, Prudhoe Bay, Barter Island, and the DEW Line sites. The 1970 population of the North Slope Burough was 3,385 (Alaska Census). With the additional petroleum installation at Prudhoe Bay, the present population along the coast is estimated at more than 6,000. Therefore, the low rate of return is expected in this remote area. Most drifter returns were from releases in nearshore areas; a situation common to surveys of this type (Kolpack, 1971; Conomos and others, 1971). Release and recovery data are summarized in Table 1.

The late summer (September) release of many of the surface drifters limited the time for transit to the beaches prior to freeze-up when surface water motion ceases and the drifters could have been incorporated into the coastal ice or the polar pack. Although cards have been found and returned from five consecutive summers following their release, there is no data to suggest that the drifters were not already ashore before freezeup in 1972.

Table 1. Drifter release and recovery data

SURFACE DRIFTERS

Date Released	Number Released	Number Recovered	Percent Recovered
8 August - 11 Sept., 1972	2925 (released from ice breaker in waters deeper than 20 m)	13	.4%
21 August - 6 Sept., 1972	1275 (released from coastal vessel in water depths less than 20 m)	72	5.6%
TOTALS	4200	85	2.0%

BOTTOM DRIFTERS

30 June, 1977	489	41	8.4%

Table 2. Summary of Surface Drifter Movements

Direction of movement	Number	Percent
East along coast	8	10(20%)
Onshore	45	52(___)
West along coast	32	38(80%)

Bottom drifters were released during the initial stages of sea-ice breakup (July), thus, they had a full open-water season in which to drift. Returns have only come from the summer season in which they were released (1977). However a greater percentage (8.4) were returned suggesting that an early release of surface drifters might have been more successful. Release and recovery data are given in Table I.

Direction of Drift

Surface drifters move predominantly in a westerly direction with secondary directions onshore and easterly (Fig. 2). Four times as many drifters moved to the west as to the east (see Table 2).

The direction of surface drift as indicated by the displacement of sediment plumes in LANDSAT imagery demonstrated the same basic water movement patterns as can be seen in surface drifters. Westerly movements dominate in the surface water while easterly displacements were observed in the central and eastern portion of the shelf (see Fig. 3). Sediment plume data is restricted to within 10--15 km of the coastline except in the vicinity of Pt. Barrow.

The bottom drifters all indicated westerly movements in Harrison Bay. A portion of the drifters moved essentially directly westward to the southwest portion of Harrison Bay while another group moved northwestward around the tip of Cape Halkett and were recovered in the vicinity of the DEW Line Station at Pitt Point (Fig. 4).

Rate of Drift

Velocity data are sparse for surface drifter returns. Only nine cards were found prior to freeze-up in 1972, the year when they were released. On the basis of these drifters calculated rates of drift range from less than 1 cm/sec to almost 38 cm/sec. The lowest velocities are associated with two drifters that moved essentially southward (onshore). Drifters traveling to the west had the highest velocities; averaging 18 cm/sec. The one drifter that moved eastward showed an average velocity of 7.5 cm/sec. The tabulated velocities (Table 3) should be considered minimum velocities as the cards may have been on the shore for some period prior to their discovery.

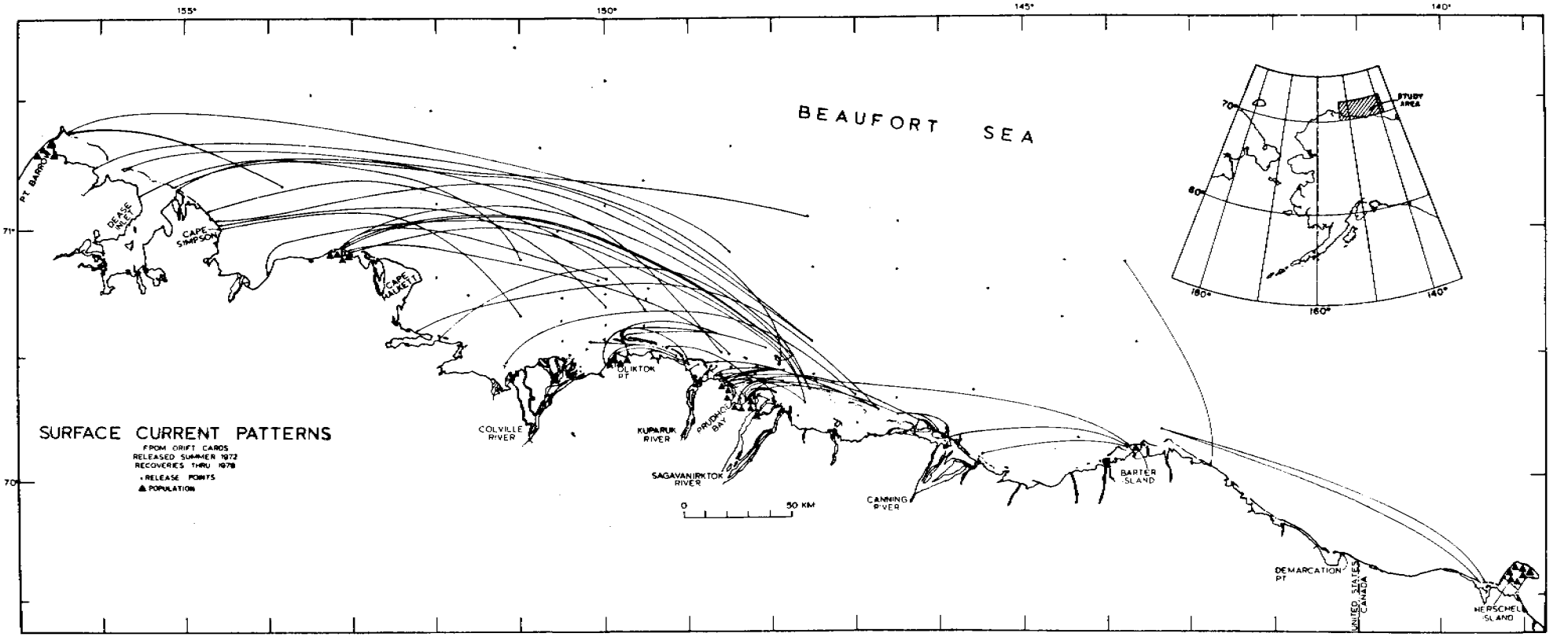

Figure 2. Idealized drift trajectories for surface drifters released in 1972, showing recovery locations through 1978. Population triangles are not represenative of population density.

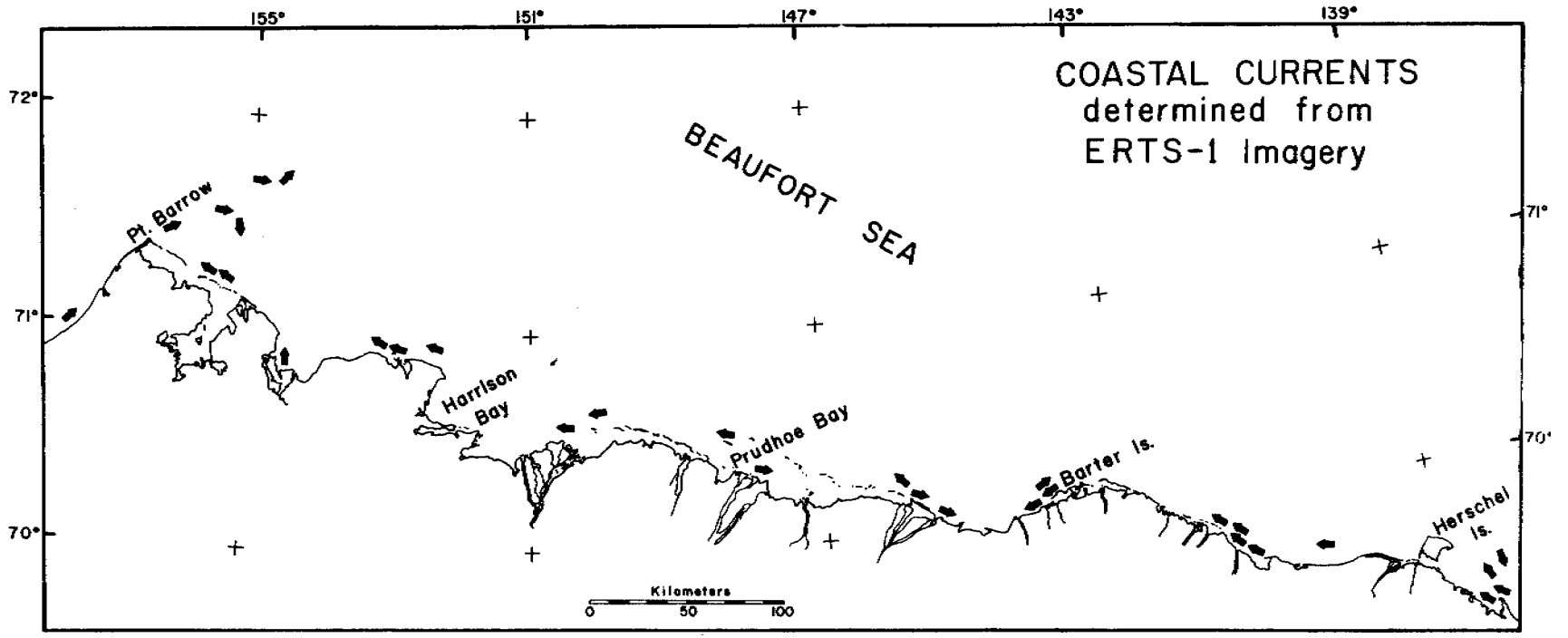

Figure 3. Coastal currents as determined using the displacement of turbid water plumes on LANDSAT imagery during summers of 1972 and 1973.

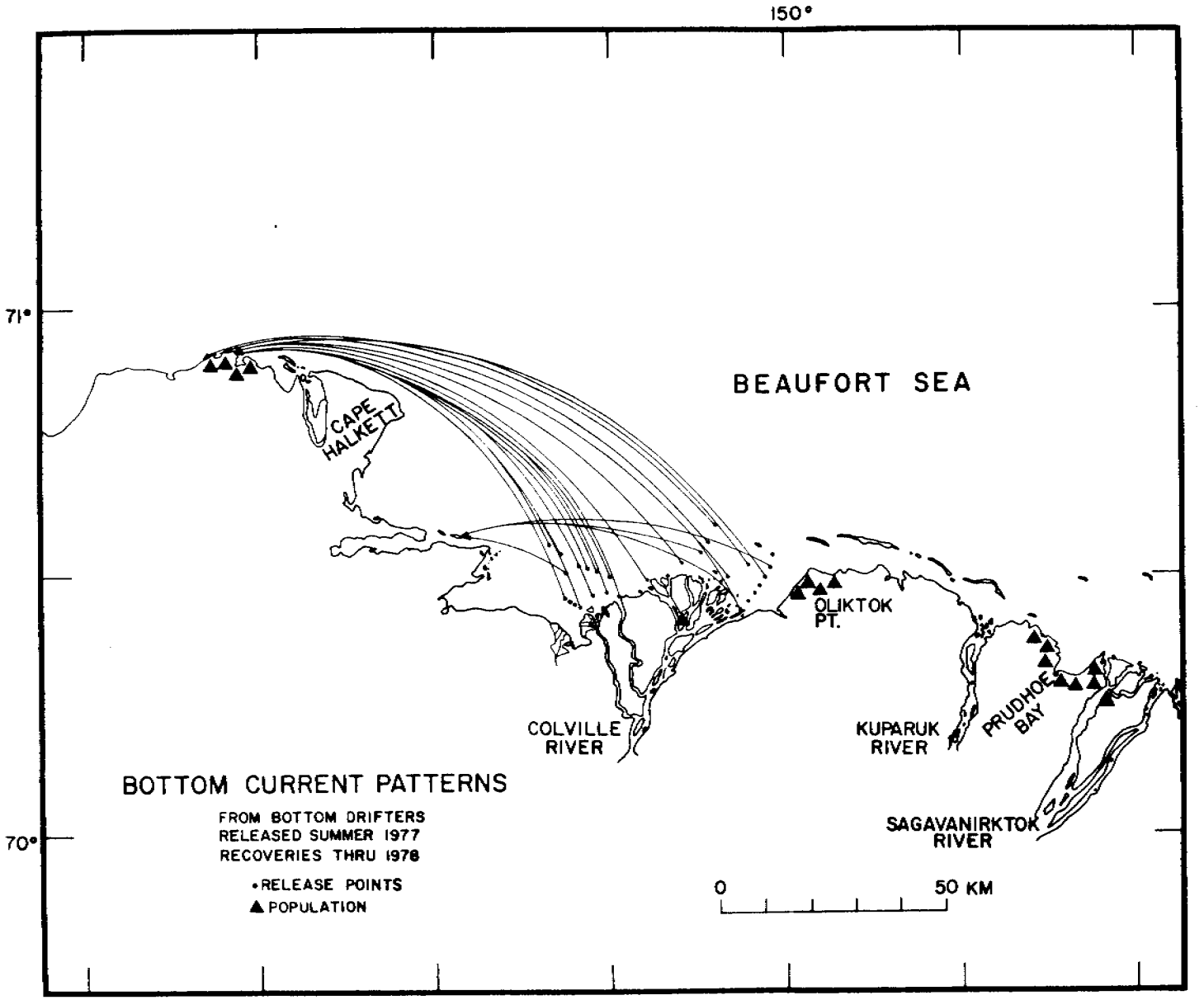

Figure 4. Idealized drift trajectories for bottom drifters released in July 1977, showing recoveries from the same summer.

Table 3. Drifter velocity data for 1972 and 1977

SURFACE DRIFTERS

Release Date-1972	Recovery Date	Days adrift	Distance (km)	Rate (km/day)	Rate (cm/sec)	Direction	Recovery Location
21 Aug.	22 Aug.	1+	28	28+	32.0+	West	Lagoon
21 Aug.	27 Aug.	6	32	5.4	6.3	West	Lagoon
21 Aug.	27 Aug	6	44	7.4	8.6	West	Oliktok
23 Aug.	26 Aug.	3	31	10.5	12.0	West	Kuparuk River
23 Aug.	28 Aug.	5	15	3.0	1.3	South(onshore)	Prudhoe Bay
23 Aug.	9 Sept.	16	13	0.8	0.9	South (onshore)	Prudhoe Bay
29 Aug.	19 Sept.	21	135	6.4	7.5	East	Barter
3 Sept.	11 Sept.	8	198	24.8	29.0	West	Cape Simpson
6 Sept.	9 Sept.	3	98	32.7	38.0	West	Barrow
					Aug. 15.1 cm/sec		

BOTTOM DRIFTERS

-1977	-1977						
31 June	14 Aug.	45	74-120	1.6-2.7	1.9-3.1	Northwest	Pitt Point
31 June	20 Aug.	51	56	1.1	1.3		
					Aug. 1.9 cm/sec		

The bulk (78%) of the bottom drifters were found by one person 45 days after their release. The distance covered by the bottom drifters during this period ranged from 74 to 120 km. Corresponding minimum velocities were 1.9 and 3.1 cm/sec (Table 3).

DISCUSSION

Surface current directions

The data are limited in both spatial and temporal resolution thereby limiting discussion to general considerations. Surface drifters were released only in 1972, imagery was examined only for 1972 and 1973, while bottom drifters were releasd in 1977. Seasonal variations are known to be significant (Hufford and others, 1974). Both the surface drifters and the sediment plume displacements show a westward dominance to the movement of shelf surface waters (Figs. 2 and 3). The U.S. Hydrographic Office data (1968) show that currents on the Beaufort shelf are variable, although the winds are from the east and wind drift of the polar pack is to the west at this season (ibid, p. 13 and p. 100). Drifter data and the displacement of sedi ment plumes as seen on satellite imagery both indicate that surface motion from the Sagavanirktok River near Prudhoe Bay is commonly to the east and eastward. This suggests that there may be a divergence in surface flow off the Sagavanirktok River.

In the same year that surface drifters were released, oceanographic observations also suggest a change in character off the Sagavanirktok River. Minimum surface salinities and temperatures and maximum ice concentrations and dissolved oxygen concentrations were observed in this region (Hufford and others, 1974).

Examination of surface wind data from the airport at Prudhoe Bay for 1972 shows no obvious correlation between wind direction and surface drifter movement in the days following their release. This suggests that the drifters were not responding only to short-term wind forces, but that long term processes were involved. A partial explanation for the observed divergence might be found in the work of Schwerdtfeger (1974). He noted that the mountain barrier effect of the Brooks Range causes dominant northeasterly geostrophic winds to become ageostrophic from the west at Barter Island. This phenomenon is well documented for the winter season but has not been studied in the summer season.

We conclude that there is a recurring divergence in surface drift patterns on the inner portion of the central Beaufort Shelf. Westerly currents are overwhelmingly dominant on the western portion of the shelf and eastward drift is common on the eastern portions of the shelf.

Surface current velocities

In an intensive study of surface currents in the Canadian Beaufort Sea, using much more elaborate drifters, MacNeill and Garrett (1974) found surface currents generally moving at about 5 percent of the wind speed and less than 45^{o} to the right of the wind direction. The surface drifter velocities that these workers reported are similar (ranging from 2-70 cm/sec and averaging around 20 cm/sec)to the velocities that we observed (Table 3). However, values reported in Table 3 are not based on a sufficient number of recoveries nor on recoveries associated with a single wind event to warrant comparisons with wind data.

Bottom currents

Considering the shallow depths of water, the dominant westerly drift observed in surface drifter movement, and the westerly deflection of sediment

plumes, the westward bottom water drift shown by the bottom drifters is not surprising. The clustering of recoveries along a short stretch of coast to the west of Harrison Bay appears to be more than fortuitous, as much of the coast from the Colville River west to Barrow was visited during the summer following the release of drifters. A possibililty exists that the section of coast where the drifters clustered may represent a point where an eddy in the bottom water circulation out of Harrison Bay impinged on the coast during 1977.

The rates of bottom water drift observed in our data are on the same order as for non-tidal drift speeds noted in other inner shelf bottom waters (Conomos and others, 1971) and are approximately an order of magnitude less than the drift observed for surface waters (1.9 cm/sec vs 15.1 cm/sec, Table 3).

CONCLUSIONS

In the inner shelf region to the west of the Sagavanirktok River both surface and bottom water movements are dominantly to the west during the summer. Sediments or entrained pollutants at the surface or at depth will move in a westerly direction at rates of from 1 to 30 km per day (Table 3).

To the east of the Sagavanirktok River the net water transport vectors on the inner shelf are more complex and commonly contain easterly components for the surface drift. The motion of bottom water in this area is unknown.

REFERENCES

Bumpus, D.F., 1965, Residual drift along the bottom on the continental shelf in the middle Atlantic bight area, Amer. Soc. of Limnology and Oceanography, v. 10, supp., p. R50-R53. Carlson, P.R., 1974, Surface currents along the California coast observed on ERTS imagery, Proc. of the Ninth International Symposium on Remote Sensing of Environment, Environmental Research Inst. of Michigan, Ann Arbor, p. 1279-1288.

Conomos, T.J., McCulloch, D.S., Peterson, D.H., and Carlson, P.E., 1971, Drift of surface and nearbottom waters of the San Francisco Bay system, California: March 1970 through April 1971, U.S. Geolological Survey, Misc. Field Studies Map MF-333.

Hufford, G.S., Fortier, S.H., Wolfe, D.E., Doster, J.F., Nobel, D.L., 1974, Physical Oceanography of the Western Beaufort Sea, in WEBSEC 71-72, An Ecological Survey in the Beaufort Sea, U.S. Coast Guard Oceanographic Report No. CG 373-64, p. 176.

Hufford, G.L., Lissauer, I.M., and Welch, J.P., 1976, Movement of spilled oil over the Beaufort Sea shelf--a forecast, U.S.C.G. Special Report D-101-76, 90 p.

Kolpack, R.L., 1971, Oceanography of the Santa Barbara Channel, in Biological and Oceanographical Survey of the Santa Barbara Channel Oil Spill 1969-1970, R. L. Kolpack (ed.), v. II, p. 90-180.

Lee, A.J., Bumpus, D.F., and Lauzier, L.M., 1965, The seabed drifter, Int. Comm. Northwest Atlantic Fish. Res. Bull., v. 2, p. 42-47.

MacNeill, Margaret, and Garrett, John, 1974, Open-water surface currents; Interim report of Beaufort Sea Project, Study D3, Beaufort Sea Project, Federal Building, Victoria, B.C., 50 p.

Mountain, D.G., 1974, Preliminary analysis of Beaufort shelf circulation in summer, in The Coast and Shelf of the Beaufort Sea, Reed J.C., and Sater, J.D., (eds.), Arctic Inst. of North Am., Arlington, Va., p. 27-48.

Schwerdtfeger,W., 1974, Mountain barrier effect on the flow of stable air north of the Brooks Range in Climate of the Arctic, Geophysical Institute, Univ. of Alaska, Fairbanks, p. 204-208.

U.S. Navy Hydrographic Office, 1968, Oceanographic Atlas for the Polar Seas Part II Arctic: H. O. Pub. No. 705, 149 p.

Wright, F.F., Sharma, G.D., and Burbank, 1973, ERTS-1 observations of sea surface circulation and sediment transport, Cook Inlet, Alaska, Freden, S.C., Mercanti, E.P., and Becker, M.A., eds., Symposium on significant results obtained from ERTS-1, Vol. I, Sec. B, National Aeronautics and Space Administraton, Washington, D.C., p. 1315-1322.

Diving observations on the soft ice layer under the fast ice at DS-11 in the Stefansson Sound Boulder Patch.

Attachment D.

By Erk Reimnitz and Ken Dunton

INTRODUCTION

The first major OCSEAP winter field program in the Beaufort Sea led to the discovery of anchor ice, or an underwater ice phenomenon. In the American Arctic anchor ice has only been suspected to occur, but solid evidence is lacking. In other polar regions the process of anchor ice formation, under conditions of supercooling of the sea-water column, has been observed and described. In Siberian waters, stakes driven into the sea floor have been extracted by the buoyant force of ice forming on the sea floor below water (Zubov, 1945), and according to some sources the term anchor ice is related to the fact that ships' anchors have been lifted to the sea surface by ice accretion. Diving observations by Dayton et al. (1969) in McMurdo Sound show that the formation of anchor ice affects the distribution of the benthic community, and is significant as a sediment transport agent. A bottom dredge, estimated to weigh 150 lbs, was found lifted to the undersurface of the fast ice in McMurdo Sound, and when shaken by divers, fell back to the sea floor (Gordon Robilliard, oral communication, 1979). Diving observations made in the Boulder Patch this winter indicate that some type of underwater ice formation did occur early in the season and these observations have far-reaching implications for most scientific disciplines involved in OCSEAP studies.

In this report the occurrence of a thick layer of soft ice under the fast ice, and pertinent observations made by divers, is briefly described. We will also discuss a few possible mechanisms that could have led to the formation of underwater or anchor ice in this particular setting, list other observations from the American Arctic that suggest underwater ice formation, and list certain implications of the phenomenon. The poor organization and rough discussion of our observations and thoughts we apologized for; we just returned from a diving investigation of the phenomenon. The principal purpose of this report is to stimulate colleagues working in the Arctic to remember observations or data pertinent to the formation of underwater ice in the Beaufort Sea, so that the phenomenon may be properly evaluated and studied.

DIVER OBSERVATIONS AT THE BOULDER PATCH

The observations pertinent to the underwater ice phenomenon at the Boulder Patch is divided into those made in early

November, 1978, and those made in late February/early March, 1979. Both sets of observations were made at one particular site in the Boulder Patch, marked by an underwater beacon, at a water depth of 4.8 m (Fig. 1). At the site the bottom is a substrate of very stiff, overconsolidated, cohesive mud, overlain by scattered pebbles, cobbles, and small boulders. This coarse material covers about 50 to 60% of the mud substrate, and individual clasts are partially embedded, or resting loosely upon the overconsolidated mud. The undersurfaces of clasts are black, suggesting reducing conditions. The upper surfaces provide the basis for a rich and varied benthic community, including several varieties of kelp with fronds a meter long, of sponges, soft corals, sea anemones, bryozoans, and many others. The biological community, and the habitat, found here are unique for the inner shelf of the Alaskan Beaufort Sea, as far as we know now, and is the focus of the study that led to the discovery of underwater ice.

Under summer conditions, when rivers and coastal erosion are supplying sediments to the sea, when waves and currents rework bottom sediments, the water at the Boulder Patch has relatively high light transmissivity and provides good visibility for divers, as compared to other areas of the inner shelf.

Early November Observations. -To locate the beacon at dive site 11 (Fig. 1) about 20 holes were augered through the ice, generally eastward of the site, at distances of up to 1.5 km. On Nov. 6th the ice was about 50 cm thick, and the ice shavings produced by the auger showed variable ice turbidity (sediment inclusions), ranging from clear to very turbid at the dive site. The general impression was that the ice farthest to the east was the cleanest, but there were variations in the ice turbidity from one hole to another, even within a few hundred meters of the site. At the site the ice had a rough surface, with ice slabs of about 10 cm thickness protruding from the thin snow cover. At a distance of 35 m to the south of the site was a 200 m wide, re-frozen lead, with smooth clean ice about 40 cm thick.

Most diving observations were made within a radius of 25 m of the access hole. The underwater visibility was only about 1-2 m, due to large amounts of fine suspended matter, making conditions much worse for diving observations than during summer. Red encrusting algae, and large brown kelp fronds, were covered with a millimeter-thick ooze, and a sediment collecting tray set on the bottom in August had collected .5 cm of fine sediment. Currents were not noticed.

A layer of slushy soft ice of highly variable thickness, generally ranging between .5 and 1.5 m, but projecting down to within 2 m of the sea-bottom, covered the undersurface of the .5 m thick massive ice canopy. A crossectional sketch of the two-layer ice canopy at the site is shown in figure 2. The slushy ice consisted of a loose aggregate of plate-like ice particles of

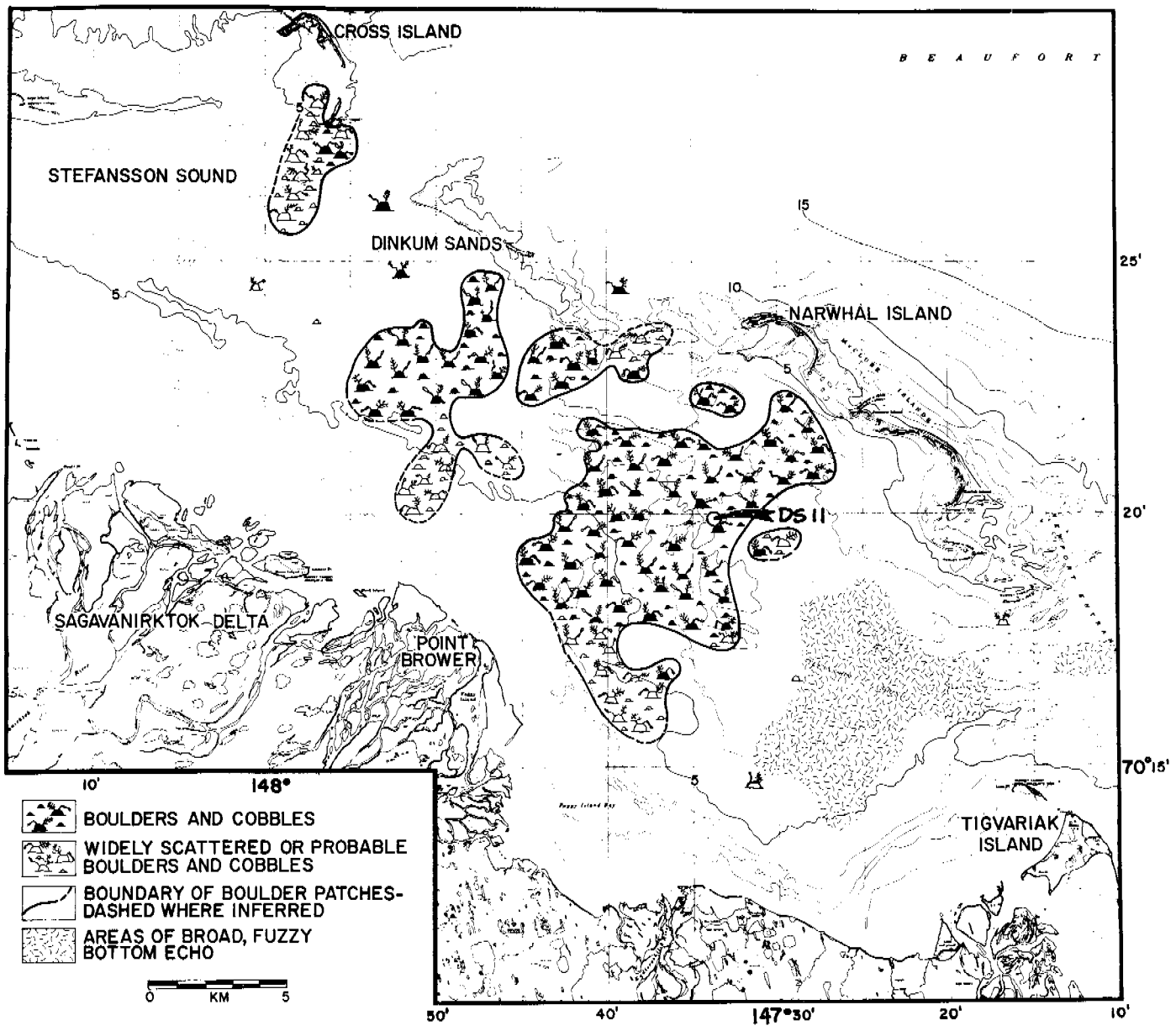

Figure 1. The Boulder Patch and location of divesite 11.

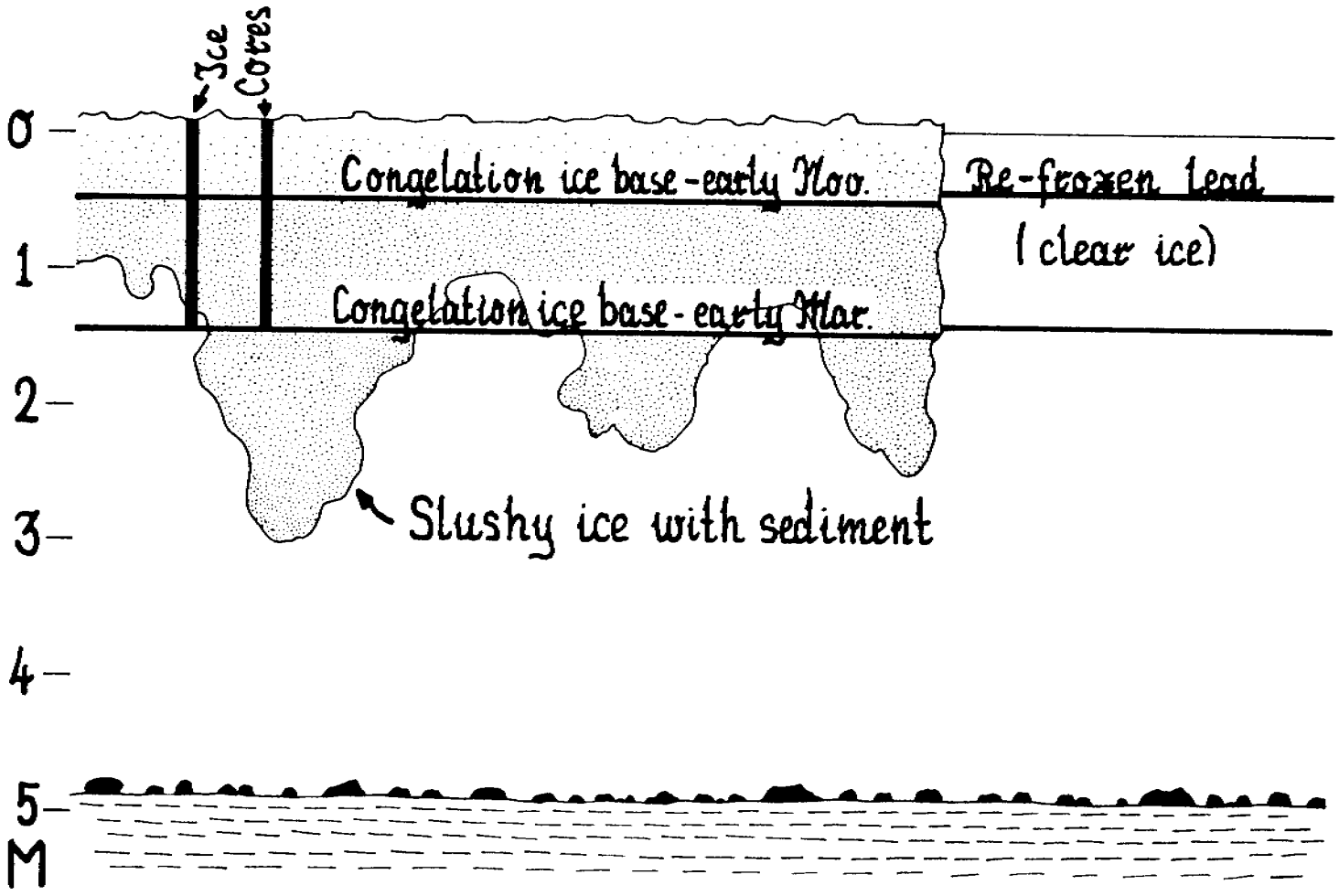

Figure 2. Schematic diagram of the relation between congelation ice and the soft ice layer at DS-11 in November and March. Two ice cores, one through a solid ice-water interface, the other into soft ice, and a nearby re-frozen lead with clear ice are shown.

about 1-5 cm average diameter, with enough interstitial water so that a diver could disappear within the deposit. An overall view and a closeup view are shown in two photos (Figs. 3 and 4). No stalactites, wide spread under the fast ice in an earlier diving observation in May, 1978, (Fig. 5) were noted. When disturbed by divers, the slushy ice contributed fine suspended matter to the water column, with the largest particles having noticeable settling velocity. Pebbles, shells, or other macroscopic particles were not included in the slushy ice. In numerous diving days, none of four divers noticed ice crystals on the benthic community under study, nor on the rocks, nor in the underlying stiff mud. Also, no frazil ice was seen in the water column.

At a nearby study site on the re-frozen lead mentioned above, a "jigger board" (used to move a line along the undersurface of the ice) functioned properly. This device only works under the smooth firm surface, and therefore could not have been used at the dive site. The ice bottom within the re-frozen lead must have been hard and smooth, like "normal" undeformed first- year sea ice. In another diving investigation the ice base at the EXXON ice island under construction in Stefansson Sound, about 30 km west of our dive site, was also found to be clean, smooth, and firm. There the water depth is only 3 m, and the bottom consists of fine muddy sand.

Late February/early March Observations.- The ice surface at the dive site had undergone no noticeable changes, except for a slight increase in snow depth. The diver access hole was cut adjacent to a flag, marking the November dive hole. This flag had moved about 5 m in a southerly direction, as shown by the relative position of the bottom-mounted beacon.

Diving observations again were made within a 25 m radius of the access hole, but one of us (K.D.) swam a 50 m traverse to the refrozen lead south of the hole. The most notable contrast with the fall conditions was the clear water, allowing about 6 m of visibility in the undisturbed water column. No frazil ice was noted in the beam of our search lights. Almost total darkness prevails under the ice, in spite of the abnormally thin snow cover this year. Only after about 3 minutes with the flash light turned off, could the eye detect patches with a hint of daylight, but not enough to illuminate objects. Some of the ooze film covering the bottom, plants, and animals appeared to have been rinsed off by currents, fish, or seals moving about. The sediment collecting tray had trapped only about one millimeter of fine sediment. The fronds of the large brown algae were oriented, pointing 270° T.

The high-relief, undulating soft-ice layer below the solid fast ice canopy still was very conspicuous (Fig. 3). But about half of the overhead area consisted of smooth and solid congelation ice. This had shallow, irregular grove features, outlined only when filled with diver exhaust air, similar to the

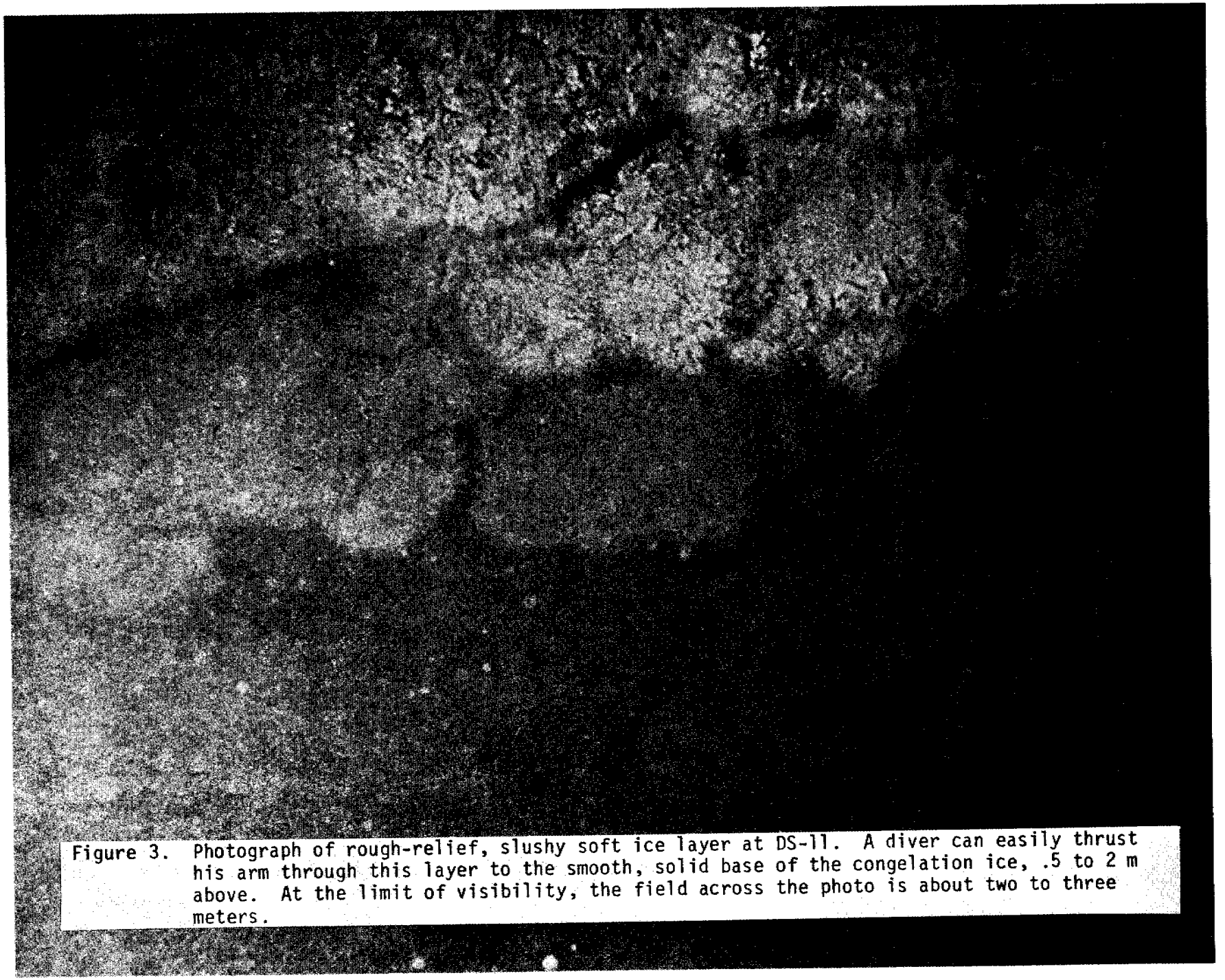

Figure 3. Photograph of rough-relief, slushy soft ice layer at DS-11. A diver can easily thrust his arm through this layer to the smooth, solid base of the congelation ice, .5 to 2 m above. At the limit of visibility, the field across the photo is about two to three meters.

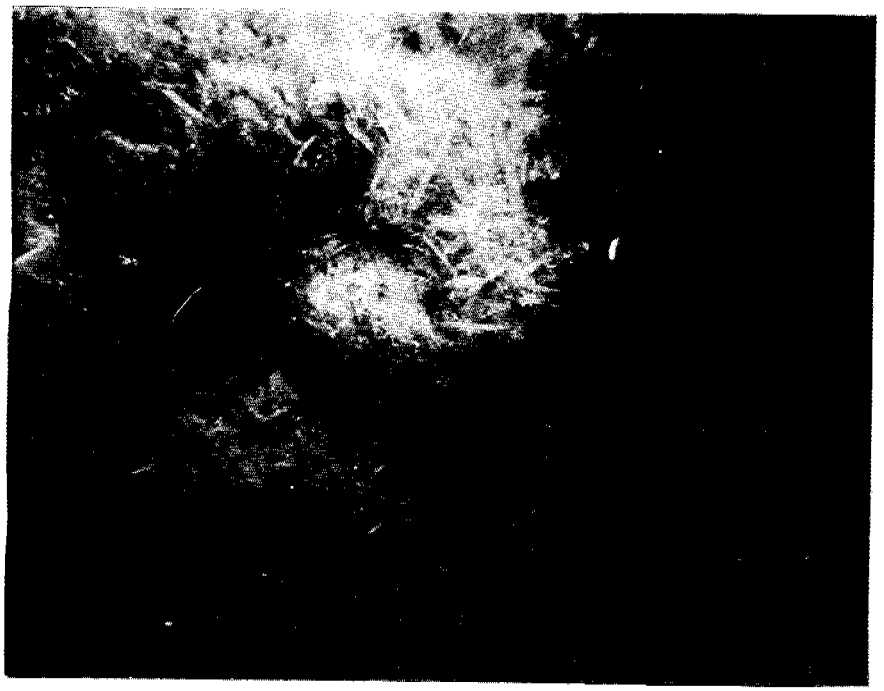

Figure 4. Close-up view of the soft ice layer crystal lattice, showing very fine-grained mushy ice, and randomly oriented ice platlets up to 15 cm in diameter. In this photo most of the large platelets are oriented with the edges toward the viewer. The elongate bright spot to the right of the ice aggregate is a 3 to 4 cm long amphipod, practicing his swimming.

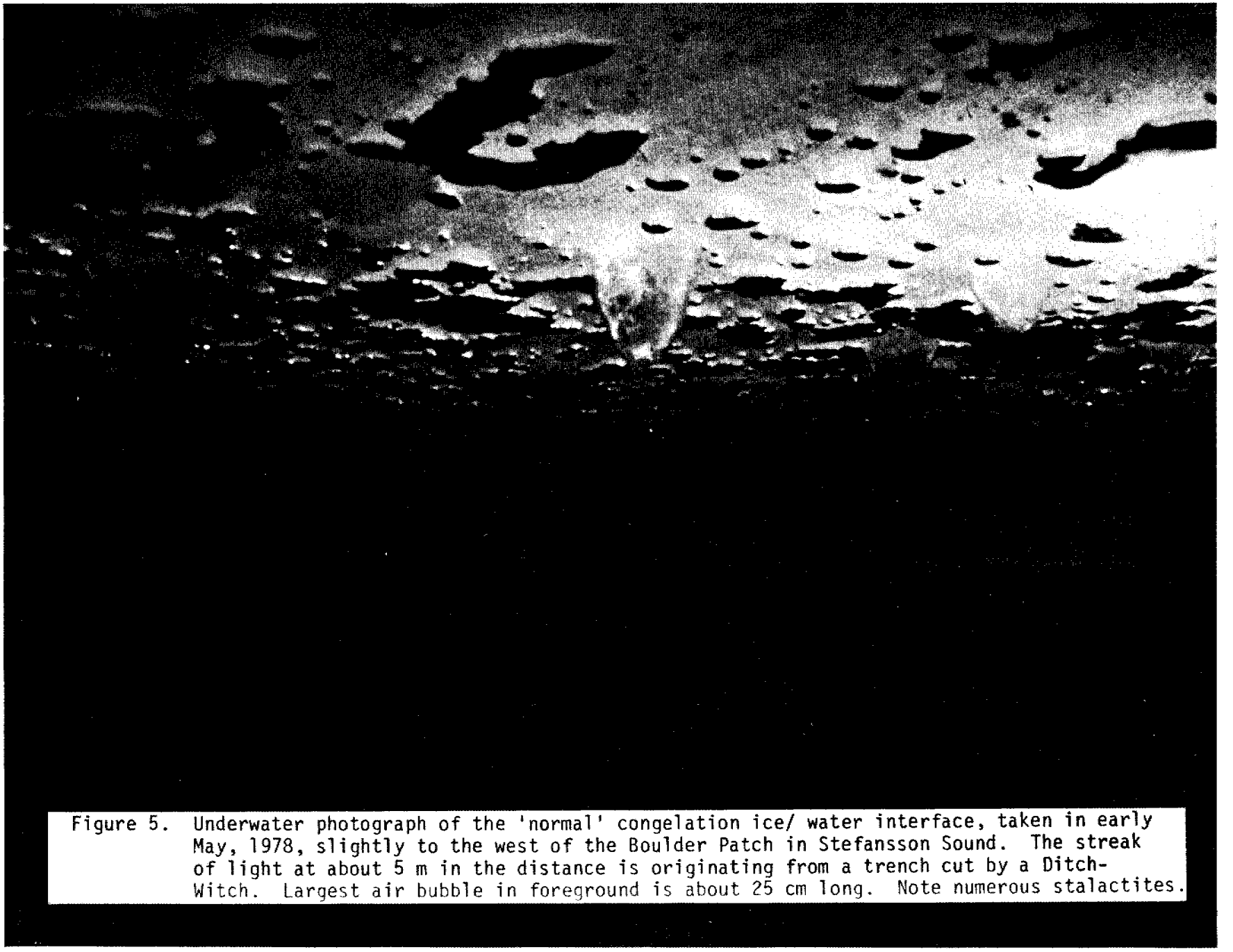

Figure 5. Underwater photograph of the 'normal' congelation ice/ water interface, taken in early May, 1978, slightly to the west of the Boulder Patch in Stefansson Sound. The streak of light at about 5 m in the distance is originating from a trench cut by a Ditch-Witch. Largest air bubble in foreground is about 25 cm long. Note numerous stalactites.

photo in figure 5. Even on days when six tanks of air (approximately 300 cubic feet) were used up under the ice, no large pools were noted, implying that gasses escape freely through the ice canopy. The soft ice layer, on close observation, again consisted of a lattice of 1-15 cm platelets on very fine-grained slush, forming a loose, dirty-appearing aggregate, containing more than 50% interstitial water. One of us (E.R.) has the impression that the coarser crystal aggregates occur in a 5 to 10 cm thick, sediment-free surficial layer covering the dirty, finer-grained slush ice. The amplitude of the soft ice mounds below sea level apparently had not changed since November; peaks reached to within 2 m of the sea floor. In one area, about 15 m south of the dive hole, a number of stalactites occurred; one exceptionally large one had a diameter of about 20 to 25 cm at the base and a length of .5 m. Some of the larger ones were protruding from soft ice, others grew out of congelation ice. No brine drainage, easily detectable from the light refraction at the interface of a settling plume of brine and sea water, was noted at the time of observation.

One of our theories to explain the highly undulating relief of the soft ice layer underneath a smooth fast ice canopy, involves ice nucleation from supercooled water onto a heterogeneous seafloor, with protruding rocks and a variety of biological growth. We therefore looked for clues on the seafloor that might be correlated to downward projecting peaks of soft ice, but no clues were found that would explain variations in the accumulation rates of frazil ice to form slush ice.

On one particular day, under optimum conditions at the southern perimeter of the study site, an eerie bluish light was noted still farther to the south. This phenomenon was investigated on the last diving day by swimming toward the light with a 50 m long tether. Sky light was coming through the clean, smooth ice of the lead, separated by a sharp straight boundary from the slush ice region. The ice bottom in the lead was smooth and firm. The light penetrating the ice illuminated the sea scape similar to summer conditions, so that no search lights or strobes for photography were required.

Two ice cores were taken of the solid ice by use of a CIPRE corer in the area near the dive hole. One of these was located over a thick slush ice accumulation (Fig. 2). The core penetratead 143 cm of solid ice (the slush ice cannot be collected with this tool). The upper 10 cm of the core were clear ice. From that point downward the ice gradually became turbid, with a sharper turbidity gradient at about 30 cm. The lower part of the core was uniformly turbid, with particles of up to 1 mm size. The other core, located over ice with a smooth, hard base (Fig. 2) penetrated 157 cm of solid ice. The turbidity-distribution within this core was similar to that of the first one, except that the bottom 10 cm appeared slightly clearer than the turbid ice above.

Salinity measurements were made by use of a simple temperature-conductivity-salinity-meter on a number of days, as shown in Table 1. The data of March 8 definitely is bad, possibly due to ice crystals being stuck within the sensor element; but we believe that the slight salinity increase from 2 m, below the disturbing effect of the dive hole, to 5 m is real. The large day-to-day variations in bottom-water salinity also seem to be real (except for March 8), as are the variations below the ice canopy and within the soft ice on February 28. Accurate temperatures, taken with a string of thermisters provided by Tom Osterkamp, have not yet been calculated.

OTHER OBSERVATIONS FROM THE ARCTIC

Numerous clues lead us to believe that supercooling of the water column, resulting in anchor ice formation, is not uncommon in the Arctic.

Ice forming on nets and lines. -Reports of ice forming on nets and lines submerged in the shallow waters of the inner shelf in the period from February through May are so numerous, that we can only list a few here. Such observations were made along the Chukchi Sea and the Beaufort Sea shores. According to Jim Helmericks, such ice forms primarily within a few meters of the hole cut through the ice, generally on both net ends. Occasionally ice crystals form along the entire cork line, if this is within 20 cm of the ice base, and under severe cold ice forms on the entire webbing, bunching up the web and raising the net to the ice base. During February, 1979, 1.8 m high nylon gill nets set on the bottom in Stefansson Sound, directly north of Prudhoe Bay, had ice crystals at all knots within 16 hours, and within three days had the webbing so plugged with ice that fish no longer could be caught in them. Fyke nets, of heavier webbing and impregnated with a tar-like substance, did not accumulate ice during the same period. In that same area we observed ice growth on a submerged line off the West Dock within a 7 day period in early May, 1978. During only one night in early March a line extending from the seafloor to the ice surface at dive site 11 in the Boulder Patch had ice growth along the upper two meters. A week earlier, the same line had accumulated a very few small ice crystals during a 5 day period of cold and windy weather, while about 30 cm of ice grew over the dive hole within the diving hut. An ice cube of about 700 cc of fresh water, anchored about 15 cm above the bottom at the site, did not show any ice growth during a 7-day period in early March.

During the night of September 6th to 7th, 1975, we had a small gill net at a 1 m water depth in a narrow channel adjacent to a gravel spit at Point Thompson. During the following night the winds were about 20 knots (easterly) and the temperature -6^{0}C. Short, choppy waves were breaking against the spit. Next morning the entire webbing and lead line were ice covered and floating on the surface. At that time the bottom, in .5 to 1 m water depth, felt hard and slippery, as if sheeted with ice.

Table 1. Salinity Data (‰) collected at DS-11 in February and April with a simple conductivity-salinity-temperature probe. The readings on 3/8 must be in error due to ice within the sensor element.

	2/27	2/28	3/7	3/8		3/9	3/10	3/11	3/12	3/13
In dive hole				0 m	27.5					
				1 m	27.6	31.6		31.8		32.2
In soft ice		4-28.5		2 m	27.2					
Under hard ice		33.5		3 m	27.2					
Under soft ice		24.0		4 m	27.3					
Bottom	33.0	33.5	29.7	5 m	27.5	34.4	32.0	31.8	31.9	32.2

We are unaware of occurrences of ice growth on metallic or plastic submerged surfaces, but are wondering if the "unexplained" loss of some of our current meter moorings may not be attributable to anchor ice formation.

Coarse sediment and kelp raised to the sea surface. - During one Spring, Lou Shapiro noticed pebbles and mollusk shells on the surface of the undeformed first-year ice within 50 m of the beach at Barrow, where the water depth is 2-4 m (oral communication). An Eskimo told him that these coarse clasts are raised to the sea by ice forming on the sea bottom during cold storms of the previous Fall, and that such occurrences are not at all uncommon.

During May of 1973, while cutting a 1 m^2 hole in the undeformed first-year ice due north of Oliktok, we found several pebbles with attached brown kelp fronds in the upper 10 cm of the ice. Similarly, we found brown kelp fronds in the upper 10 cm of the undeformed fast ice in Stefansson Sound in May, 1978. Kelp in these waters does not float on the sea, even without attached pebbles, and therefore must be due to the formation of anchor ice on kelp or pebbles, raising these from the bottom to the surface.

Ice on the sea bottom. - Tom Osterkamp reports (personal communication) that in eastern Harrison Bay and western Simpson Lagoon, at water depths of less than 3 m, about 100 ice cores were taken during May in 1969 through 1971. Attempts were also made to collect sediment samples at the sites, with a sampling tube on a long rod. At about half of the site, the sea floor contact produced a sharp, clinking sound, and the sediments could not be penetrated by pushing downward. Osterkamp believes that ice sheeted the bottom at these sites; he almost retrieved one ice sample which had gotten caught in the sampling device, but then slipped out. We should note that in numerous shallow water coring and seafloor probing operations across the Colville Delta, in eastern Harrison Bay, in eastern Simpson Lagoon, in Prudhoe Bay, and in Stefansson Sound, mainly during May of various years, but also in April, we have not noted ice on the sea floor. In the last three areas, and at the Boulder Patch, we also have direct bottom observations made by diving, and found no anchor ice.

Lou Shapiro was present while a man studying amphipods at about 2 m water depth off Barrow was hitting the seafloor with a rod through a large hole cut in the ice. Irregularly shaped, shard-like pieces of porous ice of 10 to 15 cm diameter, were rising to the surface. These pieces of ice had the appearance of ice that has been lying in the sun, melting. The time of these observations of anchor ice at Barrow was June, 1976.

Frazil Ice in the Water Column. - Jim Helmericks reports that frazil ice commonly is seen rising from holes cut through the ice, and believes that this frazil ice is not released by disturbing the walls around the hole. We have commonly seen such frazil ice rising from holes in April and May, but were never able to verify that such ice is actually part of the undisturbed water column. Brian Mathews states that he saw frazil ice in the water column in his November, 1978, diving operations off Oliktok, in Egg Island Channel, and at the Boulder Patch. Such occurrences, of course, imply that the water column is very close

or at the point where anchor ice could form.

Fine Sediment in the Undeformed Fast Ice and High Water Turbidity in Winter. - Turbidity of the upper section of the fast ice was widespread during the Spring of 1978 (Barnes and Fox, Attachment E of this report). This turbidity was due to inclusions of fine sediment particles, and near the coast was found in up to 1 m or more of the upper ice. But the very top 10 cm generally had clear ice. Several large ice blocks lifted near the West Dock by EXXON Corporation in 1978 showed the boundary between the turbid ice and the clear ice below as a wavy surface. This wavy boundary was similar to a hypothetical boundary that would be formed, if all of the undulating slush ice layer at the Boulder Patch were incorporated into the solid ice by downward advance of the ice front. Thus, layers of diffuse fine sediment inclusions in the first year ice could be related to an anchor ice process raising fine sediment to the ice canopy above; but the turbid ice could also represent slush ice with sediment inclusions drifted against the coast during late Fall storms (if one could explain the clear ice often observed above the turbid ice). A third explanation, namely that the turbid ice represents normal ice growth in waters turbid from Fall storms, would seem difficult to accept. One meter into the seasonal ice growth cycle (about early January) the inner shelf waters should have had ample time to clear by settling under the shelter of the ice canopy. The discussion of ice turbidity is given in more detail by Barnes and Fox (Attachment E).

David Drake, in an unpublished report, shows that the waters of Norton Sound during Winter contain as much suspended matter as during Summer. This finding to us is suggestive of some underwater ice growth process, as Yukon River sediment input has been eliminated, and bottom reworking by wind induced currents and waves cannot be a factor. The winter water-turbidity of Norton Sound thus would have a similar cause as that observed at the Boulder Patch in November.

Under-ice Observations by Divers in the MacKenzie Bay. - Interesting observations of several types of underwater ice formation were made by the divers Ward and McGowan in MacKenzie Bay region during April, 1971 (Kovacs and Mellor, 1971). An important point to remember here is that the water salinity was measured at about 3 ppm, (p.7). We may assume that at their dive site, at a water depth of 12 m, only the upper layer was nearly fresh, while normal salinity water lies below the thermocline. The divers noted what must be the thermocline as a layer of light refraction (blurry vision) and concentrations of plankton at a depth of about 3 m.

The divers report that the keel of a multi-year ridge, and much of the surrounding under-ice terrain, was covered by an undulating layer of interlacing ice crystal platelets of 10 to 15 cm diameter, with the largest measuring 45 to 60 cm in diameter (p.99). This aggregate of ice crystals and water in places was

90 to 120 cm thick, as the divers could not thrust their arms through to a solid ice boundary. The divers also noted the "clouding effect they (the ice crystals) produced upon impact", reducing the visibility. Kovacs and Mellor (p.17) called this thick layer of mushy ice of undulating relief and sediment inclusions "deteriorated ice". The similarities of this layer with the "platelet layer" in McMurdo Sound (Dayton et al. 1969), and the slush ice layer in the Boulder Patch, suggests to us that an anchor ice process is responsible and the layer is actually depositional (upside down).

Not far from the site of the above observations the divers studied the near-vertical walls of two adjacent ice island fragments. The water depth (13 m) was similar, and as the time of observations was only two days after the first described observations, we may assume that the water structure was similar, with fresh water overlying salt water. The divers report a "definite water stratum", about .6 m thick, marked by concentrations of plankton, with the appearance of an oil/water suspension (light refraction), about 7 to 8 m from the surface. Corresponding with this thermocline was a 1-m thick ice ledge, protruding about 1 m from the sheer faces of ice, around virtually all but the down-current sides of the ice island fragments. The outermost edge of this ice ledge is characterized as a "rim of ice-crystals" appearing "as a very enormous hoarfrost with 2 x 5-inch platelets" (p.106). The ice of the protruding ledge felt relatively soft. Above the thermocline, and the ice ledge, the texture of the ice was mushy, and could be penetrated to about 10 cm, while the surface of the ice island from the ledge to the seafloor had a pockmarked texture, with 15-cm diameter pockets of smooth hard ice.

The ledge, with coarse cyrstal around the rim, appears to us as an ice growth feature at the interface between the upper fresh water and the lower, colder seawater. The deep water cools the freshwater to, or below, its freezing point, and the ice island provides the nucleating surface. Analogous conditions may occur in Stefansson Sound if river discharge were to increase temporarily shortly after the freeze-up.

Some possible causes for the underwater ice formation at DS-11.- Before considering the most likely causes, which at the particular setting of dive site 11 could have resulted in underwater ice formation, a time frame should be established.

The ice thickness of 50 cm at DS-11, measured on November 5, lies near the ice thickness curve for the Arctic coast (Fig. 6) compiled from several years of data by Schell (1974). When we last saw Prudhoe Bay, on September 26, freeze-up appeared eminent. Thus, last winter's ice growth in Stefansson Sound may also have begun on October 1. A 10 cm ice thickness difference between dive site 11 and the nearby lead (Fig. 2), suggests that the lead may have formed on October 8 to 10. Also, the thickness of slightly rafted ice at DS-11 suggests that breaking of the ice

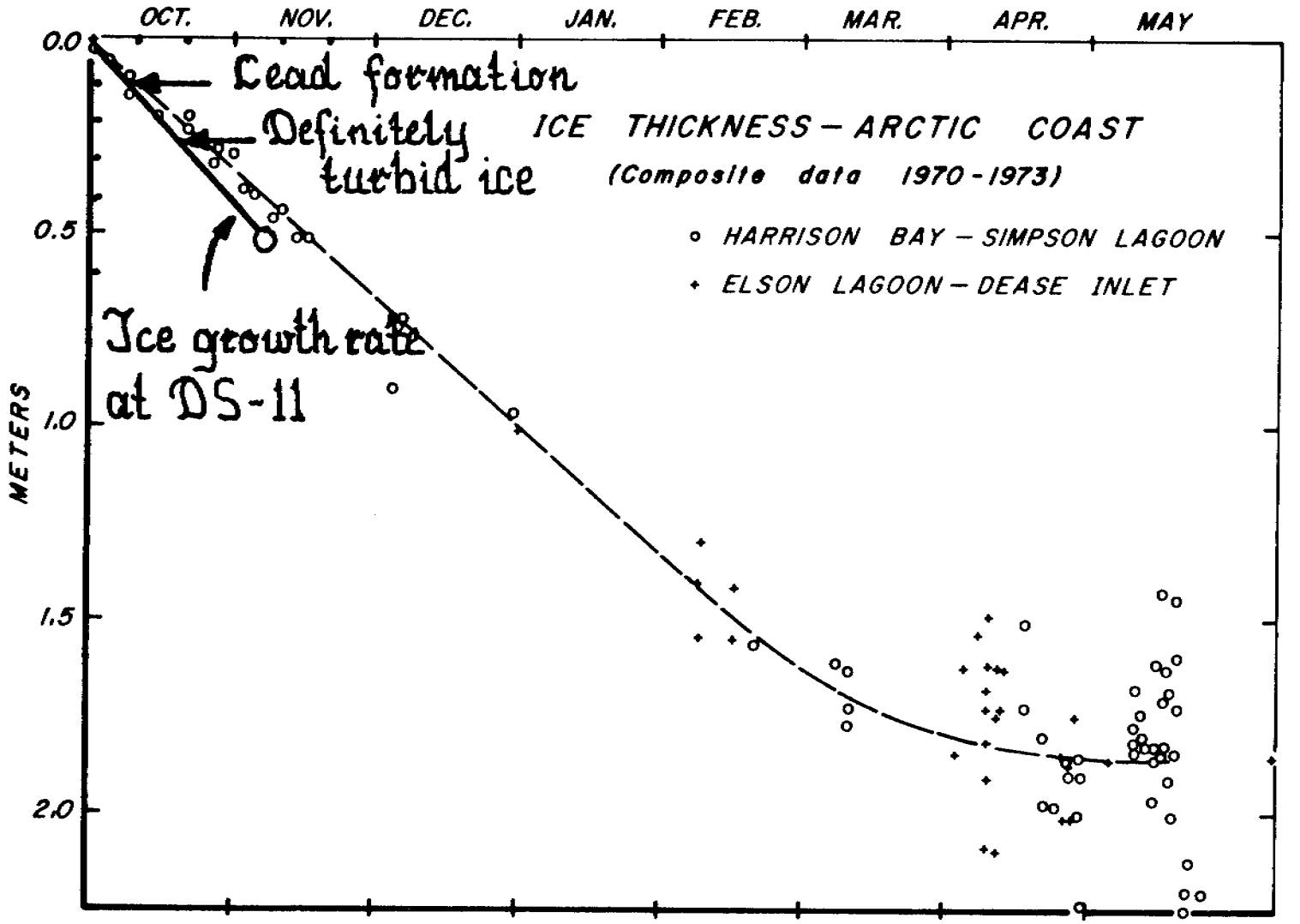

Figure 6. Seasonal ice thickness growth rate, compiled by Schell(1974), with the November,1978 measurement at DS-11. This data, together with the depth points of ice turbidity increase, establish a time-frame for the underwater ice production event.

occurred about that time. Barrow recorded easterly winds of 20 to 30 mph for the period from October 6 through the 8th, and Barter Island showed easterly winds of 28 to 35 mph, gusting to 46 mph, suggesting these three days as a likely time for ice deformation in Stefansson Sound. A slight increase in ice turbidity started about the same time, but the ice was definitely turbid by October 15. According to diving observations, an increase in ice turbidity should be a result of underwater ice formation; it represents incorporated soft ice with sediments. Thus underwater ice formation started between October 10 and 15. But since the ice of the re-frozen lead, formed on about October 10, is clear, the slush ice event was over by the time of re-freezing. This line of reasoning suggests that soft ice formed within a period of only several days, possibly during the easterly storm of October 6 to 8th, just prior to opening of the lead.

During the last winter, the accumulation of underwater ice may have been restricted to the Boulder Patch. North of Prudhoe Bay the Stefansson Sound fast ice had a firm, smooth base, and augering 1.5 km east of DS-11 in November showed the ice was clean. This might suggest that the mechanism of underwater ice formation was related to a unique bottom type and benthic community. The fact that the soft ice has a highly undulating and even rough relief, suggests that the soft ice did not accumulate by individual ice crystals rising from the water column; the resulting deposit would form a uniform blanket under the solid ice. Moreover, neither previous observations nor laboratory experiments have provided clear evidence for ice nucleation on suspended sediment particles (heterogeneous nucleation) (Osterkamp, 1975, Al'tberg, 1938, Benedicks and Sederholm, 1943), to account for the sediment content of the slush ice. Even if supercooling of the order of a degree were achieved to trigger heterogeneous nucleation (Muller, 1978, p.250), we have the problem of finding a mechanism to first put the sediment into suspension. As outlined earlier, the waters should be very clear under an ice cover in this locality. Let us, therefore, look at the surface of the Boulder Patch as a nucleating surface.

Individual ice crystals nucleating preferentially on certain objects or substances covering a heterogeneous bottom, could conceivably incorporate small sediment particles and rise with these to the surface. This kind of mechanism would explain the lack in the slush ice layer of particles larger than those which individual ice crystals can raise. This mechanism would also explain the random orientation of individual platelets, and the undulating relief. But this mechanism would not explain the almost jagged relief in the slush ice in many areas. Also, underwater ice nucleating on the bottom (anchor ice) is not known to rise individually, but rather in sheets or masses (Dayton et al., 1969, Benson and Osterkamp, 1974, Osterkamp et al., 1975, Zubov, 1945). Such masses of ice rising to the ice bottom would result in the kind of relief seen in the slush ice layer (Figs.

2, 3, and 4). But the lack of evidence for ripping out by ice in the benthic community and the lack of large inclusions within the slush ice layer, indicate that large masses of ice had not accumulated on the sea floor. We will have to leave this question unanswered for now. Anchor ice formation is about the only reasonable mechanism to account for the drastic increase in November water turbidity and the ooze blanket covering fauna and flora, as compared to summer conditions.

Conditions of supercooling, leading to the formation of underwater ice, could result from a number of different causes. Some of these possibilities can be eliminated since they are unlikely to occur in the Boulder Patch.

The normal process of salt exclusion during the formation of congelation ice, and the settling of cold brine to the seabed, seems unlikely as a cause, since the formation of anchor ice would be very widespread on the inner shelf. The nearby lead, formed about October 10, could have resulted in supercooling at the surface (Coachman, 1966), and the supercooled water may have been carried downward by convection; but we believe the lead would have remained open for too short a time to account for the volume of underwater ice produced. Up-welling of deep, cold oceanic water from the continental slope, and the resulting rise in freezing point from the decrease in hydrostatic pressure (about $0.007^{o}C$ per atmosphere) remains a possibility. But this would also be a more widespread phenomenon than our observations indicate. A late-fall pulse in the discharge of the Sagavanirktok River could result in a thin layer of fresh water spreading seaward below the ice canopy. Such a lense of fresh water could be cooled along the interface with the underlying salt water, to result in frazil ice formation (Pekhovich and Shatalina 1978); but this process would not result in a highly variable slush-ice thickness, and the observed steep relief.

Pekhovich and Shatalina (1978) describe several processes of ice production in the mouths of Arctic rivers. One of these involves the cooling of the riverbed by a bottom-hugging saltwedge, which advances and retreats with the tides. When the tide falls, fresh water advances across the bed, which was cooled by salt water during flooding, and results in anchor ice formation. A similar process, with another variation, could be envisioned for the shallow shelf, fringed by numerous lagoons. Bays and lagoons opening into Stefansson Sound are characterized by very high salinities, and low temperatures, during the freezing cycle. Five measurements made across Prudhoe Bay in May, 1978, showed an average temperature of $-2.5^{o}C$, and a salinity of 66.1 pm. Spilling such cold brine out of a lagoon into a basin like Stefansson Sound, could well result in the formation of frazil ice along the interface with the waters of the sound; but the transit of such a mass of cold brine across a particular area of sea floor could also result in subsequent anchor ice formation. The easterly storm that occurred during the period of October 6 through 8, would have resulted in a sea

level drop of perhaps .5 m, and the shallow bodies of water east and west of Point Brower therefore may have spilled cold saline water into Stefansson Sound at the right time.

Other methods of spilling cold brine into Stefansson Sound involve flooding of bottom-fast ice during storm-generated surges (Reimnitz and Maurer, 1978). On about November 11, 1978, up to 60 cm of water was standing on top of the fast ice surrounding the Exxon drilling pad (Duck Island) in Stefansson Sound. Because some freezing would occur on top of the fast ice during such flooding, the free water remaining, as sea level falls again, would drain as a cold brine. The November flood, however, does not fit the time frame we established for the underwater ice production at dive site 11.

IMPLICATIONS

The implications of the winter observations made at the Boulder Patch are far reaching. Only a few can be listed here.

Deltaic processes: For many years we have puzzled over the apparent lack of sediment accretion around Arctic deltas (including the Yukon and the MacKenzie). Reimnitz and Ross (1979), in their study of the Boulder Patch, point out the enigma of extensive lag deposits, and relict sediments, across the entire "delta front" of the Sagavanirktok River. Although cobbles and boulders are lacking where the Kuparuk River discharges from Simpson Lagoon onto the open shelf, relict deposits are widespread in the very area flooded during spring overflow, where most of the sediment discharge takes place. Are anchor ice processes at work seasonally, increasing the water turbidity and making sediments available for removal by subsequent currents? Is the very existence of the Boulder Patch due to the observed process? Can the fast ice turbidity, widespread in some years (Barnes and Fox, this report), be related to underwater ice production?

Biologic Environment: The effects of anchor ice processes on benthic biology of McMurdo Sound was demonstrated by Dayton, et al. (1969). Very little is now known of the possible effects of the process observed at dive site 11. However, the light reduction, owing to the thick layer of turbid soft ice, on photosynthesis and primary productivity must be drastic.

Pollutant Dispersal: The possible effect of underwater ice formation on the transport of potential pollutants may be similar to the effects on sediments, and could have serious consequences. Discharge temperatures for drilling muds, and drill cuttings may have to be controlled to avoid anchor ice formation.

Offshore construction: A better understanding of possible mechanisms of underwater ice formation on the inner shelf of the Beaufort Sea might lead to cheaper, and more efficient means of

constructing artificial ice islands. As with hydraulic power plants in northern streams, frazil ice formation may lead to the clogging of water intakes on pumping systems.

Ice gouging and related processes: Our understanding of the processes of ice gouging is far from complete. One unexplained observation, pertinent to this report, is the common occurrence of gouge terminations with well defined terminal moraines, that leave absolutely no clue as to how the ice flow continued to move after finishing the gouging job. A few floes may lift out of the gouge vertically by surface melting, quietly skipping over the terminal moraine without leaving a trace. However, there are just too many of these types of gouge terminations to be explained by this process, as the ocean during summer is not absolutely calm to allow the vertical departure of ice. Another fact, reported by our Canadian colleagues, remains a great puzzle to us: the dominant trend of ice gouging in the MacKenzie Bay area is about NW-SE. On this course ice is moving either up-slope or down-slope. Ice-gouging down-slope is rather unlikely. The average length of gouges and the average slope of the bottom is such that a floe cutting a particular gouge is moving through a depth range of several meters. In order to maintain bottom contact, ice would have to be added to the sail to increase the draft. On the other hand, moving all grounded ice several thousand meters, shoreward and up-slope through a depth range of several meters, would require tremendous forces, and also seems unlikely to us. Is it possible that the underwater addition of ice to the bottom of floating ice, as is suggested by Untersteiner and Sommerfeld (1964), observed by divers in MacKenzie Bay (Kovacs and Mellor, 1971), and observed in the Boulder Patch, can raise the ice freeboard enough to lift floes out of their gouges, and to allow long range gouging up-slope?

Conclusions

In this report on the soft ice in the Boulder Patch and on related problems, we have raised many questions and have not provided any answers. We hope that this discussion will convince our colleagues of the significance of the problems raised, and will stimulate some to provide constructive criticism.

REFERENCES

Al'tberg, V.I.A., 1938, On the center or nuclei of water crystallization: Meteorologiia i Gidrologiia, No. 3, p. 3-12. 1972 CRREL translation.

Benedicks, Carl, and Sederhelm, Per, 1943, Regarding the formation of anchor (ground) ice: Archiv för Matematik, Astronomi och Physik, v. 29 A, No.22, p. 1-7.

Benson, C.S., and Osterkamp, T.E., 1974, Underwater ice formation in rivers as a vehicle for sediment transport, in: Oceanography of the Bering Sea, D.W Hood, and E.J Kelley, (Eds.), p. 401-402.

Coachman, L.K., 1966, Production of supercooled water during sea ice formation, in: Proceedings of the Symposium on the Arctic Heat Budget and Atmospheric Circulation, J.O. Fletcher, (Ed.), Rand Corp., Santa Monica, California, Memo RM-5233-NSF, p. 497-529.

Dayton, P.K., Robilliard, G.A., and DeVries, A.L., 1969, Anchor ice formation in McMurdo Sound, Antarctica, and its biological effects: Science, v. 163, no. 3864, p. 273-274.

Kovacs, Austin, and Mellor, Malcolm, 1971, Sea ice pressure ridges and ice islands: Science and Technology, Creare Inc., Hanover, New Hampshire, Technical note TN-122, 127 p.

Lewis, E.L., and Lake, R.A., 1971, Sea ice and supercooled water: Jour. Geophysical Research, v. 76, no. 24, p. 5836-5841.

Osterkamp, T.E., and Lake, Gilfilian, R.E., and Benson, C.S., 1975, Observations of stage, discharge, pH, and electrical conductivity during periods of ice formation in a small subarctic stream: Water Resources Research, v. 11, no. 2, p. 268-272.

Müller, A., 1978, Frazil ice formation in turbulent flow: 5th International Symposium on Ice Problems, Luleå, Sweden, Proceedings, Part 3, p. 250.

Pekhovich, A.I., and Shatalina, I.N., 1978, Formation of frazil ice in the mouths of regulated rivers: 5th International Symposium on Ice Problems, Luleå, Sweden, Proceedings, Part 3, p. 27-34.

Reimnitz, Erk, and Maurer, D.K., 1978, Storm surges in the Alaskan Beaufort Sea: U.S. Geol. Survey open-file report 78-593, 26 p.

Reimnitz, Erk, and Ross, Robin, 1978, The Flaxman boulders in Stefansson Sound: a survey of the boulder patch, in: Barnes, P.W., and Reimnitz, Erk, Geologic Processes and Hazards of the Beaufort Sea Shelf and Coastal Regions, Quarterly Report to Nat'l. Oceanic and Atmospheric Admin., Principal Investigator's Reports, Oct. thru Dec., 1978. Attachment B, 17 p.

Schell, Donald, 1974, Seasonal variation in the nutrient chemistry and conservative constituents in coastal Alaskan Beaufort Sea waters, in: Environmental studies of an arctic estuarine system, Univ. of Alaska, Inst. of Marine Sciences, Report No. R-74-1, Chap.7, p. 233.

Untersteiner, N., and Sommerfeld, R., 1964, Supercooled water and the bottom topography of floating ice: Jour. Geophysical Research, v. 69, no. 6, p. 1057-1062.

Zubov, N.N., 1945, Arctic sea ice, Translated by Naval Ocean. Office and American Meteorological Society under contract to Air Force Cambridge Research Center, 1963. U.S. Naval Electronics Laboratory, San Diego, Calif., 491 p.

ATTACHMENT E

Sediment-laden first-year sea ice, central Beaufort Coast, Alaska

by Peter Barnes and Dennis Fox

INTRODUCTION

During three winter and spring field operations on the sea ice off the northern coast of Alaska, which involved extensive ice drilling and coring operations, only scattered occurrences of sediments and pebbles were seen in the nearshore ice. In contrast, during an ice operation in the spring of 1978, a considerable quantity of sediment was present in the ice canopy both locally and on a regional basis. As this was apparently an anomalous situation, based on our earlier observations, the distribution, content, and character of the sediment included in the ice canopy were studied.

The presence of abundant sediment in the ice canopy is important from both a standpoint of biological and physical processes, but also from practical aspects of potential development activities on the inner shelf. The presence of sediment in the ice excludes, or greatly diminishes, light transmission in the ice canopy thereby limiting or eliminating the growth of flora on the undersurface of the ice and on the seabed in shallow water. The strength and character of the ice sheet must be affected by sediment included within the ice crystals. From a geological point of view, the sediments transported when the ice canopy is in motion may comprise a significant part of the sediment transport regime where this process is effective.

BACKGROUND

The fact that sea ice in the arctic oceans commonly contains sediment of varying quantities and textures has been observed by many workers from the earliest days of exploration (Kindle, 1924). Most observers have generalized the process of rafting by having sediment adfrozen to the ice during periods when ice is in contact with the seabed or to be carried to the ice by wind and water when ice is in close proximity to the coast. Subsequently these sediments are transported by movements of the ice. During transit sediments are thought to be brought to the surface by the seasonal cycle--melting at the surface in summer and accretion of new ice in winter along the lower surface of the ice (Sverdrup, 1956).

A careful reading of the early literature suggests that there are two common forms of sediment in the ice that are readily distinguishable. The first (as above) occurs where ice contains heavy concentrations of a variety of grain sizes: pebbles, mud, kelp--clearly indicative of material brought in toto directly from the sea floor or the coast (Kindle, 1924; Sverdrup, 1935; Campbell and Collin, 1955). The second occurrence is surficial deposits of evenly distributed silts and clays, either on or within the ice (Campbell and Collin, 1955; Polunin, 1949; Tarr, 1897; Kindle, 1909; Barnes and Reimnitz, 1974). Sharma (1974), noted the presence of sediments in the sea ice of the Bering Sea that were finer textured than in the underlying bottom sediments. He concluded that the sediments must have been brought into the ice canopy from turbulent suspension but he could not conceive of a system whereby this would happen during the season of ice cover when turbulence is reduced.

Ice Regime

In our study area, the seasonal growth and zonation of the nearshore ice follows a regular pattern (Reimnitz and others, 1978). With the onset of freezing in the fall, ice initially grows in the vicinity of the coastline and river mouths where lower salinities and higher freezing temperature occur. The ice canopy continues to grow seaward incorporating varying quantities of ice, remnant from previous years, until a solid canopy is formed which then interacts with the encroaching polar pack, forming a grounded ridge zone, called the stamukhi zone, along the seaward edge of the stable ice canopy. Inside of the stamukhi zone the stable ice canopy, called the fast-ice zone, continues to grow through the winter, reaching thicknesses of 1.5-2 m (Kovacs and Mellor, 1974). Oceanographic conditions at the formative stages of the fast-ice zone are critical to the ultimate character of this zone. Winds, currents, and waves during the formative stages, can alter this zone by piling ice into ridges or rotating and transporting segments of the canopy.

The fall of 1977, when the ice canopy we sampled was formed, was unique in several respects. Except for grounded remnants of the stamukhi zone, there was no ice on the shelf at the initiation of freezeup in late September-early October. These unusual open-water conditions allowed for the development of larger than normal waves due to the increased fetch. Furthermore, it allowed for a complete mixing of the water column prior to the initiation of freezing. There were several storms that passed through the area with recorded wind speeds in excess of 40 knots at Prudhoe Bay airport.

METHODS

The data in this report are based on ice cores which were examined for sediment content and character. The cores were obtained using an electrically driven Sipre corer at sites chosen to represent different hydrographic and geographic environments. Subsequently the 5-cm diameter cores were visually described, photographed and subsampled in 10 to 20 cm segments which were placed in waterproof plastic containers. Core melt water was shipped to the laboratory for further analysis.

Sediment concentrations were determined after vigorously homogenizing the sample by shaking and then decanting a 30-100 ml aliquot which was filtered through a 47-mm diameter 0.4μ filter. Salt was removed by washing the filters with distilled water. The filters were then oven dried at 50°C and weighed on an electrobalance to the nearest 0.01 mg. After calculating the sediment concentration in the aliquot, the weight of sediment in the core was computed. An ice concentration value was also derived using the sediment concentration and ice volume. The technique used essentially followed Drake and others (1972).

Salinities were determined on core samples in an attempt to assay whether sediment may have been derived from fresher river waters. These were determined using conductivity measurements with a cell of 5 ml volume and a cell constant of 0.5. The conductivities were then compared to distilled water dilutions of standard Copenhagen water whose chlorinity is accurately known. The salinity was then determined using the formula:

$$S\ ^{o}/_{oo} = 0.03 + 1.805\ C\ ^{o}/_{oo}.$$

OBSERVATIONS

We attempted to sample a variety of environments. These environments included a semi-enclosed bay, Prudhoe Bay, the open lagoon environment of Stefansson Sound, and a restricted lagoonal environment, Simpson Lagoon. Additionally, cores were obtained from the vicinity of both Colville River delta and the Sagavanirktok River delta as shown in Figure 1.

Salinities

Ice core salinities were typically between 4-7 $^{o}/oo$ which is characteristic of first-year ice (Zubov, 1943). One marked exception was one core taken seaward of the Sagavanirktok delta, which was characterized by clear ice from 50-110 cm which was composed of non-saline waters. This freshwater layer may be related to the freshwater pool located off the Sagavanirktok delta and reported on by Kovacs and Morey (1979). Under-ice water salinities varied from 34 $^{o}/oo$ to over 60 $^{o}/oo$ in Prudhoe Bay (see Appendix).

Sediments

The vertical distribution of sediments in the ice cores creates a stratigraphy which can be generalized as 1) a relatively clear surface layer, 10-15 cm thick underlain by 2) a 'dirty' ice zone with pronounced discoloration by sediments. This zone ranges from a few cm to over 1 m in thickness and 3) a clear brine-rich ice underlying the 'dirty' ice zones. The upper boundary of the dirty layer, between the surface and the dirty layer was often a gradational boundary with sediment concentrations increasing downward, whereas the bottom boundary layer was often rather abrupt and in many instances contained relief indicating that at the time of solidification the bottom of the dirty layer may have been undulating (see Appendix, Core #5).

The variable morphologic character of the 'dirty' ice within the ice canopy was observed at several sites where 1 m^2 x 2-m thick blocks of ice were removed from the canopy during preparations for diving activities. In these blocks we observed the thin cleaner surface layer overlying the discolored zone, often in gradational contact. The undulating nature at the base of the 'dirty' ice contact had relief of several centimeters as shown in Figure 2.

The sediment within the ice on almost all occasions, appeared to be difused through the ice. The 'dirty' ice zone was blotchy as if ice particles of a few centimeters dimension with varying concentrations of sediment were welded together. Isolated bands of frozen sediment were not found except where ice was in contact with the seabed (Core #9).

Concentrations of sediment in the 'dirty' ice zone varied from less than 3 gm/m^3 of ice to values in excess of 2,000 gm/m^3 of ice (Table I). By comparison, oceanic values for suspended sediment are typically less than 1 gm/m^3 (Drake and others, 1972; Drake, 1977; Buss and Rudolfo, 1972). From these observations it would appear that the clearer lower portions of the ice canopy contain oceanic concentrations of suspended sediment. In contrast, the sediment-enriched zones of varying thickness contain many times the oceanic concentration and indeed many times the coastal or estuarine concentrations of suspended sediment load.

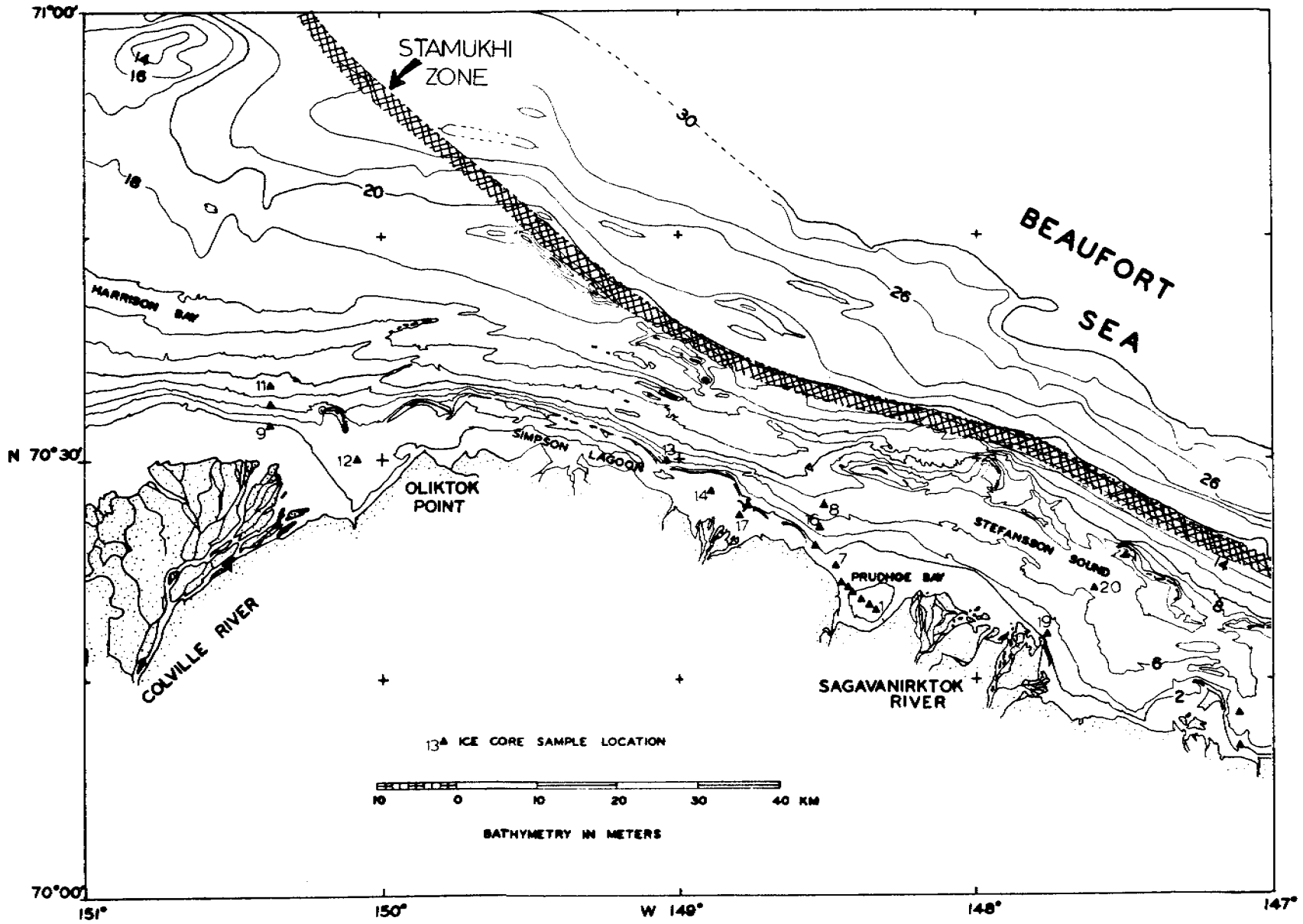

Figure 1. This map shows the location of the ice cores and the approximate location of the stamukhi zone (hatchered pattern). Note that all of the ice cores are not numbered.

Figure 2A. Weathered ice block cut from the fast ice northwest of Prudhoe Bay in Stefansson Sound. Block is about 130 cm high. Note cleaner surface ice layer and undulating relief to the abrupt contact at the base of the 'dirty' ice.

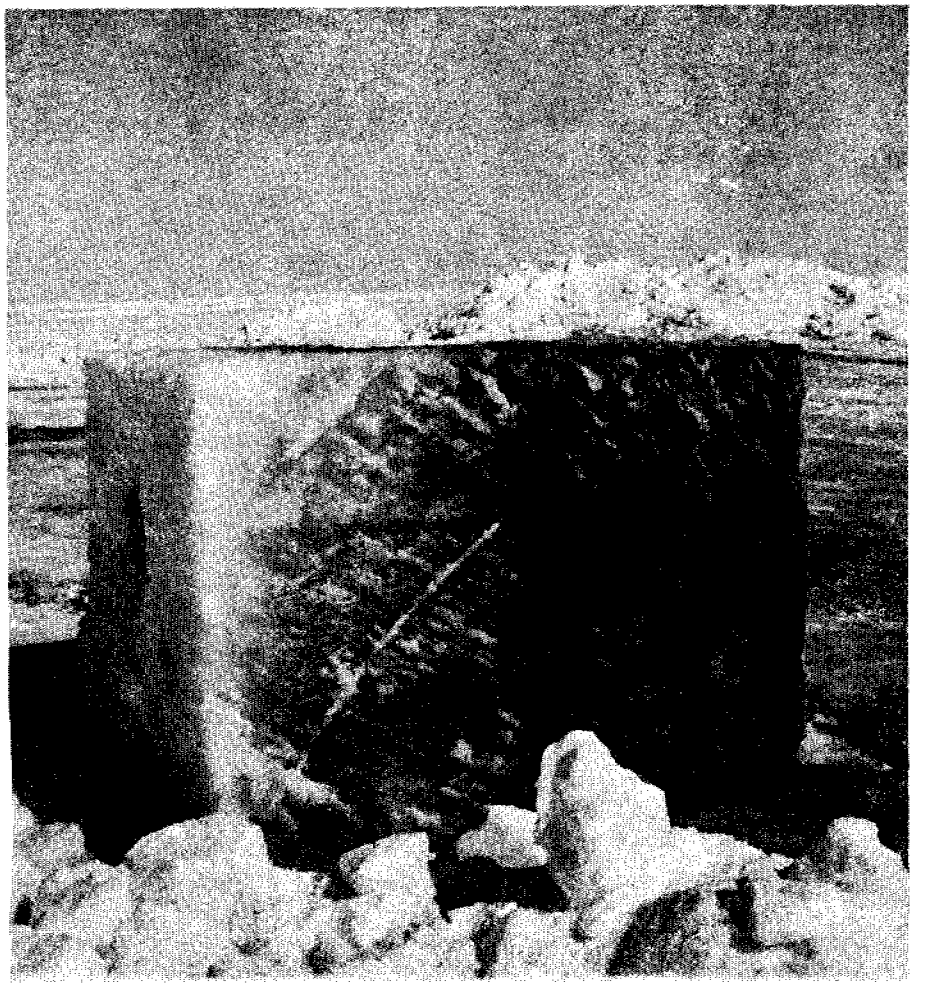

Figure 2B. Freshly cut ice block from inlet to Simpson Lagoon. Top surface is to the right. Cleaner surface layer is not present. Note irregular relief to the base of the dirty layer.

TABLE I. Weighted average sediment concentrations and potential sediment iceload.

PRUDHOE BAY

Core number:	1	2	3	4	5	6	7	Avg. all cores	
	223 g/m^3	152	625	947	1615	1644	770	865	Upper "dirty" core segment
	3.4	3.4	3.4	3.4	3.4	3.4	3.4	3.4	Lower "clean" core segment
	62	48	264	469	670	420	273	314	Avg. sediment concentration in core.

STEFANSSON SOUND

Core number:	8	15	16	19	20	21	Avg.	
	16	790	166	112	83	146	324	(as above)
	3.4	3.4	3.4	3.4	3.4	3.4	3.4	
	5.4	517	71	33	10	97	122	

SIMPSON LAGOON

Core number:	14	17	18	Avg.	
	915	912	628	818	(as above)
	3.4	3.4	21	9.2	
	865	132	315	443	

HARRISON BAY

Core number:	10	12	Avg.	
	3	119	96	
	3.4	3.4	3.4	
	9.6	29	20	(as above)

Regional Distribution

There is considerable lateral variability to the character of the 'dirty' zone. This can be seen in the five cores taken from Prudhoe Bay where the 'dirty' ice zone varies in thickness from 10->60 cm in thickness even in this restricted, rather uniform environment. On the other hand, the presence of the sediment zone within the ice is very widespread. Examining the first-year ice blocks that comprised the zone (Fig. 2), we observed that this ice contained appreciable quantities of the sediment with the same dispersed character that we observed in our ice cores inshore. In addition, areas were found where sands and shell debris suggested that some of the sediments in the stamukhi zone ice were derived directly from the bottom. The occurrence of ridged ice blocks containing dispersed 'dirty' sediment were all along the stamukhi zone (Fig. 1) from Stamukhi Shoal east to the vicinity of Flaxman Island. From these observations it would appear that the entire first-year ice cap had considerable concentrations of dispersed sediment contained within it.

The sediment load of the fast-ice canopy was estimated using the weighted average concentrations of sediment within the cores. Within the rather small environments of Prudhoe Bay, Stefansson Sound, and Simpson Lagoon (Fig. 1), in excess of 10^5 tonnes of sediment are contained in the ice canopy. The highest concentrations, on the average, occur in Prudhoe Bay and the lowest concentrations are found in Stefansson Sound (Table I). Adding a conservative estimate for the fast-ice area seaward to the stamukhi zone, the ice load is nearly 0.5×10^6 tonnes (Table II). By way of comparison, the annual Colville River discharge is estimated to be approximately 6×10^6 tonnes (Arnborg and others, 1967).

Composition

Filters containing sediment from the 'dirty' ice zones were examined under a petrographic microscope and with a scanning electron microscope in an attempt to estimate the organic composition and the textural character of the sediment. These examinations showed that the sediments are composed dominantly of silts and clay-size material with an omnipresent organic fraction which never amounts to more than a few percent of the total volume. A scanning electron micrograph of two core segments is shown in Figure 3.

To summarize, the fast-ice zone, in the winter of 1977-78, contained a fine-grained, dispersed sediment zone up to 1 m thick. Sediment in ice was observed over a wide area of the shelf, yet thickness and concentration seem unrelated to rivers, water depth, wave exposure, or distance from shore.

Discussion

The omnipresence of an abundant sediment load in the fast-ice canopy,--a load that apparently is not present in all winters--requires an explanation of formation which in many ways is problematical. The wide regional distribution with apparent disregard for concentrations near river mouths would indicate that river input is not a dominating factor in the formation of 'dirty' ice. Very high concentrations an order of magnitude higher than normal inner shelf waters in the area (Drake, 1977) suggest that there is

Table II. Estimated sediment content of fast ice - Spring 1977

	Area	Average sediment concentration	
Prudhoe Bay	26 km^2	314	.09 x 10^5 tonnes
Simpson Lagoon	146 km^2	443	.92 x 10^5
Stefansson Sound	473 km^2	122	.80 x 10^5
Fast ice (Islands to stamukhi)	1172 km^2	(122)	2.9 x 10^5
		TOTAL	4.7 x 10^5

Colville River

Suspended load 1962 (Arnborg and others, 1967) 58. x 10^5

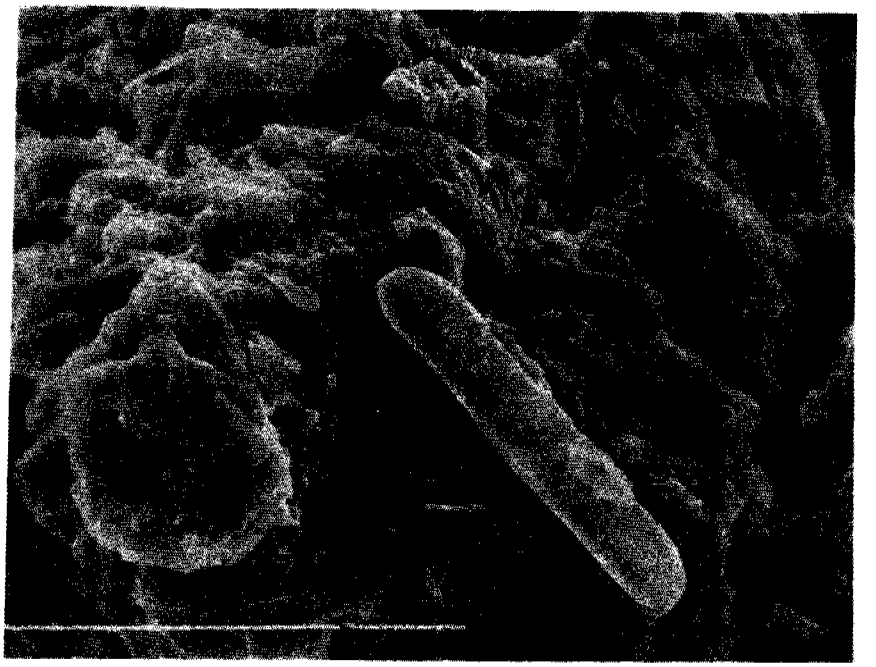

Figure 3A. Scanning electron micrograph of ice core sediments in Prudhoe Bay. Core 4, 23 - 48 cm. The short bar at bottom center is 5 microns and the space before the bar is 0.5 microns. Grain size is mostly silts and clays.

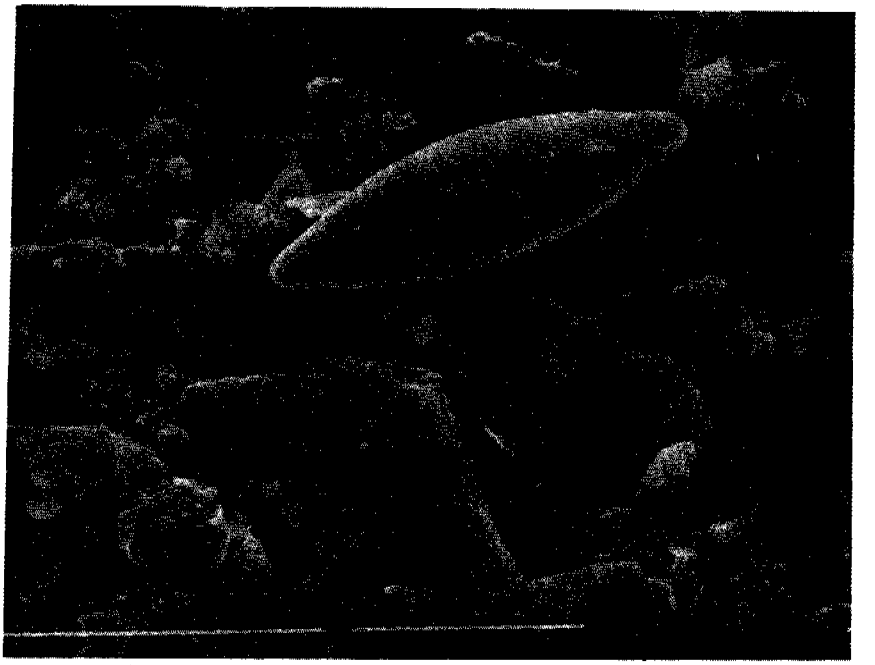

Figure 3B. Scanning electron micrograph of ice core sediments from Stefansson Sound. Core 18, 70 - 80 cm. Space and bar indicate same scale as in figure 3A. Mostly clay size material. Small holes in background are the filter openings.

some concentration process if ice and sediment are derived directly from the freezing of sea water. The uniform, difuse character of sediment within the ice cores along with the rather uniform size distribution of the sediments themselves suggest that a storing process has occurred. This is not the character to be expected if ice were formed on the sea floor and lifted to the undersurface of the ice as in the formation of anchor ice--one mechanism to concentrate sediments in the ice canopy (Dayton and others, 1969). Two other characteristics must be included in the formative story: 1) the local (cm) and regional (100s of m) variability in the thickness of 'dirty' ice and 2) the process whereby sediment is concentrated within the ice canopy must be capable of working in areas offshore in water depths approaching 20 m.

The apparently cleaner ice that occurs at the surface would seem to preclude turbulence as a contributing factor. Intuitively, it would seem that once an ice cover had formed, that water turbulence would be reduced due to reduced wave activity and reduced wind stress, with the result that available quantities of suspended sediment for inclusion in the ice canopy would be reduced. As a result the concentrations of sediments in the ice canopy should be decreasing downward, rather than increasing, as observed.

Several of the potential mechanisms operating to form undulating layers of sediment-ridged ice have been discussed in Attachment D. One possible mechanism can be described briefly as follows. The extreme open water conditions and storms in the fall of 1977 allowed for a complete mixing of the water column, reducing the entire water column on the inner shelf to near freezing temperatures. The removal of all sensible heat from the water column has been discussed by Lewis and Lake (1971). Untersteiner and Sommerfeld (1964), point out that once this has occurred, cold brine-rich packets released during initial stages of ice formation, can withdraw more heat from the water and could cause freezing or underwater ice formation. Because of their high-density the brine packets sink to the bottom or the depth of mixing. If underwater ice formation occurs in a zone of high turbidity, in a near-bottom turbid layer or on the bottom, sediment would be included with this turbid layer and carried with it to the undersurface of the growing ice canopy. Large grain sizes might not be included, either because of insufficient ice crystal growth on the seabed to buoy large grains, or the formation of ice crystals occurs at some distance above the actual seabed. With this mechanism the undulating relief to the 'dirty' ice zone would result from variabilities in the centers of nucleation intensity for the formation of the ice.

The accumulation and relief may be in part caused by advective processes during the initial stages of ice accumulation whereby 'dirty' ice formed in shallow water is then advected offshore during storms. The vertical gradations in sediment density, the regional distribution of 'dirty' ice, and the apparently cleaner surface layer are not readily explained by this mechanism. High-density brines, excluded during ice formation, may have a pronounced effect on increasing the turbulence and buoyancy factors for fine-grained sediments near the sediment/water interface. A high density salt-rich layer near the seabed could aid in keeping fine-grained sediments in suspension during initial stages of ice formation when ice growth is rather rapid (Zubov, 1943) thereby allowing ice formation at these water depths to entrap larger quantities of sediment than might ordinarily be available under conditions not involving a high density salt layer.

A natural concentrating mechanism from the water column into the ice canopy could occur if sediment acted as nuclei for ice crystallization. We attempted to test this hypothesis by freezing oceanic concentrations of sediment under turbulent and non-turbulent conditions in the laboratory and then testing the water and ice for sediment content before and after freezing had occurred. Our results showed no significant segregation of sediment and ice during the freezing process in either the turbulent or non-turbulent experiment.

SUMMARY

Implications

The fast-ice canopy from the coast out to and including the stamukhi zone during 1977-78 contained a large quantity of sediment in the upper part of the ice canopy. The source and mechanisms of accretion of the well-sorted silt and clay-size material within the ice is not fully understood (see Attachment D). In addition to problems of understanding the mechanisms of accretion, the ultimate fate of sediments in spring is poorly known - whether they melt in place or are transported away from or along the coast after breakup.

The fact that sediment is included in the ice canopy reduces light transmission to the undersurface of the ice. Observations by Don Schell (personal communication) show that virtually no biota existed on the underice surface where the ice is turbid, whereas elsewhere there was an abundant biota. Thus sediment in the ice canopy is a major factor affecting spring photosynthetic productivity.

The presence of sediment-laden ice has several implications for development activities on the inner shelf because the exact cause and effect relationships for generation of a turbid ice layer remain unknown. If developmental activities create conditions either of turbid water or of thermal alteration of the nearshore hydrologic regime, as might be incurred by large seawater intakes for water injection facilities, turbid ice layers could be created which would then have a detrimental effect on sub-ice biota and may significantly influence established sediment transport patterns as well as possibly having detrimental effects on developmental activities. Furthermore, any hydrocarbon materials that become adsorbed onto the surface of fine-grained particles in the sediment could be mobilized into the fast-ice canopy if this process is occurring at a time when there has been an oil spill and sediments are interactive with the oil. On the other hand, the presence of sediment within the ice may have positive effects from a developmental standpoint. The albedo could be lowered thereby causing earlier melting of sea ice in the vicinity of structures or shipping lanes. The strength properties of the sea ice might be altered in a favorable manner. Or, pollutants might be scrubbed from sediments or the water column by forcing the process to occur. Thus both favorable and unfavorable implications can be considered.

REFERENCES

Arnborg, L., Walker, H.J., and Peippo, J., 1967, Suspended load in the Colville River, Alaska, 1962: Geografiska Annaler, v. 49, ser. A, p. 131-144.

Barnes, P.W., and Reimnitz, Erk, 1974, Sedimentary Processes on the arctic shelf off the northern coast of Alaska in: Reed, J.C., and Sater, J.E., eds., The Coast and Shelf of the Beaufort Sea, Arctic Institute of North America, Arlington, Virginia, p. 439-476.

Buss, B.A., and Rodolfo, K.S., 1972, Suspended sediments in continental shelf waters off Cape Hatteras, North Carolina, in: Swift, D.P., Duane, D.B., Pilkey, O.H., eds., Shelf Sediment Transport: Process and Pattern, Dowden, Hutchinson, and Ross, Inc., Stroudsberg, Pennsylvania, 656 pp.

Campbell, N.J., and Collin, A.E., 1955, A preliminary report on some of the oceanographic features of Foxe Basin: St. Andrews, N.B., Joint Committee on Oceanography, Atlantic Oceanographic Group, May, 1956, iii, 64 pp.

Dayton, P.K., Robilliard, G.A., and DeVries, A.L., 1969, Anchor ice formation in McMurdo Sound, Antarctica, and its biological effects: Science, v. 163, p. 273-274.

Drake, D.E., 1977, Suspended matter in nearshore water of the Beaufort Sea: U.S. Geological Survey Open-File Report 77-477, p. C1-C13.

_____, Kolpack, R.L., and Fischer, P.J., 1972, Sediment transport on the Santa Barbara-Oxnard Shelf, Santa Barabara Channel, California, in: Swift, D.P., Duane, D.B., and Pilkey, O.H., eds., Shelf Sediment Transport: Process and Pattern, Dowden, Hutchinson, and Ross, Inc., Stroudsberg, Pennsylvania, 656 pp.

Kindle, E.M., 1924, Observations on ice-borne sediments by the Canadian and other arctic expeditions: American Journal of Science, Series 5, v. 7, no. 40, p. 249-286.

_____, 1909, Diatomaceous dust on the Bering Sea ice floes: American Journal of Science, Series 4, v. 28, p. 175-179.

Kovacs, A., and Morey, R., 1979, Remote detection of a freshwater pool off the Sagavanirktok River delta, Alaska: Arctic, in press.

_____, and Mellor, M., 1974, Sea ice morphology and ice as a geologic agent in the southern Beaufort Sea, in: Reed, J.C., and Sater, J.E., eds., The Coast and Shelf of the Beaufort Sea, Arctic Institute of North America, Arlington, Virginia, p. 113-161.

Lewis, E.L., and Lake, R.A., 1971, Sea ice and supercooled water: Journal of Geophysical Research, v. 76, n. 24, p. 5836-5841.

Polunin, N., 1949, Arctic unfolding, Huchinson, London, 348 pp.

Reimnitz, Erk, Toimil, L.J., and Barnes, P.W., 1978, Arctic continental shelf morphology related to sea-ice zonation, Beaufort Sea, Alaska: Marine Geology, v. 28, p. 179-210.

Sharma, G.D., 1974, Contemporary depositional environment of the eastern Bering Sea, in: Hood, D.W., and Kelley, E.J., eds., Oceanography of the Bering Sea, University of Alaska, Fairbanks, p. 517-537.

Sverdrup, H.U., 1956, Arctic sea ice, in: The Dynamic North, Book I, Technical Assistant to Chief of Naval Operations for Polar Projects (Op-03A3), June, 1956, 17 pp.

_____, 1935, Notes on erosion by snow and transport of solid material by sea ice: American Journal of Science, Series 5, v. 35, p. 370-373.

Tarr, R.S., 1897, The Arctic Sea ice as a geological agent: American Journal of Science, v. 3, n. 15, p. 223-229.

Untersteiner, N., and Sommerfeld, R., 1964, Supercooled water and the bottom topography of floating ice: Journal of Geophysical Research, v. 69, n. 6, p. 1057-1062.

Zubov, N.N., 1943, Arctic Ice, translated by Naval Oceanographic Office and American Meteorological Society, 1963, pub., Naval Electronics Laboratory, San Diego, California, 491 p.

APPENDIX

Ice Core Descriptions

For each core a field description of the core is included along with a graphic drawing and photograph. Where available, temperature and salinity of the water below the core hole are also included. Each core subsample (set off in brackets) was tested for salinity and sediment content. These values plus a comparative value are listed next to the brackets.

Ice Core #1

70° 19.5'N 148° 20.2'W

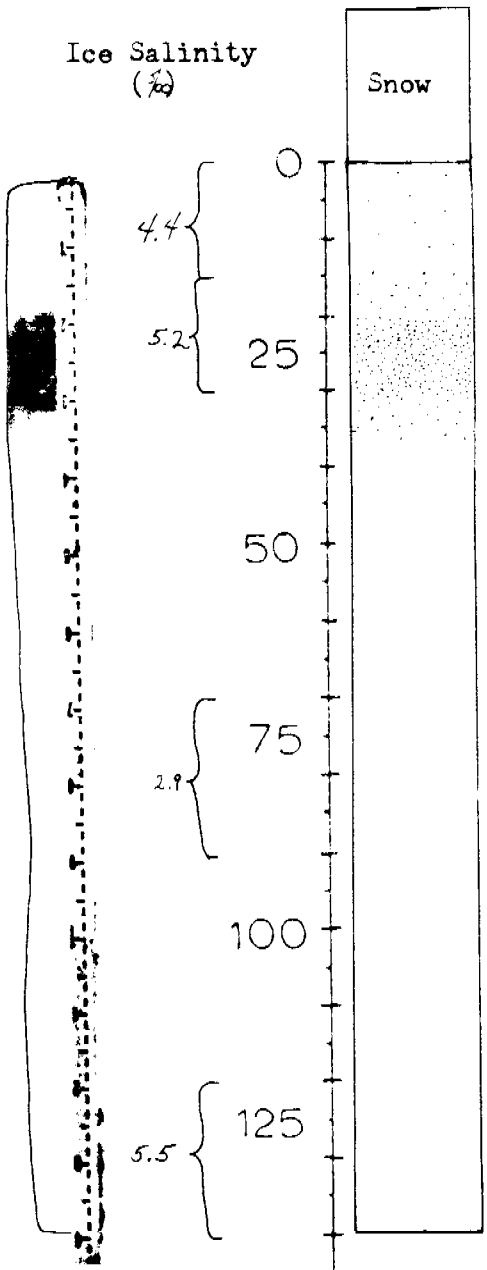

Sediment Concentration

	Observed (mg)	Comparative Value (g/m^3 of ice)
0 – 25 cm	73.8	99
25 – 50 cm	303	406
75 – 100 cm	3.39	3.4
125 – 150 cm	1.32	1.3

Dirty Layer 15 - 35 cm
Pronounced 20 - 30 cm below ice surface
Ice Thickness 140 cm
Snow cover 20 cm

Water Properties at 2 m

S 64.1 ‰

T -2.2 °C

Ice Core #2

70° 19.8'N 148° 21.8'W

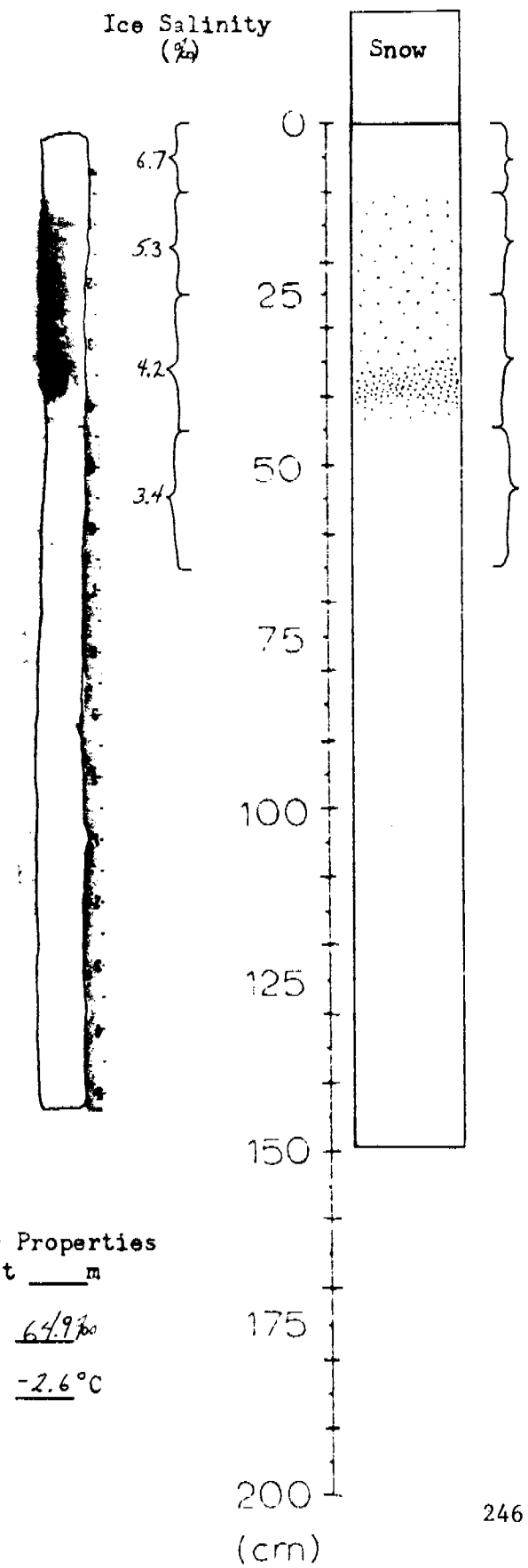

Sediment Concentration

	Observed (mg)	Comparative Value (g/m^3 of ice)
	2.39	4.8
	138	185
	199	200
	4.55	4.6

0 - 11 cm clean
11 - 40 cm dirty ice
45 - 150 cm clean
Ice Thickness 150 cm
Snow cover 17 cm

Water Properties at ____ m

S 64.9‰

T -2.6°C

Ice Core #3

70 20.1'N 148 23.4'W

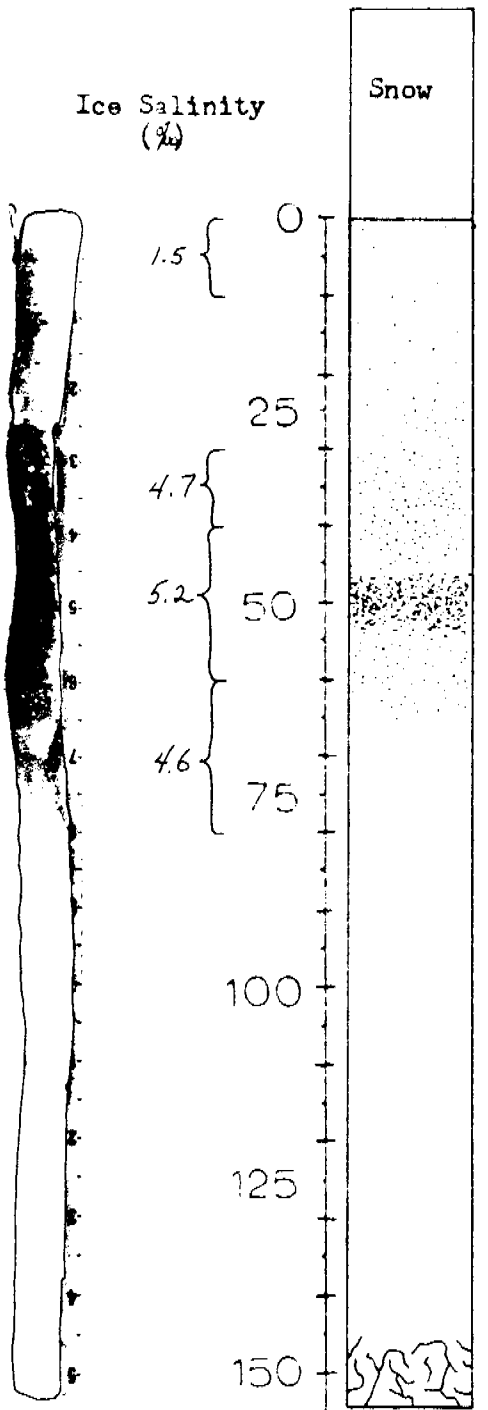

Ice Salinity (‰)

1.5
4.7
5.2
4.6

Sediment Concentration

	Observed (mg)	Comparative Value (g/m^3 of ice)
0 - 25 cm	79.8	161
25 - 50 cm	234	471
50 - 75 cm	1350	1360
75 - 100 cm	379	382

Water Properties at ____ m

S 66.7‰

T -2.5 °C

0 - 25 cm murky ice; evenly distributed through ice
25 - 65 cm darker zone of dirty ice with dirtiest ice at about 50 cm. No layering discernable.
65 - 80 cm ice on half the core blotches of mud--but clearly in core and not an artifact of coring.
80 - 155 cm clear ice. Brine channels in lower 10 cm are very learly seen.
Ice Thickness 155 cm
Snow cover 28 cm

Ice Core #4

70° 20.7'N 148° 25.2'W

Ice Salinity (‰)

Sediment Concentration

	Observed (mg)	Comparative Value (g/m^3 of ice)
3.4	1310	1060

Snow

0
25
50
75
100
125
150
175
200
(cm)

0 - 8 cm fairly clean ice--may have slight discoloration
8 - 75 cm muddy ice although not as muddy as core #3 in upper parts.
75 - 152 cm cleaner ice. Boundary fairly clean at 75 cm. Another boundary at 90 cm.
Ice Thickness 152 cm
Snow cover 12 cm

Water Properties at ____ m

S 67.3‰

T -2.6 °C

Ice Core #5

70° 21.0'N 148° 26.0'W

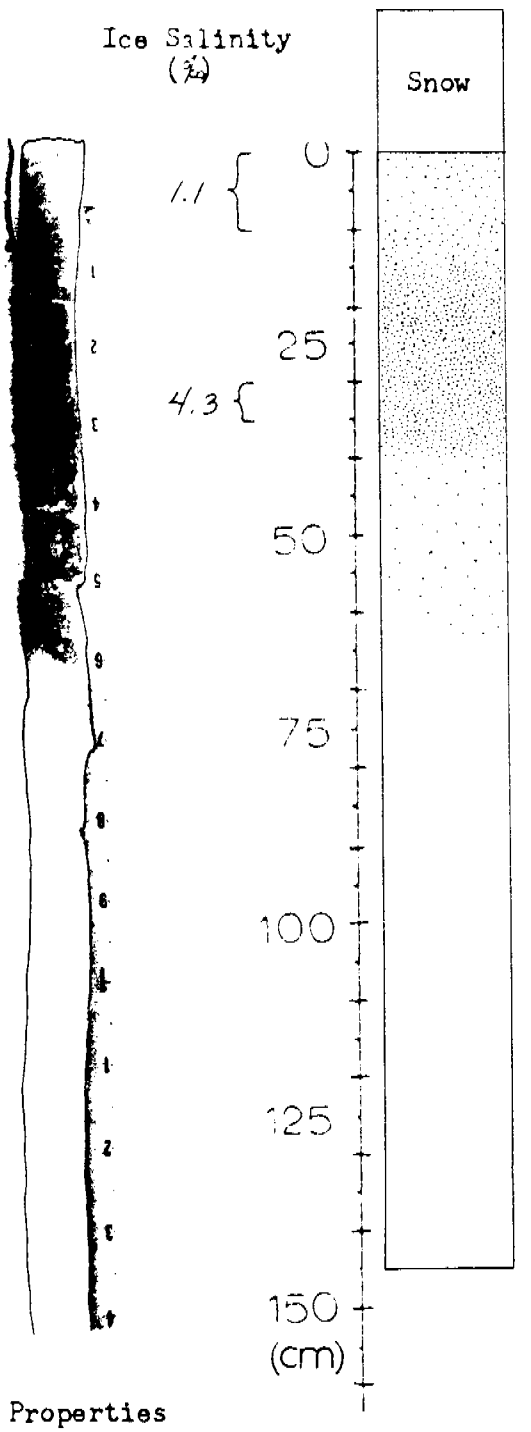

Sediment Concentration	Observed (mg)	Comparative Value (g/m^3 of ice)
0 – 25 cm	342	690
25 – 50 cm	723	2910

Water Properties
at ____m

S ____‰

T ____°C

Ice resting on bottom. No noticable change at ice-water contact.
Possibly 2 cm between ice and bottom.
0 - 15 cm increasingly muddy ice right from the surface.
15 - 40 cm 'very' muddy ice
40 - 60 cm 'less' muddy ice. Lower contact dipping at about 45°.
60 - 145 cm clear ice. Sediment not adfrozen nor lenses of sediment in lower part of core. That is, ice core appeared clean.
Ice Thickness 145 cm
Snow cover 19 cm

Ice Core #6

70° 21.6'N 148° 27.8'W

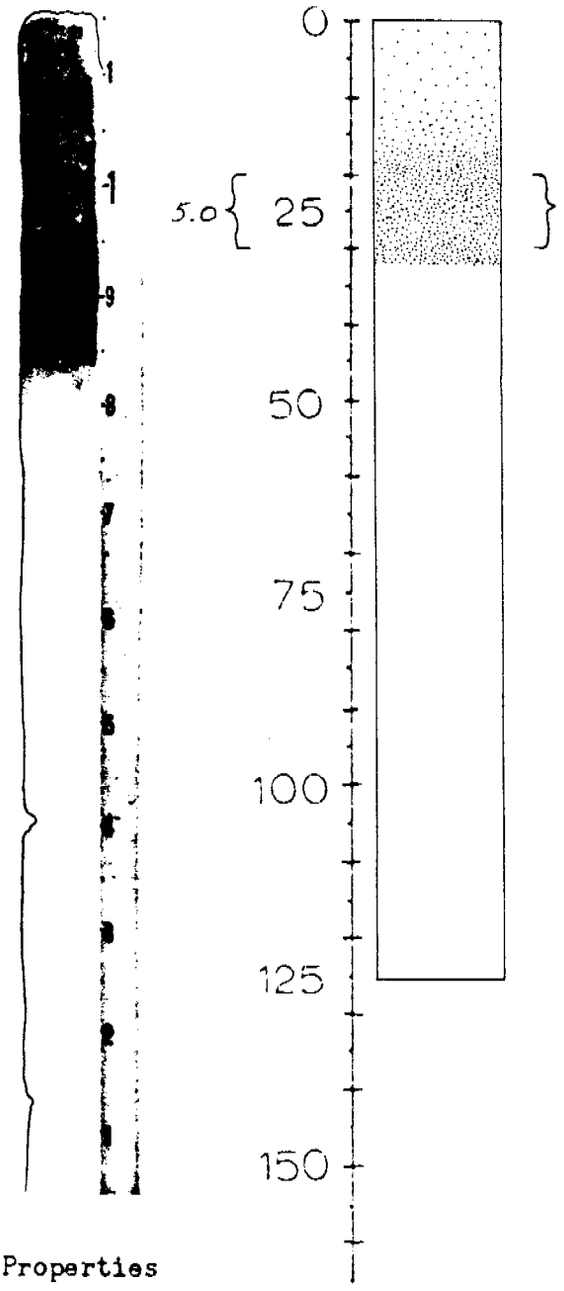

Water Properties
at ____m

S ____‰

T ____°C

0 - 17 cm muddy ice--'light'--vaguely getting dirtier with depth.
17 - 32 cm dirtiest ice in core. Sharp contact at base.
32 - 120 cm clean ice.
Ice Thickness 126 cm

Ice Core #7

70° 22.7'N 148° 29.1'W

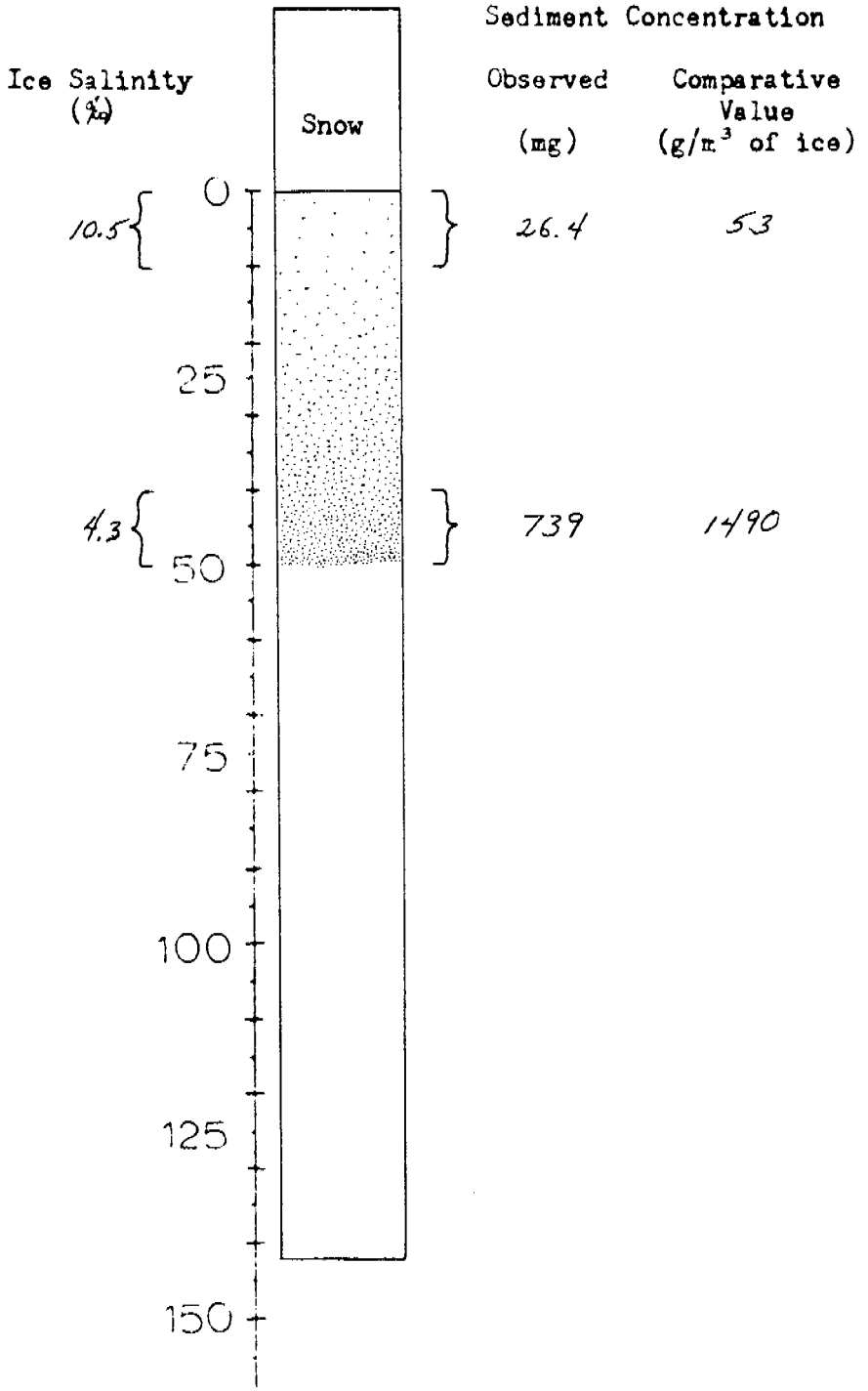

Water Properties at ____ m

S 52.2 ‰

T -3.0 °C

Turbidity increasing from surface to 50 cm. Sharp contact with clean ice.

Ice Thickness 142 cm

Snow cover 25 cm

Ice Core #8

70° 25.8'N 148° 30.2'W

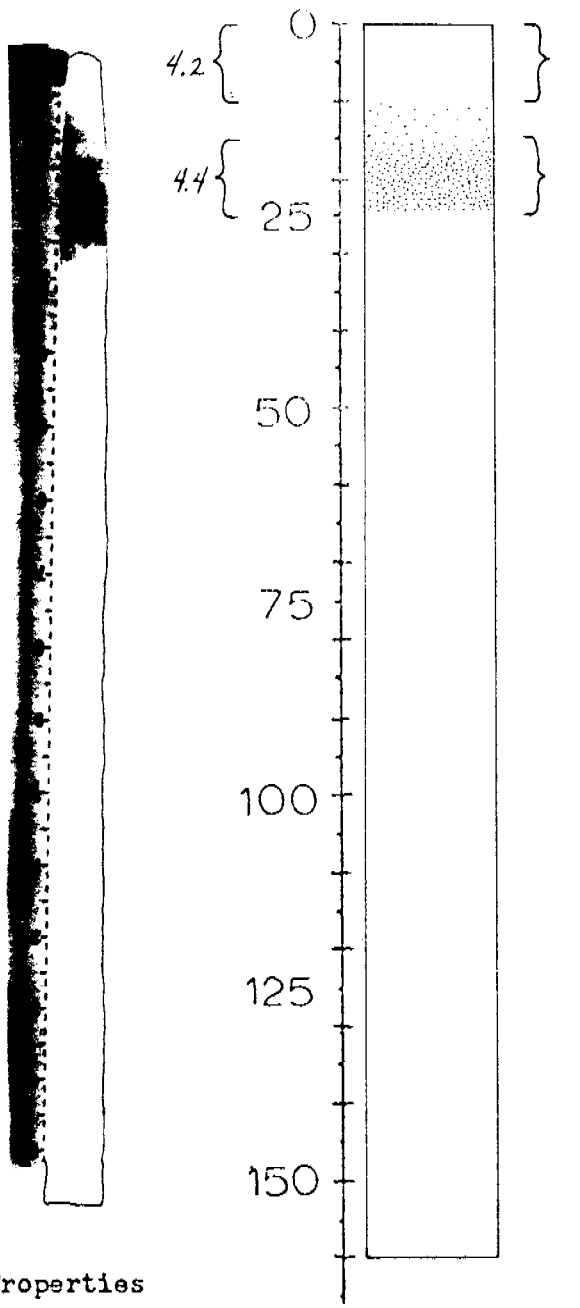

Water Properties at ____ m

S 38.4‰

T -2.5 °C

Upper 10 cm clear, gradually getting dirtier to maximum at 16 cm.
25 cm sharp contact. Clear to bottom
Ice Thickness 160 cm

Ice Core #9

70° 32.2'N 150° 22.5'W

Ice Salinity (‰)	Sediment Concentration Observed (mg)	Sediment Concentration Comparative Value (g/m³ of ice)
1.3	>2740	4600
0.0	101	140

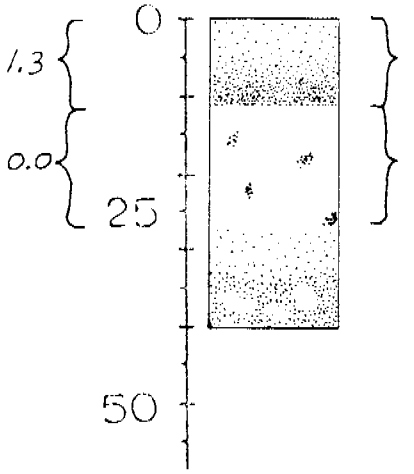

0 - 5 cm clear.
5 - 12 cm very dirty.
12 - 27 cm clear with pockets of sediment.
27 - 40 cm sediment with ice lenses and ice cracks running vertically.
Ice Thickness 40 cm

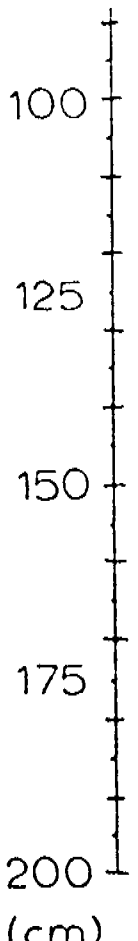

Water Properties at ___m

S ___‰

T ___°C

Ice Core #10

70° 33.7'N 150° 22.7'W

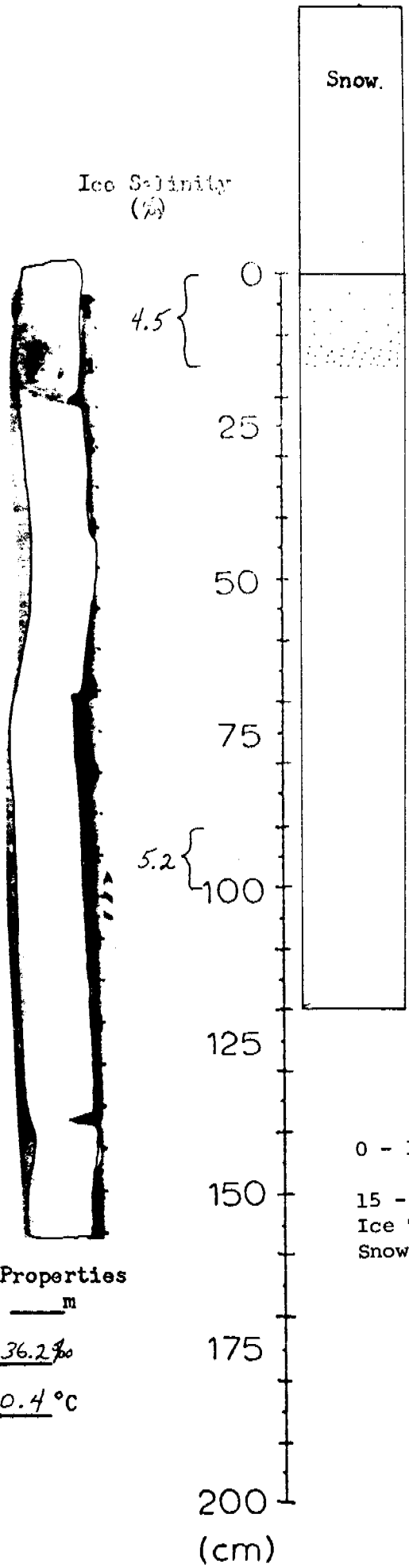

Sediment Concentration	Observed (mg)	Comparative Value (g/m³ of ice)
0 – 45 cm	39.4	53
90 – 120 cm	0.949	1.9

0 - 15 cm core discolored increasing with depth.
Contact? at break in core.
15 - 120 cm clear ice.
Ice Thickness 120 cm
Snow cover 45 cm

Water Properties at ____m

S 36.2‰

T -0.4 °C

Ice Core #11

70 35.0'N 150 22.8'W

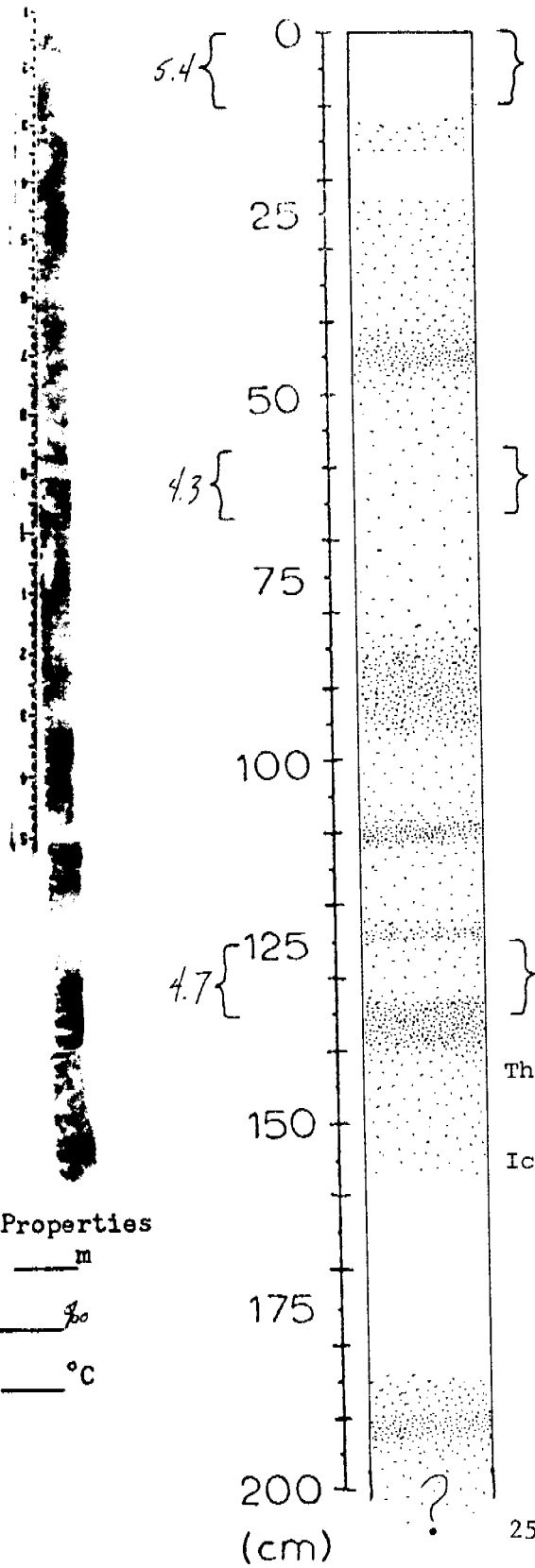

Sediment Concentration	Observed (mg)	Comparative Value (g/m³ of ice)
0 – 50	50.2	101
50 – 75	21.4	48
125 – 200	159	320

Repeated layers?

Thin whiskers of discoloration some of which is less than 1 cm thick to 5 cm thick. Possibly repeated layers form ice piles in the fall.
Ice Thickness >200 cm

Water Properties at ____m

S ____‰

T ____°C

Ice Core #12

70° 30.0'N 150° 05.0'W

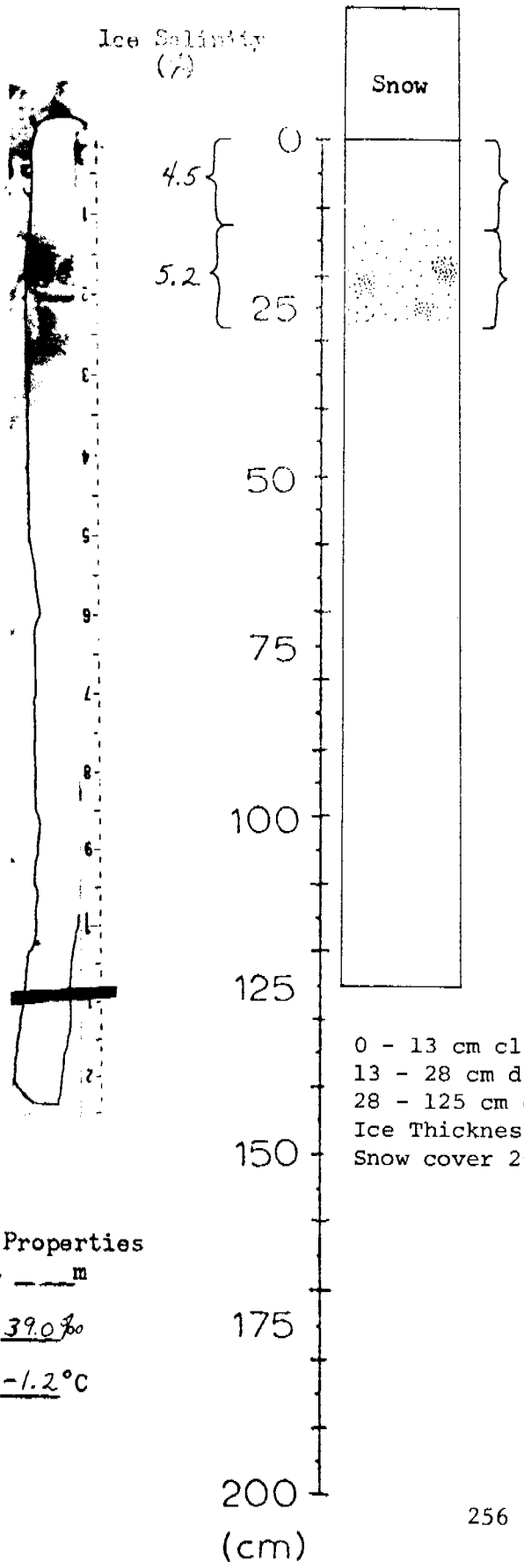

0 - 13 cm clear ice with gradual contact with next lay
13 - 28 cm dirty ice with sediment pockets.
28 - 125 cm clear ice.
Ice Thickness 125 cm
Snow cover 20 cm

Water Properties at ___m

S 39.0‰

T -1.2°C

Ice Core #13

70° 29.8'N 149° 02.5'W

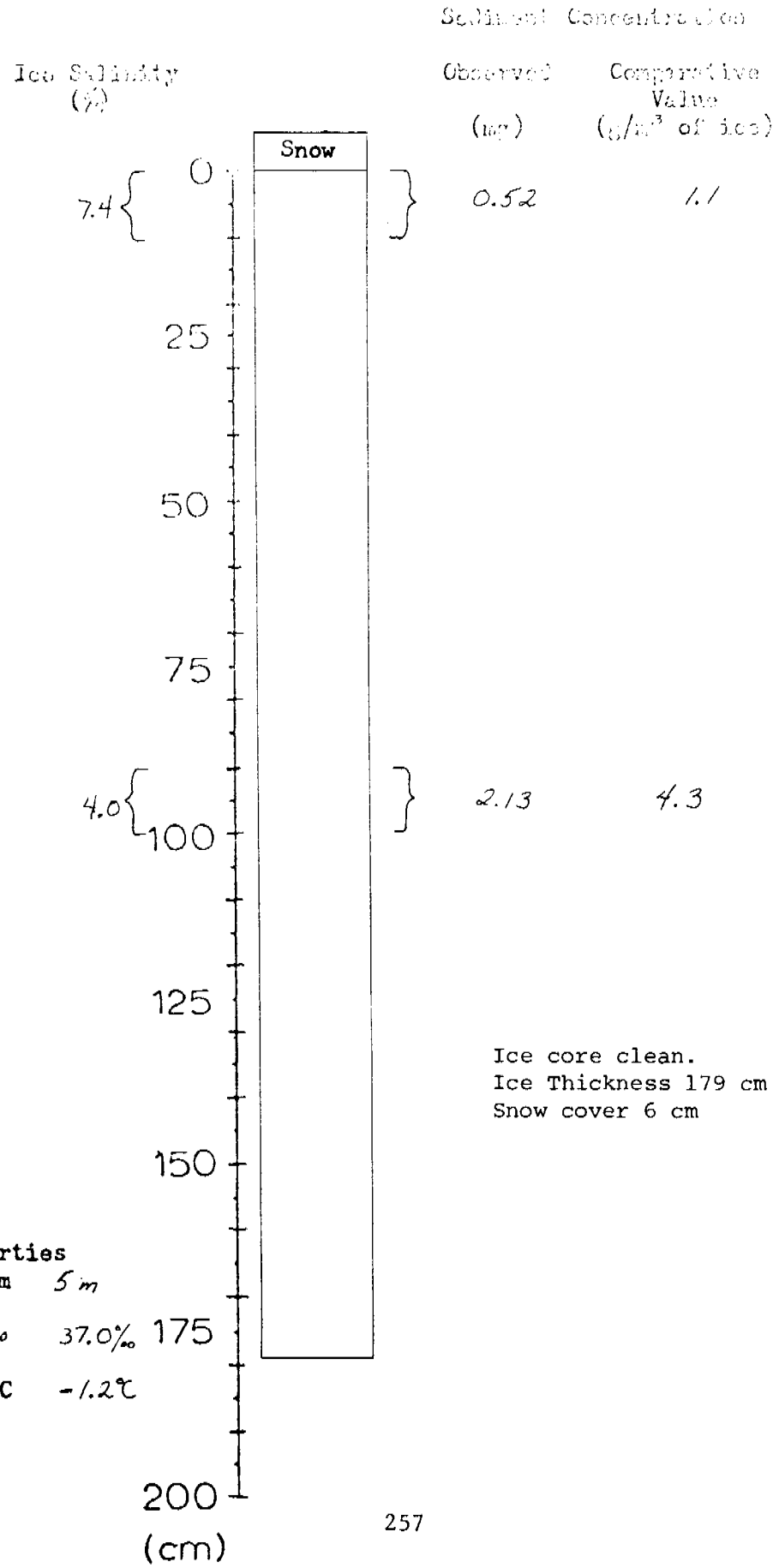

Ice core clean.
Ice Thickness 179 cm
Snow cover 6 cm

Water Properties

	at 2¼ m	5 m
S	33.7‰	37.0‰
T	0.5 °C	-1.2°C

Ice Core #14

70° 27.8'N 148° 54.4'W

Ice Salinity (‰)

5.3
7.0
4.5
5.4
3.8

Sediment Concentration

Observed (mg)	Comparative Value (g/m^3 of ice)
382	770
734	1480
461	930
7.89	16
>2400	>4800

upper 50 cm contain grass and stems up to 2cm long

0
25
50
75
100
125
150
175
200
(cm)

Water Properties at ____ m

S 49.1‰

T -2.0°C

0 - 120 cm murky core with vague banding at 30 - 40 c
120 - 150 cm clean ice.
150 - 155 cm dirty ice grading down to sediment lens
155 to 156 cm. Cleaner ice below.
Organic material particularly noticable in upper 50 c
core--grass and stems up to 2 cm long.
Ice Thickness 165 cm

Ice Core #15

70° 24.0'N 148° 32.6'W

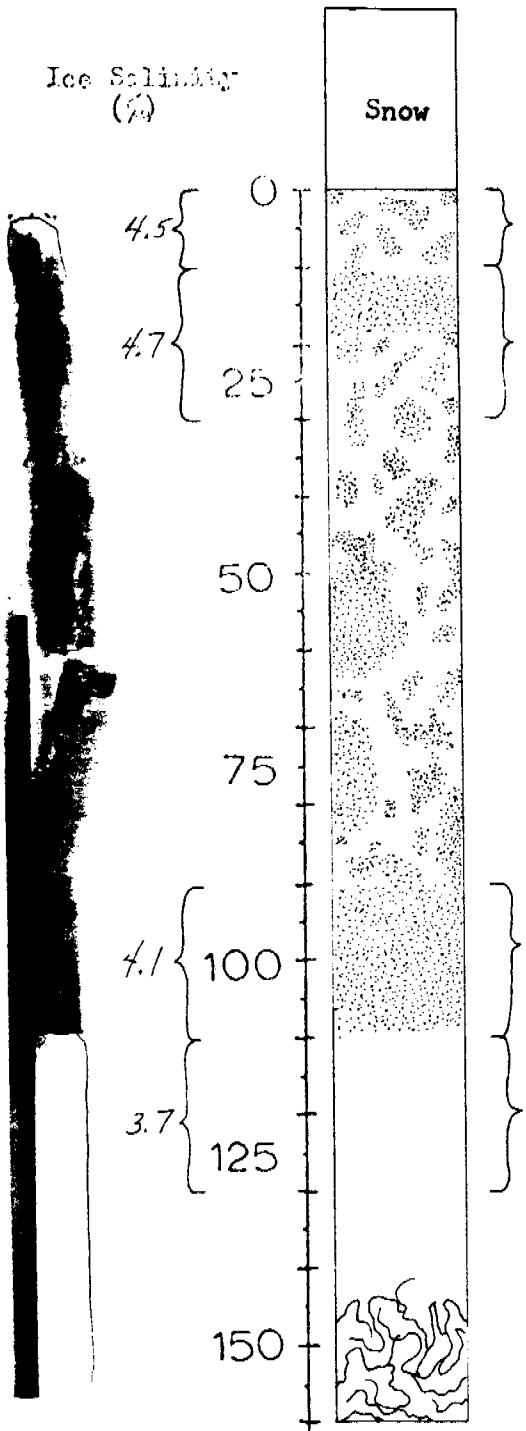

Sediment Concentration	Observed (mg)	Comparative Value (g/m² of ice)
0 - 25 cm	371	750
25 - 100 cm	874	880
100 - 125 cm	618	620
125 - 150 cm	7.90	7.9

Water Properties at ____m

S ____‰

T ____°C

0 - 110 cm dirty ice--dirtied by specks of dirt giving muddy appearance to core. Individual flecks rather than even turbidity to ice. Particularly dirty at 10 - 20 cm and 90 - 110 cm.

Sharp contact at 110 cm with clean ice. Clean to bottom of core. Ice is honeycombed at bottom with brine channels.

Ice Thickness 160 cm

Snow cover 24 cm

200 ⊥

(cm)

Ice Core #16

70° 25.1'N 148° 31.5'W

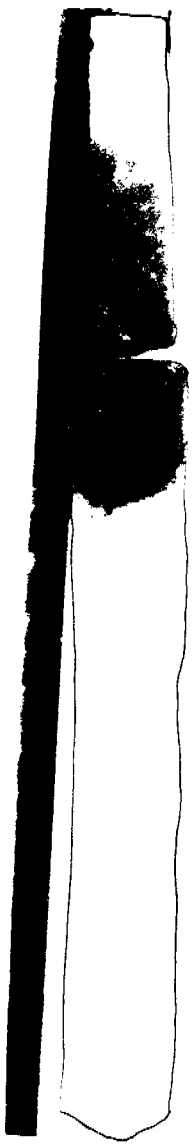

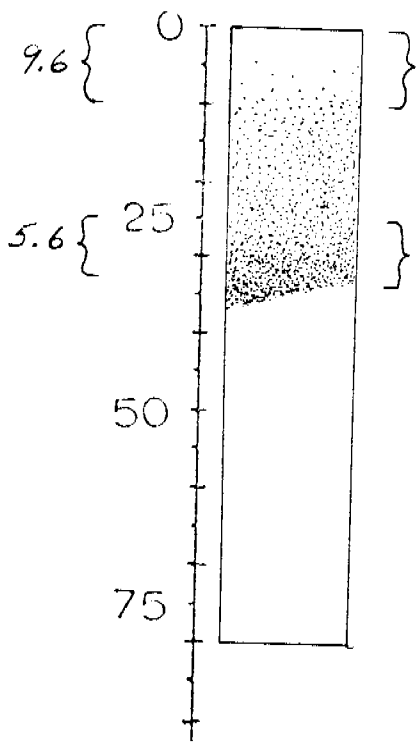

Sediment Concentration		
	Observed (mg)	Comparative Value (g/m³ of ice)
0–25 cm	7.43	15
25–33 cm	132	330

Clean ice down to 7 cm. Gradual contact with dirty ice which gets darker with depth to 33 cm where there is a sharp but slightly sloping contact with underlying clean ice. Noted several times that coring will break the core at the dirty ic contact. Noted that 16 broke cleanly at 33 cm when struck.

Ice Thickness 80 cm

Water Properties at ___m

S ___‰

T ___°C

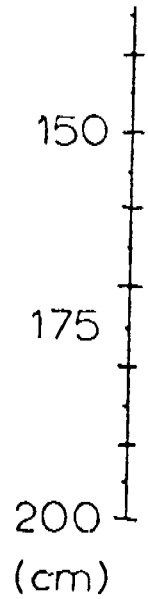

Ice Core #17

70° 26.2'N 148° 47.2'W

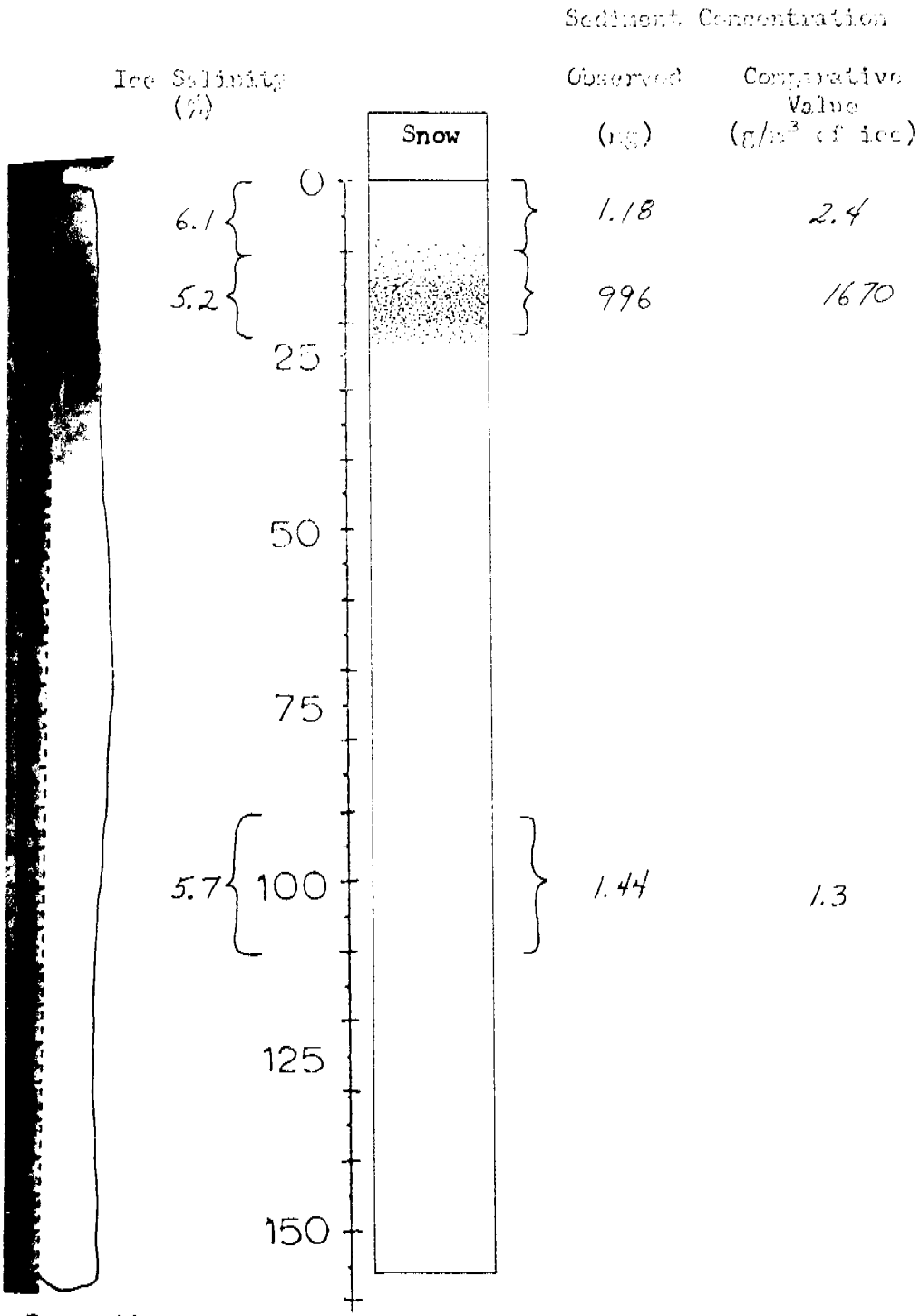

Water Properties at ___m

S 37.7‰

T -1.6 °C

Clean ice to 7 cm. Gradual contact with dirty layer at 10 - 22 cm but much thinner than at two dive blocks at site #3. Sharp contact at base of darkest ice.

Ice Thickness 156 cm

Snow depth 10 cm

Ice Core #18

70° 26.8'N 148° 45.6'W

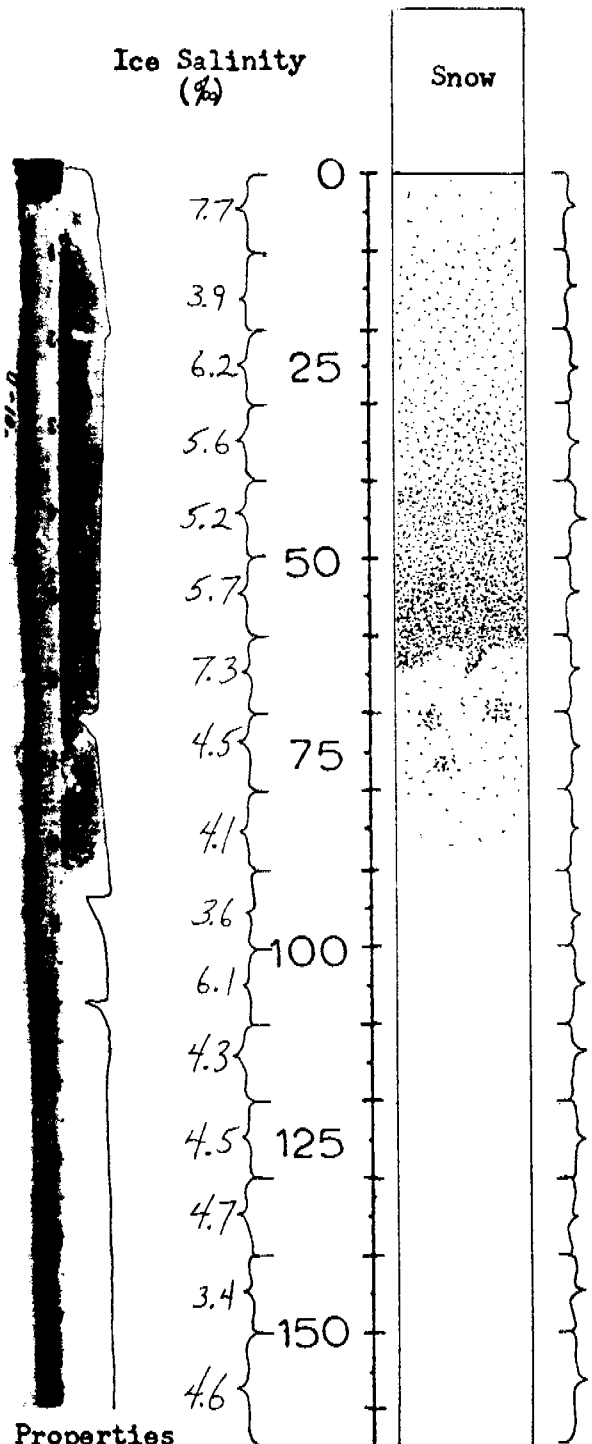

Ice Salinity (‰)	Sediment Concentration Observed (mg)	Comparative Value (g/m³ of ice)
7.7	13.1	26
3.9	104	210
6.2	129	260
5.6	186	370
5.2	294	590
5.7	638	1280
7.3	1010	2030
4.5	131	260
4.1	73.9	150
3.6	3.60	7.2
6.1	3.64	7.3
4.3	1.97	4.0
4.5	1.52	3.1
4.7	1.30	2.6
3.4	2.9	5.7
4.6	1.02	1.5

Water Properties at ____ m

S 38.0‰

T -2.2°C

0 - 62 cm turbid layer increasing with depth. No obvious lenses o
layers.

62 - 81 cm less turbid and slightly blotchy zone with irregular lo
contact.

81 - 164 cm 'clear' ice.

Ice Thickness 165 cm

Snow cover 22 cm

200 ⊥
(cm)

Ice Core #19

70° 17.9'N 147° 46.9'W

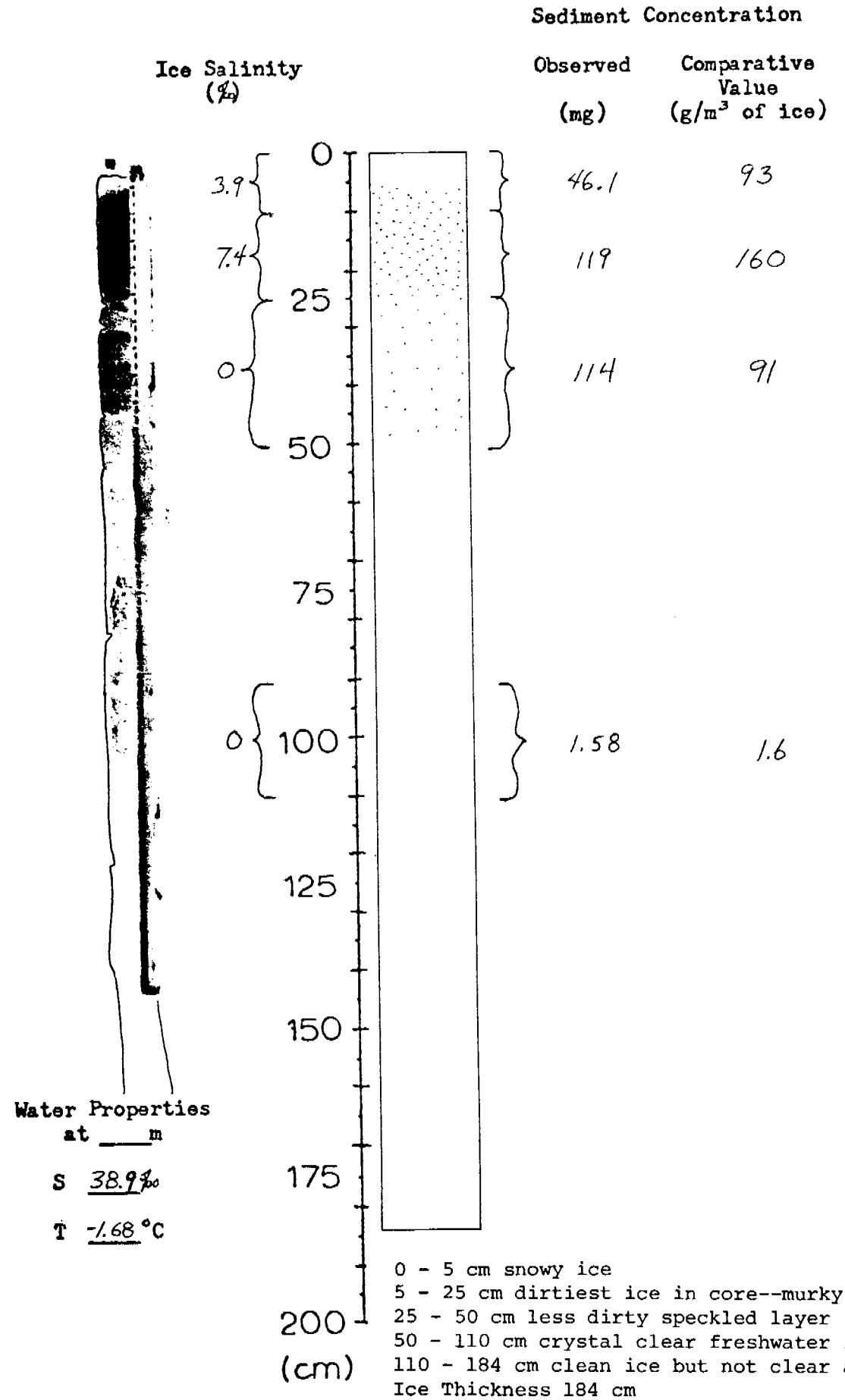

0 - 5 cm snowy ice
5 - 25 cm dirtiest ice in core--murky.
25 - 50 cm less dirty speckled layer
50 - 110 cm crystal clear freshwater ice.
110 - 184 cm clean ice but not clear as in above section.
Ice Thickness 184 cm

Ice Core #20

70° 20.6'N 147° 38.6'W

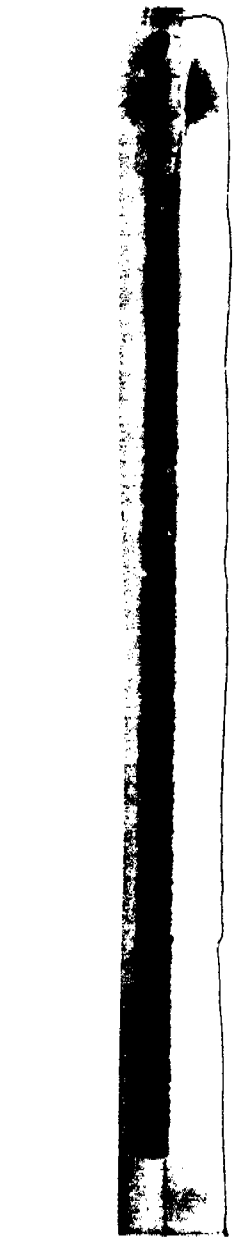

Ice Salinity (‰)

7.0

3.8

3.9

Snow

0

25

50

75

100

125

150

175

200

(cm)

algae in bottom

Sediment Concentration

	Observed (mg)	Comparative Value (g/m³ of ice)
0 - 25 cm	17.5	35
25 - 100 cm	44.8	60
100 - 150 cm	1.82	1.8

0 - 5 cm slightly dirty snowy ice
5 - 15 cm murky layer
15 - 160 cm clear ice
160 - 170 cm algae in bottom
Ice Thickness 181 cm
Snow cover 12 cm

Water Properties at 3 m

S 38.5‰

T -1.9°C

Ice Core #21

70° 23.2'N 147° 29.7'W

Ice Salinity (‰)

5.7

6.2

4.3

6.2

Water Properties at 3 m 7m

S 37.5‰ 38.7‰

T -2.0°C -2.0°C

0 Snow

25

50

75

100

125

150

175

200

(cm)

Sediment Concentration

	Observed (mg)	Comparative Value (g/m³ of ice)
	4.7	9.5
	169	170
	148	150
	1.28	1.3

0 - 5 cm snowy clean ice
5 - 110 cm dirty ice--coarsening at bottom
110 - 168 cm clean ice
Ice Thickness 168 cm
Snow cover 5 cm

Kovacs Core #125

70° 10.5'N 147° 06.6'W

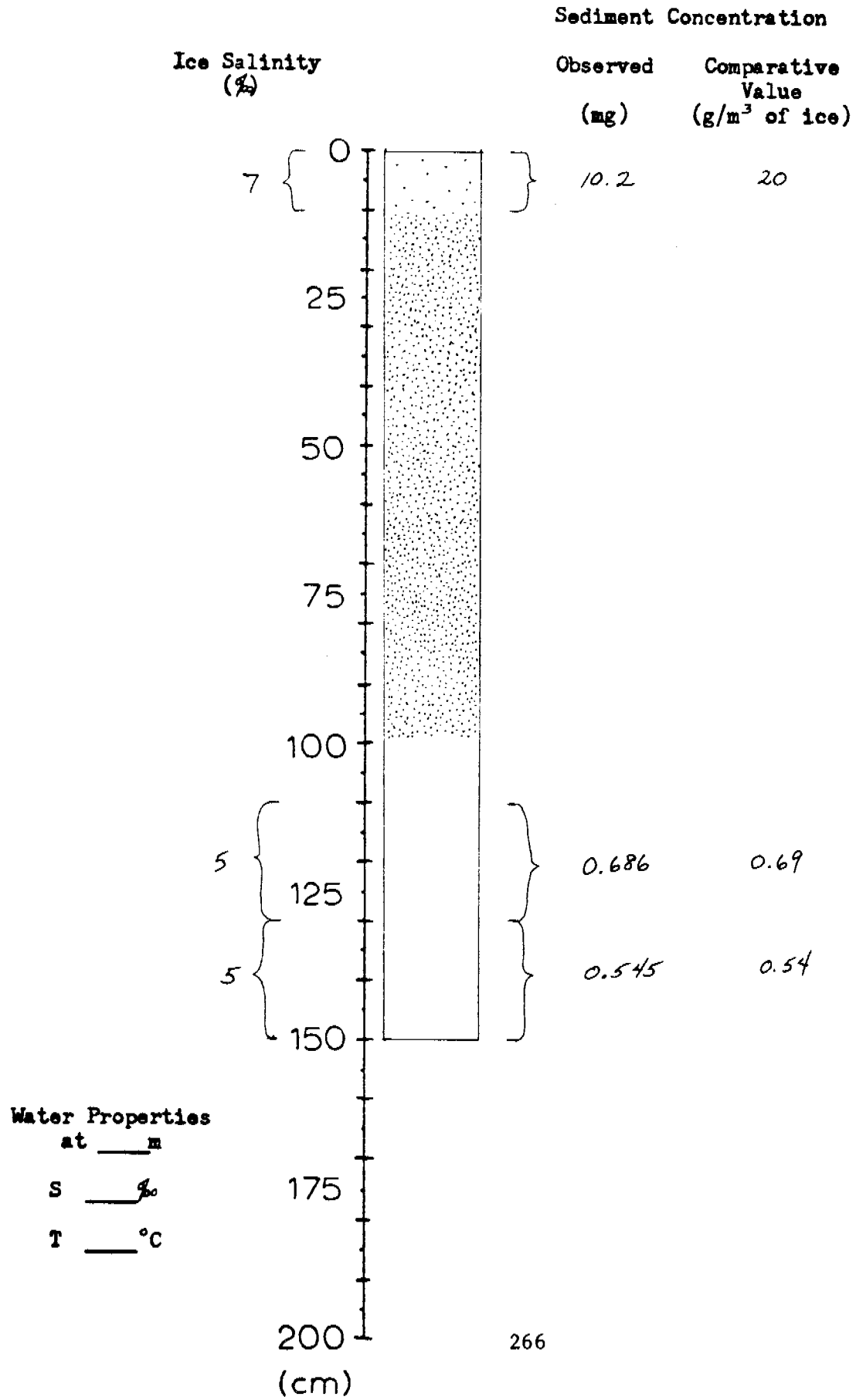

Kovacs Core #186

70° 12.7'N 147° 06.7'W

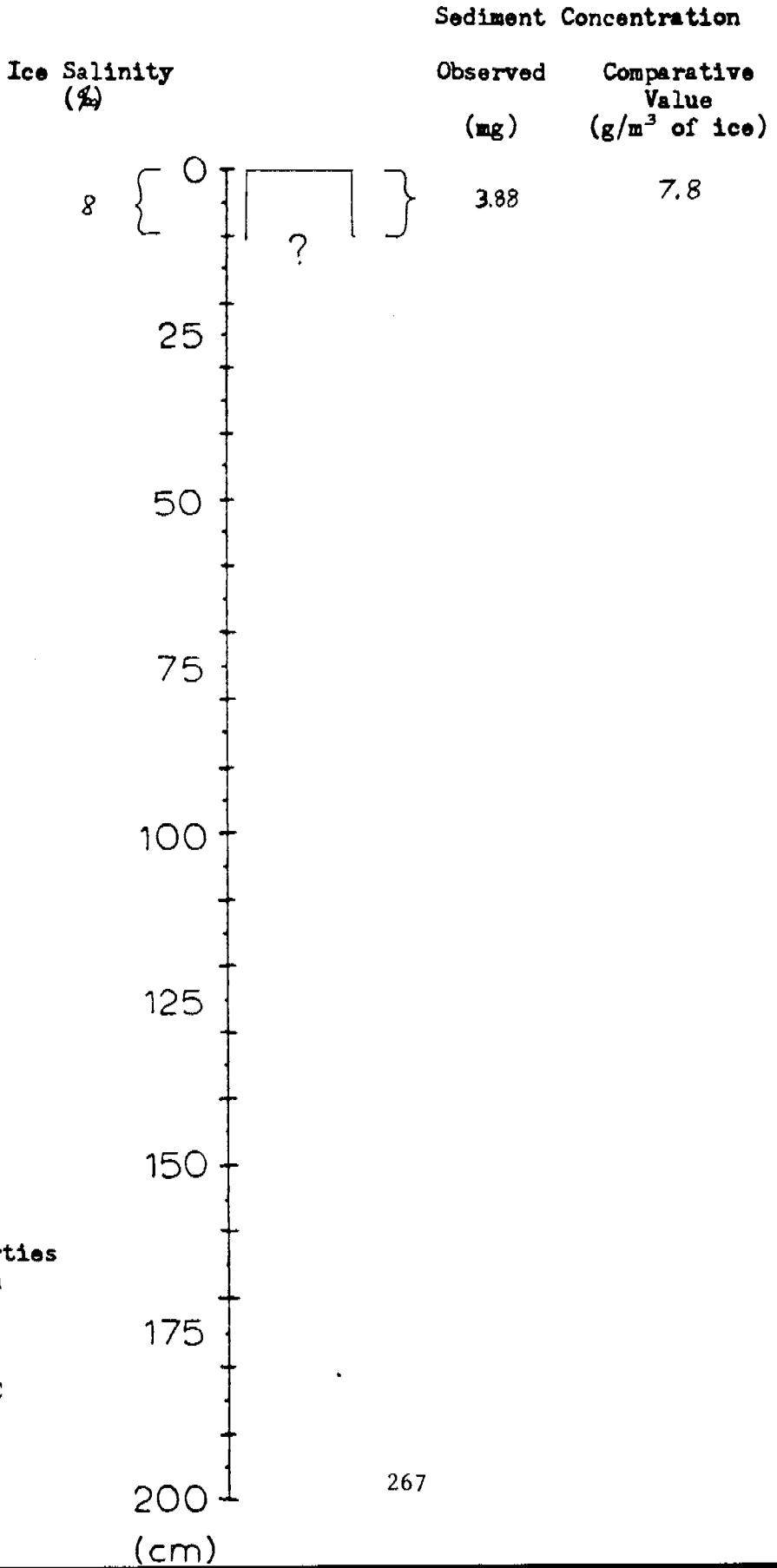

Water Properties at ___m

S ___‰

T ___°C

ANNUAL REPORT

YUKON DELTA COASTAL PROCESSES STUDY

William R. Dupré

Department of Geology
University of Houston
Houston, Texas

April 7, 1978

Prepared for

U.S. Department of Commerce
National Oceanic and Atmospheric Administration
Environmental Research Laboratories
Boulder, Colorado 80302

Research Unit: 208

I SUMMARY

Objectives

The overall objective of this project is to provide data on geologic processes in the Yukon-Kuskokwim delta region in order to better evaluate the potential environmental impacts of oil and gas exploration and production. The specific objectives of the study include the following:

1) Study the processes along the delta shoreline (e.g., tides, waves, sea-ice, river input) to develop a coastal classification including geomorphology, coastal stability, and dominant direction of sediment transport.
2) Study the processes active on the delta plain, including river breakup, river bank erosion and sedimentation, and the hydrology of the interconnected lakes and abandoned river channels.
3) Make a tectonic map of the delta region, delineating areas of Quaternary volcanism and faulting.
4) Make a geologic map of the delta area, emphasizing the delineation of depositional systems, in order to:
    a) establish a chronology of delta sublobes to serve as a datum by which the relative age of Quaternary faulting and volcanism can be measured.
    b) establish a chronology of storm-induced erosional events recorded in chenier-like sequences along the coast to estimate the recurrence interval of major storms in the region.
    c) determine the physical properties of the different geologic units, including the depth and stability of permafrost.
    d) aid in the definition and extrapolation of biological habitats throughout the region.

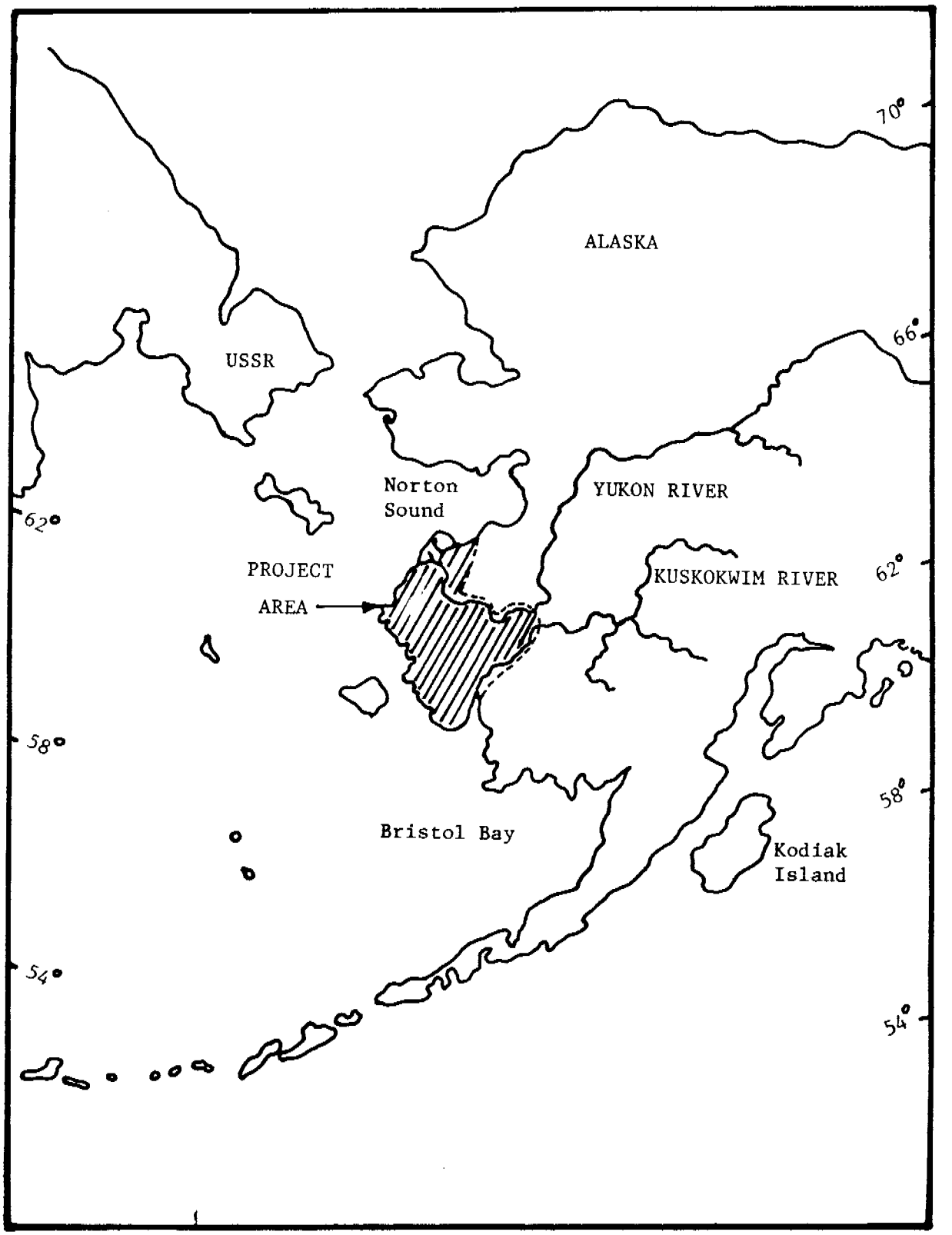

Figure 1: Location of project area - Yukon Delta Coastal Processes Study (R.U. 208).

Conclusions:

The Yukon-Kuskokwim delta region is characterized by widespread Quaternary tectonism. Evidence of Holocene faulting, coupled with the high potential for liquefaction of most of the Holocene fluvial and deltaic sediments, constitute serious geologic constraints both in the selection of transportation corridors and the design of offshore structures. The risk from explosive volcanism, however, appears slight.

Non-tectonic geologic hazards also exist throughout the region. Of these, permafrost may be one of the more difficult to predict, as it appears to be present in various degrees in most areas except along large rivers, deep lakes, and rapidly prograding shorelines. Other geologic processes which must be considered in any site selection include: 1) flooding, both along the rivers and the coast, 2) erosion and sedimentation along rivers, sub-ice channels, and the shoreline, and 3) ice-related problems such as rapidly moving pack ice and ice gouging. It is also extremely important to recognize that these processes vary temporally, as well as spatially. The seasonality of processes must be properly understood, both in the selection and design phase of offshore and onshore facilities as well as modeling the predicted dispersion and impacts of potential oil spills.

Lastly, it should be noted that the depositional environments of the modern Yukon Delta differ significantly from most previously described deltas. Failure to recognize these differences could seriously aggravate the already difficult problem of siting offshore facilities in this region.

Implications:

The siting of offshore facilities (e.g., drilling platforms, underwater pipelines) must take into account the mobility and deformation of seasonal pack ice, the extent and variability of shorefast ice, the probability of offshore permafrost, and the possible effects of altering offshore bathymetry in changing coastal stability. In addition, the evaluation of possible oil spills must take into account not only the dominant northward drift of water and suspended sediments, and the local and seasonal variability of current patterns, but also the role of sub-ice channels in affecting bedload transport.

The selection of shoreline sites (e.g., docking and pipeline terminals) must take into account the present coastal stability, including the possibility of erosion associated with major storm surges, even in an area of long-term progradation. The effects of shorefast ice for over half of the year must also be considered. The heterogeneity of the shoreline must also be considered in determining oil spill vulnerability.

Much of the delta is underlain by the on-land extension of the Nunivak Arch; this would seem to exclude most of the region for serious consideration for exploration. Nevertheless, the Quaternary faults and volcanoes which characterize the zone constitute geologic constraints on the selection of transportation corridors. The discontinuous permafrost and the complex hydrology of the delta further complicate the location of such corridors, as well as making it difficult to predict the effects of oil spills.

Lastly, an understanding of the geologic processes and products within the delta region will greatly aid in the definition and regionalization of biological habitats, as well as help in the development of depositional models for sedimentation in an ice-dominated coastal environment.

II. INTRODUCTION

The overall objective of this project is to provide data on geologic processes in the Yukon-Kuskokwim delta region in order to better evaluate the potential environmental impacts of oil and gas exploration and production. The specific objectives of the study include the following:

1) Study the processes along the delta shoreline (e.g., tides, waves, sea-ice, river input) to develop a coastal classification including geomorphology, coastal stability, and dominant direction of sediment transport.
2) Study the processes active on the delta plain, including river breakup, river bank erosion and sedimentation, and the hydrology of the interconnected lakes and abandoned river channels.
3) Make a tectonic map of the delta region, delineating areas of Quaternary volcanism and faulting.
4) Make a geologic map of the delta area, emphasizing the delineation of depositional systems, in order to:
    a) establish a chronology of delta sublobes to serve as a datum by which the relative age of Quaternary faulting and volcanism can be measured.
    b) establish a chronology of storm-induced erosional events recorded in chenier-like sequences along the coast to estimate the recurrence interval of major storms in the region.
    c) determine the physical properties of the different geologic units, including the depth and stability of permafrost.
    d) aid in the definition and extrapolation of biological habitats throughout the region.

This project was designed to provide as much information as possible to the problems of petroleum development in the region. A better understanding of the tectonic framework of the delta region should aid in the exploration of oil and gas. Those same tectonic features, to the

extent to which they are active today, also provide serious constraints to the selection of transportation corridors, as does the existence of extensive permafrost and the actively shifting river courses.

A better understanding of coastal processes will aid in the siting of shoreline installations (e.g., docking and transfer facilities), as well as in evaluating the possible impacts of such facilities on coastal stability. The siting of offshore facilities (e.g., drilling rigs, underwater pipelines) must take into account frequency and magnitude of a variety of nearshore processes, including those associated with sea-ice. An understanding of these processes, including their seasonal variability, will also aid in predicting the paths of possible oil spills. An inventory of coastal materials and landforms will also serve as baseline data should spills come onshore.

Lastly, a better understanding of the sub-arctic coastal processes by which the present coastal depositional systems formed, will aid in the interpreting older, potentially oil-bearing units which may have been formed under similar climatic conditions.

III. CURRENT STATE OF KNOWLEDGE

The Yukon River is the 17th largest river in the world providing over 90% of the sediment introduced into the Bering Sea (Lisitzin, 1972), however, relatively little is known of its Quaternary history or of the process by which it was formed.

The ancestral Yukon River emptied into the Pacific in the vicinity of Cook Inlet during early Cenozoic time. Late Miocene uplift of the Alaska Range resulted in the diversion of the drainage system into the Bering Sea, where it has remined to the present (Nelson et al., 1974). Gradual submergence during late Miocene and Pliocene time was followed during the Pleistocene by repeated glacio-eustatic fluctuations of sea-level. River vallys cut into the exposed continental shelf during the last low-stand of sea-level were subsequently filled during rising sea-level with estuarine and marine sediments (e.g., Moore, 1964; Creager and McManus, 1967; Knebel and Creager, 1973). This rise in sea-level was apparently accompanied by a general northward shift of the Yukon River to the north (Knebel and Creager, 1973; Shepard and Wanless, 1971).

Much work has been done on studying the Cenozoic sedimentary and tectonic history of the Bering Sea (e.g., Nelson and others, 1974; Marlow and others, 1976), including studies of the Holocene sediments of the Yukon River at its mouth (Matthews, 1973) and on the Bering Sea shelf (e.g., Moore, 1964; McManus and others, 1974; Nelson and Creager, 1977). However, geologic mapping in the delta region (Hoare, 1961; Hoare and Coonrad, 1959a, 1959b; Hoare and Condon, 1966, 1968, 1971a, 1971b) has largely emphasized the pre-Quaternary history of the region. This study is the first, to deal in detail with the processes and events by which the Yukon-Kuskokwim delta complex was formed.

IV. STUDY AREA

The combined Yukon-Kuskokwim delta complex (Figure 1) is an area of unique natural resources covering over 31,000 square miles. It has a large native population living in large part on a subsistence economy. It provides access to most of the spawning areas for salmon in the region. It is, in addition, one of the most significant breeding grounds for migratory birds in North America.

The delta region is largely a flat, featureless plain consisting of wet and dry tundra, interrupted by innumerable lakes, many of which are oriented. Many of these lakes have coalesced laterally to form very large bodies of water (e.g., Baird Inlet) connected to the sea by a series of ancient river channels. The flatness of the delta complex is interrupted by numerous small Quaternary shield volcanoes, the major uplifted massifs of the Askinuk and Kuzilvak Mountains, and the Quaternary volcanic complex which forms Nelson Island.

The coastline is extremely varied, in part because of the complex geology along the coast, and in part because of the lateral variability of sediment sources and tidal range. For example, broad tidal flats, locally bordered by short barrier islands, flank the macro-tidal Kuskukwim delta, whereas the micro-tidal Yukon delta is fringed by distributary mouth bars and interdistributary tidal flats. Sandy beaches are present near Hooper Bay, where Wisconsinan(?) sand dunes provide the source of sediments, whereas steep gravel beaches and rocky headlands form along the cliffed shorelines at Cape Romanzof, Point Romanof, and Nelson Island. Elsewhere most of the coast consists of low, eroding bulffs cut into poorly consolidated Pleistocene deposits.

V. SOURCES, METHODS, AND RATIONALE OF DATA COLLECTION

Hydrologic data on discharge are available in published form for the Kuskokwim River at Crooked Creek (1951-1965) and for the Yukon River at Kaltag (1957-1965). More recent data are presently unpublished, but are available from the Water Resources Division of the U.S. Geological Station in 1974, providing additional information on suspended and bedload sediment as well as discharge. Additional samples of both the bedload and suspended load of the Yukon and Kuskokwim Rivers are being collected as part of the field work.

Much of the region has been mapped and published at a scale of 1:250,000 by Dr. Joe Hoare and associates at the U.S. Geological Survey. I have been using these maps in conjunction with aerial photography and LANDSAT imagery, to prepart a geologic map of the delta region emphasizing the Quaternary depositional systems.

Field work is providing the ground truth for the mapping as well as samples for textural and mineralogic analyses and radiocarbon dating. Samples for dating are being selected to document the frequency of major shifts in the rivers course as well as major coastal storms. The distribution of permafrost is also being studied, with special emphasis on defining the relationships between geomorphology, vegetation, and extent of ground ice. Hopefully the geologic mapping can be combined with data on morphology, vegetation, and physical properties to ais in the characterization of biological habitats and the definition of resource capability units.

Part of the field work consisted of coring a volcanic lake in the center of the delta region and another in the vicinity of St. Michaels Island. The cores are presently being analyzed by Dr. Tom Ager (U.S. Geological Survey) to determine frequency of volcanism in the region (via ash content), sources and rates of sedimentation, and evidence of climatic change (via pollen analysis).

Existing imagery is being used in combination with coastal overflights in a light plane and helicopter to develop a coastal classification scheme. Baseline coastal stations were established to characterize homogeneous intervals of the coastline. Approximately twelve such stations were established in 1976; an additional thirty were set up in 1977. Approximately two thirds of those were reoccupied in 1978. Beach profiles are measured at each station using a modified Emery method - some offshore profiles were obtained in 1976 with a Zodiac and fathometer. Sediment samples and process measurements (e.g., winds, waves) are also collected.

Bathymetric maps (dating back to 1898) are being used in conjunction with aerial photos (1954, 1973, and 1976) and beach profiles to determine rates and directions of shoreline change as well as dominant directions of nearshore sediment transport. Bathymetric profiles from the R/V KARLUK are also available to determine rate of offshore changes. The KARLUK also collected 22 vibracores taken on the sub-ice platform, which, when combined with offshore cores taken by C. Hans Nelson and onshore cores taken during this project, should provide a good overview of the patterns of sedimentation in the delta.

LANDSAT imagery is also being used, and has proven invaluable in defining offshore sediment plumes as well as studying the development and mobility of ice in the region. NOAA VHRR(I-2) weather satellite imagery is also being used in combination with synoptic weather data to aid in interpreting ice patterns in the Norton Sound region.

VI. RESULTS

Many of the results of this project (e.g. tectonic and gologic maps; maps of coastal morphology, and rates of shoreline change) will not be completed until the Final Report at the end of the year, hence the reader is referred to earlier Annual Reports for a description of those aspects of this study. This project has, however, produced some results during the past year which should be specially noted. These include:

1) A reassessment of rates of ice wedge formation based on new radiocarbon dates (Fig. 2) demonstrating that moderately large ice wedges (>1 m across at top) have formed within the last 4,500 years in the southern Norton Sound region.

2) A compilation of over 300 grain-size analyses which demonstrate the marked paucity of clays in the sediment (Fig. A2), reflective of the dominance of mechanical weathering processes, and an unusual offshore increase in percent of sand offshore of the modern Yukon delta (Fig.A6), probably reflecting the increased wave energy on the outer edge of the delta front (sub-ice) platform.

3) A better understanding of the depositional environments within the modern Yukon delta (Fig. A5), suggesting it may represent a type of ice-dominated delta, morphologically distinct from previously described wave-, river-, and tide-dominated deltas (Appendix A).

4) An evaluation of patterns of ice movement in the vicinity of Norton Sound (Appendix B), demonstrating previously unrecognized complications in the kinds of ice-related geohazards which might characterize the Norton Basin.

5) A better understanding of the seasonality of deltaic processes which are probably characteristic of many high-latitude, epicontinental seas (Appendices B and C).

VII. DISCUSSION

Tectonic Framework:

The Yukon-Kuskokwim delta complex is located within the Koyukuk volcanogenic province which has been characterized by recurrent faulting and syntectonic volcanic activity throughout Mesozoic and Cenozoic time (Patton, 1973). Most of the major faults in the region (e.g., the Kaltag fault) formed were most active during late Cretaceous and early Tertiary time (Hoare, 1961), however, many of these structures have remained active, albeit at reduced levels of activity, to the present (e.g., Hoare, 1961; Patton and Hoare, 1968; Grim and McManus, 1970).

Most of the newly recognized faults, photo-linears, and measured joint sets within the Quaternary deposits are parallel to or are extension of previously mapped faults. There is no evidence of the Kaltag fault passing through the modern lobe of the Yukon delta, as previously suggested by Hoare and Condon (1971), however this may simply be the result of masking by the relatively young (<2500 yrs) delta. Alternatively the Kaltag may splay into a series of southwest-trending faults which transect the Andreski Mountains and continue across the delta plain.

The age of the most recent faulting remains uncertain, however at least some of the faults appear to cut Holocene deltaic and fluvial deposits. Thus it seems clear that the selection of potential transportation corridors must take into account the possibility of significant ground movement along at least some of the fault zones in the area. In addition, all site investigations must evaluate the potential for ground shaking and liquefaction due to such an event, even though the historical seismicity is relatively low. This is particularly important as almost all of the Holocene fluvial and deltaic sediments are characterized by grain size distributions which suggest they are highly susceptible to liquefaction.

The Quaternary volcanism probably occurred over a wide period of time, as evidenced by the various degrees of weathering and slope modification; however paleomagnetic data indicate that almost all of the basalts are normally polarized, hence are younger than 700,000 years old (Hoare and Condon, 1971b). A core taken from a volcanic lake in the middle of the delta complex contains an ash deposit which is approximately 3500 years old. However, the composition of the ash suggests it was derived from a distant source (e.g. Alaska Peninsula). There is no other evidence of volcanism preserved in the core, which probably records an interval of approximately 24,000* years, suggesting either that the most recent volcanism in the region was far removed from the lake or that it predates the core. The latter seems most likely, however there are some extremely young looking flows near St. Micahels which are probably younger than any of the volcanic activity in the delta region. Thus is seems likely that, with the possible exception of the area around St. Michaels, the risk due to volcanic activity should be considered slight.

* previously stated as 40,000-60,0000 years

Permafrost:

Previous Annual Reports have described the variability in the kinds and extent of permafrost in the delta region. The Pleistocene deposits are extensively underlain by permafrost, locally up to 200 m thick. Permafrost also underlies much of the Holocene deposits, where it is typically 2 - 10 m thick. I previously reported that moderately large ice wedges (e.g. >1 m wide) were probably restricted to Wisconsinan age sediments. This appears to have been an error.

A series of radiocarbon dates run by Sam Velastro at the Radiocarbon Laboratory of the University of Texas at Austin clearly demonstrate that such ice wedges have formed at least twice during the Holocene (Fig.). The presence of such large ice wedges in the Holocene deposits in an area whose mean annual temperature (approx -2°C) was previously thought to have been too warm for their formation, suggests the need for a reassessment of the paleo-climatic significance of large ice wedges. It should also be noted that the estimated rates of ice wedge growth (1.2 - 1.6 mm/yr), between approximately 4500 and 2300 yrs BP are comparable with rates presently forming along some areas of the North Slope of Alaska (Dave Hopkins, personal communication).

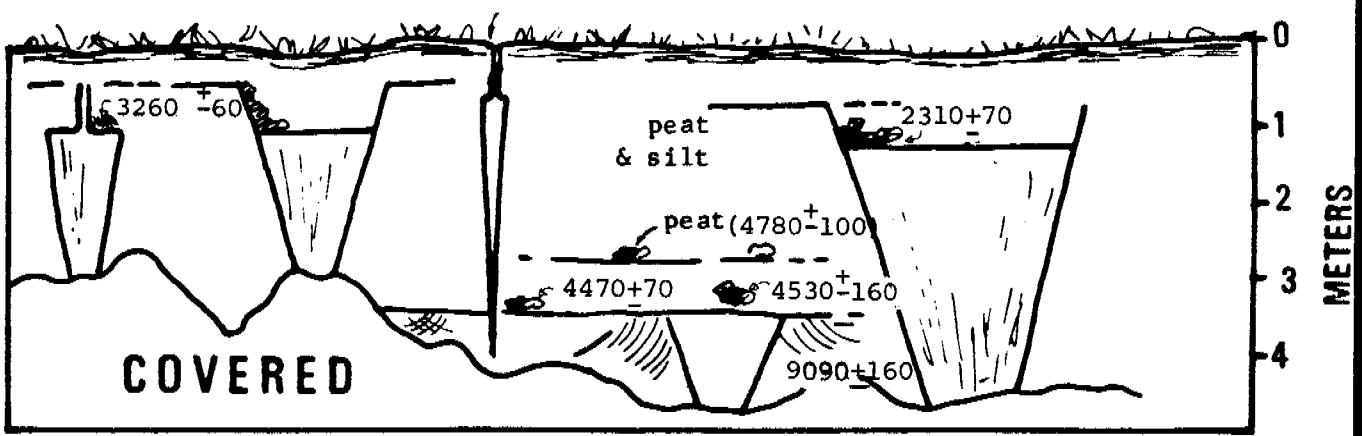

Figure 2.: Holocene ice wedge sequence exposed in sea cliff approximately 10 km northeast of Pt. Romanoff.

VIII. CONCLUSIONS

The Yukon-Kuskokwim delta region is characterized by widespread Quaternary tectonism. Evidence of Holocene faulting, coupled with the high potential for liquefaction of most of the Holocene fluvial and deltaic sediments, constitute serious geologic constraints both in the selection of transportation corridors and the design of offshore structures. The risk from explosive volcanism, however, appears slight.

Non-tectonic geologic hazards also exist throughout the region. Of these, permafrost may be one of the more difficult to predict, as it appears to be present in various degrees in most areas except along large rivers, deep lakes, and rapidly prograding shorelines. Other geologic processes which must be considered in any site selection include: 1) flooding, both along the rivers and the coast, 2) erosion and sedimentation along rivers, sub-ice channels, and the shoreline, and 3) ice-related problems such as rapidly moving pack ice and ice gouging. It is also extremely important to recognize that these processes vary temporally, as well as spatially. The seasonality of processes must be properly understood, both in the selection and design phase of offshore and onshore facilities as well as modeling the predicted dispersion and impacts of potential oil spills.

Lastly, it should be noted that the depositional environments of the modern Yukon Delta differ significantly from most previously described deltas. Failure to recognize these differences could seriously aggravate the already difficult problem of siting offshore facilities in this region.

IX. NEEDS FOR FUTURE STUDY

It has become increasingly apparent that the process of sediment transport and deposition (and resuspension) is far more complex than previously thought. The extreme seasonality of processes, including those associated with river influx, wind and waves, oceanic and tidal currents, and ice must be studied in more detail if predictive models of sediment (and pollutant) transport are to be properly developed. This will necessitate the funding of a series of coordinated studies of in situ monitoring of processes during several periods of the year. I strongly recommend serious consideration be given to the following type of program.

1) Winter-dominated period: this would include both lab studies of weather patterns and ice movement as detectable on satellite imagery, as well as field studies to measure ice thickness and patterns of ice movement and deformation, as well as sub-ice processes such as oceanic currents and tides in a variety of environments such as sub-ice channels, the delta front, and prodelta.

3) Breakup: This period is of extreme importance in establishing and maintaining many of the environment which appear unique to ice-dominated coastal zones. In situ monitoring of currents and sediment transport on top of the fast ice and below the ice canopy, both in sub-ice channels and in the sub-ice platform.

3) River-dominated period: This is a period dominated by the high sediment discharge of the Yukon. Studies emphasizing the pattern of sedimentation during this time would be extremely useful. Offshore wave and current meters would be installed at this time.

4) Storm-dominated period: Late summer and early fall is a period dominated by the combined effects of decreasing sediment input and increasing storm frequency (hence sediment reworking). In situ monitoring of offshore processes is particularly important at this time.

5) Freezeup: It also would be useful to study the processes by which the shore-fast ice forms and expands over the sub-ice platform and associated channels. This also would require in situ monitoring during late October to early November.

X. SUMMARY OF JANUARY - MARCH QUARTER

The last quarter was spent at the Pacific-Arctic Branch of Marine Geology, U.S. Geological Survey, where I have been working on data collected both as part of my project and data from the offshore portions of the delta, collected by Jim Howard and Hans Nelson. Work has been completed on describing the types of sedimentary structures found in the subaqueous delta facies; textural analyses of sediments are planned for the near future. Work also continues on finishing the tectonic and geologic maps, as well as the maps of coastal morphology and coastal processes.

BIBLIOGRAPHY

Beikman, H.M., 1974, Preliminary geologic map of the southwest quadrant of Alaska; USGS open file map (2 sheets).

Carey, S.W., 1958, A tectonic approach to continental drift, in Continental Drift, a symposium, University of Tasmania, pp.177-355.

Creager, T.S. and McManus, D.A., 1967, Geology of the floor of Bering and Chukchi Seas - American studies; in Hopkins, D.M. (ed.) The Bering Land Bridge, Stanford Univ. Press, Stanford, Calif., pp. 32-46.

Fisher, W.L., and others, 1969, Delta systems in the exploration for oil and gas: a research colloquium, Bureau of Economic Geology, Univ. of Texas, Austin.

Galloway, W.E., 1975, Process framework for describing the morphologic and stratigraphic evolution of deltaic depositional systems: in Broussard, M.L. (ed.) Deltas: Models for Exploration; Houston Geol. Soc., pp. 87-98.

Grim, M.S. and McManus, D.A., 1970, A shallow-water seismic-profiling survey of the northern Bering Sea; Marine Geology, vol. 8, pp. 293-320.

Hamilton, T.D. and Porter, S.C., 1975, Itkillik glaciation in the Brooks Range, Nortern Alaska; Quaternary Research, vol. 5, pp. 471-497.

Hayes, M.O., 1975, Morphology of sand accumulation in estuaries: in Cronin, L.E. (ed.) Estuarine Research, vol. II, Geology and Engineering, Academic Press, New York, pp. 3-22.

Hill, D.E., and Tedrow, J.C.F., 1961, Weathering and soil formation in the Arctic environment: Amer. Jour. Sci., vol. 259, pp. 84-101.

Hoare, J.M., 1961, Geology and tectonic setting of lower Kuskokwim-Bristol Bay region, Alaska; Am. Assoc. Petroleum Geologists Bull., vol. 45, pp. 594-611.

Hoare, J.M. and Condon, W.H., 1966, Geologic map of the Kwiguk and Black Quadrangles, western Alaska; USGS Misc. Geol. Invest. Map I-469.

Hoare, J.M. and Condon, W.H., 1968, Geologic map of the Hooper Bay Quadrangle, Alaska; USGS Misc. Geol. Invest. Map. I-523.

Hoare, J.M., and Condon, W.H., 1971(a), Geologic map of the St. Michael Quadrangle, Alaska; U.S.G.S. Misc. Geol. Invest. Map I-682.

Hoare, J.M., and Condon, W.H., 1971(b), Geologic map of the Marshall Quadrangle, western Alaska; USGS Misc. Geol. Invest. Map I-668.

Hoare, J.M., and Coorad, W.L., 1959, Geology of the Bethel Quadrangle, Alaska; USGS Misc. Geol. Invest. Map I-285.

Hoare, J.M., and Coonrad, W.L., 1959, Geology of the Russian Mission Quadrangle, Alaska; USGS Misc. Geol. Invest. Map I-292.

Knebel, H.J., and Creager, J.S., 1973, Yukon River: evidence for extensive migration during the Holocene Transgression; Science, vol. 79, pp. 1230-1231.

Lisitzin, A.P., 1972, Sedimentation in the world ocean; Soc. Economic Paleontologists and Mineralogists Spec. Pub. No. 17, 218 p.

MacKay, J.R., 1971, The origin of massive icy beds in permafrost, western Arctic coast, Canada: Canadian Jour. EArth Sci., vol. 8, no. 4, pp. 397-422.

Marlow, M.S. and others, 1976, Structure and evolution of Bering Sea shelf south of St. Lawrence Island: Amer. Assoc. Pet. Geologist, vol. 60, pp. 161-183.

Matthews, M.D., 1973, Flocculation as exemplified in the turbidity maximum of Acharon Channel, Yukon River delta, Alaska; Unpublished Ph.D., dissertation, Northwestern Univ., 88 p.

McManus, D.A., Venkatarathnam, K., Hopkins, D.M., and Nelson, C.H., 1974, Yukon River sediment on the northernmost Bering Sea shelf; Journal of Sed. Petrology, vol. 44, pp. 1052-1060.

McManus, D.A., and others, 1977, Distribution of bottom sediments on the continental shelf, northern Bering Sea: U.S. Geol. Survey Prof. Paper, 759-C, 31 p.

Moore, D.G., 1964, Acoustic reflection reconnaissance of continental shelves: eastern Bering and Chukchi Seas; in Moore, R.L. (ed.) Papers in marine geology, MacMillan Co., N.Y., pp. 319-362.

Muench, R.D. and Ahlnas, K., 1976, Ice movement and distribution in the Bering Sea from March to June, 1974: Jour. Geophys. Research, vol. 81, no. 24, pp. 4467-4476.

Nelson, C.H., 1978, Faulting, sediment instability, erosion, and depositional hazards of the Norton Basin sea floor, in Annual Reports of Principal investigators for year ending March 1978, NOAA-OCSEAP.

Nelson, C.H., and Creager, J.S., 1977, Displacement of Yukon-derived sediment from Bering Sea to Chukchi Sea during Holocene time: Geology, vol. 5, pp. 141-146.

Nelson, C.H., Hopkins, D.M., and Scholl, D.W., 1974, Cenozoic sedimentary and tectonic history of the Bering Sea; in Hood, D.W., and Kelley, E.J. (ed.), Oceanography of the Bering Sea; Inst. Marine Sci., Univ. of Alaska, Fairbanks.

Patton, W.W. Jr. and Hoare, J.M., 1968, The Kaltag fault, west-central Alaska, U.S. Geol. Survey PM Paper 600-D, pp. D147-D153.

Patton, W.W. Jr., 1973, Reconnaissance geology of the northern Yukon-Koyukuk Province, Alaska; U.S. Ge-l. Survey Prof. Paper 774-A, 17 p.

Péwé, T.L., 1948, Terraine and permafrost of the Galena Air Base, Galena, Alaska; U.S. Geol. Survey Permafrost Program Program Rept. 7, 52 p.

Péwé, T.L., 1975, Quaternary geology of Alaska: U.S. Geol. Survey Prof. Paper 835, 145 p.

Reed, J.C., and Sater, (ed.), 1974, The coast and shelf of the Beaufort Sea; Arctic Institute of North America, 750 p.

Reimnitz, E., and Barnes, P., 1974, Sea ice as a geologic agent on the Beaufort Sea; in Reed and Sater (ed.), The coast and shelf of the Beaufort Sea; Arctic Institute of North America.

Reimnitz, E., and Bruder, K.F., 1972, River discharge into an ice-covered ocean and related sediment dispersal, Beaufort Sea, coast of Alaska; Geol. Soc. Amer. Bull, vol. 83, pp. 861-866.

Reimnitz, E., Toimil, L.J., and Barnes, P.W., 1977, Stamukhi zone processes: implications for developing the Arctic coast: in Proceedings of the Offshore Technology Conference, May 2-5, 1977, OTC 2945, pp. 513-518.

Scholl, D.W., Buffington, E.C., and Hopkins, D.M., 1968, Geologic history of the continental margin of North America in the Bering Sea; Marine Geology, vol. 6, pp. 297-330.

Scholl, D.W., and Hopkins, D.M., 1969, Newly discovered Cenozoic basins, Bering Sea shelf, Alaska; Amer. Assoc. Pet. Geol. Bull., vol. 53, pp. 2067-2078.

Shapiro, L.H., and Burns, J.J., 1975, Satellite observations of sea ice movement in the Bering Strait Regions, in Weller, and Bowling, S.A. (ed.), Climate of the Arctic; Geophysical Institute, Univ. of Alaska, Fairbanks, pp. 379-386.

Shepard, F.P., and Wankss, H.R., 1971, Our changing coastlines: McGraw Hill, New York, 579 p.

Smith, M.W., 1976, Permafrost in the Mackenzie delta, Northwest Territories: Geological Survey of Canada, Paper 75-28, 34 p.

Walker, H.J., 1973, The nature of the seawater-freshwater interface during breakup in the Colville River delta, Alaska: in Permafrost: the North American contribution to the Second International Conference; Nat'l Acad. Sci., pp. 473-476.

Williams, J.R., 1970, Groundwater in the permafrost regions of Alaska: U.S. Geol. Survey Prof. Paper 696, 83 p.

Wright, L.D., and Coleman, J.M., 1973, Variations in morphology of major river deltas as functions of ocean wave and river discharge regimes: Am. Assoc. Petroleum Geologists Bull., v. 57, pp. 370-398.

APPENDIX A

Dupre', W.R. and R. Thompson (1979). "The Yukon Delta: A Model for Deltaic Sedimentation in an Ice-Domicated Environment," Proceedings of the 11th Annual Offshore Technology Conference in Houston, Texas, April 30 - May 3, 1979. 9 pp.

Verna M. Ray and William R. Dupré

INTRODUCTION

General background and purpose

Three regimen have been proposed by Dupré (1978), in defining the Yukon Delta coastal processes, one of which is the ice-dominated regimen (fig. B1). This paper is intended to describe in more detail the processes which characterize the ice-dominated regimen. This regimen is in turn divisible into three phases: freezeup, winter, and breakup (fig. B2). Because the federal government is in the process of evaluating the Norton Sound-Yukon Delta area for potential oil and gas exploration lease tracts, the nature of ice-related hazards are important considerations. In this study data from 1973 to 1977 Landsat and NOAA imagery wereused to observe the extent of shorefast ice, the patterns and velocity of pack ice movement, and how weather conditions effect these phenomena throughout the ice-dominated regimen. The months of interest were October through June, however the satellite cameras are not in operation from late-November through January, due to the Arctic Night.

Geographic setting

The study area includes the Norton Sound of northeastern Alaska, the offshore area to the west of the sound to St. Lawrence Island, and the area south to Nunivak Island. Norton Sound is an east-west trending arm of the Bering Sea. The embayment is bounded on the north by the Seward Peninsula and on the south by the Yukon River Delta.

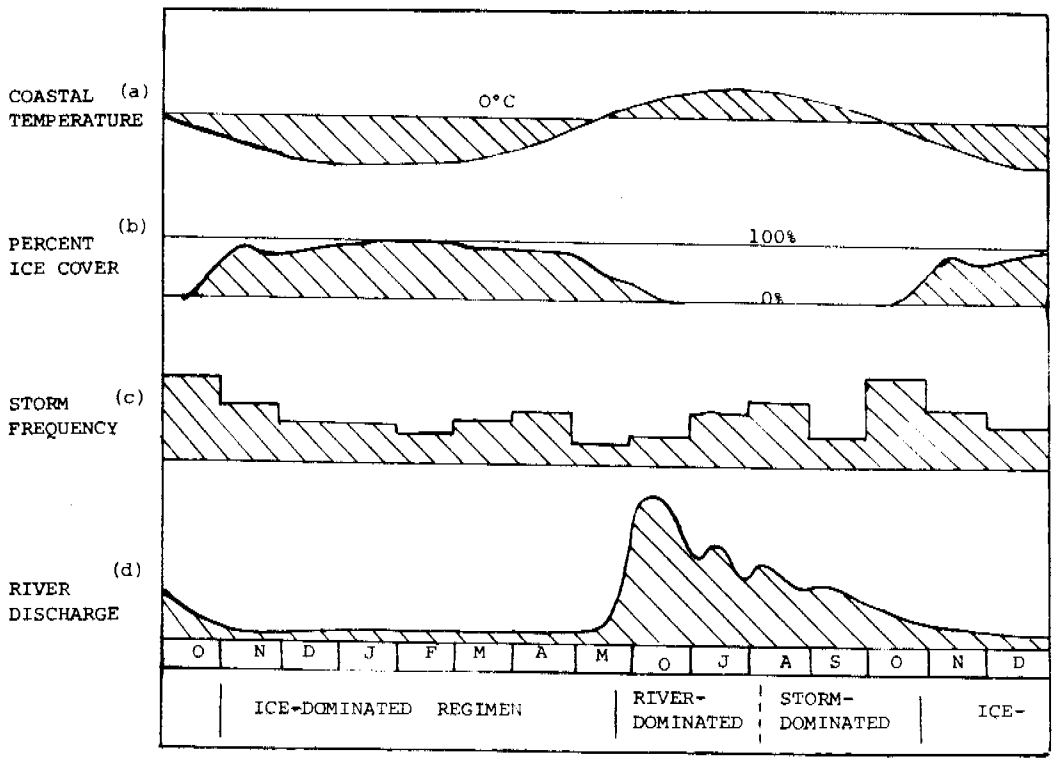

Figure B1.: Diagram illustrating the seasonality of processes in the Yukon Delta - Norton Sound region of the Bering Sea. Sources of data include: (a) Summary of average monthly temperatures at Unalakleet, 1941-1970, (NOAA); (b) Summary of ice observations for Yukon Delta region from Brower et al. (1977); (c) Frequency of major low pressure centers in the northern Bering Sea region, from Brower et al. (1977); and (d) Discharge of the Yukon River at Kaltag, 1962 (U.S.G.S. Water Resources Data).

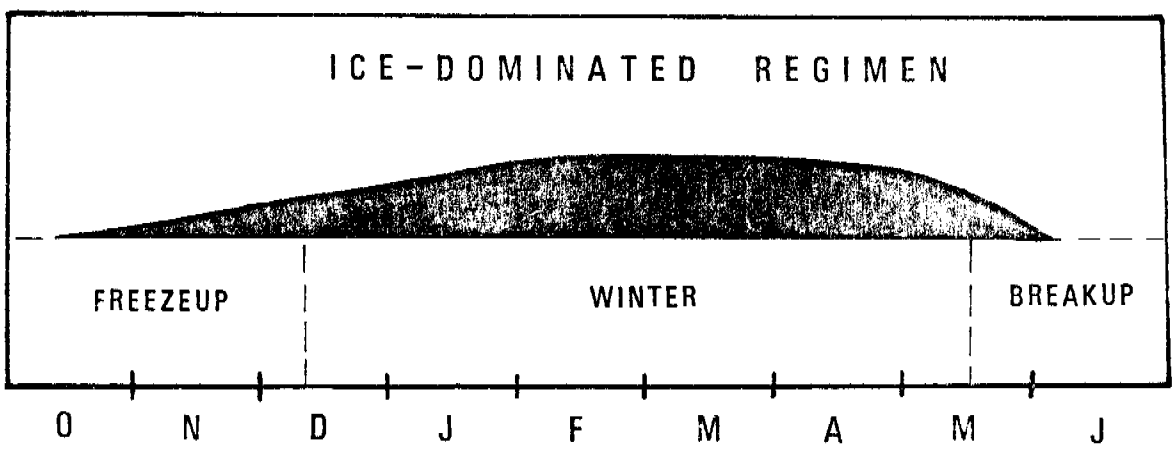

Figure B2.: Three phases of the ice-dominated regimen.

Most of Norton Sound is shallower than 20m, and the surrounding offshore area of interest is less than 40m deep.

Previous work

Norton Sound basin is a potential site for offshore oil and gas exploration. The accompanying construction of offshore facilities requires knowledge of ice-related hazards. Extensive previous research has been concentrated on ice dynamics in Arctic regions such as the Beaufort Sea. Among others studying ice-related problems in the Arctic, Erk Reimnitz and Peter Barnes have compiled a significant amount of data concerning sea ice as a geologic agent on the Beaufort Sea Shelf of Alaska (Reimnitz and Barnes, 1974). However, very limited research has been done in subarctic regions such as the Bering Sea and Norton Sound. Devin Thor, Hans Nelson, and others (1977, 1978) are presently engaged in an extensive sonographic study of ice gouge in the Norton Sound region. They are dealing with the actual measurement of ice gouges, and the frequency with which they occur in different areas. This study looks more closely at the patterns and intensity of ice movement that might be responsible for this sediment deformation.

Patterns of ice movement in the northern Bering Sea have been defined by Muench and Ahlnas (1974) for a 3 month period in 1974, using NOAA imagery. Because Landsat data offers better resolution for observing ice floe movement, this study provides a more detailed analysis of ice movement over a 4-year period.

Shapiro and Burns (1975) used Landsat for March 1973, to observe a short-term ice deformation event north of the Bering Strait. A similar

1976 event of massive ice fracture in the Chukchi Sea and rapid advection through the Bering Strait is documented in this study, which further extends the effects of ice deformation into the Bering Sea.

Stringer (1977), has mapped a variety of ice-related features in the Beaufort, Chukchi, and Bering Seas using Landsat imagery. His maps of the Bering Sea show the distribution of the edge of "contiguous ice" as well as the patterns of ice morphology. These maps, in combination with the interpretation of Landsat imagery of the Yukon Delta region by Dupré (1977, 1978), provide the only existing detailed data on ice conditions in the study area. This study is designed to expand on these works, as well as provide data on rates of ice movement.

Methods of study

The data used in this study were compiled from the photographic products of imagery acquired by the Multispectral Scanner system of the Landsat and NOAA-2, 3, 4 satellites. Meteorologic data also were taken from daily surface synoptic charts from the National Climatic Center in North Carolina. The extent of shorefast ice and ice floes was mapped from Landsat images to acetate overlays, which could be superimposed on standard bathymetric base maps of the same scale, 1:1,000,000, of the northern Bering Sea. Overlays for successive days could be superimposed to chart the movement of particular ice floes over an approximate 24-hour period. Ice vectors as seen in Figure B9 for example, represent the magnitude and direction of displacement of pack ice floes from 14 March to 15 March. Images had to be registered with respect to landforms in order to map the positions of the ice floes on successive days. In general, sea

ice movement cannot be accurately monitored by referencing the scenes to coordinates, as coordinates provided on the margin of Landsat images allow for only approximate registeration (Colvocoresses and McEwen, 1973).

The Landsat images were band 5 and 7, 9x9-inch positive prints. The images and the base map appeared to be perfect overlays. The band-5 images proved to be most useful in defining nilas ice. These areas of very new ice appeared as dark, open-water areas on band 7 (infrared) images. However, for defining the sea-ice boundary in distinguishing pack-ice floes and shorefast-ice areas, the band 7 images were much more useful. There is no distinction made between newly formed ice and open water on most maps in this paper, because of the difficulty in distinguishing the two. According to Colvocoresses and McEwen (1973), the systematic, root mean square error of position for points on the satellite images ranges from 200-450 meters, with no detectable additional error associated with image duplication. The sea ice is moving on the order of kilometers per day, hence this error should be considered as insignificant for the purposes of this paper.

The NOAA 10x10-inch satellite photoprints (infrared) furnished only general meteorological information. However, they did provide a good overview of ice movement, although they were not used for detailed rate evaluation. Wind patterns and weather systems could be observed from NOAA, but wind velocity and directional information was obtained from daily surface synoptic charts. Some weather station readings are influenced by local orographic conditions, but in general, most of the information is believed to be useful for the purposes of this study.

FREEZEUP

Ice crystals typically begin to form and accumulate as new ice along the shore of Norton Sound in late October, as coastal temperatures drop below 0°C (Fig. 1). Bottomfast ice forms along the shallow margins of the delta (e.g. on intertidal mudflats and subaqueous levees). Some of the smaller sub-ice channels begin to be covered by floating fast ice as well. The larger sub-ice channels offshore from the main distributaries continue to maintain a channelized flor of freshwater offshore, hence are the last of the nearshore areas to freeze.

The shorefast ice continues to expand farther offshore in November, until it reaches its maximum width of from 15 to 30 km. Most of the shorefast ice is floating fast ice (Fig. B3), separated from the bottomfast ice by active tidal cracks which coincide approximately with the 1 m isobath. The seaward expansion of the shorefast ice continues until it encounters mobile, seasonal pack ice, at which time pressure ridges develop and become grounded and a seaward accreting stamukhi zone develops. This generally occurs by the beginning of December, and for the purpose of this report, marks the beginning of the winter period.

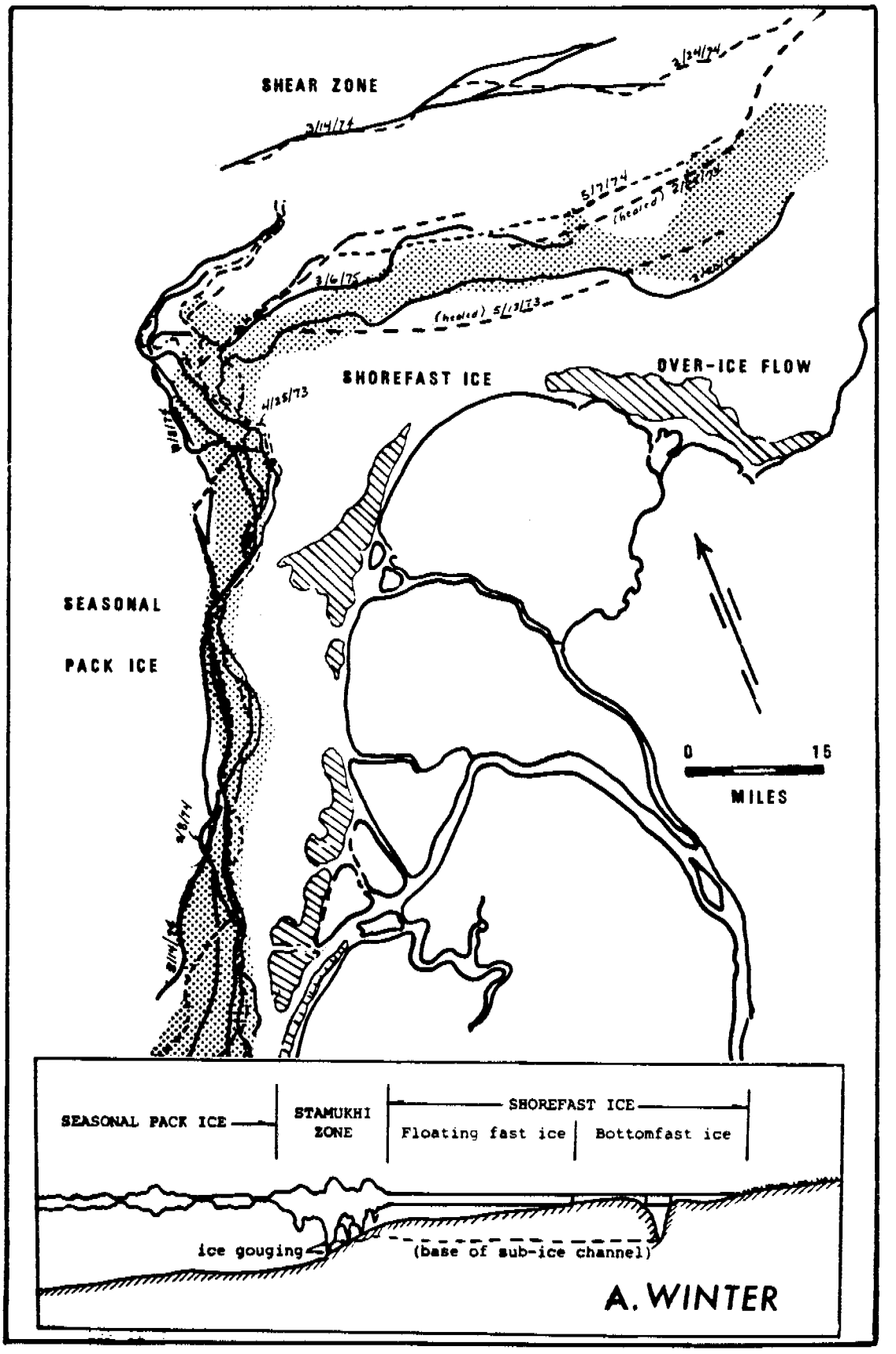

Figure B3

Location of shear zones as determined from LANDSAT imagery, 3/13/73 - 3/6/75. Hatching delineates aufeis. Dots delineate the 5 - 10 m bathymetric interval.

WINTER

The winter phase of the ice-dominated regimen is characterized by shorefast ice zones which extend up to 40 km offshore along the Yukon Delta (fig.B3). This broad zone of ice buildup is an area of fast ice compaction under the impact of converging pack ice, much or all of which originated in northeastern Norton Sound. Landsat for 23-27 February 1976 illustrates these zones of divergence and convergence as seen in Figure B4. As ice is pushed out of the Norton Bay region of the sound by geostropic winds and the water current gyre, nilas (i.e. new ice) forms a blanket over the newly opened body of water. Although ice is moving slowly to the east in Norton Sound on February 25th through 27th, it does not appear to have originated outside the sound. This pack ice has probably temporarily changed direction due to a wind shift, opening an area of water just to the west of Nome, separating in situ ice formed in Norton Sound from Bering Sea ice.

Shorefast ice is cleaved from the northern shore and pushed south to converge on the Yukon delta front. This ice pile-up creates areas of pressure ridging along the shear zone, as seen in Figure B4. Ice pile-up and associated deformation can be observed in Landsat all the way through the winter phase. These areas are sites of ice gouging, as observed by Thor and others (1978) in their data collected by side-scan sonographs. This pressure ridging produces numerous parallel furrows in the sediments (Reimnitz and Barnes, 1974).

During this season the winds are predominantly from the north, however, between 25 and 26 February 1976, winds suddenly shifted toward

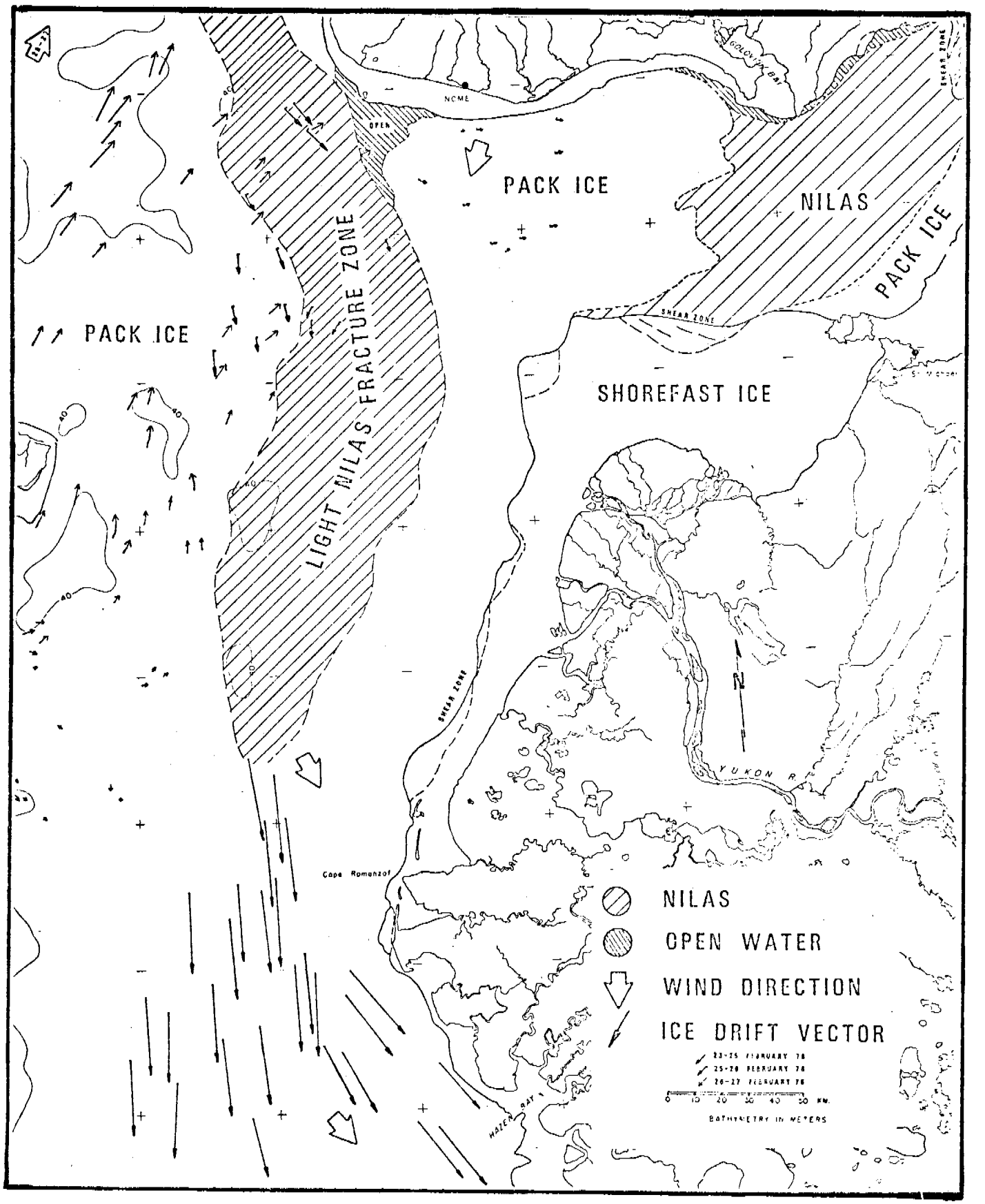

Figure B4. Patterns of ice movement from 23-27 February 1976. Length of ice drift vectors measures distance ice moved in one day. Dashed lines within the shorefast ice zone to the west of the delta are inactive shear zones. The configuration of shear lines to the north of the delta indicates stamukhi.

the north, reaching velocities up to 25 knots through the Bering Strait, according to the U.S. Surface Synoptic charts for 27 February 1976. This abrupt change apparently reversed the movement of floes from St. Lawrence Island to the Bering Strait (fig.B4). Meteorologic data shows that for 23-25 February, the counterclockwise winds of a low pressure system (a) centered over the Gulf of Alaska were responsible for pushing the floes southward in the Bering Sea (figs.B5 and B6). A second low pressure system (b) was developing to the east with a center over eastern China and accompanying winds up to 35 knots. A high pressure system was developing between these two zones of low pressure (fig.B7) with a center of high pressure over central Siberia. As low pressure system "a" moved eastward, the high pressure system was centered directly over the Bering Sea on 26 February 1976 (fig. B4). Anticyclonic winds generated within this high pressure center began to push ice northward in the northern Bering Sea (fig. B4). As a result, the floe velocities recorded in Figure B4 for February 26th to 27th are as much as 15 km per day toward the Bering Strait. Such a phenomena is significant in that it illustrates the dynamic influence of meteorologic patterns on ice movement, and thus on potential ice gouge and associated hazards which could impair petroleum exploration.

Landsat for the month of February (1973-1976), is interesting in several other respects. Pack ice shears down the western coast of the Black chenier plain and Cape Romanzof, along the 10-m isobath. The "Light Nilas Fracture Zone" in Figure B4, seems to be indigenous to this season. This appears to be an area of rapid ice floe movement where ice opens frequently, and the lead is closed by new ice. The new ice

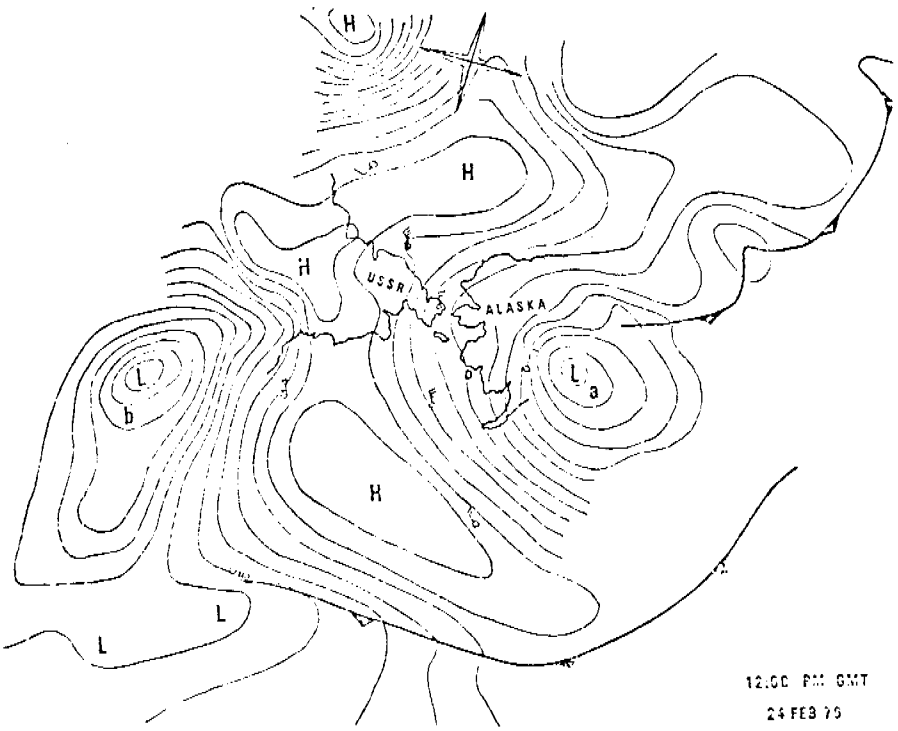

Figure B5: From surface synoptic chart.

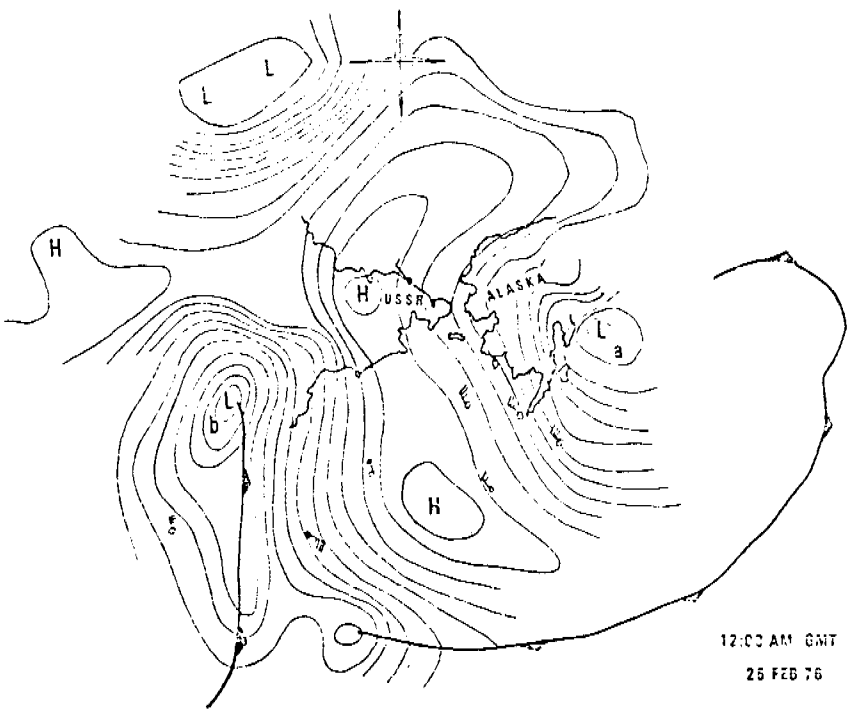

Figure B6: From Surface synoptic chart.

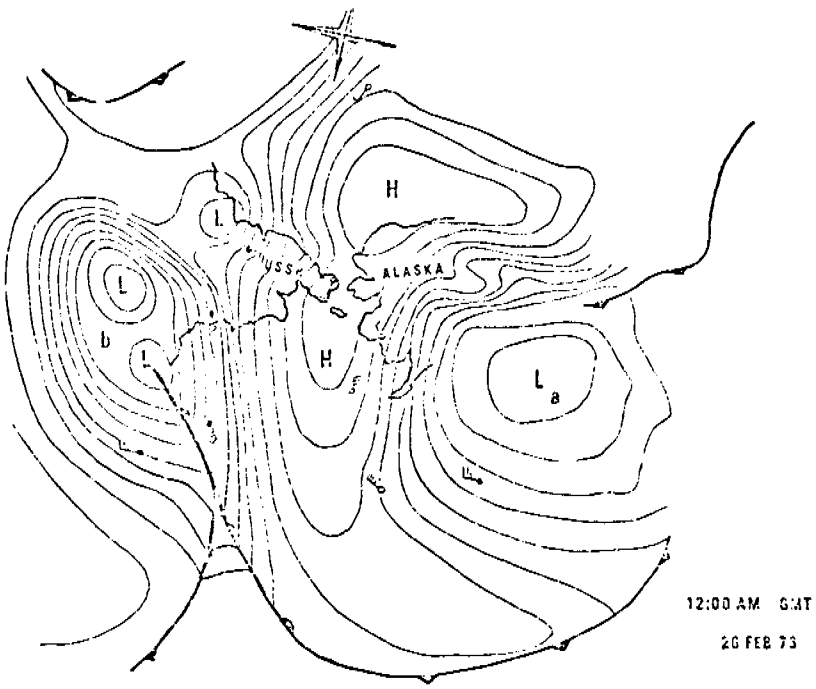

Figure B7: From surface synoptic chart.

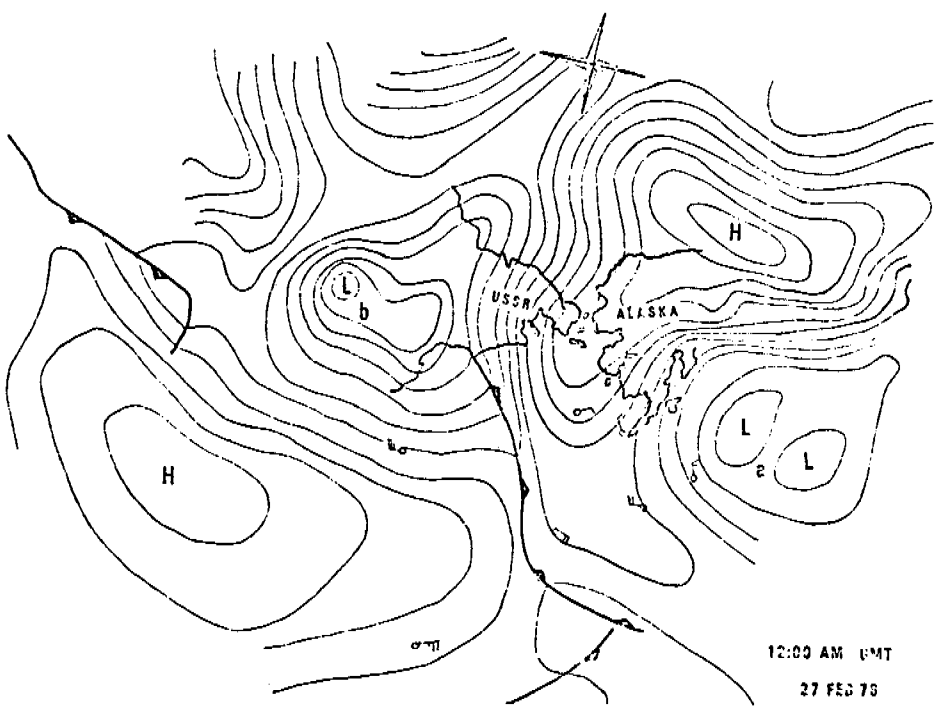

Figure B8: From surface synoptic chart.

is highly fractured. Fractures trend approximately 20°-30° NNW. One possible explanation for this "racetrack" zone might be that pack ice from the northern Bering Sea is pushed southward by strong northerly winds along this path, shoving aside slower, consolidated pack ice occupying the area. Alternatively, it may simply represent flow in water depths too great to allow grounding of the pack ice. NOAA and Landsat imagery for February 1974, show this highly fractured nilas area, originating in the Northern Bering Sea, and following the same path down the coast as seen in 1976 data. It is noted that the path bordering Norton Sound follows on its eastern margin. The geometry of ice pile-up around St. Lawrence Island tends to direct rapid ice movement from the west. St. Lawrence Island acts like a splitter placed beneath a funnel to obstruct or deflect the path of material passing through. Thus the bathymetry of Norton Sound and St. Lawrence Island appear to control the location of the "racetrack".

During the month of March, pack ice tends to pile up at the Bering Strait constriction as it moves south in response to strong northerly winds. This pile-up creates a fracture pattern in the Chukchi Sea resembling the geometry set up by funneling a semi-viscous material. Such an event has been studied and documented by Shapiro and Burns (1975) with Landsat imagery. The rapid movement of ice floes to the southwest of Seward Peninsula is recorded from LANDSAT Figure B9 and is believed to be attributed to ice deformation in the Chukchi Sea.

NOAA (VHRR) data for 13-15 March 1976 shows such a deformation event in the Chukchi Sea, with the ice being "funneled" through the Bering Sea and down the western Alaskan coast. During this event, ice floes were recorded to

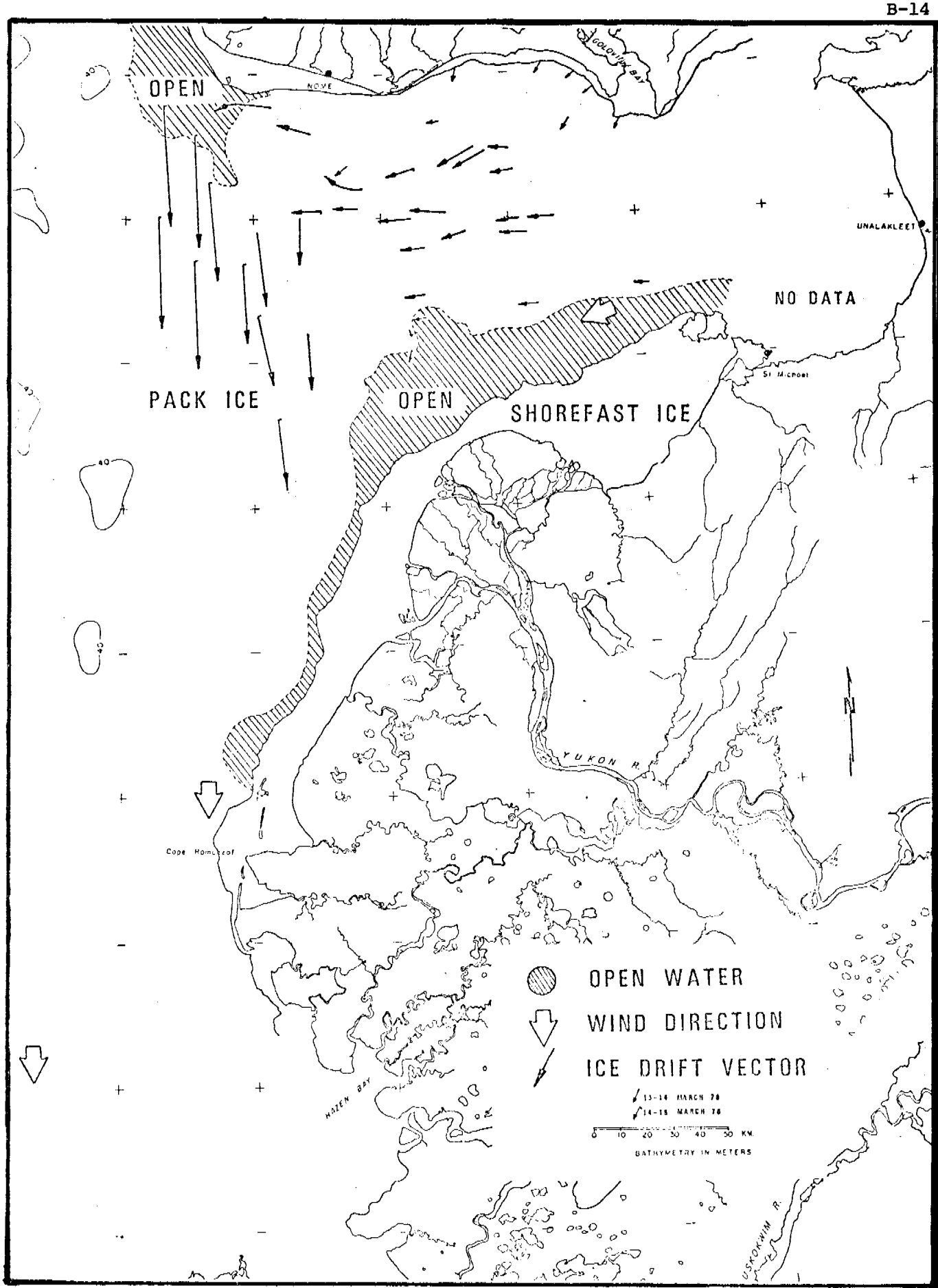

Figure B9: Patterns of ice movement from 13-15 March 1976. Length of ice drift vectors measure distance moved in one day.

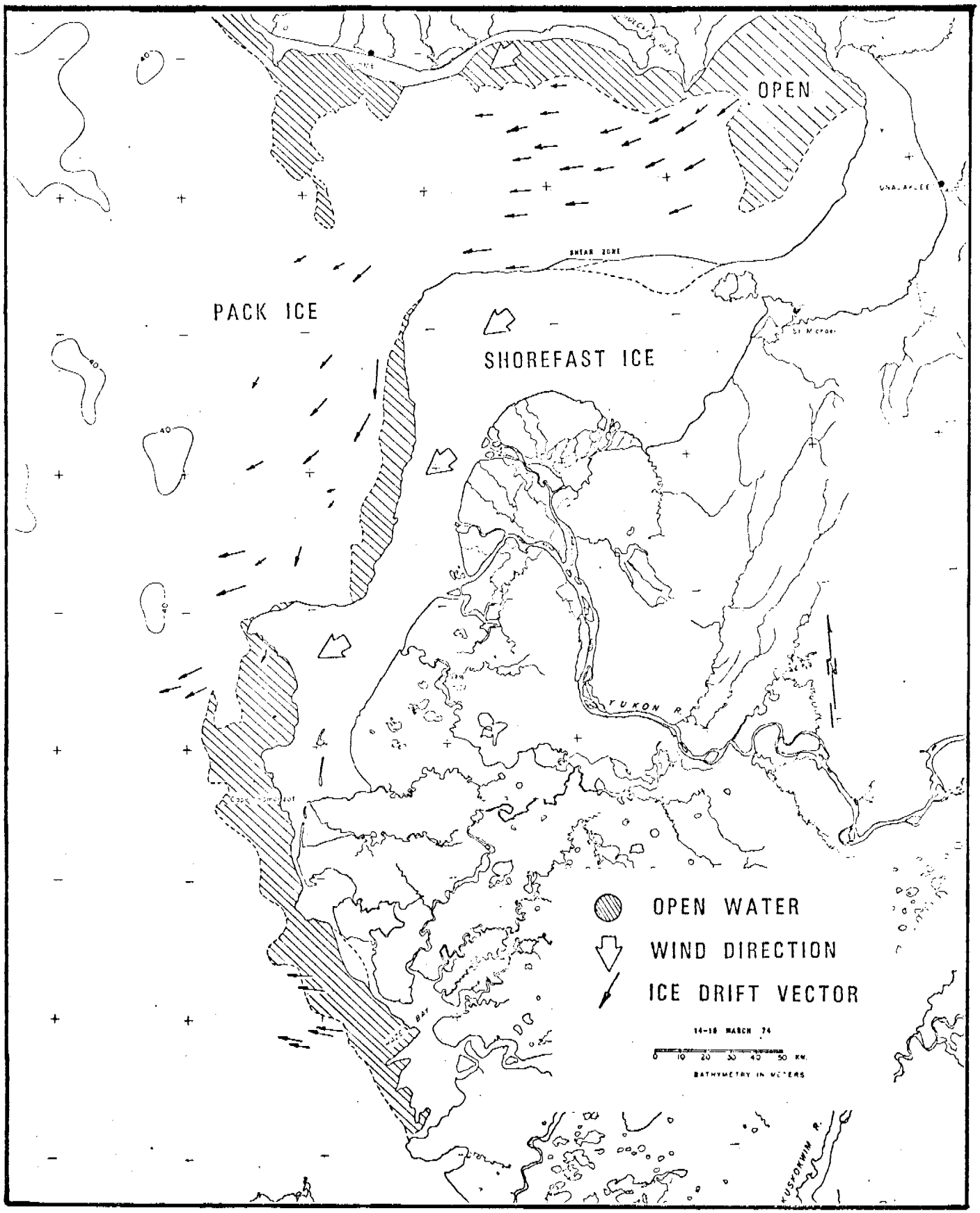

Figure B10:Patterns of ice movement from 14-16 March 1974. Length of ice drift vectors measures distance moved in one day.

move as much as 45 km per day. Even with this rapid migration of ice from the Bering Sea region, no ice was observed to be moving into Norton Sound. Shoals partially block the entrance to the Sound, and may be in part responsible for keeping pack ice out. Floes within the sound consistently moved westward, out of the embayment (fig. B9).

Shapiro and Burns (1975) concluded that a relatively stationary high pressure system centered over northwestern Siberia was responsible for the strong northerly winds, which pushed masses of pack ice out of the Chukchi Sea in March 1973. The event recorded in Figure B9 occurred under similar meteorologic conditions. Again, a stationary high pressure system was centered over northeastern Siberia, with persistent northerly winds up to 20 knots over the Chukchi Sea, and down the western Alaskan coast. The presence of a low pressure system to the east was responsible for the more westward oriented winds, which blew across Norton Sound.

In Figure B10 no episode of rapid southward displacement of sea ice through the Bering Strait seems to dominate ice movement. For this period in March 1974, ice is diverging from the northeastern Norton Sound and converging along a shearing, ridging zone along the northern Yukon Delta. The northeasterly winds, which "herd" ice along these patterns throughout much of the winter phase, also cause ice divergence along the western side of the Yukon Delta.

The data for April, 1973 (fig. B11) illustrates a very different

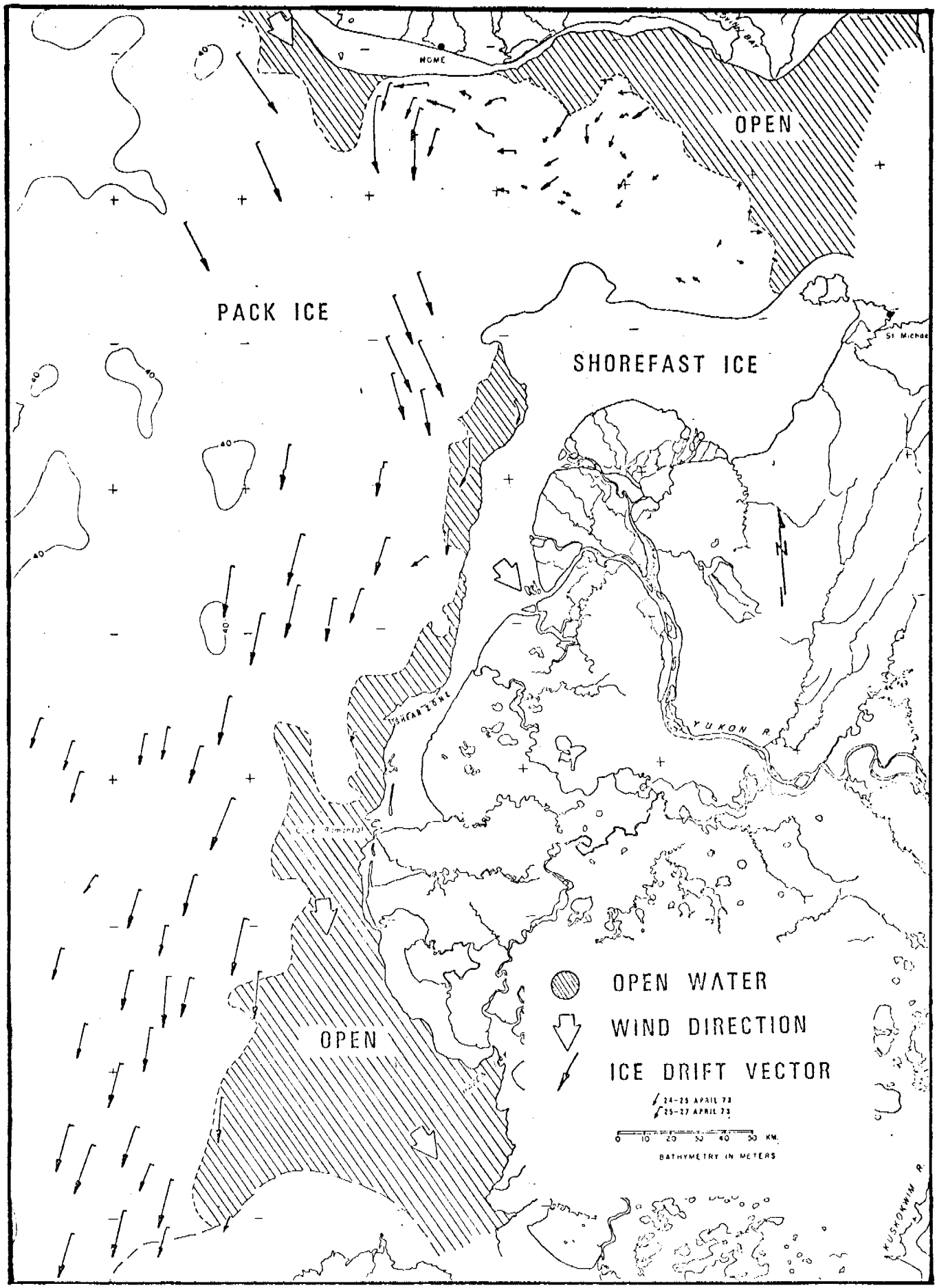

Figure B11:Patterns of ice movement from 25-27 April 1973. Length of ice drift vectors measures distance moved in one day.

pattern in this area. Northwesterly winds are again attributed to a high pressure system over the Chukchi Sea 26-27 April 1973. They are bringing pack ice from the Bering Sea down the western coast, which at this time is an area of ice convergence, although there is some deflection of ice, presumably due to bathymetric ridges. Such ridges also may be creating an area of stationary, grounded ice floes about 40 km north of Cape Romanoff, as seen in Figure B12.

Areas of grounded ice are sites of potential ice gouging, (Reimnitz and Barnes, 1974). According to a sonographic study by Thor and others (1978), ice gouging "is related to: 1) water depth and geomorphology, and 2) location of shear zone and oceanographic conditions." (p. E-4). In April, 1973 (fig.B11) a shear zone is located in the approximate area of the April, 1976 grounded floes (fig.B12).

Ice in Norton Sound is of a different origin, and follows different patterns of movement than ice farther to the west. In Figures B11 and B12 in situ ice in Norton Sound is observed to be moving slowly in somewhat of a counterclockwise gyre. This motion suggests that some of the ice within the shelter of this embayment is responding to water currents. Because the nature of ice within the sound differs from ice without, the geologic hazards differ from those along the west coast of the Yukon Delta. In particular, the intensity and density of gouging should differ between the northern and western margins of the delta region.

Some ice floes from outside the sound appear to be caught up in the gyre and pulled into the sound in Figure B12. Short-lived events of

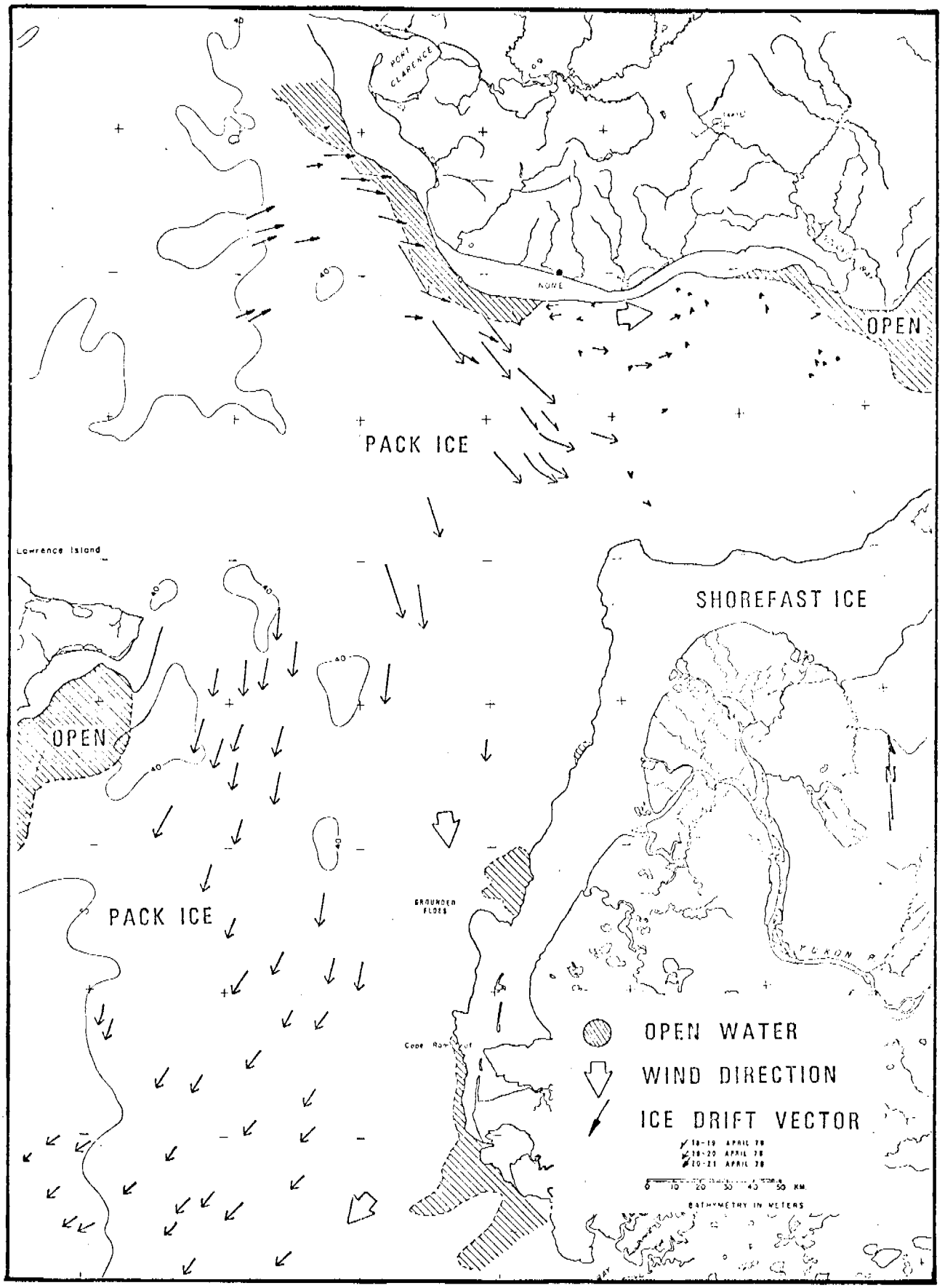

Figure B12 Patterns of ice movement from 18-21 April 1976. Length of drift vectors measures distance moved in one day.

ice movement into the sound seem to occur with undetermined frequency throughout the ice-dominated regimen. Meteorologic conditions apparently control these events. The April 1976 movement of ice into Norton Sound was probably triggered by a wind shift toward the east. Usually onshore winds from the northeast direct ice away from the sound during this time of the year.

BREAKUP

Breakup along the coast is a relatively brief event which marks the transition between the ice-dominated and river-dominated regimens, however its significance far outweighs its brevity.

River breakup along the Yukon (as with most of the coastal rivers in northern Alaska) occurs due to inland melting of river ice, hence it works its way downstream, preceeding the removal of the shorefast ice. It is marked by a tremendous increase in sediment and water discharge, resulting in ice jams, extensive inland flooding, and river bank erosion.

As river discharge begins to increase, floating fast ice begins to lift, both in the river and along the coast. The thalweg of the sub-ice channels are especially well delineated by the floating fast ice at this time. The bottomfast ice begins to be flooded by an over-ice flow (Fig. B13) which has been described on the North Slope by Reimnitz and Bruder, 1972; Walker, 1974.

Some sediment is carried onto the ice, thereby effectively bypassing much of the inner sub-ice platform. Much of the sediment appears to remain in the sub-ice channels, which cross the sub-ice platform. Some of the sediment is probably deposited from suspension on subaqueous levees farther offshore, however much of it probably bypasses the sub-ice platform completely, to be deposited on the delta front or prodelta. The role of sub-ice sediment transport during breakup is particularly intriguing, yet it remains almost unknown.

The floating ice that marks the sub-ice channels soon breaks up and is removed to sea. Much of the over-ice flow may drain through strudel holes (Reimnitz and Bruder, 1972) or cause the bottomfast ice to melt in place. Large pieces of floating fast ice break off to be transported farther offshore. Grounded ice may remain in some shallow areas to the northwest of the delta:

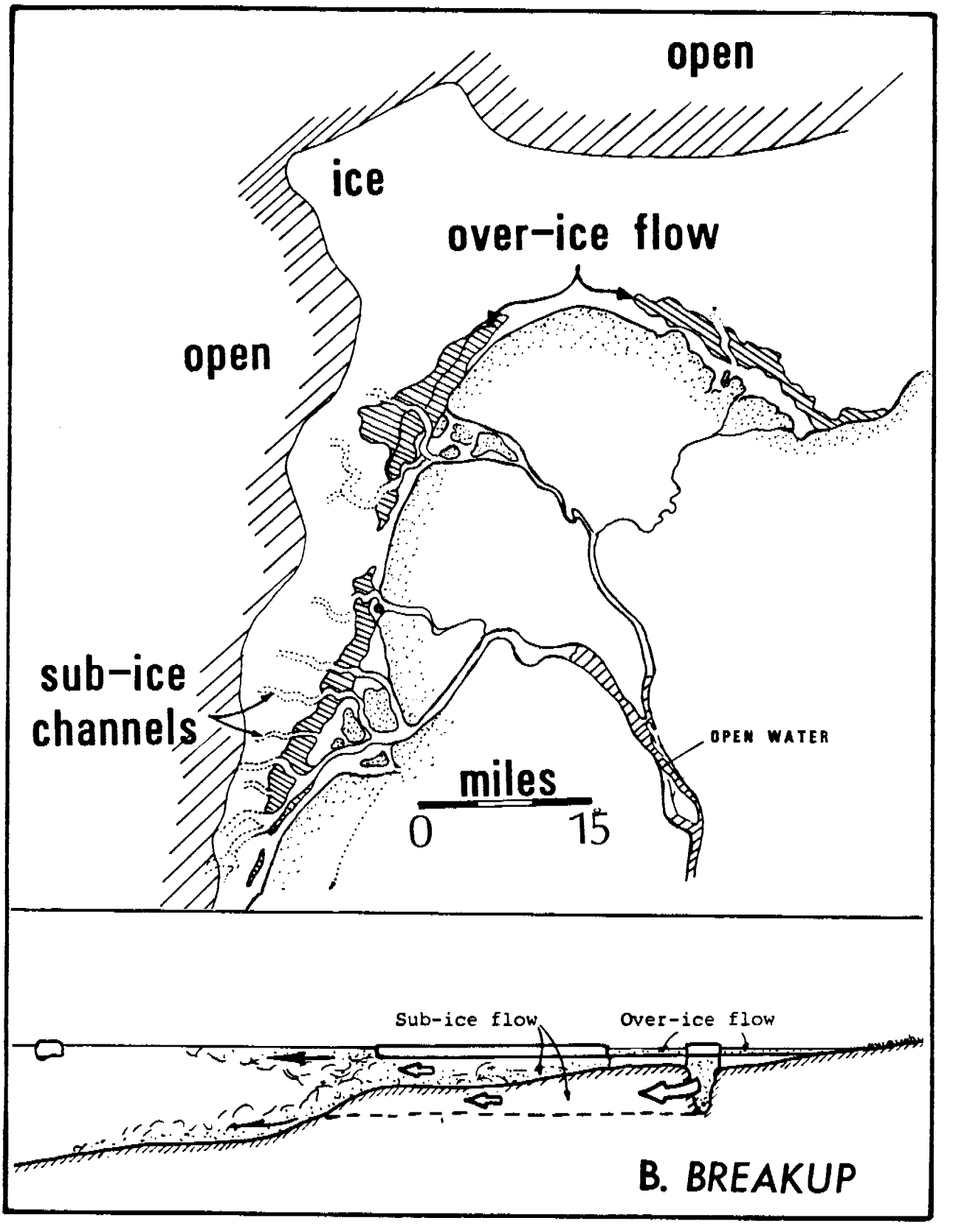

Figure B13

Diagram of over-ice flow and sub-ice channels, which provide two mechanisms for sediments to by-pass the sub-ice platform.

floating pack ice may remain trapped in the middle of Norton Sound because of the sluggish currents.

Figure B14 illustrates LANDSAT and weather data, which are typical of this season. Floe movement has changed to a northward direction, north and west of the Yukon Delta. Winds are 5 knots and less in the Bering Sea-Norton Sound area on 7 May 1974. The floes are moving as much as 20 km per day. A low pressure system moved into the area 8 May 1974, bringing a temporary restoration of "winter phase" northerlies. Muench and Ahlnas (1974) observed that after 14 May 1974, the reversal of motion from southerly to northerly through the Bering Strait was established with westerly drifting pack ice south of St. Lawrence. In contrast, during late May, 1976 (fig.B15) a stamukhi zone is still observed to the southwest of Stuart Island, due to ice convergence and shear along the Yukon prodelta. The winds are from the north due to a low pressure system working its way eastward across the Bering Sea. This low pressure system was followed by a high pressure system, bringing southerly winds, which tended to break up the ice.

By mid-June 1976 (fig.B16) no shorefast ice is recorded around the Yukon Delta. Only some isolated floes, which are grounded on shoals around Stuart Island, linger along the periphery of Norton Sound. Most of the area labeled "pack ice" is made up of unconsolidated, diminished pack-ice floes, many of which are fine enough to be aligned along water waves. The distributary channels of the Yukon Delta have been cleared of ice and are sending an apron of sediment-laden fresh water over the prodelta region. Although weak winds are moving some floes to the south in Figure , most floes are moving with the water currents. The "river-dominated regimen" (fig.B1) has begun.

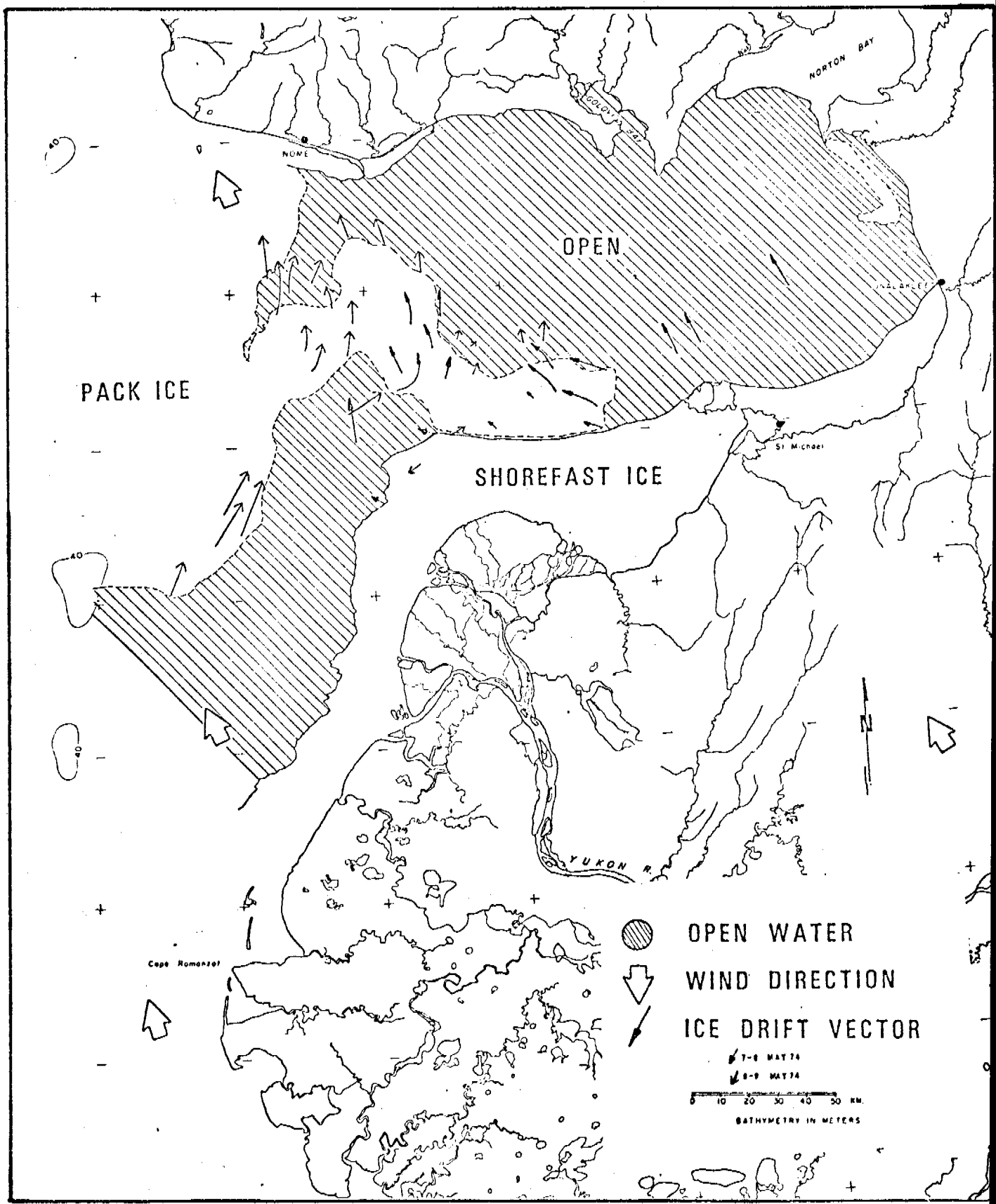

Figure B14: Patterns of ice movement from 7-9 May 1974. Length of ice drift vectors measures distance moved in one day. Pack ice is less consolidated than earlier in the year.

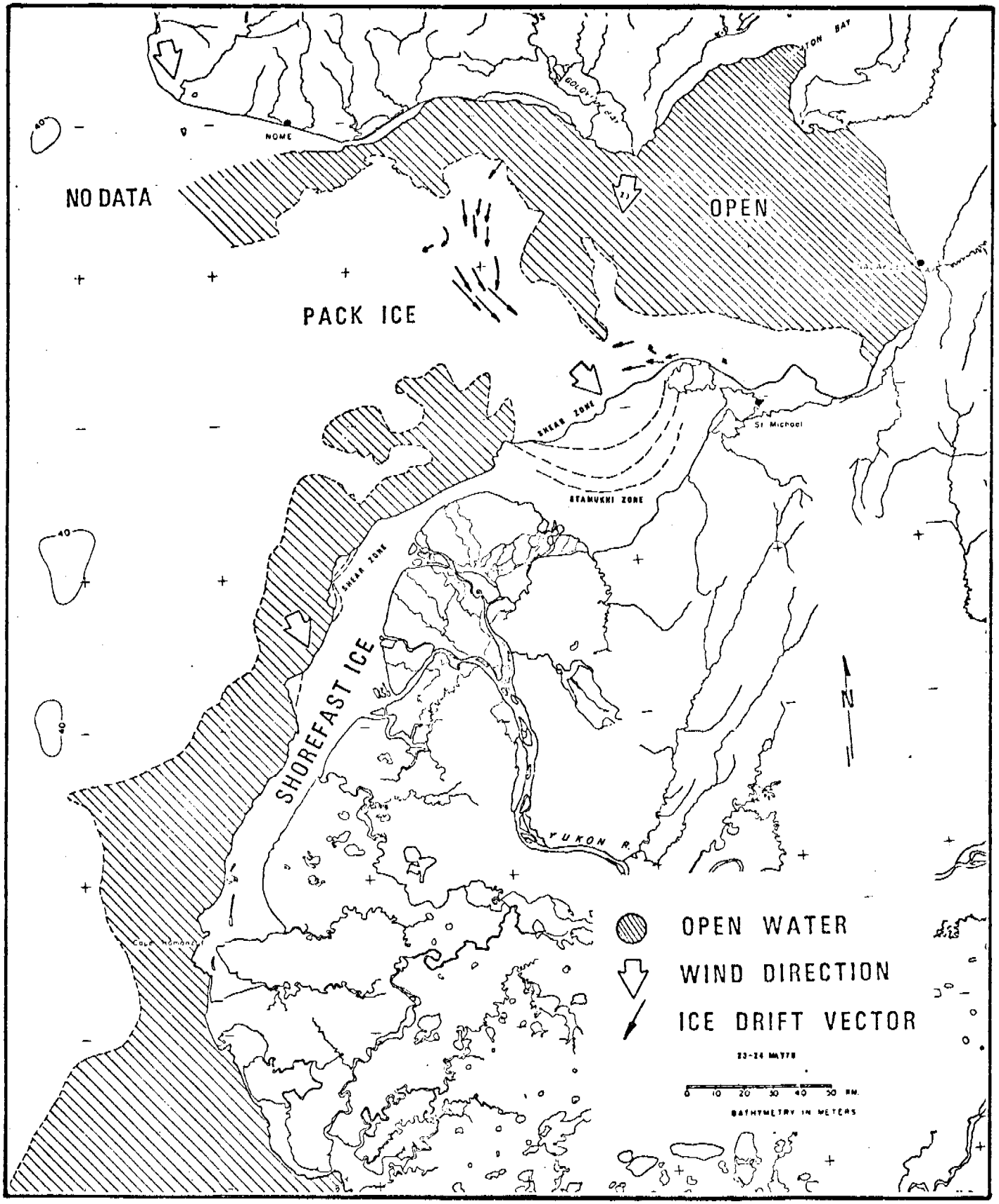

Figure B15: Patterns of ice movement from 23-24 May 1976. Length of ice drift vectors measures distance moved in one day.

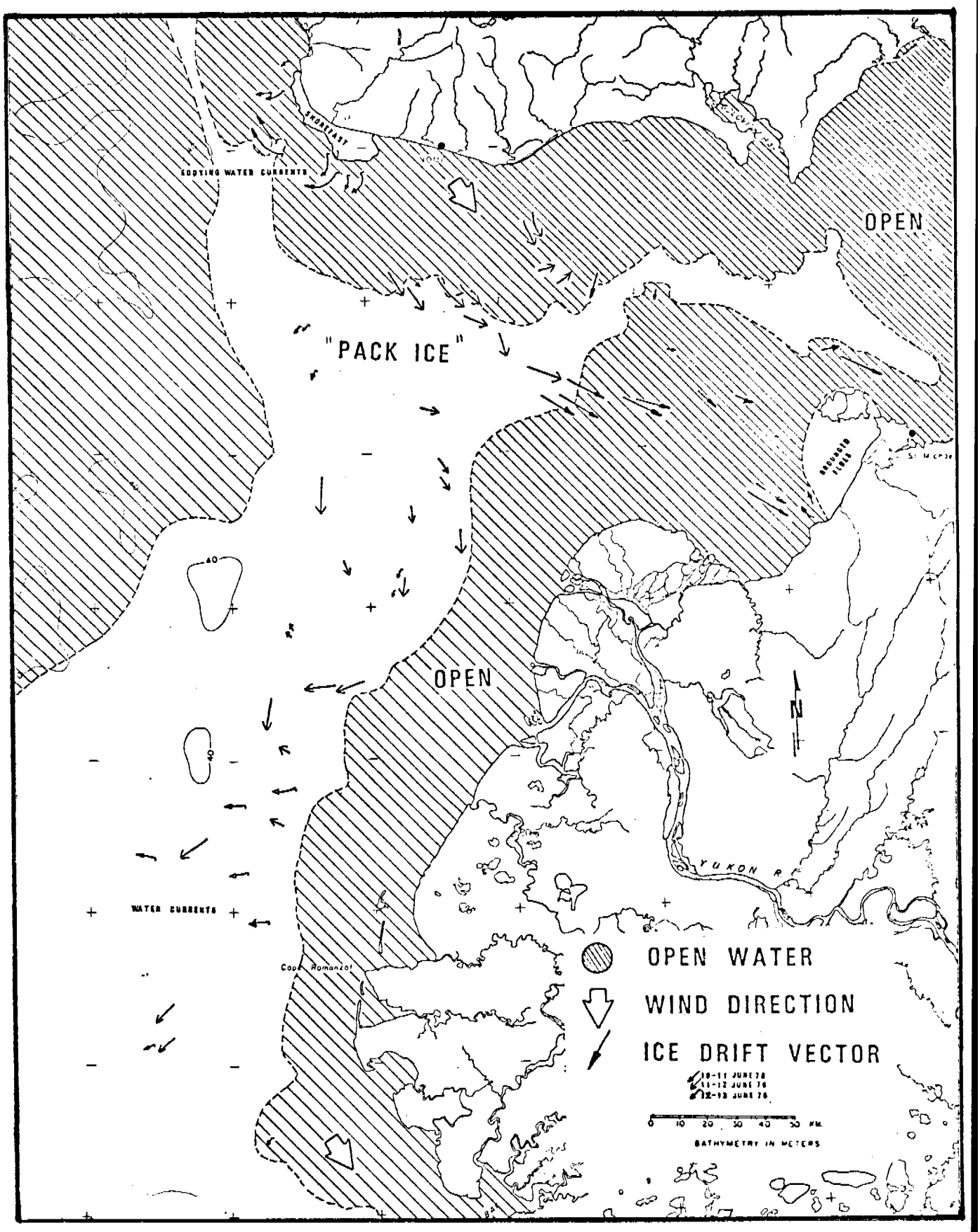

Figure B16:patterns of ice movement from 10-13 June 1976. Length of ice drift vectors measures distance moved in one day. The pack ice has become very diminished and totally unconsolidated.

DISCUSSION OF ICE GOUGING

Throughout the winter phase of the ice-dominated regimen, shorefast ice stretches to the 5 - 10 m isobath, and follows it around Norton Sound and down the western edge of the Yukon Prodelta. In situ ice approximately 0.7 - 1.2 meters thick (Brower and others, 1977) diverges from the Norton Bay area, compacting ice to form stamukhi and pressure ridge zones against the modern Yukon sub-delta. These zones become incorporated into the shorefast ice zone, stabilizing the fast-ice edge (Reimnitz and others, 1977). The impact and subsequent deformation of ice convergence can cause pressure ridge raking, producing numerous parallel furrows as the keels plow through the bottom sediments (Reimnitz and Barnes, 1974). Solitary, or single-keel ice gouge is also ubiquitous in Norton Sound (Thor and others, 1978).

Seasonal pack ice shears past the grounded, or fast ice along the 5 - 10 m isobath, which trends nearly north-south from Shpanberg Strait to Etolon Strait. Thick Bering Sea ice, or advected Chukchi Sea ice up to 12 m and 20 m thickness respectively (Thor and others, 1978) becomes caught up in this shear zone, as floes are propelled southward by Arctic northerlies, during the ice-dominated regimen. In the dynamic zone where moving sea ice collides with stationary fast ice, high energy is expended on the sea floor. The result is an area of intense gouge between the 10 m and 20 m isobaths. Thor and others (1978) observed this phenomena in the Norton Basin. A corresponding area of intense gouging between the 10 m and 20 m water depths was studied earlier by Reimnitz and others (1977) on the Beaufort Sea continental shelf.

The Yukon prodelta is the site of 85% of all ice gouges measured by Thor and others (1978), with 78% of the ice gouging in water 10 - 20 m deep. For the most part, the major gouge trends parallel isobaths, as would be expected based on the bathymetric contour of the stamukhi zone marking the interface between stationary and moving ice along this contour. None of the data collected by Thor and others (1978) were in water depths of less than 10 m, hence the potential for ice gouging in more shallow depths is uncertain. Nonetheless, the inner part of the stamukhi zones typically begin at 5 - 7 m water depths, hence some gouging would also be expected (Fig. B7) in this zone as well.

REFERENCES

Brower, W.A., Jr., and others, 1977, Climatic Atlas of the Outer Continental Shelf Waters - Coastal Region of Alaska: Vol. II - Bering Sea; Arctic Environmental Information and Data Center, Anchorage.

Colvocoresses, A.P., and McEwen, R.B., 1973, Progress in cartography, EROS program. Symposium on Significant Results Obtained from ERTS-1 NASA/GSFC, March 5-9, 1973.

Dupré, Wm. R., 1977, Yukon Delta coastal processes study, in Annual Reports of Principal Investigators for year ending March, 1977, NOAA-OCSEAP.

Dupré, Wm. R., 1978, Yukon Delta coastal processes study, in Annual Reports of Principal Investigators for year ending March 1978, NOAA-OCSEAP.

Kovacs, A. and Mellor, M., 1974, Sea ice morphology and ice as a geologic agent in the southern Beaufort Sea, in Reed and Sater (eds.), The coast and shelf of the Beaufort Sea; Arctic Institute of North America.

Muench, R.D. and Ahlnas, K., 1976, Ice movement and distribution in the Bering Sea from March to June, 1974: Jour. Geophys. Research, vol. 81, no. 24, pp. 4467-5576.

Reimnitz, E., and Barnes, P., 1974, Sea ice as a geologic agent on the Beaufort Sea; in Reed and Sater (eds.), The coast and shelf of of the Beaufort Sea; Arctic Institute of North America.

Reimnitz, E., and Bruder, K.F., 1972, River discharge into an ice-covered ocean and related sediment dispersal, Beaufort Sea, coast of Alaska; Geol. Soc. Amer. Bull., vol. 83, pp. 861-866.

Reimnitz, E., Toimil, L.J., and Barnes, P.W., 1977, Stamukhi zone processes: implications for developing the Arctic coast: in Proceedings of the Offshore Technology Conference, May 2-5, 1977, OTC 2945, p. 513-518.

Shapiro, L.H., and Burns, J.J., 1975, Satellite observations of sea ice movement in the Bering Strait Regions, in Weller, and Bowling, S.A. (eds.), Climate of the Arctic; Geophysical Institute, Univ. of Alaska, Fairbanks, pp. 379-386.

Shapiro, W.J., 1977, Morphology of Beaufort, Chukchi, and Bering Seas; Nearshore ice conditions by means of satellite and aerial remote sensing, in Environmental Assessment of the Alaskan Continental Shelf, Annual Report of Principal Investigators for year ending March, 1972, v. 15, p. 42-180.

Thor, D.R., Nelson, H., and Evans, J.E., 1977, Preliminary assessment of ice gouging in Norton Sound, Alaska, in Annual Reports of Principal Investigators for year ending March 1977, NOAA-OCSEAP.

Thor, D.R., Nelson, H., and Williams, R.O., 1978, Potential hazards of ice gouging over the Norton Sound Basin sea floor, in Annual Reports of Principal Investigators for year ending March 1978, NOAA-OCSEAP.

Walker, H.J., 1973, The nature of the seawater-freshwater interface during breakup in the Colville River delta, Alaska: in Permafrost: the North American contribution to the Second International Conference; Nat'l Acad. Sci., pp. 473-476.

Zubov, N.N., 1943, Arctic Sea Ice, Transl. by Naval Oceanographic Office and Am. Meteorological Soc. under contract to Air Force Cambridge Res. Ctr., Naval Electronics Lab., San Diego, Calif. (1945), 491 p.

APPENDIX C: SEASONAL VARIATIONS IN DELTAIC SEDIMENTATION ON A HIGH-LATITUDE, EPICONTINENTAL SHELF*

WILLIAM R. DUPRE'

Department of Geology, University of Houston, Houston, Texas 77004

The Yukon Delta provides approximately 90% of the sediment presently entering the northern Bering Sea. Much of that sediment is initially deposited in the subaqueous portion of the Yukon Delta, the morphology of which is significantly affected by the climatic extremes in this high-latitude, epicontinental shelf. The subaqueous profile of the delta differs from those of most previously described deltas in that the shoreline is separated from the prograding margin of the delta front and prodelta by a delta front platform which is typically 2-3 m. deep and extends up to 30 km offshore. The platform is crossed by a series of subaqueous channels which extend up to 20 km beyond the mouths of the major distributaries. The platform and associated offshore channels are in large part the result of the shorefast ice which fringes the delta for half of the year. Their presence suggests that the Yukon Delta may represent a type of ice-influenced delta, morophologically distinct from previously described wave-, river-, and tide-dominated deltas.

Ice is but one of the processes which combine to shape the delta and disperse its sediment, however. The depositional basin (Norton Sound) is relatively shallow (typically less than 20 m), thus much of the sediment initially deposited by deltaic processes is reworked by waves, tidal and storm-induced currents, and oceanic currents, as well as processes associated with ice. The relative importance of these processes systematically varies throughout the year; this seasonal variability can best be described in the context of an ice-dominated, river-dominated, and storm-dominated regimen.

The ice-dominated regimen begins with freezeup along the coast in late fall. The delta front platform is covered by shorefast ice which extends 10-30 km offshore to where it is terminated by a series of ice pressure and shear ridges (Stamukhi zone) formed by the interaction between fast ice and highly mobile, seasonal pack ice. Ice deformation in

* Abstract submitted to International Assoxiation of Sedimentologists - NORTHSEA '79 Symposium September 17-23, 1979, Texel, The Netherlands.

this zone results in extensive ice gouging along the outer edge of the delta front. It provides a mechanism for the resuspension of sediments which may be reworked by relatively weak, sub-ice currents such as those associated with tides and oceanic currents (e.g. Alaska Coastal Water).

River breakup typically occurs in early May, and marks the beginning of the river-dominated regimen. During breakup, much of the river sediment bypasses the inner part of the delta front platform by a combination of flow over the bottom-fast ice and sub-ice flow through channels which empty near the outer edge of the delta front. Once the shorefast ice is removed, sedimentation is dominated by normal deltaic processes influenced mainly by the high sediment discharge of the Yukon River. Wave attenuation across the delta front platform further reduces the nearshore wave energy, which when combined with the high sediment input results in relatively rapid progradation of the shoreline. Elsewhere sedimentation is dominated by the combined efforts of tides and the Alaska Coastal Water.

Increasingly frequent southwesterly winds, waves, and major storms in late summer and early fall characterize the storm-dominated regimen. High wave energy and decreasing sediment discharge from the Yukon River result in significant coastal erosion and reworking of deltaic sediment. Some of the resuspended sediment remains trapped in Norton Sound, however much is removed to be ultimately deposited in the Chukchi Sea, almost 1,000 km to the northwest. Sediment reworking continues until freezeup when ice-related processes regain their dominance.

ANNUAL REPORT

Title: Earthquake Activity and Ground Shaking
in and along the Eastern Gulf of Alaska

Report by: Christopher Stephens and John C. Lahr

Principal Investigators: John C. Lahr and Christopher D. Stephens
Office of Earthquake Studies
U.S. Geological Survey
Menlo Park, California 94025

Research Unit: 210

Reporting Period: April 1, 1978 through March 31, 1979

Number of Pages: 77

18 April, 1979

CONTENTS

ILLUSTRATIONS

TABLES

APPENDICES

Page

I. Summary of objectives, conclusions, and implications with respect to OCS oil and gas development.

The objective of this research is to analyze the earthquake activity in the Northeast Gulf of Alaska (NEGOA) and adjacent onshore areas in order to develop a better model for the current tectonic framework. This information is critical to the establishment of criteria for the safe development of oil and gas.

Seismic data since September 1974 from the USGS regional network indicates that the distribution of seismic activity is generally diffuse, although local areas of relatively high rates of activity have been identified near Icy Bay and northeast of Kayak Island. Most of the earthquakes have magnitudes less than about 4. Large temporal variations in the rate of activity do occur, and thus the general absence of earthquakes in particular areas of the NEGOA does not in itself indicate the absence of faults capable of generating potentially damaging earthquakes. For some mapped surface faults, however, sufficient geological and geophysical information may be available or attainable to conclude that the fault is inactive because of the lack of fault movement over a suitably long interval of time.

The spatial distribution of earthquakes in the magnitude range 1.0 to 4.5 and focal mechanisms for some of the larger earthquakes suggest that the regional north-south compression of the continental margin in the NEGOA is accommodated both by shallow underthrusting of the Pacific plate on a plane dipping at a low angle to the north-northwest and by reverse faulting at shallower depths on nearly vertical, east-west trending planes. A great earthquake ($M > 8$) associated with low-angle oblique underthrusting of the sea floor beneath the continental shelf could be accompanied by strong ground shaking throughout much of the eastern Gulf of Alaska, possibly from Cross Sound to Kayak Island (Page, 1975) and could trigger tsunamis, seiches, and submarine slumping, any of which could be hazardous to offshore and coastal structures (Meyers, 1976).

On 28 February 1979 a magnitude 7.7 (Ms) earthquake occurred beneath the St. Elias mountains with an epicenter about 50 km north of Icy Bay. The primary rupture mechanism of this earthquake has been inferred to be shallow thrusting on a plane dipping at a low angle to the north. The observed effects of ground shaking from this earthquake indicate intensities as high as VII, with relatively higher intensities in a south to southeast direction from the epicenter (C. Stover, personal communication, 1979). The rupture surface of this earthquake extended over only the extreme eastern portion of a zone that has been identified by previous authors as a seismic gap for large earthquakes (e.g., Sykes, 1971). If a simple application of the gap hypothesis is appropriate to this region, then a major seismic gap still remains between about Icy Bay and Kayak Island, and another magnitude 7.7 or larger earthquake may occur here within the next decade or two, and possibly within the next few years.

II. Introduction

A. General nature and scope of study.

The purpose of this research is to investigate the earthquake potential in

the NEGOA and adjacent onshore areas. This will be accomplished by assessing the historical seismic record as well as by collecting new and more detailed information on both the distribution of current seismicity and the nature of strong ground motion resulting from large earthquakes.

B. Specific Objectives.

1. Record the locations and magnitudes of all significant earthquakes within the NEGOA area.

2. Prepare focal mechanism solutions to aid in interpreting the tectonic processes active in the region.

3. Identify both offshore and onshore faults that are capable of generating earthquakes.

4. Assess the nature of strong ground shaking associated with large earthquakes in the NEGOA.

5. Compile and evaluate frequency vs. magnitude relationships for seismic activity within and adjacent to the study areas.

6. Evaluate the observed seismicity in close cooperation with OCSEAP Research Units 16 and 251 towards development of an earthquake prediction capability in the NEGOA.

C. Relevance to problem of petroleum development.

It is crucial that the seismic potential in the NEGOA be carefully analyzed and that the results be incorporated into the plans for future petroleum development. This information should be considered in the selection of tracts for lease sales, in choosing the localities for land-based operations, and in setting minimum design specifications for both coastal and offshore structures.

III. Current state of knowledge

The eastern Gulf of Alaska and the adjacent onshore areas are undergoing compressional deformation caused by north-northwestward migration of the Pacific plate with respect to the North American plate (Figure 1). Direct evidence for continued convergent motion comes from studies of large earthquakes along portions of the Pacific-North American plate boundary adjacent to the eastern Gulf of Alaska.

The 1958 earthquake on the Fairweather fault in southeast Alaska was accompanied by right lateral slip of as much as 6.5 m (Tocher, 1960). The 1964 Alaska earthquake resulted from dip slip motion of about 12 m (Hastie and Savage, 1970) on a fault plane dipping northwestward beneath the continent from the Aleutian Trench and extending from eastern Prince William Sound to southern Kodiak Island. In the intervening region between these earthquakes, from approximately Yakutat Bay to Kayak Island, the precise manner in which this convergent motion is accommodated is not known. There are some indications that a broad region is involved, extending from the continental shelf inland to the Totschunda and Denali faults. Slip on the Totschunda and Denali faults has been right lateral during Quaternary time as would be

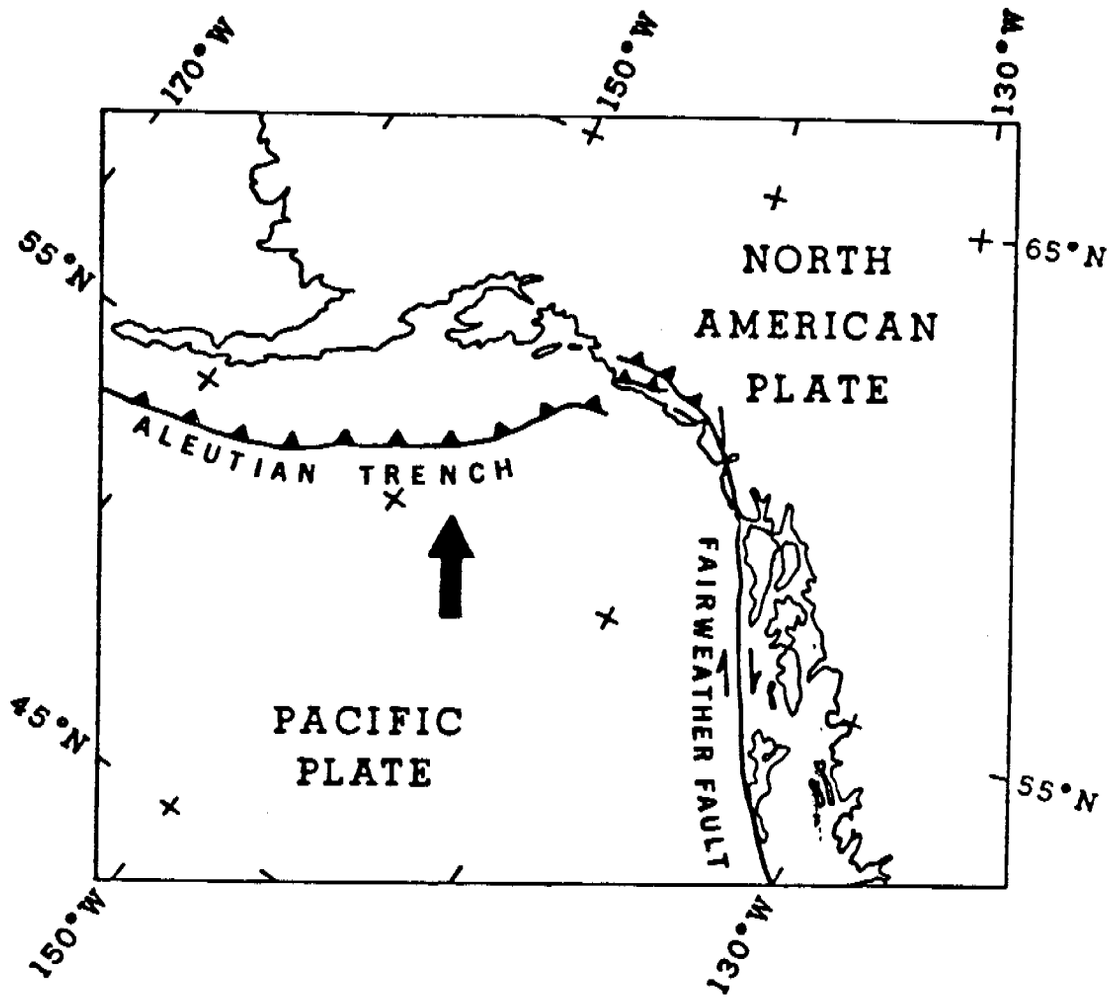

Figure 1. Plate tectonic relationships in the northeast Pacific. Large arrow indicates the the motion of the Pacific plate relative to a stationary North American plate. Small arrows indicate the sense of slip on faults; barbs are on upper edge of thrust fault.

expected if the southern margin of Alaska were partially coupled to the Pacific plate (Richter and Matson, 1971). The eastern Gulf of Alaska is bounded to the north by the young Chugach and St. Elias mountain ranges (Figure 2).

The historic record of instrumentally located earthquakes in the vicinity of the eastern Gulf is probably complete only for events larger than magnitude 7-3/4 since 1899, earthquakes larger than 6 since the early 1930's and larger than 5 since 1964. The events contained in the NOAA Earthquake Data File for 1900 through January 1979 are plotted in Figure 3. Each number corresponds to the decade in which the event occurred. The coordinates of epicenters prior to about 1960 were often rounded to the nearest tenth of a degree. To avoid plotting epicenters on top of one another, the second and subsequent epicenters to be plotted at a given point have been randomly scattered by up to 4 km. The apparent increase in seismicity in the 1960's and 1970's is due in part to aftershocks of the 1964 Prince William Sound earthquake and in part to establishment of seismograph networks in southern Alaska in 1967 by NOAA (Palmer Observatory) and the Geophysical Institute of the University of Alaska. The seismograph stations closest to the region of study prior to 1972 were located on Middleton and Kodiak Islands and near Palmer, Alaska. Before 1967 the closest permanent stations were at Sitka and College, Alaska.

Prior to the magnitude 7.7 (Ms) earthquake of 28 February 1979, the largest historic earthquakes in the vicinity of the eastern Gulf of Alaska were three magnitude 8 earthquakes in the Yakutat area in 1899 and 1900 (Tarr and Martin, 1912; Richter, 1958), the magnitude 8.5 Prince William Sound earthquake of 1964 and the magnitude 7.9 earthquake on the Fairweather fault in 1958. Shorelines were uplifted as much as 14 meters in the Yakutat Bay area and about 1 meter at Cape Yakataga during the 1899-1900 earthquakes (Tarr and Martin, 1912). Coastal uplift during the 1964 earthquake ranged from 19 meters at Montague Island to less than 3 meters at Kayak Island (Plafker, 1969).

Based on this historic record, the region between the 1958 and 1964 earthquakes has been identified as a likely location for a magnitude 7 or 8 shock within the next few decades (e.g., Kelleher, 1970; Sykes, 1971). The distribution of aftershocks from the 28 February earthquake suggests that the rupture surface from this earthquake included only the extreme eastern portion of the seismic gap. If simple application of the gap hypothesis is appropriate to this area, then a major gap still remains between about Icy Bay and Kayak Island.

The Chugach and St. Elias Mountains are bounded on the south and southwest by the Gulf of Alaska Tertiary province. Many north-dipping thrust faults have been mapped in this Tertiary province (Plafker, 1967), but it is not known which are currently active. A few of these faults are indicated on Figure 2.

Available information on the offshore structure has been summarized by Bruns and Plafker (1975), Molnia and others (1976), Carlson (1976), and Molnia and others (1978). The location of near-surface offshore faults, interpreted largely from minisparker records, are shown in Figure 2. None of these faults was found to offset Holocene sediments at the sea floor with great certainty, so their current state of activity may best be determined by earthquake investigations.

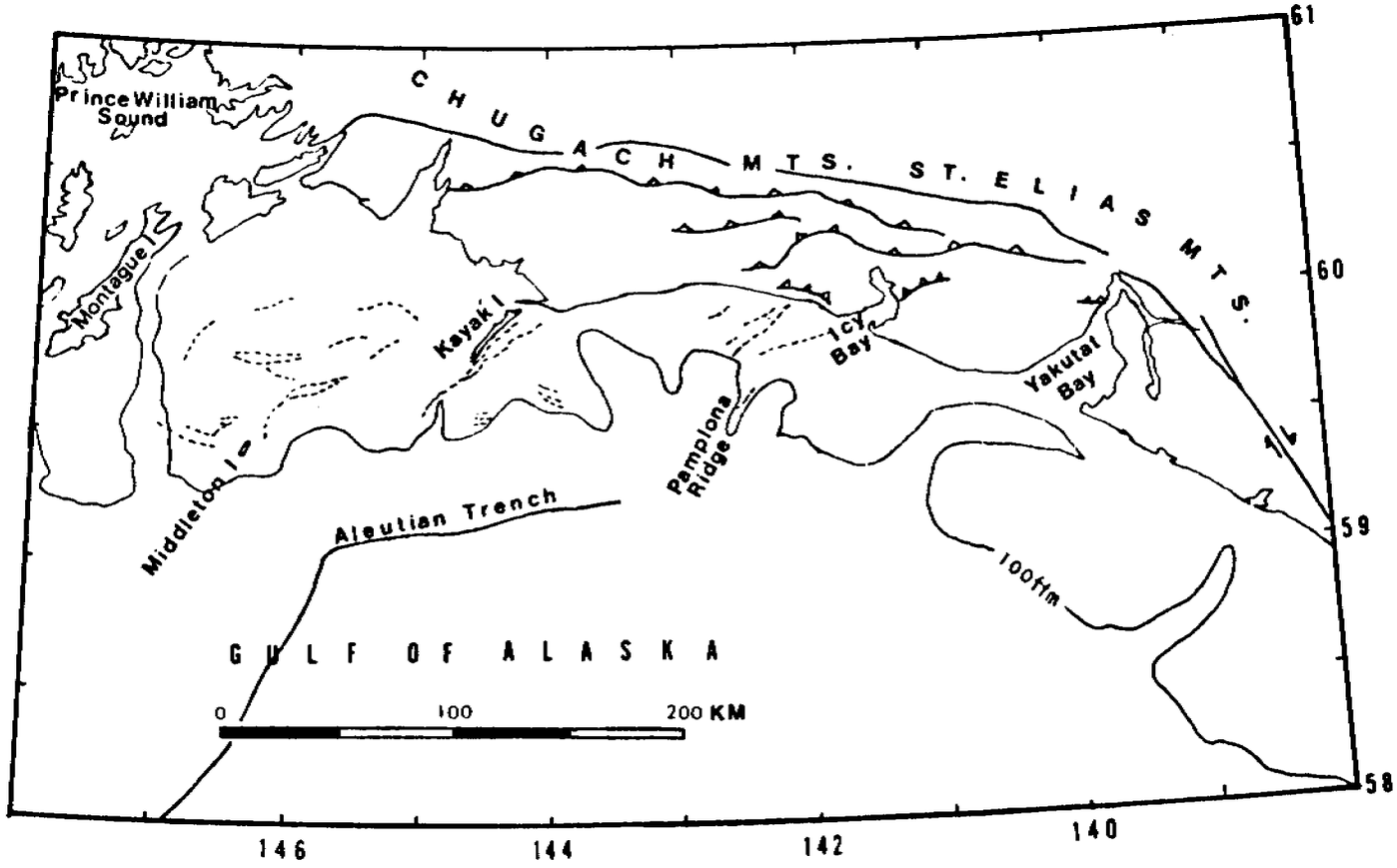

Figure 2. The eastern Gulf of Alaska region showing offshore faults and selected onshore faults (from Carlson, 1976).

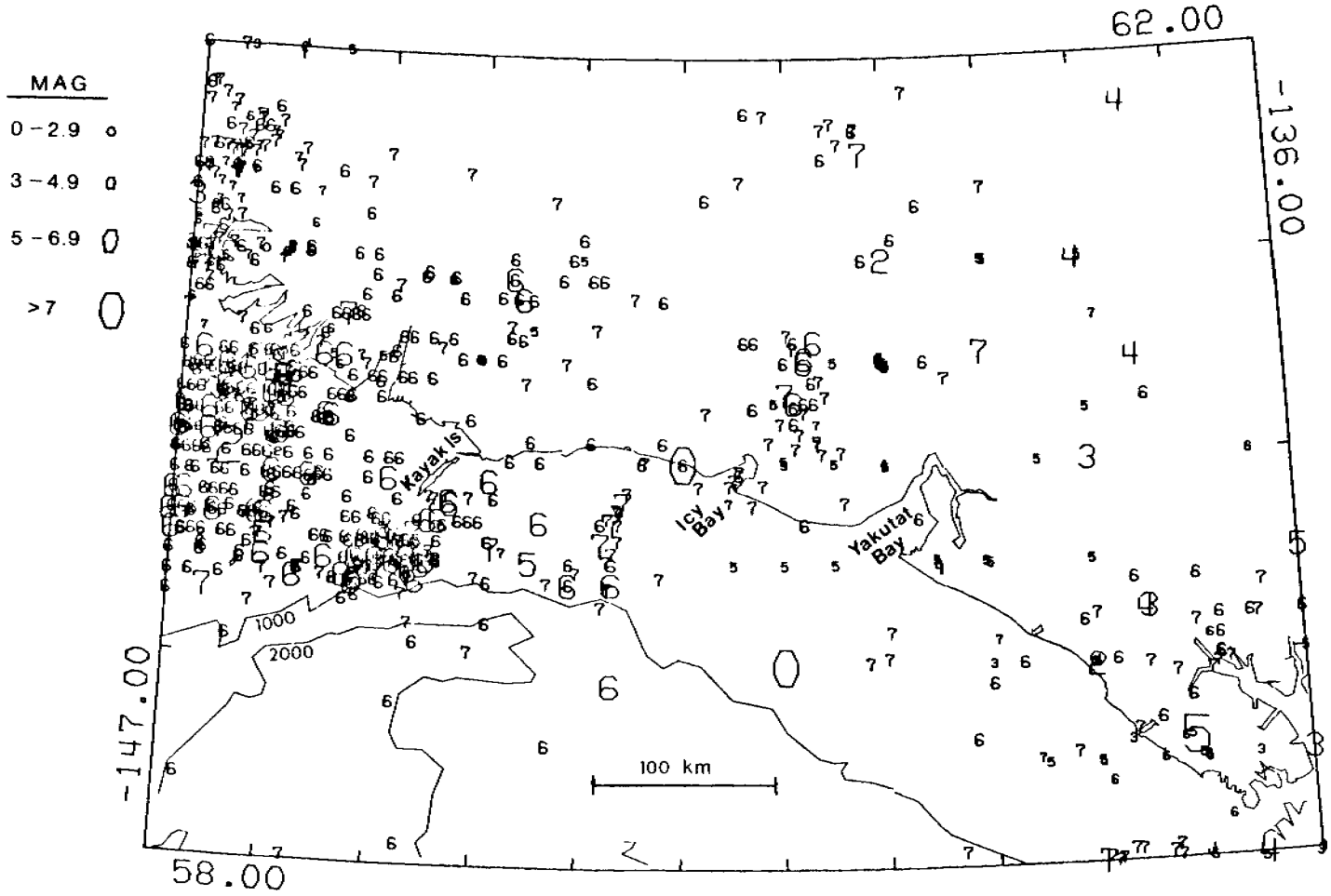

Figure 3. Map of epicenters for the eastern Gulf of Alaska for the period 1900 - January 1979. The plotting symbol is the first digit of the decade in which the event occurred (e.g. the symbol 5 corresponds to an earthquake that occurred between 1950 and 1959), and the size is proportional to magnitude. Depth contours are in fathoms.

IV. Study Area.

This project is concerned with the seismicity within and adjacent to the eastern Gulf of Alaska continental shelf area. This is the southern coastal and adjacent continental shelf region of Alaska between Montague Island and Dry Bay (Figure 2).

V. Methods and rationale of data collection.

The short-period seismograph stations installed along the eastern Gulf of Alaska under the Outer Continental Shelf Environmental Assessment Program as well as the other stations operated by the USGS in southern Alaska are shown in Figure 4. Single-component stations record the vertical component of the ground motion, while three-component stations have instruments to measure north-south and east-west motion as well. Data from these instruments are used to determine the parameters of earthquakes as small as magnitude 1. The parameters of interest are epicenter, depth, magnitude, and focal mechanism. These data are required to further our understanding of the regional tectonics and to identify active faults.

A network of strong motion instruments is also operated by the Seismic Engineering Branch (Figure 5). These devices are designed to trigger during large earthquakes and give high-quality records of large ground motions which are necessary for engineering design purposes.

VI. Results.

Preliminary data on earthquake parameters for the periods October-December 1977 and January-March 1978 were presented in quarterly reports and have been published in catalogs (Fogleman and others, 1978; Stephens and others, 1979). Preliminary data for the period September-December 1978 are listed in Appendix I. Earthquake epicenters for this latter data are plotted in Figure 6.

A report summarizing our early results on the study of the 28 February 1979 St. Elias earthquake has been released (Lahr and others, 1979). The report includes a review of the geologic and historical earthquake data available for the epicentral region, and preliminary data on aftershocks, focal mechanism, moment, and strong motion recordings. A copy of the report is included as Appendix IV.

Installation of the new AlVCO amplifier-calibrator units (Roger and others, 1979) at 18 of our stations last summer (Figure 7) has dramatically improved the reliability of the stations as well as provided daily calibration of the instruments. The gain ranging capability of these units has been used in recovery of S-wave information which previously was not possible. This latter feature is proving particularly valuable in studying the aftershock sequence of the 28 February earthquake.

A new format for storing seismic data is being implemented. The structure of this new data base is illustrated in Figure 8. The new structure will allow rapid determination of variation of derived parameters, such as station residuals with respect to time, region, or azimuth. Computing time will be significantly reduced when locations are recomputed because good starting locations will be available. Another important advantage of this new system is that it will allow us to systematically develop a more accurate method for determining magnitudes.

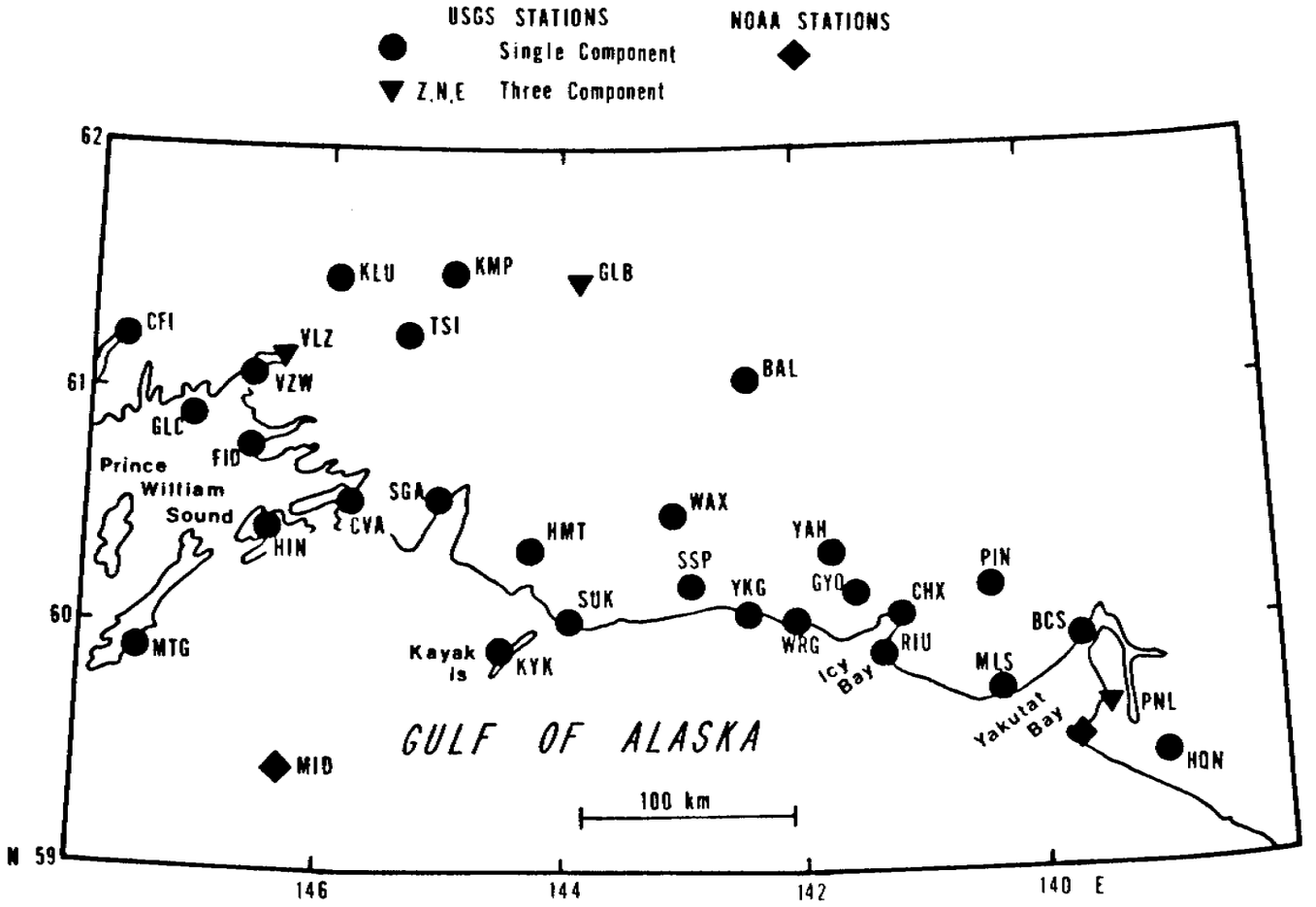

Figure 4. Seismic stations operated by the USGS in eastern southern Alaska during September-December 1978. These stations are supported in part by OCSEAP.

Table 1.

USGS SEISMIC STATIONS SUPPORTED IN PART BY OCSEAP AND OPERATED DURING SEPTEMBER - DECEMBER 1978

STA CODE	STATION NAME	LAT N DEG	LAT N MIN	LONG W DEG	LONG W MIN	ELEV M	TDLY SEC	MAG @ 1HZ
BAL	BALDY	61	2.17	142	20.67	1300	0.00	117000
BCS	BANCAS POINT	59	56.90	139	37.00	10	0.30	29700
CFI	COLLEGE FIORD	61	10.96	147	45.99	2	0.00	117000
CHX	CHAIX HILLS	60	4.00	141	7.10	793	0.30	59400
CVA	CORDOVA	60	32.79	145	44.96	90	0.30	59400
FID	FIDALGO	60	43.73	146	35.79	488	0.30	234000
GLB	GILAHINA BUTTE	61	26.51	143	48.63	845	0.00	234000
GLC	GLACIER IS.	60	53.44	147	4.35	3	0.30	117000
GYO	GUYOT HILLS	60	8.78	141	28.79	183	0.30	117000
HIN	HINCHINBROOK	60	23.81	146	30.10	611	0.30	234000
HMT	MT. HAMILTON	60	20.19	144	15.64	620	0.30	117000
HQN	HARLEQUIN LAKE	59	27.10	138	52.62	372	0.30	117000
KLU	KLUTINA	61	29.57	145	55.21	1012	0.00	234000
KMP	KIMBALL PASS	61	30.79	145	1.09	1143	0.30	117000
KYK	KAYAK IS.	59	52.10	144	31.39	375	0.30	59400
MLS	MALASPINA	59	45.80	140	9.00	2	0.30	14700
MTG	MONTAGUE IS.	59	54.71	147	29.82	31	0.30	59400
PIN	PINNACLE	60	5.80	140	15.40	975	0.30	59400
PNL	PENINSULA	59	40.12	139	23.82	579	0.30	59400
RIU	RIOU	59	52.70	141	13.70	15	0.30	7400
SGA	SHERMAN GLACIER	60	30.07	145	12.42	424	0.30	59400
SSP	SUNSHINE POINT	60	10.80	142	50.30	732	0.30	117000
SUK	SUCKLING HILLS	60	4.60	143	47.00	427	0.30	117000
TSI	TSINA	61	13.57	145	20.24	1113	0.30	117000
VLZ	VALDEZ	61	7.89	146	19.92	10	0.30	7400
VZW	VALDEZ WEST	61	3.54	146	33.24	796	0.30	234000
WAX	WAXELL RIDGE	60	27.00	142	51.10	975	0.30	0
WRG	WHITE RIVER GLCR	60	2.27	142	1.90	550	0.30	29700
YAH	YAHTSE	60	21.80	141	44.70	2135	0.30	59400
YKG	YAKATAGA	60	4.20	142	25.33	60	0.30	7400

This table lists geographical coordinated and other pertinent information for USGS seismic stations in eastern southern Alaska. TDLY is the telephone delay in seconds. The magnification (MAG) of the vertical component seismometer is given at 1 Hz.

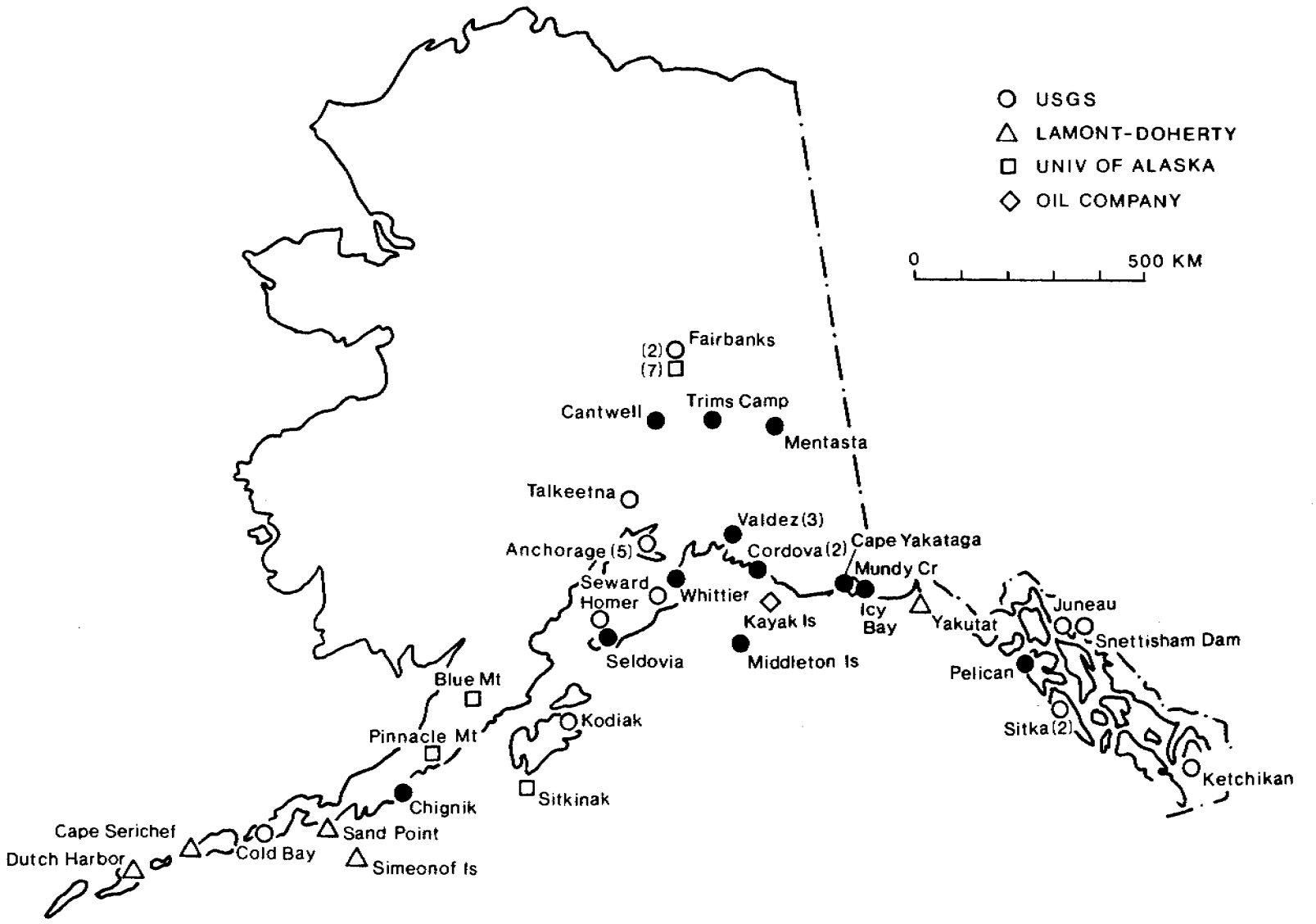

Figure 5. Distribution of strong-motion instruments in Alaska in 1978. Solid symbols indicate locations of the twelve instruments that were purchased with OCSEAP funding.

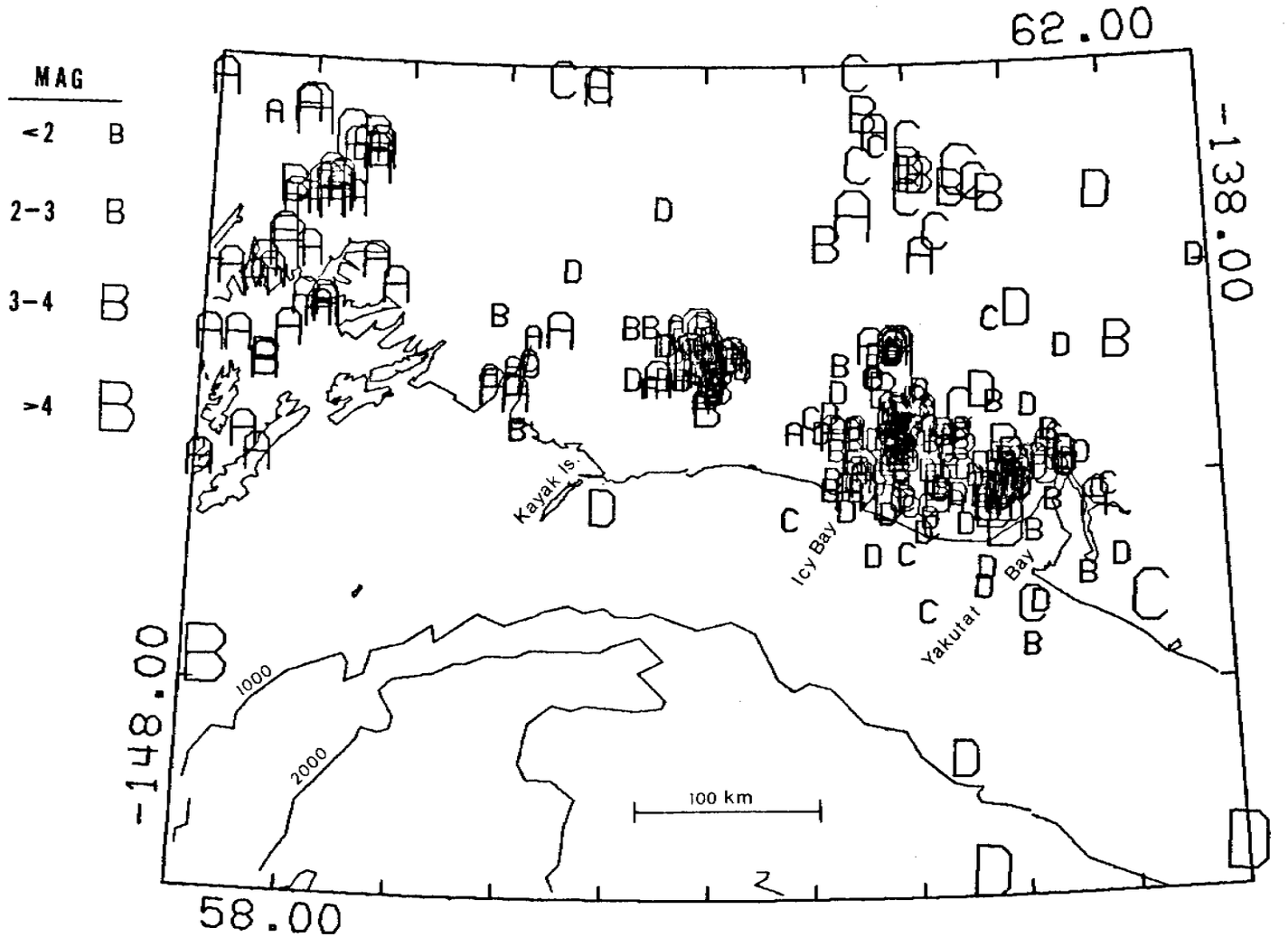

Figure 6. Map of earthquake epicenters in the NEGOA during September-December 1978. The plotting symbol represents the quality of the solution (see Appendix I), and the size is proportional to the magnitude. Depth contours are in fathoms.

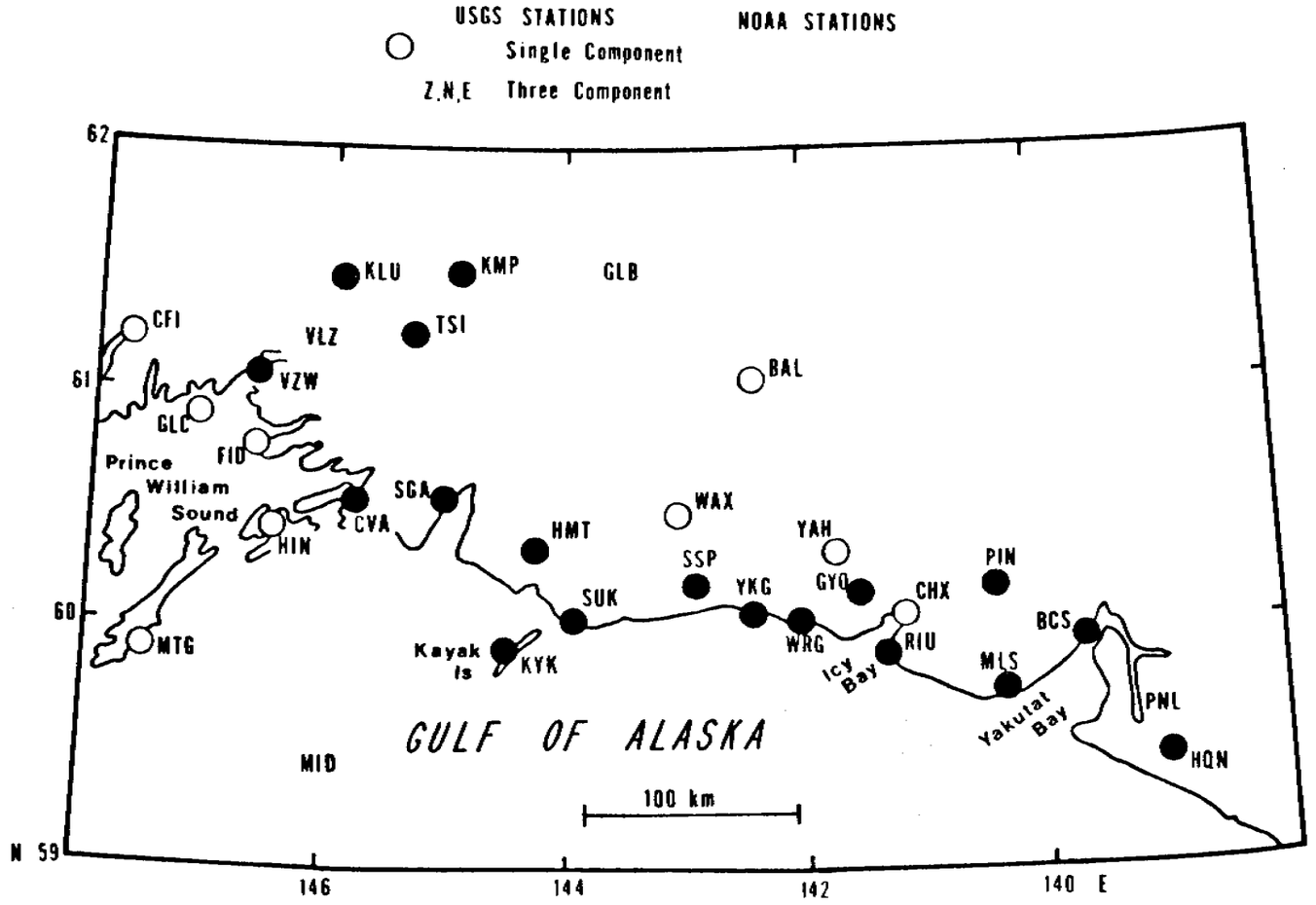

Figure 7. Map showing the USGS seismic stations in eastern southern Alaska in which the new AlVCO amplifier-calibrator unit has been installed (solid symbols).

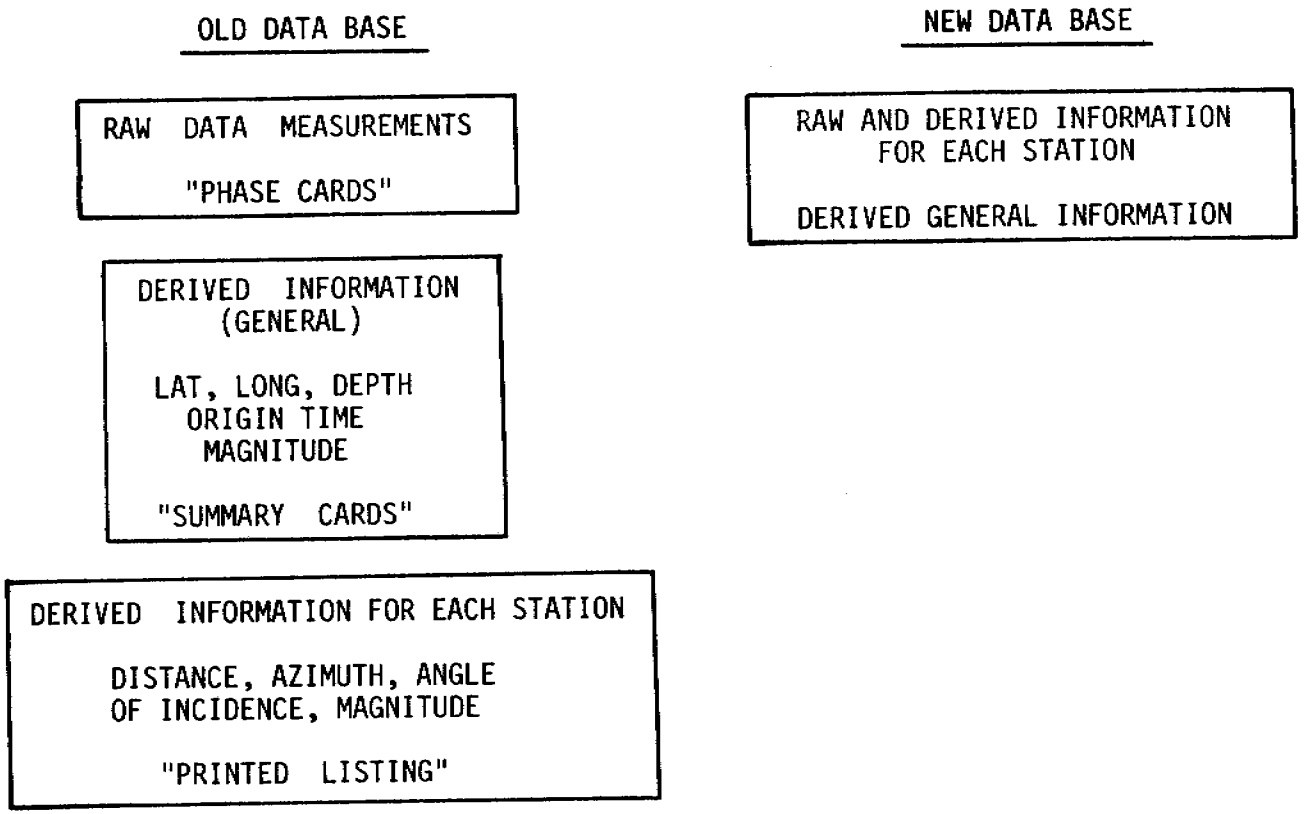

Figure 8. Schematic showing the organization of the old and new data base structures. Raw and derived data that was previously stored in three files is now combined into a single data file.

Travel times to distant stations from earthquakes that are well located using only the closest stations are being used to study the seismic velocity structure in the NEGOA. Earthquakes near Icy Bay and Yakutat Bay have been used as sources. Our results suggest that significant lateral variations occur in the velocity structure. For earthquakes that occur beneath Icy Bay, P-wave residuals at stations near Yakutat Bay to the east are generally negative (early) relative to stations to the west. Some preliminary observations of teleseismic P-wave residuals at the NEGOA stations also show relatively early arrivals at the eastern stations. A more detailed study of this area is being made in an attempt to model the structure responsible for these observations.

VII. AND VIII. Discussion and Conclusions

Comparisons of individual quarters of data with all of the data collected from the regional network since September 1974 indicate that the general distribution of seismic activity has remained nearly the same over this time period, at least up to the time of the 28 February 1979 earthquake. Most of the earthquakes have magnitudes less than about 4 and the largest earthquakes have magnitudes of about 4.5. Relatively high rates of activity have persisted near Icy Bay and northeast of Kayak Island since at least 1974. Significant temporal variations in the rates of activity do occur locally, as exemplified by the recent sequence of earthquakes that occurred about 20 km northwest of Yakutat Bay during October and November 1978 (Figure 6). The relatively short duration of this latter sequence emphasizes the need for continuous long-term monitoring to identify areas of active faulting, especially in areas where it is difficult to obtain any geologic evidence on faulting.

The magnitude 7.7 (Ms) earthquake that occurred on 28 February 1979 beneath the Chugach and St. Elias mountains is an important event in terms of understanding the tectonics of the NEGOA and in terms of assessing whether an earthquake of the same magnitude or larger can be expected to occur within the next few decades. A detailed presentation of preliminary results of the study of this earthquake is presented in Appendix IV. The distribution of aftershocks and the focal mechanism determined from P-wave first motions for the earthquake have been used to infer that the primary rupture mechanism was shallow thrusting on a plane dipping at a low angle to the north-northwest. This mode of deformation is consistent with the results found for other teleseismically recorded earthquakes from this area (O. Perez, personal communication, 1979). Associated activity on the nearly vertical, east-west trending reverse faults that have been mapped in the area (e.g., Plafker, 1967) cannot be precluded at the present and indeed there is some evidence from earlier, locally recorded data that some of these faults are currently active (Stephens and others, 1979; see Figure 9). Based on a preliminary estimate of the moment and the extent of the aftershock zone, an average slip of about 4 ¼ meters has been inferred for the 28 February earthquake. This displacement is close to the amount of strain accumulation expected since the 1899-1900 great (M 8) earthquakes based on geologic evidence for recent motion along the Fairweather fault (e.g., Plafker and others, 1978). The rupture surface did not extend through the entire region that has previously been identified as a seismic gap (e.g., Kelleher, 1970, Sykes, 1971), so simple application of the gap hypothesis would imply that another magnitude 7.7 or larger earthquake may occur between about Icy Bay and Kayak Island within the next decade or two, and possibly within the next few years.

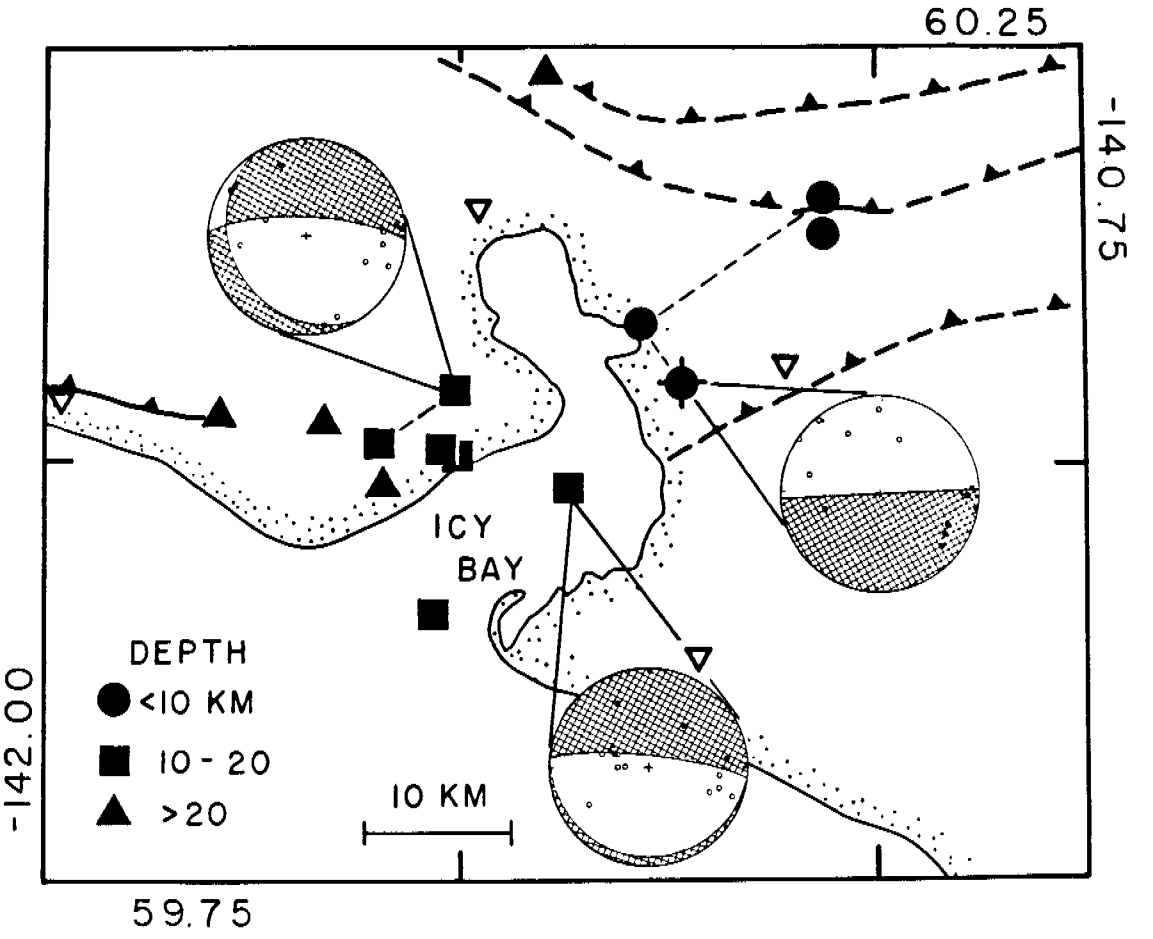

Figure 9. Composite and single-event P-wave first motion plots for earthquakes with relocated hypocenters that occurred near Icy Bay. Compressions are shown as small solid circles and dilatations as open circles. The plotting symbol for the epicenter varies with the depth of the hypocenter. Seismic stations are represented by inverted open triangles, and mapped or inferred faults are indicated by heavy solid or dashed lines, respectively. The epicenter of the earthquake used as a master event is shown as a cross. Seismic data from regional stations only were used.

Earthquakes that occur at depths less than about 10 km have focal mechanisms that are compatable with reverse motion on nearly vertical faults. This sense of motion is consistent with geologic observations in the region. Earthquakes that occur at depths of 10 to 20 km have focal mechanisms that, considering the uncertainty in constraining the dips of the low-angle planes, are compatable with shallow thrusting to the north. Teleseismically recorded earthquakes from this region also have focal mechanisms that indicate shallow thrusting to the north (O. Perez, personal communication, 1979).

IX. Needs for further study

Post-earthquake studies of the 28 February 1979 earthquake.

Study of the aftershocks from the 28 February earthquake can provide valuable constraints on the mechanism and extent of rupture of the main shock, as well as provide a basis for inferring the state of stress in the epicentral region. The present distribution of stations cannot be used to accurately resolve the depths of the aftershocks. Aftershocks from this earthquake are likely to continue to occur through the summer of 1979, and we are planning to install temporary stations in the epicentral region to provide better depth control. A few well-located aftershocks can then be used as master events toimprove the accuracy of previously recorded aftershocks. Geologic investigations of the epicentral region should also be conducted to search for evidence of surface faulting related to this earthquake.

Since the potential is high for another magnitude 7 or greater along the NEGOA within the next decade or two, if not the next few years, continued monitoring of the seismic activity should be supplemented with other geophysical measurements and geologic studies. For example, tide gauges and geodetic networks should be established to monitor regional and local strain variations. Evidence for the temporal and spatial patterns of uplift from past earthquakes might be obtained from the study of terraces. In addition to the above investigations, the existing network of strong motion instruments should be augmented so that in the event of a large earthquake, a more complete record of the variation of strong ground motion can be obtained.

Seismic Velocity Structure

The seismic velocity structure below a few kilometers depth is not well known in the NEGOA. Such information is important to understanding the tectonic structure of this region and in helping to improve the accuracy of both absolute and relative earthquake locations. This latter point is particularly important when attempts are made to identify active faults on the basis of earthquake locations. One way to obtain this information is by the study of travel times to more distant stations from earthquakes located using only a few close stations, as is currently being done for earthquakes near Icy Bay. Preliminary work indicates that significant lateral variations in the velocity structure do exist, although they are not well mapped. Further studies of this type are necessary to help resolve these variations.

A more satisfactory but also more expensive way to obtain the information is to record the signals from a few large explosions detonated at critical locations within the study region. Explosions are preferable to earthquakes because both the location and origin time are very accurately known.

Ocean Bottom Seismic Recording and Offshore Seismicity

The land-based network of seismic stations has a limited capability for detecting and accurately locating small magnitude earthquakes that occur offshore. The use of ocean bottom seismometers (OBS) can improve our detection capability in offshore areas, as well as improve the accuracy with which these events can be located. Offshore recording of earthquakes that occur in onshore areas and are well located by the land-based stations will provide some information about the seismic velocity structure in the offshore region. This summer we are planning to deploy five OBS units about 40 km

south of Yakutat Bay (Figure 10).

Magnitude-Frequency Relationships

Evaluation of magnitude-frequency relationships in the NEGOA is being delayed until we have completed our revisions to the methods used to compute magnitudes and we have recomputed locations and magnitudes for all of our data. A- and B-values, which describe the log number versus magnitude recurrence relationship, will be computed for different regions. Temporal variations in B-values that may be related to the 28 February 1979 earthquake will also be considered. Because the data for these determinations will cover a relatively short time period and include few earthquakes with magnitudes greater than about 4.5, estimates of the return rates of larger magnitude earthquakes based on recurrence curves are not expected to be very reliable.

Strong Motion Recording

The strong motion recordings obtained for the 28 February 1979 earthquake will be digitized and analyzed by the Seismic Engineering Branch of the Office of Earthquake Studies. Copies of the results of these studies will be made available to OCSEAP.

X. Summary of January-March 1979 Quarter Activities

A. Laboratory and Field Activities

1. Ship or Field Schedule
   N. A.

2. Personnel

a) Laboratory

John Lahr, USGS, Geophysicist
Project Chief

Christopher Stephens, USGS, Geophysicist
Asst. Project Chief

Kent Fogleman, USGS, Geophysicist
Data Processing Supervisor

Suzanne Helton, USGS, Physical Science Aide, Data Processing

Richard Archdeacon, USGS, Physical Science Aide, Data Processing

Kathy Baldonado, USGS, Physical Science Aide, Data Processing

Mark Smetana, USGS, Physical Science Aide

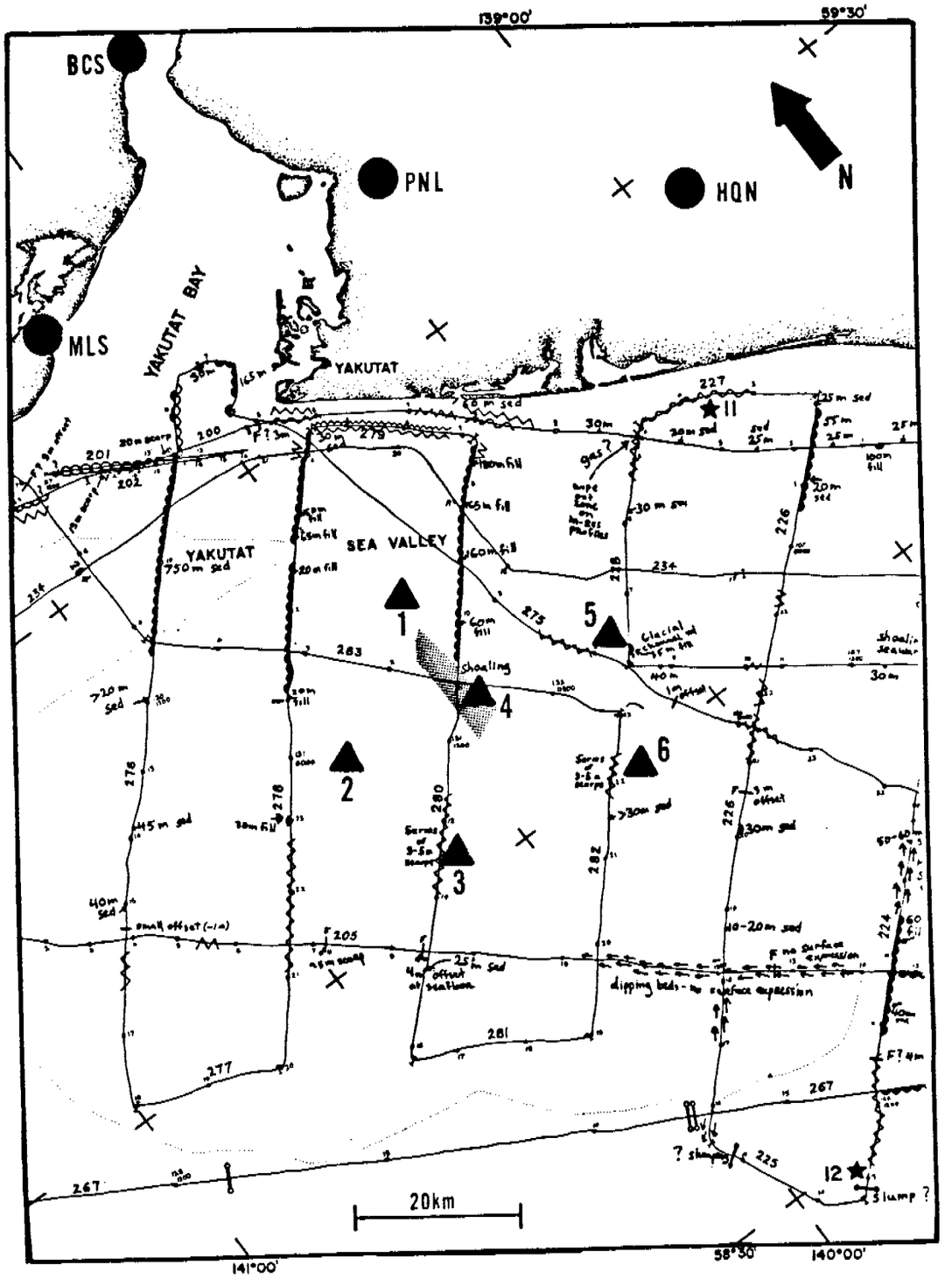

Figure 10. Map showing the proposed locations of the five ocean bottom seismometers (OBS) that will be deployed during the summer of 1979. USGS land-based stations currently operating are shown as solid circles. Stippled area indicates extent of relocated epicenters from a 1974 sequence of earthquakes. (Base map after Molnia and others, 1978).

b) Technical and Field Party

John Roger, USGS, Electronics Engineer, Coordinator, Field Operations

Marion Salsman, USGS, Electronics Technician, Station Maintenance

Tom Walker, USGS, Physical Science Aide, Instrument Maintenance

Tom Cleese, USGS, Physical Science Aide, Instrument Maintenance

3. Methods

a) Field Activities

- Data from the stations GLB and BAL were interrupted due to a power supply failure at TOA. The power supply has been temporarily replaced with lead-acid batteries.

- The stations CVA and YKG were visited and repaired.

- A site for a new station along the Alaska-Canada border has been selected. The electronic equipment for the station is being repaired at Menlo Park.

- The problem of interference by a National Weather Service transmitter at Yakutat has been resolved by installing notch filters in our antenna lines. NWS has agreed to reimburse our project for the installation costs.

b) Laboratory Activities

Several VHF radio receivers have been tested in an effort to find improved performance over the currently employed unit. The General Electric Master II base station receiver meets our specifications and has demonstrated the most satisfactory performance of the units tested. Four additional units are on order and will be installed this summer.

New transmitters have been installed at MLS and BCS for evaluation as a possible replacement of the units presently used.

Twenty additional A1VCO units are under construction and will be installed this summer.

A new calibration card incorporating solid state CMOS memory that will allow programmable calibration cycles has been designed and is being evaluated.

b) Laboratory Activities (continued)

A computer program to be used in the analysis of the AlVCO calibration signals is being developed. The program has been successfully used to extract several of the desired parameters from a calibration cycle generated by the station HQN.

4. Sample Localities

See Figure 4 for a map of the location of stations. The stations are also listed in Table 1.

5. Data Collected or Analyzed

A list of preliminary earthquake parameters for the period 1 September-31 December, 1978 is given in Appendix I. A map of the epicenters of these earthquakes is shown in Figure 6.

XI. Auxiliary Material

A. References

Bruns, T. R., and Plafker, George, 1975. Preliminary structural map of part of the offshore Gulf of Alaska Tertiary province: U.S. Geological Survey Open-File map 75-508.

Carlson, P. R., 1976. Submarine faults and slides that disrupt surficial sedimentary units, northern Gulf of Alaska: U.S. Geological Survey Open-File Report 76-294.

Eaton, J. P., O'Neill, M. E., and Murdock, J. N., 1970. Aftershocks of the 1966 Parkfield-Cholame, California, earthquake: a detailed study, Bull. Seism. Soc. Am. 60, 1151-1197.

Fogleman, Kent, Stephens, Christopher, Lahr, J. C., Helton, Suzanne, and Allan, Mary, 1978. Catalog of earthquakes in southern Alaska, October-December 1977: U.S. Geological Survey Open-File Report 78-1097, 28 p.

Hastie, L. M. and Savage, J. C., 1970. A dislocation model for the 1964 Alaska earthquake: Bull. Seism. Soc. Am., 60, 1389.

Kelleher, J. A., 1970. Space-time seismicity of the Alaska-Aleutian seismic zone: J. Geophys. Res., 75, 5745.

Lahr, J. C., Plafker, George, Stephens, C. D., Fogleman, K. A., and Blackford, M. E., 1979. Interim report on the St. Elias earthquake of 28 February 1979: U. S. Geological Survey Open-File Report 79-670, 35 p.

Lee, W. H. K., and Lahr, J. C., 1972. HYPO71: a computer program for determining hypocenter, magnitude, and first motion pattern of local earthquakes, U.S. Geological Survey, Open-File Report, 100 p.

Lee, W. J. K., Bennett, R. E., and Meagher, K. L., 1972. A method of estimating magnitude of local earthquakes from signal duration, U. S. Geological Survey, Open-File Report, 28 p.

Meyers, H., 1976. A historical summary of earthquake epicenters in and near Alaska: NOAA Technical Memorandum EDS NGSDC-1.

Molnia, B. G., Carlson, P. R., and Bruns, T. R., 1976. Report on the environmental geology OCS area, eastern Gulf of Alaska: U. S. Geological Survey Open-File Report 76-206.

Molnia, B. G., Carlson, P. R., and Wright, L. H., 1978. Geophysical data from the 1975 cruise of the NOAA ship Surveyor in the northern Gulf of Alaska: U.S. Geological Survey Open-File Report 78-209.

Page, R. A., 1975. Evaluation of seismicity and earthquake shaking at offshore sites: in Offshore Technology Conference, 7th, Houston, Texas, Proc., v. 3.

XI. Auxiliary Material

A. References (continued)

Plafker, George, 1967. Geologic map of the Gulf of Alaska Tertiary province, Alaska: U.S. Geological Survey Miscellaneous Geologic Investigations Map I-484.

Plafker, George, 1969. Tectonics of the March 27, 1964, Alaska earthquake: U. S. Geological Survey Professional Paper 543-1.

Plafker, George, Hudson, Travis, Rubin, Meyer, and Bruns, Terry, 1978. Late Quaternary offsets along the Fairweather Fault and crustal plate interactions in southern Alaska: Can. J. Earth Sci., 15, p. 805-816.

Richter, C. F., 1958. Elementary Seismology, W. H. Freeman and Co., Inc. San Francisco.

Richter, D. H. and Matson, N. A., 1971. Quaternary faulting in the eastern Alaska range: Geol. Soc. Am. Bull., 82, 1529.

Roger, J. A., Maslak, Sam, and Lahr, J. C., 1979. A seismic electronic system with automatic calibration and crystal reference: U.S. Geological Survey Open-File Report (in prep).

Stephens, C. D., Horner, R. B., Lahr, J. C., and Fogleman, K. A., 1979. The St. Elias, Alaska, earthquake of 28 February 1979: Aftershocks and regional seismicity: Abstract submitted to Amer. Geophys. Union for Spring 1979 Meeting.

Stephens, C. D., Lahr, J. C., Fogleman, K. A., Allan, M. A., and Helton, S. M., 1979, Catalog of earthquakes in southern Alaska, January-March 1978, U. S. Geological Survey Open-File Report 79-718, 31 p.

B. Papers in Preparation or Print

Hasagawa, Henry, Stephens, C. D., Lahr, J. C., 1979. Focal parameters of the St. Elias, Alaska, earthquake of 28 February 1979: Abstract submitted to Seismol. Soc. America for Spring 1979 Meeting.

Lahr, J. C., Fogleman, K. A., Stephens, C. D., Helton, S. M., Archdeacon, Richard, Allan, M. A., 1979, Catalog of earthquakes in southern Alaska, September-December 1978: U. S. Geological Survey Open-File Report (in prep).

Lahr, J. C., Horner, R. B., Stephens, C. D., Fogleman, K. A., 1979, Aftershocks of the St. Elias, Alaska earthquake of 28 February 1979: abstract submitted to Seismol. Soc. America for Spring 1979 meeting.

Lahr, J. C., Plafker, George, Stephens, C. D., Fogleman, K. A., Blackford, M. E., 1979, Interim report on the St. Elias earthquake of 28 February 1979: U. S. Geological Survey Open-File Report 79-670, 35 p.

Roger, J. A., Maslak, Sam, Lahr, J. C., 1979, A seismic electronic system with automatic calibration and crystal reference: U. S. Geological Survey Open-File Report (in prep).

Stephens, C. D., Horner, R. B., Lahr, J. C., Fogleman, K. A., 1979, The St. Elias, Alaska, earthquake of 28 February 1979: aftershocks and regional seismicity: Abstract submitted to Amer. Geophys. Un. for Spring 1979 Meeting.

Stephens, C. D., Lahr, J. C., Fogleman, K. A., Allan, M. A., and Helton, S. M. , 1979, Catalog of earthquakes in southern Alaska, January-March 1978: U. S. Geological Survey Open-File Report 79-718, 31 p.

C. Oral Presentations

Review of seismicity of NEGOA presented at OCSEAP Review Meeting, Boulder, CO. by J. C. Lahr and C. D. Stephens, March 1979.

APPENDIX I

Preliminary earthquake locations along the NEGOA
September - December 1978

This appendix lists origin times, focal coordinates, magnitudes, and related parameters for earthquakes which occurred in the eastern Gulf of Alaska region. The following data are given for each event:

(1) Origin time in Universal Time (UT): date, hour (HR), minute (MN), and second (SEC). To convert to Alaska Standard Time (AST) subtract ten hours.

(2) Epicenter in degrees and minutes of north latitude (LAT N) and west longitude (LONG W).

(3) DEPTH, depth of focus in kilometers.

(4) MAG, magnitude of the earthquake.

(5) NP, number of P arrivals used in locating earthquake.

(6) NS, number of S arrivals used in locating earthquake.

(7) GAP, largest azimuthal separation in degrees between stations.

(8) D3, epicentral distance in kilometers to the third closest station to the epicenter.

(9) RMS, root-mean-square error in seconds of the traveltime residuals:

$$RMS = \sum_i \left[(Rp_i^2 + Rs_i^2) \; / \; (N_P + N_S) \right]$$

where Rp_i and Rs_i are the observed minus the computed arrival times of P- and S-waves, respectively, at the i-th station.

(10) ERH, largest horizontal deviation in kilometers from the hypocenter within the one-standard-deviation confidence ellipsoid. This quantity is a measure of the epicentral precision for an event. An upper limit of 99 km is placed on ERH.

Projection of ellipsoid
onto horizontal plane

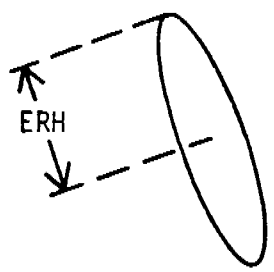

(11) ERZ largest vertical deviation in kilometers from the hypocenter within the one-standard-deviation confidence ellipsoid. This quantity is a measure of the depth precision for an event. An upper limit of 99 km is placed on ERZ.

Projection of ellipsoid onto vertical plane:

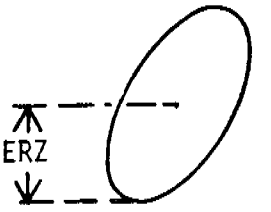

(12) Q, quality of the hypocenter. This index is a measure of the precision of the hypocenter and is calculated from ERH and ERZ as follows:

Q		ERH		ERZ
A	$\leq$	2.5	$\leq$	2.5
B	$\leq$	5.0	$\leq$	5.0
C	$\leq$	10.0	$\leq$	10.0
D	$\geq$	10.0	$\geq$	10.0

This quality symbol is used to denote each earthquake on epicenter maps.

All earthquakes were located using the following horizontally layered velocity model:

Layer	Depth to Top (km)	P velocity (km/sec)
1	0	2.75
2	0.01	6.0
3	20	7.0
4	32	8.2

This model was developed by minimizing the travel-time residuals for a group of earthquakes near Valdez. It is considered a reasonable model but not necessarily the optimum model for this region. Further modifications and refinements to the model will undoubtedly take place in the future as more data are gathered.

Whenever possible S-phase arrivals are used in addition to P-phase arrivals. The S-phase velocity is assumed to equal (P-velocity)/1.78 in each layer of the velocity model.

Magnitudes are determined from the signal duration or the maximum trace amplitude. Eaton and others (1970) approximate the Richter local magnitude, whose definition is tied to maximum trace amplitudes recorded on standard horizontal Wood-Anderson torsion seismographs, by an amplitude magnitude based on maximum trace amplitudes recorded on high-gain, high-frequency vertical seismographs such as those operated in the Alaskan network. The amplitude magnitude XMAG used in this catalog is based on the work of Eaton and his co-workers and is given by the expression (Lee and Lahr, 1972)

$$XMAG = \log_{10}A - B_1 + B_2\log_{10}D^2 \qquad (1)$$

where A is the equivalent maximum trace amplitude in millimeters on a standard Wood-Anderson seismograph, D is the hypocentral distance in kilometers, and B_1 and B_2 are constants. Differences in the frequency response of the two seismograph systems are accounted for in calculating A; however, it is assumed that there is no systematic difference between the maximum horizontal ground motion and the maximum vertical motion. The terms $-B_1 + B_2 \log_{10}D^2$ approximate Richter's $-\log_{10}A_0$ function (Richter, 1958, p. 342), which expresses the trace amplitude for a zero-magnitude as a function of epicentral distance (Δ). For small local earthquakes in central California, $B_1 = 0.15$ and $B_2 = 0.80$ for Δ = 1 to 200 km and $B_1 = 3.38$ and $B_2 = 1.50$ for Δ = 200 to 600 km.

For small, shallow earthquakes in central California, Lee and others (1972) express the duration magnitude FMAG at a given station by the relation

$$FMAG = -0.87 + 2.00 \log_{10} \tau + 0.0035 \Delta \qquad (2)$$

where τ is the signal duration in seconds from the P-wave onset to the point where the peak-to-peak trace amplitude on the Geotech Model 6585 film viewer falls below 1 cm, and Δ is the epicentral distance in kilometers.

Comparison of XMAG and FMAG estimates from equations (1) and (2) for 77 Alaskan shocks in the depth range 0 to 150 km and in the magnitude range 1.5 to 3.5 reveals a systematic linear decrease of FMAG relative to XMAG with increasing focal depth. We use the following equation, including a linear dependence on depth term:

$$FMAG = -1.15 + 2.0 \log_{10} \tau + 0.007z + 0.0035 \Delta, \qquad (3)$$

where z is the focal depth in kilometers. Incorporating the depth term in the calculation of FMAG was found to be necessary for Alaskan data.

The magnitude preferentially assigned to each earthquake in this catalog is the mean of the FMAG (equation 3) estimates obtained for USGS stations. The XMAG estimate is given when no FMAG determinations could be made. For shocks larger than about magnitude 3.0, XMAG cannot be determined because the maximum trace amplitudes are off-scale or the traces are too faint to read. For many shocks smaller than about magnitude 2.0, the trace amplitude drops below 1 cm peak-to-peak between the P and S arrivals and FMAG is not determined.

Many of the earthquakes recorded by the stations occur outside of the network, so it is difficult to establish good depth control for these events. The procedure for locating all earthquakes is to first fix the depth and determine the optimal epicentral location, and then allow the depth to vary. Frequently for earthquakes which occur outside of the network little or no improvement to the solution is found when the depth is allowed to vary. The result is that the distribution of the depths of the final hypocentral solutions may be biased toward the initial trial depth and may not reflect the true depth of the earthquakes. The trial depth used for the earthquakes occurring in the fourth quarter of 1977 was 15 km.

SOUTHEAST ALASKA SEISMICITY, SEPT-DEC 1978

1978		ORIGIN HR	MN	TIME SEC	LAT N DEG	MIN	LONG W DEG	MIN	DEPTH KM	MAG	NP	NS	GAP DEG	D3 KM	RMS SEC	ERH KM	ERZ KM	Q
SEP	1	2	42	47.3	61	58.0	141	28.6	5.0	2.3	5	2	225	189	0.39	6.0	5.0	C
	1	7	11	1.6	60	17.6	141	7.7	10.1	2.1	15	5	153	35	0.50	1.6	1.4	A
	1	10	19	54.3	58	12.1	138	0.5	49.8	4.5	9	1	181	205	0.26	24.1	98.3	D
	1	18	31	26.0	60	13.2	140	56.6	19.8	1.6	4	3	216	40	0.34	4.9	5.1	C
	2	11	15	10.0	60	38.7	143	9.0	3.2	1.7	7	4	98	62	0.46	1.4	4.3	B
	2	14	32	30.7	60	45.1	143	33.5	13.8	1.6	6	5	89	73	0.25	1.3	2.7	B
	2	17	40	60.0	59	53.4	139	15.1	0.9	2.4	17	7	131	61	0.45	1.7	1.8	A
	3	1	10	34.4	60	14.3	141	53.0	0.0	1.1	8	2	86	25	0.23	1.2	25.0	D
	3	1	57	0.9	59	54.7	141	3.8	1.7	1.7	4	2	213	49	0.40	3.5	6.7	C
	3	10	56	18.8	59	47.5	140	29.6	10.6	0.9	3	3	203	67	0.53	5.6	24.8	D
	3	18	12	9.6	61	22.1	139	4.6	24.0	2.1	7	4	185	156	0.42	9.5	12.9	D
	4	0	37	28.8	60	49.2	139	55.5	32.8	2.0	4	2	272	145	0.48	7.3	99.0	D
	5	16	23	18.3	60	27.9	143	33.5	18.2	1.7	9	7	93	51	0.51	1.7	2.0	A
	5	22	39	24.2	60	50.1	146	49.8	19.1	1.9	26	17	108	29	0.56	0.8	0.6	A
	6	1	59	54.2	61	36.8	141	16.5	0.5	0.9	3	2	260	178	0.09	4.0	7.8	C
	6	3	12	26.0	59	53.6	139	39.5	0.3	1.5	6	4	199	84	0.24	3.7	3.8	B
	6	3	57	51.1	60	4.7	140	12.1	6.0	1.9	11	6	183	62	0.45	2.6	1.4	B
	6	5	59	13.4	60	10.2	140	6.4	4.4	2.0	10	4	196	69	0.26	3.3	2.3	B
	6	7	27	43.3	61	24.5	140	32.4	0.3	2.1	6	3	199	147	0.40	3.3	2.7	B
	6	9	11	22.3	61	2.9	146	18.9	8.8	2.1	22	12	56	45	0.55	0.8	0.9	A
	6	10	53	8.2	60	51.2	147	0.7	11.5	2.7	30	8	71	34	0.63	1.0	0.9	A
	6	13	47	35.8	60	14.4	141	15.1	11.6	1.0	4	3	224	49	0.27	4.8	5.8	C
	7	2	40	47.8	61	5.1	140	52.0	0.6	2.6	18	8	90	102	0.63	1.2	1.6	A
	7	6	8	28.8	60	21.4	141	7.4	2.1	1.3	4	3	210	34	0.51	4.0	67.4	D
	7	9	5	54.4	60	12.6	140	42.6	16.7	2.2	8	5	161	43	0.29	2.0	1.1	A
	7	11	54	26.2	60	6.4	141	14.7	19.5	1.3	3	3	168	55	0.03	11.1	2.9	D
	7	15	24	34.9	60	32.0	142	55.6	4.7	1.9	7	4	130	64	0.47	1.9	2.4	A
	8	13	24	7.0	60	30.2	143	43.6	15.0	1.4	4	1	210	162	0.51	5.0	11.5	D
	8	19	11	19.8	61	35.4	146	33.9	6.7	2.3	23	16	95	61	0.54	0.6	0.9	A
	8	21	48	13.6	60	46.3	140	11.3	13.5	1.9	4	4	259	130	0.05	8.9	6.8	C
	9	5	13	7.9	60	5.9	141	34.0	13.3	1.0	5	3	157	27	0.30	2.6	2.4	B
	9	6	10	16.3	60	39.6	143	7.6	0.1	1.2	5	2	174	60	0.29	2.1	5.2	C
	9	7	54	40.3	60	33.3	142	38.8	23.0	0.8	3	2	153	142	0.29	18.4	10.8	D
	9	17	15	30.7	60	1.1	141	46.8	31.9	1.9	9	4	203	38	0.81	4.5	3.8	B
	9	18	15	41.9	60	41.6	141	3.9	21.9	1.2	4	4	207	80	0.30	2.6	44.9	D
	9	19	31	32.0	60	36.8	141	9.6	2.5	1.3	6	4	193	80	0.36	1.5	13.6	D
	9	20	16	54.9	60	7.8	141	10.3	0.8	1.6	8	4	145	41	0.61	1.4	22.9	D
	9	20	38	52.3	60	11.1	141	7.9	2.8	1.4	10	6	137	35	0.32	1.3	3.0	B
	9	22	32	46.2	60	36.5	141	10.2	0.0	1.4	5	5	192	80	0.40	1.3	4.4	B
	10	9	10	28.6	60	37.7	141	8.8	7.4	3.0	25	13	82	63	0.57	1.2	1.4	A
	10	9	31	39.9	60	17.6	141	6.0	7.5	0.9	5	4	193	37	0.39	5.1	19.4	D
	10	10	7	16.8	60	37.5	141	10.5	6.9	1.1	5	4	191	78	0.24	1.4	3.0	B
	10	19	0	47.0	60	38.8	141	8.8	4.0	2.1	15	10	195	78	0.40	1.2	1.6	A
	10	20	6	24.1	60	12.0	141	10.1	7.6	1.0	5	3	176	51	0.34	4.7	9.4	C
	10	21	57	13.4	61	20.3	146	34.8	19.9	2.0	24	18	75	39	0.48	0.8	0.8	A

SOUTHEAST ALASKA SEISMICITY, SEPT-DEC 1978 (CONT)

1978	ORIGIN HR	MN	TIME SEC	LAT N DEG	MIN	LONG W DEG	MIN	DEPTH KM	MAG	NP	NS	GAP DEG	D3 KM	RMS SEC	ERH KM	ERZ KM	Q
SEP 11	0	22	33.2	60	30.2	143	25.1	3.7	1.3	6	4	156	50	0.32	1.6	17.8	D
11	4	38	57.7	60	9.7	141	1.2	1.4	1.5	11	8	136	34	0.57	1.3	4.7	B
11	14	17	7.7	60	55.9	146	6.7	17.6	2.1	27	17	74	35	0.45	0.8	0.8	A
11	22	30	18.6	61	1.4	138	7.8	15.0	1.7	2	2	277	100	0.00	20.1	16.8	D
12	5	59	56.4	60	4.5	139	49.4	13.3	2.0	5	2	228	92	0.22	9.3	13.8	D
12	7	22	46.6	60	37.7	139	29.9	6.0	1.6	4	0	251	121	0.26	41.9	49.0	D
14	1	27	10.7	61	19.5	146	47.7	27.7	2.5	26	16	77	50	0.46	0.9	1.0	A
15	8	6	8.5	60	3.1	139	57.1	8.3	2.3	5	1	194	161	0.08	18.2	4.4	D
16	1	35	49.2	60	1.8	140	1.0	7.1	2.5	6	5	188	82	0.27	6.1	2.0	C
16	3	16	9.0	60	3.1	139	42.8	15.9	2.4	6	2	122	151	0.26	7.0	4.7	C
16	5	56	36.0	61	36.1	146	18.8	26.3	2.3	17	14	90	57	0.55	0.7	1.0	A
17	5	22	38.1	60	20.5	141	12.0	0.1	1.5	12	7	166	31	0.40	1.1	1.8	A
17	12	34	11.5	60	58.8	147	46.6	20.0	2.4	29	20	110	60	0.43	0.9	1.2	A
17	14	45	9.7	60	18.7	141	58.6	1.5	1.6	7	4	151	55	0.44	1.2	6.3	C
17	15	44	8.0	60	22.8	141	7.0	8.3	1.6	6	3	209	57	0.24	2.9	4.0	B
17	22	51	40.7	60	36.3	142	44.0	10.5	1.9	11	11	89	74	0.46	0.8	1.3	A
18	7	2	49.3	60	29.9	142	58.7	0.7	1.7	9	6	159	69	0.52	1.5	2.6	B
18	7	8	55.9	60	19.5	141	6.3	11.7	1.5	8	5	159	36	0.40	2.1	4.2	B
18	9	38	22.0	60	28.3	142	59.3	0.6	1.6	6	2	197	117	0.35	1.7	3.3	B
18	17	25	20.2	60	30.0	142	56.1	0.5	1.6	8	6	139	68	0.46	2.0	2.5	A
19	8	37	55.4	61	22.4	146	51.8	18.2	3.7	37	2	82	52	0.46	0.9	1.0	A
20	7	20	0.6	61	19.3	143	26.2	13.8	1.7	3	3	174	157	0.16	31.8	13.1	D
20	8	36	29.1	60	44.0	143	18.0	0.3	1.6	4	3	199	84	0.18	3.2	5.4	C
20	12	21	36.7	60	22.2	140	56.7	15.6	2.4	7	4	106	107	0.73	3.3	7.6	B
20	21	3	58.9	60	36.7	142	48.3	17.2	1.7	4	3	141	107	0.17	2.0	1.9	A
21	2	53	7.2	61	53.1	147	57.8	23.8	2.7	25	11	162	70	0.57	1.5	1.4	A
21	20	12	15.7	60	39.8	143	7.5	16.6	1.7	4	3	102	72	0.29	32.8	39.9	D
22	18	9	22.8	60	14.3	141	45.8	10.3	2.6	12	8	99	50	0.44	0.9	1.0	A
23	2	29	22.2	58	7.2	140	22.1	5.0	3.3	12	4	291	202	0.44	38.3	38.5	D
23	6	45	45.1	60	16.1	140	49.4	14.6	1.5	6	4	165	52	0.31	4.7	5.7	C
23	14	16	37.9	60	30.5	142	52.2	2.1	1.7	9	4	82	64	0.62	1.0	2.7	B
23	20	50	34.9	61	29.4	140	26.7	5.0	3.1	9	3	122	144	0.77	3.9	5.3	C
24	6	46	18.3	60	6.0	139	53.8	7.4	1.0	5	1	226	68	0.16	25.2	6.2	D
24	18	1	22.5	60	27.9	142	56.6	1.8	1.3	4	2	128	71	0.10	4.2	20.1	D
25	6	50	28.8	60	4.2	140	38.0	15.6	1.5	9	6	123	40	0.55	2.0	1.0	A
25	10	55	24.5	60	14.5	140	32.2	18.4	1.4	8	5	183	68	0.23	3.6	1.7	B
25	14	44	16.0	59	58.0	141	48.1	11.7	1.8	7	5	195	40	0.37	1.8	2.6	B
25	18	35	14.0	59	59.7	140	48.6	11.3	1.7	5	3	171	33	0.26	2.4	3.2	B
25	20	50	33.7	60	36.2	142	43.9	17.4	1.5	4	5	133	74	0.14	2.5	1.4	A
26	13	2	12.9	60	21.9	142	59.6	1.7	2.0	14	9	99	54	0.33	1.0	3.3	B
26	13	41	15.0	60	15.1	144	51.4	21.8	1.5	8	7	147	47	0.27	3.4	2.6	B
27	2	26	12.7	60	5.0	141	13.7	0.5	1.5	10	6	118	23	0.50	1.5	3.0	B
27	6	56	2.0	60	0.5	140	5.6	19.1	1.5	3	1	177	54	0.05	19.6	12.6	D
27	9	47	44.3	60	0.5	140	6.8	19.3	1.6	3	1	173	55	0.00	17.4	10.6	D
27	14	9	25.9	60	30.2	141	22.6	0.2	0.9	7	6	168	63	0.20	1.1	6.8	C

SOUTHEAST ALASKA SEISMICITY, SEPT-DEC 1978 (CONT)

1978	ORIGIN HR	MN	TIME SEC	LAT N DEG	MIN	LONG W DEG	MIN	DEPTH KM	MAG	NP	NS	GAP DEG	D3 KM	RMS SEC	ERH KM	ERZ KM	Q
SEP 27	19	27	55.0	60	0.3	140	2.7	7.7	1.4	4	1	185	52	0.02	2.9	3.7	B
27	19	53	47.8	59	59.9	140	2.2	7.6	1.5	4	2	184	51	0.17	2.8	2.0	B
27	19	55	39.2	60	4.8	140	19.9	31.6	1.3	3	1	263	70	0.03	10.6	3.3	D
28	1	42	6.0	61	8.8	141	48.8	1.0	2.2	8	3	217	96	0.48	2.8	3.8	B
28	2	33	50.8	59	60.0	140	3.9	6.4	1.7	6	2	179	53	0.20	2.6	2.8	B
28	9	47	9.9	60	12.5	141	16.3	0.2	1.4	5	3	159	31	0.32	2.0	99.0	D
28	13	20	52.6	60	4.9	139	55.4	6.3	1.9	7	4	199	106	0.25	8.4	2.9	C
28	13	30	6.0	60	2.9	139	59.8	9.6	2.2	9	1	191	62	0.15	5.2	2.2	C
30	13	29	22.7	60	13.0	140	41.6	15.9	1.5	7	5	163	60	0.33	5.0	3.0	B
30	15	37	55.0	60	16.0	141	32.3	7.5	1.3	9	4	132	32	0.36	2.0	1.9	A
30	18	31	54.8	59	55.2	140	21.0	0.2	1.4	7	6	160	60	0.41	1.9	4.6	B
30	18	55	12.4	60	28.3	142	56.4	1.9	1.4	4	2	129	71	0.09	4.0	19.1	D
OCT 1	0	16	18.6	61	23.3	146	47.2	24.4	3.1	36	12	82	48	0.40	0.8	1.1	A
1	2	24	22.7	59	59.2	140	5.1	16.8	1.7	10	7	137	27	0.58	1.6	0.9	A
1	9	14	46.4	59	54.0	140	35.3	4.9	1.7	10	6	159	35	0.41	1.2	1.7	A
1	17	39	28.6	59	12.2	139	54.7	17.5	1.1	5	3	243	65	0.20	4.8	4.6	B
2	12	15	26.0	61	26.0	140	18.0	2.5	2.6	11	4	111	143	0.64	4.0	5.1	C
3	11	35	6.9	60	2.6	141	31.5	12.9	3.6	30	3	125	25	0.42	1.4	0.9	A
3	18	30	58.3	60	2.3	141	31.8	12.8	2.5	25	9	127	24	0.46	1.3	0.8	A
3	18	52	10.7	59	57.3	141	37.6	15.3	2.0	8	5	175	46	0.54	2.0	1.5	A
4	2	26	30.8	59	57.8	140	5.9	16.8	1.4	5	3	160	51	0.51	4.5	2.0	B
4	16	25	17.6	59	59.2	140	7.5	15.0	1.9	6	2	158	54	0.41	2.7	1.9	B
4	16	30	27.7	59	57.7	140	7.0	8.6	2.6	8	1	130	51	0.42	2.8	2.7	B
4	17	11	36.0	61	9.8	147	14.7	0.2	2.1	23	4	67	39	0.47	1.0	1.8	A
4	18	20	57.9	60	1.6	140	1.4	16.3	3.3	14	1	160	53	0.55	2.7	1.4	B
4	18	28	30.8	59	57.4	140	8.4	16.0	1.9	6	3	162	53	0.29	4.0	2.4	B
4	18	40	48.0	60	2.2	139	59.5	3.8	2.3	6	1	164	53	0.63	4.5	3.1	B
4	18	42	27.0	59	54.6	140	10.0	7.9	1.7	6	5	167	51	0.47	2.4	2.4	A
4	19	5	19.6	59	59.7	140	4.5	14.8	2.3	8	1	143	53	0.54	2.4	1.4	A
4	19	12	20.8	59	53.4	140	16.3	0.7	2.3	5	2	196	55	0.30	4.0	6.8	C
4	19	15	13.5	59	55.9	140	7.6	15.4	1.8	5	4	188	50	0.44	3.8	1.8	B
4	19	27	22.5	59	54.3	140	13.4	7.6	1.7	5	2	193	53	0.21	2.3	3.3	B
4	19	29	11.7	59	57.0	140	7.4	16.4	1.6	6	2	162	51	0.52	5.0	2.3	C
4	19	29	49.2	59	54.3	140	14.1	0.1	1.8	6	2	169	54	0.12	3.7	5.7	C
4	19	33	46.4	60	0.2	140	3.1	14.1	2.3	9	1	152	52	0.50	2.5	1.4	A
4	19	41	48.3	60	0.8	140	2.0	15.4	2.3	7	2	155	52	0.48	2.8	1.5	B
4	19	44	54.7	59	53.1	140	13.0	1.3	1.0	5	3	171	52	0.26	1.8	4.4	B
4	20	31	14.4	60	5.8	147	23.7	8.7	2.6	24	10	189	99	0.48	1.3	1.2	A
5	1	37	45.0	59	56.8	140	8.2	8.3	2.3	6	1	159	52	0.36	2.8	2.2	B
5	2	54	28.2	59	59.4	140	2.8	11.4	2.2	7	3	146	53	0.36	2.5	1.7	A
5	5	27	37.4	60	32.2	142	56.6	8.7	1.9	3	3	185	92	0.24	4.3	6.9	C
5	11	45	40.8	59	53.4	140	16.8	2.2	2.0	6	3	177	49	0.28	1.9	3.2	B
6	7	46	4.8	61	27.5	146	48.9	24.0	2.2	21	9	89	48	0.42	1.0	1.3	A
7	0	10	4.6	59	59.6	140	6.0	10.4	2.0	7	4	138	54	0.40	2.8	3.2	B
7	0	21	29.1	59	22.4	140	53.3	29.5	1.9	4	4	249	91	0.31	8.8	7.7	C

SOUTHEAST ALASKA SEISMICITY, SEPT-DEC 1978 (CONT)

1978	ORIGIN HR	MN	TIME SEC	LAT N DEG	MIN	LONG W DEG	MIN	DEPTH KM	MAG	NP	NS	GAP DEG	D3 KM	RMS SEC	ERH KM	ERZ KM	Q
OCT 7	9	4	17.5	60	15.0	140	30.3	19.1	1.7	10	7	173	55	0.27	2.9	1.2	B
7	12	6	9.8	60	4.7	139	30.9	15.6	0.6	5	3	208	46	0.12	7.7	3.8	C
7	15	50	20.4	60	2.8	141	31.6	14.6	1.5	7	6	129	28	0.33	2.2	1.8	A
10	3	59	1.2	60	49.4	146	48.4	20.0	2.0	26	12	64	30	0.49	0.9	0.9	A
11	3	43	38.7	61	38.9	146	22.1	19.1	2.3	21	10	92	66	0.39	1.0	2.6	B
12	6	20	40.4	61	5.2	147	0.0	17.0	2.6	20	9	141	86	0.36	1.6	1.4	A
12	12	43	18.4	61	1.3	147	26.5	20.0	2.4	26	8	73	61	0.49	1.1	1.4	A
12	18	31	7.6	61	34.3	146	22.4	22.7	2.6	22	8	91	67	0.32	1.0	1.9	A
12	20	6	57.1	61	36.3	146	19.8	24.5	2.7	21	8	90	68	0.31	1.0	1.8	A
13	6	30	53.7	60	43.3	143	4.3	7.8	2.4	9	5	105	90	0.43	1.3	1.8	A
13	9	8	52.3	60	43.3	143	4.9	6.0	3.1	12	1	105	89	0.46	1.5	2.1	A
13	22	6	38.8	60	40.3	143	2.9	1.1	2.0	7	1	84	75	0.54	1.2	4.0	B
14	4	29	40.7	60	39.2	142	48.9	1.5	1.9	9	7	83	103	0.53	1.3	2.1	A
14	13	36	37.9	60	20.4	140	56.5	12.6	1.8	6	2	170	109	0.28	5.8	8.2	C
14	14	15	1.0	60	41.7	143	15.7	0.6	1.5	6	4	93	68	0.38	1.1	3.7	B
14	19	37	52.8	60	3.3	141	6.2	11.7	1.6	6	2	116	47	0.45	2.8	1.9	B
15	9	19	56.4	59	57.7	141	33.2	13.1	0.8	7	4	168	28	0.37	2.8	4.1	B
15	17	56	27.1	60	18.1	140	57.2	0.4	1.0	6	4	164	106	0.25	2.4	11.8	D
16	3	6	33.6	60	41.1	143	4.7	0.3	1.6	11	6	85	76	0.57	1.0	3.3	B
16	5	15	45.3	60	33.8	141	41.0	10.1	1.4	6	5	158	64	0.18	2.2	2.7	B
16	21	16	28.7	61	16.8	141	32.2	1.1	3.3	21	9	120	103	0.80	1.6	1.6	A
18	8	23	53.7	60	19.9	141	48.0	19.0	1.6	3	1	220	153	0.00	16.8	13.3	D
19	4	49	6.3	61	45.3	147	1.4	14.7	3.0	29	5	133	69	0.58	1.2	1.2	A
19	16	13	14.5	59	49.6	142	11.8	5.0	1.4	3	1	260	159	0.00	8.9	6.0	C
19	17	53	32.7	59	54.8	141	8.8	10.0	1.8	5	2	214	102	0.23	5.7	3.9	C
20	21	44	29.4	60	13.9	141	14.6	12.8	1.2	4	3	139	92	0.14	6.8	7.1	C
21	6	16	12.6	60	45.0	143	44.7	15.5	1.3	5	5	106	77	0.34	2.2	3.1	B
21	18	15	48.9	60	2.8	141	6.9	0.0	1.6	8	4	115	48	0.23	1.5	4.6	B
23	21	15	17.9	59	32.0	139	20.8	6.9	1.9	10	4	220	52	0.58	3.2	2.2	B
23	21	34	49.6	60	39.8	143	5.3	1.4	1.2	4	2	106	74	0.63	2.1	99.0	D
24	16	4	27.7	60	10.2	141	7.9	11.5	1.7	5	1	167	117	0.20	17.4	35.6	D
24	21	14	40.2	59	54.3	141	14.8	9.4	2.2	4	2	200	109	0.27	10.8	5.8	D
25	3	18	46.2	60	7.6	140	33.4	7.0	3.1	14	2	145	83	0.50	3.8	2.5	B
25	5	14	16.2	60	23.5	143	3.3	9.8	1.8	7	4	157	82	0.33	1.1	1.4	A
25	22	2	18.7	59	6.9	147	45.7	12.5	4.1	34	1	169	146	0.24	3.3	2.2	B
26	12	15	30.4	60	32.2	143	4.6	4.3	1.6	4	2	210	108	0.27	3.1	10.1	D
27	4	37	59.9	59	53.1	144	0.9	8.4	2.1	3	1	299	174	0.00	30.6	9.9	D
28	8	48	51.8	60	47.9	145	3.9	12.5	0.6	4	3	210	99	0.10	4.2	4.3	B
28	12	59	33.0	60	37.7	143	6.0	16.8	1.6	4	2	103	72	0.25	63.6	75.9	D
29	5	43	20.8	60	30.7	145	8.8	17.4	1.2	8	5	140	53	0.45	2.1	1.1	A
30	0	39	20.5	61	46.1	141	24.3	9.6	2.7	6	4	165	166	0.56	4.8	4.9	B
30	6	55	39.3	61	56.2	144	28.4	15.5	2.1	4	2	270	91	0.29	5.5	3.6	C
30	13	7	23.2	61	22.6	140	9.2	0.6	2.3	5	5	124	124	0.79	1.4	2.6	B
30	14	4	6.7	59	58.6	141	7.5	0.1	1.4	3	3	189	109	0.16	8.6	3.3	C
30	18	48	21.2	61	1.1	144	20.4	9.8	0.8	3	3	271	100	0.30	17.9	97.4	D

SOUTHEAST ALASKA SEISMICITY, SEPT-DEC 1978 (CONT)

1978	ORIGIN HR	MN	TIME SEC	LAT N DEG	MIN	LONG W DEG	MIN	DEPTH KM	MAG	NP	NS	GAP DEG	D3 KM	RMS SEC	ERH KM	ERZ KM	Q
OCT 31	12	37	55.0	60	28.2	144	55.1	20.6	1.6	3	2	277	124	0.10	11.3	8.7	D
31	16	50	44.4	60	40.1	143	23.3	16.7	1.6	3	2	216	89	0.20	21.8	31.6	D
NOV 1	3	31	29.3	60	16.2	140	58.6	0.0	1.7	5	4	285	114	0.13	4.4	2.7	B
1	15	0	18.3	59	24.5	138	45.8	10.8	3.2	9	1	232	143	0.44	7.3	4.5	C
1	20	6	25.7	61	35.6	140	57.6	1.3	2.2	4	4	179	153	0.55	5.5	3.2	C
2	2	15	41.6	60	27.1	142	56.7	10.3	1.9	4	2	180	74	0.09	3.7	3.5	B
2	8	38	17.4	60	33.5	144	44.5	11.2	0.9	4	3	128	105	0.25	11.2	8.6	D
2	8	39	24.4	60	25.4	144	53.3	16.8	2.0	10	7	106	65	0.45	1.4	1.3	A
2	9	42	34.5	60	35.1	144	45.7	9.8	1.4	4	3	130	106	0.46	3.8	6.4	C
2	10	46	42.8	61	34.1	146	18.9	27.1	2.6	21	9	88	60	0.56	0.9	1.4	A
2	15	22	37.5	60	25.9	142	56.5	24.6	1.8	9	5	99	67	0.30	2.1	1.8	A
3	14	53	41.5	59	57.2	139	6.7	0.9	1.2	3	2	282	215	0.15	4.8	7.2	C
3	18	3	34.5	60	38.7	141	8.5	1.3	1.6	6	5	198	79	0.27	2.1	3.3	B
4	23	43	19.7	60	37.1	142	50.0	3.4	1.7	5	1	127	106	0.16	3.2	8.3	C
5	4	4	40.0	60	39.9	143	25.7	5.0	1.6	3	1	219	89	0.55	2.8	70.2	D
5	7	53	21.1	59	55.9	141	4.3	12.2	1.0	3	2	232	114	0.20	15.9	8.1	D
6	0	48	39.9	59	53.3	140	13.1	7.2	3.0	7	4	175	160	0.53	11.1	13.6	D
6	4	3	48.8	59	52.9	140	4.0	18.4	2.1	3	1	170	179	0.00	42.7	65.5	D
6	4	54	6.1	60	39.4	147	56.3	19.1	2.1	22	11	137	63	0.44	1.0	1.0	A
6	5	30	58.1	59	56.1	140	10.5	8.9	2.7	7	3	167	155	0.30	2.9	1.8	B
6	6	15	17.7	59	58.8	139	59.4	11.0	2.5	3	2	184	175	0.29	18.0	29.6	D
6	6	58	45.3	59	47.7	140	7.1	24.0	3.0	5	2	186	169	0.53	16.6	23.4	D
6	22	17	22.1	60	32.3	147	22.8	14.4	2.9	30	4	70	75	0.43	1.0	1.4	A
7	4	2	22.0	60	34.6	143	4.8	15.0	1.2	3	2	199	104	0.36	65.4	74.4	D
7	13	51	24.5	60	45.5	143	18.2	15.0	1.8	8	5	79	80	0.57	4.0	5.9	C
8	4	28	24.1	60	6.0	139	43.7	5.5	2.3	12	8	127	52	0.32	1.9	2.2	A
8	6	19	40.5	60	42.0	144	43.4	15.4	1.8	10	7	82	67	0.35	1.0	1.3	A
8	12	21	25.9	59	51.9	141	38.9	12.4	1.5	3	3	262	93	0.27	34.7	92.8	D
9	19	21	9.8	60	10.4	139	43.8	0.2	1.6	6	5	218	51	0.11	4.0	6.2	C
9	19	53	56.2	60	3.1	140	51.0	0.1	1.7	5	3	264	36	0.41	4.8	25.0	D
9	21	34	26.2	60	48.2	146	52.7	19.0	2.2	23	13	70	64	0.40	1.0	1.2	A
9	23	2	24.7	60	29.5	141	20.9	1.4	1.7	7	5	168	63	0.24	1.4	6.7	C
9	23	17	21.9	60	30.2	141	20.8	2.5	1.8	11	6	169	64	0.20	1.5	3.5	B
9	23	43	37.5	60	30.0	141	21.1	0.5	1.4	8	5	169	64	0.17	1.2	10.5	D
10	4	6	22.7	60	33.2	142	56.8	0.5	2.3	15	9	76	69	0.51	1.1	1.6	A
10	5	46	28.7	60	11.4	140	48.6	22.4	1.4	5	3	150	98	0.17	4.3	3.7	B
10	7	19	55.4	60	14.9	140	41.2	26.2	1.2	4	2	171	122	0.18	11.1	2.6	D
10	14	41	3.1	60	27.4	145	6.6	16.1	2.1	13	5	137	73	0.47	2.0	1.3	A
10	16	3	3.0	60	4.9	139	29.1	9.2	0.8	3	2	262	46	0.14	11.3	14.7	D
11	0	6	27.9	60	24.5	140	56.5	17.5	1.7	7	5	180	51	0.34	2.0	1.9	A
11	1	19	53.9	60	41.7	143	0.6	7.9	2.1	13	9	77	79	0.44	1.2	1.6	A
11	14	50	48.8	61	40.8	141	17.5	11.1	2.7	6	6	156	136	0.78	1.8	1.7	A
11	22	0	19.4	59	55.9	140	13.2	13.7	1.4	3	3	231	55	0.11	7.5	15.4	D
11	22	50	26.5	59	56.5	139	12.5	0.4	1.9	5	6	254	61	0.23	5.6	5.1	C
12	14	17	52.2	60	3.7	139	31.4	9.3	0.7	3	2	255	44	0.15	13.7	13.7	D

SOUTHEAST ALASKA SEISMICITY, SEPT-DEC 1978 (CONT)

1978	ORIGIN HR	MN	TIME SEC	LAT N DEG	MIN	LONG W DEG	MIN	DEPTH KM	MAG	NP	NS	GAP DEG	D3 KM	RMS SEC	ERH KM	ERZ KM	Q
NOV 12	23	7	11.2	60	36.8	141	20.4	17.5	1.3	6	3	193	62	0.43	3.2	2.9	B
13	3	55	11.5	60	12.4	141	32.7	10.9	1.9	10	5	125	28	0.40	1.3	1.1	A
13	4	11	19.2	60	9.1	140	31.3	15.1	1.2	5	3	188	53	0.26	3.7	1.1	B
14	2	52	41.3	59	39.1	141	4.8	6.4	1.6	4	5	331	88	0.42	7.4	2.6	C
14	3	22	24.1	59	58.3	140	4.4	13.8	0.7	4	1	168	51	0.23	4.1	5.6	C
14	4	16	24.8	60	6.6	139	21.7	2.6	1.4	5	2	240	59	0.42	7.0	17.8	D
14	6	5	0.3	60	33.7	143	2.8	0.9	1.1	3	1	146	71	0.02	3.9	98.9	D
14	9	52	13.5	61	6.7	147	13.7	19.9	3.2	23	4	100	115	0.31	1.8	1.7	A
14	16	17	23.2	59	34.7	140	18.7	1.1	0.8	3	2	246	198	0.08	5.2	18.6	D
15	5	55	59.6	60	14.8	140	30.2	19.5	1.9	4	1	189	134	0.05	67.8	72.1	D
15	5	57	55.6	60	21.4	140	31.3	0.3	2.1	8	3	206	67	0.25	2.4	6.3	C
15	7	24	28.7	60	37.8	142	57.6	0.6	1.3	3	1	151	79	0.04	2.6	99.0	D
15	8	2	26.8	60	42.3	143	5.1	13.5	1.3	3	2	190	91	0.18	15.9	16.1	D
15	8	51	3.4	60	25.8	142	55.1	7.0	1.4	3	2	203	75	0.11	10.5	10.8	D
15	10	4	32.3	60	9.3	141	9.5	10.7	1.3	6	4	131	40	0.40	2.4	2.3	A
17	3	28	53.6	60	13.6	141	12.1	10.9	1.3	6	3	140	34	0.36	5.0	6.5	C
17	5	53	35.1	60	33.1	143	15.9	0.1	2.2	22	10	78	60	0.38	0.9	1.6	A
17	6	17	20.0	60	55.4	147	31.1	19.9	2.4	27	10	52	45	0.44	0.9	1.0	A
17	8	2	28.7	60	30.1	143	15.0	0.4	1.1	3	2	148	77	0.11	2.4	99.0	D
17	8	27	22.3	60	13.2	140	37.1	18.4	1.7	7	5	171	64	0.19	4.1	1.4	B
17	10	53	54.8	60	30.1	143	14.2	0.4	1.4	7	2	147	77	0.10	1.7	4.9	B
17	13	42	45.4	60	21.6	140	50.1	0.2	1.6	13	6	172	58	0.50	1.4	2.7	B
17	17	43	9.5	58	39.9	140	34.8	22.1	2.5	5	4	296	160	0.29	24.2	34.1	D
17	23	31	11.6	60	33.1	144	55.0	15.9	1.6	11	7	87	79	0.36	1.3	1.2	A
18	2	17	16.7	60	0.1	140	19.3	25.4	0.7	3	2	219	64	0.05	7.2	5.7	C
18	4	15	55.9	60	13.4	139	39.3	0.5	1.4	4	4	249	64	0.16	2.7	3.3	B
18	4	32	7.0	60	6.4	140	1.9	2.5	2.0	11	5	178	39	0.38	2.7	2.6	B
18	4	49	33.5	60	9.3	141	44.2	8.3	0.9	5	3	125	23	0.15	1.4	3.9	B
18	9	14	18.2	59	23.9	139	53.8	31.3	2.0	6	4	258	63	0.19	5.4	2.2	C
18	21	1	12.6	60	8.5	141	3.8	11.5	1.7	12	5	132	31	0.60	1.3	1.2	A
18	22	4	46.6	59	24.5	139	48.9	30.8	1.5	4	1	295	61	0.05	12.9	2.8	D
19	0	32	23.3	60	39.0	143	1.7	15.6	1.8	5	3	116	76	0.44	3.2	4.0	B
19	4	30	1.9	60	46.3	143	2.0	14.8	1.4	2	2	279	100	0.11	58.5	79.9	D
19	9	53	20.0	60	10.4	141	12.1	14.5	1.6	7	1	132	37	0.32	2.8	1.6	B
19	19	48	34.3	60	38.6	138	57.4	1.0	2.5	8	1	183	108	0.52	2.3	4.0	B
19	20	47	42.6	60	37.7	142	41.0	23.3	1.9	4	3	129	86	0.15	3.5	5.0	B
20	5	14	21.6	60	36.3	143	14.2	2.3	1.3	3	3	163	68	0.17	4.6	81.8	D
20	9	46	18.1	60	15.0	141	7.2	1.5	1.2	7	3	147	51	0.52	1.7	14.2	D
20	22	29	21.5	60	5.1	139	33.7	0.3	1.6	5	4	224	47	0.15	3.6	4.2	B
21	17	56	30.9	60	22.3	140	11.2	4.9	1.9	11	6	204	62	0.34	2.8	4.9	B
22	20	46	12.0	60	13.3	139	40.4	0.6	1.0	4	3	232	172	0.11	2.8	3.5	B
22	21	12	0.9	60	6.5	139	46.8	0.3	1.9	4	3	207	174	0.06	12.7	7.6	D
23	12	11	57.4	60	26.5	140	54.9	11.4	1.6	3	3	226	107	0.03	5.9	10.1	D
24	4	36	53.1	59	57.4	140	44.2	9.8	1.2	3	2	235	130	0.05	8.3	3.7	C
24	4	39	13.0	61	31.1	140	58.5	0.9	2.4	5	4	259	151	0.38	2.7	2.5	B

SOUTHEAST ALASKA SEISMICITY, SEPT-DEC 1978 (CONT)

1978	ORIGIN HR	MN	TIME SEC	LAT N DEG	MIN	LONG W DEG	MIN	DEPTH KM	MAG	NP	NS	GAP DEG	D3 KM	RMS SEC	ERH KM	ERZ KM	Q
NOV 24	8	9	46.8	59	57.8	140	5.9	7.1	2.0	8	4	145	51	0.36	2.5	2.0	B
24	8	12	1.8	60	3.2	140	3.5	0.8	2.2	14	3	164	33	0.63	2.7	1.8	B
24	8	14	45.2	59	57.3	140	7.2	4.3	1.5	7	3	117	28	0.33	1.8	2.3	A
24	8	18	5.6	59	55.7	140	12.8	0.4	1.4	4	1	170	54	0.13	2.7	6.1	C
24	10	59	35.5	60	28.5	143	0.6	9.4	1.6	3	2	150	72	0.23	7.4	13.6	D
24	15	32	36.3	60	34.6	142	43.8	10.0	2.1	12	3	89	59	0.38	1.2	1.7	A
24	17	25	18.2	60	7.9	141	10.9	9.5	1.1	4	2	223	48	0.18	5.7	3.3	C
24	17	39	34.7	59	58.2	140	43.6	10.2	1.7	6	3	180	46	0.19	3.0	2.2	B
24	20	50	39.8	59	44.9	139	50.9	14.6	1.0	4	3	166	27	0.18	1.4	4.6	B
25	2	41	58.3	61	22.5	146	43.3	19.7	2.8	27	10	80	45	0.61	1.8	1.6	A
25	9	35	14.5	60	21.0	139	51.3	0.5	1.3	4	1	304	93	0.03	7.6	16.4	D
25	18	55	37.5	59	56.1	140	45.4	11.1	2.9	19	4	149	39	0.35	3.3	3.0	B
25	19	0	28.6	59	45.4	140	54.6	15.0	0.8	3	2	280	54	0.08	27.3	72.7	D
25	19	27	20.0	60	19.3	141	4.4	15.0	1.4	3	2	251	52	0.21	20.6	31.7	D
25	20	31	2.0	60	38.0	141	9.1	2.6	0.6	6	2	196	63	0.20	5.2	99.0	D
25	21	30	35.0	60	7.6	139	37.1	0.0	1.1	5	3	222	53	0.22	8.3	6.7	C
25	22	19	35.5	59	46.8	140	49.8	9.7	1.4	5	3	261	54	0.13	7.7	5.0	C
26	13	8	56.1	60	2.5	141	19.0	0.0	0.8	6	4	133	43	0.20	3.7	9.1	C
26	19	18	16.6	60	21.4	141	8.6	11.8	1.1	3	2	204	95	0.09	27.4	81.0	D
26	20	19	6.6	60	32.2	142	55.2	0.2	1.6	14	8	94	67	0.56	1.0	2.7	B
26	21	21	49.7	60	30.2	143	29.0	0.1	2.3	16	12	89	50	0.39	0.9	1.5	A
27	12	51	24.0	60	8.8	141	34.3	0.2	1.2	5	2	206	108	0.35	20.2	11.0	D
27	16	50	4.7	60	35.7	142	44.2	1.1	1.7	3	3	216	148	0.25	7.8	13.0	D
28	3	28	37.9	60	26.0	141	42.5	3.6	0.3	5	2	142	63	0.13	7.3	18.2	D
28	16	41	50.8	61	29.8	146	21.0	22.4	2.9	30	10	81	50	0.56	1.1	1.8	A
29	3	51	50.3	60	8.2	141	6.9	16.4	1.4	8	3	129	43	0.23	3.9	2.1	B
29	11	24	14.8	60	39.2	143	7.0	16.6	1.3	5	2	103	72	0.26	65.0	74.7	D
29	13	37	31.5	61	54.9	144	5.4	9.7	2.0	8	3	252	101	0.26	5.6	4.1	C
30	15	19	10.4	61	22.0	140	59.2	1.0	2.8	13	3	229	138	0.42	8.3	4.4	C
30	23	19	40.0	60	1.3	140	23.3	8.8	0.8	4	1	152	68	0.09	8.3	10.6	D
DEC 1	6	58	0.2	60	12.4	141	16.8	13.6	1.3	6	3	134	31	0.14	4.2	3.5	B
1	7	37	6.9	60	1.0	141	28.7	13.7	2.0	8	0	137	21	0.33	2.1	1.6	A
1	10	50	24.3	60	39.7	147	39.6	14.6	2.0	19	10	84	59	0.39	1.3	1.0	A
2	13	51	39.8	61	43.6	147	26.3	17.7	1.9	21	10	137	64	0.39	1.2	1.3	A
2	14	41	43.3	60	40.1	142	58.1	11.9	2.2	9	4	117	75	0.34	1.5	2.0	A
3	15	18	59.5	60	42.0	147	9.9	20.6	2.4	29	8	88	52	0.41	1.3	1.6	A
4	13	27	52.2	60	39.1	143	1.3	0.1	1.5	5	2	158	77	0.32	1.9	5.1	C
4	20	32	51.9	61	28.5	140	56.2	4.8	2.3	3	2	289	158	0.17	10.1	9.5	D
5	8	28	24.3	60	14.2	142	8.5	14.2	1.2	5	4	193	46	0.23	1.8	2.0	A
5	14	26	39.3	59	36.9	139	1.5	0.0	1.1	4	2	328	87	0.14	7.1	22.3	D
5	17	37	18.9	59	49.5	140	50.6	4.8	1.5	3	2	255	132	0.12	11.1	7.4	D
5	20	32	44.8	60	5.9	139	31.4	0.2	2.7	7	0	250	48	0.21	8.9	7.2	C
5	21	29	4.3	59	53.0	140	53.0	12.5	1.8	4	1	194	87	0.07	9.6	4.6	C
6	2	46	45.7	60	7.6	141	8.7	14.7	1.8	9	5	127	50	0.51	3.5	1.0	B
6	7	2	6.0	60	33.2	147	22.3	19.8	2.2	22	10	173	63	0.37	1.5	2.5	B

SOUTHEAST ALASKA SEISMICITY, SEPT-DEC 1978 (CONT)

1978	ORIGIN HR	MN	TIME SEC	LAT N DEG	MIN	LONG W DEG	MIN	DEPTH KM	MAG	NP	NS	GAP DEG	D3 KM	RMS SEC	ERH KM	ERZ KM	Q
DEC 6	23	42	42.1	60	36.4	143	11.7	15.0	2.0	5	2	171	99	0.31	33.8	41.5	D
7	2	6	28.5	60	15.5	141	0.6	16.3	1.5	6	4	153	42	0.30	2.5	2.4	A
7	5	28	7.1	60	37.8	143	18.7	4.8	1.5	4	1	141	69	0.06	8.1	88.1	D
7	6	55	51.4	61	46.8	147	5.5	15.4	2.2	21	11	140	70	0.51	1.3	1.3	A
7	17	56	10.2	60	35.7	142	49.5	15.0	2.6	3	0	218	153	0.00	77.5	61.6	D
8	17	14	58.0	60	12.9	141	11.2	8.9	1.9	7	4	139	53	0.34	3.4	3.6	B
8	17	15	59.1	60	13.9	141	9.8	3.8	1.6	5	3	142	96	0.26	2.8	6.7	C
9	5	14	1.6	60	10.8	141	3.8	11.6	1.7	9	6	138	35	0.38	1.8	1.3	A
9	13	46	22.4	60	12.0	139	36.8	1.7	0.8	4	2	250	60	0.04	2.8	8.4	C
10	1	51	24.4	60	28.4	142	52.9	0.1	2.1	7	4	124	119	0.53	2.0	3.3	B
10	4	23	29.5	61	28.3	140	50.8	0.2	2.6	5	4	259	157	0.34	3.6	2.2	B
10	5	25	42.9	61	24.3	146	42.0	30.2	2.6	28	5	82	43	0.40	1.1	1.1	A
10	10	26	19.8	61	38.3	146	36.6	19.9	3.6	31	0	102	58	0.51	1.0	5.4	C
10	13	26	42.2	61	11.9	140	42.3	2.2	2.5	8	2	249	124	0.22	5.7	3.1	C
10	18	49	30.8	61	31.3	141	28.2	0.9	2.0	5	1	252	130	0.19	6.9	6.3	C
11	2	33	30.4	61	20.1	147	9.4	14.2	2.4	26	7	81	50	0.48	0.9	0.9	A
11	5	7	35.3	60	4.9	139	37.8	16.9	0.7	3	2	251	48	0.08	9.9	5.2	C
11	8	29	30.8	60	32.7	143	6.1	16.6	1.3	4	3	123	69	0.15	3.4	6.3	C
12	13	56	41.5	60	20.1	141	12.5	15.7	1.5	5	2	155	59	0.11	3.1	2.0	B
12	15	20	27.0	60	32.0	143	6.9	1.2	2.4	17	9	94	70	0.36	1.1	1.7	A
12	18	5	54.4	60	3.3	147	56.9	7.0	2.6	22	4	151	92	0.46	1.6	1.4	A
12	20	37	10.1	60	5.9	141	9.4	13.1	1.2	4	2	138	50	0.14	11.2	4.7	D
13	1	29	46.4	60	44.0	144	27.4	13.1	2.1	7	6	126	93	0.57	1.1	1.3	A
14	6	23	29.3	60	3.1	139	31.5	8.9	1.2	3	1	254	43	0.00	12.6	11.9	D
14	8	52	41.8	60	21.8	141	5.9	1.0	0.9	3	1	165	101	0.36	3.9	99.0	D
15	7	41	17.5	60	12.1	147	33.0	12.0	2.7	27	4	90	81	0.37	0.9	1.1	A
15	17	45	49.7	60	26.0	140	18.2	16.5	2.2	4	1	208	130	0.03	16.5	6.8	D
16	9	27	30.6	60	31.7	143	2.6	7.8	1.7	4	2	123	70	0.18	3.9	14.4	D
17	19	16	40.4	60	15.3	141	42.9	3.6	1.9	7	3	124	66	0.31	1.8	3.4	B
18	17	3	57.3	60	26.2	140	53.6	15.0	1.6	5	4	187	104	0.46	4.6	6.7	C
18	18	32	26.2	61	19.2	147	1.7	22.0	2.3	18	9	79	48	0.39	1.0	1.6	A
19	10	45	30.2	60	6.0	141	1.0	6.0	1.2	4	3	172	127	0.32	13.3	15.9	D
19	13	37	33.2	59	29.3	140	20.6	0.3	1.4	4	2	238	176	0.06	13.5	10.6	D
19	17	43	15.6	60	39.8	143	3.0	15.9	1.1	4	2	113	76	0.48	62.7	76.7	D
20	8	45	35.7	60	8.8	139	31.4	0.4	1.0	3	1	252	187	0.04	14.0	18.3	D
20	19	19	19.7	59	38.9	141	24.0	2.0	1.8	3	1	244	121	0.15	26.9	29.2	D
20	21	30	57.8	60	15.6	141	33.9	1.0	1.7	11	5	130	75	0.32	3.1	3.9	B
21	2	10	39.7	60	12.2	141	21.8	12.1	1.3	3	2	131	107	0.17	27.7	24.3	D
21	15	15	56.9	60	0.7	141	6.6	13.0	1.8	8	3	109	48	0.43	1.9	1.4	A
21	17	15	27.8	60	37.4	142	46.5	10.6	2.3	15	7	86	77	0.41	1.1	1.4	A
21	17	53	47.5	61	26.2	146	42.8	19.9	2.7	26	6	85	43	0.34	1.1	1.4	A
22	0	39	22.4	60	20.6	141	12.0	9.8	2.3	11	5	157	57	0.48	1.8	1.5	A
22	6	35	6.0	60	39.2	141	22.9	9.3	2.2	10	6	186	84	0.21	2.0	1.8	A
22	14	43	48.2	59	59.5	140	45.3	0.3	2.1	6	3	166	84	0.28	3.0	3.3	B
24	5	56	1.2	59	50.9	141	14.9	0.3	1.4	5	1	187	112	0.33	8.4	15.2	D

SOUTHEAST ALASKA SEISMICITY, SEPT-DEC 1978 (CONT)

1978	ORIGIN HR	ORIGIN MN	TIME SEC	LAT N DEG	LAT N MIN	LONG W DEG	LONG W MIN	DEPTH KM	MAG	NP	NS	GAP DEG	D3 KM	RMS SEC	ERH KM	ERZ KM	Q
DEC 24	9	33	25.4	60	30.6	142	58.6	0.2	1.4	7	6	120	73	0.24	2.1	5.5	C
25	6	19	8.2	60	16.6	140	59.6	0.0	1.8	5	4	157	112	0.10	6.3	5.9	C
26	1	2	44.5	60	3.0	141	36.5	7.9	1.8	8	3	134	29	0.43	2.2	2.1	A
26	7	54	48.4	60	18.6	140	53.4	1.1	2.3	12	2	169	52	0.62	1.6	2.4	A
26	16	25	57.7	60	8.5	140	40.1	22.4	1.6	4	2	176	89	0.19	5.0	2.3	C
27	3	43	58.0	60	26.5	141	16.1	3.8	2.0	8	4	214	68	0.31	2.8	2.1	B
27	11	56	11.2	60	13.3	141	1.4	10.2	1.3	5	3	184	71	0.23	6.0	4.0	C
28	5	8	39.9	61	23.4	147	11.1	19.2	2.4	20	6	49	54	0.39	1.1	3.4	B
28	13	54	24.3	59	52.8	141	1.8	7.6	1.4	4	3	225	119	0.13	5.7	3.7	C
28	14	8	15.4	61	36.1	146	28.7	17.4	2.3	15	7	81	58	0.50	1.0	1.2	A
28	19	49	1.3	61	54.1	144	7.1	12.8	2.1	5	3	251	99	0.20	2.4	1.9	A
28	22	29	52.6	60	50.8	146	49.4	19.3	2.5	24	7	113	28	0.49	1.0	0.7	A
29	2	26	16.3	60	8.7	141	9.1	1.3	1.3	8	5	130	50	0.52	2.9	7.3	C
30	2	59	25.9	60	38.0	143	5.5	16.5	1.0	3	3	190	72	0.37	63.7	75.8	D
30	7	49	42.5	59	56.0	140	33.6	11.8	0.9	4	1	180	140	0.22	20.9	25.4	D
30	10	30	30.3	60	15.0	141	35.0	0.4	0.9	5	2	128	76	0.45	4.6	14.2	D
31	9	22	27.2	60	58.3	147	21.5	4.4	2.0	17	9	100	49	0.34	1.0	2.0	A

APPENDIX II

ABSTRACT SUBMITTED TO SSA FOR SPRING 1979 MEETING

Aftershocks of the St. Elias, Alaska, Earthquake of 28 February 1979

J. C. Lahr, R. B. Horner, C. D. Stephens, K. A. Fogleman, G. Plafker

On 28 February 1979 an earthquake with surface wave magnitude (M_s) of 7.7 occurred beneath the Chugach and St. Elias mountains of southern Alaska. This region is one of complex tectonics that is located between the northwest-trending Fairweather fault and the southwest-trending Aleutian megathrust. Based on preliminary analysis of USGS and Canadian short-period seismic data from the region the parameters of the hypocenter are: 60^{o} 37.2 N, 141^{o} 30.5 W and depth 15 $\pm$ 10 km. P-wave first motions from both teleseismic and local stations give good control for what is interpreted to be the auxiliary nodal plane, with strike N 81^{o} E and dip 82^{o} SSE. The fault plane, although poorly determined, must have a shallow dip, probably to the northwest. The aftershock locations indicate that the rupture surface extended only over the eastern part of a zone previously identified as a seismic gap for large earthquakes. If simple application of the gap hypothesis is appropriate in this area, then a gap still remains between about Icy Bay and Kayak Island. The focal mechanism, aftershock locations, and extrapolated refraction data together indicate that this earthquake may be due to underthrusting of the Pacific oceanic plate beneath the region.

APPENDIX III

THE ST. ELIAS, ALASKA, EARTHQUAKE OF 28 FEBRUARY 1979: AFTERSHOCKS AND REGIONAL SEISMICITY

C. D. Stephens
R. B. Horner*
J. C. Lahr
K. A. Fogleman (all at: U.S. Geological Survey, Menlo Park, CA 94025)
(*Earth Physics Br., Dept. of Energy, Mines, and Resources, Ottawa, Canada K1AOY3)

The magnitude 7.7 (Ms) earthquake of 28 Feb. 1979 in southeastern Alaska occurred in a region of complex tectonics dominated by north-south compression. This is a region of transition from predominantly strike-slip motion on the Fairweather fault along the east to subduction at the Aleutian megathrust to the west. Analysis of seismic data since 1974 from the USGS regional network suggests that the regional compression is accommodated both by underthrusting by the Pacific plate on a plane dipping at a low angle to the NNW and by reverse faulting at shallower depths on nearly vertical, east-west trending planes. The combination of these two types of deformation may explain the generally diffuse distribution of epicenters found in this region. Short-period seismic data from USGS and Canadian regional stations are being used to monitor aftershock activity from the 28 February earthquake. Preliminary results to date for 124 aftershocks indicate that, for at least the first week following the main shock, most of the larger aftershocks occurred in a zone extending from about 50 to 100 km southeast of the epicenter of the main shock. The two largest aftershocks had magnitudes of 5, and one was located around 20 km SE of the main shock. Although depth control for shallow earthquakes is poor with the present station geometry, most of the aftershocks were located at depths less than 25 km. Together with a focal mechanism for the main shock determined from P-wave first motions, the distribution of aftershocks has been used to infer a low-angle thrust to the NNW as the primary rupture mechanism of the main shock. Associated activity on the steeply-dipping faults cannot be precluded without a careful evaluation of the data.

APPENDIX IV

Lahr, J.C., George Plafker, C.D. Stephens, K.A. Fogleman, and M.E. Blackford (1979). Interim Report on the St. Elias, Alaska Earthquake of 28 February 1979, U.S. Geological Survey Open-File Report 79-670. 35 pp.

Attention is called to the following reference:

Carlson, Paul R. (1978). "Holocene Slump on Continental Shelf Off Malaspina Glacier, Gulf of Alaska," The American Association of Petroleum Geologists Bulletin, Vol. 62, No. 12, pp 2412-2426.

ANNUAL REPORT

Contract Number: 03-5-022-55
Research Unit Number: 250
Task Order Number: 11
Reporting Period: 4/1/78-3/31/
Number of Pages: 59

MECHANICS OF ORIGIN OF PRESSURE RIDGES, SHEAR RIDGES AND HUMMOCK FIELDS IN LANDFAST ICE

Lewis H. Shapiro
Howard F. Bates
William D. Harrison

Geophysical Institute
University of Alaska
Fairbanks, Alaska 99701

May 1979

I. SUMMARY OF OBJECTIVES, CONCLUSIONS AND IMPLICATIONS

The present stage of this project has two objectives. The first is directed at the study of overriding and ridging along beaches and barrier islands. In previous years, most of the work toward this objective has been in connection with movements during break-up. However, during the winter of 1977-1978 a series of overrides occurred on the beach at the village of Barrow, at Point Barrow, and along the barrier islands which form the northern boundary of Elson Lagoon. These were studied in the field, and the resulting descriptions of the events and features are reported here. These are of interest because they include descriptions of the complete override of two barrier islands along relatively wide fronts, an event which has not previously been reported in the literature. This is important for OCS development because of the anticipated use of artificial gravel islands and barrier islands as drilling platforms during both the exploration and production phases. The potential for override is a major hazard to the use of such structures and understanding the processes through which override of natural beaches and islands occurs may provide a basis for designing structures to minimize the threat of such events.

The second phase of the study is an investigation of the relationship between long-period vibration of the ice sheet and the occurrance of relatively high levels of compressive stress. As described in previous reports, this association has been observed on several occasions, and a preliminary analysis was given in the last annual report of this project. A final version of the analysis of the problem for the elastic case is included here. The viscoelastic case will be considered in future. This

study gives promise of leading to results which are of importance for OCS development, in that it may provide the basis for an early warning system through which the build-up of stress may be predicted for a period of up to several hours prior to the peak stress being reached. This can be used to provide ample time for appropriate safety measures to be taken to protect drilling and transportation operations.

II. INTRODUCTION

A. Scope of the Study and Relevance to Petroleum Development

This project is concerned with the mechanisms and processes involved in the deformation of landfast ice, including ridging, hummocking, and interaction with beaches and with the sea floor.

The major emphasis of the project to date has been on the study of overrides of beaches and barrier islands during both the break-up period and mid-winter periods. The potential for override of structures, barrier islands and beaches is recognized as a signficant hazard to OCS development. However, it had previously been considered primarily in connection with the freeze-up and break-up periods when the ice is generally more mobile than during the winter months. In particular, the break-up period was considered to present the greater hazard because the ice is still relatively thick and yet ductile due to the warm temperatures. In this state it is flexible, and capable of bending through relatively large angles without failing and piling into ice push ridges. In contrast, movements during freeze-up generally involve thinner, colder ice, which is brittle and will generally fail and pile along beaches more readily. However, during the winter of 1977-1978, a series of ice push ridges and overrides of barrier islands were observed. These formed in late-

December at the village of Barrow, and (probably) in late-January along the barrier island which form the northern boundary of Elson Lagoon. This falls within the period which has generally been considered safe for operations and indicates that the potential for large ice movements close to shore during this time cannot be dismissed and must be considered in operating regulations and desgin considerations.

The study of ice sheet vibration forms the second object of this project. In particular, observations suggest that there is an association between rising compressive stress levels in the ice and the occurrence of vibrations with periods on the order of several minutes. If verified, this may provide a relatively simple and inexpensive method of monitoring the build up of stress in the pack ice which may ultimately be transmitted to the landfast ice. As such, it would become an operational tool for providing early warning of potentially hazardous conditions.

Finally, a cooperative study of ice gouging in the Barrow area is in progress, with P. Barnes of the U.S.G.S. The purpose of the study is to gather data on the rate of ice gouging in the sea floor through repeated side-scan sonar surveys. The University of Alaska sea ice radar system is being used to monitor ice motion in the survey area to aid in interpretation of the side-scan sonar data. The hazard which gouging presents to offshore operations is well-known and the study of gouging rates in progress will provide additional information which is required on that subject.

III. CURRENT STATE OF KNOWLEDGE

The current state of knowledge regarding the problems above has been reviewed in previous annual reports and will not be repeated here.

IV. STUDY AREA

The site of most of the field work is the Naval Arctic Research Laboratory at Barrow. Studies are also done in other areas as required.

V. SOURCES, METHODS AND RATIONALE OF DATA COLLECTION

Data for this project comes from field study, interpretation of radar data and from side-scan sonar surveys. Details are given in previous annual reports.

VI. RESULTS

Results for the present year are presented in the two reports which follow. The first, regarding override of the barrier islands and the ice push events in the Barrow area, was presented at the annual meeting of the Northwest Section of the American Geophysical Union in September 1979. The second on wave propagation in a floating ice sheet has been submitted for publication to the Journal of Geophysical Research.

ICE-PUSH AND ICE OVERRIDE IN THE POINT BARROW, ALASKA REGION

by

A. Hanson
NARL, Barrow, Alaska

R. Metzner
L. Shapiro
Geophysical Institute
University of Alaska
Fairbanks, Alaska 99701

I. INTRODUCTION

Ice push along Arctic and sub-Arctic beaches has been of interest for many years in studies of ice as an agent in shaping beaches, and for general information on the pressure which ice can exert against coastal structures. Numerous examples of damage to such structures resulting from ice push events, are documented in the literature. The study of processes associated with ice push has recently received new impetus as the result of the impending exploration for hydrocarbon deposits on the continental shelf of the Beaufort and Chukchi Seas. In particular, it is anticipated at present that for the initial stages of offshore exploration and development most drilling will be conducted from natural or man-made gravel islands. Ice push and ice override of such islands presents a major hazard to their use for this purpose, a hazard which can be minimized by proper design based upon an understanding of the process.

Five ice-push ridges formed in the Point Barrow area during the winter of 1977-1978, and the description of these forms the bulk of this report. The locations are shown in Figure 1. Two of these (Tapkaluk

and Igalik Islands) involved complete override of the barrier islands along wide fronts. Damage occurred only at the village of Barrow, where a power line along the coast was toppled. The remaining sites were unoccupied.

All of the sites were visited during the course of the study, and each site, except Point Barrow, was photographed from the air both in winter and during the melt season.

II. DESCRIPTION OF THE EVENTS

The ice push at Barrow village occurred as a series of discrete movements over a period of about 12 hours on December 30, 1977. Weather conditions at the time are shown in Figure 2, an infra-red image of the Chukchi and western Beaufort Seas acquired by a NOAA weather satellite at 1219 hrs local time on December 30. Data from previous days shows that the storm located northeast of Point Barrow had moved to that position along a generally northeasterly track off the west coast of Alaska. Peak winds associated with its passage reached 21 m/sec from the south-southwest at 0600 hrs on December 30. Note that the circulation around the storm would tend to drive the pack ice toward the coast from the west and southwest with a fetch on the order of hundreds of kilometers. Similar weather conditions have been associated with ice push events at Barrow in late Spring. Similarly, the winds associated with the passage of the storm would tend to drive the ice off the coast east of Point Barrow, and the leads in that area as shown in Figure 2 are probably the result of this effect. As described below, the closing of this lead system was probably responsible for the overrides and ice piles along the barrier islands.

The area of the ice push at the village of Barrow is shown in Figure 3. The major ice push associated with the prominent shore ice piles along the beach occurred along a front about 725 m wide, with additional minor movements along the beach for 1 km to the south and 2 km to the northeast. The thrust sheet of the major movement is bounded by fractures trending offshore, both of which appear to terminate at ridges about 700 m from the beach. The latter ridges occur along a line which is sub-parallel to the shore and a smaller ridge connecting them, but slightly offset shoreward, is visible on the thrust sheet. The large ridge just south of the thrust sheet was examined and found to be comprised of blocks of brash ice consisting of rounded fragments of ice of varying sizes in a matrix of finer-grained ice. This is characteristic of ice found in shear ridges and associated shear zones (Weeks, et al., 1971; Shapiro, 1975).

The irregular fracture which bounds the northeast margin of the thrust sheet is marked by several small pressure ridges. In addition, some buckling of the ice sheet was also observed along this line. In contrast, the southwestern boundary of the thrust sheet is a sharp, smoothly curving fracture with only minor deformation along its trace and trending toward tangency with the beach.

Based upon the observations described above, it can be deduced that the motion of the thrust sheet was parallel to the smooth crack along its southwestern boundary, with resulting high normal stress components across the northeast boundary. The latter caused the ridging and buckling along that line. Outside the limits of the thrust sheet, the motion of the advancing pack ice was taken up primarily by the formation of pressure

ridges along the line of the pre-existing shear ridge so that only minor advance of the ice up the beach occurred. The ice in the resulting pressure ridges was derived from the zone of brash ice which typically occurs on the offshore side of shear ridges.

The area shown in Figure 3 lies just out of the field-of-view of the University of Alaska sea ice radar system located at the Naval Arctic Research Laboratory, 5 km northeast of the village of Barrow. The radar data indicates that at the time of the movement, a segment of a line of ridges extending across the field of view of the radar, and about 3 km offshore, was shoved 100-200 m toward shore. Some ridge growth was also detected along other segments of this ridge line, but no motion was observed further inshore. The projection of the ridge line to the southwest passes approximately 1 km offshore from the shear ridge described above. It is clear that, in general, the impingement of the pack ice was primarily taken up by ridging offshore along the pack ice-landfast ice boundary or along the older shear ridge, except where the fracture bounded thrust sheet was formed. Within that sheet, the pre-existing shear ridge was not altered, and the motion was taken up entirely along the beach.

The area of major movement is shown in greater detail in Figure 4. The ice was about 1.3 m thick at the time of the event, and was pushed up the beach a maximum of 35 m at the northeast corner of the thrust sheet, reaching a beach elevation of 2.8 m above sea level. The heights of the shore ice ridges were generally between 4 and 6 m, with a maximum of 7 m at one point. It is of interest that gravel berms pushed up

ahead of the advancing ice sheet were generally absent, or small where present, reflecting the frozen nature of the beach surface at the time of the event.

Figure 1 shows the location of the ice push at Point Barrow. Its time of formation is unknown, except that it occurred prior to May 1, 1978, when the photograph shown in Figure 5 was acquired. This shows the high-angle fracture bounding the thrust sheet on the south, but unfortunately, the northern boundary was missed, so that the width of the push is not known. The ice reached the beach only at the southeast corner of the thrust sheet where it formed an ice cored gravel mound (Figure 6) about 1.6 m high, and 14 m long which was parallel to, and 8 m from the shore. This feature, which was similar to those described by Hume and Schalk (1964), was destroyed by wave action in late summer.

The remaining events occurred on the barrier islands which define the northern boundary of Elson Lagoon as shown on Figure 1. The exact time at which they formed is uncertain. However, they were not present during an overflight of the area on January 5, 1978, and were first observed on February 9. Examination of ice motion in the area from NOAA weather satellite imagery suggests that the movements occurred after January 18, 1979, when the lead system shown north of Elson Lagoon in Figure 2 finally closed against the coast. This coincided with the onset of a period of northeasterly winds which continued for several days, reaching velocities of over 10 m/sec at Barrow during the period from January 19 to 22. The ice motion in the area during this time involved closing of the ice along the coast north of Elson Lagoon and rapid west and southwesterly motion of the ice around Point Barrow. Based upon

this, it is reasonable to conclude that the ice push events along the barrier islands occurred during this time interval. The observation that the resulting ice push ridges and overrides affected beaches with approximately the same orientations on the three islands also implies that the events occurred at the same time.

The thicknesses of the ice in the ice push ridges on the barrier islands ranged from 0.5-0.7 m. However, the thickness of the unbroken ice sheet on Tapkaluk Island was found to be 0.9 m. The difference in observed thickness between the ice sheet and the broken blocks is probably due to horizontal splitting of the ice sheet during piling, as well as the difficulty of locating samples of the full ice sheet thickness in the snow covered ice push ridges.

The ice was thrust onto Tapkaluk Island along a front nearly 900 m wide. Figure 7 shows the area as it appeared in late winter, and Figure 8, taken in mid-June when the snow had melted off, shows the distribution of the ice push ridges relative to the island as well as the minor fractures associated with the movements. The contrast between these and the surrounding ice is probably the result of clean water freezing into the cracks formed in January, adjacent to dirtier ice formed from muddy water during freeze-up.

The island was completely overridden by three segments of the thrust. The largest of these was 120 m wide with an ice advance of about 140 m. The island was 32 m wide at the override. The smaller overrides were 43 and 34 m in width and developed where the island was about 50 m wide. Ice push ridges are distributed over the remainder of the width of the movement front. The maximum relief of these was 10 m.

Finally, Figure 9 shows another view of the Tapkaluk Island override taken in late Spring. This shows a distinct banding in the landfast ice offshore from the island. The banding probably resulted from the drift of slush ice into the area during freeze-up, and provides markers in the ice which can be used to determine the magnitude of the onshore motion through measurement of the displacement across the fractures which bound the thrust sheet. Measurement of the offset from vertical aerial photographs gives a value of about 140 m for the onshore movement. Differences between this value and the advance of the ice onto the island must be taken up by increasing the volume of ice in the ice push ridges.

The ice push ridges on Martin Island are shown in Figure 10. In this case the ice advanced a maximum of 55 m, without completely overriding the island. The width of the overthrust sheet is 215 m, and the maximum freeboard which the ice reached was 1.7 m. Note the similarity between the geometry of the cracks bounding the overthrust sheet with those of the thrusts on Tapkaluk Island discussed above.

The override at Igalik island is shown in Figure 4. The length of the beach which was affected is in excess of 1800 m, but this reflects the fact that part of the beach is at a relatively low angle to the direction of motion of the ice sheet. In addition, some motion of the ice into the pass at the southeastern end of the island is also indicated by the presence of pressure ridges in that area. The width of the segment which completely overrode the island was 400 m, with a maximum advance of 105 m.

III. SUMMARY

The pattern of the ice push events described above are sufficiently similar to permit some generalizations to be offered regarding the process.

In the Barrow area, the radar data and aerial photography show that movement occurred over a front at least 8 km wide. If it is assumed that ice push at Point Barrow occurred at the same time, then this distance is extended to about 13 km. Within this distance, the only major advance of the ice up the beach was at the village of Barrow along a 725 m front. Minor movements of less than 2-3 m occurred along an additional 3 km of the beach, but in general the motion was taken up by ridging either within the landfast ice, or at the boundary between the landfast and pack ice. Similarly, if the conclusion that all of the events along the barrier islands occurred at the same time is accepted, then the movements in that area occurred along a front about 30 km wide. However, the length of the beaches along which ice push occurred was less than 3000 m of approximately 13 km of island beaches exposed to the movement direction. No evidence of motion of the ice into the passes between the islands was found other than that noted at the south end of Igalik Island. Thus, though the satellite imagery indicates that the pack ice closed against the edge of the landfast ice along a wide front, the length of the beach along which ice push ridges formed represented only a small fraction of the length of the front. This implies that, as was true along the Chukchi Sea coast in December, the motion of the pack ice was probably taken up as ridging either in the landfast ice or along the boundary between the pack ice and the landfast ice.

The stresses required to cause the displacements and ice push ridges along the beaches can be calculated using simple physical models based

on driving slabs up inclined ramps to simulate override of the beaches, and from calculations of the work required to pile the ice to some height. The latter were based upon Parmerter and Coon's (1973) model of pressure ridge formation, modified to account for grounding of the keels in shallow water. The results provide a lower limit to the driving stresses, because the work done in breaking the ice, gouging of the sea floor and beach, overcoming hydrodynamic forces, and in other minor processes, is not accounted for. The results of the calculation indicate that the lower limits of the stresses associated with the formation of the ice piles along the beach are in the range of about 0.13 to 0.2 MPa (18-30 psi). In contrast, Parmerter and Coon (1973) calculate stresses approximately an order of magnitude lower than these as typically associated with the formation of pressure ridges in drifting pack ice, which probably represents a reasonable upper limit to the geophysical driving stress which could be expected to be transmitted from the pack ice to the landfast ice.

The discrepancy between the geophysical driving stress and the stresses required to form the overrides and ice push ridges can be accounted for by noting that, as described above, ice push ridges and overrides form along a relatively small length of beach within the area of the pack ice-landfast ice interaction. Further, those sections where large movements occur consist of ice sheets with discrete fracture boundaries giving them the general form of truncated wedges with the apex along the beach. The implication is, therefore, that the formation of wedge-shaped segments, within the landfast ice is a necessary requirement for the occurrence of major movements of the ice up the beach. That is,

segmentation of the ice sheet is the mechanism by which the geophysical driving stress is concentrated and amplified sufficiently to drive the ice up the beach.

REFERENCES

Hume, J. D. and Schalk, M., 1964, The effects of ice-push on Arctic beaches; Amer. J. Sci., v. 262, p. 267-273.

Parmerter, R. R., and Coon, M. D., 1972, A model of pressure ridge formation in sea ice; J. Geophys. Res., v. 77, p. 6565-6575.

Shapiro, L. H., 1975, A preliminary study of the formation of landfast ice at Barrow, Alaska, winter 1973-74; University of Alaska, Geophysical Institute Report UAG R-235, 44 pp.

Weeks, W. F., Kovacs, A., and Hibler, W. D. III, 1971, Pressure ridge characteristics in the Arctic coastal environment; Proc. 1st. Int. Conf. on Port and Ocean Engineering under Arctic Conditions, Trondheim, Norway, p. 152-183.

FIGURE CAPTIONS

Figure 1. Map of the Point Barrow area. Locations of ice push ridges and island overrides are indicated by x's.

Figure 2. NOAA VHRR infra-red image of the area off western Alaska acquired at 1219 hrs. AST, December 30, 1977. North is approximately at the upper-left corner of the picture. Point Barrow is indicated by the 'x'. Note the lead system along the coast east of Point Barrow.

Figure 3. Ice push at the village of Barrow. The length of coastline shown is 3 km, and north is at the lower left corner of the picture. The northeast boundary of the thrust sheet is the line of ridges extending almost normal from the coast in the northeast half of the picture. The southern boundary is a shear fracture shown as a sharp line curving toward shore from the end of the large pressure ridge in the right half of the picture.

Figure 4. Ice push ridge at the village of Barrow. The length of the coastline shown is 1 km.

Figure 5. Ice push at Point Barrow. View, is toward the southwest. Thrust sheet is along the west side of the Point, with the farthest advance at its southern end.

Figure 6. Ice cored gravel mound at the southern end of the ice push ridge at Point Barrow.

Figure 7. Override at Tapkaluk Island as it appeared in late-winter. North is towards the bottom of the picture. The length of the island beach included in the picture is about 1 km. The straight line feature to the right of the picture is the trail left by a seismic exploration party.

Figure 8. Mid-June view of Tapkaluk Island showing the relationship between the ice push ridges and the island. North is toward the bottom of the picture.

Figure 9. Oblique view to the northwest showing Tapkaluk Island in the foreground and Point Barrow in the distance. Note the banding in the ice on the north (Beaufort Sea) side of the photograph, which is enhanced by the melting which has occurred prior to acquisition of this mid-June scene.

Figure 10. Early summer view of the ice push ridge on Martin Island. Length of the island shown in the photograph is about 850 m. North is toward the bottom of the picture.

Figure 11. Early summer view of the ice push and ice override on Igalik Island. The width of the override in the center of the picture is 400 m. North is toward the bottom of the picture.

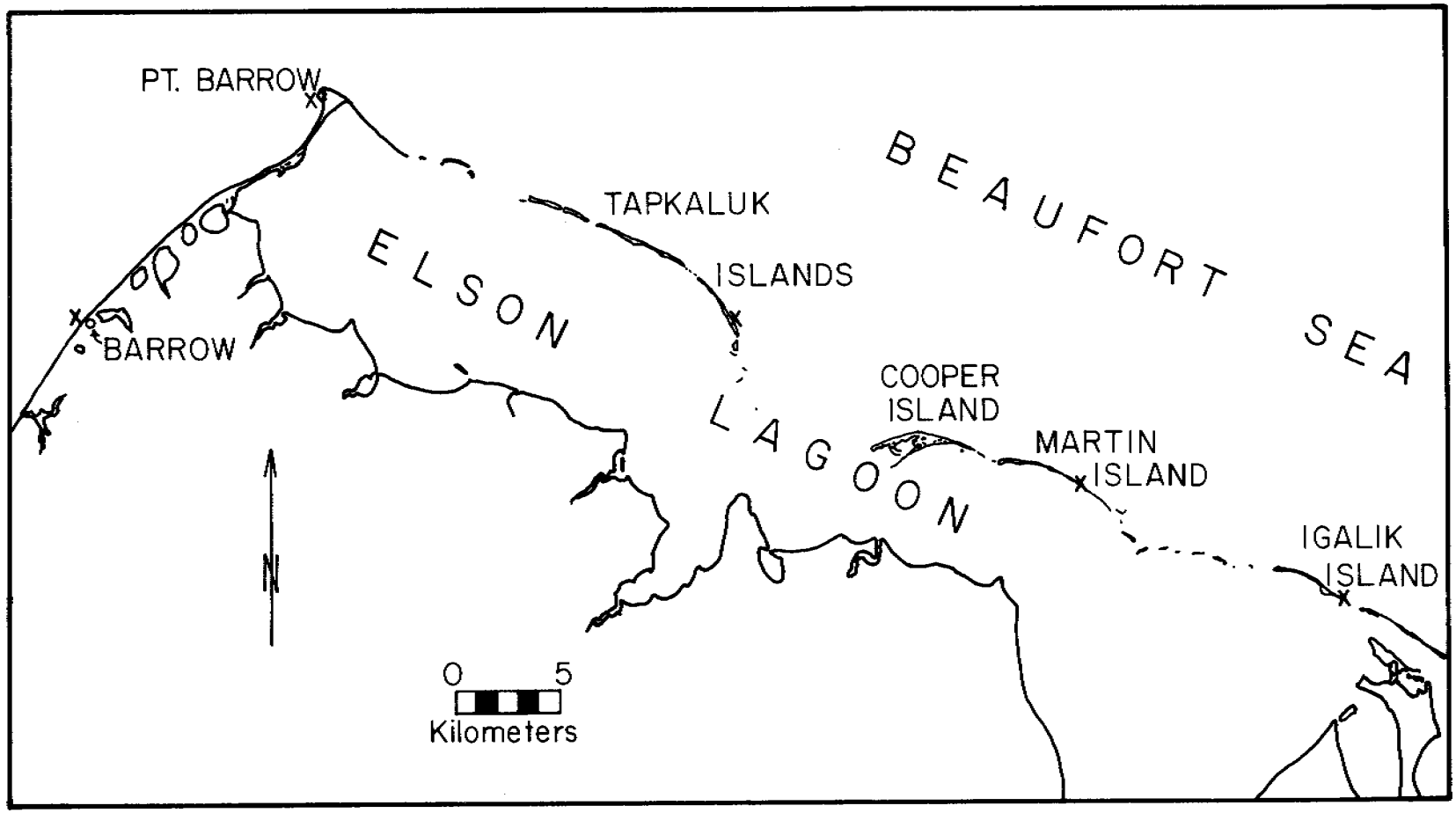

Figure 1. Map of the Point Barrow area. Locations of ice push ridges and island overrides are indicated by x's.

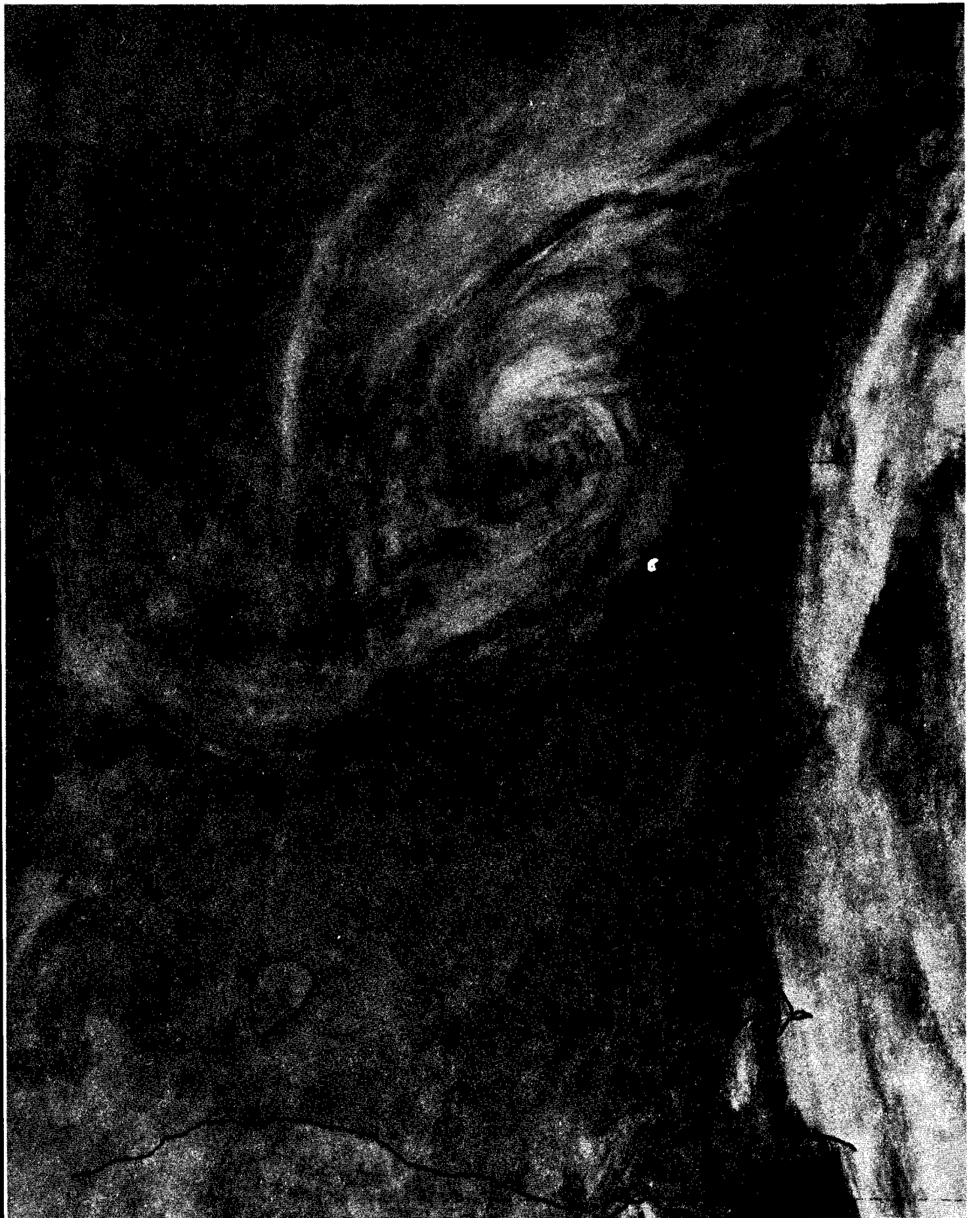

Figure 2. NOAA VHRR infra-red image of the area off western Alaska acquired at 1219 hrs. AST, December 30, 1977. North is approximately at the upper-left corner of the picture. Point Barrow is indicated by the 'x'. Note the lead system along the coast east of Point Barrow.

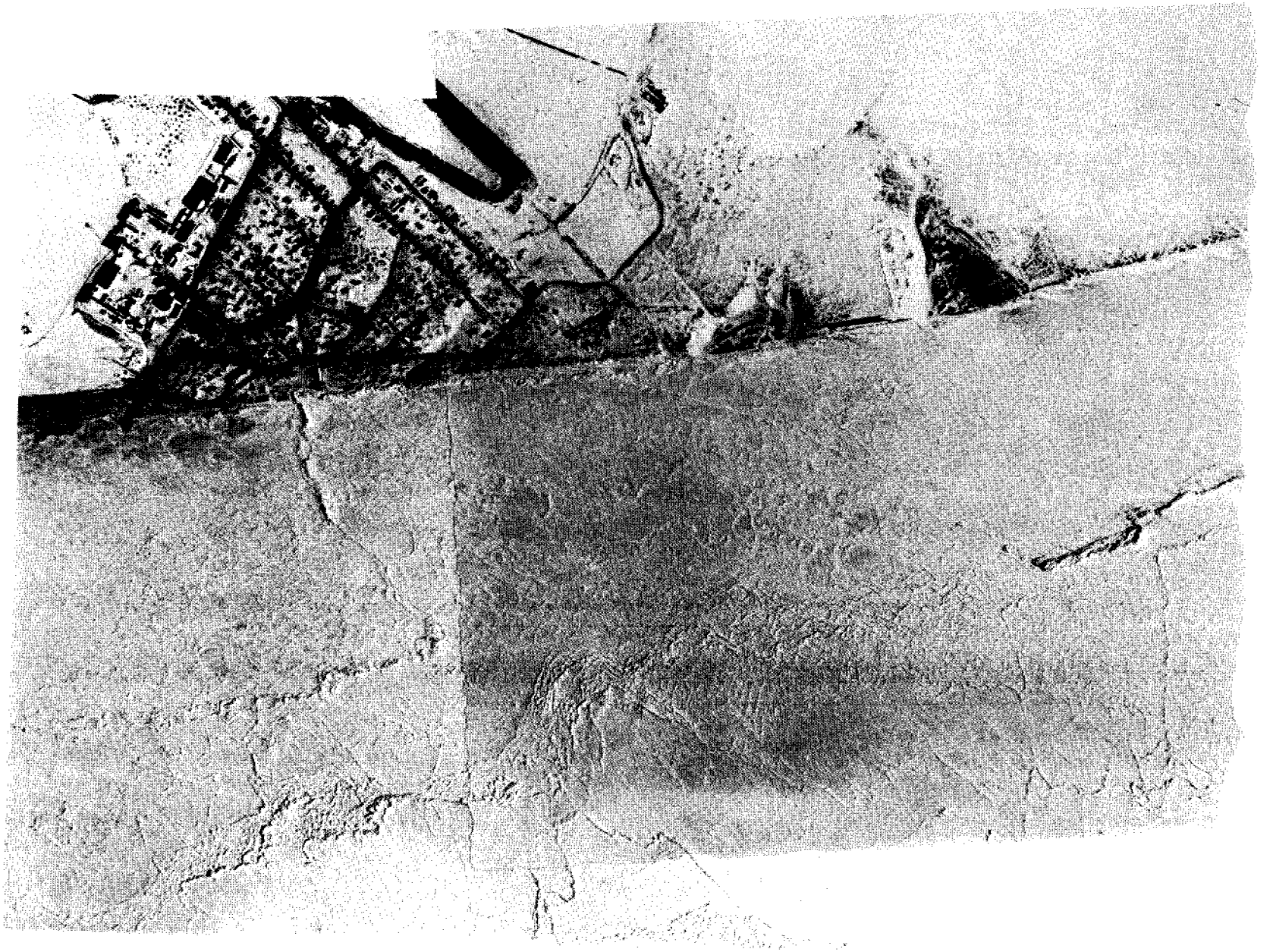

Figure 3. Ice push at the village of Barrow. The length of coastline shown is 3 km, and north is at the lower left corner of the picture. The northeast boundary of the thrust sheet is the line of ridges extending almost normal from the coast in the northeast half of the picture. The southern boundary is a shear fracture shown as a sharp line curving toward shore from the end of the large pressure ridge in the right half of the picture.

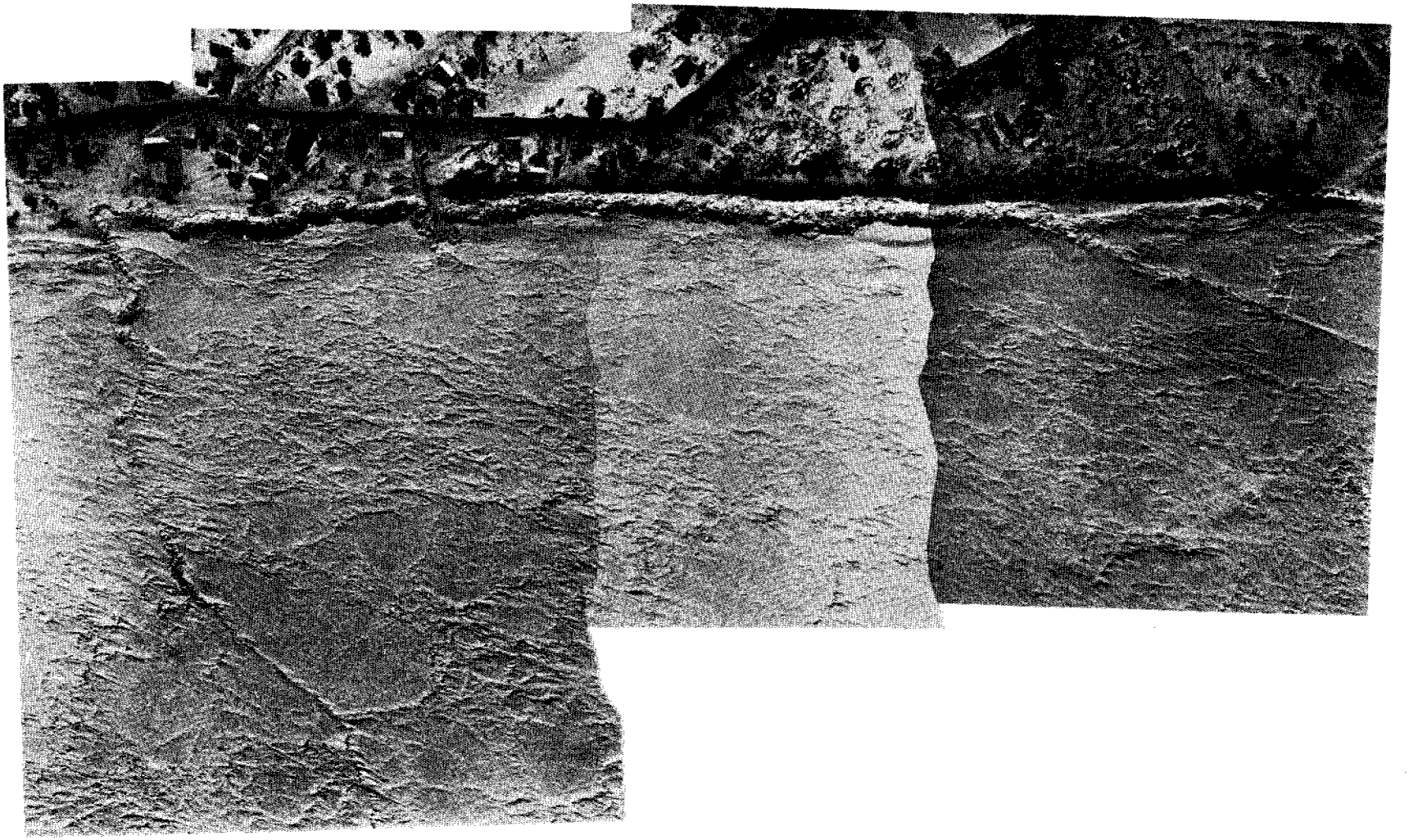

Figure 4. Ice push ridge at the village of Barrow. The length of the coastline shown is 1 km.

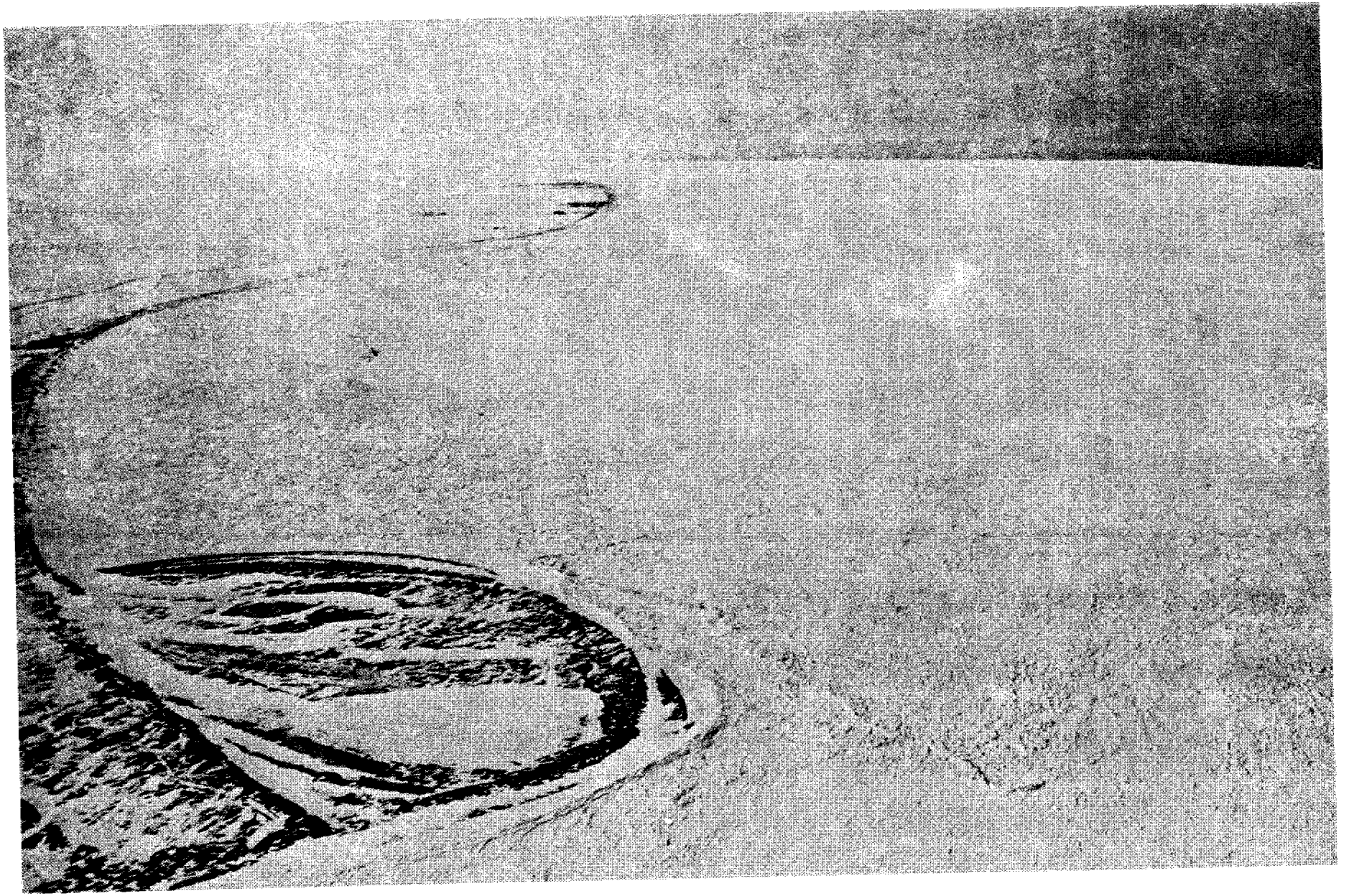

Figure 5. Ice push at Point Barrow. View is toward the southwest. Thrust sheet is along the west side of the Point, with the farthest advance at its southern end.

Figure 6. Ice cored gravel mound at the southern end of the ice push ridge at Point Barrow.

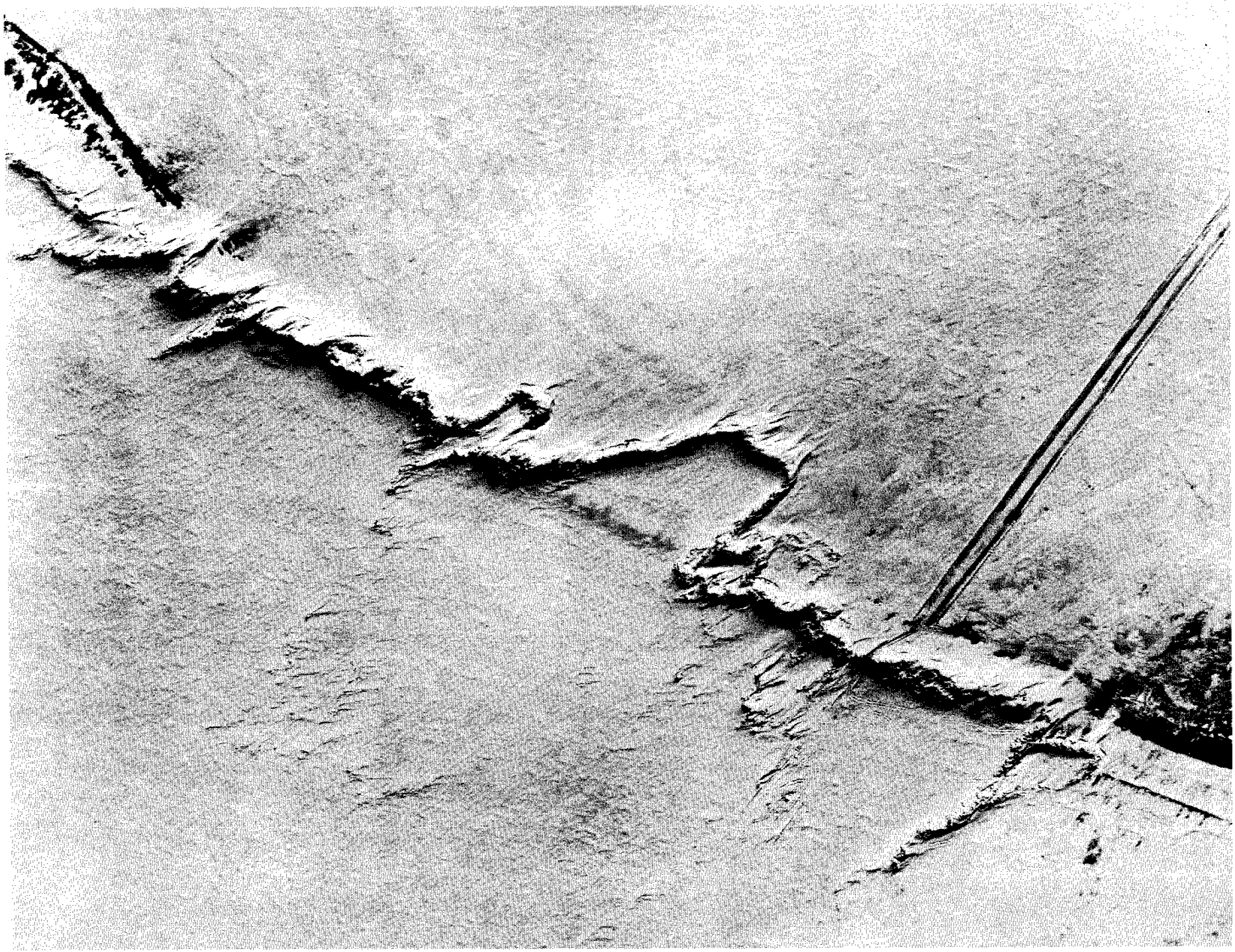

Figure 7. Override at Tapkaluk Island as it appeared in late-winter. North is towards the bottom of the picture. The length of the island beach included in the picture is about 1 km. The straight line feature to the

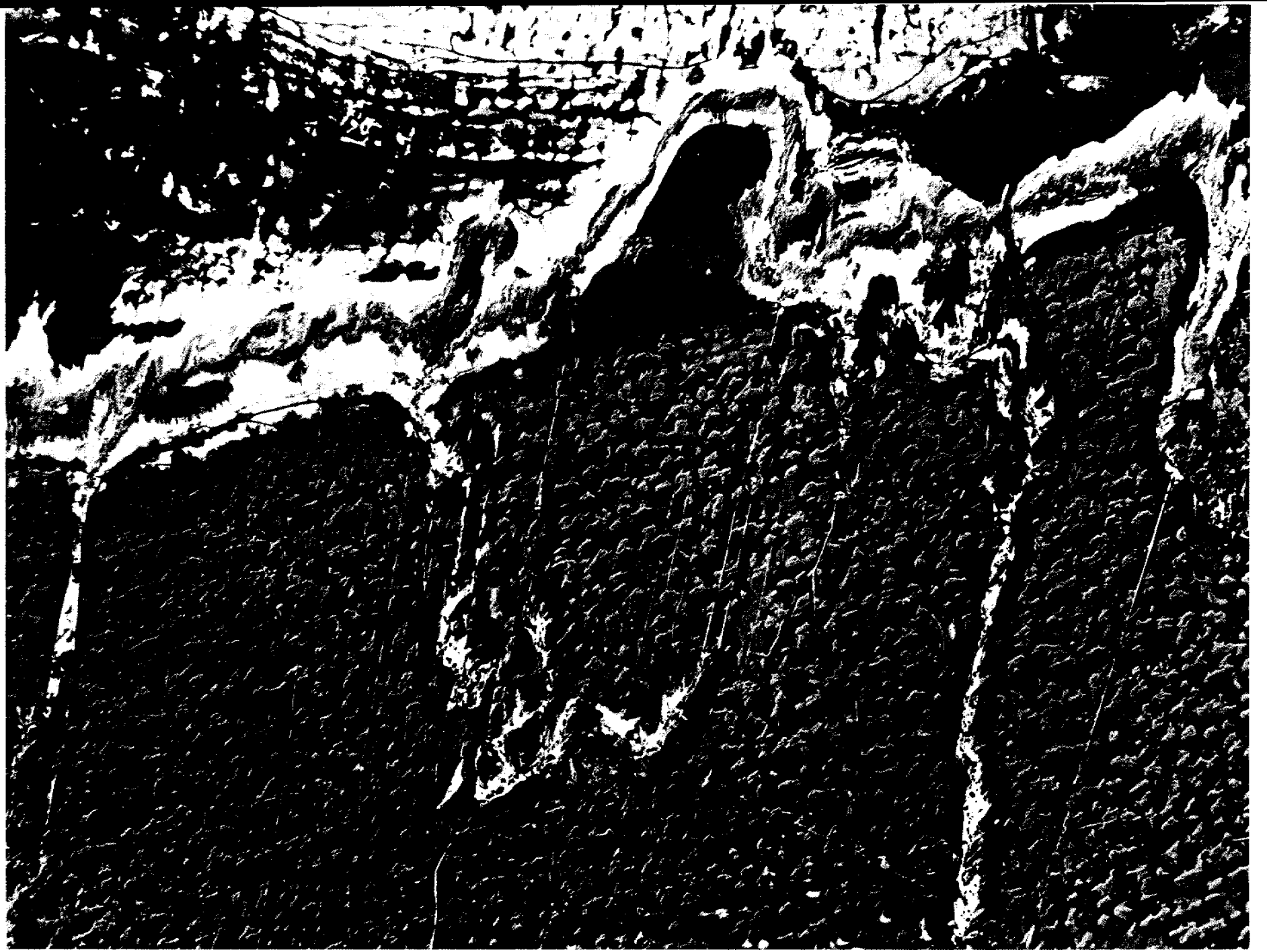

Figure 8. Mid-June view of Tapkaluk Island showing the relationship between the ice push ridges and the island. North is toward the bottom of the picture.

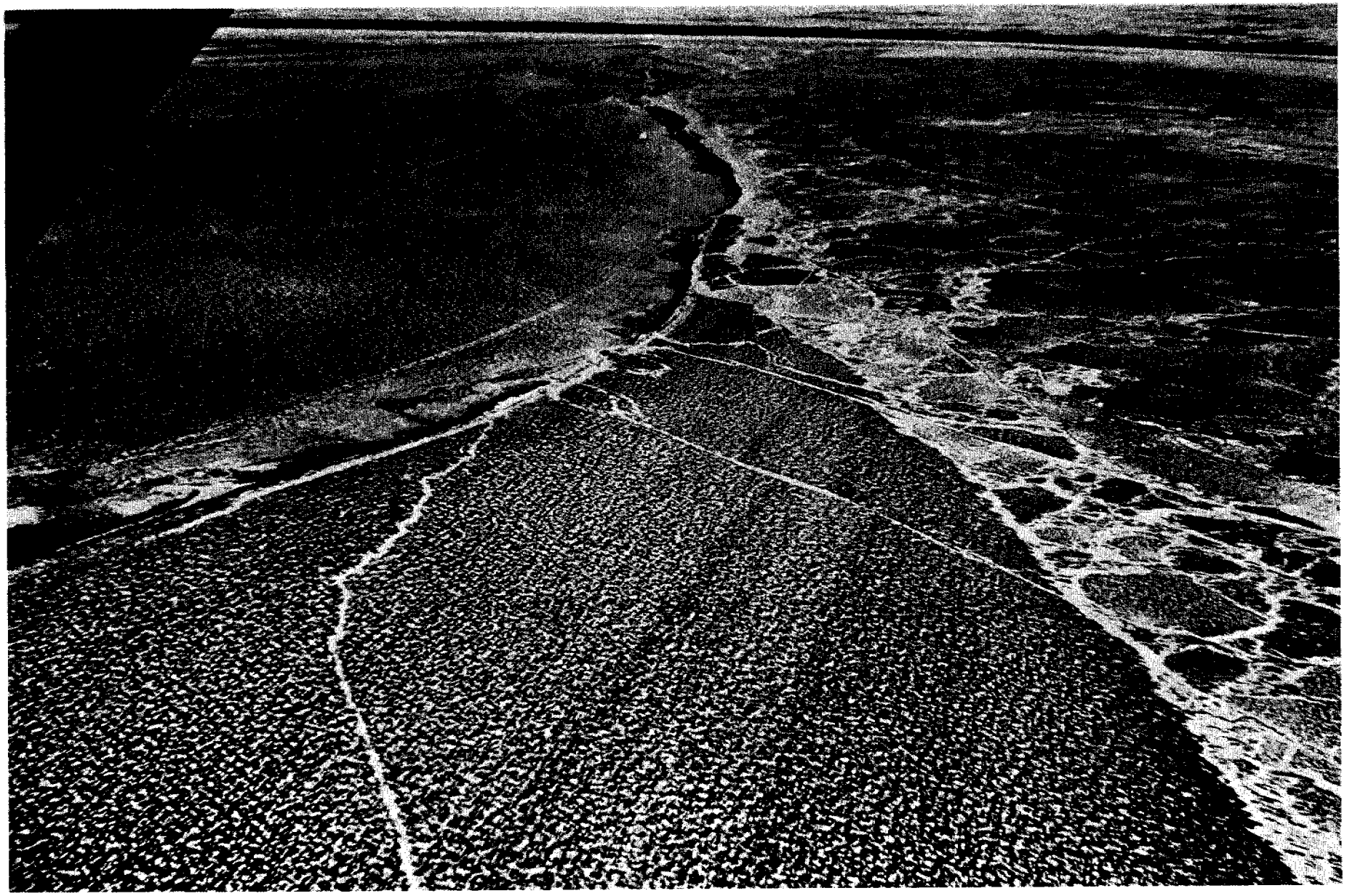

Figure 9. Oblique view to the northwest showing Tapkaluk Island in the foreground and Point Barrow in the distance. Note the banding in the ice on the north (Beaufort Sea) side of the photograph, which is enhanced by the melting which has occurred prior to acquisition of this mid-June scene.

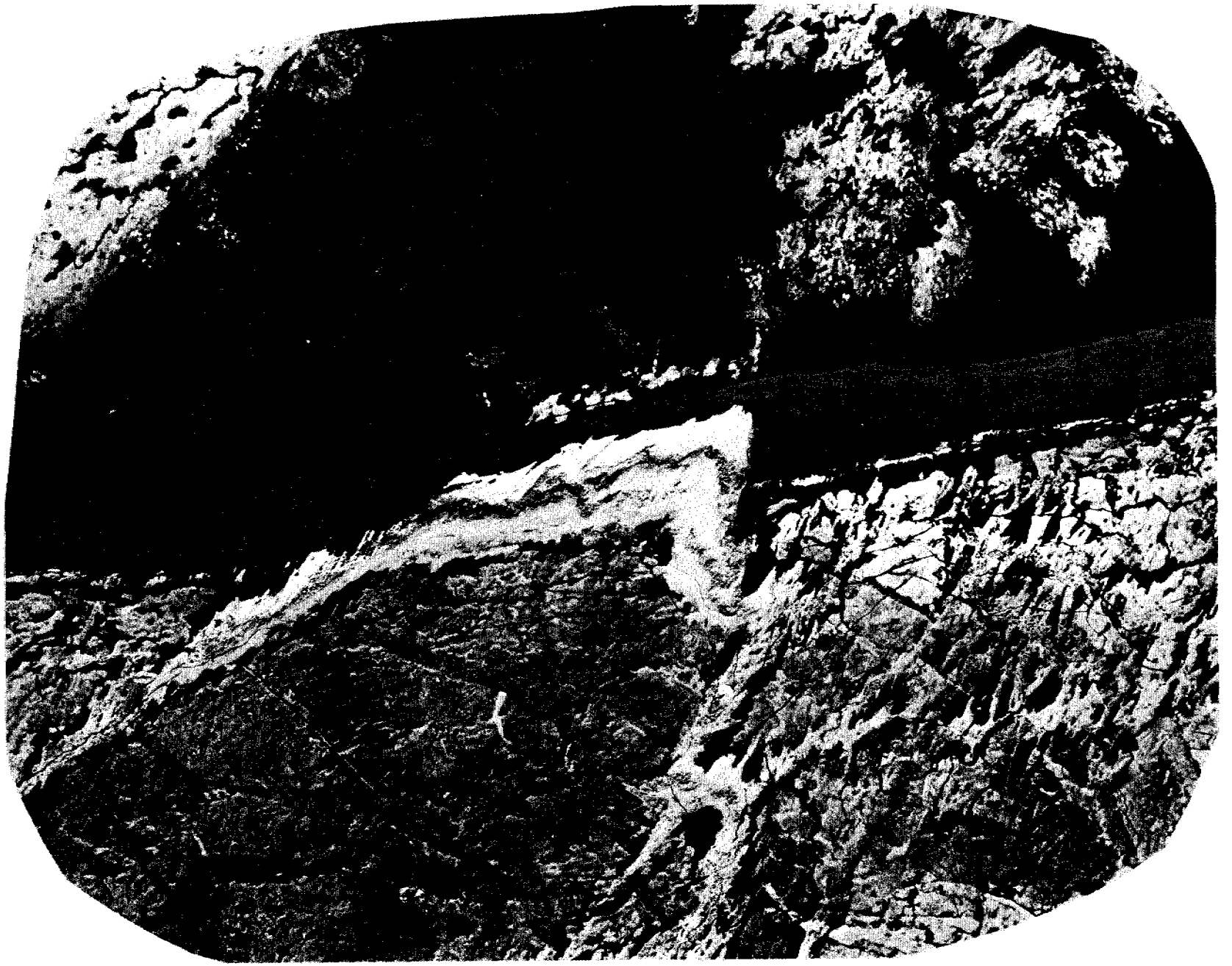

Figure 10. Early summer view of the ice push ridge on Martin Island. Length of the island shown in the photograph is about 850 m. North is toward the bottom of the picture.

Figure 11. Early summer view of the ice push and ice override on Igalik Island. The width of the override in the center of the picture is 400 m. North is toward the bottom of the picture.

Long Period Gravity Waves in Ice Covered Sea

by

Howard F. Bates and Lewis H. Shapiro
Geophysical Institute
University of Alaska
Fairbanks, Alaska 99701

ABSTRACT

A floating ice sheet under compressive stress is modelled as a laterally compressed thin linearly elastic plate floating on a compressible liquid of constant depth. Sinusoidal travelling waves having vertical planes of constant phase are sought for the impulse response of the equation of motion of the floating plate. The coupling pressure between plate and liquid is found to be a Hooke's Law force, for which the effective modulus is directly proportional to the difference between the square of the phase velocity of a wave in the floating plate and that of a free-surface gravity wave at the same wavelength. Thus, for gravity waves the analogy of an elastic plate supported on an elastic foundation is apt. A physical constraint found is that for stability, the phase velocity in the floating plate system at a given wavelength cannot exceed that in the free-surface liquid. This constraint, derived by considering the hydrodynamics of the system, has not previously been recognized. Two bands of gravity waves are found: 1) flexural and 2) floating-membrane. The highest frequency gravity wave that can propagate is the finite resonant frequency of the system, for which the coupling pressure is zero. Flexural gravity waves form a narrow band above the resonant period. Floating-membrane gravity waves exist at all

periods greater than those in the flexural gravity wave band. The results suggest that because long period wave motion accompanies lateral compression of the ice sheet, wave measurements of vibrations in the floating ice may provide a means of detecting the build-up of widespread compressive stress in the ice.

I. INTRODUCTION

On two occasions during short periods of observations a tide gauge operated by the University of Alaska under the landfast ice near Point Barrow, Alaska recorded vertical waves of several centimeters amplitude and of the order of 600 seconds period. During one event stress transducers that had been implanted in the ice indicated increasing compressive stress associated with these waves. In the other instance no stress transducers were operating; however, compressive stress is indicated because the ice moved some 10 m onto the beach as the waves reached their recorded maximum amplitude. (The record ends when the ice moved and destroyed the tide gauge.) Hunkins (1962) reported that long period waves accompanied winds exceeding 5 ms^{-1} (10 kt) over relatively continuous floating sea ice.

These events imply an association between long period waves in the ice-covered sea and rising compressive stresses in the ice sheet. This in turn suggests that a means must exist by which substantial energy is coupled through the ice to the water from the wind as it produces the compressive stress. [Calculations following Robin (1963) show that long period wave energy in the ice-covered sea travels primarily in the water].

We suggest that wave energy is introduced into the ice-covered sea by the impulsive breaking of ice during the production of pressure ridges resulting from compressive stress. During the breaking of the ice in the ridging process, blocks of ice are abruptly displaced upward and downward, with the energy necessary for this motion supplied by the impulsive release of stored elastic energy. To maintain hydrostatic equilibrium, approximately eight times the volume of the ice that is

displaced upward must be displaced downward. The pumping action represented by the abrupt vertical motion of a substantial volume of ice transforms a fraction of the released elastic energy into wave motion in the ice-covered sea. Calculations after Robin (1963) and Parmerter and Coon (1973) show that the power flow necessary to supply the energy in waves of a few centimeters amplitude is a fraction of the total needed to build, for example, ten average pressure ridges.

Thus, sufficient energy, and a means of coupling it to the water, are indeed available. Hence, the next step in solving the problem is to determine the wave propagation characteristics of the system. To study this, we seek the plane-wave impulse response (Green's function or kernel) of a linearly elastic plate floating on a perfectly compressible liquid.

The compressive stress in the ice is assumed to be due primarily to wind, although this is not a crucial assumption for our model. The coupling between wind and ice increases with the square of the wind speed and is such that a 5 to 10 m s^{-1} (10 to 20 kt) wind acting over 100 to 250 km of 1.5 m thick ice produces a compressive stress of the order of 3.5 to 35 kPa (0.5-5.0 p.s.i.) (Seifert and Langleben, 1972; Langleben, 1972).

II. PLAN OF SOLUTION

The basic notion behind the method used for finding the equation of motion of a floating ice sheet is almost a century old and is attributed to Greenhill (1887) by Ewing and Crary (1934). Recent workers to use the idea are Hunkins (1962) and Wadhams (1973). Our approach differs from that of earlier workers because we (1) include the buckling effect of an in-plane compressive stress, (2) compute the impulse response

(Green's function or kernel) of the system, (3) allow the liquid to be compressible, and (4) examine for the first time the physics of the plate-liquid coupling.

Our technique is to approximate a floating ice sheet as a lossless thin linearly elastic infinite plate of constant thickness that is floating on a perfectly compressible liquid of constant depth. The starting point is the equation of motion of a vibrating plate--a fourth order partial differential equation in time and space variables. The plate is assumed to be loaded in part by the pressure at the plate-liquid interface, a quantity that is found by solving Bernoulli's Law at the interface for a small sinusoidal displacement. It is found that the coupling pressure is proportional to the difference between the square of the phase velocity in the free-surface liquid and that in the floating plate system at the same wavelength. When the equivalent free-surface phase velocity exceeds that in the floating plate, the coupling pressure is a linear restoring force proportional to the displacement. If, however, the magnitudes of the phase velocities are reversed, the coupling pressure is proportional to the displacement and acts in the same direction. The latter case is unstable, leading to exponentially increasing solutions that must be discarded as non-physical. Thus, even before the equation of motion of the system is examined, it must be noted that a physical constraint on the system exists, such that the coupling pressure must oppose the displacement. It is this constraint, due to the hydrodynamics of the system, that none of the previous workers discovered (See Part V).

A second component of the loading is assumed to be an in-plane constant compressive component. Such a compressive stress modifies the response by increasing the tendency for the plate to buckle; however, because the compressive stress term is small in thick sea ice compared

to the inertial term, buckling appears to be a minor factor in the wave motion problem.

The desired solution of the partial differential floating-plate equation is the impulse response (Green's function) of an infinite floating plate in terms of small travelling sinusoidal waves having vertical planes of constant phase and propagating in one direction. The response for any arbitrary excitation and boundary conditions can then be obtained using superposition (convolution or hereditary integral). Because the solutions sought are one-dimensional plane waves, there is no dependence on two of the spatial coordinates; the plane-wave floating-plate equation therefore depends only on time and one spatial variable.

The next step is the reduction of the partial differential plane-wave floating-plate equation to an infinite number of ordinary differential 'reduced-floating-plate' equations. This step in the solution is accomplished by noting that the argument $t-x/v$ of a plane-wave function is a linear combination of the space and time variables that depends on the phase velocity of the wave; thus, the phase velocity enters our solution as a reduction constant.

The reduction of the partial differential equation yields an infinite set of ordinary differential reduced-floating-plate equations: each ordinary differential equation corresponds one-to-one with each possible value of phase velocity. Because each differential equation is of the fourth order, it has four plane-wave functions as solutions, each of which corresponds to one of the characteristic frequencies (eigenvalues). Thus, each value of phase velocity provides four characteristic frequencies. There are an infinite number of such possible phase velocities, so that there are correspondingly an infinite number of characteristic frequencies.

In each set of four characteristic frequencies, two lie in the negative half of the frequency domain. Because these negative frequencies yield non-physical solutions, they are discarded, leaving only the two characteristic frequencies in the positive or real half of the frequency domain. Finally, it is shown that at most one of these characteristic frequencies corresponds to a physically possible wave solution.

The linear model of the floating plate (elastic plate on an elastic foundation) is a passive system; that is, there are no internal sources of energy. Therefore, the model is analogous to a linear filter having no internal amplifiers. A plane wave launched in the linear floating-plate system will thus propagate forever with constant amplitude. No other plane-wave response is physically possible. As a result, any eigenvalue that satisfies the hydrodynamical constraint on the coupling pressure and yields a pure sinusoid as a solution is a physically possible value, whereas any eigenvalue that leads to a complex or real exponential is not.

The technique used here to find the characteristic frequencies is to Laplace transform each equation in the infinite set of reduced-floating-plate equations. The result is an infinite set of dispersion relations, each one corresponding one-to-one with a member of the infinite set of phase velocities. Each dispersion relation is a biquadratic in the Laplace variable s, so the eigenvalues are easily found.

Once the characteristic frequencies are calculated, the amplitudes of the wave solutions are readily obtained using the inverse Laplace transform. The residue of each transformed reduced-floating-plate equation at each of its eigenvalues is the amplitude of the corresponding plane-wave function.

III. SYMBOLS USED

The symbols used in this paper are listed below. [SI units are used.]

ϕ	Velocity potential	c	Speed of sound in liquid
ω	Angular frequency	λ	Wave length
v	Phase velocity in floating plate	g	Acceleration of gravity
v_w	Phase velocity in free-surface liquid	d	Liquid depth
α	Attenuation constant	D	Flexural rigidity of plate
$s=\alpha+j\omega$	Laplace transform variable	σ	Poisson's ratio
$k=\frac{\omega}{v}$	Propagation constant	η	Vertical displacement
ρ	Density of plate	E	Young's Modulus
ρ_ℓ	Density of liquid		
h	Plate thickness		
S_x	Laterally compressive stress		

IV. DEVELOPMENT OF LINEAR THEORY

A. Compressible Liquid

The first step is a brief review of the classical derivation of small amplitude, irrotational gravity waves in the sea. Because the motion is irrotational, it can be drived from a potential function. Classically, the velocity potential ϕ has been used, such that (e.g. Lamb, 1945; Stoker, 1957)

$$\vec{\nabla}\phi = \dot{\vec{x}}_j \quad . \tag{1}$$

The starting point for the derivation of water waves is the wave equation [e.g. Eq. 1.35, p. 12, Meyer and Neumann, (1972)] for the velocity potential in a perfectly (lossless) compressible fluid.

$$\frac{1}{c^2}\frac{\partial^2\phi}{\partial t^2} = \nabla^2\phi. \qquad (2)$$

A substantial simplification is possible because the solution sought is the dispersion relation for small-amplitude plane travelling waves whose surface of constant phase is a vertical plane, taken in this case to be normal to the x_1-axis. The original three-dimensional coordinate system (x_1 and x_3 horizontal, and x_2 vertical) therefore reduces to the two-dimensional system of x (horizontal) and y (vertical). Finally, the wave-solutions sought are of the form

$$\eta = \eta_0 \cos(\omega t - kx) \quad . \qquad (3)$$

When (3) is substituted into (2), the resulting ordinary differential equation is readily solved. The general solution for the velocity potential of a compressible liquid having zero vertical velocity at the bottom at depth d is

$$\phi = A \operatorname{Cosh} k\beta(y+d) \operatorname{Sin}(\omega t - kx), \qquad (4)$$

where

$$\beta^2 = 1 - \left(\frac{v_w}{c}\right)^2 \quad . \qquad (5)$$

Bernoulli's Law must be satisfied as a boundary condition at the water surface. The classical technique for accomplishing this is to evaluate the time derivative of Bernoulli's Law on the half-space y=0 for a constant pressure at the fluid surface. After being linearized (dropping the second-order velocity terms), the time derivative of Bernoulli's Law evaluated on the half-space is,

$$0 = \left[-\omega^2\phi + g\frac{\partial\phi}{\partial y}\right]_{y=0}, \tag{6}$$

The result is the usual dispersion relation, modified for the slight compressibility of the fluid, for the phase velocity of gravity waves in open water of constant depth.

$$v_w^2 = \frac{\beta g}{k} \text{ Tanh } \beta kd \quad . \tag{7}$$

B. Floating Plate Theory.

The ice sheet is approximated by a thin lossless linearly elastic plate of infinite extent. The equation of motion for the vertical displacement of such a plate driven by forces p_j is (Skudrzyk, 1968)

$$D\nabla^4\eta + \rho h\frac{\partial^2\eta}{\partial t^2} = p_j \quad . \tag{8}$$

For this problem the driving pressure p_j is assumed to be composed of three parts: (1) the waves propagating in the liquid couple an upward pressure p_1 onto the plate, (2) the plate is under a lateral compression that produces a vertical loading pressure p_2, and (3) the external driving pressure is an impulse.

In the floating-plate system (also termed just 'floating plate' below) a gravity wave travelling in the liquid exerts a force on the plate. This coupling pressure is found by noting that for an inwardly directed pressure p, the linearized Bernoulli's Law requires that on any surface,

$$p_o = -\rho_\ell\frac{\partial\phi}{\partial t} - g\rho_\ell y \quad . \tag{9}$$

The pressure p in (9) is directed downward into the liquid, so that p equals p_1, the corresponding upward-direction coupling pressure on the floating plate. Plane travelling waves with small sinusoidal surface displacements are presumed to be present in the liquid such that the surface displacement η is given by (3). Thus, the surface upon which (9) is evaluated is the surface $y=\eta$.

The first step in this process is to find the arbitrary constant in the velocity potential (4). The condition that the vertical velocity must be continuous across the plate-liquid interface yields for the velocity potential

$$\phi = \frac{\omega \eta_o}{k\beta \text{ Sinh } k\beta d} \text{Cosh } k\beta(y+d) \text{ Sin}(\omega t - kx) \quad . \tag{10}$$

Combining (9) and (10) and evaluating the result on the surface $y=\eta$ gives

$$p_1 = -p_o \eta, \tag{11}$$

where

$$p_o = \rho_\ell g\left(1 - \frac{v^2}{v_w^2}\right) \quad . \tag{12}$$

The quantity v_w in (12) is the free-surface phase velocity for the same wavelength as is propagating in the floating-plate system.

If $v<v_w$, then $p_o>0$ and the coupling pressure p_1 in (11) is oppositely directed from the displacement, in which case p_1 acts as a restoring force. Furthermore, because p_1 in this case is a restoring force proportional to the displacement, the coupling pressure represents a Hooke's Law force. The floating plate system is therefore analogous to an elastic

plate on an elastic foundation; the equivalent modulus of elasticity of the foundation is p_o and is proportional to the difference between the squared phase velocities v_w and v.

For the case $v=v_w$, the coupling force between the plate and the liquid vanishes. In that instance the system is in mechanical resonance because each element is freely vibrating at the same natural period.

Finally, consider the case $v>v_w$, for which $p_o<0$. In this situation the coupling force acts in the same direction as the displacement, thereby producing an unstable system. Such plane-wave solutions must be discarded as non-physical.

Thus, this formulation of the floating plate problem is applicable only to those eigenvalues for which p_o is non-negative. Therefore a physical constraint on the solutions is that for a given wavelength λ_i

$$v(\lambda_i) \neq v_w(\lambda_i) \ . \tag{13}$$

Returning to (8), the buckling component normal to the sheet due to lateral compression is part p_2 of the loading pressure. For a constant positive compressive stress S_x parallel to the x-axis, the component of pressure acting to produce vertical motion is [e.g. Eq. 6.7a, Jaeger (1964)].

$$p_2 = - S_x \frac{\partial^2 \eta}{\partial x^2} \ . \tag{14}$$

An impulse of unit pressure at zero time and distance is the third component p_3 of the driving pressure. Therefore, for plane waves propagating parallel to the x-axis, the floating-plate equation of motion (8) becomes, for a unit impulsive driving force,

$$\frac{\partial^4 \eta}{\partial x^4} + \frac{\rho h}{D} \frac{\partial^2 \eta}{\partial t^2} + \frac{S_x}{D} \frac{\partial^2 \eta}{\partial x^2} + \frac{p_o}{D} \eta = \frac{1}{D} \delta(t,x). \qquad (15)$$

The next step in the development is to reduce this partial differential equation to ordinary differential equations. As (3) shows, time and space are linearly related in the argument of a wave function through the phase velocity. These quantities are combined as follows to yield what is frequently termed the retarded time τ.

$$\tau = t - \frac{x}{v} \quad . \qquad (16)$$

When the retarded-time transformation is made, (15) becomes the reduced-floating-plate equations (17).

$$\frac{d^4 \eta}{d\tau^4} + \frac{\rho h v^4 + S_x v^2}{D} \frac{d^2 \eta}{d\tau^2} + \frac{p_o v^4}{D} \eta = \frac{v^4}{D} \delta(\tau) \; . \qquad (17)$$

Although it is written as a single equation, (17) represents an infinite set of ordinary differential equations, one for each possible value of phase velocity v. At this point, the phase velocity is represented by an infinite set of numbers, each corresponding one-to-one with a member of the infinite set of reduced-floating-plate equations. The phase velocity is therefore a specific number in each reduced-floating-plate equation, so that each differential equation is linear with constant coefficients. Thus, Laplace transformation provides a particularly simple way of solving (17).

A small simplification of (17) is possible. The quantity γ is defined such that

$$\gamma^2 = 1 + \frac{S_x}{\rho h v^2} \quad . \tag{18}$$

The Laplace transform of (17) for the case of zero initial conditions is

$$(s^4 + \frac{\gamma^2 v^4 \rho h}{D} s^2 + \frac{p_o v^4}{D}) H(s) = \frac{v^4}{D} \quad . \tag{19}$$

The plane-wave impulse response $h(\tau)$ is the inverse Laplace transform of $H(s)$:

$$h( ) = \mathcal{L}^{-1} [H(s)] = A_1 e^{s_1 \tau} + A_2 e^{s_2 \tau} + A_3 e^{s_3 \tau} + A_4 e^{s_4 \tau} . \tag{20}$$

An attractive feature of Laplace transform analysis is that the inverse Laplace transform in (20) is automatically the sum of four travelling wave functions. The eigenvalues s_i are the poles of the impulse response $H(s)$. For simplicity, when set to zero, the polynomial in s in (19) is defined as $N(s_i)$--the dispersion relation for wave propagation in the floating plate:

$$0 = N(s_i) = s_i^4 + \frac{\gamma^2 v^4 \rho h}{D} s_i^2 + \frac{p_o v^4}{D} \quad . \tag{21}$$

The four eigenvalues s_i of each of the infinite number of dispersion relations (21) can be found with the aid of the quadratic formula because (21) is a biquadratic. However, before doing that, it is enlightening to use stability criteria of automatic control theory to study the impulse

response. First, we note that the Hurwitz criterion [e.g. Ch. 6 Melsa and Schultz (1969)] requires that indeed p_0 be a positive quantity if the equation of motion (19) is to be stable, i.e. physically possible for the linear model.

For a floating plate there are two real (non-negative) frequencies at which the coupling-pressure coefficient p_0 is zero--at zero frequency and at the non-zero resonant frequency. (The constant hydrostatic bouyancy force is neglected here because it does not affect the impulse response of the system.) The behavior of the characteristic frequencies as p_0 varies is shown qualitatively below using the root-locus method of automatic control theory [e.g. Ch. 7, Melsa and Schultz (1969)].

Briefly, the root-locus method provides an easily applied tool for making a plot of the locus of all of the possible eigenvalues of a linear differential equation with constant coefficients as some parameter in the system varies. For example, the appropriate root-locus plot would show in a particularly simple fashion how a change in the flexural rigidity D affects the eigenvalues. Of considerable use in this problem would be a root-locus plot of the eigenvalues as the coupling coefficient p_0 changes. Unfortunately, this analysis is not directly possible because p_0 depends upon the phase velocity. Changing p_0 therefore explicity changes the phase velocity; this in turn changes the coefficient of the middle term in (21), thereby complicating the calculation. However, because the change is small as p_0 varies over its useful range, the approximate root-locus plot in Figure 1 was made by ignoring the velocity dependence.

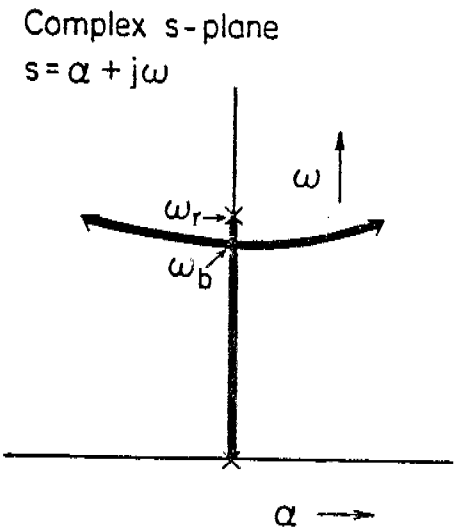

Figure 1. Approximate locus of characteristic frequencies of floating plate equation as the coupling pressure changes. Zero coupling is indicated by the x at one end of the branch, and the coupling increases as the eigenvalues move away from these points. The resonant (ω_r) and breakaway (ω_b) frequencies are shown. The upper branch is the flexural gravity wave branch; the lower is the floating-membrane gravity wave branch.

As noted in II, only sinusoids are physical solutions for the linear model, so that only those characteristic frequencies lying on the positive half of the imaginary (real-frequency) axis in the complex s-plane are admissible. Figure 1 shows that there are two distinct bands of such eigenvalues; the bands are of finite range and join at the breakaway frequency ω_b. The resonant frequency ω_r is the upper bound because greater values can be obtained only by taking $p_o<0$, a condition that is prohibited because the linear model becomes unstable. Values of p_o greater than the breakaway value lead to complex eigenvalues, also forbidden to be physical quantities. Figure 1 therefore illustrates qualitatively in a simple yet elegant way what considerable calculation is required to show in the next section.

Returning to the dispersion relations (21), the eigenvalues s_i are obtained from the quadratic formula. The two positive (upper half-plane) eigenvalues s_i of $N(s_i)$ are as follows (the negative-frequency values are ignored):

$$s_{1,2} = j\, v^2\gamma \sqrt{\frac{\rho h}{2D}} \sqrt{1 \pm \sqrt{1 - \frac{4Dp_o}{\rho^2 h^2 v^4 \gamma^4}}} \quad . \tag{22}$$

The last step in the derivation of the impulse response is the computation of the coefficients A_i of the wave functions in (20). Laplace transform theory states that the coefficients A_i are the coefficients of the partial fraction expansion of the transformed impulse response H(s) in (19). Hence, each coefficient is the residue of H(s) evaluated at its corresponding pole. The coefficients A_1 and A_2 corresponding to the eigenvalues s_1 and s_2 in the real (positive) frequency domain are

$$A_1 = \frac{v^2}{\sqrt{\rho^2 h^2 v^4 \gamma^4 - 4Dp_o}} \frac{1}{s_1} , \tag{23}$$

and

$$A_2 = - \frac{v^2}{\sqrt{\rho^2 h^2 v^4 \gamma^4 - 4Dp_o}} \frac{1}{s_2} . \tag{24}$$

C. Discussion of Linear Model.

The objective of this section is to find the physically possible solutions to the linear model and to apply the results to a representative ice sheet.

First, as shown above a basic constraint of the model is the hydrodynamical requirement that the coupling pressure between liquid and plate be a restoring force, so that it must oppose the displacement. This condition is satisfied only if the coupling-pressure coefficient p_o is non-negative. Next, because sinusoidal plane-wave solutions are sought, physical solutions to (19) are those whose eigenvalues s_i are purely imaginary. Solutions to (19) having real or complex eigenvalues s_i do not correspond to physical solutions, and they must be discarded. Finally, those eigenvalues having a negative imaginary part correspond to characteristic frequencies in the negative frequency domain; these are discarded.

If the relation $s_i = jvk_i$ is used, the characteristic frequencies of (22) can be transformed into the following relation that depends solely upon the characteristic wave-number k_i for each given v.

$$k_i = v\gamma\sqrt{\frac{\rho h}{2D}}\sqrt{1 \begin{matrix} + \\ - \end{matrix}\sqrt{1 - \frac{4D\rho_\ell g}{\rho^2 h^2 v^4 \gamma^4}\left(1 - \frac{v^2}{v_w^2(k_i)}\right)}} \quad . \qquad (25)$$

The free-surface phase velocity v_w, given by (7), is a transcendental function of characteristic wave-number k_i, so an explicit solution of (25) in terms of wavelength is not possible. However, computing the characteristic values k_i from (25) is a simple task with an iterative technique.

It is shown in the dicussion of (30) below that the minus sign before the inner radicals in (22) and (25) provides the characteristic frequencies in the lower band in Figure 1. Sample computations with (25) show that if a value of phase velocity is chosen such that one of the characteristic frequencies given by (22) lies in the lower band in Figure 1, the other root k_i of (25) is real, but the corresponding v_w is less than the value of v used to find the pair of roots. Thus, if one characteristic frequency lies in the lower band in Figure 1, the other is unstable because it violates the hydrodynamical constraint (13).

The plus sign before the inner radical in (22) and (25) provides the characteristic frequencies in the upper band. Computations with (25) show that if v is chosen such that one eigenvalue of (22) lies in the upper band, the other root of (25) is complex, even though $p_0>0$. This effect exists because the value of p_0 necessary to obtain the second characteristic value exceeds the maximum value allowable for p_0 (occurring at ω_b in Figure 1) for physically possible characteristic values, as discussed below. Furthermore, the eigenvalue s_i corresponding to this complex root of (25) has a positive real part, so that the corresponding wave function grows without bound. Thus, when one eigenvalue is in the upper band in Figure 1, the second eigenvalue is in the right half of the complex s-plane and leads to an unstable wave solution that must be discarded.

In summary, therefore, each dispersion relation (22), corresponding to one value of phase velocity, has two eigenvalues in the real-frequency part (upper half) of the s-plane. One of these eigenvalues always leads to an unstable wave function that must be discarded, while the other value may or may not be physically possible, depending on the phase velocity. Thus, for each value of phase velocity, at most one physical eigenvalue exists. This result could have been anticipated directly from the physical constraint $p_o \neq 0$. Because v_w [given by (7)] decreases monotonically with frequency and the characteristic values ω_i and k_i obey $\omega_i = vk_i$, the hydrodynamical constraint that v never exceed v_w requires that the eigenvalues s_i be single-valued functions of the phase velocity.

The next step in the analysis is to examine the behavior of the physically possible characteristic frequencies in detail. As noted above, the liquid and the plate vibrate freely at the non-zero frequency ω_r for which the coupling pressure vanishes. This is the condition for which the system is in mechanical resonance; the phase velocity in the floating plate then equals that in the free-surface liquid at the same frequency and wavelength. The resonant frequency ω_r is electrically analogous to parallel resonance. From (22) the resonant frequency is

$$\omega_r = v_w^2 \gamma \sqrt{\frac{\rho h}{D}} \quad . \tag{26}$$

When (7) and $\omega_r = v_w k_r$ are combined with (26), the resulting equation contains only the resonant wavelength as an unknown and is readily solved numerically.

$$\lambda_r^3 - \frac{8\pi^3 D}{\rho g h \gamma^2} \operatorname{Coth} \frac{2\pi d}{\lambda_r} = 0 \quad . \tag{26}$$

Characteristic frequencies greater than the resonant frequency are obtainable from (22) only for negative p_0. Thus, because physical solutions to (17) do not exist for $p_0<0$, the resonant frequency is the upper bound of the eigenvalues, as illustrated in Figure 1. The band of frequencies for which gravity waves can propagate in the floating plate is therefore finite. This conclusion is contrary to earlier work, as is discussed in the last section.

As the coupling pressure coefficient p_0 increases, the characteristic frequencies in each band in Figure 1 approach a common value (known in control theory as the breakaway frequency), for which the inner radical in (22) and (25) vanishes. For values of p_0 greater than that of the breakaway value, the inner radical of (22) and (25) becomes imaginary, thereby leading to complex eigenvalues. Furthermore, for real frequencies the real part of the eigenvalue is then positive, so that the corresponding solutions grow without bound. As noted above, such solutions are not physically possible for our linear model, so they must be discarded. Thus, a maximum p_0 exists, beyond which wave propagation is not possible in the linear model.

Physically the breakaway frequency corresponds to the maximum difference that can occur between the free-surface and floating-plate phase velocities. Waves for which the difference is greater than that at the breakaway value will not propagate in the linear model of the floating plate discussed here.

As the breakaway frequency is approached, the wave amplitudes--(23) and (24)--increase without bound because the same radical that goes to zero in (22) for the breakaway condition occurs in the denominator of each coefficient. Thus, the breakaway point is another resonance of the system, analogous in network theory to series resonance.

The breakaway eigenvalue s_b is found from (22) by setting the inner radical to zero. Two relations result:

$$s_b = j\, v_b^2 \gamma \sqrt{\frac{\rho h}{2D}} \quad \text{and} \quad 4Dp_o = {}^2h^2 v_b^4 {}_\gamma {}^4. \tag{28}$$

The combination of (7), (12), (28) and $\omega_b \lambda_b = 2\pi v$ leads to a transcendental equation whose only unknown--the breakaway wavelength λ_b -- is easily found numerically:

$$\lambda_b^4 - \frac{16\pi^3 D}{\rho h g \lambda^2}\, \lambda_b \operatorname{Coth} \frac{2\pi d}{\lambda_b} = \frac{16\pi^4 D}{\rho_\ell g} \quad . \tag{29}$$

In summary to this point, it has been shown that each dispersion relation provides at most one physically possible eigenvalue so that each value of phase velocity corresponds to at most one physical eigenvalue. The characteristic frequencies lie in two adjacent finite bands, one of which extends to zero frequency. The two bands join at the breakaway frequency. The upper bound of the upper frequency band is the resonant frequency, above which plane waves cannot propagate in the linear model used. As the breakaway frequency is approached, a vanishingly small excitation produces a finite output.

The next step in discussing the eigenvalues is to identify the type of waves in the two bands; that is done as follows. Over much of each band the coupling pressure is small enough that the inner radical in (22) is sufficiently close to unity that a first order approximation can be made. Hence, for small p_o the characteristic frequencies in the upper--ω_f and lower--ω_g--bands are approximately

$$\omega_f = v^2\gamma\sqrt{\frac{\rho h}{D}} \quad \text{and} \quad \omega_g = \frac{1}{\gamma}\sqrt{\frac{\rho_\ell g}{\rho h}\left[1 - \left(\frac{v^2}{v_w}\right)\right]}. \tag{30}$$

The upper branch frequencies ω_f contain the ratio of mass to flexural rigidity, the quantity that determines how an elastic plate freely vibrates. To a first order approximation the lower branch frequencies ω_g contain no information about the elastic properties of the plate. Thus, considering only small coupling pressures, the floating plate behaves almost as a freely vibrating laterally compressed elastic plate for the upper branch eigenvalues, while for eigenvalues on the lower branch the plate acts approximately as a floating membrane with mass but no elastic properties. The upper and lower branch wave functions for small coupling pressure therefore respectively represent flexural gravity waves and floating-membrane gravity waves.

The term 'flexural wave' in this paper is used in the customary sense: at a wave crest the top surface of the plate expands while the bottom surface contracts. Thus, a flexural wave is that wave for which any plane initially normal to the unflexed neutral surface in the plate will remain normal to that neutral surface as the wave flexes the plate. This behavior is contrasted with that of an elastic shear wave (i.e. seismic S_V wave), for which vertical planes in the unflexed material remain vertical as the wave passes.

In the final part of this section we apply the results of the linear model to a floating sheet of sea ice under lateral compressive stress. To produce illustrative numerical results, the following values were used:

$d=50m$,

$h=1.5m$,

$\sigma=0.30$,

$\beta=1.00$,

and $D=\frac{Eh^3}{12(1-\sigma^2)}$

The values computed from these quantities for the resonant and breakaway periods and speeds are shown in Table 1. To account for the probable non-continuity of ice sheets in the polar sea, we use values of Young's modulus that range over an order of magnitude downward from that obtained from the speed of sound in ice.

Calculations for various water depths show that little change in wave characteristics occurs for water deeper than about 30m. Thus, the data above obtained for 50 m depth are representative of those for deep water. Computations show that as the water depth decreases, the periods T_r and T_b increase, and the phase velocities v_r and v_b decrease and move together; decreasing water depth therefore narrows the flexural gravity wave band and moves it lower in frequency. The data in Table 1 show that the flexural branch wave solution is narrow in spectral width and is nearly insensitive to moderate changes in elastic modulus or ice thickness in deep water.

V. DISCUSSION

The goal of this study to find the plane-wave impulse response (Green's function) of a lossless floating linearly elastic plate has been realized. Two infinite sets of positive characteristic frequencies associated with propagating plane-wave functions result. The upper band of characteristic frequencies (the flexural gravity wave branch) is narrow in spectral

Table 1

Stress (kPa)	70		35		0	
Youngs' Modulus (Nm^{-2})	6.00×10^8					
Period (s)	9.6	11.4	9.8	11.6	10.0	11.8
Speed (ms^{-1})	14.7	16.2	14.9	16.4	15.2	16.6
γ	1.11	1.09	1.06	1.05	1.00	1.00
	1.90×10^9					
	12.5	15.4	12.8	15.6	13.0	16.0
	17.4	18.8	17.6	19.0	17.8	19.1
	1.08	1.07	1.04	1.03	1.00	1.00
	6.00×10^9					
	17.6	22.9	18.0	23.4	18.4	23.9
	19.7	20.6	19.8	20.7	19.9	20.8
	1.06	1.06	1.03	1.03	1.00	1.00

Table 1. The resonant and breakaway periods and speeds for several compressive stresses. Young's Modulus ranges over an order of magnitude downward from approximately the value derived from the speed of sound in ice. The highest stress is near the upper stress limit for ridging events in pack ice.

width; the system resonant frequency is the upper bound, and the breakaway frequency is the lower bound. The resonant period for sea ice floating in deep water is near 10 s and is relatively insensitive to changes in system parameters. The lower frequency band (identified as the floating-membrane gravity wave branch) extends to zero frequency from its junction at the breakaway frequency with the flexural gravity wave band.

The buckling effect of compressive stress on the wave motion is shown in Table 1. Increasing the compressive stress reduces the period and the speed of the flexural gravity wave, but the effects are small. However, the buckling effect coupled with the wave motion may substantially affect the ease with which the ice breaks; in turn this might increase the power flow into the wave motion, thereby increasing the wave amplitude and hence the buckling. We have not addressed that problem in this study.

The data presented in the previous section show that the maximum difference between the phase velocities v_w and v that can produce propagating plane waves in the model is a few-tenths ms^{-1} (a few per cent of v_w) in deep water, and the difference decreases as the water depth decreases. Therefore the gravity waves propagating in the floating plate are very nearly those that would propagate in the free-surface liquid in the pass band of the floating plate. Hence, the main effect of floating a plate on a liquid is to cause a stop band for which gravity wave propagation is not possible, whereas in the free-surface liquid, gravity wave propagation is possible at all frequencies.

A recent study (Wadhams, 1973) of sea waves propagating into pack ice provides experimental support for the gravity wave behavior deduced above. To show this, let us consider a semi-infinite elastic plate with vanishing lateral compression (γ=1) floating on the infinite surface of an incompressible

liquid (β=1) in which free-surface gravity waves propagate perpendicularly toward the plate. Waves with periods less than the resonant period cannot propagate in the floating plate (because p_o is negative), so they are completely reflected at the edge of the plate; however, motion due to the resulting evanescent waves at these periods extends a few wavelengths (hundreds of meters) into the plate-fluid system with a high attenuation rate. This situation is analogous to that occurring in electromagnetic waveguides at frequencies below cut-off.

Waves at the resonant period propagate through the free-surface--plate interface as though the plate did not exist, because the same phase velocity exists on either side of the interface. Waves above the resonant period undergo a small amount of reflection that depends upon the difference in phase velocity across the interface. The standard reflection and transmission coefficients of wave propagation theory that depend only on the phase velocities in the media involved are strictly applicable to this situation, because the free-surface sea and the ice-covered sea are each types of waveguides.

Thus, according to the linear model developed here, wave measurements made in the ice-covered sea a few wavelengths from the edge of the ice would show the following during periods when sea waves are incident upon the ice sheet in deep water. The resonant wave has the peak amplitude because it passes into the ice-covered sea with no reflection; all other waves in the two pass bands suffer some loss of amplitude at the interface due to the reflection caused by the differing phase velocities in the two media. The evanescent waves (periods less than the resonant period) are attenuated rapidly with distance from the interface, while those with periods greater than the resonant period will undergo only the small attenuation of the system (primarily bending losses in the ice).

The predictions above agree with Wadhams (1973) listed results:

1. A spectral peak existed near periods of 12 s.
2. Wadhams' ice-creep model predicted the observed attenuation rate for periods greater than about 10s.
3. For periods less than about 10 s, the measured attenuation rate was far too great to be explained by his ice-creep model of bending losses in the ice.

Thus, we conclude that Wadhams' results confirm the existence of a pass band with periods above approximately 10 s and a stop band below it.

Hunkins (1962) reported that the long period waves he observed had amplitudes that appeared to fit an inverse frequency dependence. Away from the breakaway frequency, (23) and (24) show that the amplitude of the wave functions in the impulse response varies inversely with the characteristic frequency. This inverse frequency dependence arose because the driving force was assumed to be an impulse (a ramp in displacement). If, for example, the driving function were an impulse in velocity (a step in displacement), the inverse frequency dependence disappears. This is easily seen by differentiating (20), because the response of any linear system to the derivative of a driving function is the derivative of the response to that driving function. Thus, the stressed floating-plate theory developed here and Hunkins' (1962) observations taken together suggest that the driving force is basically impulsive in nature. This result, if confirmed by more observations, greatly simplifies solutions involving the superposition integral, because only the initial and boundary conditions will have to be considered to obtain a physical solution.

Our conclusion that gravity wave propagation cannot exist above the resonant frequency does not agree with the results of Greenhill (1887),

Ewing and Crary (1934), Hunkins (1962), or Wadhams (1973), all of whom found no upper bound for gravity waves in a floating plate. The key to identifying the discrepancy lies in Figures 13 of Hunkins and 4 of Wadhams: each plot can be interpreted as showing that above some frequency, the phase velocity in the floating plate exceeds that in the free-surface liquid. As discussed at length above, that situation cannot exist physically, because the coupling pressure must act as a restoring force for stability.

The waves discussed above are denoted gravity waves because they are driven by gravity waves in the liquid, and they have the basic characteristics (i.e. phase velocity and wavelength) of free-surface liquid waves. Another type of flexural wave can exist in the ice--flexural elastic waves--and these waves have been examined by a number of authors in the past [e.g., Ch 6-3, Ewing, et al., (1957)]. A basic difference between these two types of flexural waves is the phase velocity (10 to 20 m s^{-1} for the gravity wave and 1 to 2 km s^{-1} for the elastic wave). It is to flexural elastic waves that Ewing and Crary (1934) applied their floating plate theory, derivable as a special case from the theory presented above. Because our results indicate that the elastic and gravity wave branches do not join for the linear model, Ewing and Crary's application appears questionable.

In summary, two adjoining frequency bands of travelling gravity waves form the plane-wave impulse response of a lossless linearly elastic plate that is laterally compressed and is floating on a perfectly compressible liquid. For small coupling pressures one set of waves represents floating-membrane gravity waves, and the other set represents flexural gravity waves. The flexural gravity waves exist over a narrow band of frequencies between the resonant and breakaway frequencies of the floating plate, and

for deep water this band of frequencies is relatively insensitive to moderate changes in plate thickness or elastic modulus. The floating-membrane gravity waves exist at all frequencies below the band of flexural waves. For small coupling pressures the floating-membrane gravity waves are, to first order, independent of the elastic properties of the plate; for these waves the plate acts as a non-elastic membrane with mass. No gravity waves can exist in the linear model above the resonant frequency. These conclusions are supported by published reports of observational results obtained from sea waves incident on floating sea ice.

We therefore conclude that in-plane compressive stress in the ice can produce two bands of gravity waves: (1) a narrow band of flexural gravity waves near 10 s period, and (2) a broad band of floating-membrane gravity waves with periods of tens of seconds through tens of minutes and longer. (The actual frequencies propagating in a physical situation depend upon the boundary conditions of the ice.) Thus, an easily implemented means of detecting widespread high compressive stress in the ice is to measure long period wave motion in the ice-covered sea with a sensitive tide gauge. We suggest that such a system could provide early warning of possibly destructive ice movements into island and shore installations in the Arctic Ocean.

ACKNOWLEDGEMENTS

We thank William D. Harrison and Ronald C. Metzner for their stimulating discussions.

This research was supported by the National Oceanic and Atmospheric Administration under contract NOAA 03-5-022-55, and by the National Science Foundation, Division of Polar Programs under grant DPP 78-01806.

REFERENCES

Ewing, M. and A. P. Crary, Propagation of elastic waves in ice., Part II, Physics, 5, 181, 1934.

Ewing, W. M., W. S. Jardetsky, and F. Press, Elastic Waves in Layered Media, McGraw-Hill, New York, 1957.

Greenhill, A. G., Wave motion in hydrodynamics, Am. J. Math., 9, 62, 1887.

Hunkins, K., Water waves in the Arctic ocean, J. Geophys. Res., 67, 2477, 1962.

Jaeger, L. G., Elementary Theory of Elastic Plates, McMillan, New York, 1964.

Lamb, Hydrodynamics, Dover, New York, 1945.

Langleben, M. P., A study of the roughness parameters of sea ice from wind profiles, J. Geophys. Res., 77, 5935, 1972.

Melsa, J. L., and D. G. Schultz, Linear Control Systems, McGraw-Hill, New York, 1969.

Meyer, E. and E.-G. Neumann, Physical and Applied Acoustics, Academic Press, New York, 1972.

Robin, G. DeQ., Wave propagation through fields of pack ice, Phil. Trans. A., 255, 313, 1963.

Seifert, W. J., and M. P. Langleben, Air drag coefficient and roughness length of a cover of sea ice, J. Geophys. Res., 77, 2708, 1972.

Skudrzyk, E., Simple and Complex Vibratory Systems, Pennsylvania State University Press, Univesity Park, 1968.

Stoker, Water Waves, Interscience, New York, 1957.

Wadhams, P., Attenuation of swell by sea ice, J. Geophys. Res., 78, 3552, 1973.

Unpublished Reference:

Parmerter, R. R. and M. D. Coon, Mechanical models of ridging in the Arctic sea ice cover, AIDJEX Bulletin No. 19, University of Washington, Seattle, Washington, 98105, March 1973.

ANNUAL REPORT

Contract Number: 03-5-022-55
Research Unit Number: 251
Reporting Period: 4/1/78 - 3/31/79
Number of Pages: 69

SEISMIC AND VOLCANIC RISK STUDIES - WESTERN GULF OF ALASKA

H. Pulpan
J. Kienle

Geophysical Institute
University of Alaska
Fairbanks, Alaska 99701

May, 1979

I. SUMMARY OF OBJECTIVES, CONCLUSIONS AND IMPLICATIONS WITH RESPECT TO OCS OIL AND GAS DEVELOPMENT

The objectives of this research are to evaluate geologic hazards to offshore petroleum development due to earthquake and volcanic activity in the lower Cook Inlet, Kodiak Island, Shelikof Strait and Alaska Peninsula offshore and onshore areas.

Seismicity studies, based on both historic data and data accumulated from the operation of a high resolution network over the past four years, show that the greatest seismic risk is associated with the shallow seismic thrust zone of the subducting Pacific plate. This thrust zone is laterally segmented and individual segments appear to release accumulated strain independently. The segment immediately west of the great 1964 Alaskan Earthquake aftershock zone, the Shumagin gap, has not broken since 1938. Therefore, there is a high probability that a great ($M > 7.8$) earthquake will occur in the Shumagin gap within the lifetime of any potential petroleum development in that area. There is one area, at the western end of the 1964 Alaskan earthquake thrust zone, which over the years has had an unusually high rate of seismic strain release, as seen both in the historic as well as our own more recent earthquake data. This intense earthquake activity appears to be associated with ongoing localized shallow thrusting beneath the Kodiak shelf, off southwestern Kodiak.

The deeper portion of the Benioff zone (deeper than 50 km) seems not capable of generating great earthquakes, even though beneath certain volcanoes, such as Iliamna, we have observed intense clusters of earthquake activity, which in the case of Iliamna, have frequent events with magnitude greater than 6. In Cook Inlet, which lies within a recently

filled gap, the aftershock zone of the great 1964 Alaska earthquake, activity like that below Iliamna could be the prime contributor to the seismic risk within the stipulated timespan of petroleum development.

The shallow (less than 50 km deep), crustal seismicity, aside from the subduction thrust zone, in general is diffuse and does not correlate with the major mapped faults, most of which, based on geologic evidence, show no offsets in their more recent geologic history. With a few exceptions, we also see no clear correlation of the shallow seismicity with recently mapped smaller faults offshore.

Among the 14 active volcanoes in the Katmai-Cook Inlet region, Augustine volcano with its very active recent eruptive history and close proximity to lower Cook Inlet lease areas perhaps presents the most obvious volcanic risk to petroleum development in the western Gulf of Alaska. Its eruptions are typically Pelean, i.e., glowing avalanche and glowing cloud activity are the most serious volcanic hazards. In the past, glowing avalanches have typically travelled to distances of 7 to 10 km from the summit vent. Associated glowing clouds would probably travel further. Being an island volcano, one of its past eruptions has been tsunamigenic. Augustine appears not to erupt without warning as shown during the recent eruptions in 1976 which were preceeded by 8 months of precursor seismicity. The volcano should be monitoried geophysically (seismically) throughout the lifespan of petroleum development nearby.

A special hazard exists at Redoubt Volcano, where volcanogenic floods threaten the currently existing tanker loading facility at the mouth of Drift River. Redoubt had 3 major eruptions in this century, the last one in 1966-68.

II. INTRODUCTION

We attempt to contribute towards the assessment of seismic risk to offshore development in the following ways:

1. by providing seismological input parameters required by different analytical risk assessment schemes, such as recurrence rates of earthquakes, maximum size of earthquakes likely to occur, relationships describing the attenuation of certain strong ground motion parameters as a function of distance, etc.; and

2. by providing input towards the development of a seismotectonic model of the area, that permits detailed delineation of seismic source zones.

To meet these objectives we have installed and continue to operate a network of high-gain, short period, vertical component seismic stations and three strong motion instruments in lower Cook Inlet, Kodiak Island and on the Alaska Peninsula (Fig. 1).

The goal of the volcanic risk assessment portion of this program is to define and quantify the parameters necessary to estimate the most likely type of future eruptions, their magnitude, their recurrence rate and their associated hazards. So far we have concentrated primarily on Augustine Volcano, but have begun to work on Redoubt Volcano as of last year.

Our present risk assessment of Augustine Volcano greatly benefits from the results of the past 9 years of multidisciplineary research which included (1) a study of the geologic record, e.g., type, chemistry, volume and age of historic eruptive products, and (2) geophysical studies, designed to identify the structure, configuration and size of its plumbing system and possible eruption precursors. Only a small portion

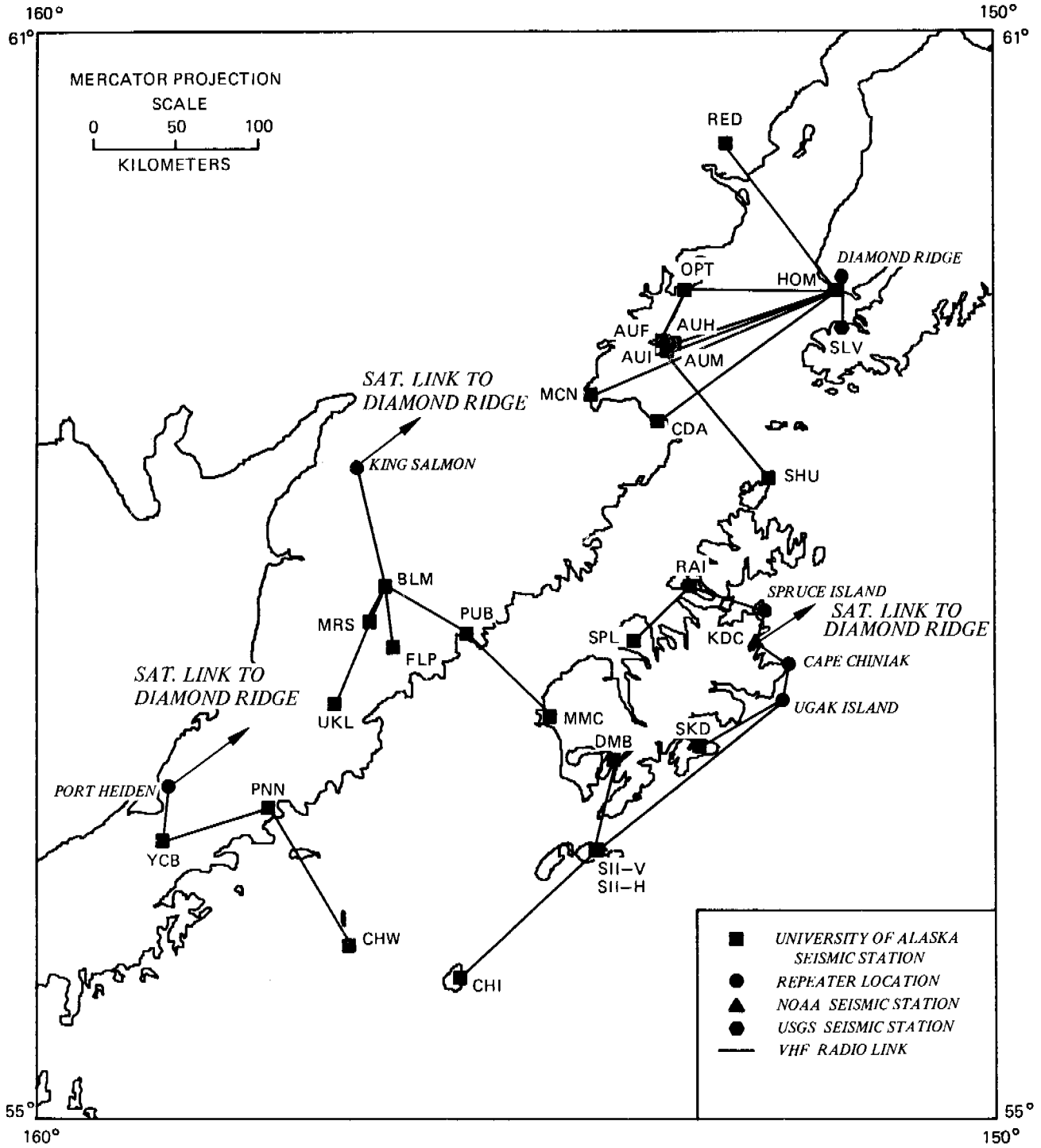

Figure 1. Present configuration of the seismic networks in Cook Inlet, on Kodiak and on the Alaska Peninsula.

of this research has been funded by OCSEAP but it is difficult to discuss the risk without considering the total picture. Because many of the results are unpublished, often contained in theses, Table 1 summarizes the Augustine volcanologic work from 1970 to 1978, identifies the contributing scientists and students and gives their principal sources of funding. Naturally, the following discussions draw heavily on the work of these researchers, whose contributions we gratefully acknowledge.

Since 1976, OCSEAP has been principally involved in the seismology aspects, a special study of the 1976 eruption, certain aspects of the pyroclastic flow problem, and has supported part of the analysis of an explosion seismic experiment, designed to derive a 3-dimensional velocity structure of the volcano.

The Redoubt work, started in 1978, has two major aspects, one geological, the other glaciological. To date, OCSEAP has only supported part of the geologic effort and some of the photogrammetry required for the glaciologic work. Table 2 lists the scientists and students now involved in the program and their sources of funding.

III. CURRENT STATE OF KNOWLEDGE

A. Tectonics

The tectonics of the eastern Aleutian arc is dominated by the interaction between the North American and Pacific plates (Fig. 2). Along the Queen Charlotte-Fairweather faults the two plates are slipping past one another along a right lateral transform fault system. Along the Aleutian island arc and the Aleutian-Alaska Range, up to Mt. McKinley, the oceanic Pacific plate is underthrusting the continental North American plate. The Aleutian trench axis marks the initial downbending of the

TABLE 1

Augustine Research 1970-1978

Studies	Year	Principal Personnel	Principal Funding
Seismology	1970-1971	D. Harlow, J. Kienle	USGS
	1972	J. Kienle	U/A Sea Grant Prog., NSF-1
	1973	J. Kienle	NSF-1
	1974	J. Kienle	NSF-2
	1975-1976	J. Kienle, D. Lalla	OCSEAP, ERDA
	1977-1978	J. Kienle	OCSEAP
		D. Lalla	Unfunded
Petrology and Geochemistry	1970-1974	R. Forbes, J. Kienle	NASA, NSF-1, U/A Sea Grant Prog.
	1974	R. Buffler	State of Alaska-DGGS
	1975	D. Johnston	Unfunded
	1976	R. Forbes, D. Johnston, J. Kienle	OCSEAP, State of Alaska-DGGS
	1977	D. Johnston	USGS, State of Alaska-DGGS
		J. Kienle	OCSEAP
	1978	D. Johnston	USGS
Eruptive History	1970-1978	R. Forbes, D. Johnston, J. Kienle	All listed grants
1976 Eruption	1976-1978	R. Forbes, D. Johnston, J. Kienle, D. Lalla	Emergency grants OCSEAP and State of Alaska-DGGS
		G. Shaw	State of Alaska
Pyroclastic Flows			
(1) Onshore Petrology, Structure, Texture	1976	D. Johnston	State of Alaska-DGGS
		H.-U. Schmincke	Unfunded
Cooling of 1976 Flows	1976-1978	J. Kienle, D. Lalla	OCSEAP
Dating	1978	J. Kienle	OCSEAP
Volume Calculations (1963/64, 1976 Eruptions)	1978	J. Kienle	OCSEAP
(2) Offshore	1978	J. Kienle, J. Whitney	USGS, Conserv. Div., Anch.
Summit Heat Flow	1974	J. Kienle, D. Lalla	NSF-2

Studies	Year	Principal Personnel	Principal Funding
Geodesy			
(1) Surveying	1970-1978	J. Kienle, D. Stone	All listed grants
(2) Gravimetry	1972, 1974, 1975	J. Kienle	NSF-1, NSF-2, ERDA
(3) Photogrammetry			
Post 1963/64 Eruption Summit Topog. Map	1973-1974	J. Kienle	ERDA
Post 1976 Eruption Summit Topog. Map	1976	J. Kienle	State of Alaska-DGGS
1976 Flows, NE Sector, Topog. Map	1978	J. Kienle	OCSEAP
Structure			
(1) Velocity Structure	1975-1976	J. Kienle C. Pearson	ERDA OCSEAP
(2) Magnetic Structure	1975-1976	S. Barrett, D. Stone	State of Alaska
(3) Magnetotelluric Structure	1972-1973	R. Metzner, D. Stone	NSF-1, U/A Sea Grant Prog., State of Alaska

TABLE 2

Redoubt Research 1977-1978

Studies	Year	Principal Personnel	Principal Funding
Petrology and Geochemistry	1977	D. Johnston	State of Alaska-DGGS
	1978	R. Forbes	Unfunded
		J. Kienle	OCSEAP
Glaciology			
Summit Crater	1977	C. Benson	State of Alaska (logistics:
		J. Kienle	State of Alaska-DGGS U.S. Army)
Motion Study of Drift River Lobe of N. Glacier	1978	C. Benson	State of Alaska (logistics:
		P. MacKeith	NSF OCSEAP, Cook
		R. March	NSF Inlet Pipeline
		R. Motyka	NSF Company, Drift River)
Photogrammetry			
Aerial Photography of Redoubt 1977	1977		State of Alaska-DGGS
Aerial Photography of Redoubt and Drift River	1978		OCSEAP

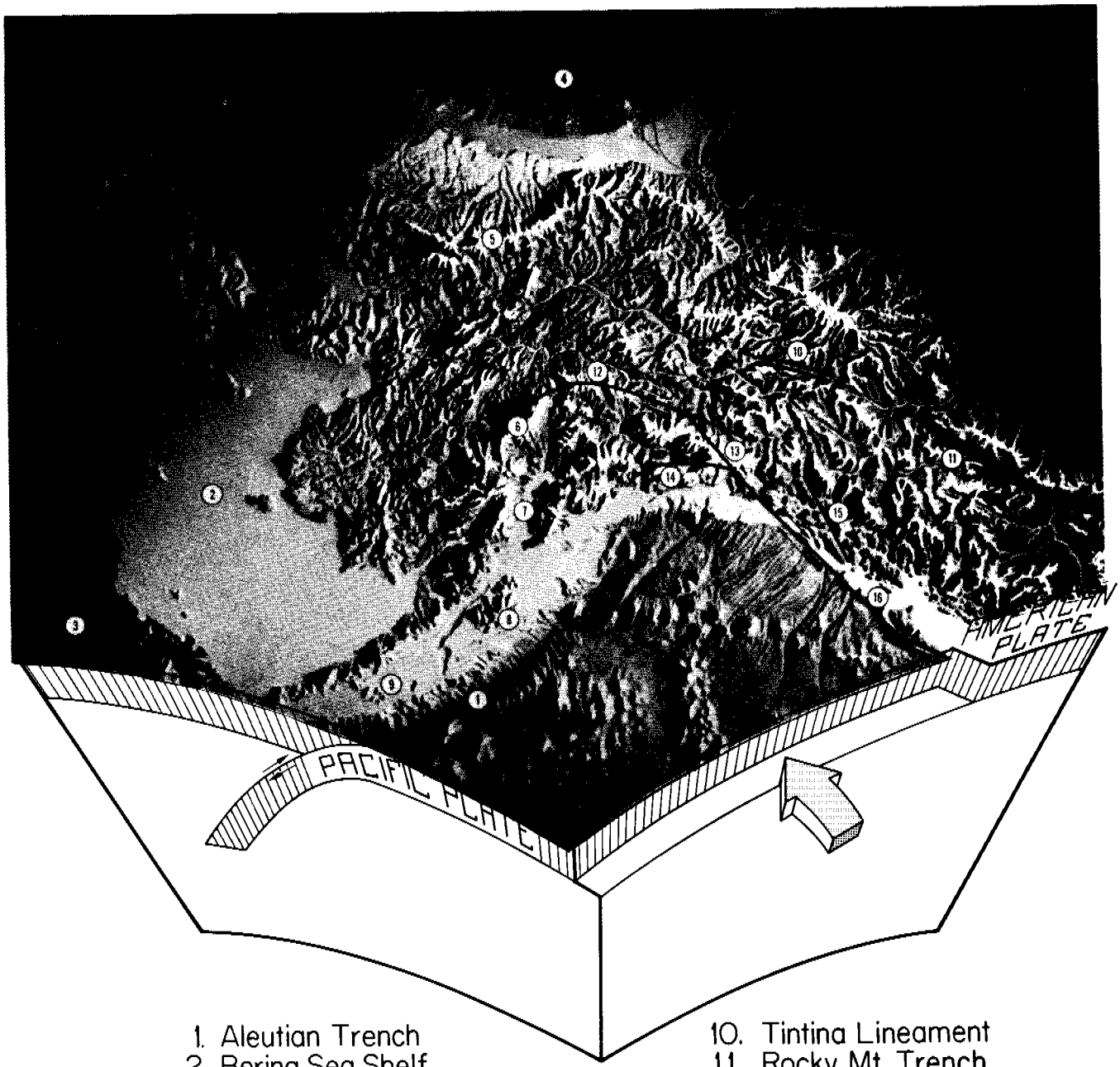

1. Aleutian Trench
2. Bering Sea Shelf
3. Bering Sea Basin
4. Arctic Basin
5. Brooks Range
6. Alaska Range
7. Cook Inlet
8. Kodiak
9. Shumagin Islands
10. Tintina Lineament
11. Rocky Mt. Trench
12. Denali Fault
13. Fairweather Fault
14. Chugach – St. Elias Thrust
15. Chatham Strait Fault
16. Queen Charlotte Fault

Figure 2. Plate convergence in southern Alaska.

oceanic plate, and the active volcanic arc approximately traces the 100 km depth contour of the subducted plate. The transition zone between these two distinct tectonic regimes lies between the Denali fault and the Gulf of Alaska and contains a complicated system of thrust and strike slip faults.

In our study area three major fault systems have been mapped: the Castle Mountain fault, the Bruin Bay fault and the Border Ranges fault (Figures 3 and 4); in addition a major unnamed thrust fault separates the Mesozoic and the Cenozoic in southern Kodiak. The trace of the Castle Mountain fault cuts the grain of the arc system at an oblique angle of 20 degrees and transects the volcano line just south of Mt. Spurr volcano. The relative motion along this fault is right lateral strike slip. Fairly recent displacements have occurred along the Castle Mountain fault as indicated by offset Pleistocene glacial deposits and lineations (Evans et al., 1972). Both, the Bruin Bay and the Border Ranges faults are thrusts that follow essentially the trend of the arc structure. However, neither of these faults shows any evidence of recent displacement: the Border Ranges fault has been inactive since late Mesozoic-early Tertiary time and the Bruin Bay fault is not offsetting any strata younger than 25 million years (Magoon et al., 1976).

With regard to the offshore areas, seismic reflection surveys indicate little recent surface faulting in the lower Cook Inlet (Magoon et al., 1979). A few small faults have been observed north of the Augustine-Seldovia arch. Normal faults associated with horst and graben tectonics are common near Augustine Island (Fig. 3). Surface faulting of the seafloor is indicated in Shelikof Strait between Cape Douglas

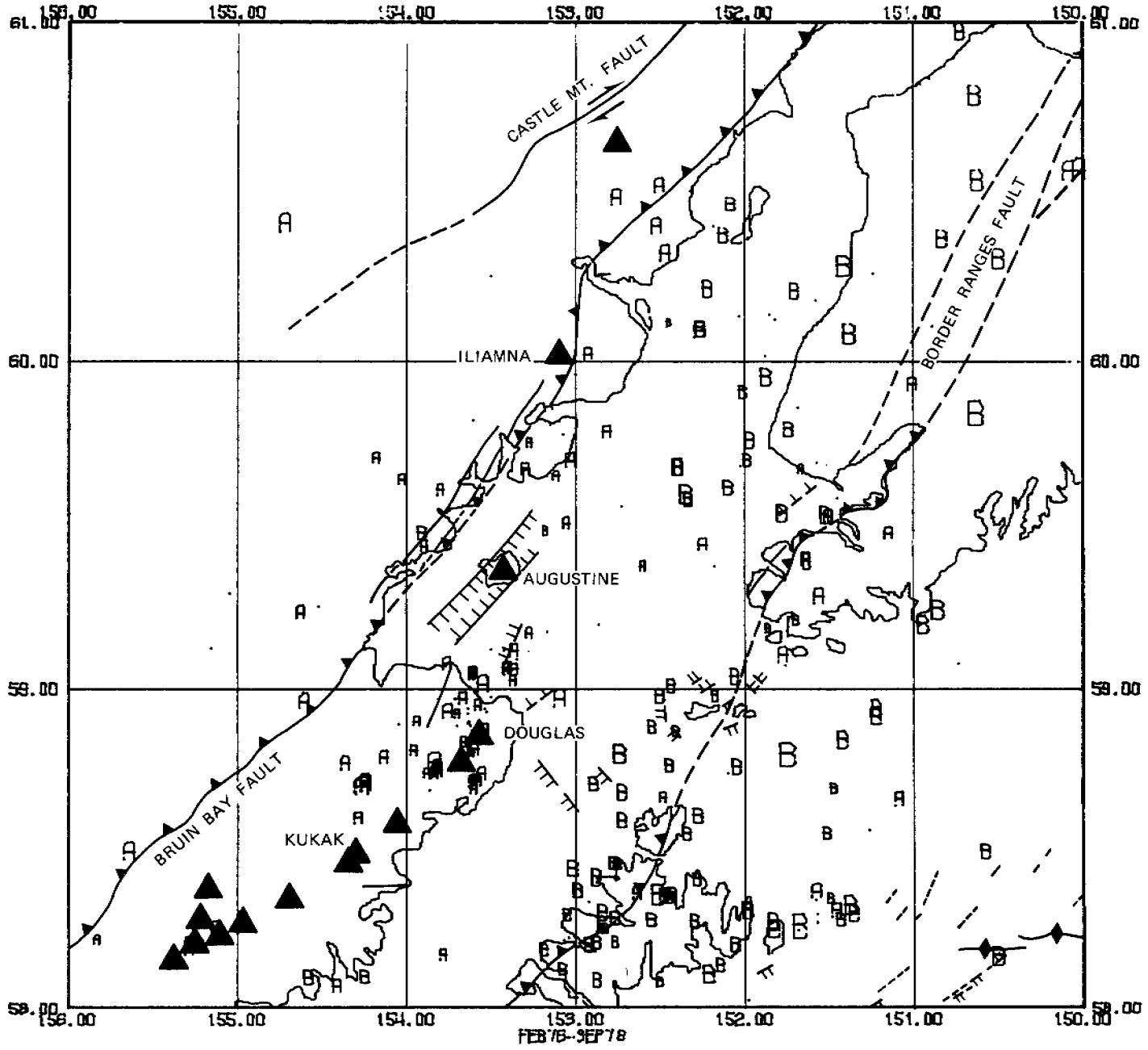

Figure 3. Epicenters (0-50 km depths, class 1) in relation to faults and volcanoes in the Cook Inlet region. Faults from Magoon et al., 1979 and Hampton et al., 1979. Appendix I gives the definition of the letter code used in all the following epicenter plots and the definition of class 1 events.

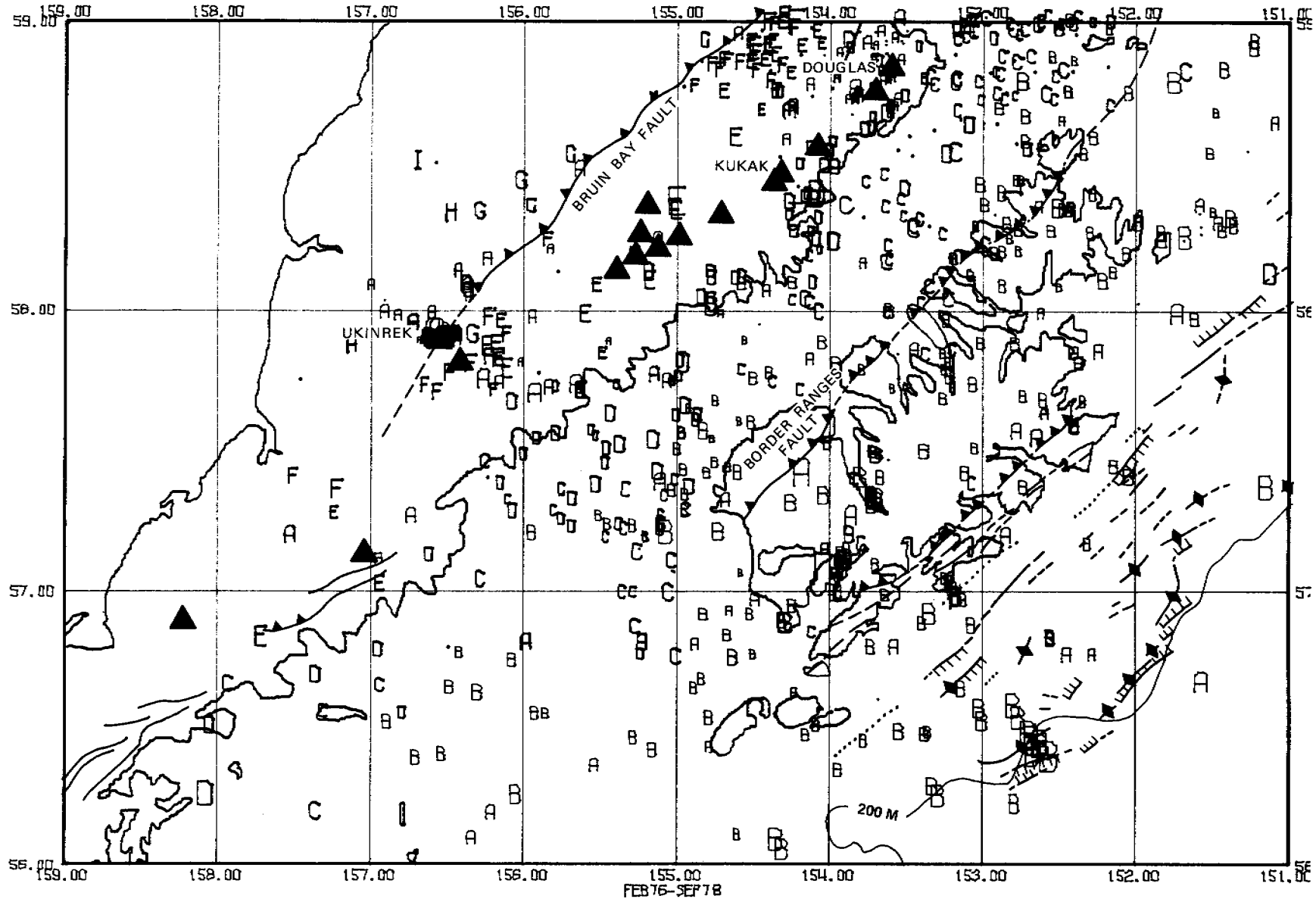

Figure 4. Epicenters (all depths, class 1) in relation to faults and volcanoes on the Upper Alaska Peninsula, Shelikof Strait, Kodiak Island and Kodiak Shelf. Faults from Burk, 1965, Magoon et al., 1979 and Hampton et al., 1979.

and Shuyak Island (Magoon et al., 1979). A major zone of normal faulting trends northeasterly along the Kodiak shelf edge (Fig. 4), where individual faults offset the sea floor by as much as 10 m (Hampton et al., 1979). This faulted zone could be contiguous with faults to the northeast, off Montague Island, which were active during the 1964 Alaska earthquake (Malloy and Merrill, 1972).

B. Shumagin Islands Seismic Gap

Along convergent plate boundaries most of the seismic energy is released during great (magnitude > 7.8) earthquakes (Kanamori, 1977). The aftershock zones of these great earthquake do not overlap, suggesting that the areas left between them, so called seismic gaps, are the most likely sites for the next great earthquake. The longer the time interval since the occurrence of the last great earthquake in a given gap the higher is the probability for a next great earthquake. Unfortunately, the recurrence rate of great earthquakes is poorly known. Estimates range from maximum of 800 years, based on geological evidence (Plafker, 1971), to a minimum of 33 years, based on seismic patterns over the past 80 years (Sykes, 1971). In Alaska there is the additional problem that aftershock zones of great earthquakes before 1964 are poorly defined. In spite of these shortcomings the seismic gap concept is useful for determining the likelihood of the occurrence of the next great earthquake. It is noteworthy that the only earthquakes above magnitude 7 that occurred in Alaska in the past years were located precisely within the two gaps identified by Sykes (1971). These two events were the 1972 magnitude 7.6 earthquake near Sitka and the February 1979 magnitude 7.7 earthquake near Mt. St. Elias (Lahr et al., 1979).

Two well-defined aftershock zones dominate the historic seismicity of the eastern Aleutian arc. One is associated with the 1957 Andreanof-Fox Islands event, magnitude 8.2, the other with the 1964 Prince William Sound earthquake, magnitude 8.5 (Fig. 5, bottom). Sykes (1971) did not identify the area between these two zones as a seismic gap because he considered the possibility that most of it ruptured during the 1938 magnitude 8.7 event. The aftershock zone of this event is rather poorly defined but is frequently delineated as indicated in Fig. 5 (bottom). The gap between the western boundary of the 1938 event and the eastern boundary of the 1957 aftershock zone is called the Shumagin gap. It seems justified to extend this gap to the southwestern margin of the 1964 aftershock zone, as the entire area is experiencing a period of relative quiescence. This quiescence is indicated both by the historic seismicity (Fig. 5, top) and by our own studies which show a definite change in the level of seismicity along a line that transects the arc close to the southwestern margin of the 1964 aftershock zone (Figure 4). This line also coincides with pronounced geologic changes on the Alaska Peninsula near Wide Bay (Burk, 1965). The fact that this line is nearly congruent with a major seaward offset of the volcano line lends further support to the notion that a transarc boundary exists near the western edge of Kodiak.

Archambeau (1979) computed the stress drop for recent earthquakes in the Aleutian-Alaska arc system and found high stress levels from Kodiak Island to the end of the Alaska Peninsula, i.e., in the area of the extended Shumagin gap. If we assume that petroleum development off the Kodiak shelf will take place over the next 40 years (i.e., up

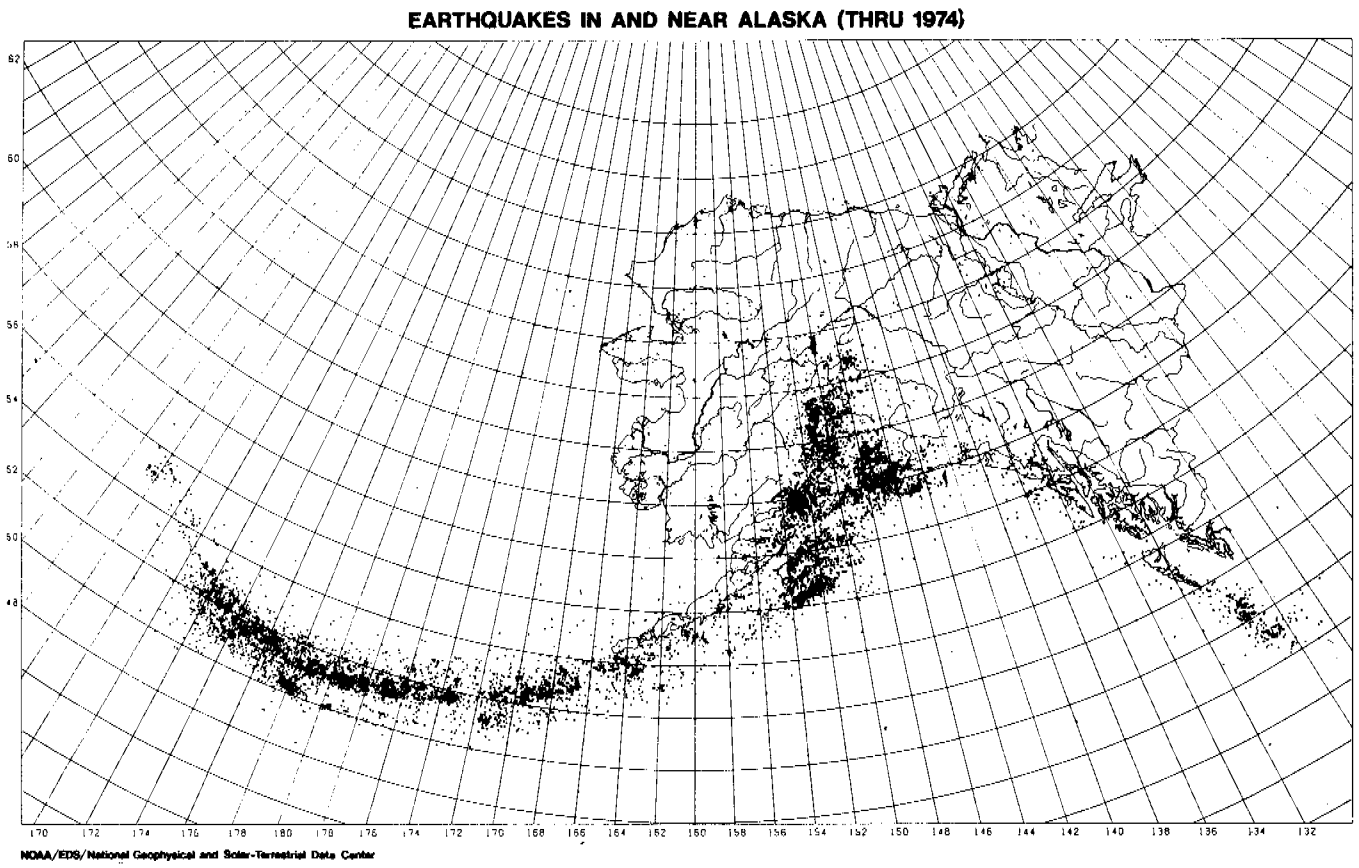

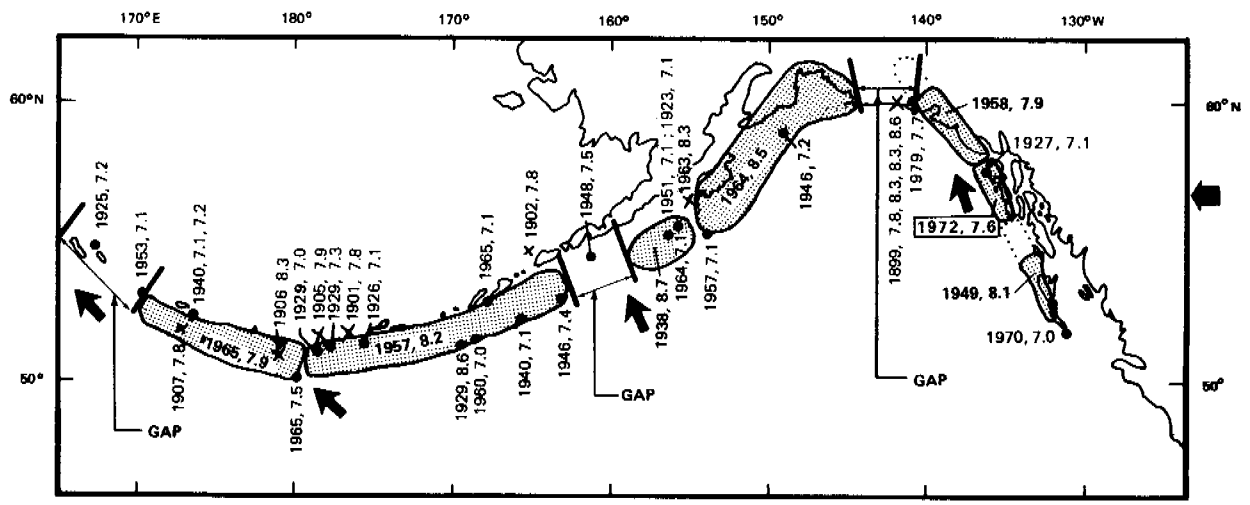

Figure 5. Historic seismicity (top, from NOAA/EDS) and aftershock zones of great earthquakes, modified from Sykes, 1971 (bottom). Other major Alaskan earthquakes are also shown.

to 80 years following the 1938 event) it seems clear, that the greatest seismic risk to offshore development in this area would be associated with the highly probable next great earthquake in the Shumagin gap. The hypocenter of such an event would almost certainly be located on the shallow thrust portion of the subducting Pacific plate and be tsunamigenic. If Kelleher's (1970) observation holds that rupture zones of great earthquakes propagate away from the focal zone of the previous adjacent large earthquake, that event would then be located close to the southwestern edge of Kodiak Island. Kelleher's (1970) space time studies led him to believe that a major earthquake will occur between 1974 and 1980 in the region southwest of the 1964 earthquake zone with an epicenter near 56°N and 158°W.

C. Volcanology

Calc-alkaline volcanism along the Aleutian arc is the result of plate convergence between the North American and Pacific plates (Fig. 2). Nineteen volcanoes form the eastern Aleutian arc from the Upper Alaska Peninsula to Cook Inlet. Of these, eight have erupted in this century and another six have active fumarole fields. The 1912 Katmai eruption was one of the largest eruptions in the world in this century. So far we have only considered two of the most active Cook Inlet volcanoes, Augustine and Redoubt.

Augustine Volcano: We have now a reasonable understanding of (1) its eruptive history, (2) its geology and geochemistry, (3) its internal structure, (4) its recent (past 9 years) seismicity and (5) we have just witnessed a major eruptive cycle 3 years ago:

(1) Augustine's eruptions are typically Pelean, characterized by moderate to violent ejection of solid or very viscous hot fragments of new lava, the ejecta being typically glassy to lithic blocks, ash and pumice, glowing avalanche activity and extrusion of domes or short very thick flows (MacDonald, 1972). Since its discovery and naming by Captain Cook in 1778, 200 years ago, Augustine has erupted 5 times (1812, 1883, 1935, 1963/64, 1976) with repose times between eruptions as short as 12 years and as long as 71 years. The volumes of uncondensed ejecta has been 0.1 km^3 for the 1963/64 eruption (Detterman, 1968) and 0.1 to 0.2 km^3 for the 1976 eruption (Johnston, 1978; Kienle and Shaw, 1979) indicating that the feeding magma chamber is relatively small. In contrast, the volume of the 1912 Mt. Katmai eruption for example is about 2 order of magnitude greater than that for typical Augustine eruptions.

(2) Augustine is a calc-alkaline stratovolcano that erupts predominantly andesitic and dacitic magma (Kienle and Forbes, 1976; Johnston, 1978). The basement in sedimentary; Jurassic and Cretaceous sandstones and shales have been uplifted on the southern flank of the volcano where they crop out (Buffler, 1975).

(3) Pearson (1977), Pearson and Kienle (1978) and Lalla (1979) have determined the shallow seismic velocity structure of the volcano. The little more than 1000 m high cone consists of a central andesitic-dacitic dome complex (V_p = 2.3 to 2.6 km/sec) that is mantled by very low velocity (1.2 km/sec) pyroclastic debris flow and pumice flow material on the lower flanks. Zeolitized high velocity (5.1 km/sec)

sediments underlie the volcano at 0.9 km depth below sea level and the sediments from 0 to 900 m depth have an intermediate velocity of 2.6 to 3.4 km/sec. The volcano may have a small (less than 200 m) higher P-velocity (4.4 km/sec) conduit.

(4) The shallow seismicity observed over the past 9 years at Augustine has been classified by Lalla (1979) into 2 categories, both of swarm type: (1) Surface activity correlating strongly with below-freezing temperatures and probably originating in pockets of the winter ice pack near the shoreline of the volcano and (2) volcanogenic earthquakes from depths shallower than 6 km. Most of the type 2 shallow seismicity originates in a very shallow (0 to 1 km deep) postulated hydrothermal system that overlies an inferred shallow (less than 6 km deep) magma chamber. So far we have observed 2 periods of intense shallow earthquake swarm activity, the first in 1970/1971, and the second prior to the 1976 eruption (Lalla, 1979; Kienle and Forbes, 1976). While the first swarm was not followed by a major eruption (even though we have one report from Kamishak Bay fishermen of a minor ash eruption on October 7, 1971), the second swarm period from May 1975 to January 1976 was followed by the 1976 eruptions. Following the eruptions the volcano has again been seismically quiet.

(5) The 1976 eruption has been summarized by Kienle and Forbes (1976), Johnston (1978) and Kienle and Shaw (1979): The eruption followed a similar pattern as previous historic eruptions, starting with a set of powerful vent clearing explosions that were accompanied by strong glowing

avalanche activity between January 22 and 25, 1976; 13 major eruptions were detected in January on seismic and infrasonic arrays. The average thermal energy per eruption was about 10^{14} to 10^{15} Joules. Several of the eruptions penetrated into the stratosphere and optical effects were observed for 5 months following the eruptions at Mauna Loa, Hawaii. Glowing clouds and avalanches descended all slopes of the volcano with velocities of order 50 m/sec (Stith et al., 1977) and temperatures between 600 and 650°C (Kienle and Lalla, unpublished data). Several of the glowing clouds detached themselves from the debris avalanches, which were originally directed north through a breach in the summit crater but then veered toward the east, and some of these clouds overran our Burr Point shelter, 6 km from the summit, causing heavy damage due to hot air blasts. After 12 days of quiescence, Augustine erupted again culminating with the extrusion of a hot (about 600 to 800°C) viscous andesitic-dacitic lava dome. This phase was accompanied by pyroclastic avalanche activity but of a different type, the feeding mechanism not being column collapse or directed blasts as in January but dome collapse. Renewed dome growth occurred in April 1976, after which phase the eruptions ended.

The principal hazards of Augustine Island are glowing avalanches (pyroclastic flows), mudflows and floods, minor lava flows, bomb and ash falls, noxious fumes, poisonous gases and acid rains, and tsunamis. Of these, the most serious hazard to offshore oil and gas development are glowing avalanches. Ballistic studies indicate that the ejection range of large bombs is mainly restricted to the Island itself. Ash from the

past eruption spread all over southern Alaska, as far north as Anchorage and Talkeetna, and as far east as Sitka, 1100 km away. The ash dispersal is strongly dependent on the prevailing wind directions. Near the island ash falls can be heavy accompanied by acid rains and clouds of noxious fumes. It is clear that no place on the Island itself is safe to erect permanent or semi-permanent structures. The 1883 eruption produced tsunamis that crossed the entire lower Cook Inlet.

Redoubt Volcano: Unlike Augustine Volcano, the much higher peak of Redoubt (10,197 feet) is covered by glaciers which adds hazards due to floods and massive mudflows. During the January 1966 eruptions excessive meltwater may have accumulated in the summit crater (1 x 1.6 km in size, at an elevation of 8,000 to 8,500 feet) and then drained catastrophically. The outburst of water and ice from the crater apparently caused the Drift River to break up in mid-winter. Two separate flash floods reached the mouth of the Drift River the first of which carried large ice blocks. Such flooding may pose a serious threat to the Drift River Tanker Terminal, which was constructed after the 1966 floods.

Another flood hazard arises from the fact that the glacier that descends from the summit crater due north, the North Glacier, could dam up the Drift River. If an advance occurs, the river could get dammed creating a lake that could drain catastrophically. Little is known about the geology of Mt. Redoubt, which has never been mapped in detail. Historic eruptions occurred in 1778, 1819, 1902, 1933 and 1965-68 with eruption intervals ranging from 31 to 83 years.

IV. STUDY AREA

The areas of detailed studies are the on- and offshore areas of lower Cook Inlet, Kodiak Island and the Alaska Peninsula and Augustine and Redoubt Volcanoes.

V. SOURCES, METHODS AND RATIONALE OF DATA COLLECTION

The principal source for the study are the data collected by a network of 25 high-gain, short-period, vertical-component seismic stations. Operation, maintenance and annual service of this system constitutes a major portion of our effort. This year's annual service required a longer than normal time span in the field due to a combination of unusually adverse weather conditions, aircraft breakdown and station equipment failure. The latter was largely caused by late arrival of newly ordered equipment, which could not be tested before field deployment. As a consequence, annual service required 50 days in the field.

No major modifications in station location or technical layout were made. The only station relocation occurred within the small aperture network on Augustine Island, were the station near the summit of the volcano (AUP) was moved to a lower elevation, because the original station environment (weather, snow, rime ice, corrosive gases) was too severe and because of difficulties in reaching the site. The three letter code for the new station is AUH. Throughout much of the Cook Inlet network the older Motorola VHF radio gear was replaced with the more reliable Monitron units. With the conversion of the leased communications lines from the old troposcatter system to satellite transmission our field installation at Kodiak and Port Heiden had to be relocated. In King Salmon this relocation will take place during this years service period.

The system has continued to operate at a high level of reliability. The Kodiak Island portion operates trouble free. On the Alaska Peninsula we still experience VHF noise under certain adverse weather conditions, but only minor improvements will be needed to remedy that problem. A number of stations have been lost in lower Cook Inlet during the latter part of the winter, due to what we believe was a hasty installation at the end of a long field operation. These station losses do not effect the regional coverage but rather the seismology aspect of the volcanic risk studies at Augustine Volcano.

Several recent increases in lease rates for commercial communication lines has led us to initiate the development of a new recording system that will permit operation of the present network without commercial lines. This system will meet a need of the University of Alaska seismology program as a whole and is not being developed with OCSEAP funding.

The new system will use several recording centers throughout the state. On the Alaska Peninsula, one recording center will be set up in King Salmon (KSL) to receive all signals from that network via the VHF links only. Other such centers will eventually be located at Kodiak (for the Kodiak Island network) and at Homer for the lower Cook Inlet network. However, actual recording will not be continuous. The data will be compressed using a seismic event detector. A microprocessor will scan all incoming data, buffer it and start the recording medium, a tape recorder, only in the case of a seismic event. Thus only "useful information" will be recorded. This scheme will allow elimination of expensive commerical circuits and will also permit us to abandon the present film recorders which are notoriously difficult and expensive to maintain in a field site environment. Tape recording of events has the

additional advantage of allowing automatic data processing or more rapid manual processing, requiring less manpower than now to read the film for routine hypocenter locations.

The event detection system is presently in the debugging state in the seismology laboratory. This summer we expect to have the first system deployed in the field. There will, of course, be a time period during which the old and the new system will have to be operated in parallel, but we hope to be able to drop all commercial lines and the film recorder system by the end of the next contract period.

The three strong motion instruments located at SII, PNM and BLM were replaced with different units. The failure of the instrument at SII to trigger during the M_B = 6.5 event on April 12, 1978 off Kodiak Island was traced to an exhausted battery supply. We are now adding power supplies to the units and will make some installation modifications to assure proper functioning of these instruments in the future.

Figure 1 shows the present layout of the seismic system and table 3 provides the station coordinates.

Other, volcanological-glaciological field work, was carried out last year on Augustine and Redoubt Volcanoes in Cook Inlet.

Augustine Volcano: In June 1978, a joint field team of U.S. Geological Survey geologists from the Conservation Division, Anchorage (J. Whitney, M. Lynch and D. Thurston) and from the University of Alaska (J. Kienle) spent 9 days on the Augustine Island to investigate possible sub-marine pyroclastic avalanches on the east side of Augustine Island (Fig. 6), to try to establish their relationship to outcrops onshore and to estimate their age. Dredging the hummocky

TABLE 3

UNIVERSITY OF ALASKA

LOWER COOK INLET, KODIAK ISLAND,

AND ALASKA PENINSULA SEISMIC NETWORK

MARCH 1979

STATION NAME	CODE	LATITUDE (NORTH)	LONGITUDE (WEST)	ELEVATION (METERS)	COMPONETS
AUGUSTINE IS. DOME H	AUH	59 21.83	153 26.61	899	SPZ
AUGUSTINE IS. FLOW	AUF	59 23.27	153 27.45	166	SPZ
AUGUSTINE IS. KAMISHAK	AUI	59 20.05	153 25.62	259	SPZ
AUGUSTINE IS. MOUND	AUM	59 22.26	153 21.17	106	SPZ
BLUE MOUNTAIN	BLM	58 02.8	156 20.2	548	SPZ
CAPE DOUGLAS	CDA	58 57.32	153 31.77	386	SPZ
CHIRIKOF ISLAND	CHI	55 48.5	155 38.6	250	SPZ
CHOWIET ISLAND	CHW	56 02.0	156 42.7	160	SPZ
DEADMAN BAY	DMB	57 05.23	153 57.63	300	SPZ
FEATHERLY PASS	FLP	57 42.7	156 15.9	485	SPZ
HOMER	HOM	59 39.50	151 38.60	198	SPZ
MAARS	MRS	57 51.40	153 04.82	131	SPZ
MCNEIL RIVER	MCN	59 06.06	154 11.99	273	SPZ
MIDDLE CAPE	MMC	57 20.00	154 38.1	340	SPZ
OIL POINT	OPT	59 39.16	153 13.78	625	SPZ
PINNACLE MOUNTAIN	PNN	56 48.3	157 35.0	442	SPZ
PUALE BAY	PUB	57 46.4	155 31.0	280	SPZ
RASPBERRY ISLAND	RAI	58 03.63	153 09.55	520	SPZ
REDOUBT VOLCANO	RED	60 25.14	152 46.32	1067	SPZ
SHUYAK ISLAND	SHU	58 37.68	152 20.93	34	SPZ
SITKINAK ISLAND	SII	56 33.60	154 10.92	500	SPZ,SPE-W
SITKALIDAK ISLAND	SKD	57 09.85	153 04.82	135	SPZ
SPIRIDON LAKE	SPL	57 45.55	153 46.28	600	SPZ
UGASHIK LAKE	UKL	57 24.1	156 51.3	410	SPZ
YELLOW CREEK BLUFF	YCB	56 38.9	158 40.9	320	SPZ

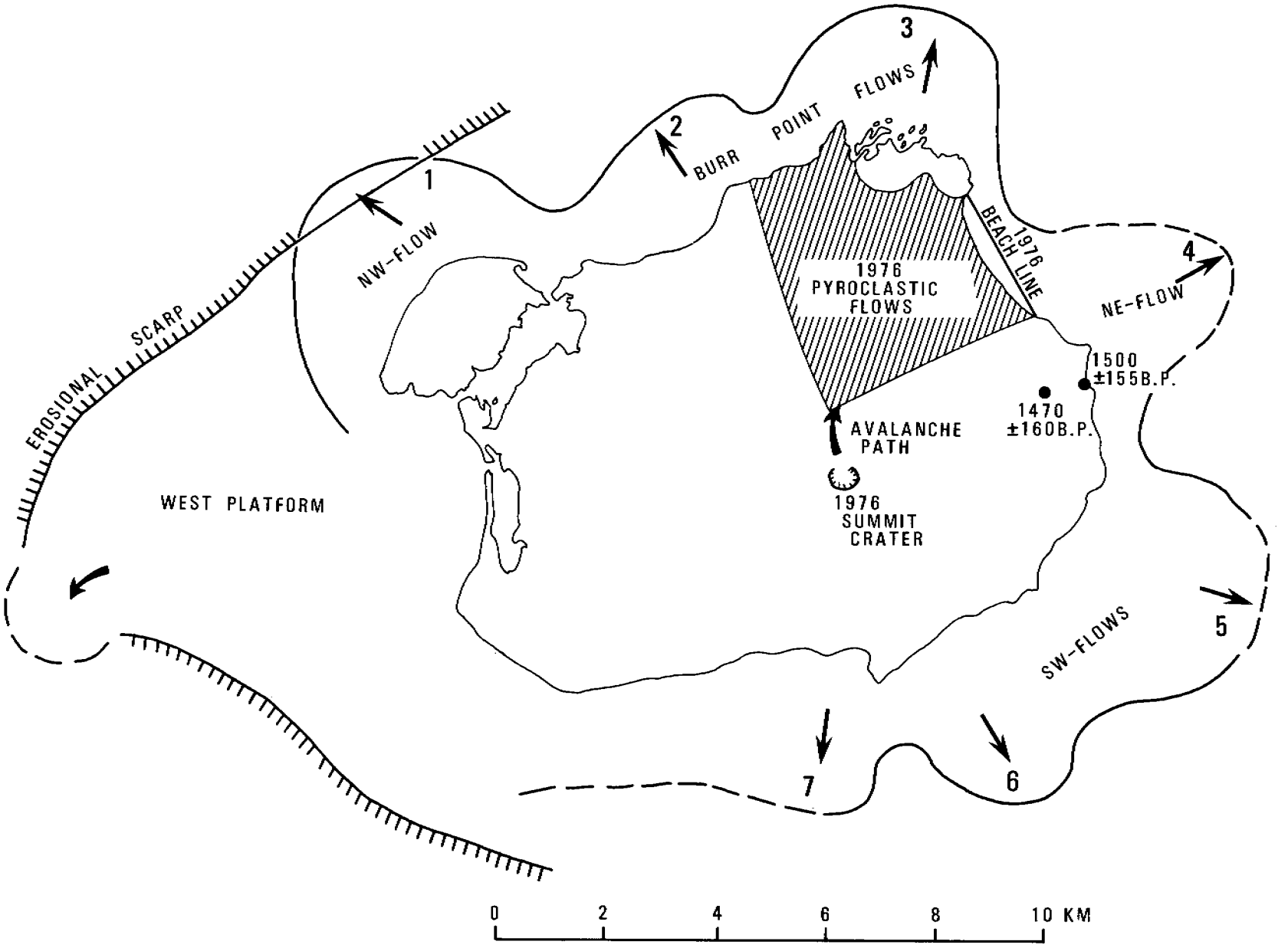

Figure 6. Preliminary sketch map of 7 suspected offshore debris flows at Augustine Volcano, also showing the extend of a large submerged platform on the west side of the Island, henceforth called the "West-Platform". Sketch is based on an advance information copy of NOAA-NOS hydrographic survey H-9073, contoured by the U.S. Geological Survey, Conservation Division, Anchorage. The location and C^{14} radiometric age of a soil and a wood sample collected at the base of a major tephra sequence on the east side of the island is also shown.

terrace offshore with a home-made small dredge and using a Zodiac raft proved not to be very successful. However, the few small pebbles that were recovered were all andesitic. Later, ocean bottom TV-footage acquired aboard the Sea Sounder (OCSEAP, RU 327) also showed very rough hummocky terrace, which we tentatively interpret to be the distal ends of the glowing avalanches. Unfortunately, to date, we still do not have a representative rock specimen from the offshore flows confirming their suspected volcanic nature.

The Burr Point Base camp which was severely damaged during the 1976 eruptions was rebuilt during the June field trip and it is now again in reasonable enough shape to provide shelter. During the Augustine seismic station service (August 31-September 2) we also disassembled and relocated a small building left by NOAA ERL/WPL, Boulder, to a permanent site on the west side of Augustine Island. We plan to rebuild the structure during the 1979 field season.

Redoubt Volcano: During last years (1978) field season the volcano was visited twice, once from July 3 to 13, the second time from September 11 to 16. In July, color vertical aerial photo coverage was obtained of Redoubt Volcano and the Drift River Valley.

During the July trip two University of Alaska graduate students (R. Motyka and P. MacKeith) and a field assistant (R. March) established geodetic benchmarks and planted and surveyed 15 stakes to monitor the movement of the Drift River Valley terminal lobe of the North Glacier (the name "North Glacier" is unofficial and is introduced here for our convenience). The glacier is heavily covered with surface moraine

and volcanic ejecta and therefore most poles were planted in this debris. Most of these stakes will only be useful to measure ice movement. A few stakes were drilled into steep ice for direct ablation measurements and a stake was installed horizontally into the river cut wall of ice at the terminus. In addition, 2 baseline benchmarks and 4 photo-control points were established in the area. In late July, North Pacific Aerial Surveys obtained vertical photo coverage of the North Glacier.

A party of four revisited to North Glacier terminus in September to (1) resurvey the 15 stakes on the glacier terminus (C. Benson and P. MacKeith) and (2) to conduct reconnaissance volcanologic field studies and to collect a suite of rock samples around the base of Redoubt Volcano (R. Forbes and J. Kienle).

VI. RESULTS

A. Seismic Source Areas

The most dominant source of earthquakes in our study area is the Benioff zone, which consists of an upper shallow thrust portion extending from the trench to about the Border Ranges Fault, and a more steeply dipping portion that reaches a maximum depth of about 200 km behind the volcanic arc. Shallow, less than 30 km deep earthquakes occur in the overlying crust. The wedge-shaped mantle region between the crust and the top surface of the Benioff zone is aseismic and therefore called the aseismic wedge. In addition to these 2 main seismogenic tectonic environments, the crust and the Benioff zone, tightly clustered earthquakes occur beneath many of the active volcanoes. In the following we discuss each tectonic environment separately.

1. Shallow Thrust Zone

The shallow thrust zone is that portion of a subduction zone which generates the great destructive earthquakes. The zone is not well defined in the Cook Inlet area (Fig. 7), partly because it lies outside the area covered by the seismic network, but also because the zone is relatively quiet in this area. Figure 5 (top) shows quite clearly the lower level of seismic activity in the central portion of the 1964 Prince William Sound earthquake aftershock zone covered by our array. Jacob et al. (1977) have shown that the main differences of the seismic zones along the Aleutian arc are associated with the morphology of the shallow thrust zone, widening from west to east as the distance between the volcanic arc and the trench axis (arc-trench gap) increases. In our study area this gap widens from 300 km at the western end of Kodiak to 450 km at the upper end of lower Cook Inlet.

In contrast to Cook Inlet, the shallow thrust zone is very well defined beneath and trenchward of Kodiak Island, dipping at an angle of about five degrees (Fig. 8). There is an area of an unusually high rate of strain release on the southwestern Kodiak shelf, south of 17°N and between 152°W and 154°W (Figures 4 and 9). Figure 10 shows the historic seismic activity for various time periods since the turn of the century, indicating that this concentration of activity reaches back to that time. Only events of magnitude greater than 5 were used. Hypocenter locations shown in this figure for the period between 1944 and 1963 are based on the relocations by Tobin and Sykes (1966). Magnitude determinations for the period before 1963 are rather incomplete but still appear to be sufficiently homogeneous to meaningfully delineate areas of high con-

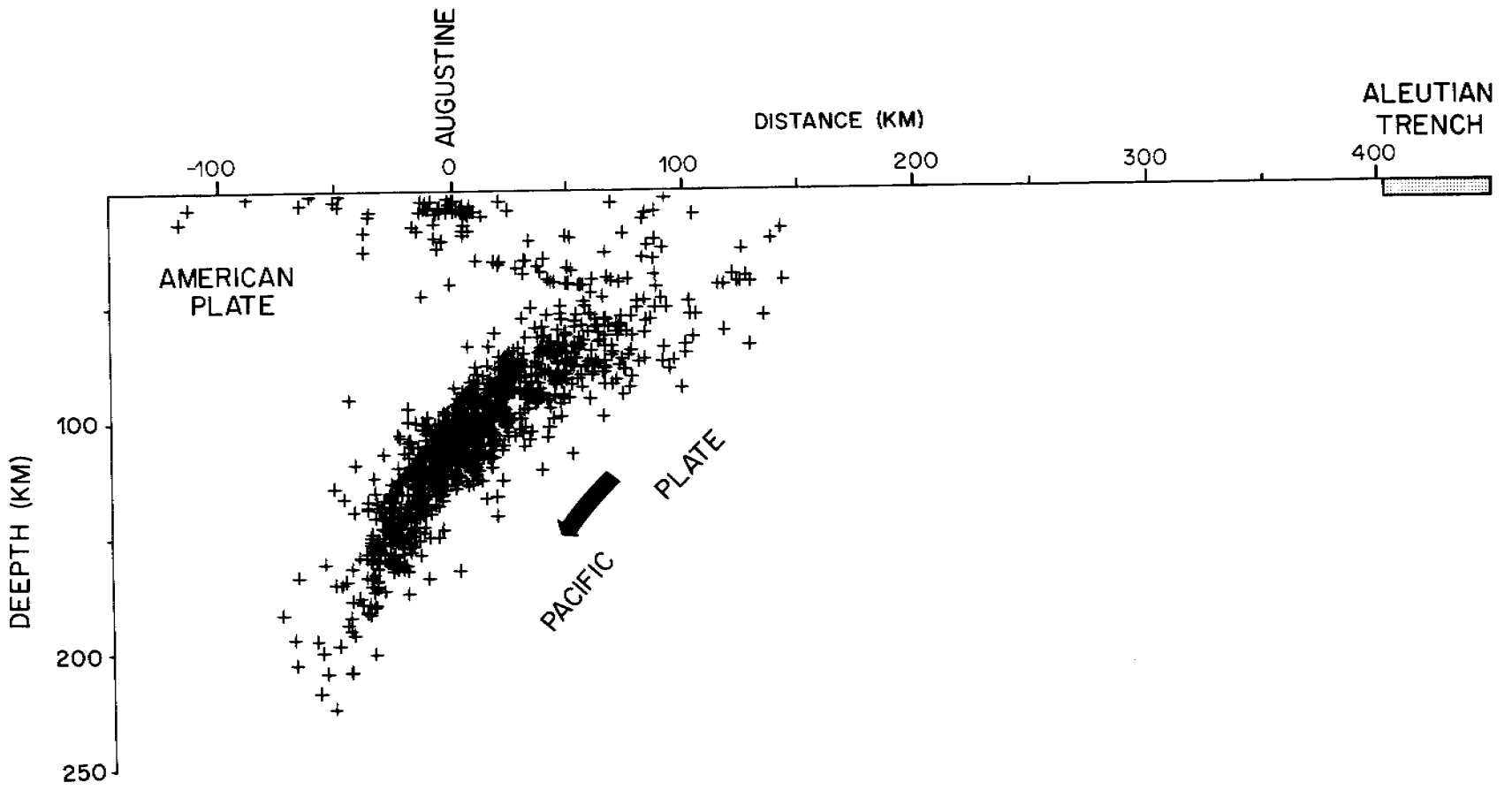

Figure 7. Benioff zone in Cook Inlet, class 1 events, February 1976-September 1978.

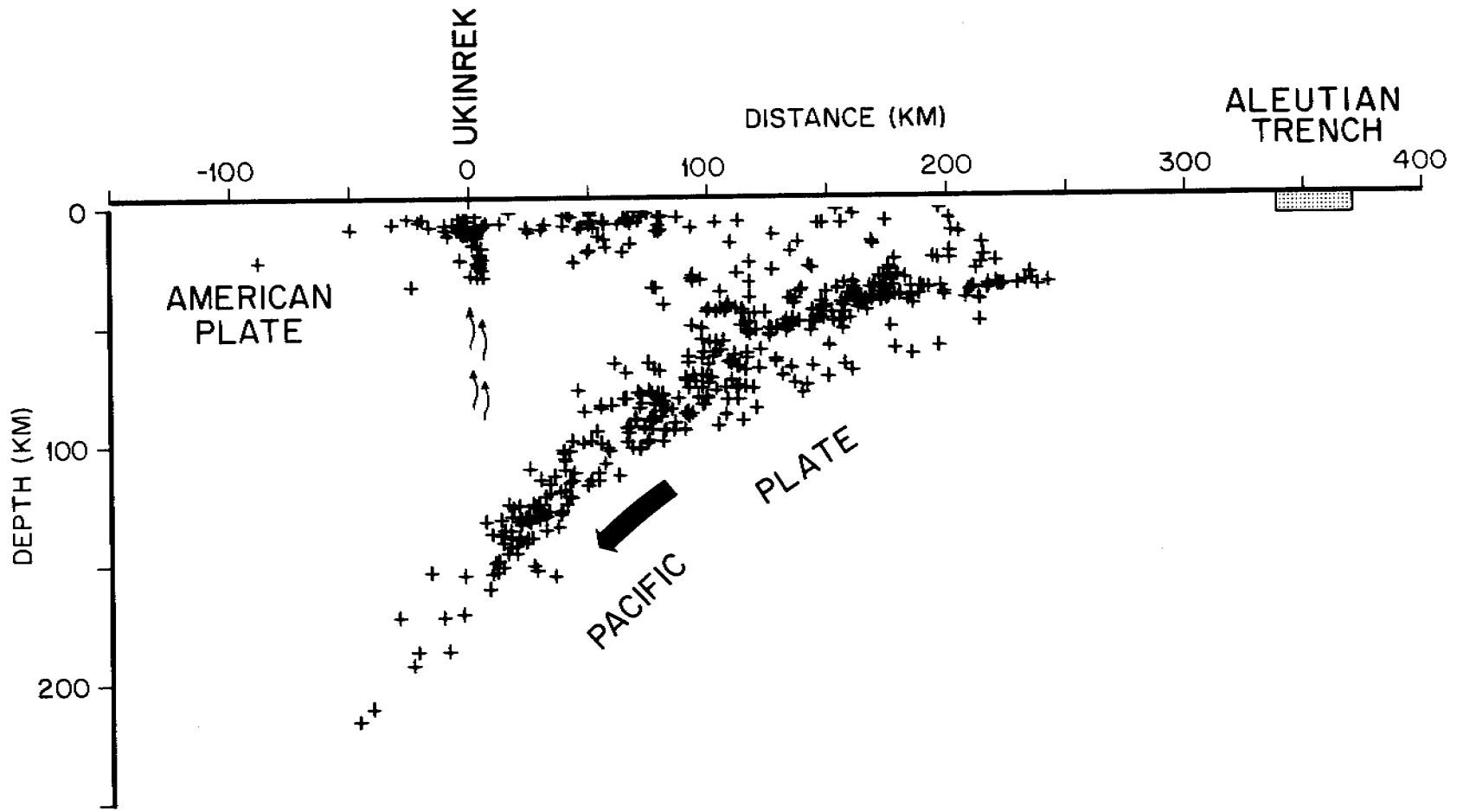

Figure 8. Benioff zone in the Upper Alaska Peninsula-Kodiak region, class 1 events, February 1976-September 1978.

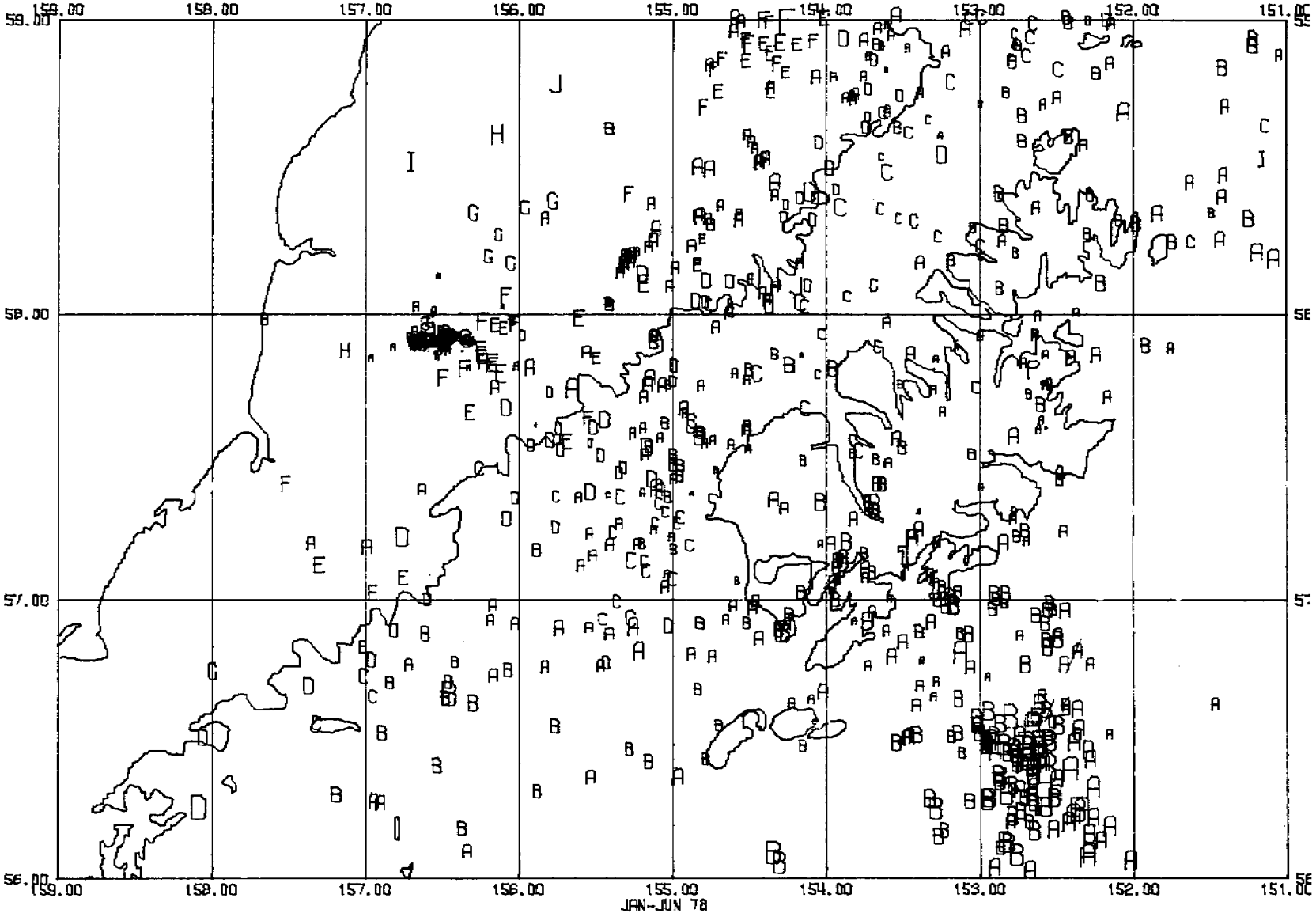

Figure 9. Epicenter map for Kodiak Island and the Alaska Peninsula, all events January to June 1978. Note, intense aftershock sequence of the magnitude 6.5 April 12, 1978 event off Kodiak and shallow cluster of events at the Ukinrek maars (near 156.5 W, 57.9 N).

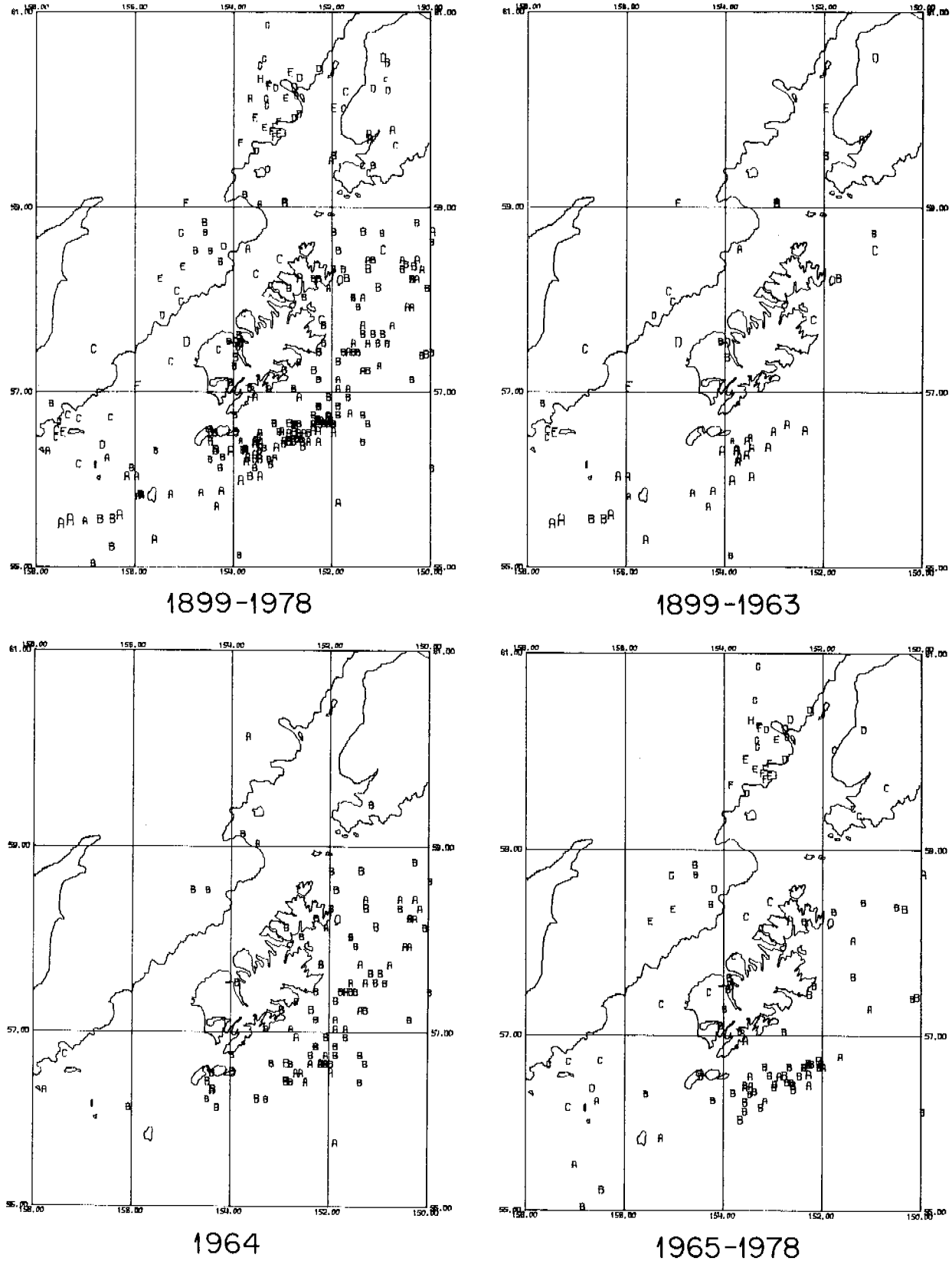

Figure 10. Earthquakes above magnitude 5 for different time periods. Note, that the cluster of events on the Kodiak shelf appears already prior to the great 1964 Alaskan earthquake.

centration of seismic activity at the magnitude level shown. Clearly, the pre-1963 plot represents a minimum level of seismicity. The zone of high activity is fairly sharply bound by the southwestern margin of the 1964 aftershock zone and the 152°W meridian, and may indicate a further transverse segmentation of the shallow thrust zone within the 1964 aftershock block. This motion is supported by sea floor studies of Hampton et al. (1979) which also indicate a sharp change in the style of deformation at the northeastern boundary of the zone of high seismic activity. Many of the events in the active seismic zone reflect the plate subduction process, i.e., they represent thrusts on gently dipping fault planes. First motion studies conducted by Stauder and Bollinger (1966) for events in the 1964 aftershock zone show a remarkably consistent picture of shallow dipping thrust solutions (Fig. 11). A magnitude 6.5 event that occurred in April 1978 also fits this pattern. First motion studies of this event and two major aftershocks do not permit a unique fault plane solution, but the first motion distributions (Fig. 12) are compatible and highly suggestive of a gently dipping thrust mechanism for these events. The lack of proper constraint for the fault planes is a consequence of the unfavorable azimuthal distribution of the seismic stations with respect to the epicenter. The postulated shallow thrust solution seems to be confirmed by the hypocentral distribution of aftershocks along the thrust plane (Figure 8).

2. Deep Benioff Zone

The lower portion of the Benioff zone is well defined throughout the study area. It is about 30 km thick, dips at an angle of 40 to 50 degrees into the mantle and reaches a maximum depth of about 200 km. There appears to be a steepening of dip near a depth of 100 km. Similar

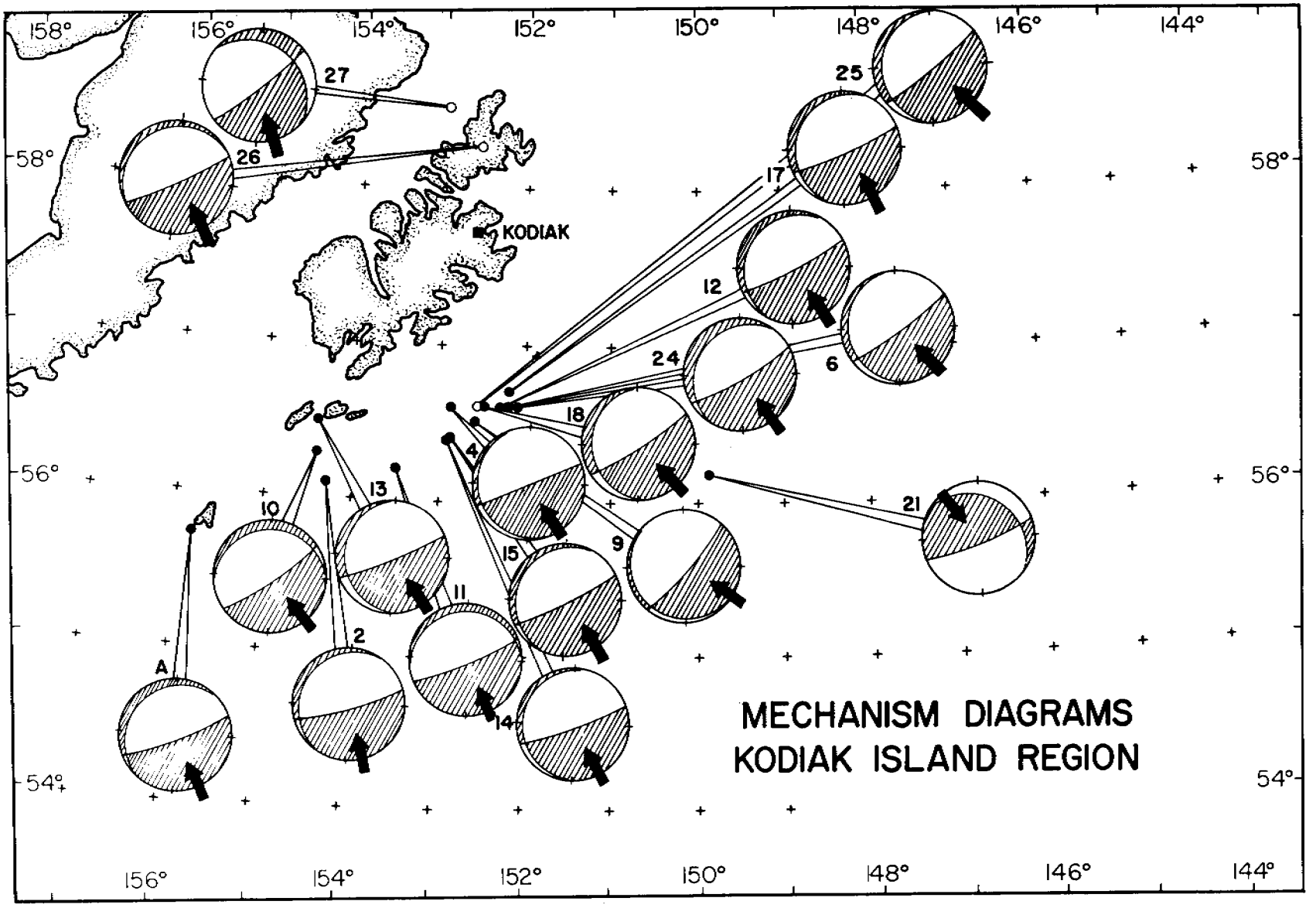

Figure 11. Consistent shallow thrust mechanisms for earthquakes in the 1964 aftershock zone, after Stauder and Bollinger, 1966.

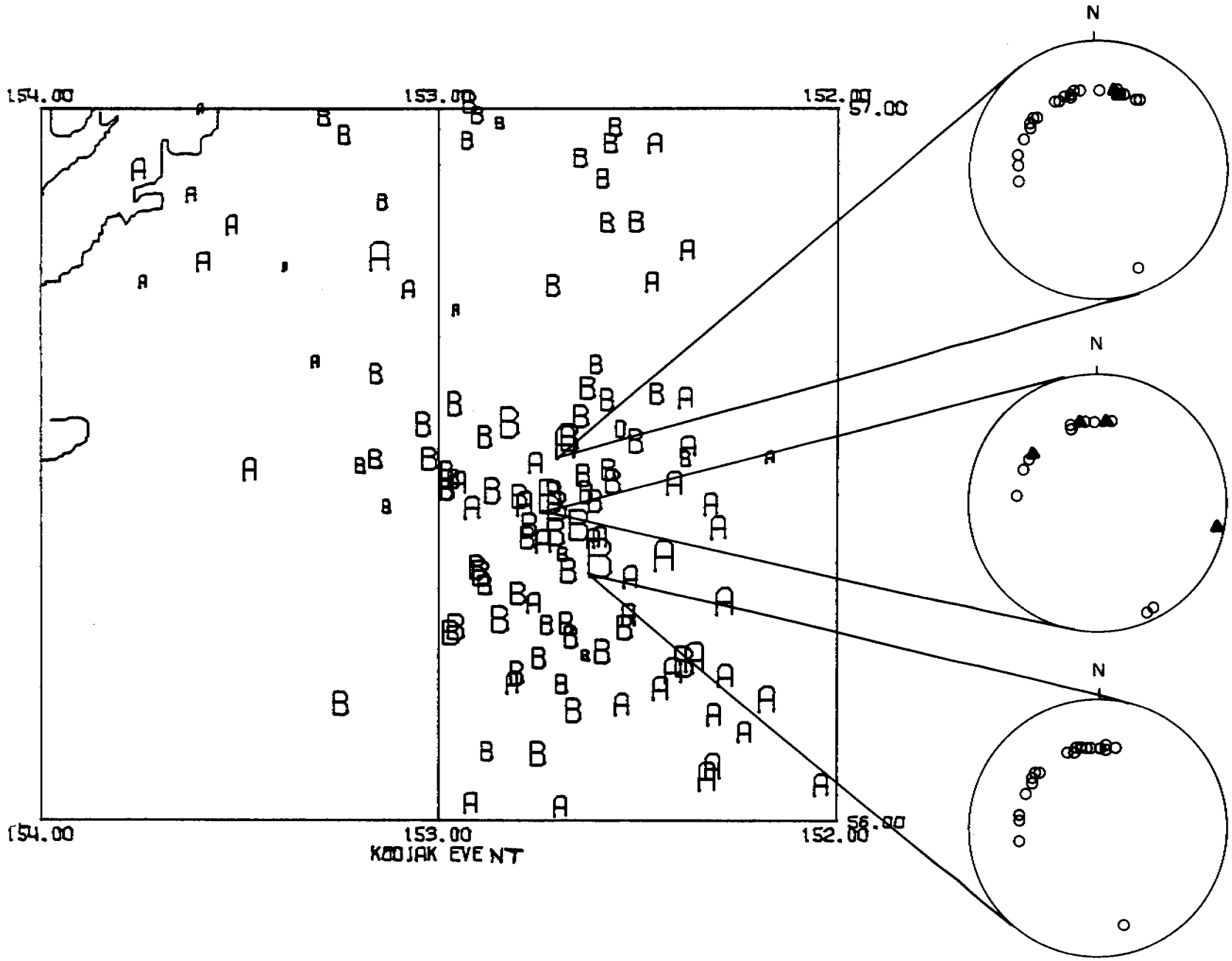

Figure 12. April 12, 1978, magnitude 6.5 earthquake off Kodiak Island--aftershock zone (all events) and first motion distribution (open circles-compressional arrivals, filled triangles--dilational arrivals).

changes in dip at that depth have been observed elsewhere in the Aleutian arc (Davies, 1979; Engdahl, 1977). There is some question whether or not this change in dip is real or represents an artifact of using over-simplified two-dimensional velocity models in locating earthquakes.

The seismicity in the deeper portion of the Benioff zone is not uniform in space but tends to cluster beneath certain volcanoes. The most prominent of these clusters lies below Mt. Iliamna, an active volcano, with frequent events in the magnitude 5-6 range (Fig. 13) but no great earthquakes are associated with the cluster. This cluster of activity appears to have developed post-1950 (Fig. 10). Less intense deep clusters occur beneath Augustine, Douglas and Peulik Volcanoes. Similar clustering of deep mantle earthquakes beneath volcanoes has been observed by Engdahl (1977) in the central Aleutian arc.

As in the shallow seismicity, there also seems to be a general decrease in the Benioff zone seismicity as one crosses from the western end of the 1964 aftershock zone into the extended Shumagin gap.

The aseismic wedge, a zone devoid of seismic strain release between the Benioff zone and the zone of shallow (less than 50 km) seismicity landward from where the Benioff zone bends into the mantle is clearly mapped out in Figures 7 and 8.

3. Shallow, Crustal Seismicity

Aside from the intense seismicity in the shallow thrust zone, the general shallow seismicity (hypocentral depth less than 50 km) in our area is diffuse and not preferentially associated with the major fault systems (Figures 3 and 4). This does not necessarily imply that these faults are indeed seismically inactive but rather that

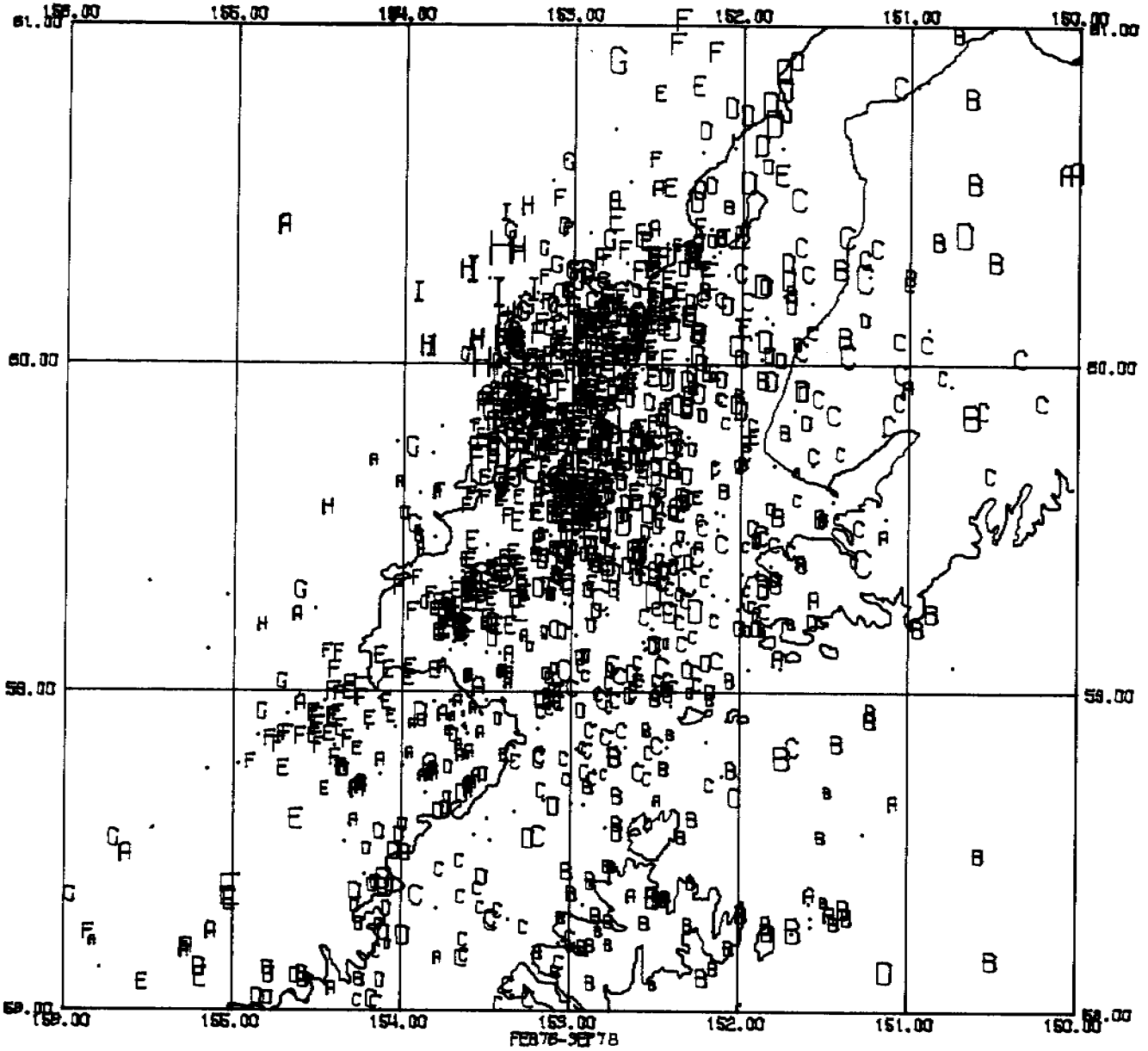

Figure 13. Epicenter map for Cook Inlet, class 1 events, February 1976-September 1978, showing the dominating deep cluster near Iliamna volcano and less intense deep clusters beneath Augustine Volcano and Mt. Douglas.

within the limited time period of operation of the high resolution seismic network we have no indication that these fault systems constitute important seismotectonics features. The concentration of activity in the shallow thrust zone off Kodiak underlies an area of intense sea floor deformation on the southwestern Kodiak shelf. In Figure 4 the many faults, offsets of the seafloor and submarine slides mapped by Hampton and Bouma (1979) have been plotted on the epicenter map to see if there is any correlation of seismic activity with individual mapped faults. To date we see no correlation. However, a few linear seismic trends in lower Cook Inlet might be associated with recently mapped offsets of the sea floor.

The only clear seismic trend that might indicate a seismically active fault is located on Kodiak Island, striking approximately N10°E from Deadman Bay (17°N, 154°W, Fig. 4). No fault has been mapped in this area. Though this linear is of no consequence with respect to the seismic risk associated with offshore development, it indicates that our system is capable of detecting faults that are seismically active, at least within the networks. To determine whether or not the mapped faults on the Kodiak shelf are seismically active, the present network needs to be extended with ocean-bottom seismometers.

4. Shallow Volcanic Clusters

Over the past 4 years we have located tight clusters of earthquakes beneath several volcanoes. In Cook Inlet, intense shallow (less than 10 km deep) precursor seismic activity was observed for an 8 month period prior to the 1976 eruptions of Augustine Volcano. On the Alaska Peninsula, we are still observing earthquake swarms near the Ukinrek Maars which newly formed during 10 days of phreatomagmatic activity in April 1977

(Kienle et al., 1978). In Katmai, shallow clusters of seismicity have been detected beneath or near the following volcanoes, from east to west: Mt. Douglas, Kaguyak Crater, Kukak Volcano, Snowy Mt., Trident, Mt. Mageik and Mt. Martin. We suspect that this seismicity is the result of hydrofracturing in shallow magmatic-geothermal reservoirs beneath the volcanic centers. So far we have not detected any volcanogenic earthquakes beneath the recently active volcanoes Katmai and Novarupta. The fact that we are locating the events beneath the volcanoes gives us confidence in our precision of earthquake locations.

B. Volcanology

1. Augustine Volcano

Offshore Flows: The main discovery of the past year, made through joint work with personnel (J. Whitney and his staff) from the U.S. Geological Survey, Conservation Division, Anchorage and R.U. 327 (M. Hampton and A. Bouma) was the tentative identification of extensive offshore pyroclastic flow deposits. Evidence for the existence of these features comes from the very detailed NOAA-NOS hydrographic survey H-9073, released last year, and reflection seismic data.

Several lobate, hummocky bathymetric features, that morphologically resemble the onshore Burr Point glowing avalanche terrane can be seen to extend up to 4 km offshore on almost all flanks of Augustine Volcano (Fig. 6) but expecially on the east flank. Whitney and Kienle suspect these features to be sub-marine pyroclastic flows. The integrated area of these deposits is about again the size of the exposed Island. In addition, a large submerged platform of unknown origin was discovered to extend 10 km offshore west of the Island (Fig. 6).

At the eastern flank of Augustine the shoreline, consists of a steep wave-erosional scarp with good outcrop, about 50 feet (15 m) high. These outcrops have been mapped by Detterman (1973) as andesitic to rhyodacitic lava flows but we found them to be andesitic-dacitic debris avalanches and lahars that appear to be the onshore equivalents of the suspected offshore flows. The flows were overlain by a well developed tephra sequence containing various soil horizons. We recovered a wood and a soil sample from the pyroclastic flow--tephra layer interface, which was C^{14}-dated at 1470 $\pm$ 160 and 1500 $\pm$ 155 years B.P. (Fig. 6). Since the 2 dates are in such good agreement we can be fairly sure that the underlying pyroclastic flow unit on the northeast side of Augustine has a minimum age of about 1500 years B.P., and that the overlying tephra sequence represents 1500 years of eruptive history. Kienle and S. Swanson, our new staff petrologist, will study this tephra sequence in detail during the 1979 field season.

Eruption Volumes: Figure 14 is a post-1976 eruption NOAA-NOS photograph of Augustine Volcano. The light colored materials are the deposits of pyroclastic avalanches. The bulk of these avalanches overran the northeast flank of the volcano but considerable pyroclastic flow activity also affected the eastern and southwestern flank of the volcano. These are the 3 flanks that face the lease areas. Decidedly fewer avalanches descended the western flank of the volcano. This distribution of pyroclastic flows is similar to the pattern mapped by Detterman (1968) following the 1963/64 eruptions. The directionality of pyroclastic flows from the last 2 major Augustine eruptions (1963/64, 1976) appeared to

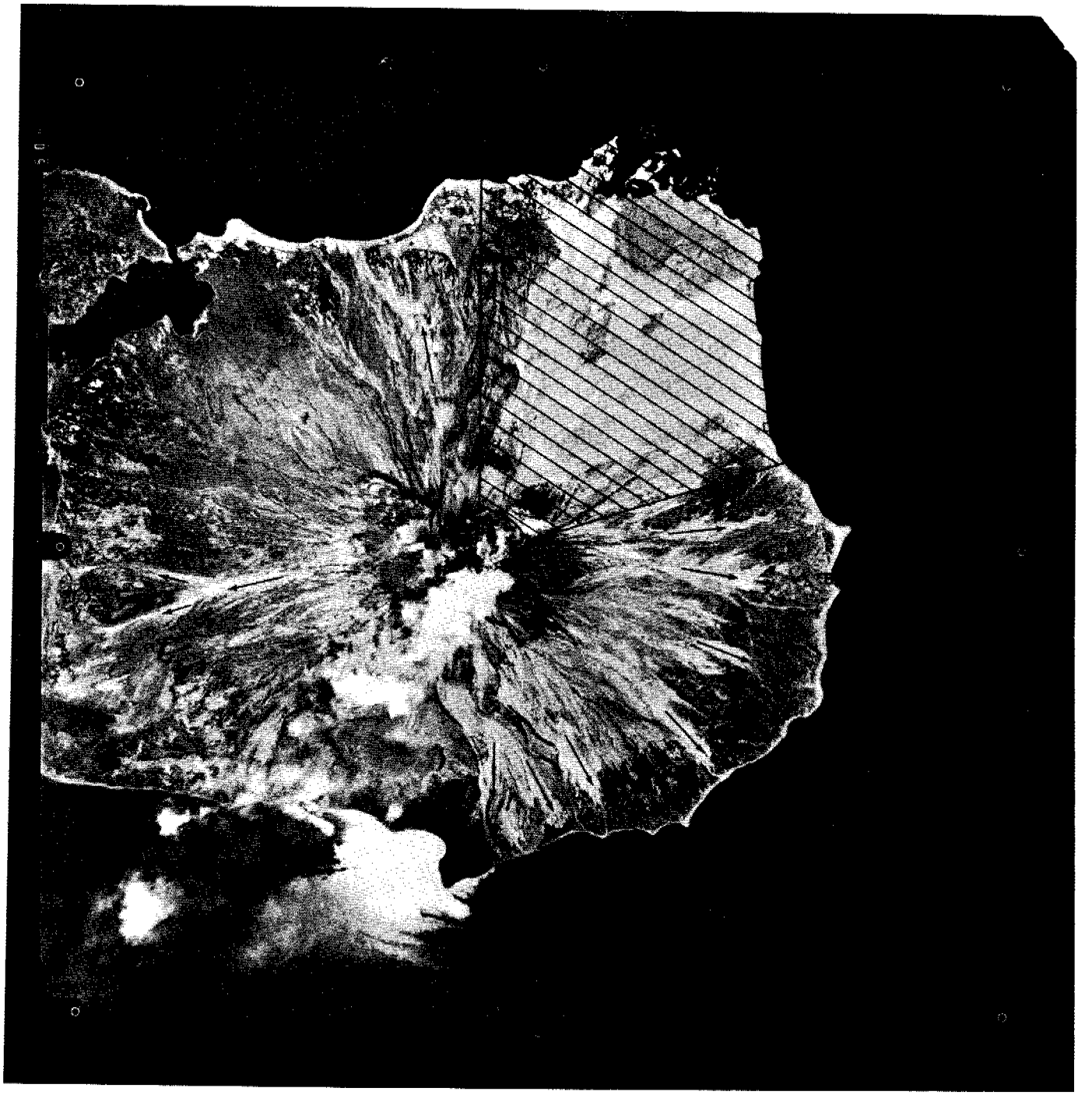

Figure 14. National Ocean Survey (NOS) photograph of June 11, 1976 of Augustine Volcano, showing the principal pyroclastic flow deposits (arrows and "ruled" area). The "ruling" actually indicates the exact location of 21 profiles along which the pre-1963/64, pre-1976 and post-1976 topography was digitized from air-photos in order to obtain volume estimates of the 1963/64 and 1976 debris. Also shown are the former NE-camp, now buried by pyroclastic avalanches and the Burr base camp, damaged heavily by glowing clouds.

be governed by the shape of the summit crater. We have now digitized the topography along 21 profiles crossing the north-northeastern pyroclastic fan terrane, based on aerial photography taken in 1957, 1974 and 1976. The location of the profiles is also shown in Figure 14. From this data we will obtain pyroclastic flow volumes for the 1963/64 and 1976 eruptions in the northeast sector of the volcano, where the flows were most voluminous, at least in 1976. A detailed (c.i. 10 m) topographic map of this sector of the volcano was prepared from the post-1976 eruption photogrammetric data (Figure 15).

1976 Precursor Seismicity: Lalla (1979) has now analysed the temporal and spatial distribution and the seismic energy release of the 1976 eruption precursor seismicity as a function of time. Knowing the three-dimensional structure of the volcano, as determined by the active seismic experiment discussed in the background section, it was possible to resolve the position of the precursor events to within half a kilometer. The precursor seismicity occurred in swarms and began eight months prior to the eruptions. It is epicentrally restricted to the central conduit system and is shallower than 6 km. From July to December, 1975, the monthly seismic energy release increased by three orders of magnitude from 6×10^{11} ergs to 4×10^{14} ergs. From January 1 to 22, 1976, when the eruptions began, the volcano entered a period of relative quiescence and the energy release (6×10^{13} ergs) dropped by a factor of 6, compared to December. The conduit system finally failed in a major earthquake swarm ten hours prior to the vent clearing explosions of January 23. That swarm released two orders of magnitude more energy (5×10^{16} ergs) than was released for the entire month of December. However, the total seismic precursor energy was

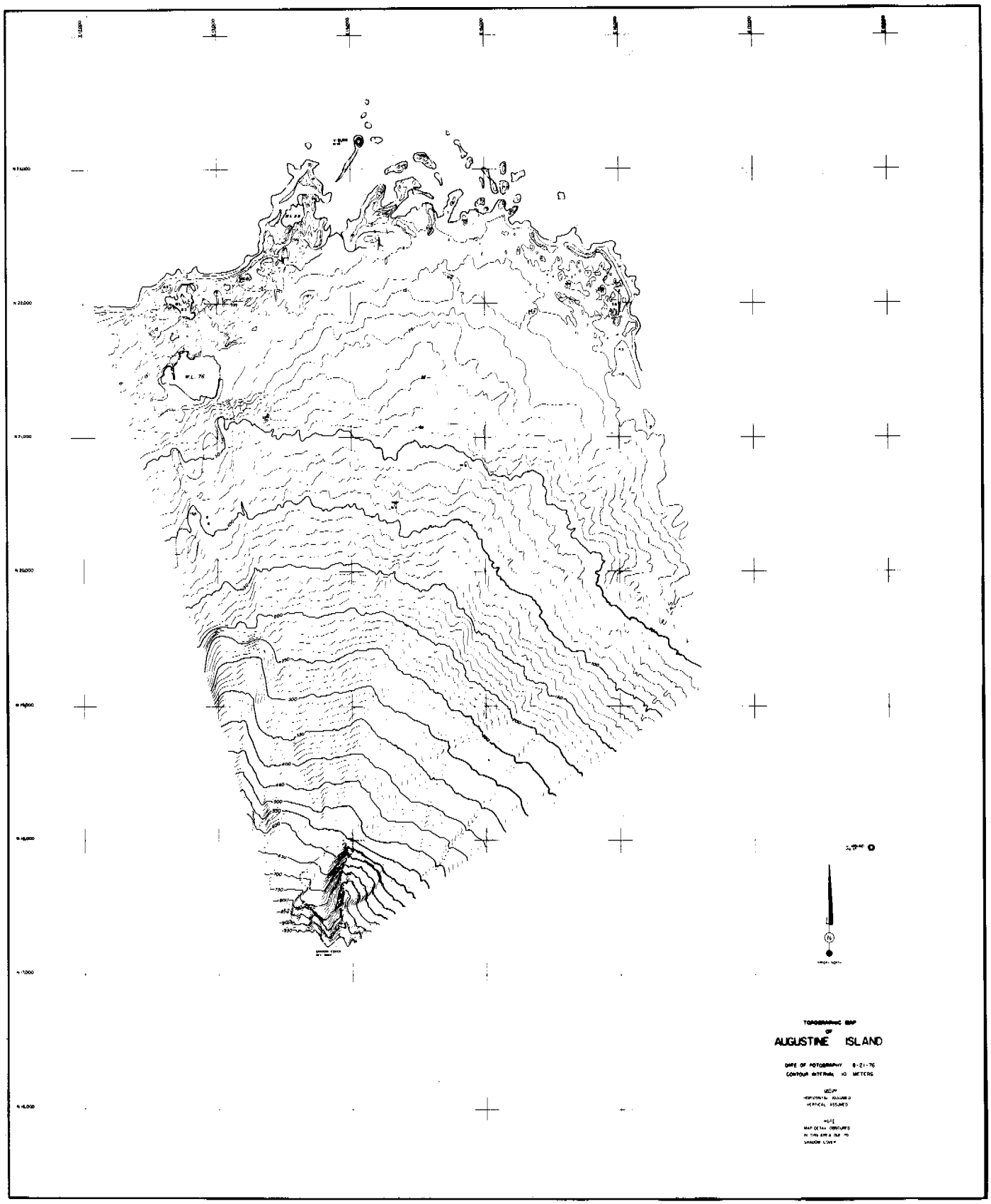

Figure 15. Post-1976 eruption topography of the NE sector of Augustine Volcano, covering 18 km^2, contour interval 10 m. The distance between tick marks is 1000 m. This was the area of most intense pyroclastic flow activity during the 1976 eruptions.

still seven to eight orders of magnitude lower than the thermal energy released in the eruptions. Figure 16 is a summary plot of the September to December 1975 precursor seismicity showing the tight clustering of epicenters near the center of the volcano (top) and a E-W cross sectional view of the hypocenters (bottom).

C. Redoubt Volcano

1. Petrology

Last year, R. Forbes and J. Kienle collected a first suite of rocks from Redoubt Volcano.

Prior to the 1978 field season, our knowledge of the petrology of Redoubt volcanic rocks was confined to that gained from a few samples collected during the 1966 eruption, and one collected from the summit dome by Kienle in 1977. Additionally, an ash sample collected from the deck of a ship in Cook Inlet during the eruption of 1902 has been acquired and analyzed. Whole rock chemical analyses of these samples are listed in Table 4. Selected samples collected in 1978 are awaiting analysis. However, some preliminary conclusions are merited by the data shown in Table 4.

(1) The bulk chemistries of samples (1) and (2) are remarkably similar, although sample (1) was erupted in 1902, and (2) was thought to be of the dome emplaced during the eruptions of 1966-68. Since the two analyses are nearly indistinguishable the dome may already have been extruded in 1902.

(2) Samples (3), (4) and (5) are chemically and mineralogically similar, and represent pumiceous vs. blocky variations in the initial ejecta of 1966.

(3) All of the above samples are hornblende bearing two pyroxene andesites, an ejecta type which appears to be dominant throughout the Redoubt volcanic pile. This magma type has a relatively high explosivity index, and an eruptive style characterized by turbulent ash cloud production, block avalanches, ash flows, lahars and endogenous dome formation.

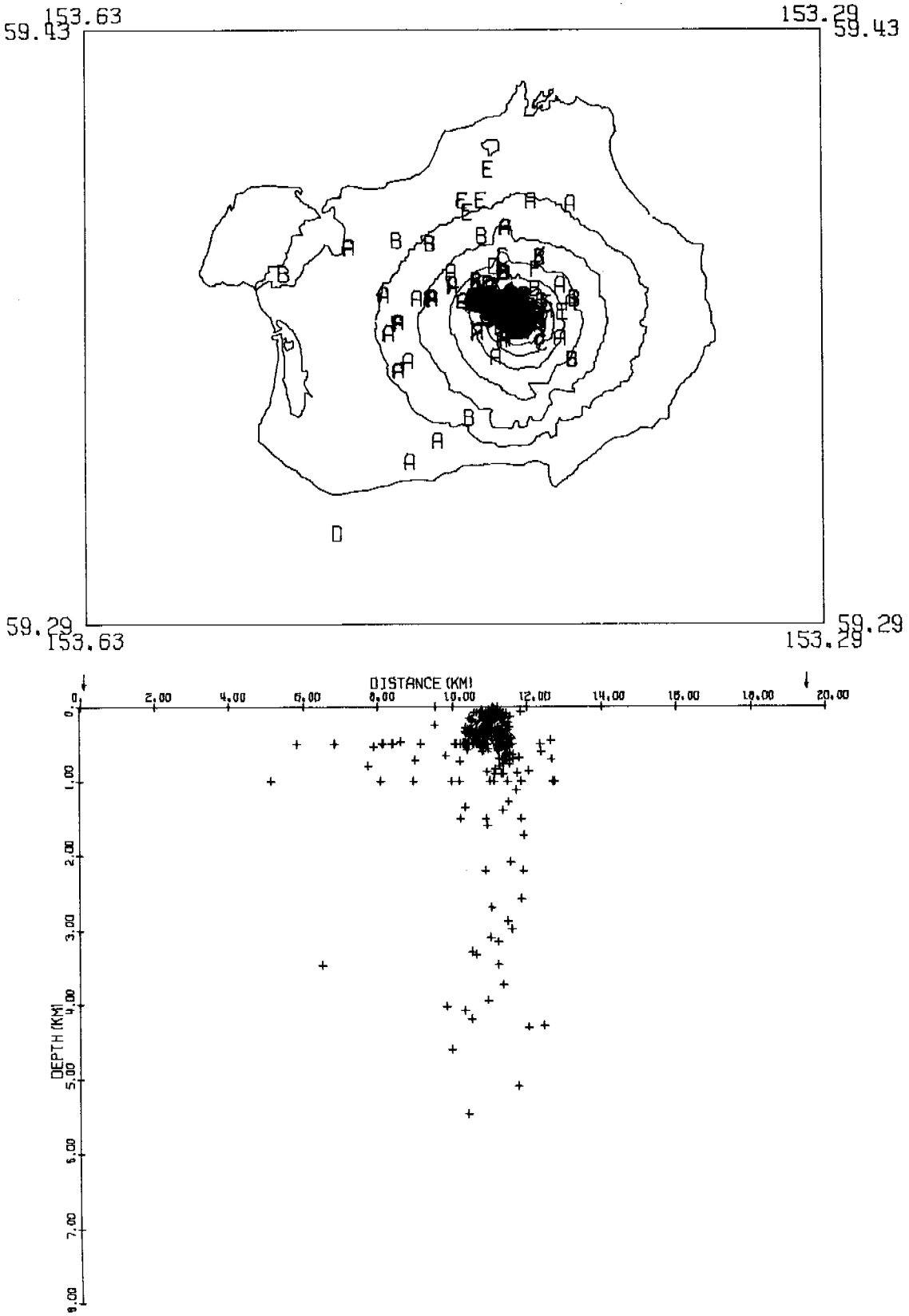

Figure 16. Epicentral (top) and E-W cross sectional view (bottom) of Augustine eruption precursor seismicity, September to December, 1975 (D. Lalla, personal communication).

Table 4 Whole rock chemical analyses of ejecta from Redoubt Volcano.

	(1)	(2)	(3)	(4)	(5)
SiO_2	60.46	60.40	59.46	59.92	59.72
Al_2O_3	18.16	18.20	18.10	17.83	18.20
TiO_2	0.56	0.54	0.74	0.65	0.68
Fe_2O_3			2.75	3.01	3.63
FeO	*6.14	*5.81	2.91 *5.39	3.13 *5.84	2.13 *5.40
MnO	0.15	0.15	0.14	0.15	0.14
MgO	2.51	2.34	2.60	2.59	2.24
CaO	6.80	6.82	7.14	6.70	6.95
Na_2O	4.19	4.08	3.94	3.99	4.16
K_2O	1.40	1.41	1.58	1.61	1.73
H_2O+	0.53	0.14	0.12	0.18	0.30
H_2O-	0.48	0.2	0.03	0.05	0.02
P_2O_5	0.23	0.22	0.20	0.20	0.21
Total	101.61	100.37	99.71	100.01	100.11

(1) Ash deposited on deck of ship in Cook Inlet during 1902 eruption: Analyzed by G. G. Cunningham.

(2) Andesite from summit dome of Redoubt Volcano: Collected by J. Kienle: Analyzed by G. G. Cunningham.

(3) Andesite block erupted by Redoubt Volcano in February, 1966, collected by R. B. Forbes: Analyzed by H. Haramura.

(4) Andesite block erupted by Redoubt Volcano in February, 1966, collected by R. B. Forbes: Analyzed by H. Haramura.

(5) Andesitic pumice erupted by Redoubt Volcano in February, 1966, collected by R. B. Forbes: Analyzed by H. Haramura.

* Σ Fe as FeO

Figure 17 shows the sample locations of the 1978 field study. Based on a suite of float samples collected from a stream bed near the base camp (Station #1-1), the flow units of the volcanic pile range from olivine theoleiite through hornblende bearing two pyroxene andesite to hornblende dacite. To date, rhyolite and rhyodacite indicative of highly explosive eruptions have not been detected in the sequence.

Sub-volcanic basement samples were collected from Stations #1, #2, and #6. On the north flank of the mountain, the granitic basement ranges from quartz monzonite to hornblende diorite. Basement rocks exposed in a deeply incised ravine on the south side of the peak (Station #6) are particularly interesting, as they appear to represent an igneous complex which includes plagiogranites and diorites.

Field work in 1978 indicated that olivine basalt flows and agglomerates were among the earliest units composing the Redoubt volcanic pile (Station #2). Andesite flows were also discovered which overlay glacial outwash (Stations #2, #9, #10); and these flows have in turn been glaciated by another ice advance. Based on these relations, we hypothesize that the eruptive history of Redoubt Volcano might extend back to Pre-Illinoian time. Attempts to date the andesites overlying the glacial outwash were unsuccessful due to an excessively young age, but olivine basalt collected from Station #2 was dated at 340,000 $\pm$ 10,000 years.

2. State of North Glacier

Last year Dr. Benson and his students (with logistic support from OCSEAP) surveyed the Drift River terminal lobe of North Glacier (Figure 18). Their results are summarized below.

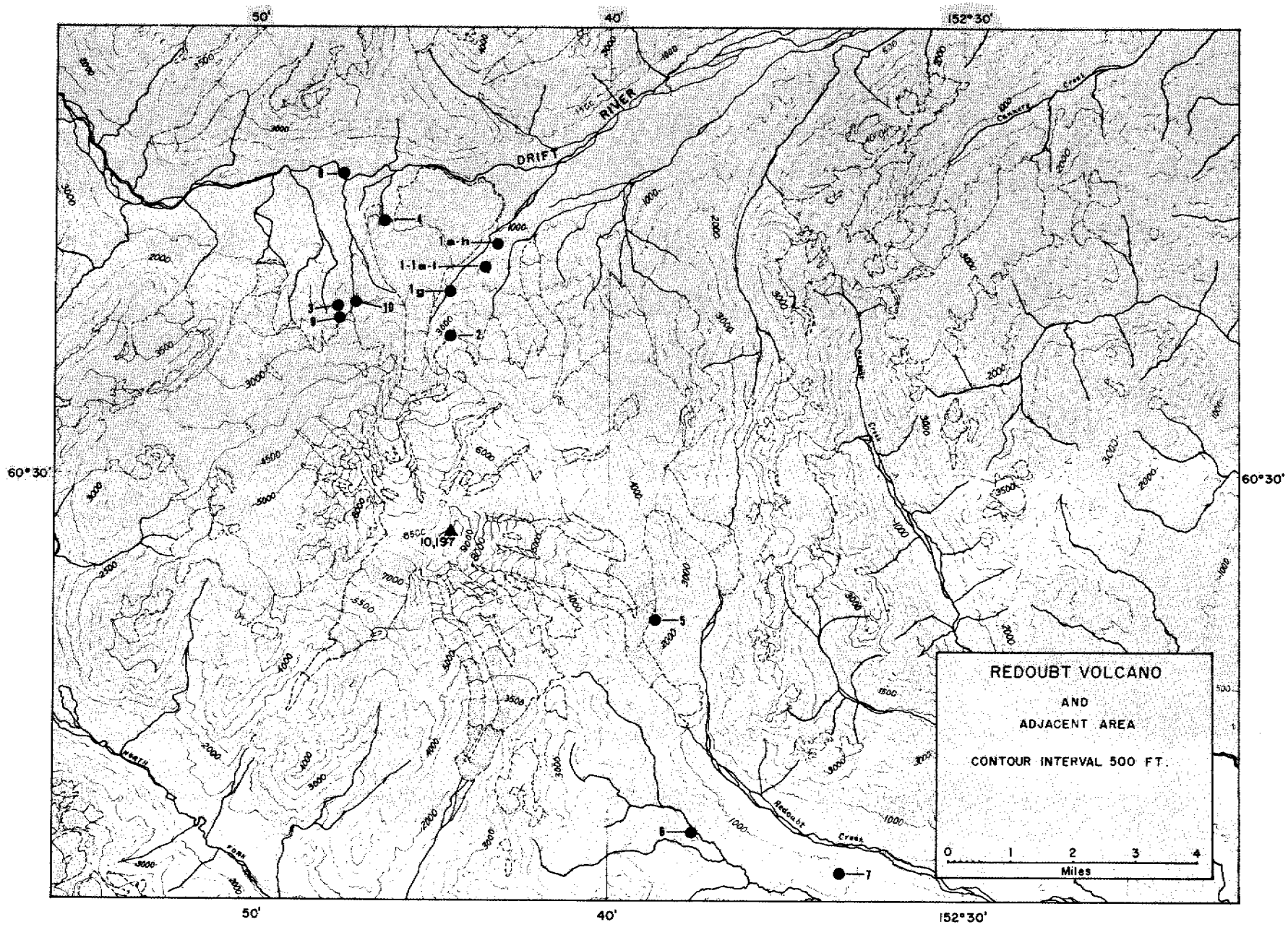

Figure 17. Location map of rock specimen collected at Redoubt during the 1978 field season.

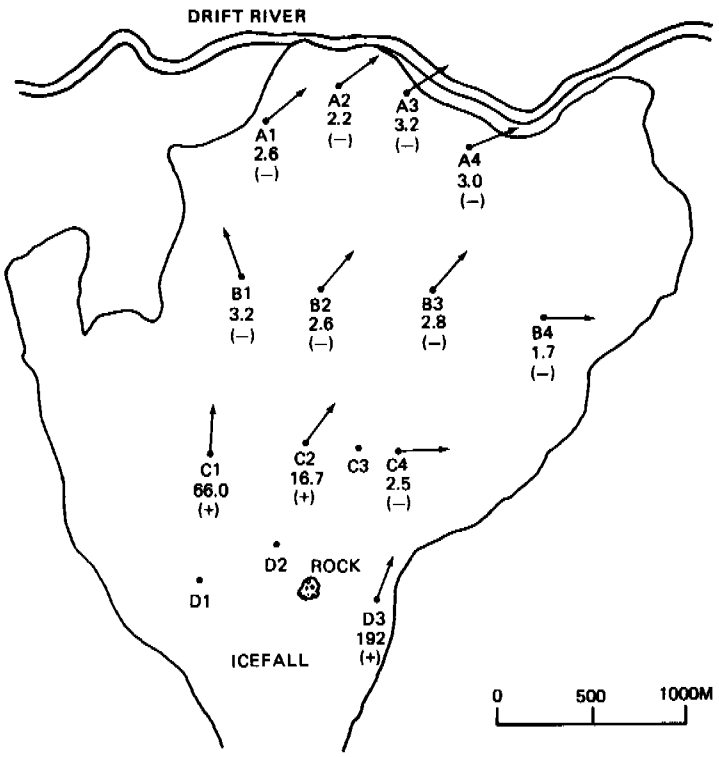

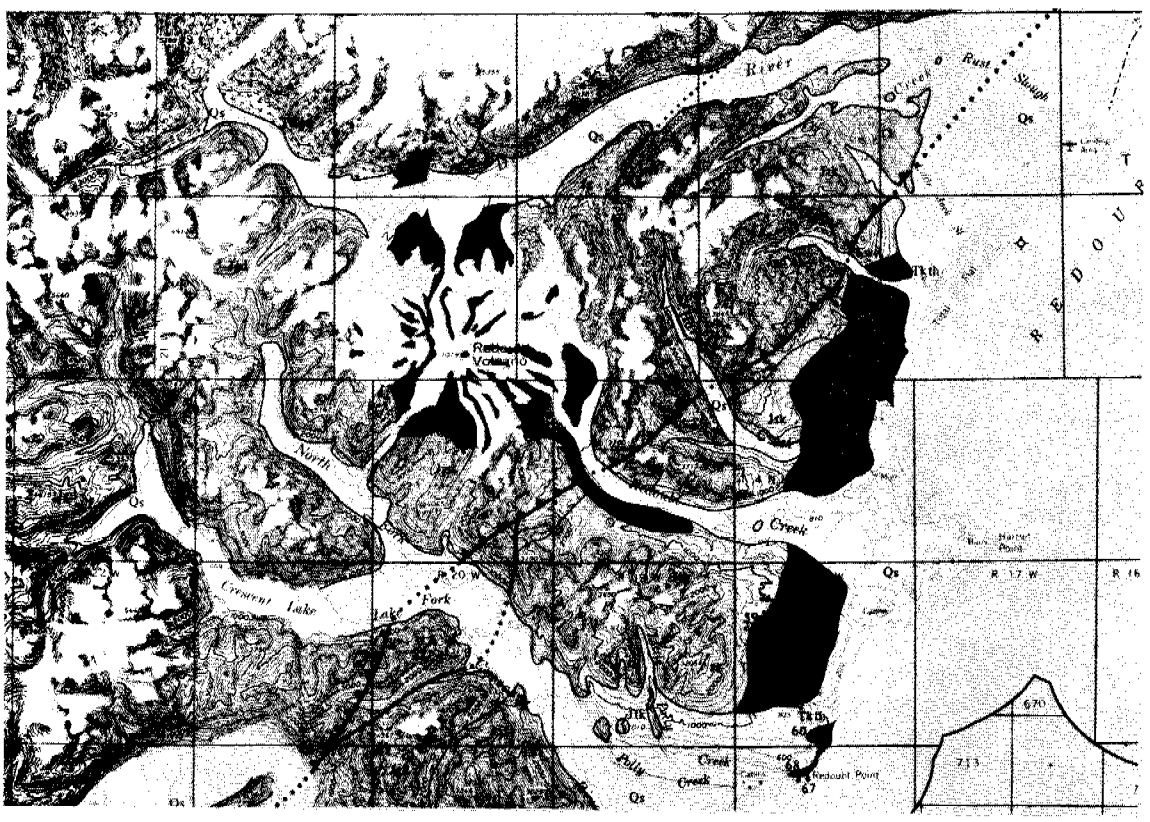

Figure 18. Location of the "North Glacier" on Redoubt Volcano (arrow, top) and close-up of "Drift River" glacier lobe (bottom). Arrows indicate flow directions deduced by comparing surveys taken in July and September, 1978. Stakes are letter-coded, numbers below letter-code indicate the stake velocity, converted to m/year. The + and - signs indicate thickening and thinning of ice, respectively.

Ablation: Near the river the vertical ice cliff had melted back 4.4 m between July and September, while at the icefall a pole that in July had been sunk 4 m into the ice had melted out completely by September.

Horizontal ice motion: Within 1.5 km of the river the motion was between 2 and 3 m/yr (0.33 to 0.5 m measured in 2 months). At a distance of 2.5 km from the river it was 66 m/yr on the west side and 2 m/yr on the east side, while at the icefall, 3 km from the river, one stake recorded a motion of 192 m/yr!

Vertical ice motion: As could be expected, the ice was thinning in the areas of slowest motion while in the area of faster movement on the west side, the ice was thickening.

Preliminary interpretation: The rate of melting at the terminus is 4.4 m horizontally, which at the moment is not quite balanced by about 3 m per year advance. This fits with the observation that the ice in the lower 1.5 km appeared to be thinning. However, a patch of debris from the 1966 eruption is moving down the steep portion of the glacier below the summit crater. The probably thickened ice beneath this insulating patch of debris has not yet reached the lower parts of the glacier and it is therefore important that we observe ice motion and thickening higher up. On the west side of a rock outcrop near the icefall (Figure 18) the ice moves rapidly as shown by stakes C1 and C2. This area must be carefully watched in future years to determine whether or not a pulse or wave of thickened ice is travelling down glacier that might eventually reach the glacier terminus potentially creating a flood hazard by damming up Drift River.

VII. DISCUSSION

Our rather short term data base already allows a closer look at the seismotectonics of the study area. Although we cannot give a deterministic description of the occurrence of earthquakes in time and space, the framework of plate tectonics, the historic earthquake data and the data from our high resolution seismic network define an important set of input parameters for seismic risk studies. Future analyses and seismic risk maps should take into account the high probability for a great earthquake in the extended Shumagin gap as we have delineated it, rather than just reflect the occurrence of great historic earthquakes. The postulate that such a great earthquake will most likely occur along the shallow thrust zone provides important constraints on the location and focal mechanism of such an event and hence on the ground-motions likely to be generated at a particular site.

The deeper portion of the Benioff zone (deeper than 50 km), though very active beneath certain volcanoes, seems not capable of generating great earthquakes. However, within recently filled gaps, such as Cook Inlet, activity like that below Iliamna volcano, with frequent events greater than magnitude 6, could be the prime contributor to the seismic risk within the stipulated timespan of petroleum development.

According to our findings, the shallow seismicity outside the shallow thrust zone is best modelled as diffuse, i.e., by specifying an equal probability for the occurrence of an earthquake of a given magnitude throughout the area. The large known fault systems do not have any higher probability of generating given magnitude earthquakes than the

rest of the area. This lack of correlation between seismicity and the known faults is probably sufficiently explained by the fact that these faults are old. On the other hand, it is not yet clear, whether the time period of operation of the high-resolution network has been sufficiently long to rule out the existence of any faults that will eventually have to be considered as seismic source areas.

Of all active volcanoes in Cook Inlet and Katmai Augustine poses the most immediate hazard to offshore petroleum development. We now understand its geochemical make-up and eruption behavior fairly well, having monitored the volcano through one major eruptive cycle. The 1976 eruption were preceded by 8 months of precursor earthquake swarm activity from the vicinity of a shallow magma chamber beneath the center of the volcano. We now feel confident that through continued seismic monitoring we could at least anticipate, if not predict, future eruptions.

Hazard map report: Plans are now firming up to publish all the hazard related data for Augustine, collected by various individuals with different sources of funding, in one map report. Negotiations are underway with the State of Alaska, Department of Natural Resources, Geological and Geophysical Surveys to produce the report and cover the publication costs. The principal contributors to this report will be D. Johnston, U.S. Geological Survey, Menlo Park; J. Kienle, University of Alaska, and J. Whitney, U.S. Geological Survey, Conservation Division, Anchorage. As we see it now, the report will probably cover the following subjects:

(a) eruptive history

(b) distribution geology, geochemistry, and geochronology of historic ejecta

(c) offshore volcanic deposits (dependent on this years (1979) field work)

(d) individual hazards (maps and tables)

The Redoubt work has just begun and we therefore only have a very preliminary idea what geologic hazards are of concern. A major flood hazard exists in the valleys radiating from the volcano, particularly in the Drift River Valley, where the flood waters associated with the 1966 eruptions reached the shore of Cook Inlet, 45 km from the volcano. There is also evidence that prehistoric lahars have travelled along river valleys and eventually reached Cook Inlet, 35 km from the volcano, as for example along the Crescent River Valley (J. Riehle, personal communication). These hazards would have to be taken into account if other landfall facilities for offshore oil production, such as the Drift River Tanker Terminal, were to be constructed at the mouth of valleys radiating from Redoubt.

VIII. CONCLUSIONS

Seismicity studies, based on both historic data and data accummulated from the operation of a high resolution seismic network, provide some important input into quantitative seismic risk studies for areas of offshore petroleum development in lower Cook Inlet, Shelikof Strait and off Kodiak Island. The greatest seismic risk is associated with the shallow seismic thrust zone of the subducting Pacific plate. There is a high probability that a great ($M > 7.8$) earthquake will occur in the

Shumagin gap within the liftetime of any potential petroleum development in that area. The relative sharpness of the transarc boundaries of the aftershock zones of great earthquakes in the Aleutians suggests that the shallow thrust zone is segmented into separate tectonic blocks which release accumulated strain independently. There is geologic and seismic evidence that one such boundary traverses the arc near the southern edge of Kodiak and separates the 1964 aftershock zone from the Shumagin gap. Additional segmentation may exist within the 1964 aftershock zone. Seismic risk appears lower in the other offshore areas which do not overlie the shallow subduction thrust zone, but the risk is still primarily associated with the subduction process. The shallow, crustal seismic activity (less than 50 km hypocentral depth) outside the subduction thrust zone does not correlate with the major known fault systems of the area, and is of a more diffuse nature.

Augustine volcano with its very active recent eruptive history presents perhaps the greatest volcanic risk within the lower Cook Inlet and Shelikof Strait lease areas. Being an island volcano its eruptions can be tsunamigenic as in 1883. Based on its eruptive history in this century Augustine can be expected again to erupt within the lifetime of potential petroleum development in lower Cook Inlet. Having monitored the volcano for 9 years through its last major eruptive cycle in 1976 we now have learned what eruption precursors to expect before a major eruption, thus enhancing our chances of perhaps predicting the next one through careful geophysical monitoring.

IX. NEEDS FOR FURTHER STUDY

The area of high seismic activity off Kodiak Island lies outside the present high resolution network. To provide better source identification in that area the land-based system should be complimented by ocean bottom seismometers (OBS's) at least temporarily. Artificial explosions, preferably along with the deployment of OBS's, are necessary for finer resolution of the seismic velocity structure in order to provide hypocenter location accuracy.

During our investigation of the historic seismicity off Kodiak and near Iliamna volcano we used the present NOAA catalogue of historic earthquakes. The catalogue is estimated to be complete since 1899 for magnitudes greater than 7, since 1978 for magnitudes 6, and since 1969 for magnitudes 3.5. This requires the estimation of recurrence rate to be made from rather short and non-homogeneous records (with the added problem of poor location accuracies), thus limiting the space-time studies greatly. It might be of great value for many seismic risk studies to reevaluate the present historic (pre-1963) catalogue, by relocating hypocenters and determine the magnitudes of below 7 and 6 shocks (our search of the very limited number of other catalogues accessible to us, yielded a magnitude 7.2 event in 1938 off Kodiak, a magnitude 6 event in 1959 in Shelikof Strait and a magnitude 6.1 event in 1959 on the Kenai Peninsula).

Since strong motion data are of prominent importance to seismic risk assessment an increased number of strong motion instruments in the area seems warranted.

Augustine Volcano: Extensive (in area nearly the size of Augustine Island itself) offshore deposits were discovered last year and are suspected to be submerged glowing avalanche deposits. These deposits need to be sampled and mapped. During the 1979 field season we will attempt with supplemental OCSEAP and State of Alaska funds to dive on the Augustine offshore deposits, probably again joined by J. Whitney and other staff from the U.S. Geological Survey, Conservation Division, Anchorage. The objectives will be to (1) to verify the volcanic nature of the suspected debris flows offshore Augustine Island (2) to determine the geology of the West Platform and (3) to investigate Augustine rocks south of the Island.

Tephrachronologic studies to date and determine the recurrence rate of prehistoric eruptions over the past 1500 years will begin in the 1979 field season and should continue.

Redoubt Volcano: To date, the Redoubt study has received very little funding by OCSEAP, barely supporting the geologic work. Whether or not OCSEAP should support the glaciologic aspect of this work, which so far was accomplished largely with outside help (C. Benson and students), depends on whether or not OCSEAP should concern itself with landfall industry operations, such as the Drift River tanker terminal. If it does, the program needs to be scaled up. Assessment of the future flooding potential in the Drift River Valley would require a study of the flood deposits in the valley and of the mass balance of the entire North Glacier.

Other Volcanoes: So far only 2 of the most active Katmai and Cook Inlet volcanoes have been considered. Because Shelikof Strait is now being considered for leasing, reconnaissance geologic studies need to be made on some of the Katmai volcanoes, particularly Mt. Douglas and the volcanoes at the head of Hallo Bay.

X. SUMMARY OF JANUARY-MARCH QUARTER

Laboratory activity involved primarily prepartory work for the annual seismic network service trip and redepth of the interfocusing of the strong motion instruments with the high gain system. Reactive minute operations continued at the Homer recording site. Routine data processing is on schedule. Figures 19 through 22 show epicenter maps for the time period October 1978 through December 1978.

Work has continued towards the preparation of the joint USGS-State of Alaska and University of Alaska Augustine Volcano Hazard Report. Last years Redoubt rock samples have been petrologically analysed.

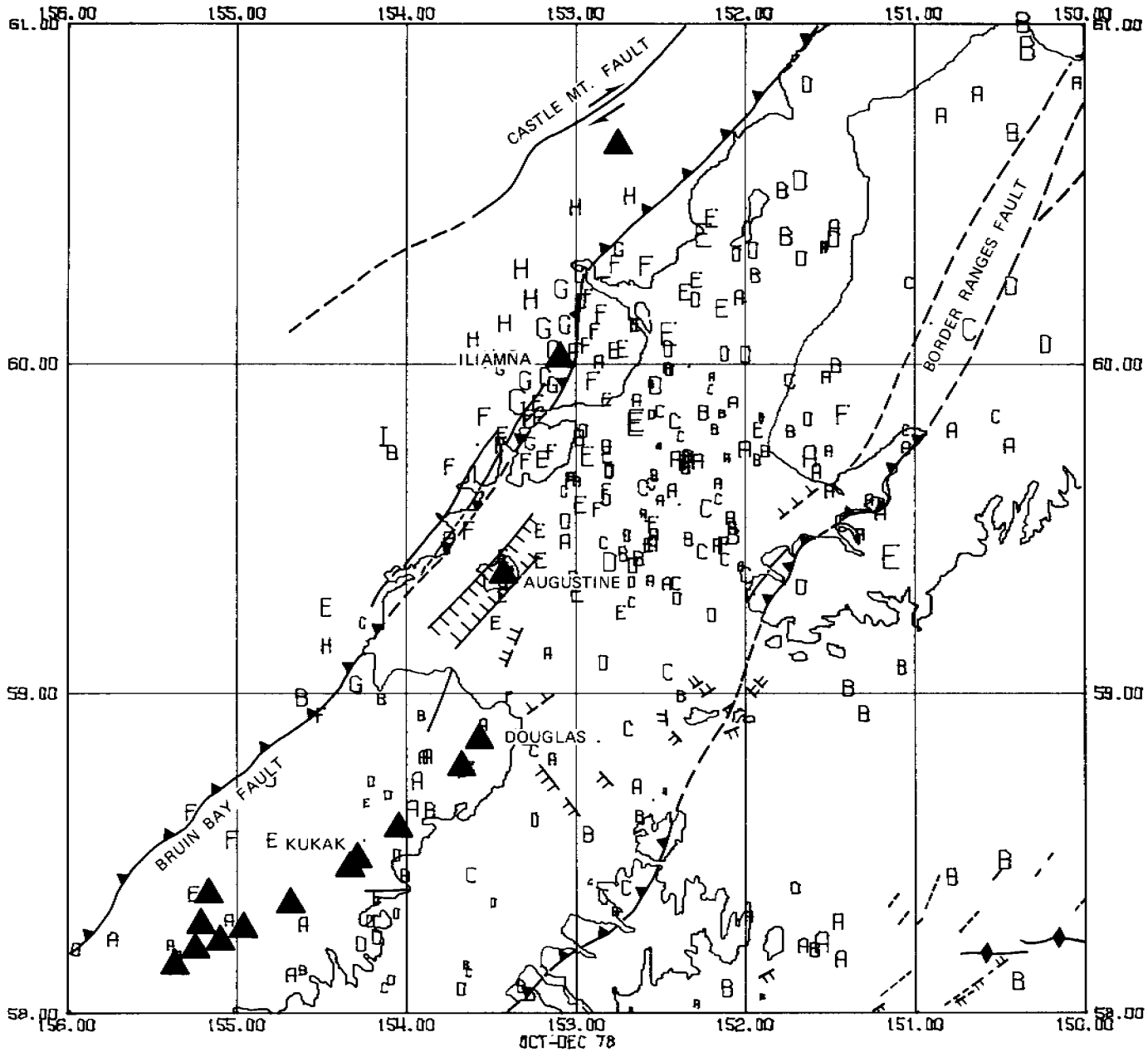

Figure 19. Epicenters (all depths, all events) in relation to faults and volcanoes in the lower Cook Inlet region, October to December, 1978.

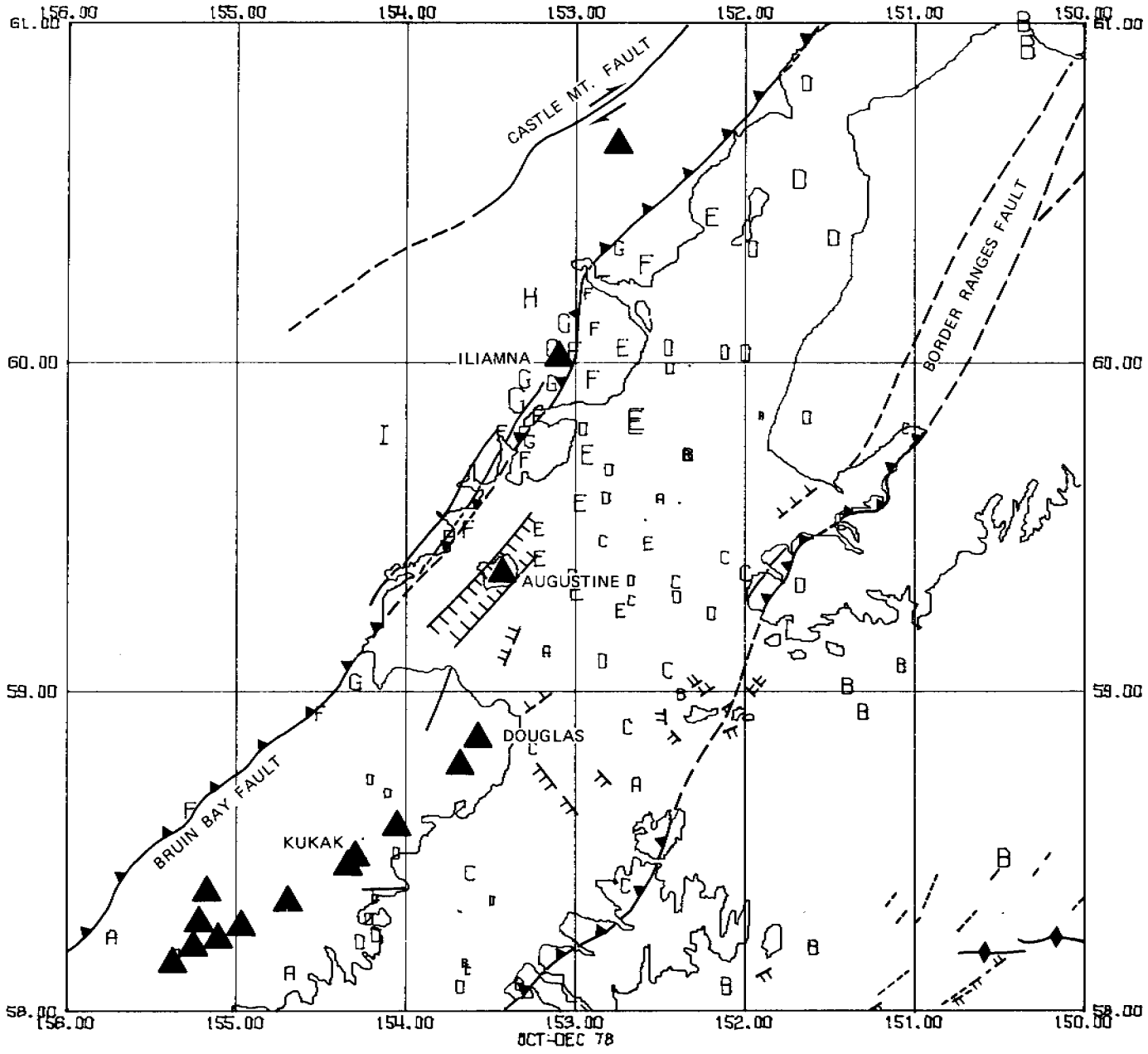

Figure 20. Epicenters (all depths, class 1 events) in relation to faults and volcanoes in the lower Cook Inlet region, October to December, 1978.

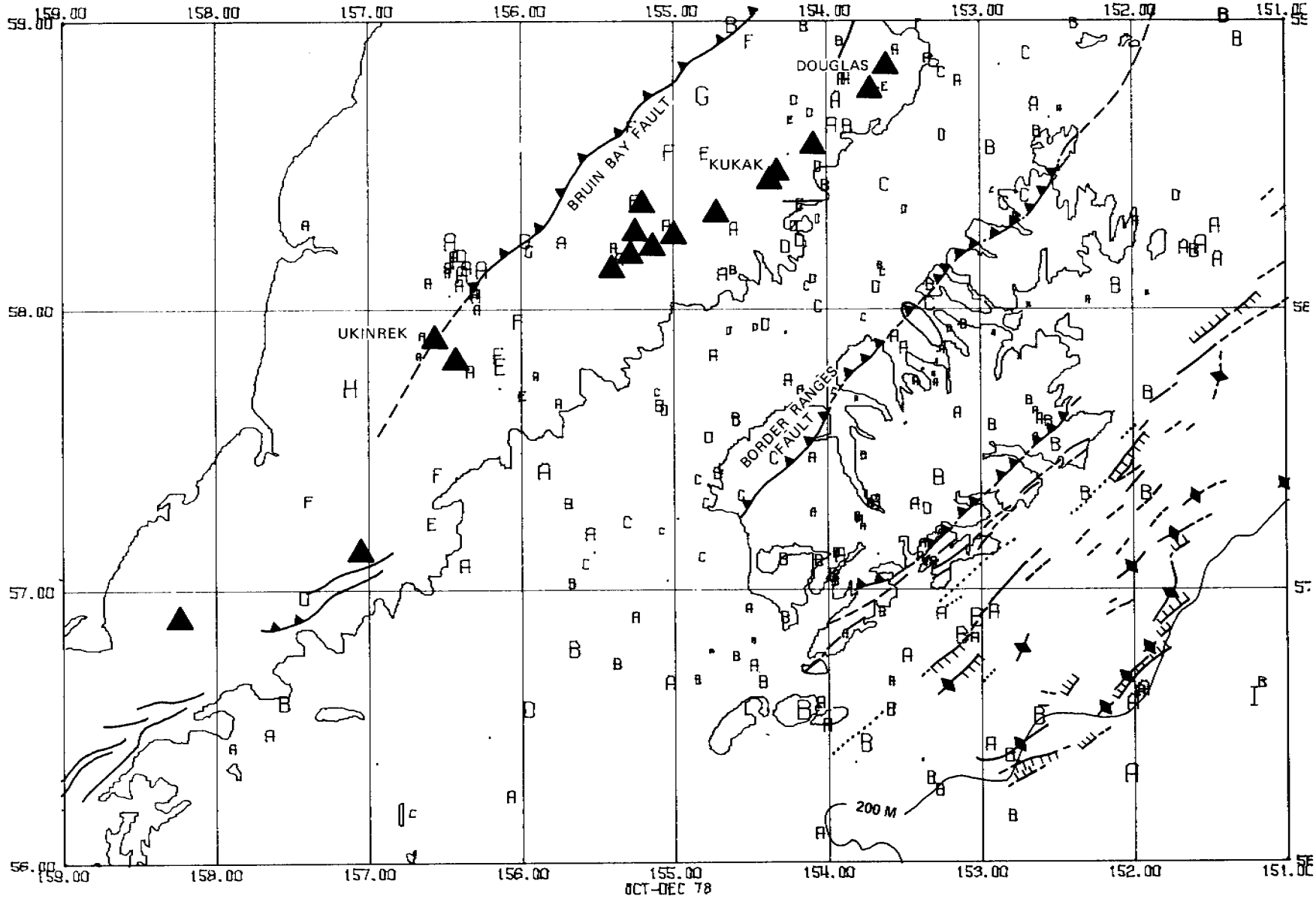

Figure 21. Epicenters (all depths, all events) in relation to faults and volcanoes in the Kodiak-Shelikof Strait-Alaska Peninsula region, October to December, 1978.

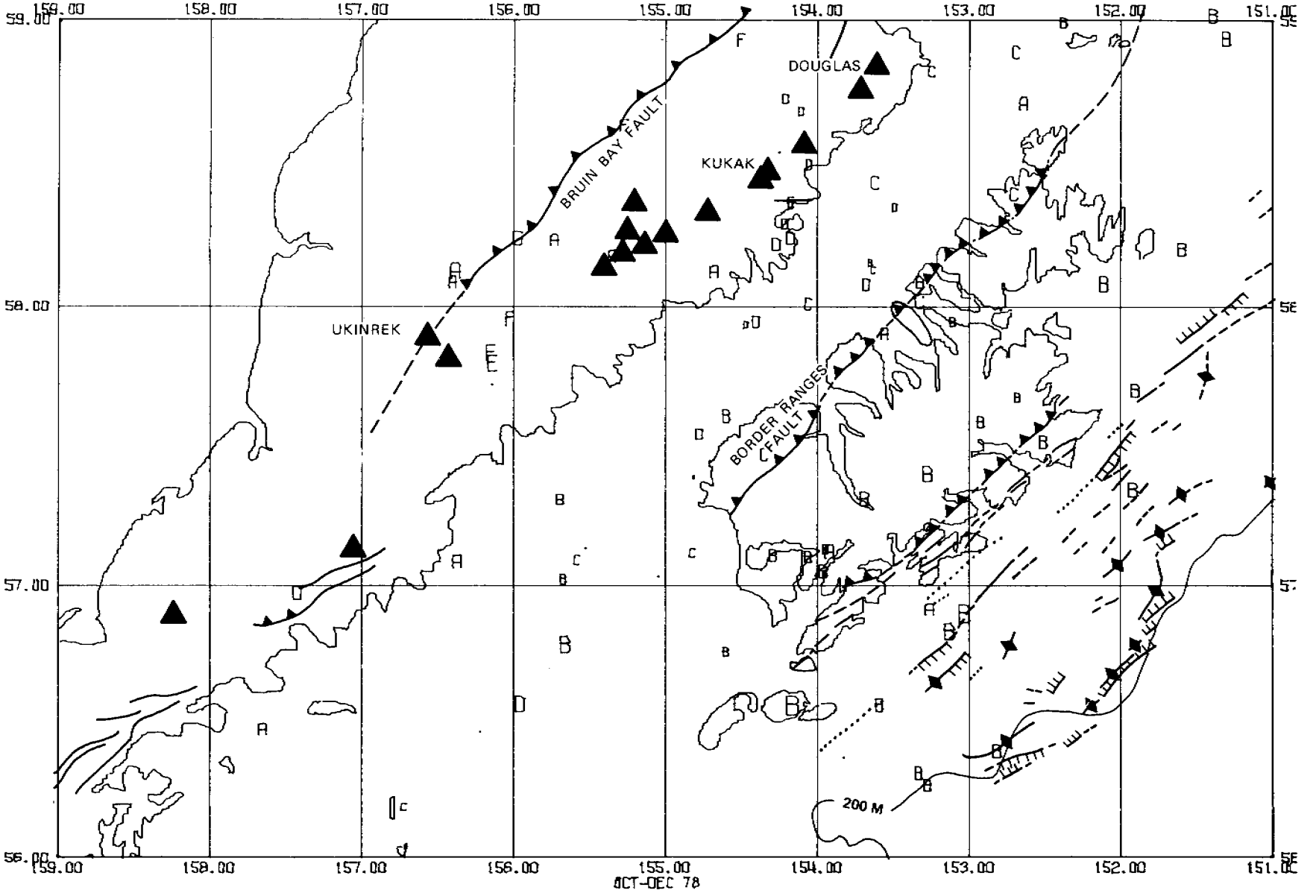

Figure 22. Epicenters (all depths, class 1 events) in relation to faults and volcanoes in the Kodiak-Shelikof Strait-Alaska Peninsula region, October to December, 1978.

XI. AUXILIARY MATERIAL

A. References

Anderson, T. and J. S. Flett, 1903, Report on the Eruptions of the Soufrière, in St. Vincent, in 1902, and on a Visit to Montagne Pelée, in Martinique - Part 1, Phil. Trans. of the Royal Soc. of London, Series A, Vol. 200, pp. 353-553.

Archambeau, C., 1978, Estimation of Non-hydrostatic Stress in the Earth by Seismic Methods: Lithospheric Stress Levels along Pacific and Nazca Plate Subduction Zones, in Proceedings of Conference VI, National Earthquake Hazards Reduction Program, U.S. Geological Survey Open-File Report 78-943, 47-138.

Buffler, R. T., 1976, Geologic Map of South Augustine Island, Lower Cook Inlet, Alaska, State of Alaska, Dept. of Natural Resources, Div. of Geological and Geophysical Surveys, AOF-96, 3 pp. and map.

Burk, C. A., 1965, Geology of the Alaskan Peninsula-Island Arc and Continental Margin (Part 1), Geological Society of America Memoir No. 99, 250 pp.

Davies, J. N., and House, L., 1979, Aleutian Subduction Zone Seismicity, Volcano-Trench Separation and Their Relation to Great Thrust Type Earthquakes, J. of Geophys. Res., in press.

Detterman, R. L., 1968, Recent Volcanic Activity on Augustine Island, Alaska, U.S. Geological Survey Prof. Paper 600-C, C126-C129.

Detterman, R. L., 1973, Geological Map of the Iliamna B-2 Quadrangle, Augustine Island, Alaska.

Engdahl, E. R., 1973, Relocation of Intermediate Depth Earthquakes in the Central Aleutians by Seismic Ray Tracing, Nature Phys. Science, 245, 23-25.

Engdahl, E. R., 1977, Seismicity and Plate Subduction in the Central Aleutians, in Island Arcs, Deep Sea Trenches and Back-Arc Basins, Maurice Ewing Ser., Vol. 1, edited by M. Talwani and W. C. Pitman III, Amer. Geoph. Union, 259-272.

Evans, C. D., Buck, F. H., Buffler, R. T., Fisk, S. G., Forbes, R. B., Parker, W. B., 1972, The Cook Inlet--An Environmental Background Study of Available Knowledge, Prepared by the University of Alaska, Resource and Science Service Center, Alaska Sea Grant Program, Anchorage, Alaska, for the Alaska District Corps of Engineers, Anchorage, Alaska, 446 pp.

Hampton, M. A., Bouma, A. H., Von Huene, R., and Pulpan, H., 1979, Geo-Environmental Assessment of the Kodiak Shelf, Offshore Technology Conference, Houston, Texas, in press.

Jacob, K. A., Nakamura, K., and Davis, T. N., 1977, Trench-volcano Gap along the Alaska-Aleutian Arc: Facts, and Speculations on the Role of Terrigenous Sediments for Subduction: in Island Arcs, Deep Sea Trenches and Back-Arc Basins, Maurice Ewing Series, Vol. 1, edited by M. Talwani and W. C. Pitman III, Amer. Geoph. Union, 243-258.

Kanamori, H., 1977, The Energy Release in Great Earthquakes, J. of Geoph. Res., v. 82, 2981-2988.

Kelleher, J. A., 1970, Space-Time Seismicity of the Alaska-Aleutian Seismic Zone, J. of Geoph. Res., v. 75, 5745-5756.

Kienle, J. and R. B. Forbes, 1975-76, Augustine-Evolution of a Volcano, Annual Report, Geophys. Inst., Univ. of Alaska, 26-48.

Kienle, J., Motyka, R. J., Lalla, D. J., Estes, S. A., and Huot, J. P., 1977, Formation of Two Maars Behind the Aleutian Volcanic Arc, Alaska Peninsula, April 1977, University of Alaska, Geophys. Rep. UAG R-257, 26 pp.

Kienle, J. and G. E. Shaw, Plume dynamics, thermal energy and long distance transport of Vulcanian eruption clouds from Augustine Volcano, Alaska, J. of Volcanol. and Geotherm. Res., in press, accepted January, 1979.

Johnston, D. A., 1978, Volatiles, Magma Mixing, and the Mechanism of Eruption of Augustine Volcano, Alaska, Ph.D. Thesis, Univ. of Washington, 177 pp.

Lahr, J. C., Plafker, G., Stephens, C. D., Fogleman, K. A., and Blackford, R. E., 1979, Interim Report on the St. Elias Earthquake of 28 February 1979, U.S. Geol. Survey Open File Report 79-670, 35 pp.

Lalla, D. J., 1979, Seismologic and Thermal Studies at Augustine Volcano, Alaska, Ph.D. Thesis, Univ. of Alaska, in preparation.

MacDonald, G. A., 1972, Volcanoes, Prentice Hall, Englewood Cliffs, N.J., 510 pp.

Magoon, L. B., Adkison, W. L., Chmelik, F. B., Dolton, G. L., Fisher, M. A., Hampton, M. A., Sable, E. G., and Smith, R. A., 1976, Hydrocarbon Potential, Geologic Hazards, and Infrastructure for Exploration and Development of the Lower Cook Inlet, Alaska, U.S. Geol. Survey, Open File Report 76-449, 124 pp.

Magoon, L. B., Bouma, A. H., Fisher, M. A., Hampton, M. A., Scott, E. W., and Wilson, C. L., 1979, Resource Report for Proposed OCS Sale No. 60 Lower Cook Inlet-Shelikof Strait, Alaska, U.S. Geol. Survey, Open-File Report 79-600, 38 pp.

Malloy, R. J., and Merrill, G. F., 1972, Vertical Crustal Movement on the Sea Floor, in The Great Alaska Earthquake of 1964, Oceanography and Coastal Engineering, National Research Council, National Academy of Sciences, Washington, D.C., 252-265.

Mauk, F. J. and Kienle, J., 1973, Microearthquakes at St. Augustine Volcano, Alaska, Triggered by Earthtides, Science, 193, 420-422.

Pearson, C. F., 1977, Seismic Refraction Study of Augustine Volcano, M.S. Thesis, Univ. of Alaska, 131 pp.

Pearson, C. F. and Kienle, J., 1978, A Seismic Refraction Study of Augustine Volcano, Alaska, EOS, Trans. AM. Geophys. Union, 59(4), 311 (abstract).

Plafker, G., 1971, Pacific Margin Tertiary Basin, American Association of Petroleum Geologists, Memoir 15, 120-135.

Stauder, W., and Bollinger, G. A., 1966, The S-Wave Project for Focal Mechanisms Studies; the Alaska Earthquake of 1964, Report prepared for Air Force Cambridge Laboratories, Office of Aerospace Research, U.S. Air Force, Bedford, Massachusetts, 124 pp.

Stith, J. L., Hobbs, P. V., and Radke, L. F., 1977, Observations of a Nuée Ardente from St. Augustine Volcano, Geophys. Res. Letters, 4, 259-262.

Sykes, L. R., 1971, Aftershock Zones of Great Earthquakes, Seismicity Gaps, and Earthquake Prediction for Alaska and the Aleutians, J. of Geoph. Res., v. 76, 8021-8041.

Tobin, D. G., and Sykes, L. R., 1966, Relationship of Hypocenters of Earthquakes to the Geology of Alaska, J. of Geoph. Res., v. 71, 1659-1667.

B. Papers and Reports in Preparation or Print

1. Papers

Kienle, J. and G. E. Shaw, Plume dynamics, thermal energy and long distance transport of Vulcanian eruption clouds from Augustine Volcano, Alaska, J. of Volcanol. and Geotherm. Res., in press, accepted January 13, 1979.

Kienle, J., S. Self, R. J. Motyka, and P. R. Kyle, Ukinrek Maars, Alaska: I, April 1977 eruption, petrology and tectonic setting, J. of Volcanol. and Geotherm. Res., (submitted January, 1979).

Pulpan, H. and J. Kienle, Western Gulf of Alaska seismic risk studies, Proceedings Offshore Tech. Conf. April 30 - May 3, 1979, Houston, Texas, in press.

Hampton, M. A., Bouma, A. M., Von Huene, R., and Pulpan, H., 1979, Geo-Environmental Assessment of the Kodiak Shelf, Proceedings Offshore Tech. Conf. April 30-May 3, 1979, Houston, Texas, in press.

2. Reports

Kienle, J., R. J. Motyka, D. J. Lalla, S. A. Estes and J.-P. Huot, Formation of two maar behind the Aleutian volcanic arc Alaska Peninsula, April, 1977, Preliminary results: field reconnaissance geochemistry and seismicity, Geophysical Institute, University of Alaska, Report UAG R-257, 26 pp., 1978.

C. Oral Presentations

Lalla, D. J., and J. Kienle, Evolution of seismicity at Augustine Volcano, 1970 to 1976 eruption, Geol. Soc. of Am., Cordilleran Section, 74th Ann. Meet., Tempe, Arizona, March, 1978, Abstracts with Programs, 10(3), 113, February 1978.

Kienle, J., S. Self, R. J. Motyka, J.-P. Huot and D. J. Lalla, Formation of 2 maars behind the Aleutian volcanic arc, in April, 1977, Geol. Soc. of Am., Cordilleran Section, 74th Ann. Meet., Tempe, Arizona, March, 1978, Abstracts with Programs, 10(3), 112, February, 1978.

Self, S., J. Kienle and J.-P. Huot, Mechanisms and deposits of the 1977 Ukinrek maar-forming eruption, Alaska Peninsula, 1978 Joint Annual Meeting, Geol. Soc. of Am., Geol. Assoc. of Canada, Min. Assoc. of Canada, Toronto, October 1978, Abstracts with Programs, 10(7), 489, August 1978.

Pulpan, H., and J. Kienle, Seismic and volcanic risk studies--Western Gulf of Alaska, NOAA-OCSEAP Workshop on Alaskan OCS Seismology and Earthquake Engineering, Boulder, Colorado, March 26-29, 1979.

APPENDIX I

In the epicenter maps shown in Figures 3, 4, 9, 12 and 13 the one-letter code represents hypocentral depths as follows:

A	$0 \leq 25$
B	$26 \leq 50$
C	$51 \leq 100$
D	$101 \leq 125$
E	$126 \leq 150$
F	$151 \leq 200$

etc.

The actual location of the event is the lower left hand corner of the letter. The size of the letter is proportional to the magnitude, the size used for the geographic coordinates corresponding to a magnitude 2.

In Figure 16, the hypocentral depths are letter-coded in 1 km depth intervals A = $0 \leq 1$ km, B = $1.1 \leq 2$ km, etc., and magnitudes are not differentiated.

Class 1 events have an RMS travel time residual of less than 1 second and a relative horizontal and vertical error of less than 10 km.

ANNUAL REPORT

Contract Number:	03-5-022-55
Research Unit Numbers:	253, 255, 256
OCSEAP Task Numbers:	D8 and D9
Reporting Period:	April 1, 1978 to March 31, 1979

SUBSEA PERMAFROST: PROBING, THERMAL REGIME AND DATA ANALYSIS

W. D. Harrison
T. E. Osterkamp

Geophysical Institute
University of Alaska
Fairbanks, Alaska 99701

April 1, 1979

TABLE OF CONTENTS

I. SUMMARY OF OBJECTIVES, CONCLUSIONS AND IMPLICATIONS WITH RESPECT TO OSC DEVELOPMENT

The objectives of this study are to determine the distribution and properties of subsea permafrost in Alaskan waters, in cooperation with other OCSEAP investigators. Besides direct measurements, our program includes an effort to understand the basic physical processes responsible for the subsea regime, as a basis for predictive models.

The detailed conclusions of our recent Beaufort Sea work in Elson Lagoon, Prudhoe Bay area, far offshore from the Barrier Islands, and on the Barrier Islands themselves are summarized in Section VIII. Much of this work was planned in connection with other OCS projects, particularly the seismic mapping permafrost project. Usually the seismic interpretations are supported by our work or vice versa.

By now is should be evident from these and other OCS studies in Alaskan waters that ice-bearing subsea permafrost is widespread and may exist near the sea bed both near and very far from shore. The latter observation would not have been predicted two years ago. Compared to terrestrial permafrost, subsea permafrost is more complex because it is transient, and because salt becomes a new, important, and unpredictable variable. The subsea permafrost is also much more easily disturbed because of the salt, and because it is warmer. The permafrost-related development problems are therefore probably more serious offshore than onshore. A curious similarity is that excavation of materials may not be feasible offshore at some locations because of shallow ice-bonding.

It is found that the permafrost regime on the barrier islands can be highly variable over small distances, a fact that has to be remembered in the interpretation of seismic searches for ice-bonding, and in the siting of structures.

II. INTRODUCTION

A. General Nature and Scope of Study

This work is part of a study of the distribution and properties of permafrost beneath the seas adjacent to Alaska. The study involves coordination of the efforts of a number of investigators (RU 204, 271, 253, 255, 256, 473, 102, 407) and synthesis of the results of both field and laboratory research.

B. Specific Objectives

The specific objectives of our particular project are:

1. To investigate the properties and distribution of subsea permafrost at Prudhoe Bay through a drilling, jetting and probing program and associated interpretation and laboratory analysis.

2. To investigate boundary conditions at the sea bed relevant to the subsea permafrost regime.

3. To study heat and salt transport processes in subsea permafrost, in order to develop models to describe and predict properties and distribution. This work is supported by National Science Foundation although some preliminary results are used here.

4. To extend the area of subsea permafrost field study using simple probing techniques to determine temperature and salinity profiles, depth to any ice-bonded boundary, hydraulic conductivity, soil types, and possibly other properties.

C. Relevance to Probelms of Petroleum Development

(Much of this section was prepared in cooperation with other research units on subsea permafrost.)

Experience obtained in the terrestrial environment has indicated the necessity for careful consideration of permafrost during development activities. Both the National Academy of Sciences review of subsea permafrost problems and Canadian studies suggest that the consequences of errors in planning or design of facilities are potentially greater offshore than on land in terms of loss of human life, environmental damage, and costs.

The primary problem in any new activity in this environment will be lack of data on:

1. The horizontal and vertical distribution of subsea permafrost and the properties of this complex material.

The importance of this information is indicated below in relation to various development activities. This is based on a compilation of data from several sources (Hunter and others, 1976; Osterkamp and Harrison, 1976A; 1976B; OSCEAP reports of Chamberlain and others, 19777 (RU 105) and the National Academy of Sciences Report 1976).

2. Differential thaw subsidence and reduced bearing strength due to thawing of ice rich permafrost.

(a) Thaw subsidence around well bores causing high down-drag loads on the well casing.

(b) Differential settlement associated with hot pipelines, silos in the sea bed, and pile and gravity structures causing instability.

(c) Differential strain across the phase boundary between bonded and unbonded permafrost.

3. Frost heaving

(a) Well bore casing collapse due to freeze-back

(b) Pipelines - differential movement

(c) Gravity structures - local heaving causing foundation instability

(d) Pile structures - differential stress in pile founded structures

4. Seismic data interpretation - Data can be misinterpreted and can lead to improper design of offshore production and distribution facilities. Also, special care needs to be taken in the interpretation of seismic exploration data.

5. Excavation - (dredging, tunneling, trenching)

(a) Increased strength of material associated with bonded sediment.

(b) Over-consolidated sediment can influence excavation rates and approach

(c) Thaw can be induced in deeper sediment by removal of material at the sea bed

(d) Highly concentrated and mobile brines can be found in the sediment

(e) Insufficient data on engineering properties for design of excavation equipment and facilities

6. Gas hydrates

(a) Blowouts - can result from gas hydrate decomposition during drilling operations

(b) Fire danger

(c) Misinterpretation of seismic data

7. Corrosion - Fluids (brines) with concentrations several times normal sea water are common in shallow water (< 3m).

To develop proper precautions against these potential problems, we must obviously develop a better understanding of the horizontal and vertical distribution of subsea permafrost and the processes that control this distribution. This is no easy task in view of the $>2 \times 10^3$ km coastline subject to potential subsea permafrost problems. It should be emphasized that with the exception of some shallow data obtained two years ago in the Chukchi Sea (Osterkamp and Harrison, 1978) drilling data exist only near Barrow and Prudhoe Bay in the Beaufort Sea of Alaska and that extrapolations to other areas must be highly speculative. The present U.S.G.S. offshore drilling program will represent a substantial increase in the subsea permafrost data base.

The exact precautions to take in preventing the above problems (2-7) cannot be specified at present due to a lack of data and the obvious site specific nature of these problems. However, precautions will probably involve:

(a) An adequate casing seal to drill safely through permafrost

(b) A drilling program designed to minimize the thermal disturbance to permafrost and gas hydrates

(c) An adequate casing seal to control hydrate decomposition and other high pressure fluids from greater depths

(d) Adequate assurance of the structural stability and integrity of silos and other structures

(e) Protection against casing collapse should the well be suspended over a season

For the present the concerns are for the safety of exploratory drilling, but the eventual objective is not only to find, but to produce hydrocarbons. At that stage, permafrost and gas hydrate conditions will be even more important since hot fluids in the well are unavoidable. Thus, it is very important to maximize the derived downhole information at the intitial stage of exploratory drilling.

Because of the great variability of offshore conditions, extensive preliminary programs will be necessary at each drill site prior to the actual drilling of the well. Without such site specific information it may be difficult to assure a safe drilling program. A partial list of potential accidents is as follows:

(a) Ruptured well casings

(b) Ruptured pipelines

(c) Damage to the drilling structures

(d) Damage to the production structures

(e) Casing collapse

(f) Corrosion and resulting weakening of metals in structures, pipelines, etc.

(g) Blowouts

(h) Fires on rigs

These potential accidents could result in the loss of human life, environmental damage and considerable cost to industry in correcting the problems.

III. CURRENT STATE OF KNOWLEDGE

(Much of this section was prepared in cooperation with other research units on subsea permafrost).

Regional details concerning this areal distribution and thickness of permafrost are unknown in the Beaufort Sea, although several local studies have established its existence and local properties (Hunter and others, 1976; Osterkamp and Harrison, 1976A; Lewellen, 1976; Rogers and others, 1975; and the OCSEAP reports of Rogers and Morack (RU 271); Chamberlain and others, 1977 (RU 105); Sellmann and others (RU 105). These studies have been restricted to three sites in the Beaufort Sea along the $>2.3 \times 10^3$ km coastline from the Bering Straits to the Mackenzie Delta; Elson Lagoon, Prudhoe Bay and the Mackenzie Delta. One borehole also exists in the Chukchi Sea near Barrow (Lachenbruch and others, 1962). Additional studies were performed during the 1977 field season, in Harrison Bay in the Chukchi Sea near Kotzebue and Barrow. The U.S.G.S. has just completed an offshore drilling program involving about 20 boreholes in the proposed Beaufort Sea lease sale area. However, the results will not be available until September 1979. Even though the sites cover a very limited area they are situated in distinctly different geological settings. The Canadian study area of the Mackenzie Delta and the sites in Kotzebue Sound are situated in an area exposed to year-around river discharge.

Some data are available from direct observations that can help establish some ideas of subsea permafrost limits. The data from the drilling programs supported by NOAA at Prudhoe Bay and the Navy program at Barrow indicate that that permafrost (as defined by temperatures colder than 0°C throughout the year) is present in every hole from near the sea bed to depths at least as great as 80 meters, which is the maximum depth of the exploratory holes. However, seismic data indicate the absence of continuous ice bonding in some of these holes (Rogers and others, 1975). One additional industry hole at Prudhoe Bay on Reindeer Island suggests bonded permafrost exists in two zones from 0 to 20 m and 90 to 125 m from the surface, although this hole was never thermally logged. Borehole temperature data available prior to 1977 are given by Lewellen, 1976; Osterkamp and Harrison, 1976, 1977; Lachenbruch and Marshall, 1977 and OCSEAP reports of Sellmann and others. These data indicate permafrost is present 17 km from shore as seen in hole PB-2 at Prudhoe Bay and 11 km at Barrow at B-2. Recent OCS reports of Rogers and Morack describe seismic studies indicating widespread distribution of bonded permafrost in the proposed Beaufort Sea lease sale area, and most surprisingly, bonded permafrost as little as 5 m below the sea bed outside the Barrier Islands.

Considerable data on the extent and distribution of subsea permafrost have been obtained by Canadian government and industry studies in the Mackenzie River region. Drilling and thermal data have confirmed the presence of permafrost, and information of the upper limit of the bonded permafrost was obtained based on a study of industry seismic investigations (Hunter et al., 1976). Additional information concerning ice-bearing permafrost can be inferred from the thermal data shown earlier. Most of these records have negative thermal gradients, a suggestion of ice-bearing permafrost at depth.

The studies conducted by Osterkamp and Harrison (1976A) and by Sellmann and others (OCSEAP reports) near Prudhoe Bay across the land/sea transition established the depth to bonded permafrost along this single line in some detail out to the 2 meter water depth and less detail beyond. These studies, and those of Lewellen (1973) and Osterkamp and Harrison (OCS reports) near Barrow, indicate that bonded permafrost is found at a shallow depth beneath the sea bed in 2 m of water or less, where the sea ice annually freezes to the sea bed. There is also considerable evidence for a seasonally active layer beneath the sea bed in this region. From Pt. Barrow to Herschel Island the area from the beach to the 2 m water depth is about 3400 km^2. In this zone the limited data from the two study sites indicate that bonded permafrost will be near the surface, probably within 20 meters. This may not apply to areas near major deltas where the environment is anticipated to be modified by warmer waters during periods of discharge.

Permafrost distribution in areas other than the shallow water environments is implied from results of the drilling and seismic efforts mentioned above, from analysis of climatic and sea level history data, as well as from negative bottom water temperatures which would suggest permafrost can exist on most of the Beaufort Sea shelf.

Recent seismic studies (RU 271) have shown that the top of the ice-bonded permafrost may be quite variable with relief of several tens of meters over short distances and may be near the sea bed at sites far offshore.

Thawing at the sea bed in the presence of negative sea bed temperature has been found by Lewellen (1973), Osterkamp and Harrison (1976A) and CRREL-USGS (RU 105) drilling programs. This has been attributed to the infiltration of salts into the sea bed. The distribution of these salts in the thawed sediments has been determined by Osterkamp and Harrison (1976A) (RU 253) and by CRREL (RU 105) (Iskandar, Osterkamp and Harrison, 1978), Page and Iskandar (1978); Page (1978).

Preliminary study of seismic, sea bed temperatures and other data imply that bonded subsea permafrost is probably absent in most of the southern Chukchi Sea in the deeper waters although it may still survive in shallow nearshore waters (OCSEAP 1976 fourth quarterly report of Harrison, Dalley and Osterkamp, 1976 (RU 253, 255, 256)).

IV. STUDY AREAS

The main study areas have been in the Beaufort Sea at Prudhoe Bay and at Elson Lagoon. Figures 1 to 4 show the locations of all except one of our study sites for the 1978 field season.

We plan to drill along 2 or 3 lines in the proposed lease sale area between the Colville and Canning Rivers during the 1979 field season.

V. METHODS AND RATIONALE OF DATA COLLECTION

The basic approach is to make direct observations of temperature, salinities and subsea soil conditions in holes made with light-weight

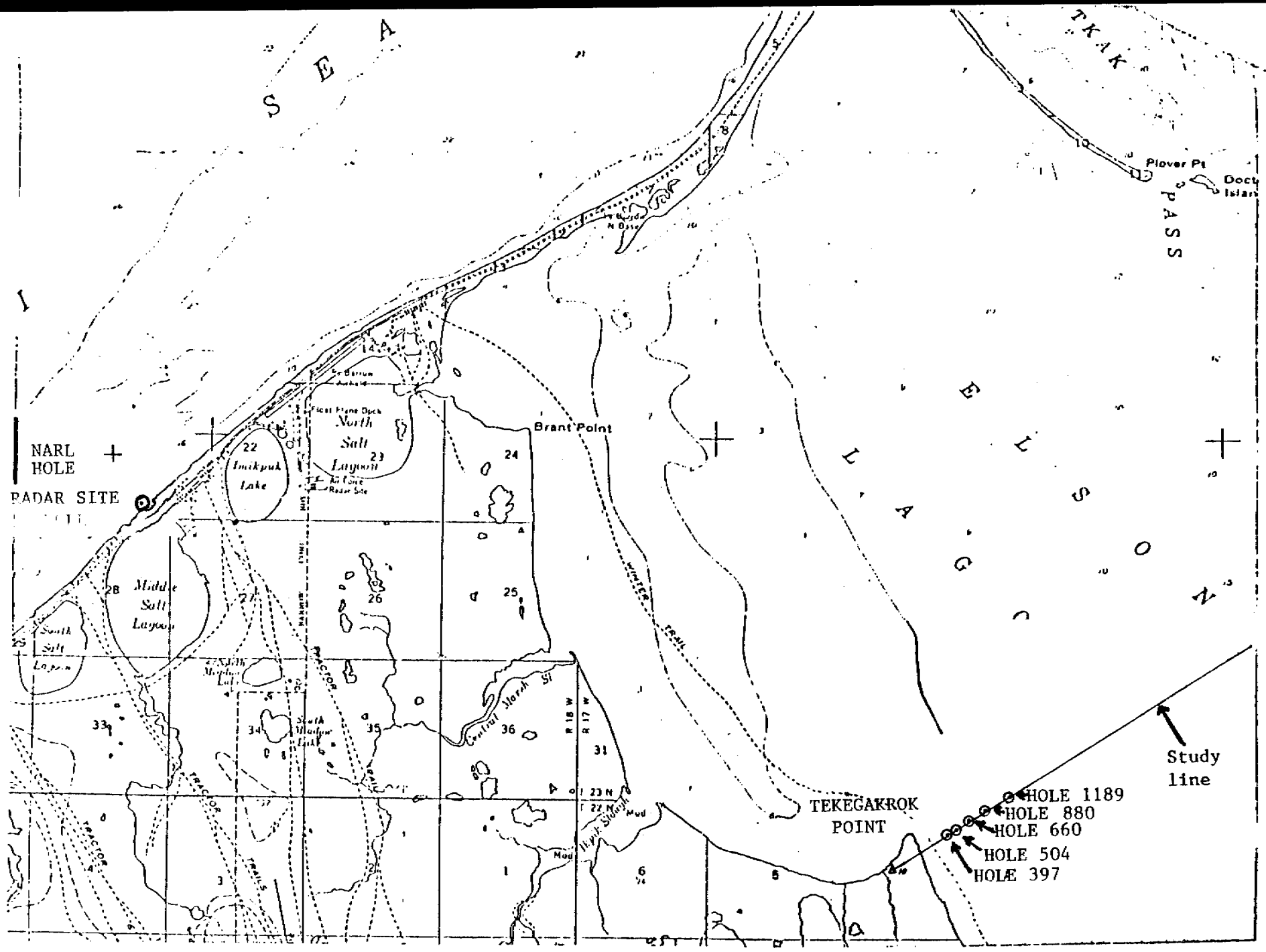
S E A
NARL
HOLE
RADAR SITE
Brant Point
North
Salt
Lagoon
Middle
Salt
Lagoon
South
Salt
Lagoon
Imikpuk
Lake
Plover Pt
PASS
L A G O O N
TEKEGAKROK
POINT
Study
line
HOLE 1189
HOLE 880
HOLE 660
HOLE 504
HOLÆ 397

FIGURE 1

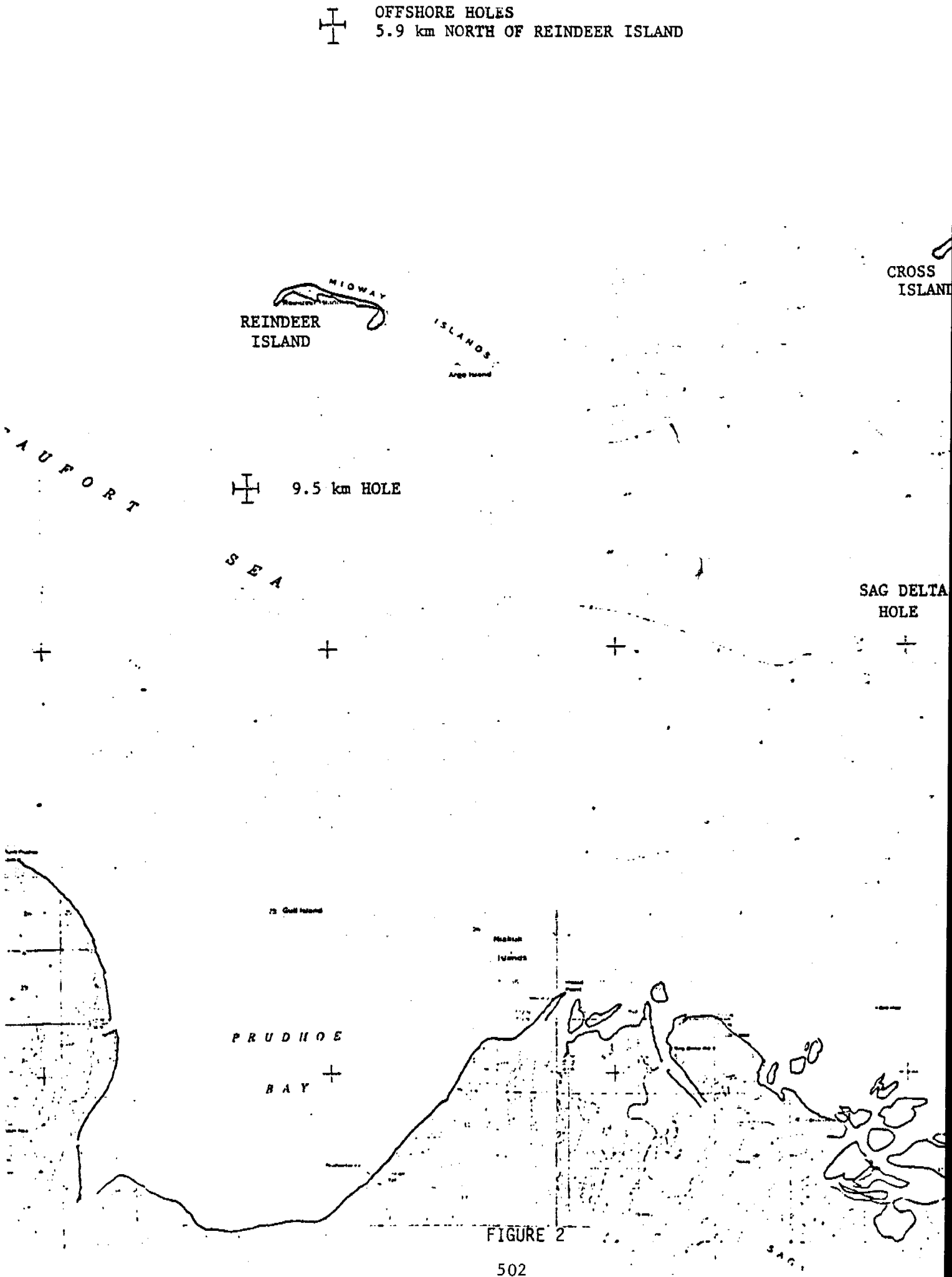
OFFSHORE HOLES
5.9 km NORTH OF REINDEER ISLAND
MIDWAY
REINDEER ISLAND
ISLANDS
CROSS ISLAND
9.5 km HOLE
SEA
SAG DELTA HOLE
PRUDHOE BAY

FIGURE 2

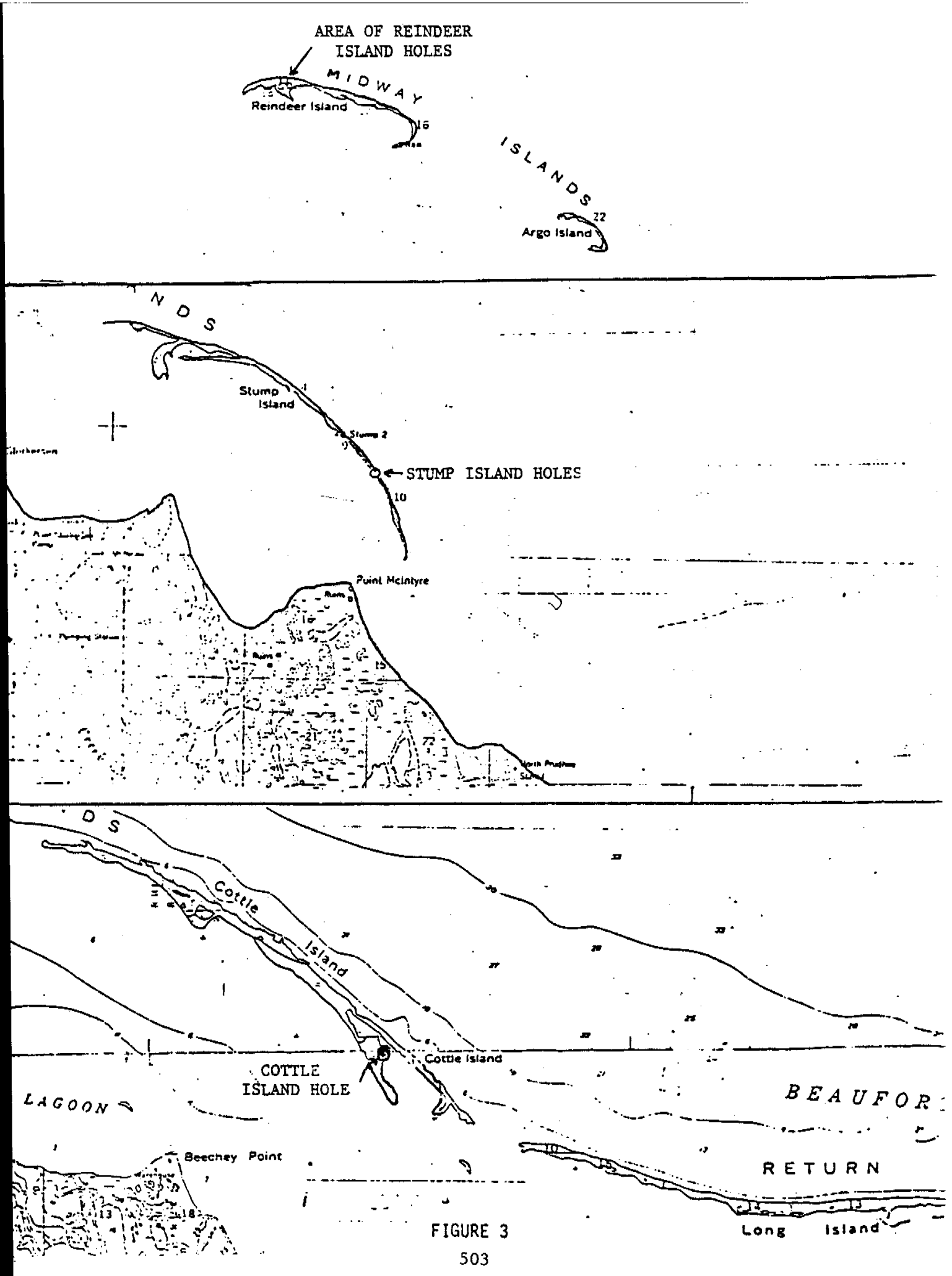
AREA OF REINDEER ISLAND HOLES
MIDWAY
Reindeer Island
16
ISLANDS
22
Argo Island
NDS
Stump Island
Stump 2
STUMP ISLAND HOLES
10
Point McIntyre
15
DS
Cottle Island
Cottle Island
COTTLE ISLAND HOLE
LAGOON
BEAUFOR
Beechey Point
RETURN
Long Island

FIGURE 3

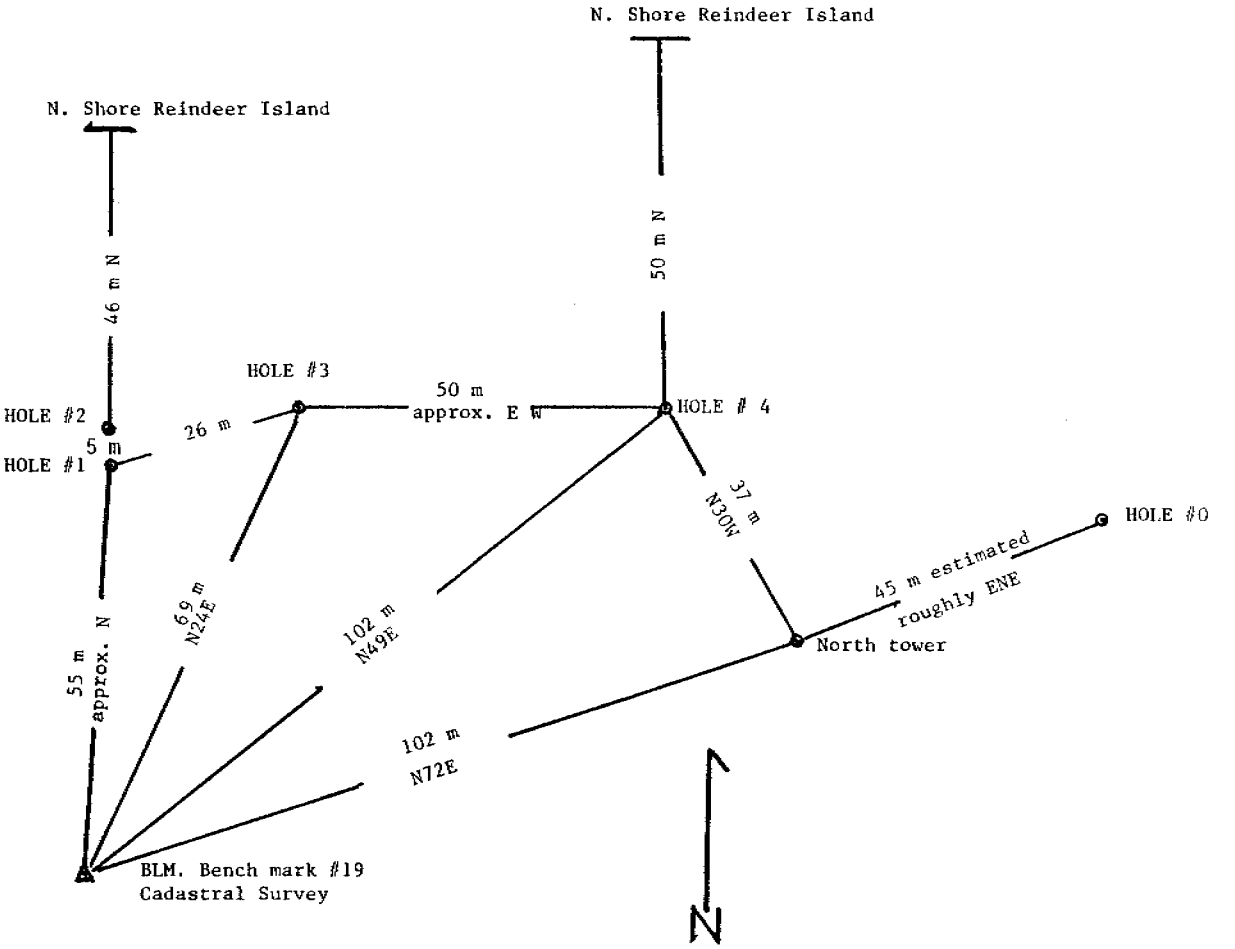

Figure 4. REINDEER ISLAND HOLE LOCATIONS

driving or jetting equipment. The technique does not permit the acquisition of the detailed data that can be obtained with a drill rig, particularly since soil samples are not taken, but it does have the advantages of speed and lightweight. Thus, data can be obtained rapidly and cheaply over a wide area. In the driving technique a portable motorized cathead and tripod set, together with a 64 kg drop hammer, are used to drive EW drill rod into the sea bed. The depth capability depends upon soil type and is optimum for the relatively coarse conditions typical of Prudhoe Bay. There we have achieved a depth of 26 m, which was determined by our available supply of drill rod. In the jetting technique 3/4 inch steel water pipe is jetted into the sea bed using a small water pump and the water from beneath the sea ice. When the pipe string is rotated, a bit open to water flow is run on the bottom; this is called jet augering. We have recently acquired other lightweight drilling equipment and are experimenting with other methods. The depth capability depends on soil type and is optimum for the fine-grained soil conditions. At Barrow we have achieved a depth of 34 m below the sea bed. The type of data that can be obtained with the driving and jetting techniques is briefly described in the following paragraphs.

Soil Conditions: Information about subsea soil conditions can be obtained from both the jetting and driving techniques, although soil samples are not taken. The experience of the driller, as in any type of drilling, is extremely important, and drilling in known material has been a factor in building up our experience. In jetting, the "feel" and sound of the drill are different in clay, silt, sand and gravel. Compact clays feel like hard rubber when the string is dropped onto the bottom of the hole; bonded materials feel more like concrete and usually drill very slowly, when, as is usual, cold water is used. Unbonded silt and silty sands usually drill rapidly, as long as the hole walls do not cave, which may happen if too much sand is present. The grains in gravel can be felt when raising and lowering the string off the bottom, and by the roughness of the drilling. Gravels are extremely hard to drill by jetting or by jet augering, due to loss of circulation, caving, and the difficulties of flushing larger soil particles from the hole. Direct identification of soil type is possible when soil cuttings are washed to the surface, as occurs on land or where the sea ice is frozen to the sea bed. Wood, shells, etc. may be recovered this way, although one must realize that they may not always come from the bottom of the hole but may be washed out of the walls.

The driving technique works best in the soils that are the most difficult to jet, sands and gravels, which can often be identified by the rapid driving progress. On some occasions clay can be identified when it comes up stuck on the drill rod. By and large, soil identification is less positive than with the jetting technique. Both techniques can detect the presence of firmly ice bonded sediments, which can be penetrated by the jetting technique if they are fine grained.

Temperatures: Both techniques are well suited to provide access for temperature measurements. In the jetting technique the pipe is left in the hole. To prevent freezing, the pipe is normally run with a check valve at the bottom, and upon hole completion a non-freezing fluid is

pumped through it. In the driving technique temperatures can be measured inside the drill rod, which has to be left in place until the temperature measurements are completed. In 1978 a new technique was developed, wherein a continuous length of 12.7 mm O.D. tubing is run inside the drill rod, and attached to a suitable driving point at the bottom. Upon completion of the hole the drill rod is removed, and the point and tubing remain behind, providing access for temperature measurement. This frees the drill rod, and the equipment needed to remove it, for immediate use elsewhere while temperatures are equilibrating. The undisturbed or "equilibrium" temperatures usually can be accurately estimated after a few days, depending upon the time spent in drilling and other factors, particularly any loss of drilling fluid. Some of the problems are discussed later. Temperature was logged inside the pipe or tubing with a single thermistor. Information about the approach to temperature equilibrium, accuracy and thermistor calibration are given by Osterkamp and Harrison (1976A). The depths on the figures are measured from the sea bed.

Soil Interstitial Water Salinity: Salinity is at least as important as temperature in determining the presence or absence of ice, and in giving clues to the past history of the soil. Therefore considerable effort has been devoted to developing techniques for determining the interstitial water salinity using the driving equipment. NSF support has been used for this phase of the work. The water is admitted into plastic tubing run inside the drill rod through a porous metal filter at the bottom, and sampled inside the tubing with a special bailer. The tubing can be cleared and closed at its lower end before the rod is driven to the new sampling depth. It is therefore not necessary to pull the drill pipe between samples.

The method has an interesting limitation if the freezing temperature of the free interstitial water is higher than the in situ temperature. Liquid will still be collected, but it will not be representative of the soil bulk H_2O salinity, because the solid phase fraction of the H_2O in the soil is not collected. There is an added complication in fine grained soils, because some of the collected water may freeze in the probe as soon as it is removed from soil particle surface effects, thereby concentrating the salt in the liquid phase until equilibrium with ice at the in situ temperature is reached. Only this liquid would be sampled by our bailer. Therefore, when the measured freezing temperature of the collected liquid is equal to the in situ temperature, one can only conclude that the soil bulk H_2O freezing temperature is higher than or equal to the in situ temperature, and that ice may be present in the soil under these conditions.

Hydraulic Conductivity: The soil conductivity (essentially the permeability) is calculated from the rate at which water from the soil enters the filter, which is determined with a water level sensor. The exact calculation is extremely difficult for some of the geometrically complicated shielded filters that we have used, but we have been able to derive a simple and reasonably accurate approximate method.

VI and VII RESULTS AND DISCUSSION

A. Barrow - Elson Lagoon - Tekegakrok Point

Data were obtained from 3 holes in spring 1978 off Tekegakrok Point (Table 1 and Figure 1). Data were also obtained from several shallow holes shortly after freeze up in fall 1978. The holes lie along the same line as the five earlier ones discussed in our last year's report. The holes along this line span the transition from cold near shore conditions where the sea ice freezes to the sea bed, to the warmer conditions in deeper water maintained by the presence of sea water of normal salinity under the ice. Measurements at this site, and at others in Elson Lagoon, have been previously made by Lewellen (1973, 1974, 1976) by Rogers and others (1975) and by Osterkamp and Harrison (1978). In the Barrow area the top 20 to 30 m of the stratigraphy consists of the Pleistocene Gubik Formation (Black, 1964), and Lewellen (1976) feels that the contact with the underlying Cretaceous (clays with some silts) is consistently at about 30 m throughout the Elson Lagoon area. His studies indicate that the shoreline is retreating about 2.4 m a^{-1} at Tekegakrok Point, and this is consistent with our own observations, which are based on a comparison of the 1955 U.S.G.S. map with present conditions.

1. Hole 660

At a site 660 m from shore, one hole was jet augered for temperature measurement, and four holes within a 1 m circle were driven for interstitial water sampling and hydraulic conductivity measurement (Table 1 and Figure 1). The drilling data are summarized in Figures 5 and 6, and are characteristic of the fine-grained sediments of this area. This site is just beyond the maximum distance from shore at which the sea ice freezes to the sea bed.

The temperature data are given in Figure 7 and Appendix I and show the rapid cooling with increasing depth characteristic of areas like this with rapidly retreating shorelines. The electrical conductivity, estimated salinity, and estimated freezing temperature of the interstitial water are given in Table 2 and Figure 8. The errors in conductivity are dominated by probe dead volume effects. In the worst case they may be about 8%, but they are usually much less, particularly when conductivity does not vary a great deal between successive depths. The freezing temperatures were calculated by using standard oceanographic tables to calculate salinity from conductivity, and the results of Doherty and Kester (1974) to calculate freezing temperature from salinity. This procedure assumes the composition of the interstitial water to be similar to that of normal sea water, and requires large extrapolation of the data used because the water is so salty. The errors may therefore be significant.

Column 4 of Table 2 shows that the interstitial water is much saltier than normal sea water, at least above 7 m. Some of this salt may have been pumped into the sea bed by the freezing of the sea ice

TABLE 1

Hole Designation	Location or Distance Offshore	Water Depth	Sea Ice Thickness	Drilling Method	Time of Drilling	Total Depth Below Sea Bed	Date of Logging
Elson Lagoon (Tekegakrok Pt.) Holes							
660 (1)	660 m	2.00 m	1.40 m	Jetted	April 25, 1978	15.0 m	April 25, 29, 1978 May 1, 3, 21, 1978
660 (2)	660	2.00 m	1.40 m	Driven	April 21-29, 1978	18.0 m	Salinity tests
880	880	2.32 m	1.45 m	Jetted	April 26, 1978	28.0 m	April 27, 30, 1978 May 4, 21, 1978
1189 (1)	1189	2.52 m	1.50 m	Jetted	April 27-28, 1978	34.5 m	May 1, 3, 21, 1978
1189 (2)	1189	2.52 m	≈ 1.40 m	Driven	April 29, - May 3, 1978	≈ 9.0 m	May 3, 1978, Salinity tests
Prudhoe Bay Holes							
SAG DELTA	11.5 km from Sag Delta #1 well	7.60 m	1.71 m	Driven	May 25-26, 1978	18.3 m	May 26, 27, 28, 29, 1978
9.5 km	9.5 km from the shore near North Prudhoe State # 1 well	6.9 m	1.60 m	Driven	May 23-25 1978	25.5 m	May 23, 26, 29, 30, 1978
Offshore Holes							
8 km	8 km true North of Reindeer Is.	21 m	≈ 1.60 m	Jetted	April 21, 1978	3.5 m	No logging
RDEE (1)	5.9 km true North of Reindeer Is.	17.0 m	≈ 1.60 m	Jetted	April 20, 1978	10.0 m	April 22, 1978
RDEE (2)	5.9 km true North of Reindeer Is. (30 m separation)	17.0 m	≈ 1.60 m	Jet-augered	May 23, 1978	12.0 m	May 26, 28, 29, 1978

-Continued on Next Page

Hole Designation	Location	Drilling Method	Time of Drilling	Depth Below Ground Level	Date of Logging
Barrier Island Holes					
Reindeer Island					
REIS 0	See Figures 3 and 4	Jetted	May 24-25, 1978	12.2 m	
REIS 1		Jetted/rotated by hand	August 19, 1978	6 m	Not logged
REIS 2		Jetted/rotated by hand	August 19, 1978	3.5 m	Not logged
REIS 3		Jetted	August 20, 1978	27 m	April 24, 26, 1978 October 26, 1978
REIS 4		Jetted	August 25, 1978	16 m	
Cottle Island					
COTT	See Figure 3	Jetted	August 24, 1978	≈ 6 m	April 26, 1978 October 26, 1978
Stump Island					
Stump I	See Figure 3	Jetted	August 21-22, 1978	10.5 m	No Pipe Left for Logging
Stump II		Jetted	August 21-22, 1978	7.5 m	

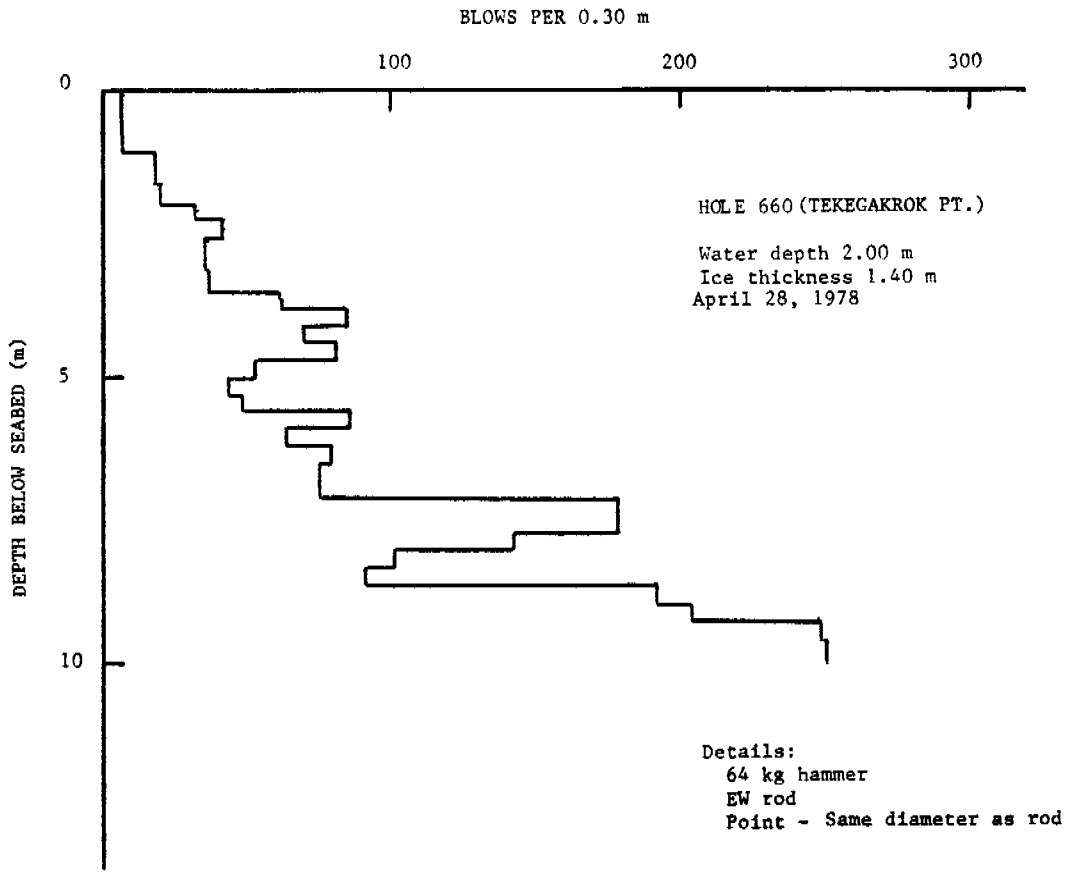
BLOWS PER 0.30 m
100
200
300
0
5
10
DEPTH BELOW SEABED (m)
HOLE 660 (TEKEGAKROK PT.)
Water depth 2.00 m
Ice thickness 1.40 m
April 28, 1978
Details:
64 kg hammer
EW rod
Point - Same diameter as rod

FIGURE 5

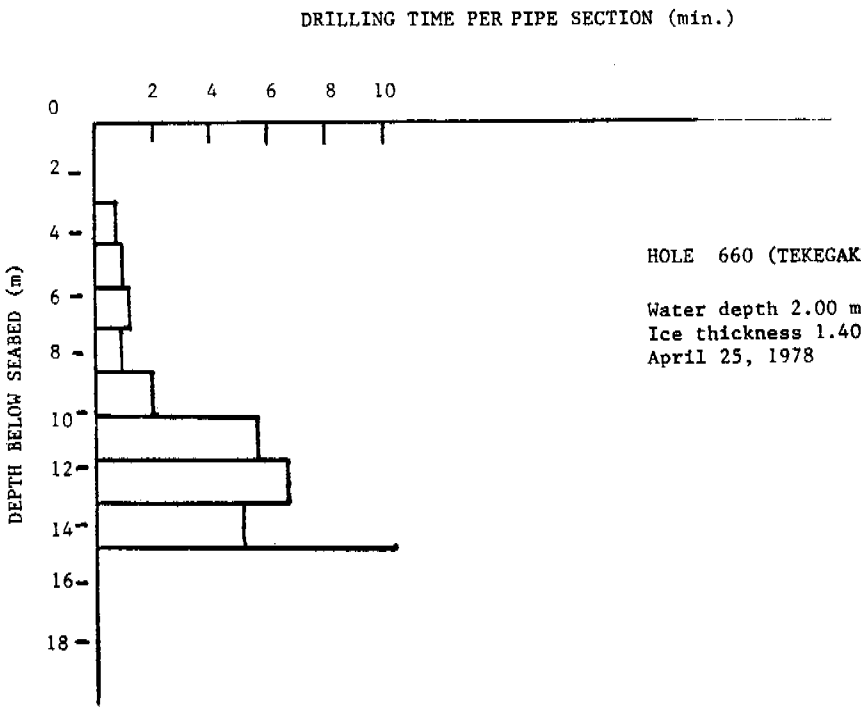

HOLE 660 (TEKEGAKROK PT.)

Water depth 2.00 m
Ice thickness 1.40 m
April 25, 1978

Details;
Deep Rock heavy duty earth probe bit.
1 pipe section = 5' = 1.53 m

FIGURE 6

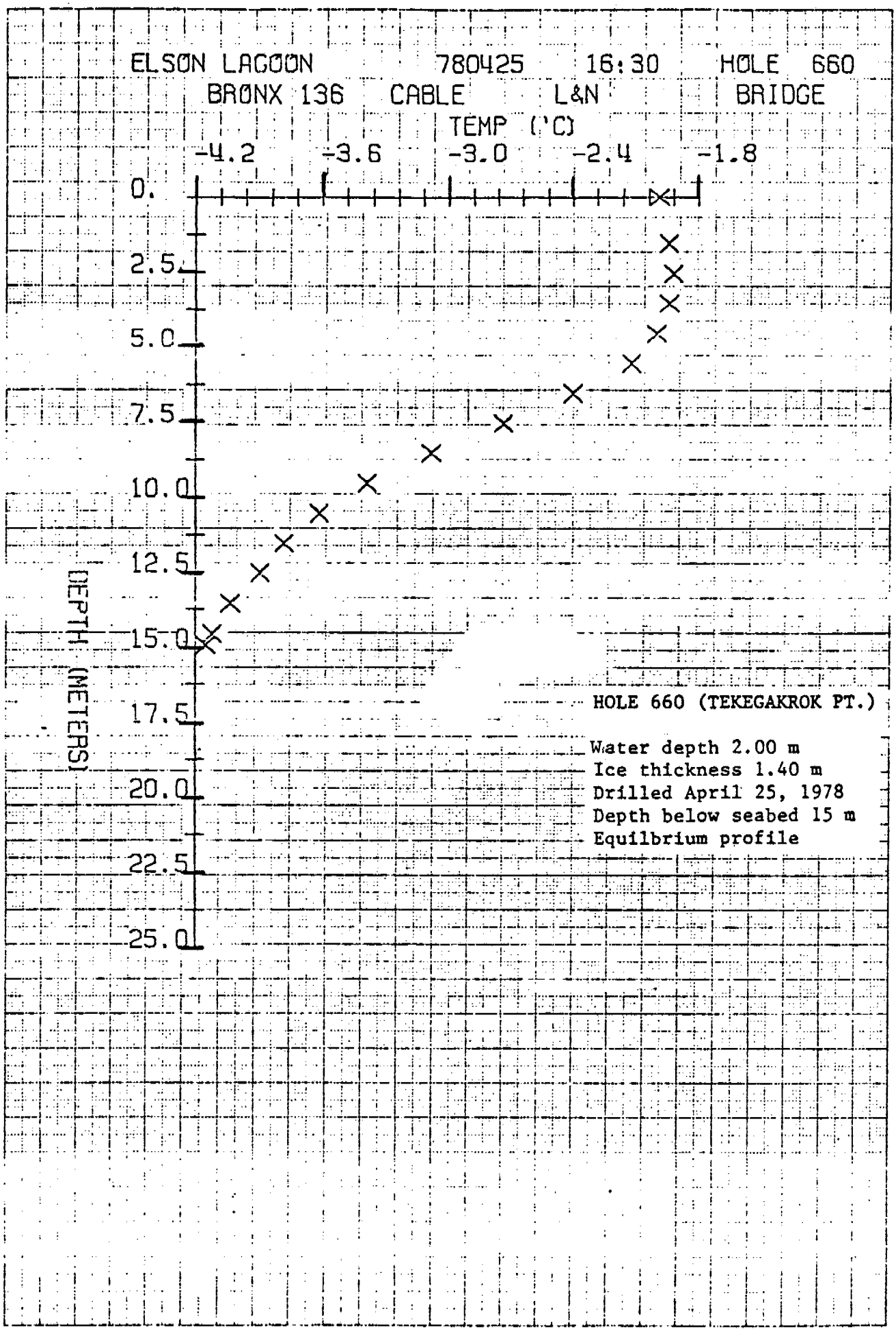
ELSON LAGOON 780425 16:30 HOLE 660
BRONX 136 CABLE L&N BRIDGE
TEMP ('C)
-4.2 -3.6 -3.0 -2.4 -1.8
0.
2.5
5.0
7.5
10.0
12.5
15.0
17.5
20.0
22.5
25.0
DEPTH (METERS)
HOLE 660 (TEKEGAKROK PT.)
Water depth 2.00 m
Ice thickness 1.40 m
Drilled April 25, 1978
Depth below seabed 15 m
Equilbrium profile

FIGURE 7

TABLE 2

HOLE 660, TEKEGAKROK POINT

Location: 660 m from shore N56°E (true, assuming 26° declination), shore to most distant bench mark = 316.6 m
Time: April 21-29, 1978
Water Depth: 2.00 m, freeboard 0.03 m
Ice Thickness: 1.40 m
Water under ice: 0.63 m
Tide peak to peak amplitude: $\sim$ 0.1 m observed, could be greater

Depth Below Sea Bed	Electrical Conductivity of Interstitial Water at 25°C	Estimated Salinity	Estimated Salinity $\div$ 34 °/₀₀	Estimated Freezing Temperature of Free Water	Hydraulic Conductivity
0 (water under) sea ice	$5.47(\Omega\ m)^{-1}$	36.2 °/₀₀	1.06	-1.99 °C	
0.7 m	7.08	48.8	1.44	-2.22	1.1 m a^{-1}
1.4	9.84	72.2	2.12	-4.14	1.9×10^{-2}
2.6	10.35	76.8	2.26	-4.43	2.8×10^{-2}
4.2	10.73	80.3	2.36	-4.66	3.2×10^{-2}
5.6	7.78	54.5	1.60	-3.06	**6.1×10^{-3}
7.1	*7.32	*50.7	*1.49	*-2.84	**6.7×10^{-3}
8.4	*7.66	*53.5	*1.57	*-3.00	**2.1×10^{-3}
9.9	*8.79	*63.0	*1.85	*-3.58	**1.0×10^{-3}

*Salinity upper limits only (lower limits for freezing temperatures). See text.

** Unreliable hydraulic conductivity values. Broken filter or irregular flow rate. Irregular rate possibly due to ice in filter.

into it, during the previous three centuries when this site was in shallower water. Figure 8 shows that below about 8 m, the freezing point of the interstitial water and the in situ temperature seem to be identical within the errors. In fact, this means only that the freezing temperature of the soil bulk H_2O is higher than, or equal to, the in situ temperature. This is due to our sampling technique, as discussed in Section V.

It is possible (neglecting soil particle surface effects) that some ice begins to occur in the soil as soon as phase conditions are right, at about 8 m. The drilling data (Figure 6) suggest that ice-bonding begins about one meter deeper, at about the same depth where a reasonably well-defined break in the temperature gradient (Figure 7) indicates a change in thermal properties and/or a heat sink. This may be another example of the difference between "ice-bearing" and "ice-bonded" permafrost.

The measured hydraulic conductivities, which are typical of fine-grained silt or clay soils, are summarized in Table 2. These values are much less than those obtained in sands and gravels at Prudhoe Bay.

2. Hole 880

A hole for temperature measurement was jet augered at a site 880 m from shore (Table 1 and Figure 1). The drilling data are summarized in Figure 9. Effects of ice bonding may be evident in the lower half of the hole and, as in hole 660, the temperature data (Figure 10 and Appendix I) show the rapid cooling with depth characteristic of areas with rapidly retreating shorelines.

3. Hole 1189

At a site 1189 m from shore, one hole was jet augered for temperature measurement, and 4 holes within a 1 m circle were driven for interstitial water sampling and hydraulic conductivity measurement (Table 1 and Figure 1). Drilling data are summarized in Figures 11 and 12. It is not easy to say with any confidence from these drilling data where ice-bonding is significant. The temperature data in Figure 13 and Appendix I show a striking discontinuity in gradient at a depth of 30 m, which must be due to a discontinuity in thermal conductivity. The ratio of the thermal conductivities above and below the break is about 1.8, assuming no heat sink is present. One interpretation, that the break could be a phase boundary with ice below 30 m, is ruled out, because the break in gradient would be in the other direction. It could possibly be a phase boundary with ice above 30 m, but this seems unlikely considering how subsea permafrost usually evolves. Most likely the effect is due to a change in lithology, probably the Pleistocene-Cretaceous contact (Black, 1964; Lewellen, 1976).

The interstitial water electrical conductivity, estimated salinity and freezing temperature are given in Table 3 and Figure 14. Since the in situ temperature is higher than the freezing temperature, no ice is

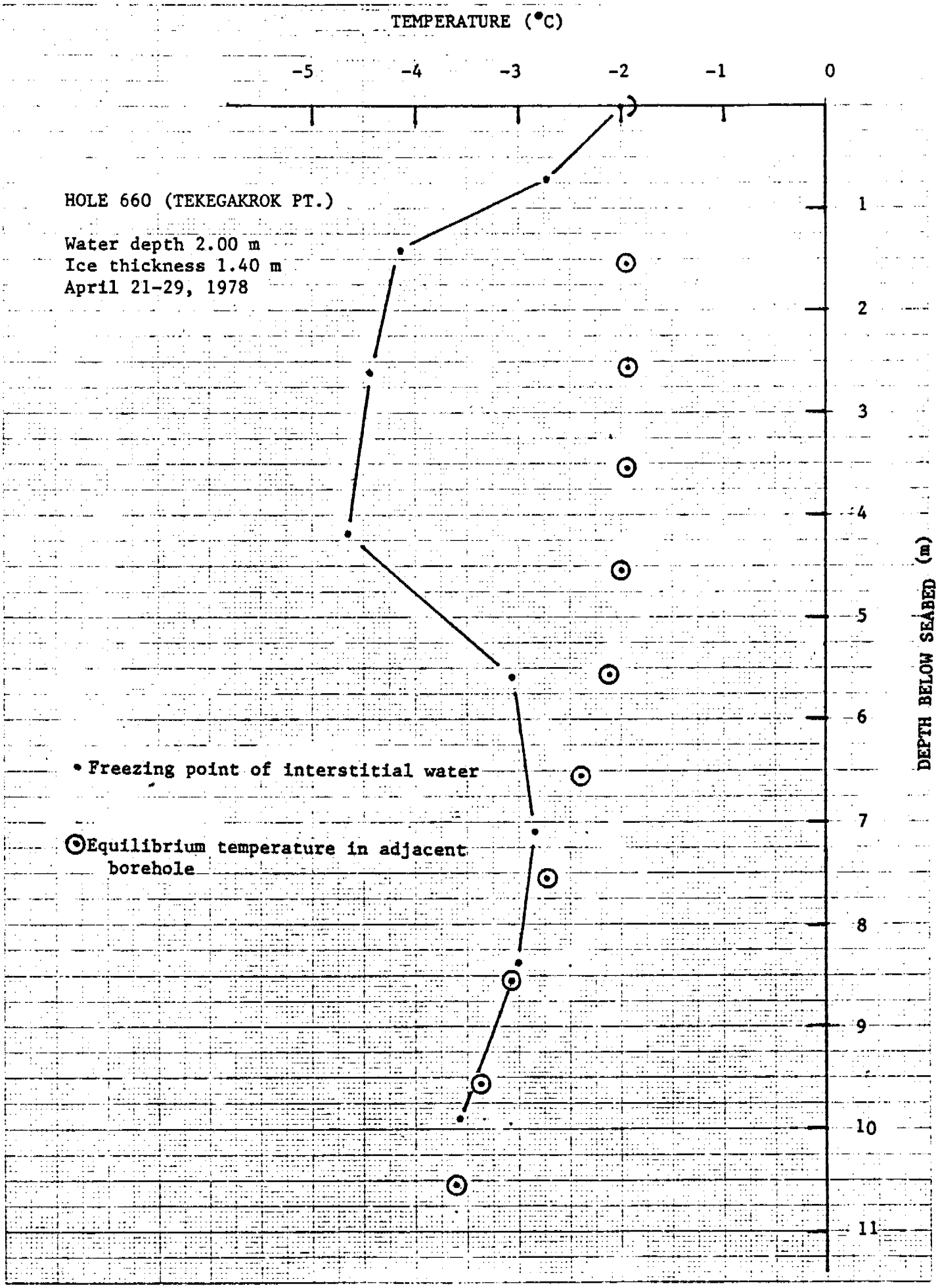
TEMPERATURE (°C)
-5
-4
-3
-2
-1
0
HOLE 660 (TEKEGAKROK PT.)
Water depth 2.00 m
Ice thickness 1.40 m
April 21-29, 1978
1
2
3
4
5
6
7
8
9
10
11
DEPTH BELOW SEABED (m)
• Freezing point of interstitial water
⊙ Equilibrium temperature in adjacent borehole

FIGURE 8

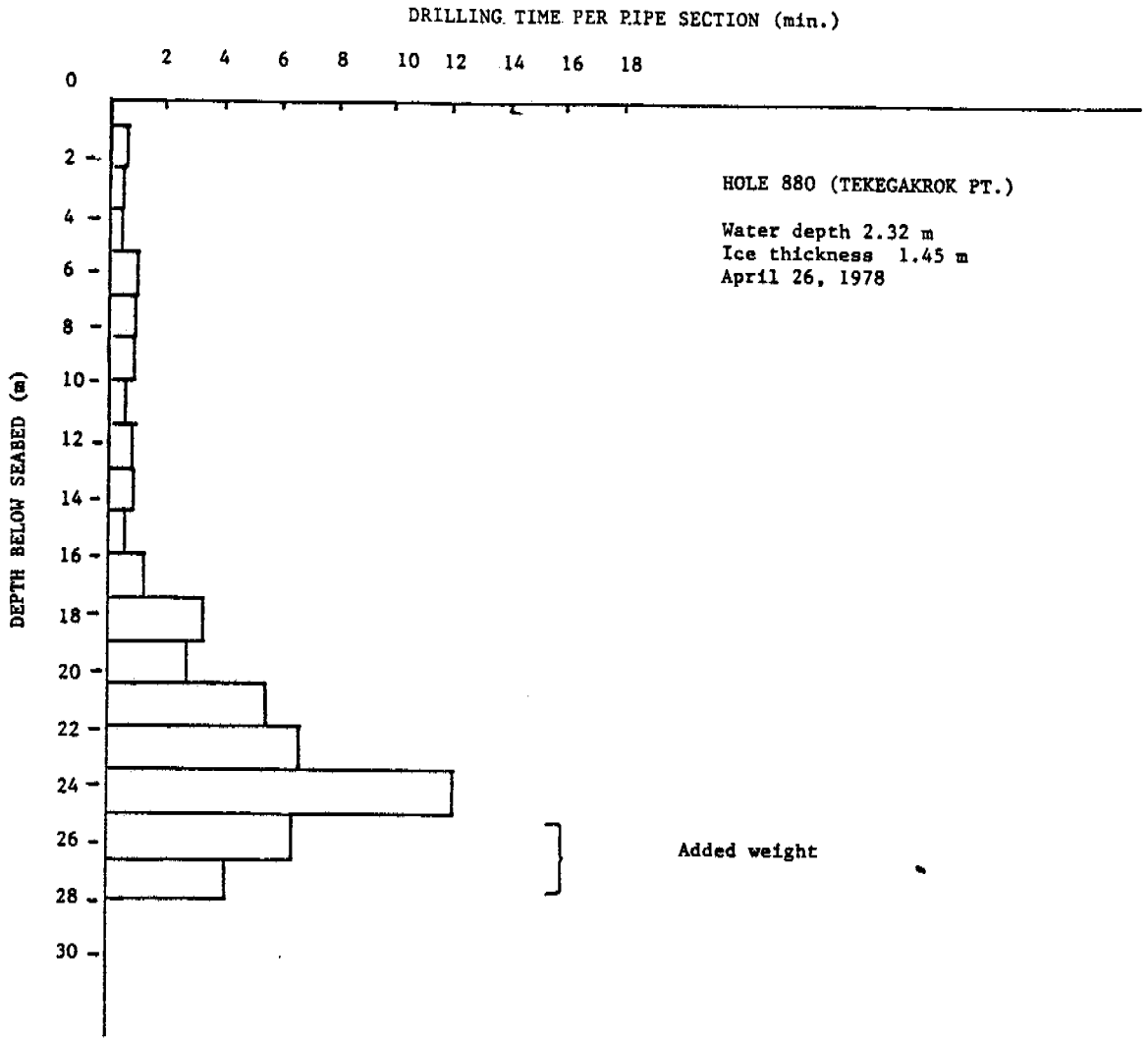
DRILLING TIME PER PIPE SECTION (min.)
2 4 6 8 10 12 14 16 18
0
2
4
6
8
10
12
14
16
18
20
22
24
26
28
30
DEPTH BELOW SEABED (m)
HOLE 880 (TEKEGAKROK PT.)
Water depth 2.32 m
Ice thickness 1.45 m
April 26, 1978
Added weight
Remarks:
Probably bit used was Deep Rock heavy duty earth probe.
1 pipe section = 5' = 1.53 m

FIGURE 9

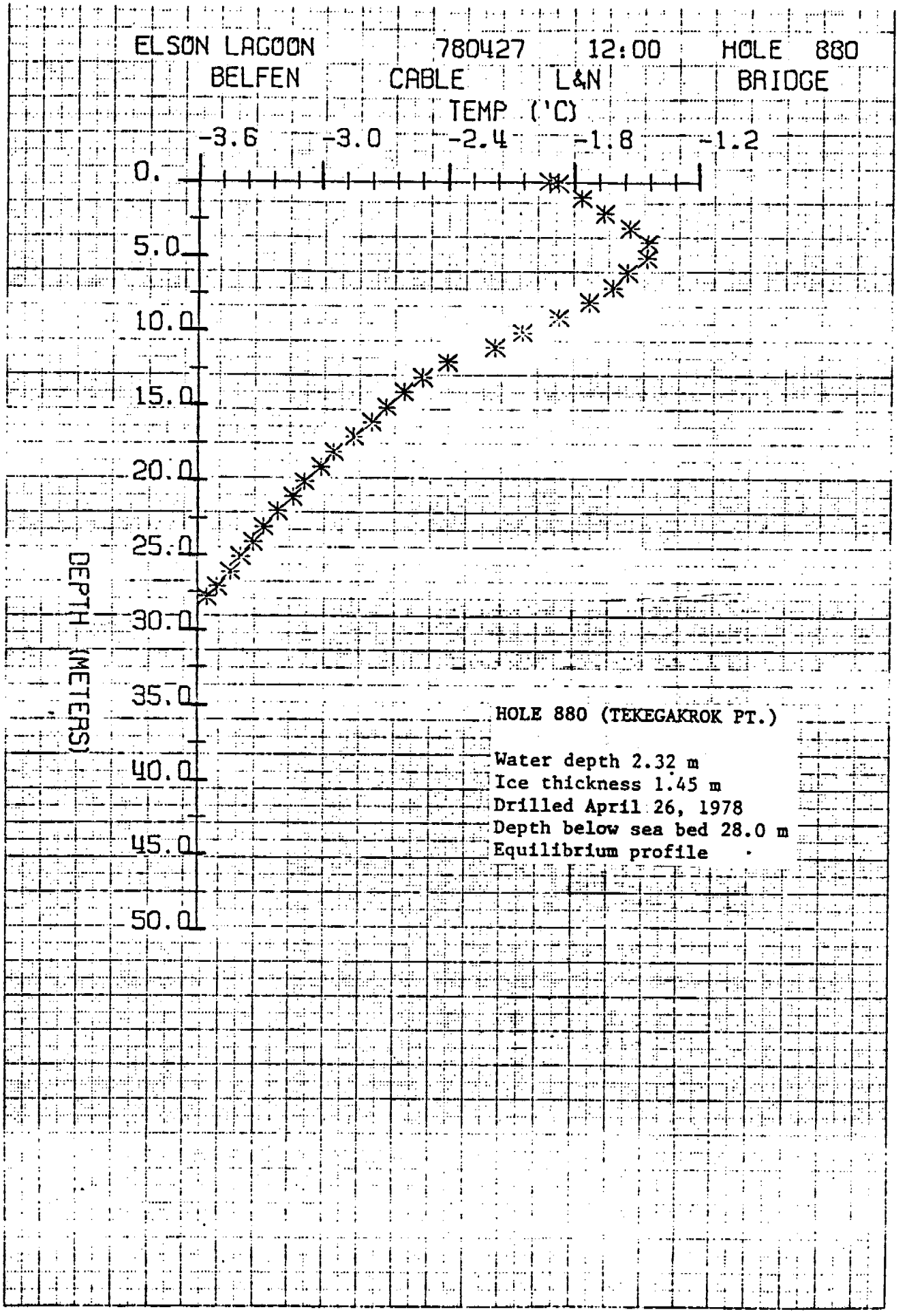
ELSON LAGOON 780427 12:00 HOLE 880
BELFEN CABLE L&N BRIDGE
TEMP ('C)
-3.6 -3.0 -2.4 -1.8 -1.2
0.
5.0
10.0
15.0
20.0
25.0
30.0
35.0
40.0
45.0
50.0
DEPTH (METERS)
HOLE 880 (TEKEGAKROK PT.)
Water depth 2.32 m
Ice thickness 1.45 m
Drilled April 26, 1978
Depth below sea bed 28.0 m
Equilibrium profile

FIGURE 10

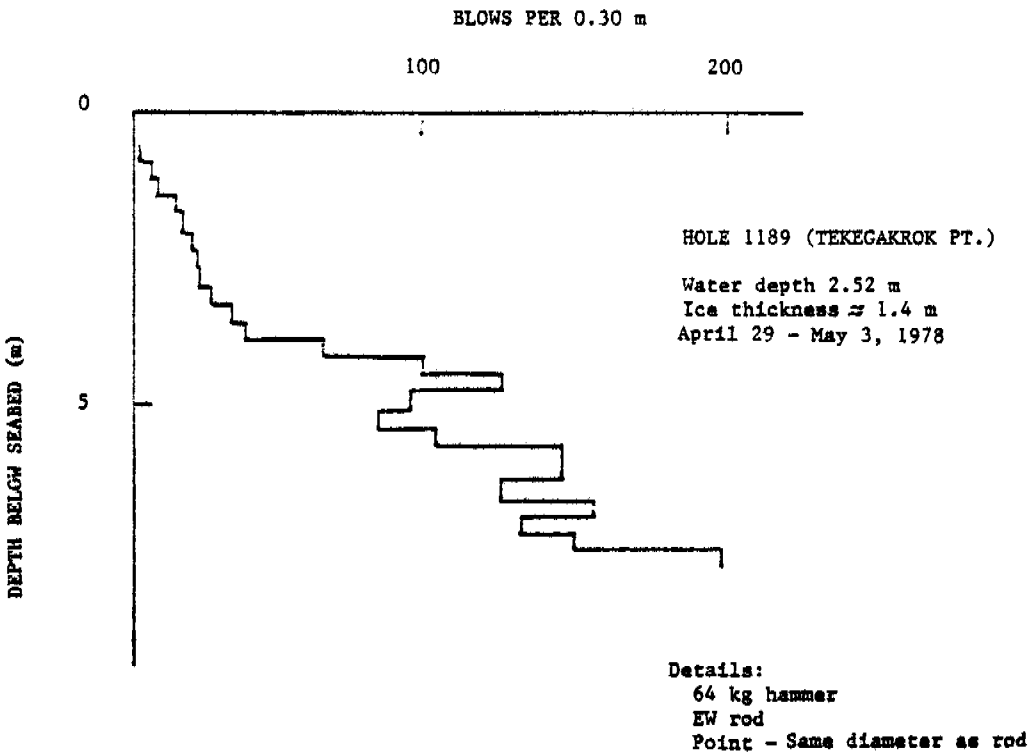
BLOWS PER 0.30 m
100
200
0
5
DEPTH BELOW SEABED (m)
HOLE 1189 (TEKEGAKROK PT.)
Water depth 2.52 m
Ice thickness ≈ 1.4 m
April 29 - May 3, 1978
Details:
64 kg hammer
EW rod
Point - Same diameter as rod

FIGURE 11

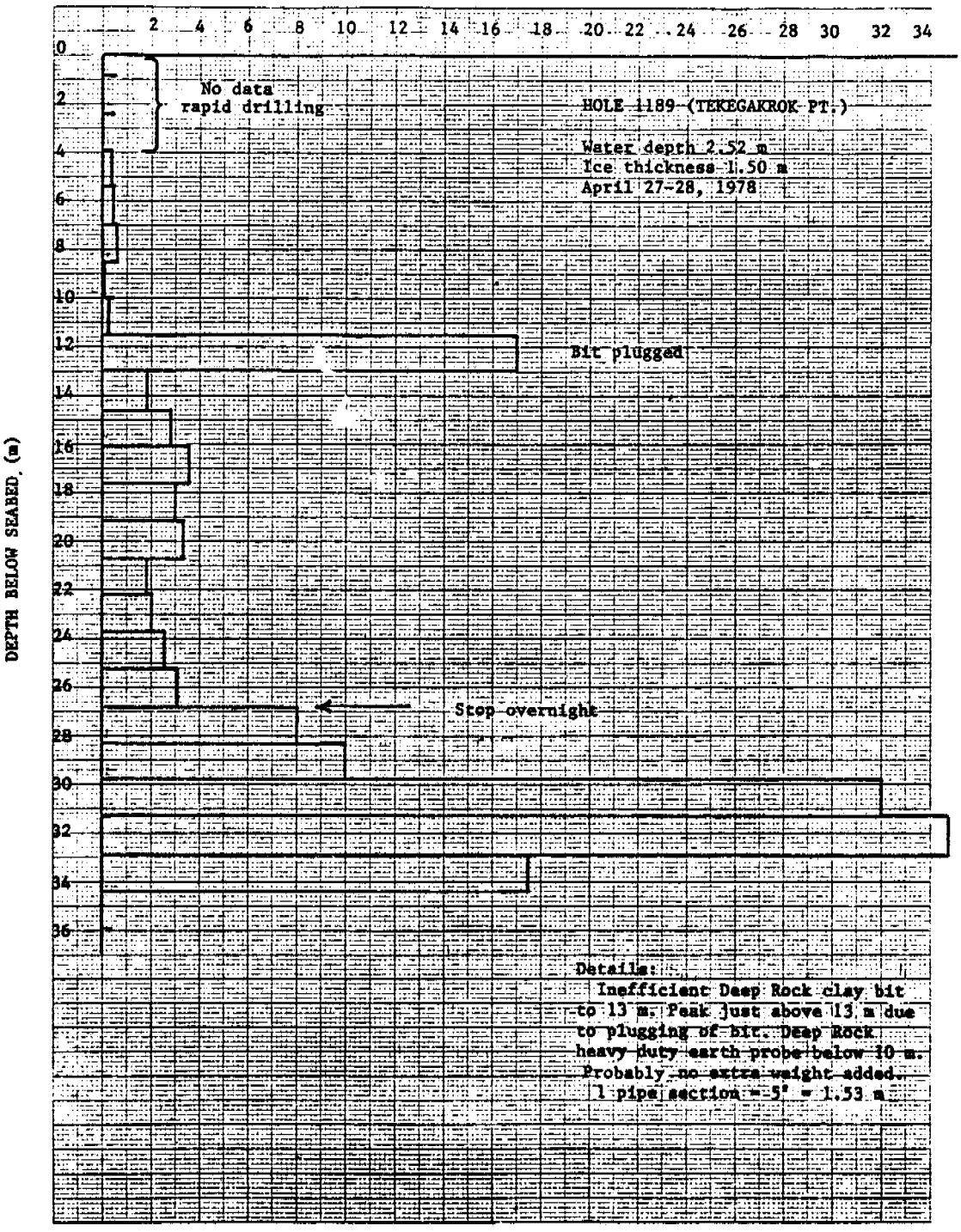

10 Millimeters to the Centimeter

FIGURE 12

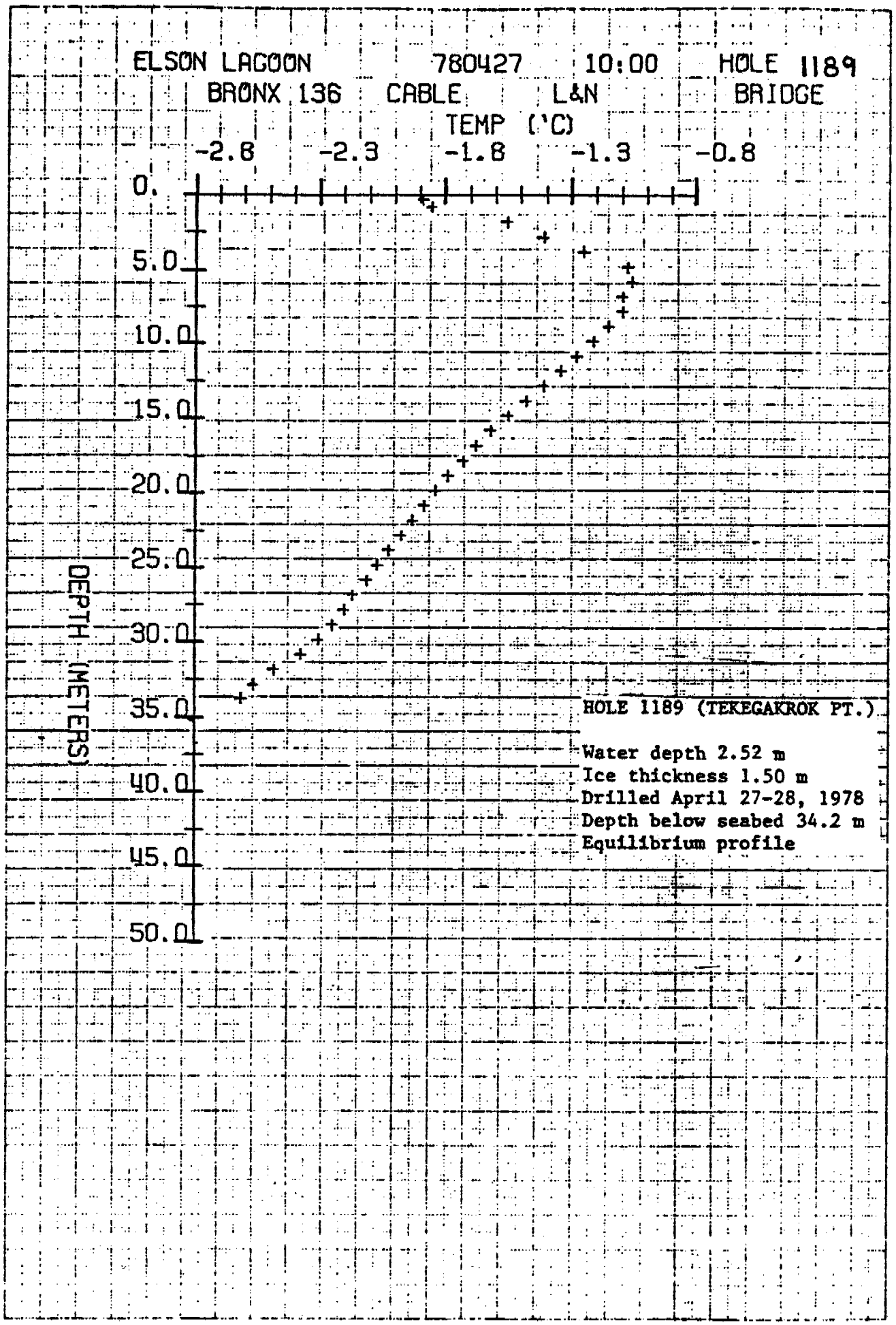
ELSON LAGOON 780427 10:00 HOLE 1189
BRONX 136 CABLE L&N BRIDGE
TEMP (°C)
-2.8 -2.3 -1.8 -1.3 -0.8
0.
5.0
10.0
15.0
20.0
25.0
30.0
35.0
40.0
45.0
50.0
DEPTH (METERS)
HOLE 1189 (TEKEGAKROK PT.)
Water depth 2.52 m
Ice thickness 1.50 m
Drilled April 27-28, 1978
Depth below seabed 34.2 m
Equilibrium profile

FIGURE 13

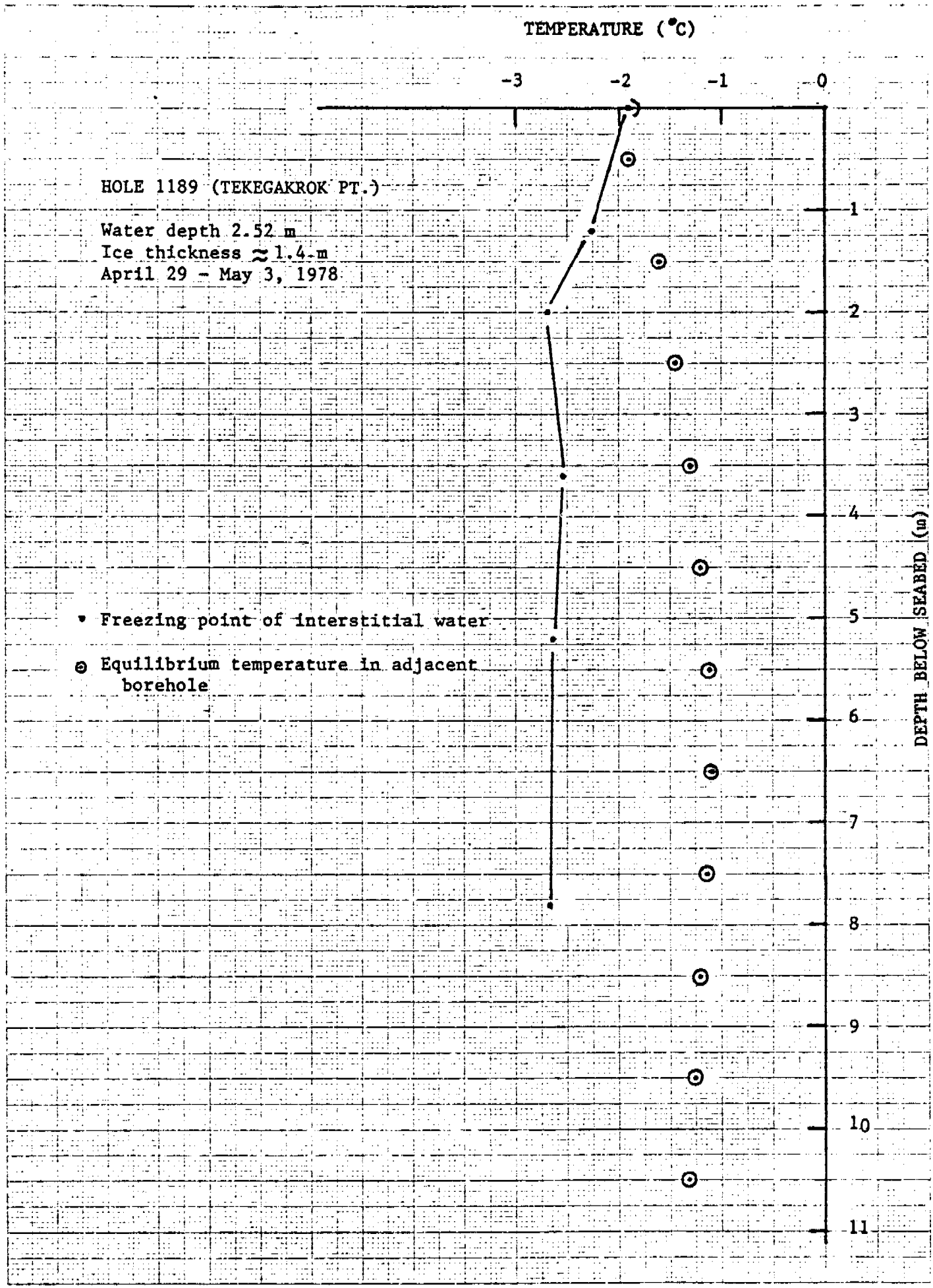
TEMPERATURE (°C)
-3
-2
-1
0
HOLE 1189 (TEKEGAKROK PT.)
Water depth 2.52 m
Ice thickness ≈1.4 m
April 29 - May 3, 1978
• Freezing point of interstitial water
⊙ Equilibrium temperature in adjacent borehole
1
2
3
4
5
6
7
8
9
10
11
DEPTH BELOW SEABED (m)

FIGURE 14

present, at least at the shallow depths sampled. Although the salinities are roughly 40% higher than that of normal sea water, they are not nearly as high as those in the upper part of hole 660. This is surprising, because roughly two centuries ago this site probably was in the same environment as hole 660 is now, and the salinity distribution should have been roughly similar. This view is supported by data at the end of Table 3 obtained from a hole 798 m from shore a year earlier; extremely high salinities at shallow depth exist here as well. The interesting question of what happened to the salt in the upper part of hole 1189, if it was ever present, remains unanswered.

The measured hydraulic conductivities for hole 1189, which with one notable exception are extremely low, are summarized in Table 3. Two values are given at a depth of 7.8 m. The first, "∞", means that the water entered the probe so rapidly that the rate may have been limited by the contuctance of the probe itself, so that no reliable soil hydraulic conductivity determination was made. The second value, 0.10 m a^{-1}, was obtained at the same depth, but in a hole roughly 1/2 to 1 m distant from the first. Evidently these data indicate the existence of a highly permeable layer at this depth!

4. Nearshore area

A preliminary investigation of the permafrost regime near shore, where the ice annually freezes to the sea bed, was carried out in May 1977, and in May and October 1978. The regime here is very dynamic in both its seasonal and secular changes. At its outer limit about 200 m from shore, the area has been innundated for 2 or 3 centuries. The high interstitial water salinities found in this area, which are probably due to seasonal freezing of the sea ice into the sea bed, persist hundreds of meters from shore, as noted in the discussion of holes 660 and 1189.

Temperature measurements were made in pipes hand driven into the sea bed in October 1978. Some interstitial water samples were obtained as well. This was accomplished by fitting the pipes with a tip in a sliding seal, driving them, and then withdrawing them slightly to break the seal. A water sample leaked in slowly and was subsequently bailed out. All these data are summarized in Table 4 and Figure 15. Also given are the estimated salinity and freezing point depression, obtained as discussed earlier.

Also shown on Figure 15 are depths to bonded permafrost, estimated with the help of hand-driven "frost" probes in holes 100, 200, 400 and 500, by jetting in hole 575, and by power driving, jetting, temperature and interstitial water measurement in hole 660 as discussed earlier. At hole 200 the presence of ice as determined by driving is confirmed by the freezing point of the interstitial water, which is the same within errors as the in situ temperature. It should be recognized, as discussed in connection with hole 660, that these boundaries are not always well defined. Also, there may be several boundaries at one site, and if they are shallow they may change seasonally. But Figure 15 still gives a good idea of the general trends.

TABLE 3

HOLE 1189, TEKEGAKROK POINT ("1250 nominal")

Location: 1189 m from shore, N56°E (true, assuming 25° declination), shore to most distant bench mark = 316.6 m
Time: April 29-May 3, 1978
Water Depth: 2.52 m
Ice Thickness: not measured but close to 1.4 m
Water under ice: 1.1 m
Tide peak to peak amplitude: $\approx$ 0.35 m observed, could be slightly larger

Depth Below Sea Bed	Electrical Conductivity of Interstitial Water at 25°C	Estimated Salinity	Estimated Salinity ÷ 34 °/₀₀	Estimated Freezing Temperature of Free Water	Hydraulic Conductivity
0 (water under sea ice)	$5.26(\Omega\ m)^{-1}$	34.7 °/₀₀	1.02	-1.90 °C	
1.2 m	6.10	41.0	1.21	-2.26	6.1×10^{-2} m a
2.0	7.02	48.3	1.42	-2.69	7.1×10^{-2}
3.6	6.73	46.0	1.35	-2.55	1.7×10^{-2}
5.2	6.91	47.4	1.39	-2.64	$*4.4 \times 10^{-2}$
7.8	7.00	48.1	1.41	-2.68	≈ 0.10

*Unreliable hydraulic conductivity value.

HOLE 798, TEKEGAKROK POINT (1977)

2.1	10.0±3.5	73.6	2.19	-4.23	
5.2	12.0±2.0	92.3	2.75	-5.43	

Table 4

NEAR SHORE AREA, TEKEGAKROK POINT

October 28 - November 4, 1978

Distance Offshore	Depth below Sea bed	Temperature	Electrical Conductivity of Interstitial Water at 25°C	Estimated Salinity	Estimated Salinity + 34 °/₀₀	Estimated Freezing Temperature of Free Water
50 m	1.56 m	-3.85°C				
100	2.46	-4.70				
200	2.44	-4.57	10.7	80.0°/₀₀*	2.35	-4.64°C*
300	3.10	-5.12				
400	3.22	-4.29(-7.2)**				
500	3.67	-4.26(-6.2)**	12.3	95.2	2.80	-5.62

*Salinity upper limit only, freezing temperature lower limit. See text.

**May 1, 1978

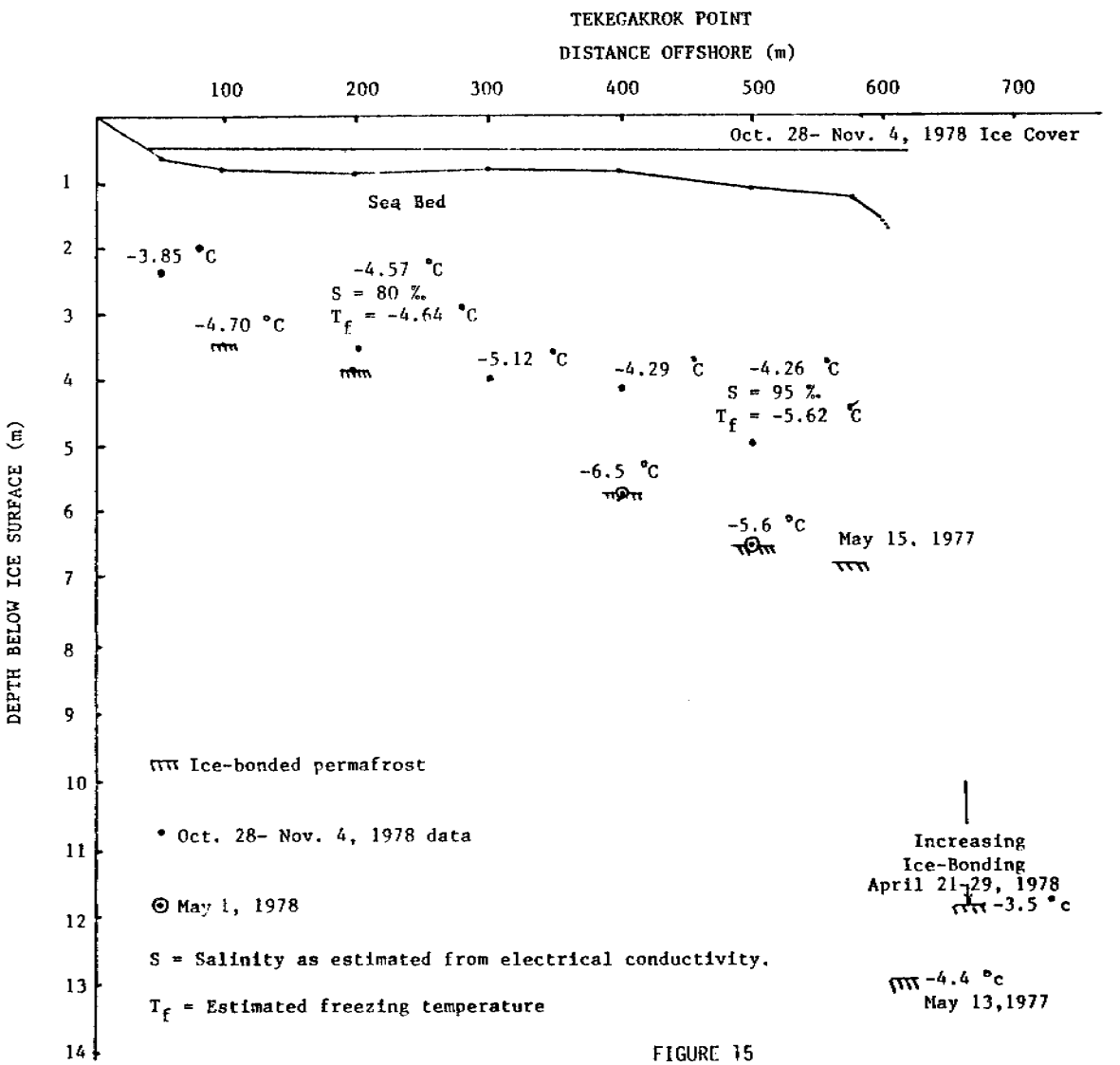
TEKEGAKROK POINT
DISTANCE OFFSHORE (m)
100
200
300
400
500
600
700
Oct. 28- Nov. 4, 1978 Ice Cover
Sea Bed
DEPTH BELOW ICE SURFACE (m)
1
2
3
4
5
6
7
8
9
10
11
12
13
14
-3.85 °C
-4.57 °C
S = 80 ‰
T_f = -4.64 °C
-4.70 °C
-5.12 °C
-4.29 °C
-4.26 °C
S = 95 ‰
T_f = -5.62 °C
-6.5 °C
-5.6 °C
May 15, 1977
Ice-bonded permafrost
• Oct. 28- Nov. 4, 1978 data
⊙ May 1, 1978
S = Salinity as estimated from electrical conductivity.
T_f = Estimated freezing temperature
Increasing
Ice-Bonding
April 21-29, 1978
-3.5 °c
-4.4 °c
May 13,1977

FIGURE 15

TABLE 5

PRUDHOE BAY SPRING 1978 HOLES

Hole	Coordinates		Water Depth	Ice Thickness
9.5 km	70° 26.90 148° 22.69	0.15'N 0.34'W	6.9 m	1.6 m
5.9 km true north of Reindeer Island	70° 32.29 148° 19.64	0.27'N 0.58'W	17 m	1.5 m
Sag Delta	70° 25.46 147° 57.90	0.13'N 0.34'W	7.60	1.71

(Errors are standard deviations.)

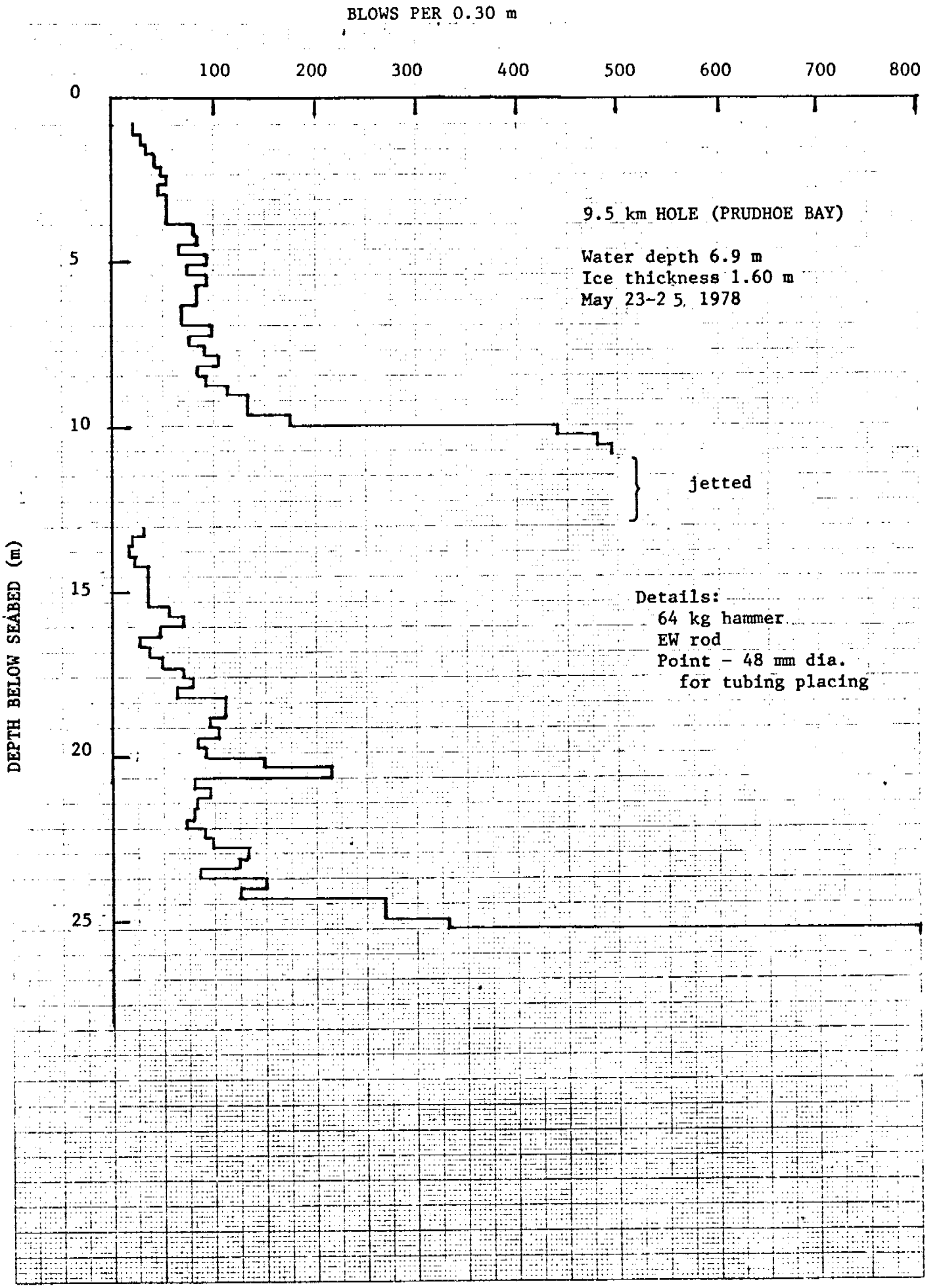

FIGURE 16

Millimeters to the Centimeter

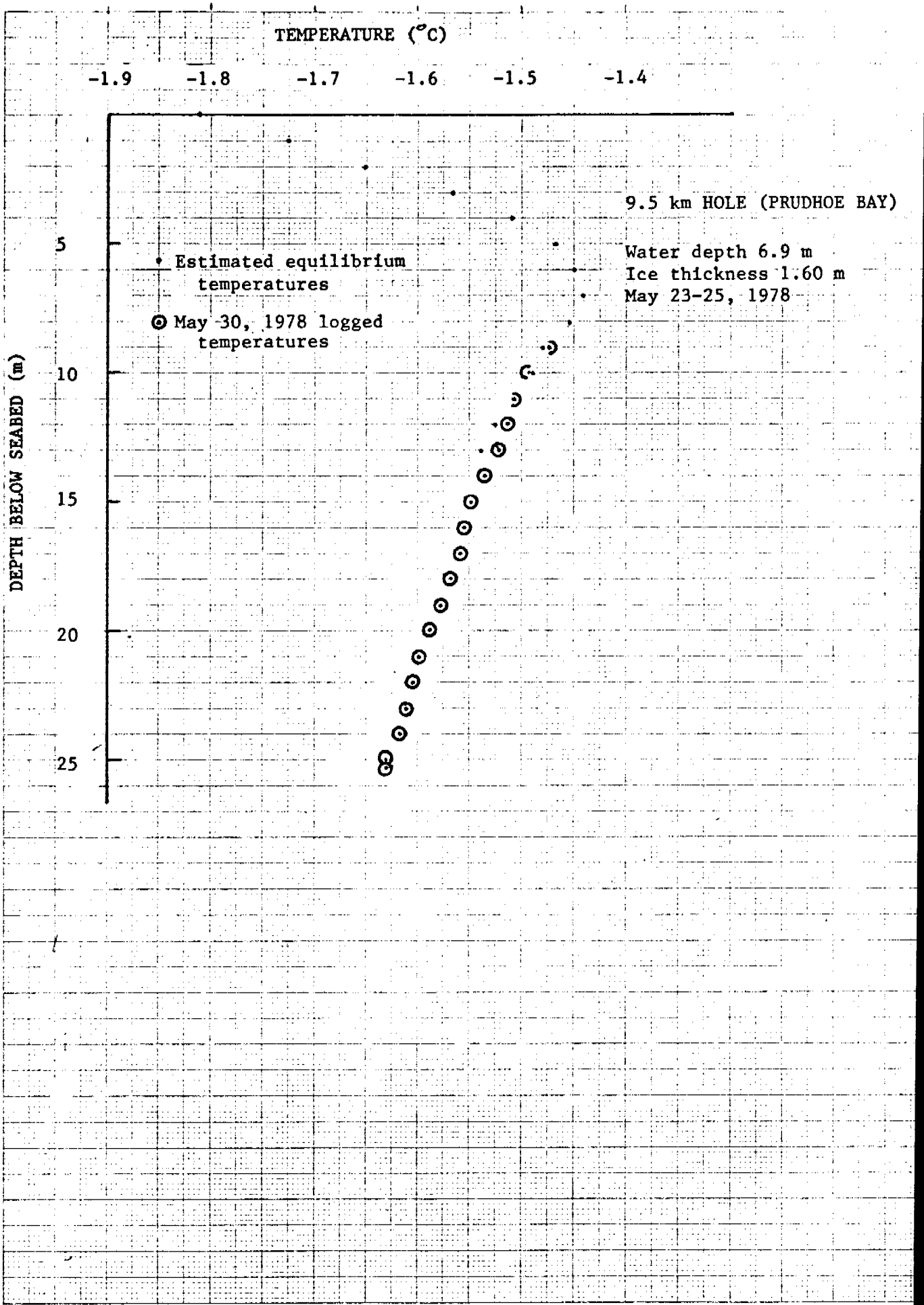
TEMPERATURE (°C)
-1.9
-1.8
-1.7
-1.6
-1.5
-1.4
9.5 km HOLE (PRUDHOE BAY)
Water depth 6.9 m
Ice thickness 1.60 m
May 23-25, 1978
Estimated equilibrium temperatures
May 30, 1978 logged temperatures
DEPTH BELOW SEABED (m)
5
10
15
20
25

FIGURE 17

B. Prudhoe Bay Area

Temperature measurements were made in holes at four sites in Prudhoe Bay (Table 1 and Figure 2) and, as discussed later, on the Barrier Islands. Hole location was chosen to give information complementary to that obtained in earlier OCS projects, particularly the seismic studies of Rogers and Morack and the USGS-CRREL drilling programs.

Three of the Prudhoe Bay sites were located by the Global Navigation System of the NOAA Bell 205 helicopter. Several independent readings (11, 7 and 2 respectively for holes 9.5 km, Sag Delta, and 5.9 km due north of Reindeer Island) were made. Also, an attempt was made to account for system drift in 5 cases. The drift correction was estimated by calibrating the system above a navigational beacon of known coordinates near the beginning of the flight, and reading the coordinates of the same point near the end of the flight. The coordinates of the three sites and estimated errors are given in Table 5.

The location of a hole 8 km due north of Reindeer Island was by helicopter dead reckoning only. However, the method was calibrated using the known coordinates of the site 5.9 km offshore of the island, and the error is unlikely to exceed 1 km.

1. Hole 9.5 km

A hole was driven and jetted 9.5 km from shore along the previous U.S.G.S.-CRREL-UA study line, bearing about N31°E (true) from North Prudhoe Bay State #1 well near the west dock (Table 1 and Figure 2). The drilling data are given in Figure 16. When the driving became hard at 11 m, the drill rod was pulled, and the hole jetted to about 13 m with the ease characteristic of silt or sandy silt soils. At 13 m the jet was stopped by caving in what was probably fine gravel or sand. Driving was successful beyond that depth to about 25 m where the blow count increased by a factor of 3. Probably some of this lower material is sand or gravel as well, considering how easily it drives; however, the reason for the large increase in blow count at 25 m is not clear.

A new technique for installing a tube for temperature logging was first employed in this hole, as discussed in Section V. It was only partially successful, as the thermistor could not be pushed below 13.3 m on the first 2 logging days. Consequently not enough data were obtained to give a good equilibrium temperature below this depth. In Figure 17 the estimated equilibrium temperatures are plotted above 13.3 m, and the May 30 logged temperatures below. The latter are probably within 0.02 deg of equilibrium. The mean annual sea bed temperature is about -1.4°C. Other temperature data are in Appendix I.

The increased blow count which terminated the driving at 25 m could be due to ice bonding, although that would be surprising given the experience along this study line. This experience also suggest -2.4°C as a lower limit on the temperature at which ice bonding begins.

Extrapolation of the temperature data indicates this would be at very roughly 110 m. This is somewhat less than suggested by the seismic evidence of Rogers and Morack (1978), but both estimates are subject to considerable uncertainty.

2. Sag Delta hole

A hole was driven and tubing placed for temperature measurement at a site off the Sagavanirktok River delta (Table 1 and Figure 2), which was chosen to coincide with one of the seismic lines of Rogers and Morack. The drilling data are in Figure 18. A well-defined boundary was found at about 17 m depth, and with rapidly increasing difficulty the rod was driven about 1 m deeper. When pulled, the last 5 sections of drill rod (each section is 1.53 m long) were covered with silty clay, or clay in the case of the bottom section. It is our opinion that the sediments were fine-grained, probably largely clay in the lower half of the hole.

The equilibrium temperatures are shown in Figure 19. The curvature below about 10 m could be an artifact of our extrapolation to get equilibrium temperatures, but it is probably a real effect. Mean annual sea bed temperature is about -1.2°C. Other temperature data are in Appendix I.

This hole location is close to the mid point of the seismic line MM' of Rogers and Morack (1978, p. 32). Their data indicate a fast layer at depths ranging from roughly 20 to 30 m below the sea surface in this region. Since the boundary we encountered was about 25 m below the sea surface, it seems fairly likely that it is the same as theirs. The boundary we encountered at 17 m could be very compact clay or ice-bonded permafrost or both.

If this boundary marks the beginning of ice-bonded permafrost, then the interstitial water salinity must be less than that of normal sea water, because the actual temperature is -1.59°C, while normal sea water begins to freeze at -1.84°C. (Since we do not have any information on the amount of freezing-point-depression due to soil particle effects, we cannot state the value for the salinity at the boundary). Extrapolation of the temperature data indicates that this conclusion is probably valid even if our identification of the boundary is incorrect, and it is in fact up to 10 m deeper.

3. Hole 8 km North of Reindeer Island

A hole was jetted 8 km due north of Reindeer Island where the water depth is 21 m (Table 1). This is the farthest offshore hole so far in Alaska waters. The material is hard clay to the 3.3 m reached (Figure 20). The compact clays were found with a few tenths of a meter of the sea bed implying that there has been very little recent sedimentation in this area.

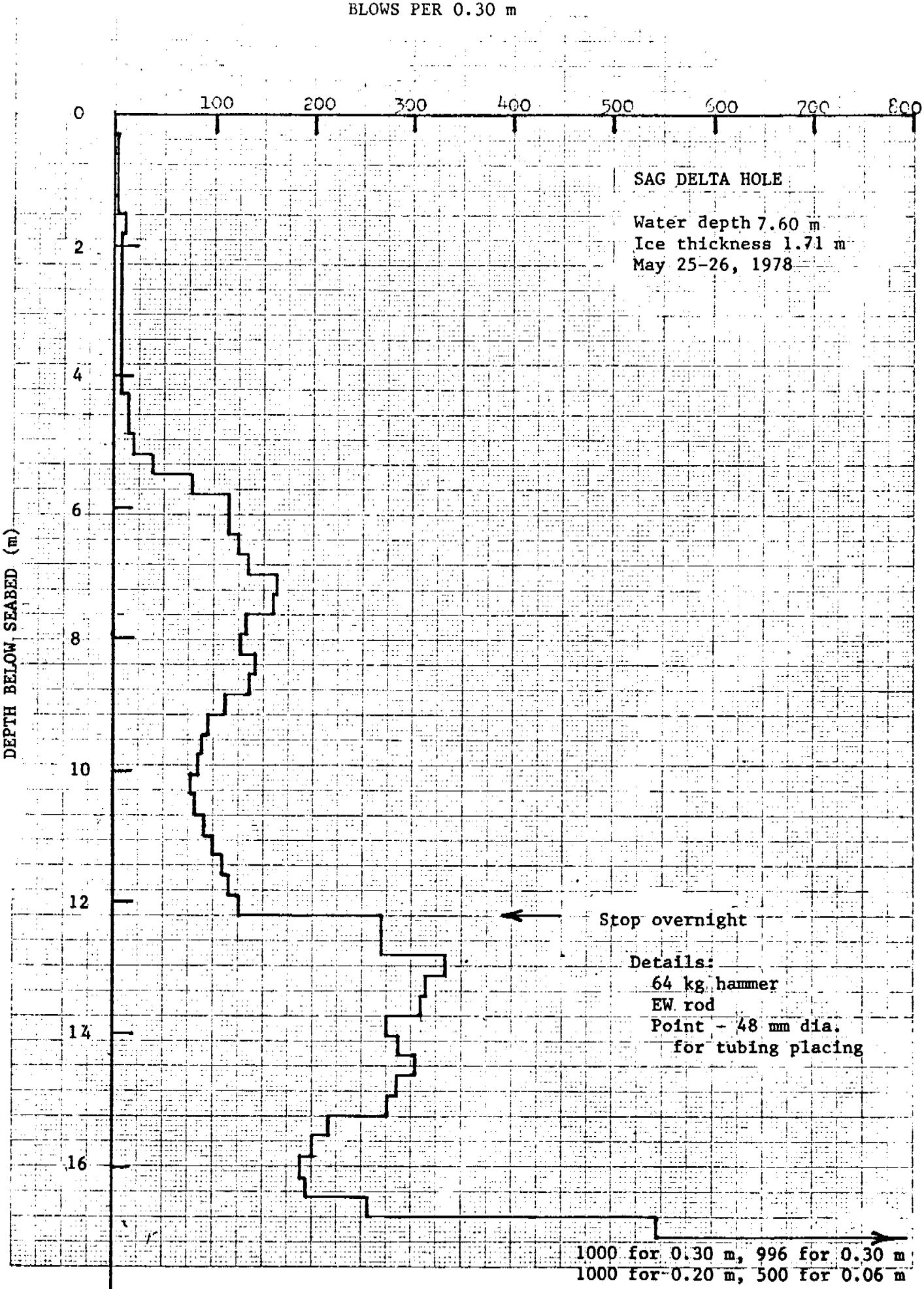

illimeters to the

FIGURE 18

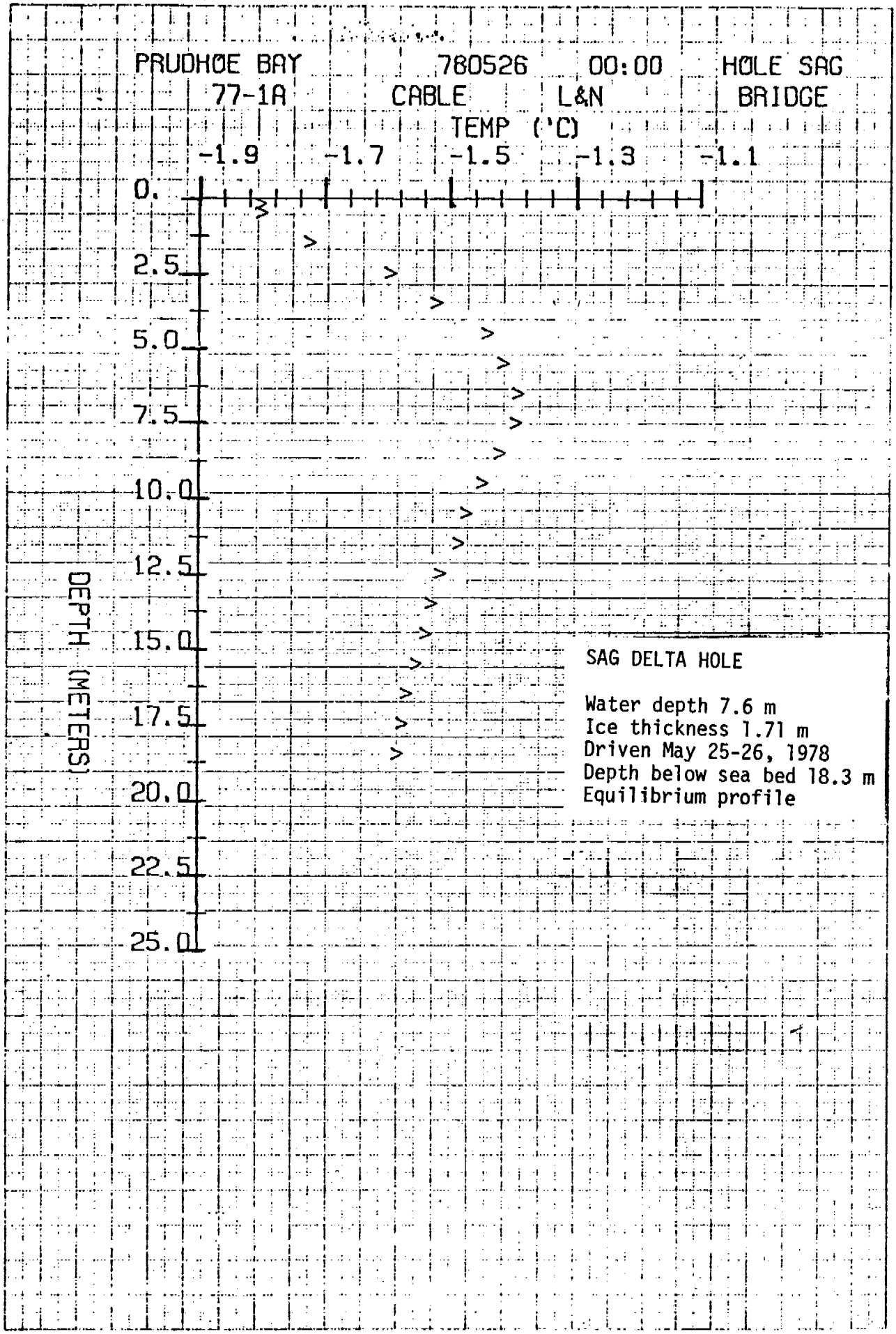
PRUDHOE BAY
77-1A
780526
CABLE
00:00
L&N
HOLE SAG
BRIDGE
TEMP ('C)
-1.9
-1.7
-1.5
-1.3
-1.1
0.
2.5
5.0
7.5
10.0
12.5
15.0
17.5
20.0
22.5
25.0
DEPTH (METERS)
SAG DELTA HOLE
Water depth 7.6 m
Ice thickness 1.71 m
Driven May 25-26, 1978
Depth below sea bed 18.3 m
Equilibrium profile

FIGURE 19

Figure 20

Holes offshore
(North) of Reindeer
Island: Lithology

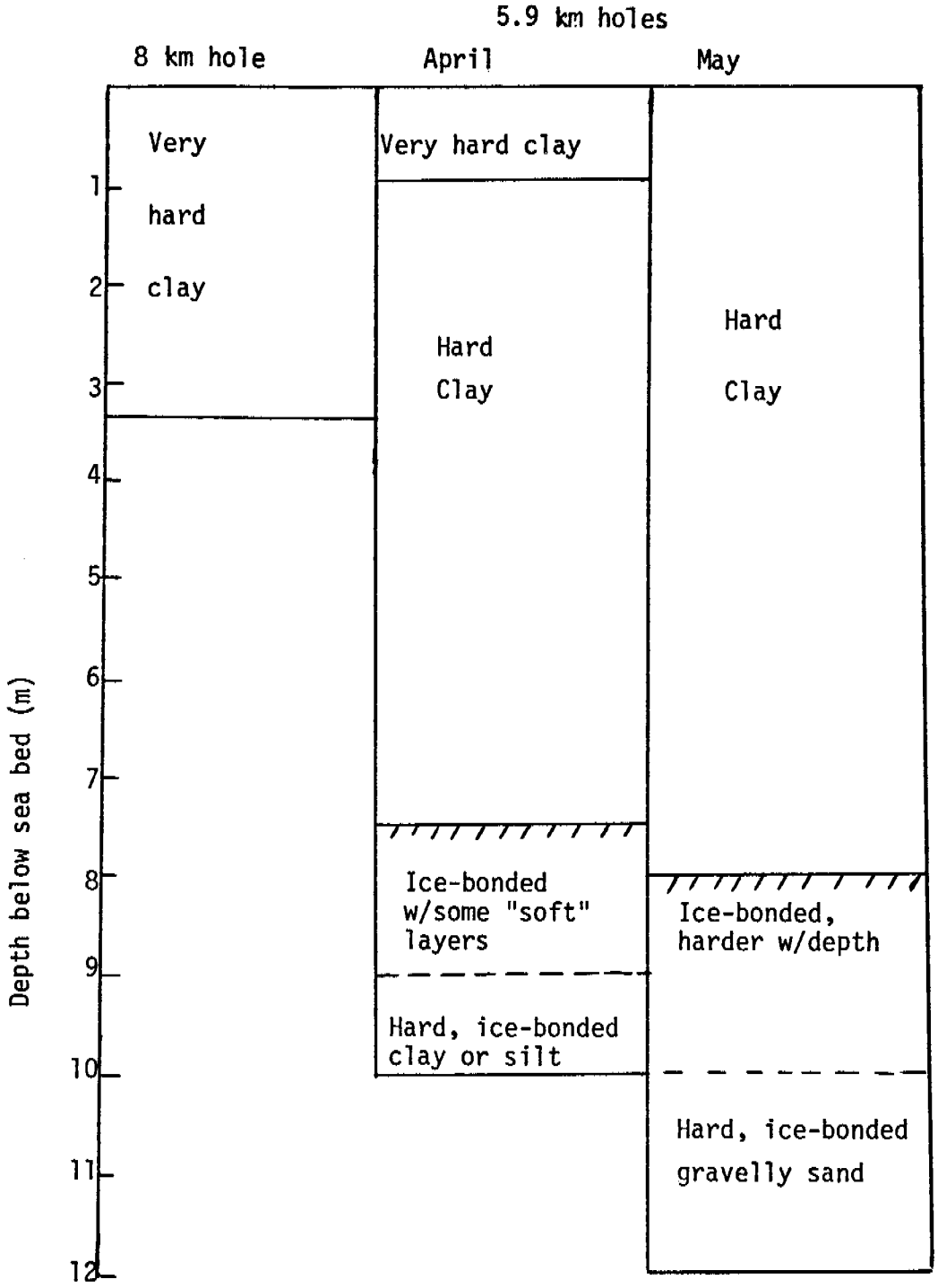

4. Hole 5.9 km North of Reindeer Island.

Two holes 30 m apart were drilled 5.9 km due north of Reindeer Island (Table 1 and Figure 2), where the water depth is 17 m. The first hole was jetted in April; the second was jet augered in May. The lithology is shown in Figure 20. No more than a few tenths of a meter of sediment overlies a 7 or 8 m thick layer of clay which in turn overlies ice-bonded material. A few m below the ice bonded boundary, hard ice-bonded gravelly sand was encountered. Temperature data for these two holes are given in Figures 21 and 22 and Appendix I. Equilibrium temperatures were not obtained. Only one logging was obtained in the April hole before it was lost. Three loggings were obtained in the May hole, but they were closely spaced in time. Both temperature profiles seem to show some evidence for the phase boundary at 7.5 m, but it would not be convincing without the drilling information. The phase boundary temperature is about -1.7°C. The upper part of the April profile is up to 0.08 degrees warmer than the May one. This probably represents a real secular change, although differences in drilling disturbances may also be a factor. The sea bed temperature was about 0.06°C colder in April. Its mean annual temperature cannot be estimated accurately, but it is probably less than -1.5°C.

The observation of shallow ice-bonded permafrost at the 5.9 km site supports Rogers and Morack's (1979) interpretation of their seismic studies in this area as indicating ice-bonded material at a depth of less than 40 m from the sea surface, which is less than 23 m below the sea bed at this site. Some of their data in this area indicate bonded materials within 5 m of the sea bed (Rogers and Morack, 1978, 1979).

The existence of shallow bonded permafrost is surprising in an area so far from shore that has been innundated on the order of 10^4 years, especially since it lies much deeper in shallower water along the study line from the west dock to Reindeer Island. Hopkins (RU 204, 473) suggests that a paleovalley of the Sagavanirktok River may have crossed this line, removing a protective cap of clay and thereby allowing subsequent infiltration of salts into the relatively permeable materials below. Where this cap remains, at our offshore holes north of Reindeer Island and probably at the Sag Delta hole, salts infiltrate very slowly, and since temperatures are negative, thawing is very slow.

The theory of Harrison and Osterkamp (1978 and Appendix II) may be applicable to the thawing rate in these clays, in which salt transport should be by molecular diffusion. If the sea bed temperature is taken as -1.70°C (about the same as the phase boundary temperature) and the sea water freezing temperature is -1.84°C, their equation (13) gives about 3 m for the thickness of the thawed layer after 10,000 years. This is the right order of magnitude, considering the many unknowns (initial salt content of the clay, soil particle surface effects, etc.).

Borehole, seismic, geologic and theoretical evidence seem to be mounting that shallow ice-bonded permafrost is widespread throughout the lease sale area.

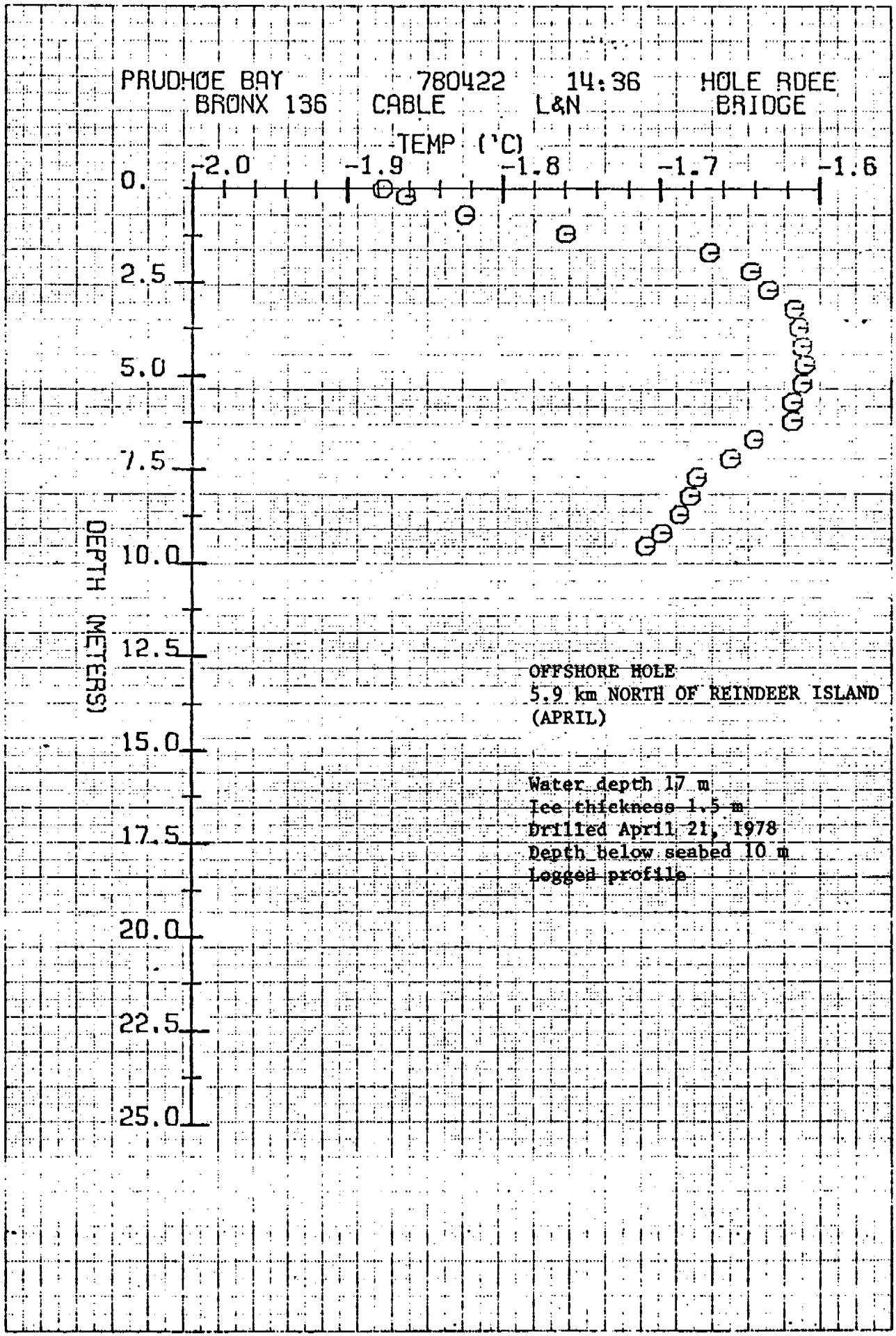
PRUDHOE BAY
BRONX 136
780422
CABLE
14:36
L&N
HOLE RDEE
BRIDGE
TEMP (°C)
-2.0
-1.9
-1.8
-1.7
-1.6
0.
2.5
5.0
7.5
10.0
12.5
15.0
17.5
20.0
22.5
25.0
DEPTH (METERS)
OFFSHORE HOLE
5.9 km NORTH OF REINDEER ISLAND
(APRIL)
Water depth 17 m
Ice thickness 1.5 m
Drilled April 21, 1978
Depth below seabed 10 m
Logged profile

FIGURE 21

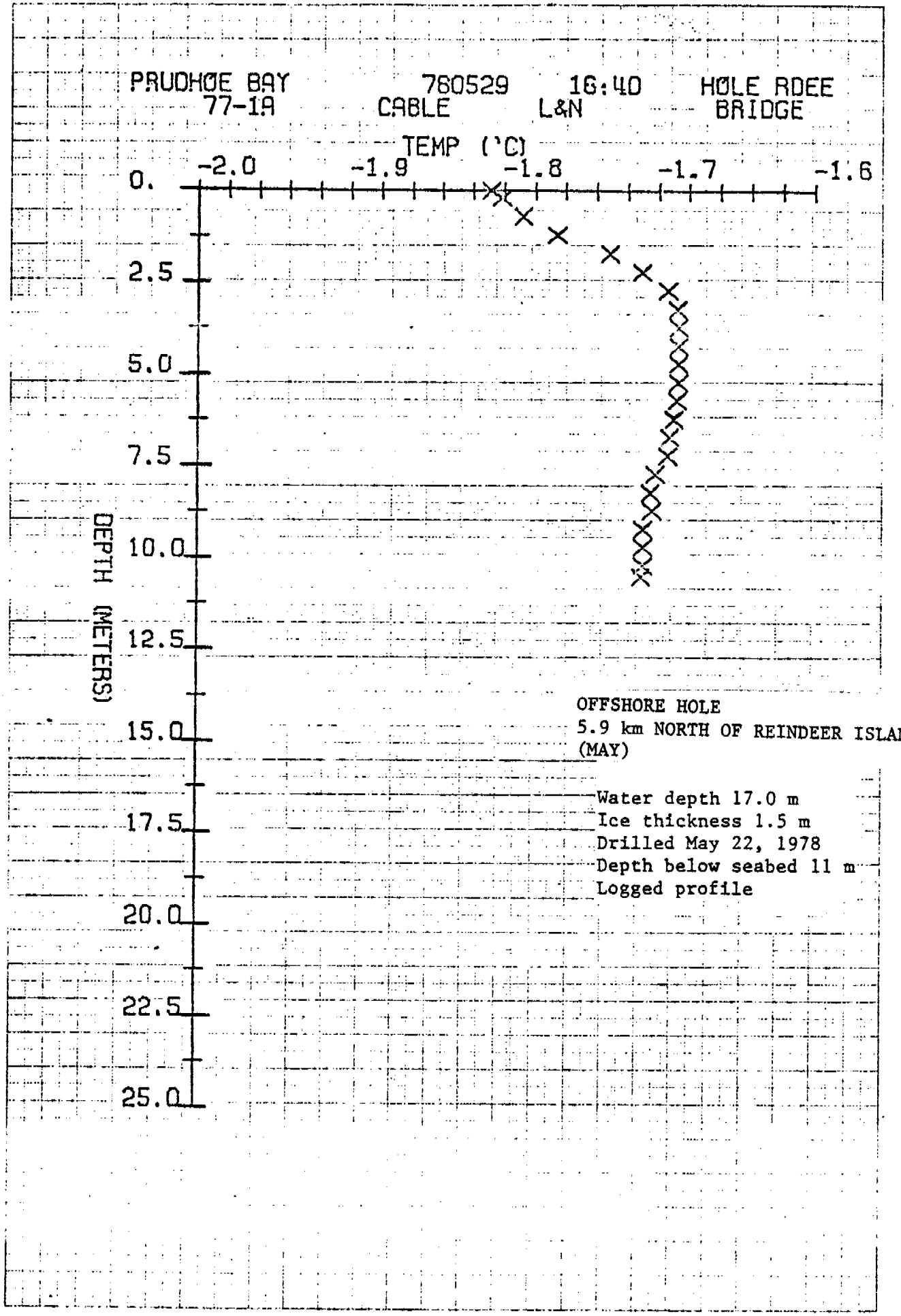
PRUDHOE BAY
77-19
760529
CABLE
16:40
L&N
HOLE RDEE
BRIDGE
TEMP (°C)
-2.0
-1.9
-1.8
-1.7
-1.6
0.
2.5
5.0
7.5
10.0
12.5
15.0
17.5
20.0
22.5
25.0
DEPTH (METERS)
OFFSHORE HOLE
5.9 km NORTH OF REINDEER ISLAND
(MAY)
Water depth 17.0 m
Ice thickness 1.5 m
Drilled May 22, 1978
Depth below seabed 11 m
Logged profile

FIGURE 22

C. Barrier Islands

Holes were jetted or jet-augered on Reindeer, Stump, and Cottle Islands in spring and summer 1978 to obtain information about soil lithology, temperature, and state of ice bondedness. Lithology and state of bondedness were interpreted as discussed in Section V.

1. Reindeer Island

Five holes were drilled in Reindeer Island at the sites shown in Figures 3 and 4. Other information is in Table 1.

The surface consists of sand with some gravel and has an elevation of 1 to 2 m. There is no vegetation. The lithology is shown in the first column of Figure 23. Although the details vary slightly from hole to hole, this general lithology is considered representative of the entire area sampled.

Hole 1 was abandoned due to caving of the loose surface active layer during a long shut down for equipment repairs. Hole 2 was abandoned when the return water flow started coming up hole 1, 5 m away. Hole 3 reached 27.7 m without difficulty but froze up at 17.1 m; the pipe is now open to 18.4 m and can probably be reopened deeper. At hole 4, only 50 m from hole 3, the drilling was completely different due to ice-bonding, and it was possible to drill only to 16 m in the time available. Hole 0 was similar to hole 4 except that the soils were harder and more bonded due to seasonal freezing.

The state of ice bondedness varies greatly, not only from hole to hole, but within a given hole as well (Figure 23). It is also likely that ice is present in areas where the sediments are not firmly ice bonded (Harrison and Osterkamp, 1977). Therefore the permafrost regime appears to be very complex, although a trend to greater ice-bonding to the east may be noted in our study area.

The temperature data from hole 3 are given in Appendix I. Equilibrium temperatures have not yet been obtained but are probably not greatly different from the logged temperatures in Figure 24. They show a sharp warming with depth, which appears to be a transient effect associated with migration of the island. The mean annual temperature at the soil surface is about -12°C or colder.

The relationship of our observations to older ones on the island needs to be discussed. In a Humble Oil test well drilled on Reindeer Island, "frozen" sediments were found from sea level to 20 m and again from 90 to 125 m (Reimnitz and Barnes, 1974). Seismic refraction and reflection studies at the well, carried out by Rogers and Morack (1977), failed to detect this "frozen" material, possibly because it was not well-bonded during the summer when their measurements were made. This hole has not yet been located with respect to our holes, but it is in the same general area.

Figure 23

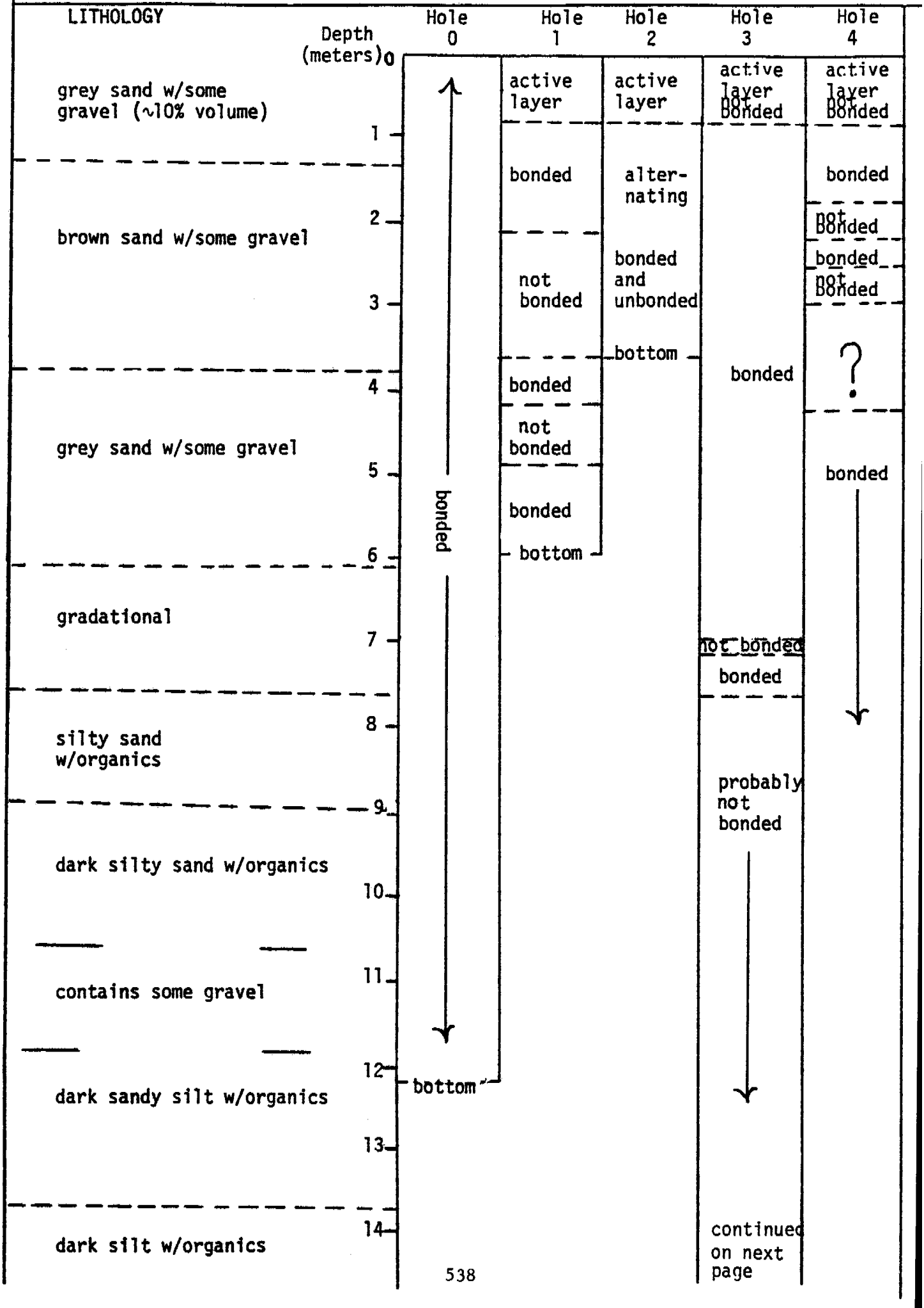
LITHOLOGY
Depth (meters)
Hole 0
Hole 1
Hole 2
Hole 3
Hole 4
grey sand w/some gravel (~10% volume)
brown sand w/some gravel
grey sand w/some gravel
gradational
silty sand w/organics
dark silty sand w/organics
contains some gravel
dark sandy silt w/organics
dark silt w/organics
0
1
2
3
4
5
6
7
8
9
10
11
12
13
14
bonded
bottom
active layer
bonded
not bonded
bonded
bottom
active layer
alter-nating
bonded and unbonded
bottom
active layer not bonded
bonded
not bonded
bonded
probably not bonded
active layer not bonded
bonded
not bonded
bonded
not bonded
?
bonded
continued on next page

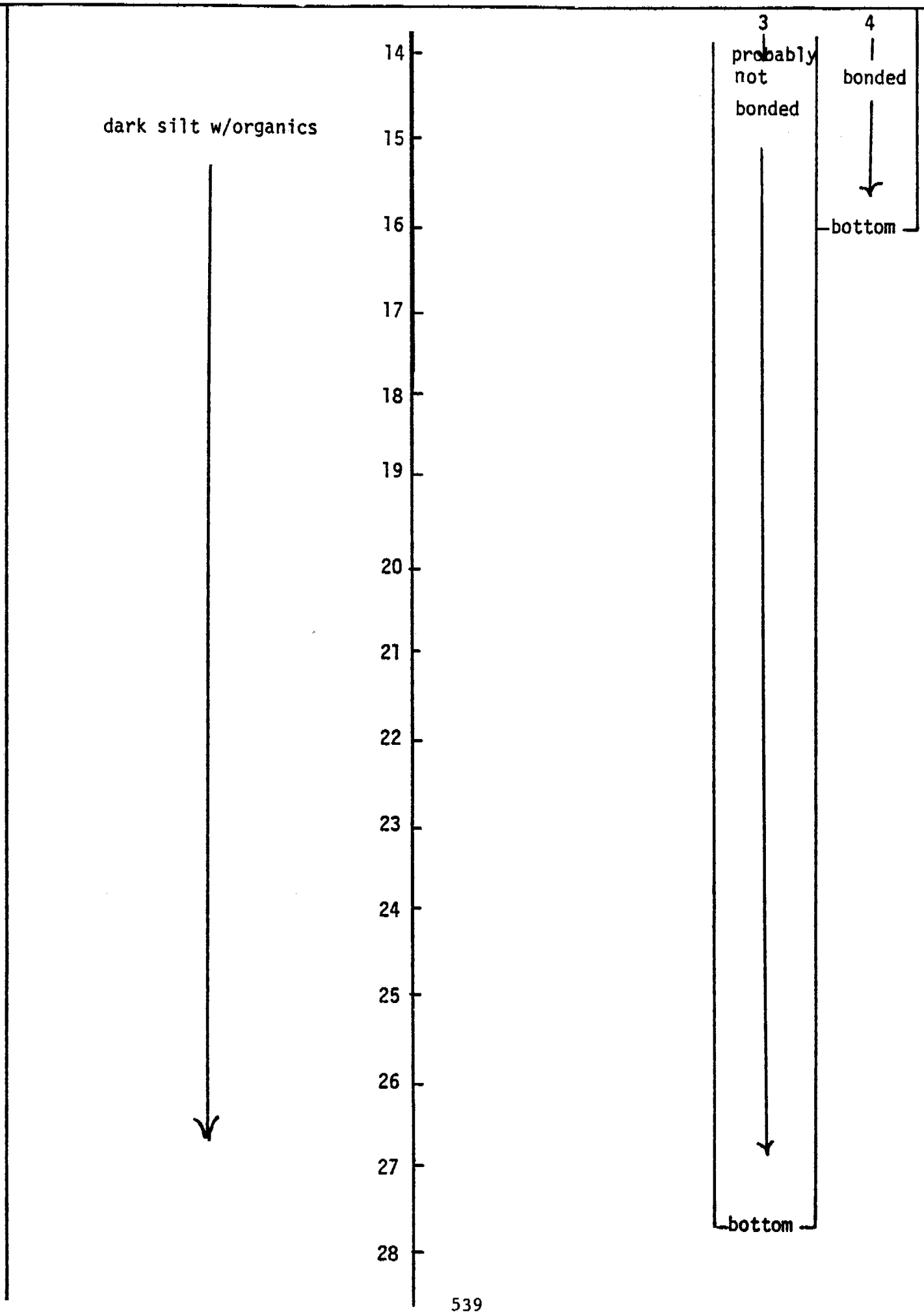
dark silt w/organics
14
15
16
17
18
19
20
21
22
23
24
25
26
27
28
3
probably
not
bonded
4
bonded
bottom
bottom

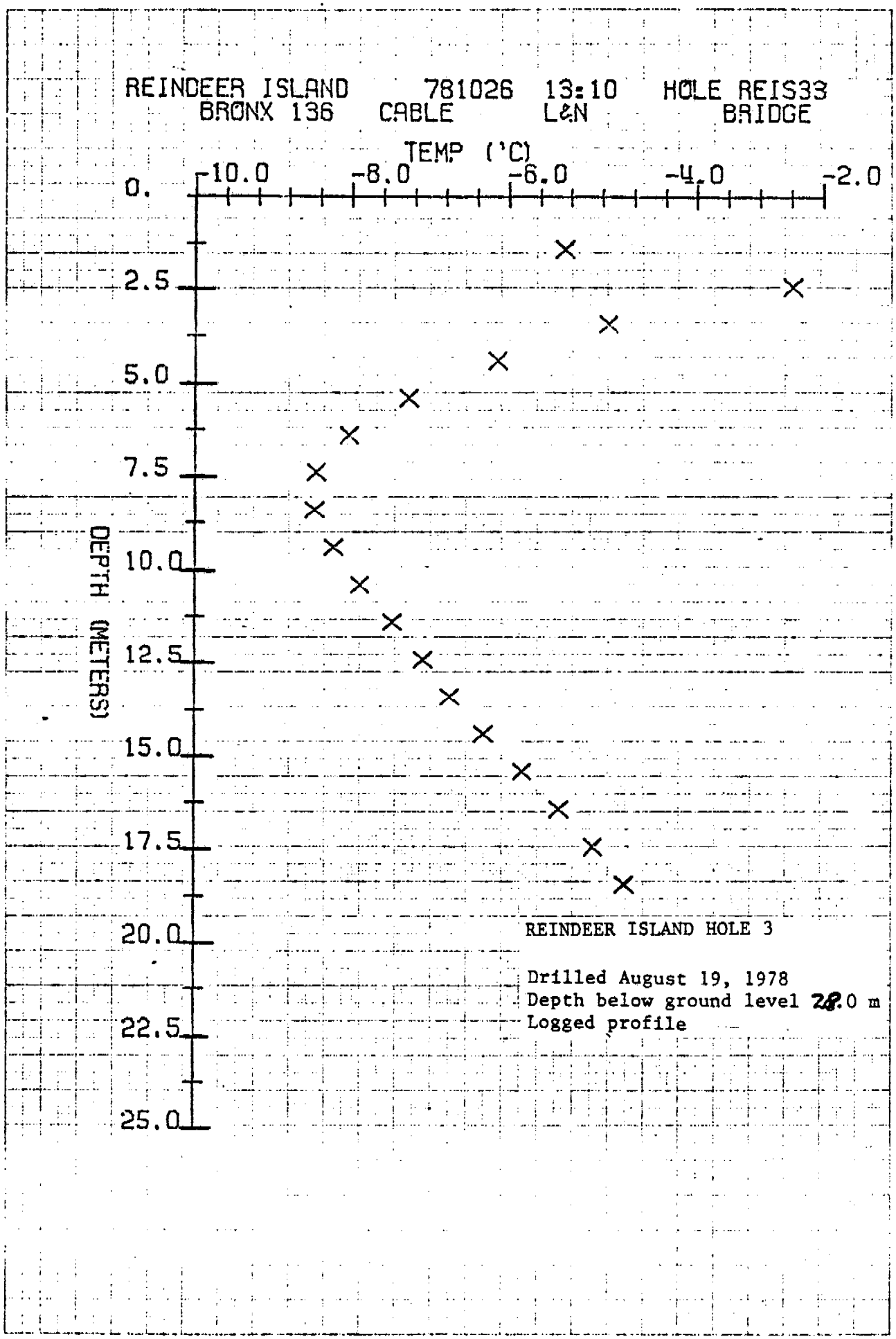
REINDEER ISLAND 781026 13:10 HOLE REIS33
BRONX 136 CABLE L&N BRIDGE
TEMP ('C)
-10.0
-8.0
-6.0
-4.0
-2.0
0.
2.5
5.0
7.5
10.0
12.5
15.0
17.5
20.0
22.5
25.0
DEPTH (METERS)
REINDEER ISLAND HOLE 3
Drilled August 19, 1978
Depth below ground level 28.0 m
Logged profile

FIGURE 24

2. Cottle Island

A hole was drilled on the tundra covered portion of Cottle Island, where the surface elevation is roughly 2 or 3 m (Table 1 and Figure 3). Cottle Island was chosen as probably being a mainland remnant and therefore having a permafrost regime different from Reindeer Island. The lithology is given in Figure 25. Below a surface layer of silt, gravel is present down to the 6 m depth penetrated. The soil seems to be well-bonded, except for the surface active layer. Some shallow temperature data are given in Appendix I, but they do not represent equilibrium conditions.

3. Stump Island

Two holes were drilled 10 to 20 m apart on Stump Island, where the surface elevation is roughly 1 to 2 m, and there is no vegetation (Table 1 and Figure 3). Stump Island was chosen because of the seismic studies of Rogers and Morack (1978) there. The lithology is given in Figure 26. Except for the top few meters, where gravel is present, the soil is basically fine grained down to the 11 m penetrated. Ice bonding of the permafrost occurs, but the details are not very well determined, due to technical difficulties during drilling.

The Stump Island holes are close to the seismic refraction line #11 of Rogers and Morack (1978), who estimated the summer depth to an ice bonded boundary to be from 2 to 4 m in this region. The drilling data indicate the boundary to be at about 1 m depth (Figure 26), and that the deeper material may have unbonded layers in it. But the interpretations seem reasonably consistent.

VIII. SUMMARY AND CONCLUSIONS

A. Barrow - Elson Lagoon

Temperature, soil interstitial water salinity, and hydraulic conductivity were studied in fine-grained sediments at a site off Tekegakrok Point in Elson Lagoon where the shoreline retreat rate is typically 2.4 m a^{-1}. Other measurements made here are described in our previous annual report (Osterkamp and Harrison, 1978). Holes into the sea bed were chosen to span the transition from cold, shallow nearshore conditions to warmer, deeper conditions where normal sea water salinity is maintained year-round under the sea ice. A thawed layer of generally increasing thickness can be traced out from shore under the sea bed, although the phase boundary may not always be sharp. Simultaneous temperature and interstitial water salinity measurements indicate that ice may be present at depths that are not well-bonded. Within roughly 600 m of shore, where the sea ice can seasonally freeze to the sea bed, interstitial water salinities in the thawed layer tend to be at least twice that of normal sea water. This high salinity persists to sediment depths of 5 to 10 m to at least 798 m from shore, but for an unknown reason it is absent at a site 1198 m from shore, where the salinities to 9 m are only about 40% higher than normal sea water. The measured hydraulic conductivites are extremely low, typical of fine-grained silts or clays, when compared to the sands and gravels at Prudhoe Bay. This must have a profound effect on salt transport processes, and therefore

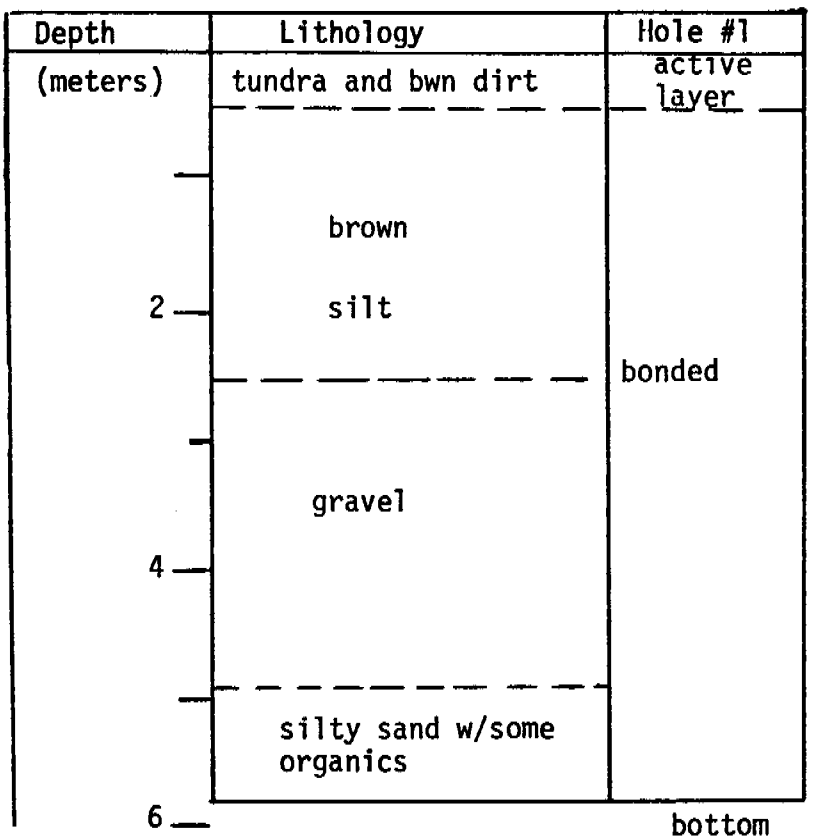

Drilling Method

Bit used: Heavy Duty Earth Probe (Deep Rock Mfg. Co.) with check valve

0-1.8 jetting water and rotating bit by hand occasionally

1.8-2.6 jetting water and rotating bit w/power-head

2.6-5.4 jetting water and rotating bit by hand

5.4-5.8 jetting water and rotating bit w/power-head

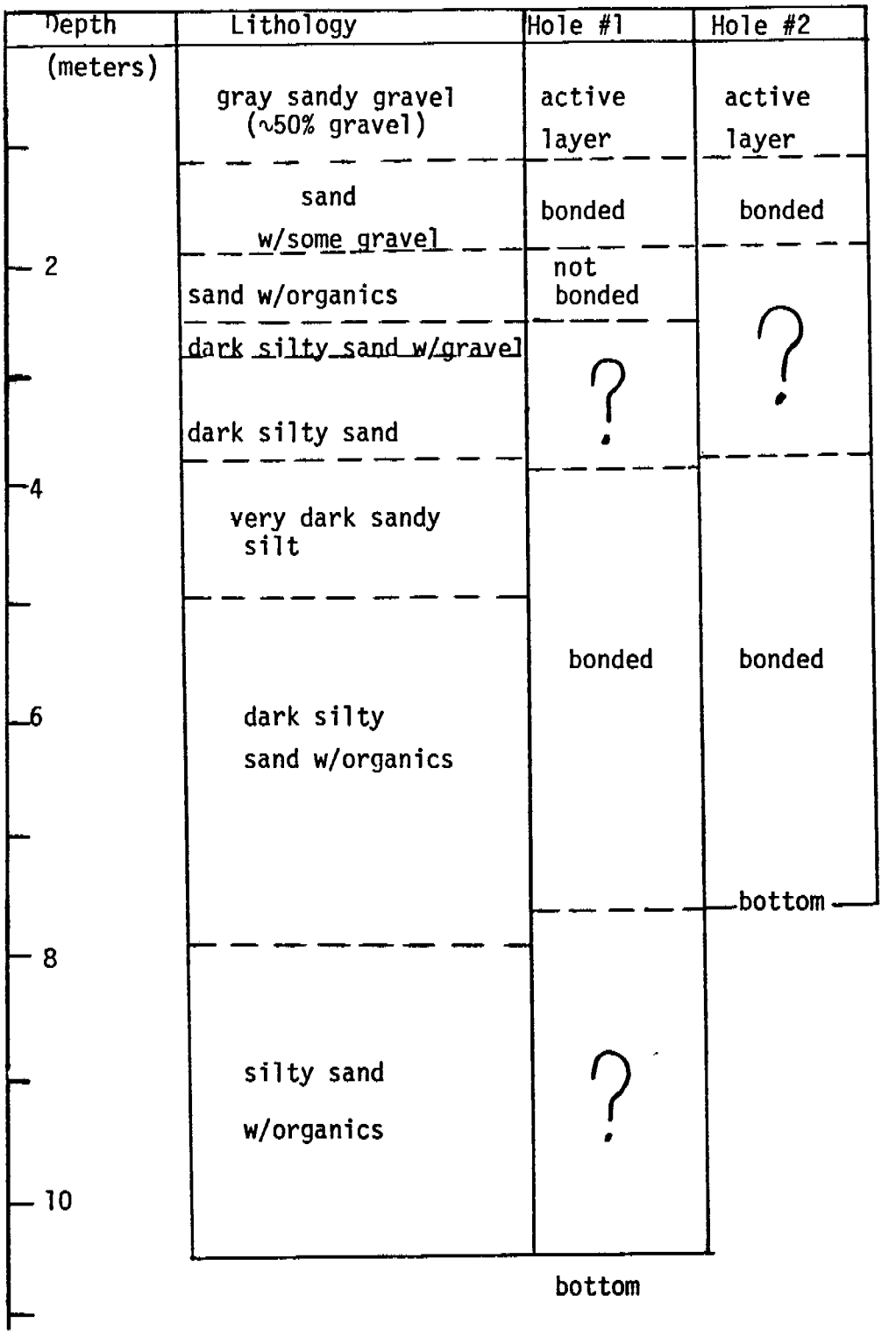

Current status: No pipe was left in the ground for temperature logging.

on subsea permafrost evolution. A striking exception to this was found 1189 m from shore, where there appears to be an extremely permeable layer 9 m below the sea bed. At the same site a sharp boundary, evidently a lithologic one between the Pleistocene and Cretaceous (Black, 1964; Lewellen, 1976), was found at 30 m depth from the temperature and drilling data.

B. Prudhoe Bay Area

Several holes were drilled in the Prudhoe Bay area at sites chosen to tie in with earlier OCS investigations. One hole was drilled for temperature measurements to fill in a gap 9.5 km from shore along the U.S.G.S./ CRREL/UA study line starting near the west dock. Another was drilled off the Sagavanirktok River delta along a seismic study line of Rogers and Morack (1978), where a fast layer varying from roughly 20 to 30 m below the sea surface was found in this particular area. A boundary was found by driving in clay or silty clay 25 m below the sea surface. The boundary temperature was -1.59°C, well above the freezing point of normal sea water. The fast layer is probably due to compact clays, ice-bonding or both. The salinity of the interstitial water at this boundary is less than that of normal sea water if the boundary is associated with ice-bonding.

Holes were also drilled at sites 5.9 and 8 km due north of Reindeer Island, farther offshore than previous holes. Soft sediments amounted to less than a few tenths of a meter at both sites. At the 8 km site hard clay was found to the 3 1/2 m penetrated. At the 5.9 km site hard clay was found to about 10 m, with ice-bonding beginning at 7 or 8 m. Below 10 m, about 2 m of hard ice-bonded gravelly sand was penetrated. This observation of ice-bonding verifies Rogers and Morack's (1979) interpretation of their seismic data as indicating the presence of ice-bonded permafrost at very shallow depths beneath the sea bed well out beyond the Barrier Islands. Hopkins (RU 204, 473) suggestion that this may be due to an impermable cap of clay that inhibits salt infiltration is also supported by our observations, and by salt diffusion theory (Harrison and Osterkamp, 1978, and Appendix II). Temperature measurements at the 5.9 km site indicate that the salinity of the interstitial water at the ice-bonded boundary is less than that of normal sea water, which is similar to the Sag delta situation.

C. Barrier Islands

Holes were drilled on Reindeer, Cottle and Stump Islands. Five holes to a maximum depth of 28 m on Reindeer Island show a complex permafrost regime. The state of ice-bondedness in a particular hole varies with depth, sometimes in a complex fashion, and with lateral position on a scale of 50 m. A hole on the tundra remnant part of Cottle Island shows firm ice-bonding to the 6 m penetrated, as might be expected. Two holes on Stump Island show a complex but mostly bonded shallow permafrost regime that seems to be consistent with the seismic interpretation (Rogers and Morack, 1978).

IX. NEEDS FOR FURTHER STUDY

The data base for the subsea permafrost assessment program continues to improve, and should continue to do so in 1979, especially when the results are available from the recent U.S.G.S. drilling program in the Beaufort Sea lease sale area. Considering the 2000 or more km of coastline and vast shelf areas of the Beaufort and Chukchi Seas that now appear to be subject to subsea permafrost, it is hardly surprising that many field problems and surprises should remain. However, enough information is available to justify a larger effort in the coming year to interpret geologic and physical conditions. This should help us to generalize on what we know.

Many problems have been only partially studied or neglected completely. These include the configuration of the base of the subsea permafrost, its ice, salt, and liquid phase contents, the influence of causeways on it, its properties in areas of extremely rapid coastline retreat, and the distribution and properties of gas hydrates.

Hydrates are combinations of hydrocarbon and H_2O molecules which form ice-like solids under temperature and pressure conditions which probably exist in many subsea permafrost areas. Hydrates represent a potential gas resource, but at the same time present certain problems, since they may expand rapidly when decomposed by the heat of drilling or hydrocarbon production. Like ice-bonded permafrost, they may complicate the interpretation of deep seismic data. Hydrates have been found in the Canadian Beaufort Sea, and phase data have been used to assess their potential distribution; they can exist at shallow depths beneath the sea bed in association with subsea permafrost. We have collected some of the Canadian information, but a similar study for the Alaskan Beaufort Sea needs to be done.

Coordination of efforts and synthesis of results with other investigators will continue to be essential.

X. SUMMARY OF FOURTH QUARTER OPERATIONS

A. Field and Lab Activity

No field work has been conducted this quarter. Equipment for probing and sampling has been overhauled, designed, and constructed. Laboratory studies of shallow soil samples are underway. Data analysis and report writing have required major efforts.

B. Research Adiministration

No changes anticipated.

C. Funded Expended

$294,613 as of March 31, 1979.

D. Problems

Coincidence of report and field preparation times.

XI. REFERENCES

Black, R. F., 1964, Gubik Formation of Quaternary Age in Northern Alaska, U.S.G.S. Professional Paper 302-C, p. 59-91.

Doherty and Kester, 1974, Freezing Point of Sea Water, J. Marine Research, Vol. 32 (2), p. 285-300.

Harrison, W. D., P. D. Miller and T. E. Osterkamp, 1977, Permafrost beneath the Chukchi Sea-preliminary report, In OCSEAP Annual Report, by T. E. Osterkamp and W. D. Harrison, 1977, Appendix II.

Harrison, W. D., and T. E. Osterkamp, 1978, Heat and Mass Transport Processes in Subsea Permafrost I: An Analysis of Molecular Diffusion and its Consequences, J. Geophys. Res., Vol. 83, No. C9, p. 4707-4712, and Appendix II, this report.

Hunter and others, 1976, The Occurrence of Permafrost and Frozen Sub-Seabottom Materials in the Southern Beaufort Sea, by J. A. M. Hunter, A. S. Judge, H. A. MacAulay, R. L. Good, R. M. Gagne, and R. A. Burns, Beaufort Sea Project Technical Report #22, Department of the Environment, Victoria, B. C., Canada.

Iskandar, I. K., T. E. Osterkamp and W. D. Harrison, 1978, Chemistry of Interstitial Water from the Subsea Permafrost, Prudhoe Bay, Alaska, Proceedings of the Third International Conference on Permafrost, p. 92-98. National Research Council of Canada, Ottawa, Ontario, Canada K1A OR6.

Lachenbruch, and others, 1962, Temperatures in Permafrost, by A. H. Lachenbruch, M. C. Brewer, G. W. Greene and B. V. Marshall, in "Temperature-its Measurement and Control in Science and Industry", Vol. 3, Part 1, p. 791-803, Reinhold Publishing Corp., New York.

Lachenbruch, A. H. and Marshall, B. V., 1977, Subsea Temperatures and a Simple Tentative Model for Offshore Permafrost at Prudhoe Bay, Alaska, U.S.G.S. Open File Report 77-395.

Lewellen, R. I., 1973, The Occurrence and Characteristics of Nearshore Permafrost, North Alaska. Permafrost: The North American Contribution to the Second International Conference, National Academy of Sciences, Washington D.C.

Lewellen, R. I., 1974, Offshore Permafrost of Beaufort Sea, Alaska, in "The Coast and Shelf of the Beaufort Sea", Proceedings of a symposium on Beaufort Sea Coast and Shelf Research, J. C. Reed and J. E. Sater, Editors, Arctic Institute of North America.

Lewellen, R. I., 1976, Subsea Permafrost Techniques, Symposium on research techniques in coastal environments, Louisiana State University, Baton Rouge, Louisiana.

National Academy of Sciences, 1976, Problems and Priorities in Offshore Permafrost Research, Committee on Permafrost, Polar Research Board, Assembly of Mathematical and Physical Sciences, National Academy of Sciences. Available from Polar Research Board, 2101 Constitution Avenue, N. W., Washington D.C. 20418

Osterkamp, T. E., and W. D. Harrison, 1976a, Subsea Permafrost at Prudhoe Bay, Alaska: Drilling report, University of Alaska, Geophysical Institute Report, UAG R-245, Sea Grant Report 76-5.

Osterkamp, T. E., and W. Harrison, 1976b, Subsea Permafrost: Its Implications for Offshore Resource Development, The Northern Engineer, Vol 8, No. 1, p. 31-35.

Osterkamp, T. E., and W. D. Harrison, 1977, Subsea Permafrost regime at Prudhoe Bay, Alaska, U.S.A., Journal of Glaciology, Vol. 19, No. 81, p. 627-637,

Osterkamp, T. E. and W. D. Harrison, 1977, Offshore Permafrost-Drilling, Boundary Conditions, Properties, Processes and Models. Delineation of Most Probable Areas for Subsea Permafrost in the Chukchi Sea from Existing Data. Subsea permafrost: Probing, Thermal Regime and Data Analysis. OCSEAP 1977 Annual Report.

Osterkamp, T. E. and W. D. Harrison, 1978, Subsea Permafrost: Probing, thermal regime and data analysis, OCSEAP 1978 Annual Report.

Page, F. W., 1978, Geochemistry of Subsea Permafrost at Prudhoe Bay, Alaska, Masters of Arts Thesis, Dartmouth College, Hanover, N.H.

Page, F. W., and I. K. Iskandar, 1978, Geochemistry of Subsea Permafrost at Prudhoe Bay, Alaska. U. S. Army Cold Regions Research and Engineering Laboratory, Hanover, N.H. Special Report 78-14.

Reimnitz, E., and P. W. Barnes, 1974, Sea Ice as a Geologic Agent on the Beaufort Sea Shelf of Alaska. Proceedings of a Symposium on Beaufort Sea Coast and Shelf Research, Edited by J. C. Reed and J. E. Sater, Arctic Institute of North America.

Rogers, J. C. and others, 1975, Nearshore Permafrost Studies in the Vicinity of Point Barrow, Alaska, University of Alaska, Geophysical Institute Report UAG R-237, Sea Grant Report 75-6.

Rogers, J. C. and J. L. Morack, 1977, Beaufort Seacoast Permafrost Studies. OCSEAP 1977 Annual Report.

Rogers, J. C. and J. L. Morack, 1978, Beaufort Seacoast Permafrost Studies. OCSEAP 1978 Annual Report.

Rogers, J. C. and J. L. Morack, 1979, Beaufort Seacoast Permafrost Studies OCSEAP Quarterly Report, January 1, 1979.

XII. ACKNOWLEDGMENTS

It is a pleasure to acknowledge cheerful and effective assistance under difficult field conditions from Rod March, Mark Smith and the NOAA helicopter crew. Mr. M. Inoue provided valuable assistance throughout the year. Essential logistics support was also provided by OCSEAP and Naval Arctic Research Lab. A substantial part of the work reported here was supported by the National Science Foundation (DPP-77-28451).

APPENDIX I

Borehole temperature data, 1978

ELSON LAGOON
HOLE 660
780429
13:00

BRONX 136 CABLE
L&N BRIDGE

TIME	DEPTH (M)	R (OHMS)	T (C)
16.55	0.55	30134.0	-1.954
16.48	1.55	30033.0	-1.880
16.33	2.55	29989.0	-1.848
16.25	3.55	30003.0	-1.858
16.18	4.55	30073.0	-1.910
15.87	5.55	30253.0	-2.041
15.68	6.55	30696.0	-2.361
15.52	7.55	31198.0	-2.717
15.30	8.55	31778.0	-3.121
15.13	9.55	32248.0	-3.443
15.03	10.55	32478.0	-3.598
14.88	11.55	32664.0	-3.723
14.75	12.55	32872.0	-3.862
14.55	13.55	33034.0	-3.969
14.47	14.55	33195.0	-4.076

HOLE 660 (TEKEGAKROK PT.)

Water depth 2.00 m
Ice thickness 1.40 m
Drilled April 25, 1978
Depth below seabed 15 m
Logged profile

ELSON LAGOON
HOLE 660
780501
13:55

BRONX 136 CABLE
L&N BRIDGE

TIME	DEPTH (M)	R (OHMS)	T (C)
13.98	0.05	30789.0	-2.427
14.10	0.55	30336.0	-2.101
14.25	1.55	30079.0	-1.914
14.30	2.55	30024.0	-1.874
14.37	3.55	30032.0	-1.880
14.42	4.55	30104.0	-1.932
14.48	5.55	30291.0	-2.069
14.53	6.55	30742.0	-2.394
14.60	7.55	31235.0	-2.743
14.67	8.55	31778.0	-3.121
14.72	9.55	32227.0	-3.429
14.78	10.55	32542.0	-3.641
14.85	11.55	32772.0	-3.795
14.90	12.55	32924.0	-3.896
14.95	13.55	33092.0	-4.008
15.02	14.55	33227.0	-4.097
15.03-05	14.93	33280.0	-4.131

HOLE 660 (TEKEGAKROK PT.)

Water depth 2.00 m
Ice thickness 1.40 m
Drilled April 25, 1978
Depth below seabed 15 m
Logged profile

ELSON LAGOON
HOLE 660
780503
07:50

BRONX 136 CABLE
L&N BRIDGE

TIME	DEPTH (M)	R (OHMS)	T (C)
8.90	0.05	30428.0	-2.168
8.98	0.55	30258.0	-2.045
9.05	1.55	30080.0	-1.915
9.12	2.55	30022.0	-1.872
9.17	3.55	30033.0	-1.880
9.22	4.55	30110.0	-1.937
9.48	5.55	30285.0	-2.064
9.57	6.55	30710.0	-2.371
9.63	7.55	31210.0	-2.726
9.72	8.55	31748.0	-3.101
9.83	9.55	32233.0	-3.433
9.92	10.55	32526.0	-3.631
10.08	11.55	32751.0	-3.781
10.15	12.55	32929.0	-3.900
10.27	13.55	33067.0	-3.991
10.40	14.55	33238.0	-4.104
10.67	14.93	33268.0	-4.123

HOLE 660 (TEKEGAKROK PT.)

Water depth 2.00 m
Ice thickness 1.40 m
Drilled April 25, 1978
Depth below seabed 15 m
Logged profile

ELSON LAGOON
HOLE 660
780521
15:40

BRONX 136 L&N

CABLE BRIDGE

TIME	DEPTH (M)	R (OHMS)	T (C)
15.82	0.05	30200.0	-2.002
15.83	0.55	30189.0	-1.994
16.00	1.55	30098.0	-1.928
16.05	2.55	30078.0	-1.913
16.12	3.55	30102.0	-1.931
16.18	4.55	30183.0	-1.990
16.23	5.55	30350.0	-2.111
16.28	6.55	30743.0	-2.394
16.35	7.55	31223.0	-2.735
16.43	8.55	31738.0	-3.094
16.52	9.55	32178.0	-3.395
16.58	10.55	32482.0	-3.601
16.72	11.55	32734.0	-3.770
16.75	12.55	32913.0	-3.889
16.80	13.55	33104.0	-4.016
16.88	14.55	33243.0	-4.107
17.00	14.93	33288.0	-4.137

HOLE 660 (TEKEGAKROK PT.)

Water depth 2.00 m
Ice thickness 1.40 m
Drilled April 25, 1978
Depth below seabed 15 m
Logged profile

ELSON LAGOON
HOLE 660
780425
16:30

BRONX 136 CABLE
L&N BRIDGE

TIME	DEPTH (M)	R (OHMS)	T (C)
0.	0.	30183.0	-1.990
0.	1.55	30122.0	-1.945
0.	2.55	30091.0	-1.923
0.	3.55	30116.0	-1.941
0.	4.55	30198.0	-2.001
0.	5.55	30365.0	-2.122
0.	6.55	30750.0	-2.399
0.	7.55	31225.0	-2.736
0.	8.55	31722.0	-3.083
0.	9.55	32167.0	-3.388
0.	10.55	32500.0	-3.613
0.	11.55	32750.0	-3.781
0.	12.55	32920.0	-3.894
0.	13.55	33134.0	-4.035
0.	14.55	33264.0	-4.121
0.	14.93	33307.0	-4.149

HOLE 660 (TEKEGAKROK PT.)

Water depth 2.00 m
Ice thickness 1.40 m
Drilled April 25, 1978
Depth below seabed 15 m
Equilbrium profile

ELSON LAGOON
HOLE 880
780430
10:21

BELDEN
L&N

CABLE
BRIDGE

TIME	DEPTH (M)	R (OHMS)	T (C)
10.43	0.10	15200.0	-2.056
10.56	0.60	15140.0	-1.970
10.63	1.10	15020.0	-1.796
10.73	2.10	14895.0	-1.613
10.83	3.10	14804.0	-1.478
10.93	4.10	14744.0	-1.389
11.02	5.10	14748.0	-1.395
13.17	6.10	14786.0	-1.451
13.23	7.10	14831.0	-1.518
13.33	8.10	14951.0	-1.695
13.38	9.10	15087.0	-1.893
13.43	10.10	15208.0	-2.068
13.53	11.10	15303.0	-2.204
13.58	12.10	15306.0	-2.208
13.65	13.10	15311.0	-2.215
13.70	14.10	15356.0	-2.279
13.80	15.10	15498.0	-2.480
13.92	16.10	15651.0	-2.693
13.98	17.10	15735.0	-2.810
14.13	18.10	15724.0	-2.794
14.22	19.10	15805.0	-2.906
14.28	20.10	15826.0	-2.935
14.38	21.10	15933.0	-3.080
14.50	22.10	15952.0	-3.106
14.55	23.10	16015.0	-3.192
14.63	24.10	16088.0	-3.290
14.67	25.10	16111.0	-3.321
14.72	26.10	16176.0	-3.408
14.77	27.10	16239.0	-3.491
14.95	27.80	16232.0	-3.482

HOLE 880 (TEKEGAKROK PT.)

Water depth 2.32m
Ice thickness 1.45 m
Drilled April 26, 1978
Depth below sea bed 28.0 m
Logged profile

ELSON LAGOON
HOLE 880
780504
08:00

BELDEN CABLE
L&N BRIDGE

TIME	DEPTH (M)	R (OHMS)	T (C
9.17	0.10	15120.0	-1.941
9.22	1.10	14995.0	-1.759
9.27	2.10	14911.0	-1.636
9.30	3.10	14823.0	-1.506
9.38	4.10	14750.0	-1.398
9.43	5.10	14750.0	-1.398
9.48	6.10	14798.0	-1.469
9.55	7.10	14865.0	-1.568
9.60	8.10	14950.0	-1.693
9.67	9.10	15049.0	-1.838
9.70	10.10	15197.0	-2.052
9.80	11.10	15292.0	-2.188
9.87	12.10	15382.0	-2.316
9.95	13.10	15417.0	-2.366
10.03	14.10	15480.0	-2.454
10.12	15.10	15582.0	-2.597
10.17	16.10	15675.0	-2.727
10.22	17.10	15747.0	-2.826
10.28	18.10	15784.0	-2.877
10.35	19.10	15846.0	-2.962
10.40	20.10	15882.0	-3.011
10.45	21.10	15955.0	-3.110
10.53	22.10	16002.0	-3.174
10.73	23.10	16052.0	-3.241
10.80	24.10	16104.0	-3.311
10.90	25.10	16143.0	-3.363
10.95	26.10	16187.0	-3.422
12.02	27.10	16243.0	-3.497
12.10	27.80	16261.0	-3.521

HOLE 880 (TEKEGAKROK PT.)

Water depth 2.32m
Ice thickness 1.45 m
Drilled April 26, 1978
Depth below sea bed 28.0 m
Logged profile

ELSON LAGOON
HOLE 880
780521
13:20

BELDEN CABLE
L&N BRIDGE

TIME	DEPTH (M)	R (OHMS)	T (C)
13.32	0.	15107.0	-1.922
13.43	0.10	15100.0	-1.912
13.50	0.60	15060.0	-1.854
13.55	1.10	15010.0	-1.781
13.62	2.10	14922.0	-1.652
13.70	3.10	14839.0	-1.530
13.77	4.10	14780.0	-1.442
13.85	5.10	14782.0	-1.445
13.90	6.10	14880.0	-1.591
13.98	7.10	14891.0	-1.607
14.03	8.10	14970.0	-1.723
14.08	9.10	15084.0	-1.889
14.17	10.10	15197.0	-2.052
14.25	11.10	15286.0	-2.180
14.30	12.10	15425.0	-2.377
14.35	13.10	15506.0	-2.491
14.42	14.10	15563.0	-2.571
14.53	15.10	15630.0	-2.664
14.58	16.10	15696.0	-2.756
14.63	17.10	15761.0	-2.845
14.70	18.10	15820.0	-2.926
14.75	19.10	15871.0	-2.996
14.80	20.10	15925.0	-3.070
14.85	21.10	15975.0	-3.137
14.92	22.10	16021.0	-3.200
14.97	23.10	16077.0	-3.275
15.02	24.10	16118.0	-3.330
15.07	25.10	16158.0	-3.384
15.12	26.10	16199.0	-3.438
15.15	27.10	16250.0	-3.506
15.20	27.80	16281.0	-3.547

HOLE 880 (TEKEGAKROK PT.)

Water depth 2.32m
Ice thickness 1.45 m
Drilled April 26, 1978
Depth below sea bed 28.0 m
Logged profile

ELSON LAGOON
HOLE 880
780427
12:00

BELDEN
L&N

CABLE
BRIDGE

TIME	DEPTH (M)	R (OHMS)	T (C
0.	0.	15107.0	-1.922
0.	0.10	15078.0	-1.880
0.	1.10	15000.0	-1.767
0.	2.10	14925.0	-1.657
0.	3.10	14843.0	-1.536
0.	4.10	14784.0	-1.448
0.	5.10	14788.0	-1.454
0.	6.10	14850.0	-1.546
0.	7.10	14898.0	-1.617
0.	8.10	14975.0	-1.730
0.	9.10	15075.0	-1.876
0.	10.10	15193.0	-2.046
0.	11.10	15283.0	-2.175
0.	12.10	15443.0	-2.402
0.	13.10	15527.0	-2.520
0.	14.10	15590.0	-2.609
0.	15.10	15649.0	-2.691
0.	16.10	15701.0	-2.763
0.	17.10	15763.0	-2.848
0.	18.10	15833.0	-2.944
0.	19.10	15880.0	-3.008
0.	20.10	15937.0	-3.086
0.	21.10	15979.0	-3.143
0.	22.10	16034.0	-3.217
0.	23.10	16085.0	-3.286
0.	24.10	16121.0	-3.334
0.	25.10	16166.0	-3.394
0.	26.10	16201.0	-3.441
0.	27.10	16251.0	-3.507
0.	27.80	16287.0	-3.555

HOLE 880 (TEKEGAKROK PT.)

Water depth 2.32 m
Ice thickness 1.45 m
Drilled April 26, 1978
Depth below sea bed 28.0 m
Equilibrium profile

ELSON LAGOON
HOLE 1189
780427
10:00

BRONX 136 CABLE
L&N BRIDGE

TIME	DEPTH (M)	R (OHMS)	T (C)
0.	0.	0.	-1.931
0.	0.50	0.	-1.896
0.	1.50	0.	-1.597
0.	2.50	0.	-1.454
0.	3.50	0.	-1.293
0.	4.50	0.	-1.189
0.	5.50	0.	-1.118
0.	6.50	0.	-1.101
0.	7.50	0.	-1.139
0.	8.50	0.	-1.195
0.	9.50	0.	-1.256
0.	10.50	0.	-1.321
0.	11.50	0.	-1.384
0.	12.50	0.	-1.452
0.	13.50	0.	-1.521
0.	14.50	0.	-1.592
0.	15.50	0.	-1.659
0.	16.50	0.	-1.715
0.	17.50	0.	-1.767
0.	18.50	0.	-1.827
0.	19.50	0.	-1.878
0.	20.50	0.	-1.923
0.	21.50	0.	-1.968
0.	22.50	0.	-2.015
0.	23.50	0.	-2.061
0.	24.50	0.	-2.106
0.	25.50	0.	-2.149
0.	26.50	0.	-2.205
0.	27.50	0.	-2.238
0.	28.50	0.	-2.285
0.	29.50	0.	-2.341
0.	30.50	0.	-2.411
0.	31.50	0.	-2.521
0.	32.50	0.	-2.605
0.	33.40	0.	-2.654

HOLE 1189 (TEKEGAKROK PT.)

Water depth 2.52 m
Ice thickness 1.50 m
Drilled April 27-28, 1978
Depth below seabed 34.2 m
Equilibrium profile

ELSON LAGOON
HOLE 1189
780521
10:16

BRONX 136 L&N — CABLE BRIDGE

TIME	DEPTH (M)	R (OHMS)	T (C)
10.38	0.	30160.0	-1.973
10.50	0.50	30000.0	-1.856
10.63	1.50	29630.0	-1.582
10.70	2.50	29453.0	-1.450
10.80	3.50	29232.0	-1.284
10.90	4.50	29096.0	-1.181
11.02	5.50	29004.0	-1.111
11.07	6.50	28982.0	-1.094
11.17	7.50	29037.0	-1.136
11.25	8.50	29119.0	-1.198
11.30	9.50	29199.0	-1.259
11.35	10.50	29286.0	-1.325
11.42	11.50	29367.0	-1.386
11.47	12.50	29458.0	-1.454
11.52	13.50	29550.0	-1.523
11.57	14.50	29645.0	-1.594
11.63	15.50	29735.0	-1.660
11.70	16.50	29810.0	-1.716
11.75	17.50	29881.0	-1.768
11.80	18.50	29959.0	-1.826
11.85	19.50	30021.0	-1.871
11.90	20.50	30089.0	-1.921
11.95	21.50	30150.0	-1.966
12.00	22.50	30215.0	-2.013
12.05	23.50	30275.0	-2.057
12.10	24.50	30340.0	-2.104
12.15	25.50	30398.0	-2.146
12.20	26.50	30465.0	-2.195
12.27	27.50	30521.0	-2.235
12.42	28.50	30589.0	-2.284
12.52	29.50	30669.0	-2.341
12.60	30.50	30770.0	-2.414
12.67	31.50	30900.0	-2.506
12.73	32.50	31030.0	-2.599
12.83	33.40	31115.0	-2.659

HOLE 1189 (TEKEGAKROK PT.)

Water depth 2.52 m
Ice thickness 1.50 m
Drilled April 27-28, 1978
Depth below seabed 34.2 m
Logged profile

ELSON LAGOON
HOLE 1189
780503
13:40

BRONX 136 L&N — CABLE BRIDGE

TIME	DEPTH (M)	R (OHMS)	T (C)
13.67	0.	30700.0	-2.364
13.87	0.50	29840.0	-1.738
14.02	1.50	29528.0	-1.506
14.10	2.50	29461.0	-1.456
14.22	3.50	29181.0	-1.245
14.30	4.50	29048.0	-1.145
14.40	5.50	28962.0	-1.079
14.48	6.50	28979.0	-1.092
14.53	7.50	29023.0	-1.125
14.58	8.50	29120.0	-1.199
14.65	9.50	29203.0	-1.262
14.68	10.50	29290.0	-1.328
14.73	11.50	29380.0	-1.395
14.78	12.50	29470.0	-1.463
14.85	13.50	29564.0	-1.533
14.92	14.50	29657.0	-1.603
14.95	15.50	29738.0	-1.663
15.00	16.50	29815.0	-1.720
15.05	17.50	29888.0	-1.774
15.10	18.50	29958.0	-1.825
15.15	19.50	30023.0	-1.873
15.23	20.50	30081.0	-1.915
15.27	21.50	30143.0	-1.961
15.30	22.50	30198.0	-2.001
15.37	23.50	30266.0	-2.050
15.42	24.50	30337.0	-2.102
15.47	25.50	30393.0	-2.143
15.55	26.50	30413.0	-2.157
15.63	27.50	30458.0	-2.190
15.75	28.50	30570.0	-2.270
15.87	29.50	30654.0	-2.331
15.93	30.50	30781.0	-2.422
16.03	31.50	30912.0	-2.515
16.00	32.50	31023.0	-2.594
16.00	33.40	31098.0	-2.647

HOLE 1189 (TEKEGAKROK PT.)

Water depth 2.52 m
Ice thickness 1.50 m
Drilled April 27-28, 1978
Depth below seabed 34.2 m
Logged profile

ELSON LAGOON
HOLE 1189
780501
08:12

BRONX 136 CABLE
L&N BRIDGE

TIME	DEPTH (M)	R (OHMS)	T (C)
8.20	0.	30102.0	-1.931
8.80	0.50	29715.0	-1.646
9.03	1.50	29488.0	-1.476
9.22	2.50	29359.0	-1.380
9.35	3.50	29176.0	-1.242
9.58	4.50	29047.0	-1.144
9.68	5.50	28960.0	-1.077
9.73	6.50	28962.0	-1.079
9.82	7.50	29022.0	-1.125
9.88	8.50	29128.0	-1.205
9.97	9.50	29212.0	-1.269
10.05	10.50	29301.0	-1.336
10.15	11.50	29380.0	-1.395
10.20	12.50	29471.0	-1.464
10.27	13.50	29566.0	-1.535
10.32	14.50	29660.0	-1.605
10.37	15.50	29741.0	-1.665
10.43	16.50	29814.0	-1.719
10.62	17.50	29886.0	-1.772
10.68	18.50	29955.0	-1.823
10.75	19.50	30014.0	-1.866
10.88	20.50	30080.0	-1.915
10.98	21.50	30137.0	-1.956
11.10	22.50	30209.0	-2.009
11.18	23.50	30270.0	-2.053
11.27	24.50	30339.0	-2.103
11.33	25.50	30385.0	-2.137
11.48	26.50	30382.0	-2.135
11.57	27.50	30441.0	-2.177
11.68	28.50	30566.0	-2.267
11.78	29.50	30647.0	-2.326
11.87	30.50	30779.0	-2.420
11.92	31.50	30880.0	-2.492
12.00	32.50	30986.0	-2.567
12.07	33.40	31102.0	-2.650

HOLE 1189 (TEKEGAKROK PT.)

Water depth 2.52 m
Ice thickness 1.50 m
Drilled April 27-28, 1978
Depth below seabed 34.2 m
Logged profile

PRUDHOE BAY
HOLE 9.5
780526
14:20

77-1A
L&N

CABLE
BRIDGE

TIME	DEPTH (M)	R (OHMS)	T (C)
14.50	0.	25104.0	-1.810
14.53	1.00	24982.0	-1.705
14.62	2.00	24881.0	-1.618
14.65	3.00	24787.0	-1.537
14.73	4.00	24723.0	-1.482
14.78	5.00	24677.0	-1.442
14.83	6.00	24654.0	-1.422
14.87	7.00	24659.0	-1.426
14.90	8.00	24666.0	-1.432
14.93	9.00	24711.0	-1.471
14.97	10.00	24743.0	-1.499
15.00	11.00	24747.0	-1.503
15.03	12.00	24751.0	-1.506
15.07	13.00	24759.0	-1.513
15.10	13.33	24764.0	-1.517

9.5 km HOLE

Water depth 6.9 m
Ice thickness 1.60 m
Driven May 23-25, 1978
Depth below seabed 25 m
Logged profile

PRUDHOE BAY
HOLE 9.5
780529
10:10

77-1A
L&N

CABLE
BRIDGE

TIME	DEPTH (M)	R (OHMS)	T (C)
10.27	0.	25113.0	-1.817
10.38	1.00	24995.0	-1.716
10.50	2.00	24898.0	-1.633
10.62	3.00	24799.0	-1.548
10.73	4.00	24733.0	-1.490
10.85	5.00	24691.0	-1.454
10.97	6.00	24670.0	-1.436
11.08	7.00	24669.0	-1.435
11.32	8.00	24679.0	-1.444
11.43	9.00	24718.0	-1.477
11.55	10.00	24738.0	-1.495
11.67	11.00	24748.0	-1.503
11.78	12.00	24764.0	-1.517
12.02	13.00	24775.0	-1.527
12.13	14.00	24788.0	-1.538
12.25	15.00	24797.0	-1.546
12.37	16.00	24814.0	-1.561
12.48	17.00	24825.0	-1.570
12.72	18.00	24830.0	-1.574
12.83	19.00	24836.0	-1.580
12.95	20.00	24845.0	-1.587
13.07	21.00	24852.0	-1.593
13.18	22.00	24864.0	-1.604
13.30	23.00	24877.0	-1.615
13.42	24.00	24889.0	-1.625
13.53	25.00	24900.0	-1.635
13.65	25.33	24900.0	-1.635

9.5 km HOLE

Water depth 6.9 m
Ice thickness 1.60 m
Driven May 23-25, 1978
Depth below seabed 25 m
Logged profile

PRUDHOE BAY
HOLE 9.5
780530
10:00

77-1A
L&N

CABLE
BRIDGE

TIME	DEPTH (M)	R (OHMS)	T (C)
10.50	0.	25103.0	-1.809
10.62	0.99	24994.0	-1.716
10.73	1.99	24904.0	-1.638
10.97	2.99	24807.0	-1.555
11.08	3.99	24743.0	-1.499
11.20	4.99	24695.0	-1.457
11.32	5.99	24672.0	-1.437
11.43	6.99	24668.0	-1.434
11.55	7.99	24677.0	-1.442
11.67	8.99	24713.0	-1.473
11.78	9.99	24736.0	-1.493
11.90	10.99	24752.0	-1.507
12.02	11.99	24760.0	-1.514
12.13	12.99	24769.0	-1.522
12.25	13.99	24784.0	-1.535
12.37	14.99	24798.0	-1.547
12.48	15.99	24806.0	-1.554
12.60	16.99	24811.0	-1.558
12.72	17.99	24821.0	-1.567
12.83	18.99	24833.0	-1.577
12.95	19.99	24846.0	-1.588
1.07	20.99	24857.0	-1.598
1.18	21.99	24864.0	-1.604
1.30	22.99	24872.0	-1.611
1.42	23.99	24881.0	-1.618
1.53	24.99	24896.0	-1.631
1.65	25.31	24896.0	-1.631

9.5 km HOLE

Water depth 6.9 m
Ice thickness 1.60 m
Driven May 23-25, 1978
Depth below seabed 25 m
Logged profile

PRUDHOE BAY
HOLE 9.5
780523
14:00

77-1A CABLE
L&N BRIDGE

TIME	DEPTH (M)	R (OHMS)	T (C)
0.	0.	0.	-1.812
0.	1.00	0.	-1.726
0.	2.00	0.	-1.652
0.	3.00	0.	-1.567
0.	4.00	0.	-1.510
0.	5.00	0.	-1.468
0.	6.00	0.	-1.450
0.	7.00	0.	-1.443
0.	8.00	0.	-1.454
0.	9.00	0.	-1.479
0.	10.00	0.	-1.489
0.	11.00	0.	-1.507
0.	12.00	0.	-1.526
0.	13.00	0.	-1.538

9.5 km HOLE

Water depth 6.9 m
Ice thickness 1.60 m
Driven May 23-25, 1978
Depth below seabed 25 m
Equilibrium profile

PRUDHOE BAY
HOLE SAG RIVER
780527
10:40

77-1A
L&N

CABLE
BRIDGE

TIME	DEPTH (M)	R (OHMS)	T (C)
0.	-0.70	25136.0	-1.837
11.72	0.30	25070.0	-1.781
11.78	1.30	24927.0	-1.658
11.87	2.30	24758.0	-1.512
11.92	3.30	24650.0	-1.418
11.97	4.30	24548.0	-1.329
12.00	5.30	24497.0	-1.284
12.05	6.30	24502.0	-1.289
12.10	7.30	24534.0	-1.317
12.15	8.30	24535.0	-1.318
12.20	9.30	24528.0	-1.312
12.25	10.30	24562.0	-1.341
12.30	11.30	24604.0	-1.378
12.35	12.30	24610.0	-1.383
12.40	13.30	24653.0	-1.421
12.45	14.30	24716.0	-1.476
12.50	15.30	24740.0	-1.497
12.55	16.30	24766.0	-1.519
12.60	17.30	24815.0	-1.561
12.65	18.30	24845.0	-1.587

SAG DELTA HOLE

Water depth 7.60 m
Ice thickness 1.71 m
Driven May 25-26, 1978
Depth below seabed 18.3 m
Logged profile

PRUDHOE BAY
HOLE SAG RIVER
780528
14:30

77-1A
L&N

CABLE
BRIDGE

TIME	DEPTH (M)	R (OHMS)	T (C)
14.50	0.00	25106.0	-1.811
14.83	0.30	25067.0	-1.778
14.90	1.30	24954.0	-1.681
14.97	2.30	24803.0	-1.551
15.03	3.30	24746.0	-1.502
15.10	4.30	24609.0	-1.383
15.17	5.30	24564.0	-1.343
15.23	6.30	24556.0	-1.336
15.30	7.30	24575.0	-1.353
15.37	8.30	24591.0	-1.367
15.43	9.30	24602.0	-1.376
15.50	10.30	24632.0	-1.403
15.57	11.30	24665.0	-1.431
15.63	12.30	24680.0	-1.444
15.70	13.30	24710.0	-1.470
15.77	14.30	24752.0	-1.507
15.83	15.30	24768.0	-1.521
15.90	16.30	24797.0	-1.546
15.97	17.30	24825.0	-1.570
16.03	18.30	24847.0	-1.589

SAG DELTA HOLE

Water depth 7.60 m
Ice thickness 1.71 m
Driven May 25-26, 1978
Depth below seabed 18.3 m
Logged profile

PRUDHOE BAY
HOLE SAG RIVER
780529
15:00

77-1A
L&N

CABLE
BRIDGE

TIME	DEPTH (M)	R (OHMS)	T (C)
15.00	0.	25106.0	-1.811
15.20	0.30	25092.0	-1.800
15.27	1.30	24981.0	-1.704
15.33	2.30	24820.0	-1.566
15.40	3.30	24725.0	-1.483
15.47	4.30	24628.0	-1.399
15.53	5.30	24591.0	-1.367
15.60	6.30	24577.0	-1.355
15.67	7.30	24594.0	-1.369
15.73	8.30	24609.0	-1.383
15.80	9.30	24625.0	-1.396
15.87	10.30	24656.0	-1.423
15.93	11.30	24681.0	-1.445
16.00	12.30	24704.0	-1.465
16.07	13.30	24732.0	-1.490
16.13	14.30	24763.0	-1.516
16.20	15.30	24785.0	-1.536
16.27	16.30	24805.0	-1.553
16.33	17.30	24830.0	-1.574
16.40	18.30	24847.0	-1.589

SAG DELTA HOLE

Water depth 7.60 m
Ice thickness 1.71 m
Driven May 25-26, 1978
Depth below seabed 18.3 m
Logged profile

PRUDHOE BAY
HOLE SAG RIVER
780526
00:00

77-1A
L&N

CABLE
BRIDGE

TIME	DEPTH (M)	R (OHMS)	T (C)
0.	0.	0.	-1.811
0.	0.30	0.	-1.810
0.	1.30	0.	-1.732
0.	2.30	0.	-1.603
0.	3.30	0.	-1.529
0.	4.30	0.	-1.449
0.	5.30	0.	-1.423
0.	6.30	0.	-1.400
0.	7.30	0.	-1.404
0.	8.30	0.	-1.429
0.	9.30	0.	-1.456
0.	10.30	0.	-1.481
0.	11.30	0.	-1.494
0.	12.30	0.	-1.523
0.	13.30	0.	-1.537
0.	14.30	0.	-1.545
0.	15.30	0.	-1.561
0.	16.30	0.	-1.577
0.	17.30	0.	-1.583
0.	18.30	0.	-1.591

SAG DELTA HOLE

Water depth 7.6 m
Ice thickness 1.71 m
Drive May 25-26, 1978
Depth below seabed 18.3 m
Equilibrium profile

PRUDHOE BAY
HOLE RDEER I+4.5N
780422
14:36

BRONX 136 CABLE
L&N BRIDGE

TIME	DEPTH (M)	R (OHMS)	T (C)
14.63	0.	30028.0	-1.877
14.67	0.20	30008.0	-1.862
14.70	0.70	29956.0	-1.824
14.73	1.20	29870.0	-1.760
14.77	1.70	29747.0	-1.669
14.83	2.20	29712.0	-1.643
14.87	2.70	29696.0	-1.632
14.90	3.20	29675.0	-1.616
14.93	3.70	29671.0	-1.613
14.97	4.20	29669.0	-1.611
15.00	4.70	29666.0	-1.609
15.03	5.20	29669.0	-1.611
15.07	5.70	29677.0	-1.617
15.10	6.20	29677.0	-1.617
15.13	6.70	29709.0	-1.641
15.17	7.20	29729.0	-1.656
15.20	7.70	29757.0	-1.677
15.23	8.20	29763.0	-1.681
15.27	8.70	29772.0	-1.688
15.30	9.20	29787.0	-1.699
15.33	9.54	29800.0	-1.709

OFFSHORE HOLE
5.9 km NORTH OF REINDEER ISLAND
(APRIL)

Water depth 17 m
Ice thickness 1.5 m
Drilled April 21, 1978
Depth below seabed 10 m
Logged profile

PRUDHOE BAY
HOLE RDEER I+4.5N
780526
09:45

77-1A
L&N

CABLE
BRIDGE

TIME	DEPTH (M)	R (OHMS)	T (C)
10.28	-0.30	25116.0	-1.820
10.35	0.20	25104.0	-1.810
10.43	0.70	25085.0	-1.794
10.53	1.20	25047.0	-1.761
10.58	1.70	25005.0	-1.725
10.65	2.20	24992.0	-1.714
10.70	2.70	24981.0	-1.704
10.78	3.20	24978.0	-1.702
10.82	3.70	24977.0	-1.701
10.90	4.20	24978.0	-1.702
10.93	4.70	24976.0	-1.700
10.98	5.20	24979.0	-1.703
11.02	5.70	24979.0	-1.703
11.07	6.20	24986.0	-1.709
11.13	6.70	24988.0	-1.710
11.17	7.20	24988.0	-1.710
11.22	7.70	24990.0	-1.712
11.28	8.20	24993.0	-1.715
11.32	8.70	24993.0	-1.715
11.33	9.20	24995.0	-1.716
11.40	9.70	24994.0	-1.716
11.43	10.20	24996.0	-1.717
11.63	10.50	24995.0	-1.716

OFFSHORE HOLE
5.9 km NORTH OF REINDEER ISLAND
(MAY)

Water depth 17.0 m
Ice thickness 1.5 m
Drilled May 22, 1978
Depth below seabed 11 m
Logged profile

PRUDHOE BAY
HOLE RDEER I+4.5N
780528
11:00

77-1A
L&N

CABLE
BRIDGE

TIME	DEPTH (M)	R (OHMS)	T (C)
11.00	0.	25111.0	-1.816
11.40	0.20	25112.0	-1.817
11.45	0.70	25092.0	-1.800
11.57	1.20	25061.0	-1.773
11.63	1.70	24994.0	-1.716
11.68	2.20	24986.0	-1.709
11.72	2.70	24980.0	-1.704
11.77	3.20	24971.0	-1.696
11.80	3.70	24971.0	-1.696
11.87	4.20	24972.0	-1.697
11.90	4.70	24973.0	-1.698
11.93	5.20	24967.0	-1.692
11.97	5.70	24975.0	-1.699
12.00	6.20	24976.0	-1.700
12.03	6.70	24981.0	-1.704
12.07	7.20	24985.0	-1.708
12.10	7.70	24989.0	-1.711
12.13	8.20	24992.0	-1.714
12.17	8.70	24990.0	-1.712
12.20	9.20	24995.0	-1.716
12.23	9.70	25000.0	-1.721
12.27	10.20	25002.0	-1.722
12.30	10.50	25002.0	-1.722

OFFSHORE HOLE
5.9 km NORTH OF REINDEER ISLAND
(MAY)

Water depth 17.0 m
Ice thickness 1.5 m
Drilled May 22, 1978
Depth below seabed 11 m
Logged profile

PRUDHOE BAY
HOLE RDEER I+4.5N
780529
16:40

77-1A
L&N

CABLE
BRIDGE

TIME	DEPTH (M)	R (OHMS)	T (C)
16.67	0.	25103.0	-1.809
16.83	0.20	25095.0	-1.802
16.87	0.70	25078.0	-1.788
16.90	1.20	25053.0	-1.766
16.93	1.70	25013.0	-1.732
16.97	2.20	24989.0	-1.711
17.00	2.70	24969.0	-1.694
17.03	3.20	24962.0	-1.688
17.07	3.70	24961.0	-1.687
17.10	4.20	24961.0	-1.687
17.13	4.70	24961.0	-1.687
17.17	5.20	24961.0	-1.687
17.20	5.70	24962.0	-1.688
17.23	6.20	24964.0	-1.690
17.27	6.70	24968.0	-1.693
17.30	7.20	24969.0	-1.694
17.33	7.70	24978.0	-1.702
17.37	8.20	24982.0	-1.705
17.40	8.70	24981.0	-1.704
17.43	9.20	24987.0	-1.710
17.47	9.70	24987.0	-1.710
17.50	10.20	24987.0	-1.710
17.53	10.50	24989.0	-1.711

OFFSHORE HOLE
5.9 km NORTH OF REINDEER ISLAND
(MAY)

Water depth 17.0 m
Ice thickness 1.5 m
Drilled May 22, 1978
Depth below seabed 11 m
Logged profile

REINDEER ISLAND
HOLE REIS31
780824
09:49

77-1A
L&N

CABLE
BRIDGE

TIME	DEPTH (M)	R (OHMS)	T (C)
9.93	0.40	21300.0	1.750
10.02	1.40	23275.0	-0.181
10.12	2.40	24486.0	-1.275
10.20	3.40	25512.0	-2.155
10.33	4.40	26137.0	-2.671
10.58	5.40	27997.0	-4.130
12.48	5.90	28584.0	-4.567
12.18	6.40	27500.0	-3.751
12.37	6.90	26440.0	-2.917
11.02	7.40	26671.0	-3.102
12.02	7.90	29925.0	-5.530
11.13	8.40	32569.0	-7.292
11.30	9.40	31974.0	-6.910
11.42	10.40	31657.0	-6.703
11.52	11.40	31268.0	-6.446
11.62	12.40	31706.0	-6.735
11.68	13.40	31353.0	-6.503
11.77	14.33	30799.0	-6.131

REINDEER ISLAND HOLE 3

Drilled August 19, 1978
Depth below ground level 20.0 m
Logged profile

REINDEER ISLAND
HOLE REIS32
780826
11:40

77-1A
L&N

CABLE
BRIDGE

TIME	DEPTH (M)	R (OHMS)	T (C)
11.85	0.40	15300.0	9.160
11.95	1.40	23578.0	-0.461
12.03	2.40	24454.0	-1.247
12.17	3.40	26053.0	-2.603
12.30	4.40	28155.0	-4.249
12.40	5.40	30419.0	-5.872
12.80	5.90	30680.0	-6.051
12.58	6.40	30356.0	-5.829
12.98	7.40	29581.0	-5.288
13.07	8.40	32952.0	-7.534
13.22	9.40	32759.0	-7.413
13.37	10.40	32292.0	-7.115
13.47	11.40	31841.0	-6.824
13.53	12.40	31867.0	-6.841
13.58	13.40	31460.0	-6.574
13.65	14.33	30865.0	-6.176

REINDEER ISLAND HOLE 3

Drilled August 19, 1978
Depth below ground level 28.0 m
Logged profile

REINDEER ISLAND
HOLE REIS33
781026
13:10

BRONX 136 CABLE
L&N BRIDGE

TIME	DEPTH (M)	R (OHMS)	T (C)
13.33	1.40	35100.0	-5.291
13.50	2.40	30725.0	-2.382
13.67	3.40	34217.0	-4.737
13.80	4.40	36512.0	-6.146
13.95	5.40	38474.0	-7.276
14.08	6.40	39861.0	-8.037
14.22	7.40	40643.0	-8.454
14.35	8.40	40680.0	-8.474
14.63	9.40	40222.0	-8.231
14.77	10.40	39591.0	-7.891
14.93	11.40	38831.0	-7.475
15.12	12.40	38137.0	-7.086
15.23	13.40	37540.0	-6.746
15.38	14.40	36795.0	-6.313
15.52	15.40	35963.0	-5.818
15.65	16.40	35191.0	-5.347
15.75	17.40	34494.0	-4.912
16.07	18.40	33866.0	-4.512

REINDEER ISLAND HOLE 3

Drilled August 19, 1978
Depth below ground level 28.0 m
Logged profile

COTTLE ISLAND
HOLE COTTL2
781026
11:25

BRONX 136 CABLE
L&N BRIDGE

TIME	DEPTH (M)	R (OHMS)	T (C)
11.70	1.00	32164.0	-3.386
11.98	2.00	31856.0	-3.175
12.12	3.00	34117.0	-4.673
12.27	4.00	35700.0	-5.658
12.38	5.00	37160.0	-6.526
12.50	5.48	37815.0	-6.903

COTTLE ISLAND HOLE

Drilled August 24, 1978
Depth below ground level 5.15 m
Logged profile

COTTLE ISLAND
HOLE COTTL1
780826
15:01

77-1A CABLE
L&N BRIDGE

TIME	DEPTH (M)	R (OHMS)	T (C)
0.	0.50	22299.0	0.749
0.	1.00	24550.0	-1.331
0.	2.00	24554.0	-1.334
0.	3.00	24799.0	-1.548
0.	4.00	24465.0	-1.256
0.	5.00	29109.0	-4.950
0.	5.48	31013.0	-6.276

COTTLE ISLAND HOLE

Drilled August 24, 1978
Depth below ground level 5.15 m
Logged profile

APPENDIX II

Harrison, W.D. and T.E. Osterkamp (1978). "Heat and Mass Transport Processes in Subsea Permafrost; An Analysis of Molecular Diffusion and Its Consequences," J. Geophysical Research, pp. 4707-4712.

ANNUAL REPORT

Contract Number: 03-5-022-55
Research Unit Number: 265
Reporting Period: 4/1/78-3/31/79
Number of Pages

DEVELOPMENT OF HARDWARE AND PROCEDURES FOR IN-SITU MEASUREMENT OF CREEP IN SEA ICE

Lewis H. Shapro

Geophysical Institute
University of Alaska
Fairbanks, Alaska 99701

Contributing Scientist:

Earl R. Hoskins

Department of Geophysics
Texas A & M University
College Station, Texas

May 1979

I. SUMMARY

The primary objectives of this project are to develop and test the procedures and hardware required for in-situ measurement of the mechanical properties and strength of sea ice, and to conduct a program of such measurements. The properties of primary interest are the strength and elastic and viscoelastic constants in uniaxial and biaxial compression, but the strength in shear and tension has also been considered. In addition, the results of the extensive series of laboratory tests done by Peyton (1966) are also being re-evaluated. The intention is to compare the results the laboratory and in-situ tests in order to determine the degree with which laboratory results on small samples are representative of those from larger samples in the field.

During the past year, a summary of the test techniques was presented at the 'Energy Technology Conference', sponsored by the American Society of Mechanical Engineers in Houston, Texas, November 5-9, 1978. A modified version of that paper has been accepted for publication in the Journal of Energy Resources Technology, and that paper is included as part of this report.

During the past year, a second task has been added to this project in which historical information regarding ice conditions in Alaskan coastal waters is being sought through interviews with local residents of the area. As a pilot project, a series of 8 interviews were conducted and the results synthesized for inclusion here. Results of interest include a report of major movement of part of the landfast ice sheet off the north coast of Alaska during the mid-winter period, and descriptions of ice overrides at Barrow and Cape Halkett.

Finally, the field program is in progress, and it is anticipated that in excess of 100 tests will be completed by its conclusion. Preliminary results are described in the third part of this report.

II. INTRODUCTION

A. General Nature, Scope and Objectives

The problem of translating results from laboratory tests to field conditions is well known in many branches of science, and forms an important aspect of studies of the mechanical properties of sea ice. It is difficult in the laboratory to simulate the effects of temperature and salinity gradients, continuous variations in grain size and ice fabric, and the presence of inhomogeneities on scales larger than laboratory samples. Further, mechanical properties of the ice can change during the processes of removal from the ice sheet, storage, and transport. Thus, a program is needed to determine the mechanical properties of the ice using large, relatively undisturbed samples, for comparison and verification of laboratory results.

The objective of this project is to develop the techniques, procedures and equipment necessary to measure as many as possible of the mechanical properties of the ice by in-situ methods; to utilize these procedures to conduct a program to obtain the relevant measurements; and to compare these results with published results of laboratory tests. In conjunction with these studies, it has also been necessary to develop the required mathematical description of the deformational properties of sea ice in order for the results of the experimental program to be interpreted.

B. Relevance to Problems of Petroleum Development

Any permanent or semi-permanent structure located off the Arctic Coast of Alaska must contend with the hazard that sea ice presents to its stability. The extent of this hazard depends on three basic parameters. First, the strength of the structure itself, with respect to its ability to withstand forces of a given magnitude. Second, the geometry of the interaction between the structure and the surrounding ice, including the state of bonding between the two and, finally, the strength of the ice, which determines the maximum force that the ice can sustain in the mode of failure which the structure is designed to induce. The first two of these parameters are determined largely by the third, the strength of the ice, and it is to this problem that the project is directed.

III. CURRENT STATE OF KNOWLEDGE

Weeks and Assur (1967) reviewed the state of knowledge regarding the mechanical properties of sea ice, and that work has been made current by Schwarz and Weeks (1977). The results of these reviews can be summarized by noting that major uncertainties of the strength of sea ice exist with respect to the effect of stress- or strain-rate, sample size, and loading direction relative to the dominant crystal orientation for all failure modes. Further, the effect of confining pressure has not been investigated, despite its importance for may applied problems.

A more complete review of previous work on the creep of sea ice has been reported in previous annual reports of this project.

IV. STUDY AREA

As in past years, the field program is being conducted in the landfast ice sheet at the Naval Arctic Research Laboratory at Barrow, Alaska.

V. SOURCES, METHODS AND RATIONALE OF DATA COLLECTION

The selection of tests to be run depends upon two factors. First, tests are chosen to fill obvious data gaps, as is illustrated by the tests on multi-year ice and oriented samples described in the last section of this report. Second, the testing program reflects progress made in the mathematical description of the deformational process as described in previous annual reports of this project.

A complete description of the test methods is given elsewhere in this report.

IN-SITU MEASUREMENT OF THE MECHANICAL PROPERTIES OF SEA ICE

by

Lewis H. Shapiro
Geophysical Institute
University of Alaska
Fairbanks, Alaska 99701

Earl R. Hoskins
Department of Geophysics
Texas A & M University
College Station, Texas 77843

Richard D. Nelson
Dynasearch Engineering
207 Washburn St.
Capitola, California 95010

Ronald C. Metzner
Geophysical Institute
University of Alaska
Fairbanks, Alaska 99701

March 1979

ABSTRACT

The objective of this report is to describe techniques for conducting measurements of several of the mechanical properties of sea ice by in-situ methods. The tests described all involve the use of flatjacks of various shapes for supplying a known load into the ice. The geometry of the sample being tested is defined by introducing internal boundaries into the ice sheet by cutting slots or installing layers of plastic film. The resulting deformation of the ice is measured by strain gauges embedded in the test sample or by LVDT's or linear potentiometers mounted on pegs which, in turn, are frozen to some depth in the sample. Test procedures for conducting uniaxial and biaxial compression tests, indirect tension tests and a simulated direct shear test are described. These yield information on Young's modulus, Poisson's ratio, creep properties, and strength under various loading conditions.

INTRODUCTION

The problem of translating the results of laboratory tests of the mechanical properties of natural materials into field applications is well known and is no less acute for the case of sea ice than for other materials. In its natural state, sea ice occurs as an ice sheet which, in the offshore areas of Alaska, may reach a thickness of about 2 meters by May of each year. Within this vertical distance grain size ranges from dimensions of a few milimeters at the surface to several centimeters at the base, with a tendency to strong preferred orientation of grains by alignment of c-axes in the horizontal plane over large areas (1, 2). Superimposed over this fabric are both horizontal and vertical variations in salinity of the ice, and a temperature gradient reflecting temperature differences which may be in excess of 40°C between the top and bottom of the ice sheet at various times during the winter. Further, the character of an ice sample collected for laboratory study may change during removal, transport and storage through loss of brine and sublimation.

Assuming that the difficulties associated with sample collection can be minimized by proper handling of the specimens, the problem still remains of devising and conducting an appropriate series of tests on small, laboratory samples, through which the properties of the entire ice sheet thickness can be deduced. Hence, there is a need for the development of methods of testing large samples in-situ. For vertical loading, which places the ice sheet into a state of bending, suitable large scale in-situ tests can be devised. The problem is more difficult for the case of in-plane loading of the ice sheet, although large scale compression tests have been run (3, 4).

The objective of this report is to describe a series of in-plane loading tests through which some of the difficulties noted above may be circumvented. To date, the tests have been run only on moderate sized samples because of limitations of manpower and equipment, but in principle there is no reason why similar tests could not be run on samples up to the full thickness of the ice sheet.

The tests are referred to as in-situ tests, although it is obviously necessary to disturb the ice in some manner in order to prepare specimens for testing. In particular, some brine drainage is inevitable as the result of drilling holes or making chain saw cuts in the ice, and in one test it is necessary to remove the test sample from the ice sheet and replace it with a layer of polyethylene film at its base. This clearly restricts further movement of the brines through the ice sheet. However, test samples are always permitted to return to temperature equilibrium before testing, so that tests are conducted at the ambient temperature gradient of the ice sheet.

The approach used in all of the tests is similar. Flatjacks are installed in the ice and expanded to provide a known load. The geometry of the resulting stress field is controlled by creating internal boundaries in the ice sheet using chain saw cuts which serve to define the geometry of the test samples. Strain sensors are embedded in the sample or attached to its surface to determine response to the applied loads. The temperature profile of the ice is monitored continuously and samples are collected from the specimen for salinity measurements. In addition, thin sections are taken before testing to determine the fabric of the sample.

EXPERIMENTAL TECHNIQUES

Loading System

Stresses are introduced into the ice sheet using flatjacks. These are simple devices and inexpensive to construct, consisting only of an envelope of thin, sheet steel (or other suitable material) welded together along the edges. Two nipples of steel tubing are attached to one edge for introduction of a loading fluid and for attachment of a pressure transducer (Figure 1). The load is applied by pumping the fluid into the envelope. Note that the properties of the fluid are not important, although of course, it must not freeze. To date, in all of our experiments pressure has been supplied by either diesel fuel loaded through a hand pump, or by high pressure nitrogen gas through a pressure regulator.

When under internal pressure, the flatjacks expand transmitting a force to the surrounding ice. If the expansion were uniform, and if the contact area between the flatjack and the ice remained constant, then the total force transmitted would simply be the internal pressure times the flatjack area. For the tests conducted to date, the strain at failure has been sufficiently small that only minimal expansion of the flatjacks has been required, so that the assumption of constant contact area between the flatjacks and the ice appears justified. However, it is known that the efficiency with which a flatjack transmits a force is dependent upon the ratio of flatjack area to edge length (5, 6). In the absence of a compression testing machine, an in-situ test was devised to provide

an approximate measure of the efficiency of the 30 x 30 cm flatjacks used in the uniaxial and biaxial compression tests conducted in this program.

The experimental procedure is illustrated in Figure 2. A block of ice 30 x 32 x 60 cm was prepared as if for a uniaxial test (as described below) with a double layer of polyethylene sheeting at its base and a 30 x 30 cm steel flatjack at each end. A 35 x 35 cm copper flatjack was then installed in a chain saw cut parallel to, and midway between the steel flatjacks, with its top edge at the surface of the ice. Chain saw cuts were then made to define the sides of the block as shown in Figure 2, thus forming two blocks, 30 x 30 x 32 cm, which separate the copper flatjack from the steel flatjacks. The copper flatjack was then expanded with diesel oil, sealed, and the pressure allowed to relax back to near zero by creep of the ice around the flatjack. These preparations thus leave the full surface area of the steel flatjacks in contact with the test block, while most of the edge area of the copper flatjack (with the exception of the edge at the surface) is outside of the test block, but confined in the surrounding ice. In its expanded condition, the copper flatjack then acts as a pressure sensor to changes in the load transmitted by the steel flatjacks.

The steel flatjacks were loaded at rates of about 14 kPa/sec (2 psi/sec) and the changes in the internal pressure of the copper flatjack was recorded. The results are shown in Figure 3, in which the data points were acquired at ten second intervals so that the loading rates can be determined.

Over the linear portions of the curves the slopes average 0.63. At the end of each loading cycle, the pressure in the steel flatjacks was held constant during which time, the pressure in the copper flatjack drifted down. This may have been in response to gradual closure of the copper flatjack as the fluid was squeezed towards the margins outside of the loaded surface. Tensile failure of the ice was noted at the tips of the copper flatjack.

The efficiency, 'e' of the flatjacks can be calculated from the equation

$$e\ P_s\ A_s = P_c\ A_c$$

where P_s and P_c are the internal pressures of the steel and copper flatjacks, A_s is the area of the steel flatjacks (30 x 30 cm), and A_c is the area of the loaded ice surface in contact with the copper flatjack (30 x 32 cm). Using the value $P_c = 0.63\ P_s$, 'e' is found to be 67% which is in agreement with that determined in (5) for flatjacks of this size and internal pressure.

This calibration procedure is approximate only, because factors such as the membrane stresses in the copper flatjack, edge effects, and the influence of the reaction forces around the edges of the copper flatjack, (where confined in the surrounding ice) are not considered. However, the experiment can be taken as implying that the application of flatjacks in this type of program does not cause excessive deviations from efficiencies which have been determined in the references cited above.

Flatjacks are limited in the extent to which they can expand and still maintain sufficiently flat faces so that the stress field in the loaded volume of the ice does not become unduly distorted. The problem may be enhanced in sea ice because of the gradients of mechanical properties. To date, we have not attempted to quantify this effect. However, examination of the flatjacks which have been used in tests indicates that the distortion present arises primarily during failure of the ice when rapid expansion of the flatjacks occurs. In addition, slow loading tests in ice near its melting temperature tend to produce overexpansion of the edge of the flatjack at the surface of the ice, due to rapid creep at the unconfined surface. With these exceptions the expansion of the flatjacks appears to be even, except at the edges. Note that for the sample sizes tested to date, the expansion of the flatjacks required to produce failure has been small (generally less than 1 cm).

Another matter of concern is the effect on the temperature profile of the ice of introducing a flatjack into the ice sheet. In particular, it is important to determine the distance from the flatjack to which the ambient profile can be disturbed. To examine this, a simple experiment was performed (8), which showed that at a distance of 8 cm from a flatjack, the disturbance to the temperature profile disappears within 24 hours of installation of the flatjack. The experiment was performed during a period when the ambient air temperature was about -15°C, and has not been repeated for other temperatures.

The effect of chain saw cuts on the temperature was examined by cutting a slit 60 cm long and 35 cm deep, centered at a distance of 7 cm from a thermistor string which had previously been frozen into the ice and allowed to come to equilibrium with the ambient ice temperatures. The string consisted of two thermistors, one at 10 cm, the second at 23 cm. Measurements of the temperatures were then made over a 24 hour period, during which time neither thermistor varied by more than 1°C. The slit was then widened to 15 cm, and the temperatures were measured over the following 12 hours. In this case, the thermistor at 10 cm showed a variation of about 1°C, while that at 23 cm cooled by 2°C. Ambient air temperature at the time of the experiment were in the range of -24°C to -28°C. In general, tests are conducted within an hour of the time the chain saw cuts are made. Thus, the experiment described above suggests that the effect of these cuts on the temperature of the test specimen are minimal.

In most of the experiments to date, the load has been applied with nitrogen gas. For creep tests, a pressure regulator has been used to maintain constant pressure in the flatjacks, and has proved to be adequate to within a few percent of the desired load. Constant loading rate tests have also been run using the pressure regulator to control the rate of application of the load. In this case, the operator simply controls the flow of the gas manually by watching the time and pressure and adjusting the regulator accordingly. Again, rates that are accurate to within a few percent can easily be achieved in this manner. Finally, a ball valve has been used to release the

gas quickly from an accumulator loaded to some desired pressure when creep-rupture tests are run at pressures which are anticipated to cause failure of the ice sample in a relatively short time. In this case, the time required to bring the flatjacks to the desired pressure by gradual release of gas through a pressure regulator would be a significant part of the total test time. In addition, tests at extreme loading rates can also be run in this manner by pressurizing the accumulator sufficiently high that failure of the ice is assured. Loading rates of about 52 MPa/sec (approximately 7,500 psi/sec.) have been reached in this manner.

In summary, flatjacks provide a relatively inexpensive and efficient method of introducing controlled stresses into an ice sheet. The details of installing them for specific tests are given below.

Deformation Measurements

The measurement of strain presents particular problems because virtually any technique used, other than simply attaching a strain sensitive instrument to the surface of the ice, must result in disturbance to the sample. In addition, because of the inhomogeneity of the ice resulting from both the structure and the temperature gradient, it is often difficult to interpret the results of such measurements.

It has not been possible to use the method of attaching a strain measuring device to the ice surface, because samples tend to bulge when loaded. Thus, a strain gauge or extensomenter oriented parallel to the loading direction often indicates tensile strain after even short durations of compressive loading at low stress.

To overcome this, a procedure was developed for installing strain gauges directly into the ice sheet, as was previously done by Vaudrey (9). The size of the samples to be tested dictated that relatively small gauges be used to minimize the disturbed volume of the ice. Accordingly, 2.5 cm and 1.25 cm strain gauges have been employed. These gauges are prepared as for any application, except that particular care must be taken in waterproofing and sealing because of the presence of concentrated brines in the ice. Epoxy sealants have been most successful.

A small cylinder of sea ice chips frozen together with water of a salinity of 6 parts per thousand is prepared, and the sealed strain gauge is then frozen to one end. The cylinder is then extended to include the gauge, forming a "strain cell". The cell is placed in a hole drilled in the sample block, with the strain gauge aligned in the desired direction. Water is added and allowed to freeze and return to thermal equilibrium with the test block.

The use of small strain gauges for measurements in a coarse, crystalline material such as sea ice introduces the possibility that the gauge may sense the strain of only a few grains and thus does not provide information on the average strain of the sample. However, by preparing a strain cell in the manner described, the gauge is placed in contact with many smaller grains, while the cell represents an inclusion of a relatively homogeneous material of properties similar to those of normal sea ice. Thus, the cell should sense the strain of the surrounding ice and average it through the small grains so that, in effect, the gauge should sense an average strain.

There are two obvious problems to be considered regarding the use of the strain cells. The first is the question of the adherence between the strain gauges and the ice. Preliminary experiments indicate that the gauges respond instantly to changes in applied loads, and recover to zero strain when loaded and unloaded rapidly. These observations support the conclusion that the gauges do indeed bond firmly to the ice. The second is the problem of determining the degree to which measured strain represents the true strain in the sample. This depends upon the difference in modulii between the strain cell and the surrounding ice. No attempt was made to resolve this, because of a decision not to use the strain cells for actual measurements during the present program. Instead, the method described below has been used.

The disadvantages to the use of strain gauges are in the time required for preparation and waterproofing, for preparation of the strain cells, and for setting gauges into the ice. In addition, care must be exercised to avoid trapping air bubbles in the ice both in the strain cell, and in the column of ice fragments used to fill the hole in the sample. The bubbles cause stress concentrations which can lead to premature failure of the ice around the strain cell.

A second method for measuring strain involves the use of linear potentiometers or LVDT's attached to pegs frozen into the ice. To measure the axial strain in a uniaxial test, two pegs are placed on the center line of the sample, and spaced so that the displacement between them is measured over the middle 1/3 of the sample (20 cm of the 60 cm samples used to date). Displacements are measured at two

heights on the pegs so that corrections can be made for rotation of the pegs due to bulging of the surface of the sample. The strain at any depth can be calculated from the resulting data. Note that a similar pair of pegs can be set along a transverse line on the sample for measurements of lateral strain.

Preliminary experiments were required to determine an appropriate depth for insertion of the pegs. For the 30 cm thick samples tested, freezing the pegs to a depth of 20 cm caused an increase in strength of 10% to 20% over tests on similar samples with no pegs. However, samples with pegs frozen to depths of 10-12 cm gave the same results as those with no pegs. These tests were conducted at a loading rate of 7 kPa/sec (1 psi/sec) which tends to induce failure by the formation of numerous small cracks of dominately horizontal orientation. These cracks amplify the vertical displacement of the sample surface, which the strength of the bond between the ice and the pegs tends to resist. Apparently, the effect is enhanced when the pegs extend below the neutral axis, accounting for the relatively large increase in strength observed.

For rapid loading, in which failure occurs in shear along a single vertical crack extending between opposite corners of the test block, the pegs have no apparent effect. In most cases, the crack passes cleanly between the pegs, as if they were not present.

The advantage of this approach to strain measurements is in the ease of field set-up when compared to the time required for preparing strain gauges. The results of strain measurements using this procedure

appear to be satisfactory, but the pegs do not always return to their original position after rapid loading and unloading at low stresses. Residual strains, however, are generally small compared to the strain reached during tests taken to failure or long creep tests.

TEST PROCEDURES

Uniaxial and Biaxial Compression Tests

Uniaxial compression tests have been conducted on specimens in two geometries; triangular prisms and rectangular prisms. In the former, triangular flatjacks are installed in the ice as shown in Figure 4. After freezing, chain saw cuts are made connecting the ends of the flatjacks and dipping into the ice sheet parallel to the edges of the jacks. This isolates a triangular prism of ice attached to the ice sheet only through the flatjacks at the ends of the sample. The test is thus relatively easy to install, but it can be difficult to control the angle of the chain saw cuts to assure a uniform test speciman with straight sides.

The rectangular prisms are prepared by removing a block of ice from the ice sheet and trimming to the desired size. Water is poured into the resulting hole and allowed to freeze to make a smooth bottom surface at a depth equal to the thickness of the sample. A double layer of polyethylene sheeting is then placed at the base of the hole and the block is replaced. The polyethylene sheeting provides a boundary between the sample and the remainder of the ice sheet across which only minimal shear stress can be transmitted. Flatjacks are installed at the ends of the blocks for uniaxial tests, while for biaxial tests, a second pair of flatjacks

is installed along the sides of the block, to be loaded through an independent system. In both set-ups fresh water is added to freeze the blocks and flatjacks together, in addition sufficient time is allowed for the sample to return to temperature equilibrium before testing. Note that the final step in preparing an uniaxial test is that of cutting loose the unbound sides of the sample leaving a clearance of about 1 cm from the edges of the flatjacks, to form the rectangular prism. A typical arrangement for a biaxial test is shown in Figure 5.

Figure 6 shows the results of a three-stage creep test under biaxial loading. Confining pressure was maintained at 0.21 MPa (30 psi) and changes in pressure of the flatjacks providing the axial pressure were accomplished within about 10 seconds. Two strain gauges were embedded in the sample for this test, one parallel to the axial (loading) direction, and one normal to it. Only the results from the former gauge are shown in Figure 6. Note that the asymptote to the recovery segment of the curve is within a few parts per million of the total strain accumulated in the segments of the creep curve. The initial elastic response to each change of load is indicated in Figure 7, in which data from the strain gauge oriented transverse to the axial load are also included. The recovery of elastic strain was virtually complete for both gauges.

Uniaxial and biaxial tests can be run at constant pressures for creep or creep-rupture tests, or at controlled loading rates for tests of strength as a function of stress rate.

Direct Shear Test

Flatjacks can also be used to simulate a test similar to that of a standard "shear box" test. The configuration used is shown in Figure 8.

The test consists simply of loading the flatjack until failure occurs at the base of the block. The "shear strength" is then calculated assuming the stress to be uniform across the failure plane. Thus, if the dimensions of the flatjack are 'a' and 'b', and the pressure at failure is 'P', then the total force is Pab. This is assumed to equal τcb, where τ is the shear strength, and 'c' and 'b' are the dimensions of the block outlined by the reliefs slots. In the tests to date, 'c' has been set equal to 'b', so that $\tau = (a/c)P$. Note that a criterion of validity of the test is that the results should agree for different values of the ratio a/c. To date, tests have been run only at ratios of 1/2 and 1/3 and the values of τ obtained are in reasonable agreement.

The geometry of the stress distribution in the test block has been examined using a 2-dimensional plane stress finite element analysis, and the results compared to similar calculations for an idealized "punch test" with uniform loading. These are shown in Figure 9. The calculations indicate that the first crack to form during the test can be expected to be a tension crack propagating downward under the flatjack into the ice sheet. Subsequently, the stress configuration near the flatjack closely resembles that of the punch test as shown in Figure 9. The vertical crack can be simulated at the time of the test set-up, by deepening the chain saw cut made to receive the flatjack and installing a piece of stiff cardboard wrapped in polyethylene sheeting in the slot below the flatjack. This provides a very low tensile strength bond assuring that the first crack will propagate in this direction. Examination of the fracture zone formed during these tests

shows it to be generally thin, involving only 2-4 centimeters of the total 15 cm thickness of the blocks tested to date. Within this zone, the ice tends to shatter into flat plates about 1 cm thick with linear dimensions of several centimeters. The base of the hole typically shows irregular "step" asperities oriented transverse to the direction of motion of the failed block, with the riser of the step facing the loading direction (Figure 10). Flat cracks extend into the ice from the base of each step, as evidenced by a distinct gray color of the ice in these areas. The failure mode represented in these tests is thus similar to that of failure in uniaxial compression tests on ice or rocks.

It should be noted that attempts to conduct this test using square flatjacks invariably resulted in tensile failure at the base of the speciman. Thus, cubical blocks simulate the bending of a thick, cantilever beam under a uniform distributed load. Tests in which the width of the flatjack was at least twice the depth however, always failed in the manner described above.

Brazil Test (Indirect Tension Test)

The possibility of running indirect tension tests in the ice sheet has also been examined, but only two tests have been performed to date. In the first of these, a circle of 59 cm in diameter was outlined on the surface, and two 15 x 60 cm flatjacks were installed on opposite ends of a diameter of the cylinder with their 15 cm edges at the ice surface. A chain saw cut 75 cm deep was then made along the circumference of the circle, and the flatjacks were then loaded until failure occurred. The cylinder failed with a single crack along the diameter, and secondary cracking near the flatjacks.

Curved flatjacks were used in the second test, in order to provide a load over 15° arcs of the tests speciman rather than along a single line. These were prepared by flattening two 46 cm lengths of 7.6 cm diameter copper tubing and then bending them to the radius of curvature of the test speciman. The ends were then silver soldered and a nipple for loading installed at one end. The test was set up and run as described above, but in this case, failure occurred as a single crack, with no secondary cracking near the flatjacks (Figure 11). Further, when sectioned with a chain saw, the test speciman separated into two blocks along that crack, with no evidence of splaying of the crack as it extended downward (Figure 12). It thus appears that plane strain conditions are achieved over a sufficient length of the sample to provide an adequate test, but further tests are required to assess repeatability.

SUMMARY

The physical properties of sea ice, and its mode of occurrence in nature dictate that determinations of the mechanical properties of the ice must be conducted in-situ, as well as in the laboratory. In-situ tests involving vertical loading of the ice sheet have been conducted by several investigators, but techniques involving in-plane loading of the ice sheet have had more limited use. The application of flatjacks to induce stress fields in the plane of the ice sheet provides a means of conducting such tests. To date tests have been run in uniaxial and biaxial compression, indirect tension, and direct shear in a horizontal plane. Similar tests in uniaxial tension and shear in a vertical plane have been devised but have not yet been tried in the field. In addition, the tests described have been run on relatively small samples, but with some additional development they could be extended to involve the full thickness of the ice sheet.

REFERENCES CITED

(1) Weeks, W. F., and Gow, A. J., "Preferred Crystal Orientations in the Fast Ice Along the Margins of the Arctic Ocean," USA CRREL Report 78-13, 1978.

(2) Weeks, W. F., and Assur, A., "The Mechanical Properties of Sea Ice," USA CRREL, Cold Regions Science and Eng., Part II, Sect. C3, pp. 6-11, 1967.

(3) Croasdale, K. R., Morgenstern, N. R., and Nuttall, J. B., "Indentation Tests to Investigate Ice Pressures on Vertical Piers," Journal of Glaciology, Vol. 19, No. 81, pp. 301-312, 1977.

(4) Croasdale, K. R., "Crushing Strength of Arctic Ice," in Reed, J. C., and Sater, J. E., eds., The Coast and Shelf of the Beaufort Sea. Proceedings of a Symposium on Beaufort Sea Coast and Shelf Research. Arlington, Virginia, Arctic Institute of North America, pp. 377-399, 1974.

(5) Deklotz, E. J., and Boisen, B. P., "Development of Equipment for Determining Deformation Modulus on In-Situ Stress by Means of Large Flatjacks;" in Determination of the In-Situ Modulus of Deformation of Rock. ASTM STP 477, American Society for Testing and Materials, pp. 117-125, 1970.

(6) Pratt, H. R., Black, A. D., Brown, W. S., and Brace, W. F., "A New Technique for Determining the Deformation and Frictional Characteristics of In-Situ Rock," in Field Testing and Instrumentation of Rock, ASTM STP 554, American Society for Testing and Materials, pp. 3-19, 1974.

(7) Shapiro, L. H., and Hoskins, E. R., "The Use of Flatjacks for the In-Situ Determination of the Mechanical Properties of Sea Ice," in Burrell, D. C., and Hood, D. W., eds. "Proceedings of the Third International Conference on Port and Ocean Engineering Under Arctic Conditions," Vol. 1, pp. 427-436, 1976.

(8) Vaudrey, K. D., "Development of a Sea Ice Strain Transducer," Naval Civil Engineering Command, Technical Note N-1310, 1973.

FIGURE CAPTIONS

Figure 1. 45 x 45 cm square flatjacks.

Figure 2. Plan view and cross-section of flatjack calibration installation.

Figure 3. Results of calibration experiment. Flatjack #1 is the steel flatjack pair; flatjack #2 is the copper flatjack.

Figure 4. Set-up for uniaxial compression test using triangular flatjacks.

Figure 5. Biaxial compression test installation. Sample dimensions are 30 x 30 x 60 cm. The two linear potentiometers are at heights of about 4 cm and 20 cm.

Figure 6. Strain-time data for axial strain gauge of a three-stage creep-recovery test, under confining pressure.

Figure 7. Stress-strain curve for rapid load changes on both axial and transverse strain gauges of the test shown in Figure 6.

Figure 8. Set-up for direct shear test.

Figure 9. Results of finite element analysis of punch test (solid line) and direct shear test (dashed line). Calculations refer to a surface just below the dashed lines on the diagrams. The slot below the flatjack represents either the first crack or the prepared crack as described in the text.

Figure 10. Results of a shear test with load applied from lower left to upper right. Cracks in the surface below the block are indicated by light colored bands. Note size and shape of fragments broken from the base of the test block at left.

Figure 11. Results of an indirect tension test using curved flatjacks. Failure occurred along a single crack shown as a faint line across the surface of the test block connecting the flatjacks.

Figure 12. Test block of Figure 11 after sectioning the crack appears as a thin, vertical line in the center of the block.

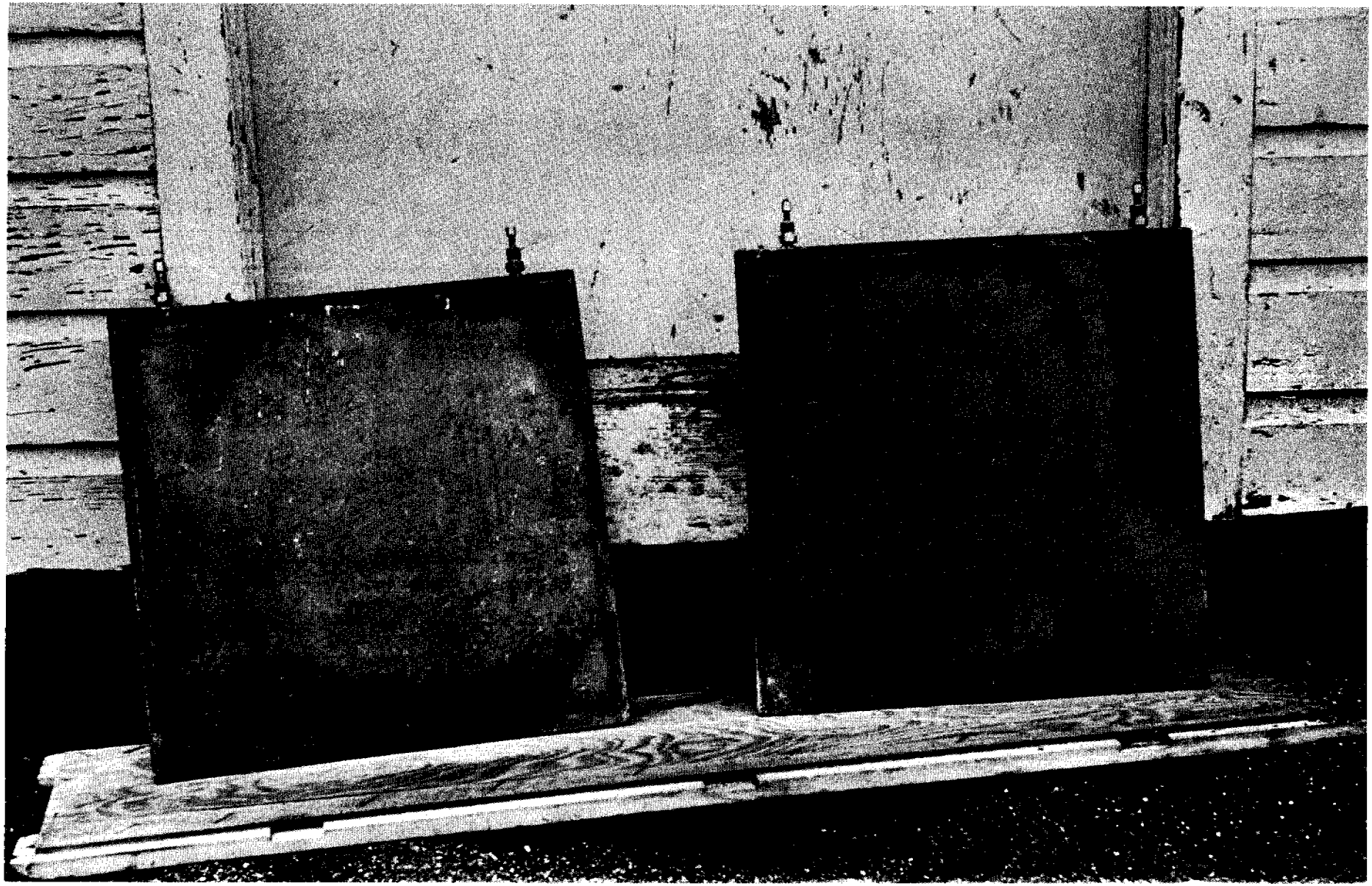

Figure 1. 45 x 45 cm square flatjacks.

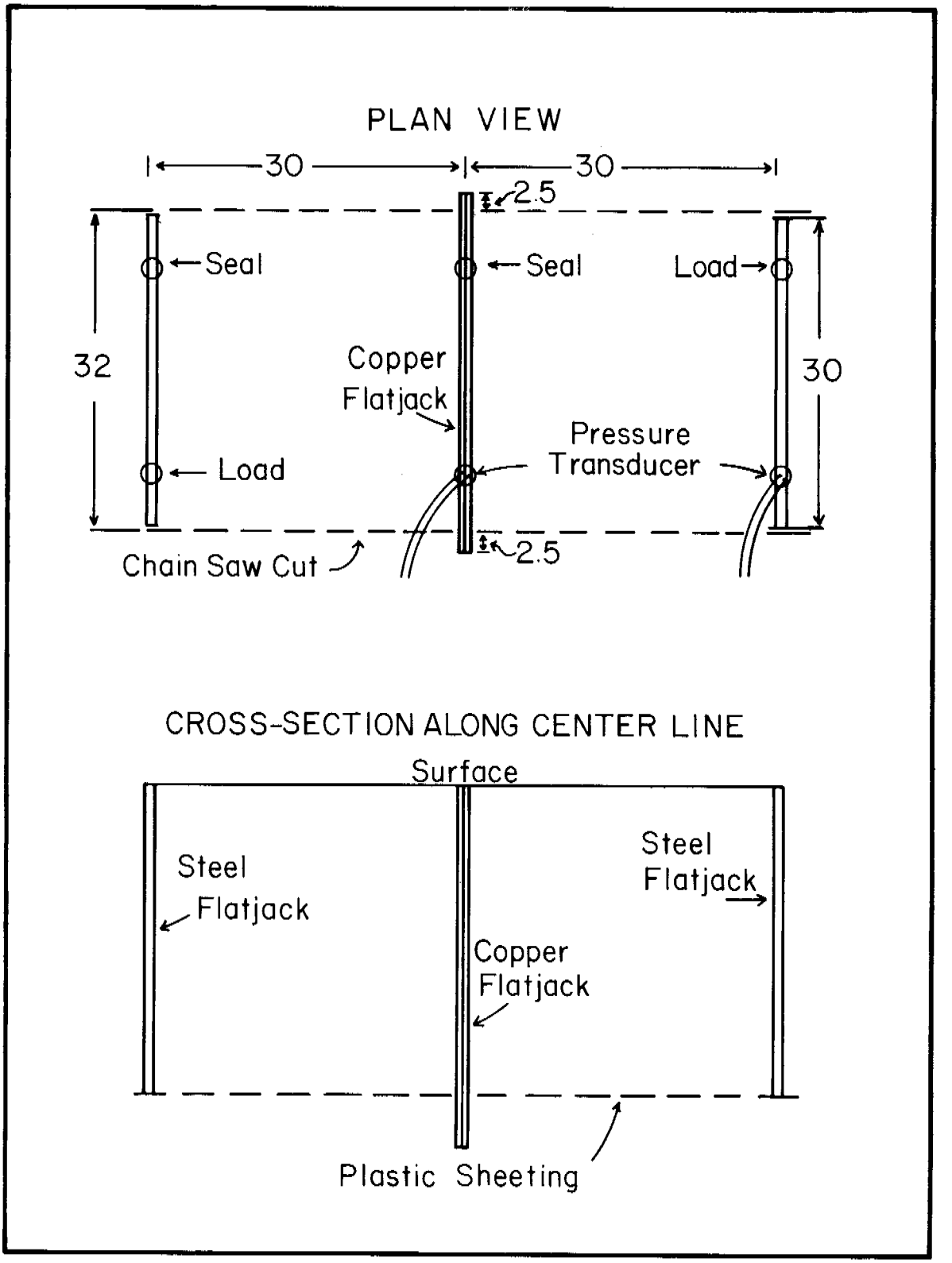

Figure 2. Plan view and cross-section of flatjack calibration installation.

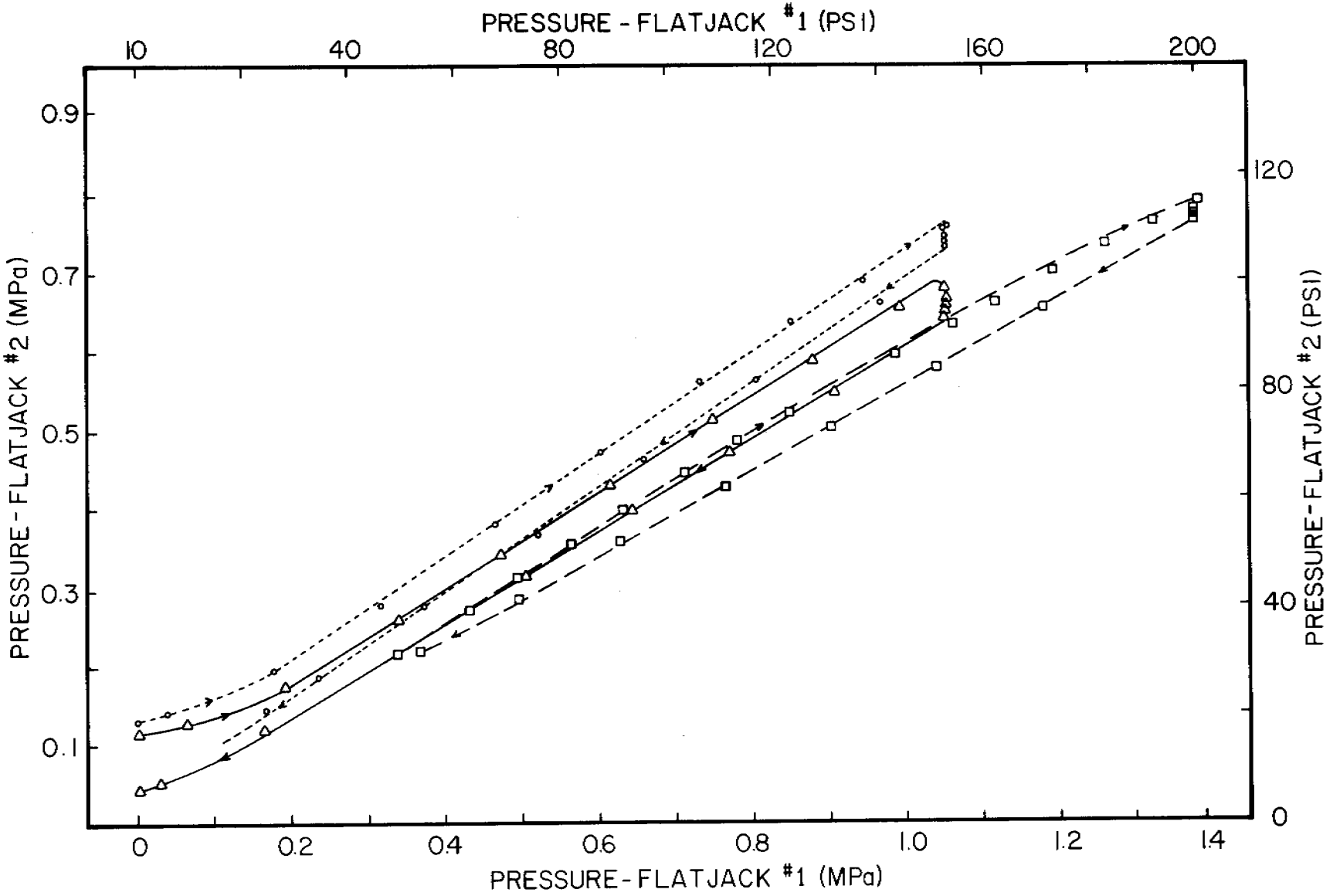

Figure 3. Results of calibration experiment. Flatjack #1 is the steel flatjack pair; flatjack #2 is the copper flatjack.

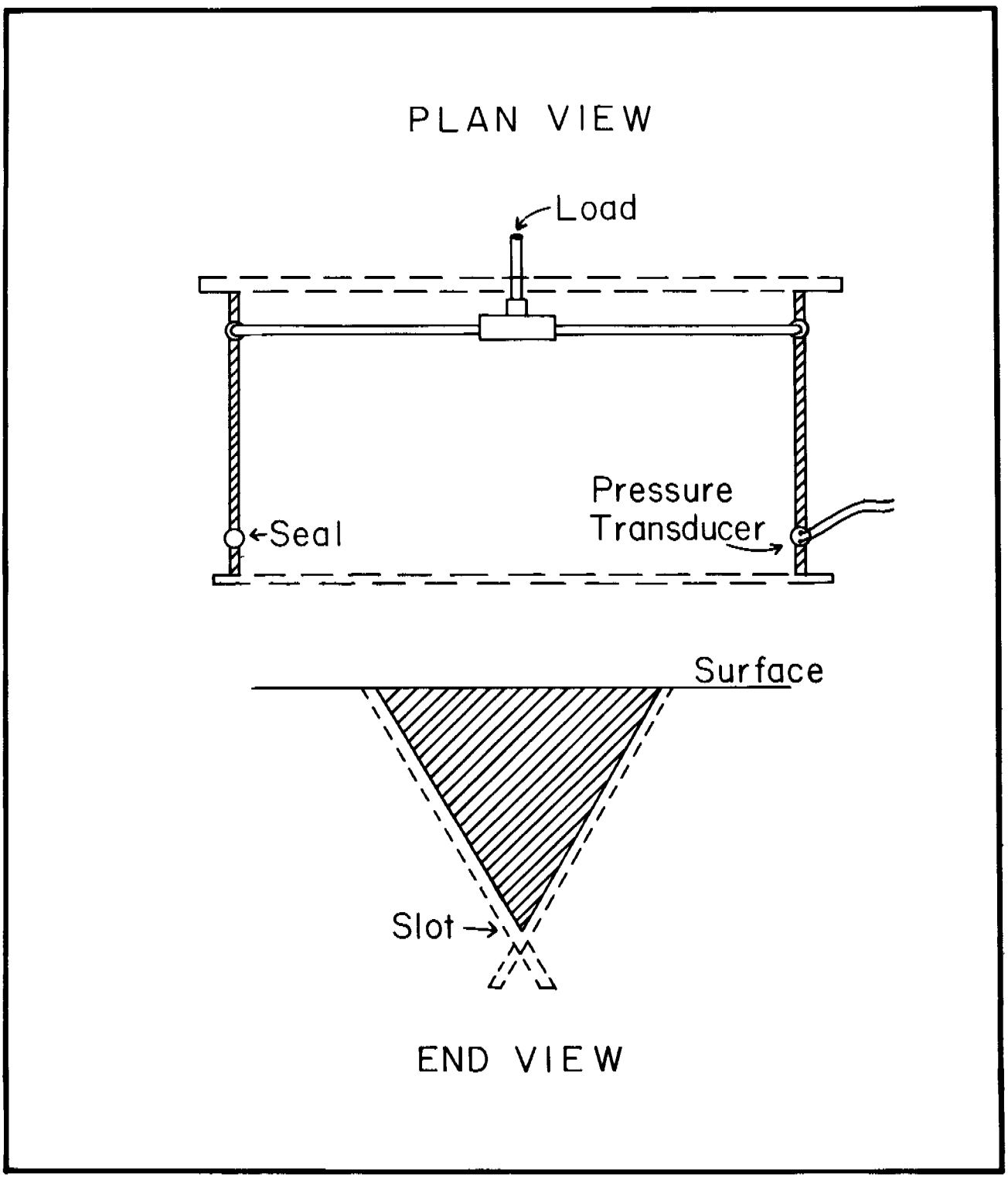

Figure 4. Set-up for uniaxial compression test using triangular flatjacks.

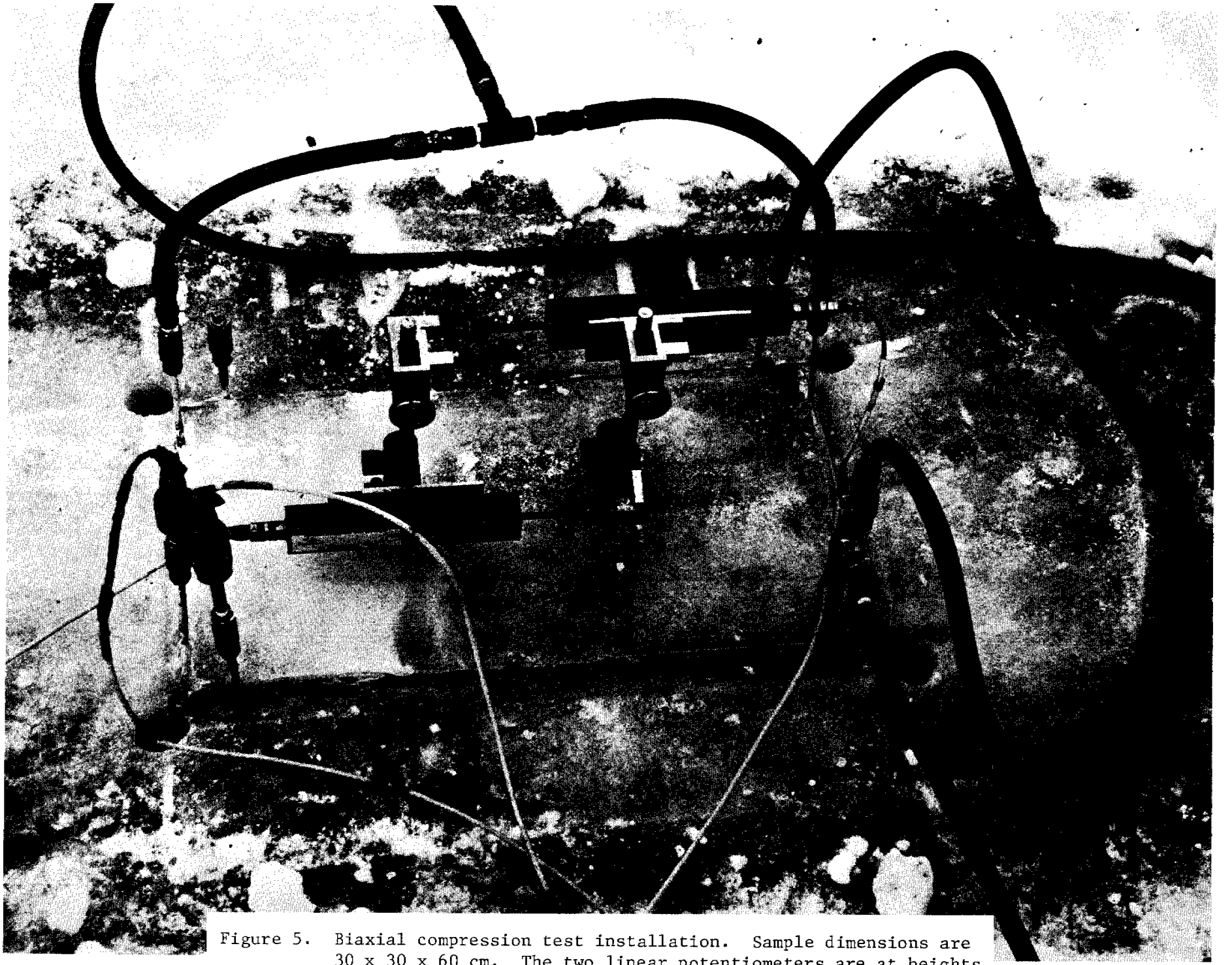

Figure 5. Biaxial compression test installation. Sample dimensions are 30 x 30 x 60 cm. The two linear potentiometers are at heights of about 4 cm and 20 cm.

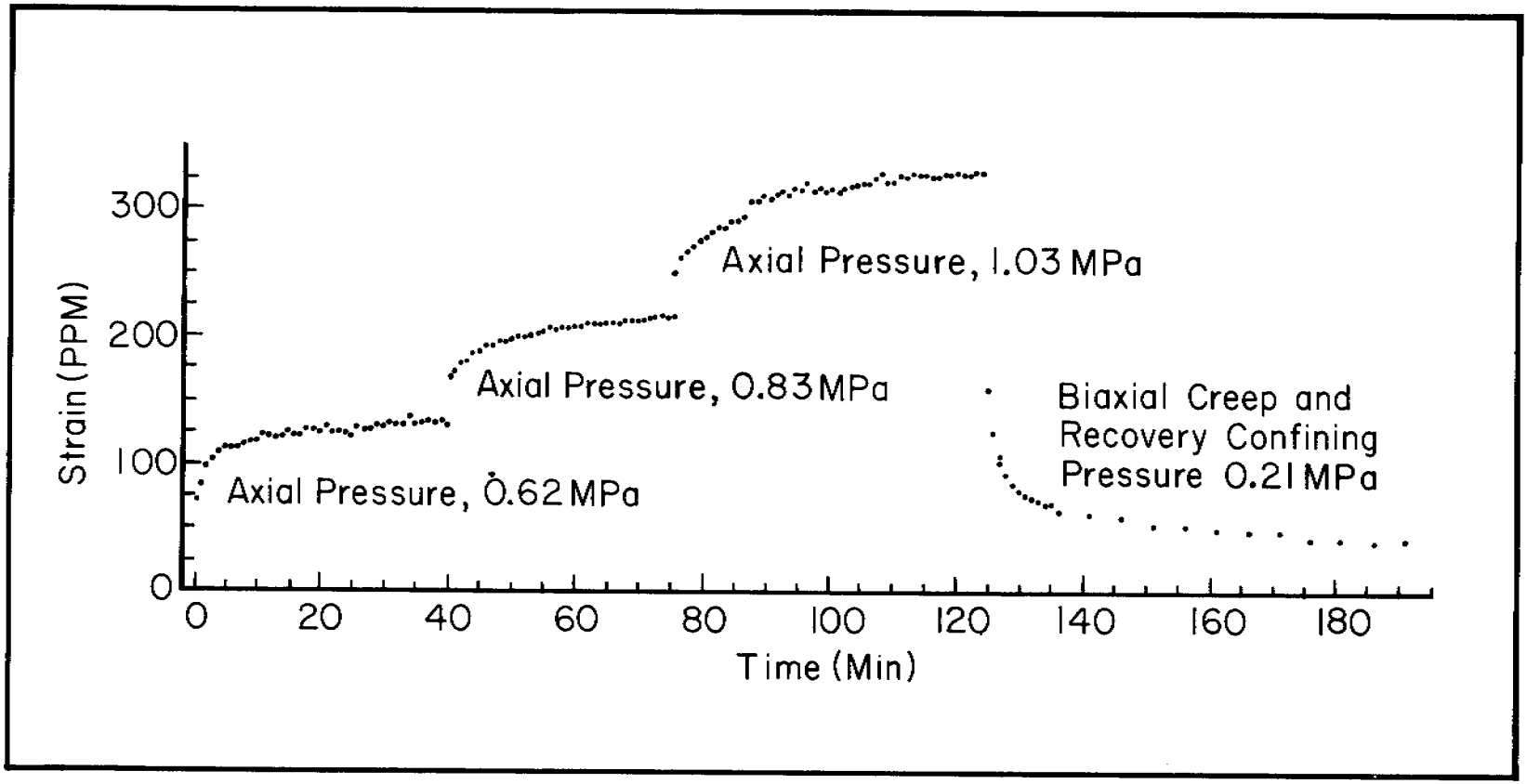

Figure 6. Strain-time data for axial strain gauge of a three-stage creep-recovery test, under confining pressure.

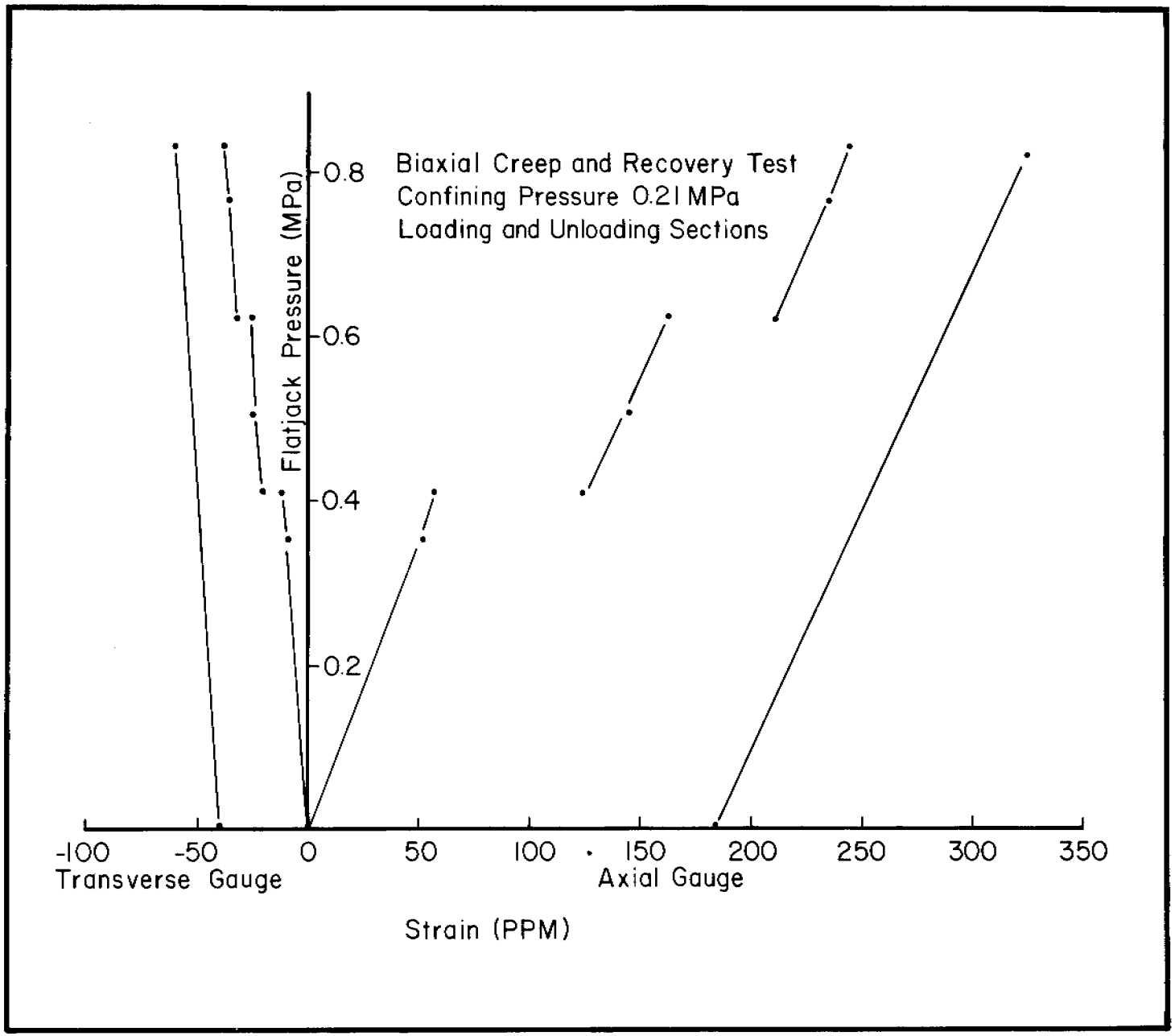

Figure 7. Stress-strain curve for rapid load changes on both axial and transverse strain gauges of the test shown in Figure 6.

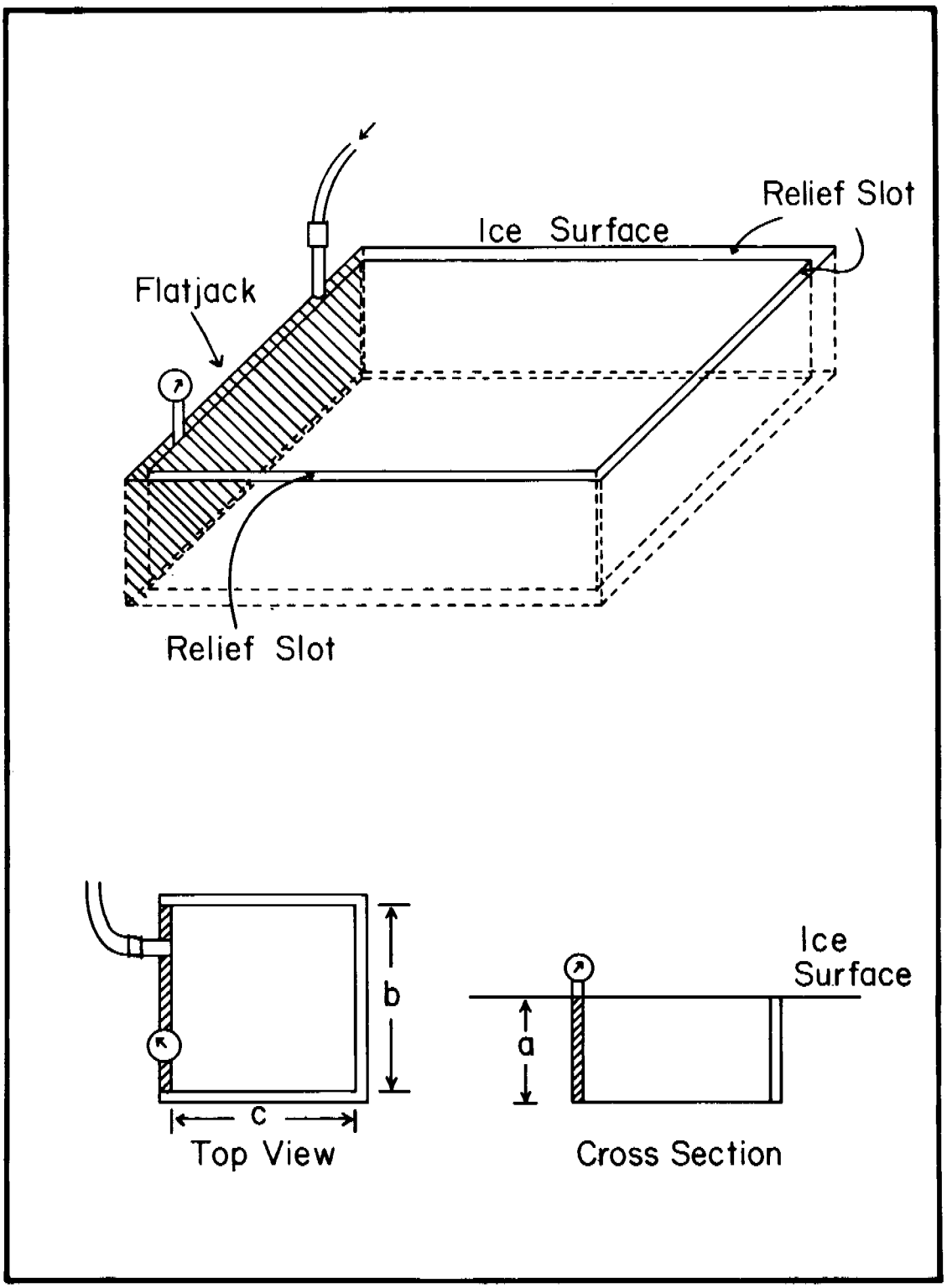

Figure 8. Set-up for direct shear test.

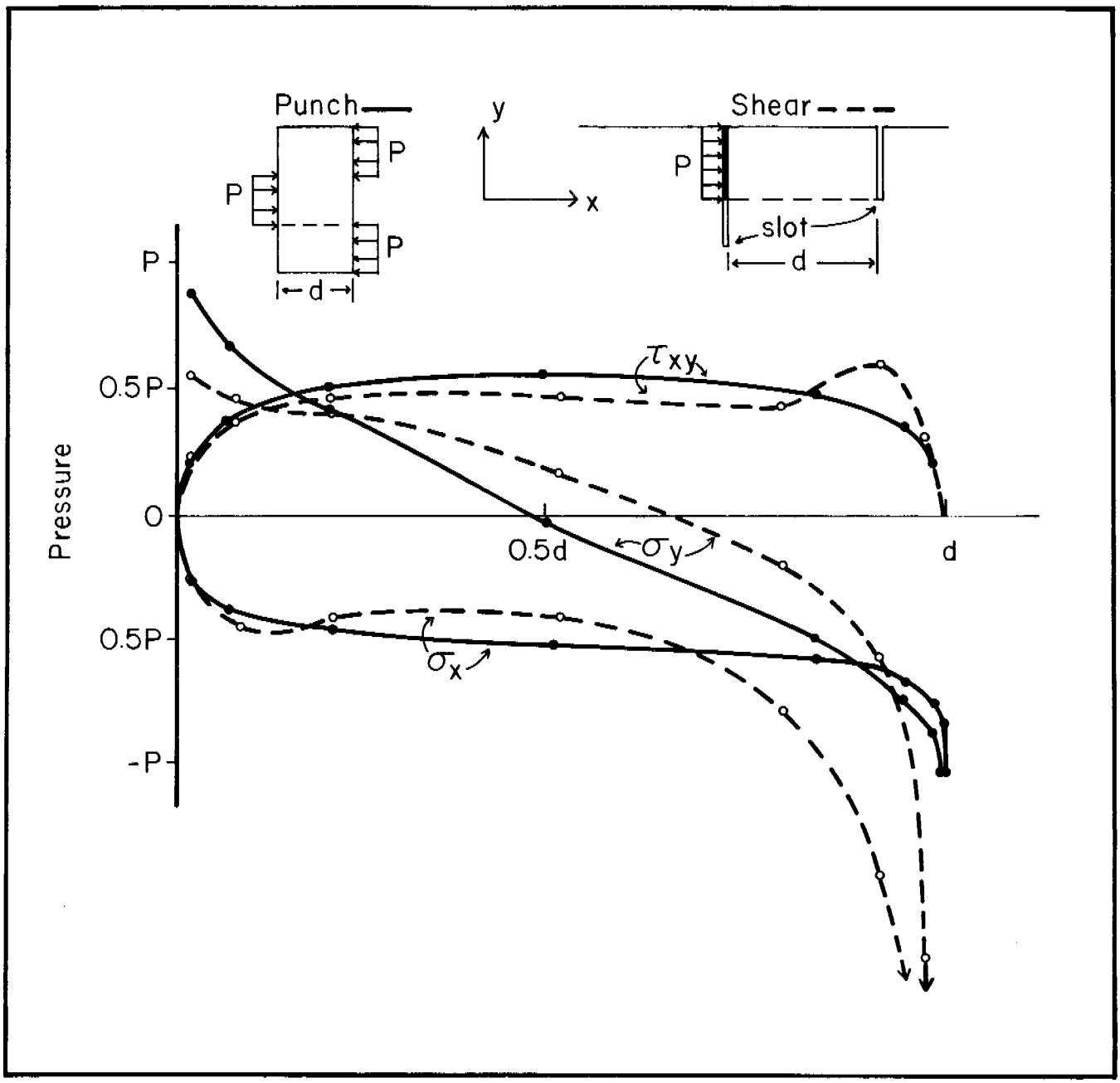

Figure 9. Results of finite element analysis of punch test solid line) and direct shear test (dashed line). Calculations refer to a surface just below the dashed lines on the diagrams. The slot below the flatjack represents either the first crack or the prepared crack as described in the text.

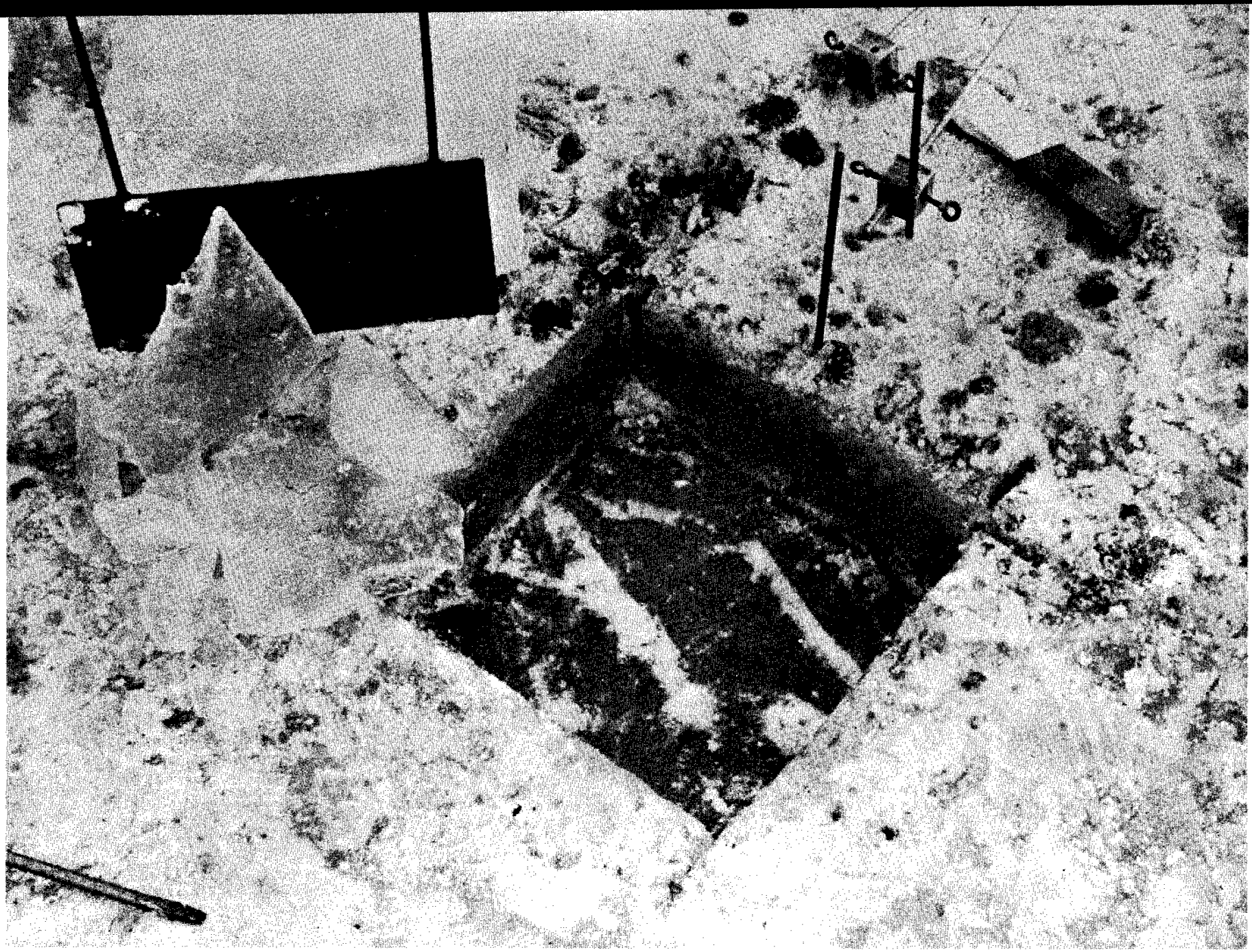

Figure 10. Results of a shear test with load applied from lower left to upper right. Cracks in the surface below the block are indicated by light colored bands. Note size and shape of fragments broken from the base of the test block at left.

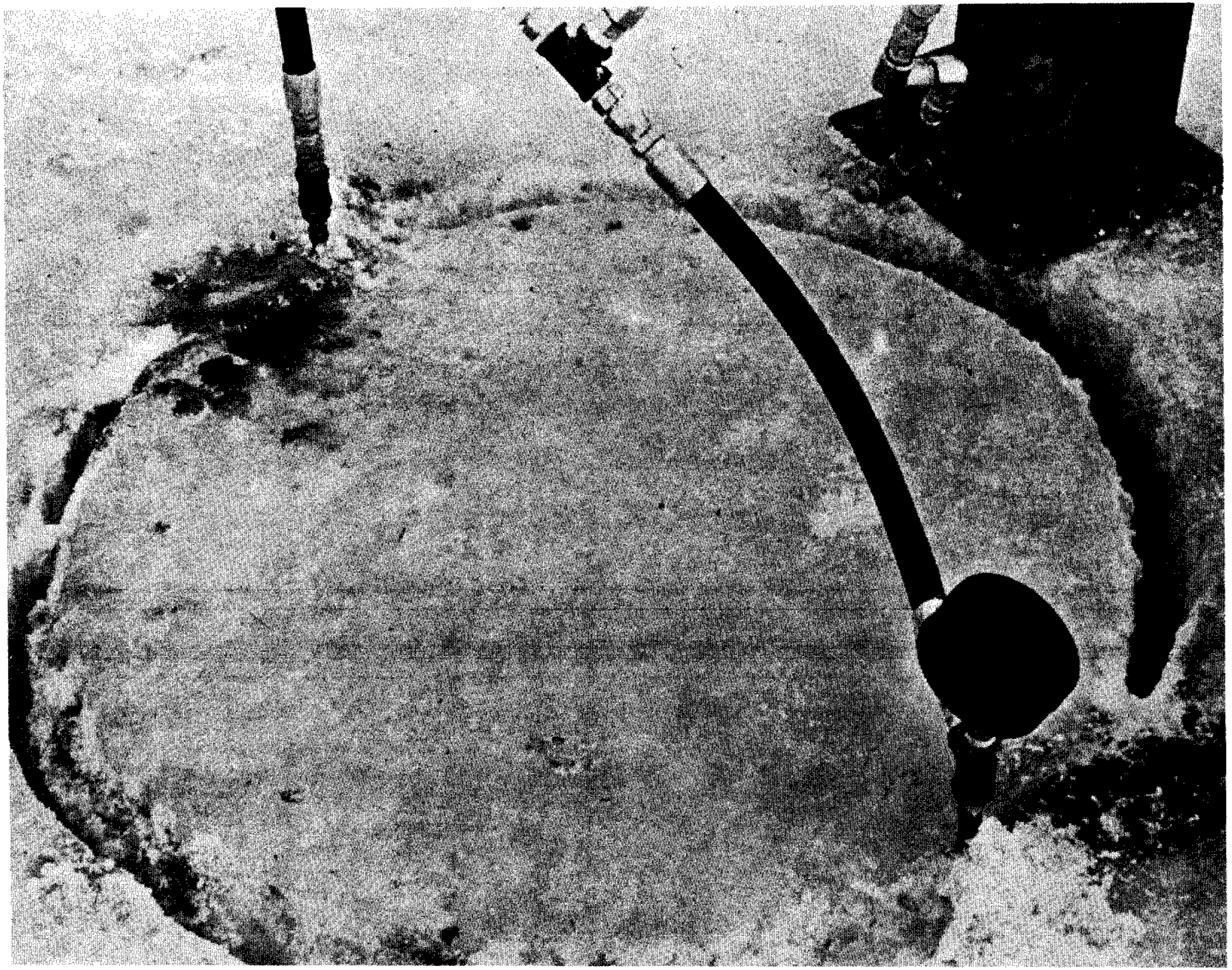

Figure 11. Results of an indirect tension test using curved flatjacks. Failure occurred along a single crack shown as a faint line

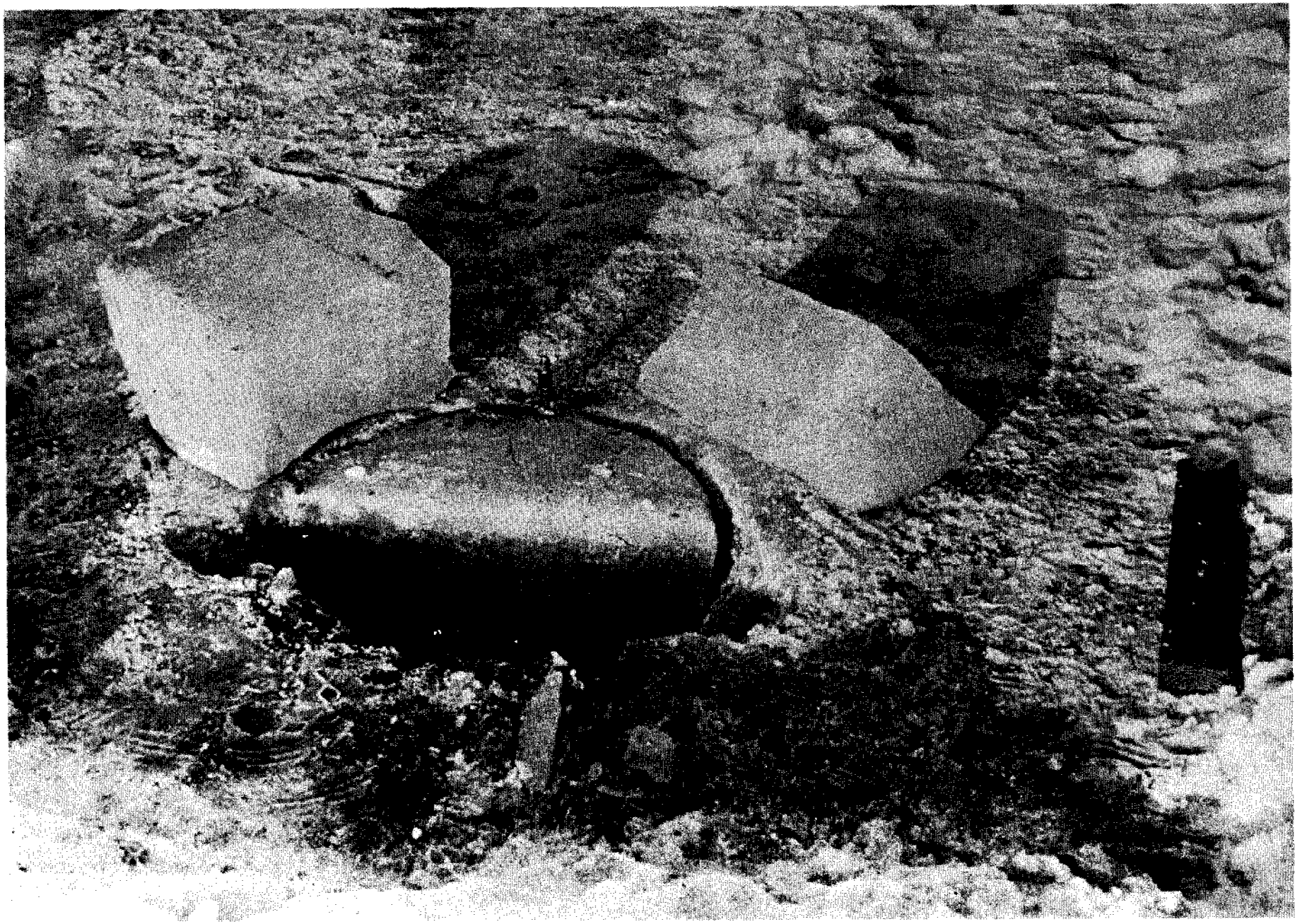

Figure 12. Test block of Figure 11 after sectioning the crack appears as a thin, vertical line in the center of the block.

PARTIAL SUMMARY OF 1979 FIELD PROGRAM

by

Lewis H. Shapiro

I. INTRODUCTION

A. Objectives

The field program during the present year has three primary objectives. The first is to conduct a series of tests in biaxial compression to assess the dependence of ice strength on the intermediate principal stress. Second, a series of uniaxial compression tests is to be run on multi-year ice samples to determine the strength vs. load rate relationship for ice of this type. The number of tests will be limited, so that it is not likely that temperature effects can also be examined. The third objective is to investigate variations in ice strength with respect to depth in the ice sheet and orientation of the load relative to the dominant c-axis direction of the ice fabric. Finally, a limited number of uniaxial compression tests on surface ice are being run to provide a comparison with the ice tested during the 1978 field season.

B. Procedures and Test Conditions

The test procedures being employed have been described in earlier reports of this project, and are included elsewhere in this report. The samples being used are all 30 x 32 x 60 cm in size, installed for testing at the surface. Most of the tests will be at constant loading rates, although a few creep-rupture and creep tests are also planned.

Temperatures have been generally colder this year than in 1978, so that it has not yet been possible to repeat tests at the warmer ice

temperatures which prevailed then. Structurally, the ice is similar to that in 1978, with a layer of fine-grained ice at the surface, becoming columnar with a tendency for the c-axes to orient parallel to the coast within the top 10-15 cm. The salinity of the ice is lower than that of 1978, with an average value in the range of 4.5-5 ppt as against the average 6.5 ppt of the previous year.

II. RESULTS AND DISCUSSION

A. Introduction

The results for all the test series to date are described below. These are limited by the available data, and in general there are too few tests to permit firm conclusions to be drawn. However, some preliminary interpretations are offered as an indicator of what further work is required during the remainder of the field season.

Note that all of the strength data reported has been corrected for variations in width of the sample blocks, so that they represent values for a standard block of 30 x 30 cm cross-section. However, no correction for the efficiency of the flatjacks has been made.

B. Uniaxial Compression Tests

A total of 20 tests in uniaxial compression have been run on samples of surface ice, in order to provide a comparison with the results of the 1978 tests. Of these, 17 have been on samples with an average temperature of less than -16°C. These are plotted in Figure 1 as strength vs. time to failure, and in Figure 2 as strength vs. loading rate. Data from the 1978 field program has been added for comparison.

The figures indicate that the ice may be stronger at the higher loading rates this year than was true for the higher salinity ice tested in 1978. However, this may not be the case at low loading rates. Unfortunately, the 1978 data set is limited in this temperature range, so that the comparison is not as exact as would be desirable. However, it is hoped that an additional series of tests can be run later in the field season to match the larger 1978 data set at temperatures in the range of -10° to -15°C.

C. Biaxial Compression Tests

The program of biaxial compression tests was planned to consist of tests at 5 loading rates (.69, 6.9, 69, 690 and 6900 kPa or 0.1, 1.0, 10, 100 and 1,000 psi/sec) at each of 3 different confining pressures (30%, 60% and 100% of the uniaxial compressive strength at each loading rate). In addition, each test was to be duplicated, so that a total of 30 tests was required to complete the program. This number of tests will be exceeded, but the program objectives had to be modified. First it was simply not possible to conduct the entire test series at comparable temperatures. More important however, the ice strength in confinement is so great, in the temperature range in which tests have been conducted, that the limits of bottle gas pressure available is approached for biaxial tests at loading rates of only .35 MPa (50 psi/sec). Internal flatjack pressures of up to 11.0 MPa (1600 psi) have been reached, and at these pressures the edge weld of the flatjacks, which is at the ice surface, tends to fail prematurely by overexpansion resulting from the absence of confinement. At warmer temperatures the ice can be expected to fail at lower pressures, so that the available gas pressure should be adequate. However, it is not certain that the ice will be sufficiently

strong at the surface to contain the flatjacks and prevent premature rupture of the jacks. Thus, for the present, .35 MPa (50 psi/sec) is considered to be the upper limit of loading rates which for which tests can be successfully completed, and the program has been modified accordingly.

When under biaxial load the ice samples do not tend to fail by the formation of through-going cracks, as is the case with samples tested in uniaxial compression at high loading rates. Instead, cracking is pervasive throughout the block, turning the color of the ice to a milky white. Thin cracks are visible on the surface which, in turn is bulged up. Strain in the lateral and vertical directions tends to increase at a high rate as failure is approached, but the stability of the axial strain measuring system is usually disturbed by cracks before failure. Finally, as the peak stress is approached, the axial flatjacks begin to expand rapidly, so that it is difficult to maintain the loading rate. This rapid expansion results from the decrease in load carrying capability of the sample which, in constant strain-rate tests conducted in a laboratory, is indicated by a gradual drop in stress with increasing strain following the peak stress. The loading system used in this program, however, lacks the stiffness of a laboratory system so that the gradual drop in the stress magnitude following peak stress does not occur. However, it is reasonable to interpret tests in which the milky color of the ice develops as having reached a stress comparable to the peak stress in a constant strain-rate test. Comparison with tests in which the flatjacks failed prematurely indicates that these often leave the block totally intact, even though the stress reached is within 10-15% of the peak stress reached in a comparable test which clearly failed by the criterion given above.

Most of the data acquired were used to prepare the plots shown in Figures 3 and 4. The results, while inconclusive, are suggestive and some speculations can be made regarding the implications.

The plot of Figure 3 shows axial pressure vs. temperature for two combinations of confining pressure and loading rate. Note that a straight line fit to the data of both plots would have the same slope, representing the increase in strength with decreasing temperature. The value is about .17 MPa/°C (25 psi/°C). Unfortunately, there is not yet enough data from uniaxial tests to provide a comparison.

The effect of confining pressure on the strength is shown in Figure 4a,b,c. Note that the confining pressure in a biaxial test is the intermediate principal stress with the axial stress as maximum and the vertical stress across the surface taken as zero. From the results in Figure 4b and c, there is little or no apparent variation in strength with changes in the intermediate principal stress. Further, if the values of the peak stresses which reached failure are averaged for each plot (including Figure 4a) the result is a value which ranges from 46% to 57% greater than the uniaxial strength for all three cases.

The bars on the graph of Figure 4b represent the results of 4 tests in which the confining pressure was supplied only by the reaction force of the ice surrounding the test sample. In two of these, the confining pressure flatjacks were left in place but not pressurized. In the remaining two tests, the confining pressure flatjacks were removed and replaced by a double layer of polyethylene sheeting. The test results

were plotted as horizontal lines (dotted for the blocks with the flatjacks in place, solid for the blocks with no flatjacks) to indicate the magnitude of the axial pressure reached, although the value of the confining pressure is not known. Note that these four tests give an average result which is about 32% of the uniaxial strength, less than than when a confining pressure is applied.

In summary, the results suggest that any applied lateral pressure, other than a simple reaction pressure, leads to an increase of about 50% of the uniaxial strength, and that the increase is independent of the confining pressure. Further, this percentage increase is independent of variables of temperature or loading rate.

Additional tests to evaluate the results described above are in progress.

C. Multi-Year Ice Tests

Multi-year ice samples were collected from a single multi-year ice floe which was frozen into the landfast ice sheet near the test site. The floe was about 1.4 m thick when it was frozen in, and about .6 m of oriented first-year ice has been added to the bottom since that time. Samples were collected from the upper .3 m of the floe. These include a thin layer of fine-grained refrozen meltwater about 1-2 cm thick overlying ice which appears similar to first-year ice with the absence of platelet structure or brine pockets. Crystal sizes average about 2 cm and there is no preferred alignment of c-axes. Salinity through the top 30 cm ranged from 0.0 at the surface to about 2.0 ppt at the base, although one sample had an average value of 4.5 ppt for the bottom 5 cm.

A total of only four tests have been run on multi-year ice samples to date, and these have been at low loading rates. The results indicate that there is little difference between the strength of the multi-year ice and first year ice tested at the same temperatures and loading rates.

Ten additional multi-year ice samples have been prepared for testing at a later stage in the program. These will be run alternately with first year ice samples to check the above result under a wider range of loading rates.

FIGURE CAPTIONS

Figure 1. Peak Flatjack PRessure (corrected to a standard 30 x 30 cm area) vs. Time to rupture.

Figure 2. Peak Flatjack Pressure (corrected to a standard 30 x 30 cm area) vs. Loading rate.

Figure 3. Peak Flatjack Pressure (corrected to a standard 30 x 30 cm area) vs. average sample temperature. Note lateral pressures and loading rates.

Figure 4. Peak Flatjack Pressure (corrected to a standard 30 x 30 cm area) vs. Lateral Pressure for three different combinations of average sample temperature and loading rate.

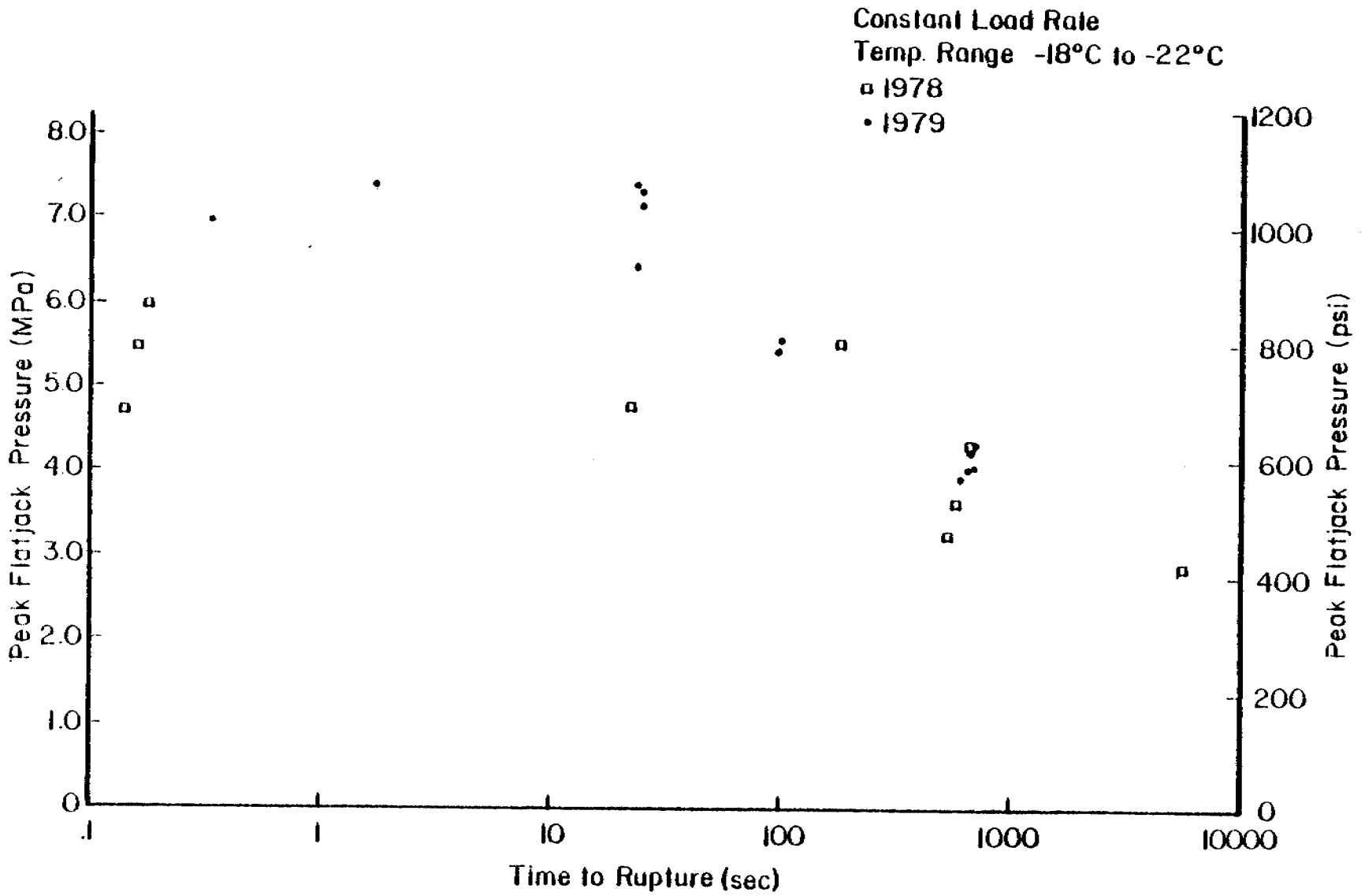
Constant Load Rate
Temp. Range -18°C to -22°C
1978
1979
Peak Flatjack Pressure (MPa)
8.0
7.0
6.0
5.0
4.0
3.0
2.0
1.0
0
Peak Flatjack Pressure (psi)
1200
1000
800
600
400
200
0
.1
1
10
100
1000
10000
Time to Rupture (sec)

Figure 1

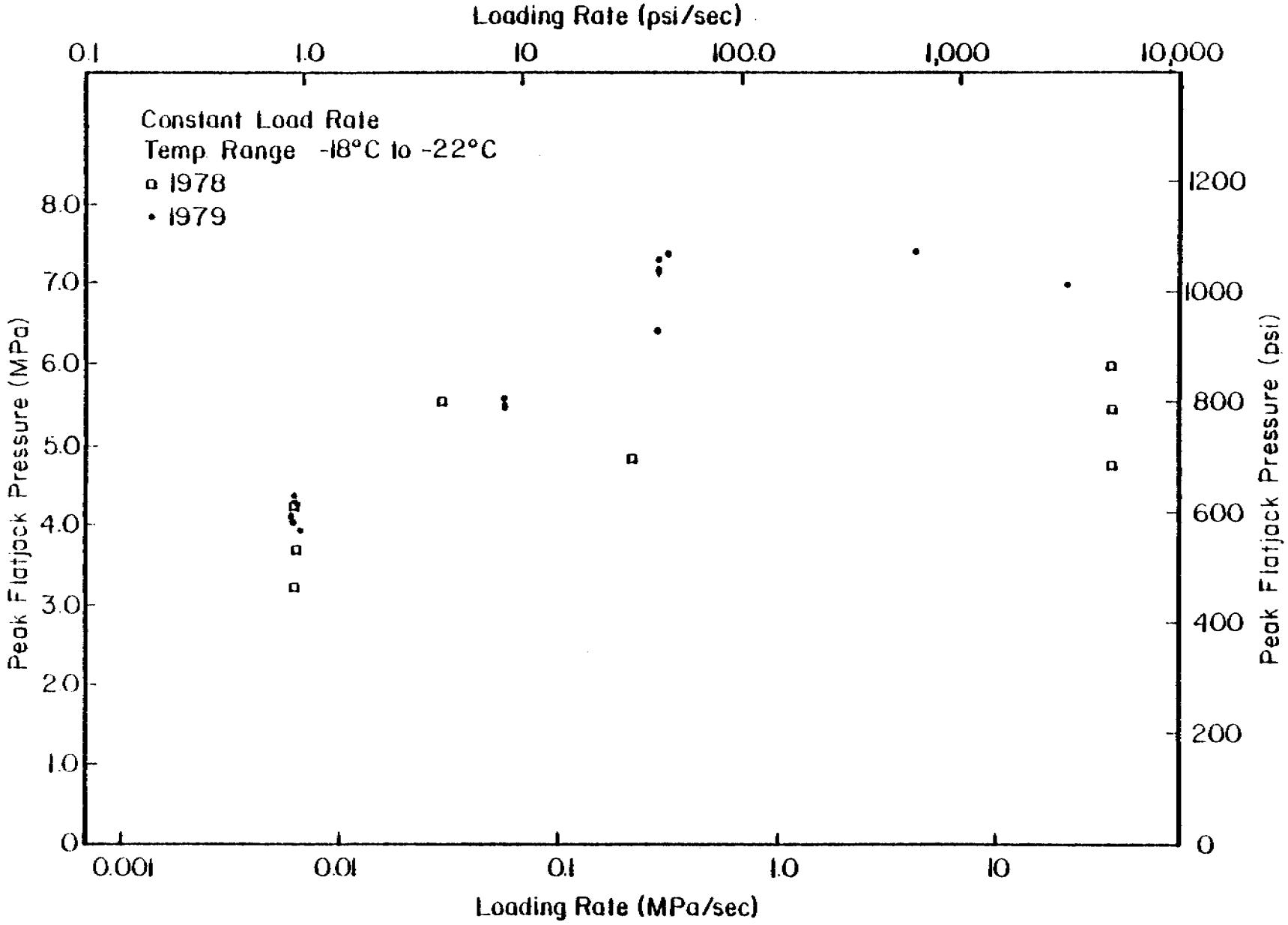
Loading Rate (psi/sec)
0.1
1.0
10
100.0
1,000
10,000
Constant Load Rate
Temp Range -18°C to -22°C
1978
1979
Peak Flatjack Pressure (MPa)
8.0
7.0
6.0
5.0
4.0
3.0
2.0
1.0
0
1200
1000
800
600
400
200
0
Peak Flatjack Pressure (psi)
0.001
0.01
0.1
1.0
10
Loading Rate (MPa/sec)

Figure 2

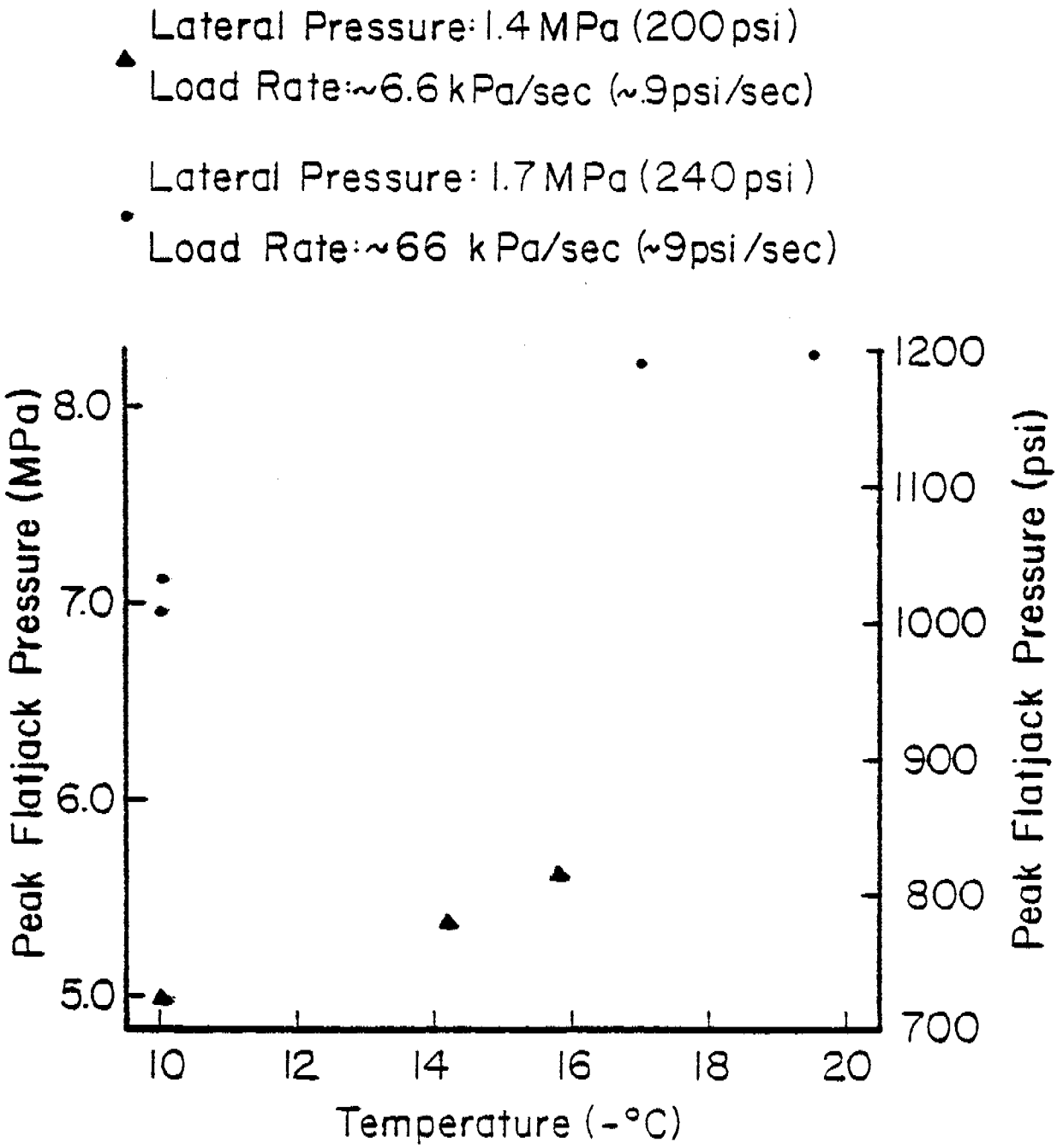
Lateral Pressure: 1.4 MPa (200 psi)
Load Rate: ~6.6 kPa/sec (~.9 psi/sec)
Lateral Pressure: 1.7 MPa (240 psi)
Load Rate: ~66 kPa/sec (~9 psi/sec)
Peak Flatjack Pressure (MPa)
8.0
7.0
6.0
5.0
1200
1100
1000
900
800
700
Peak Flatjack Pressure (psi)
10
12
14
16
18
20
Temperature (-°C)

Figure 3

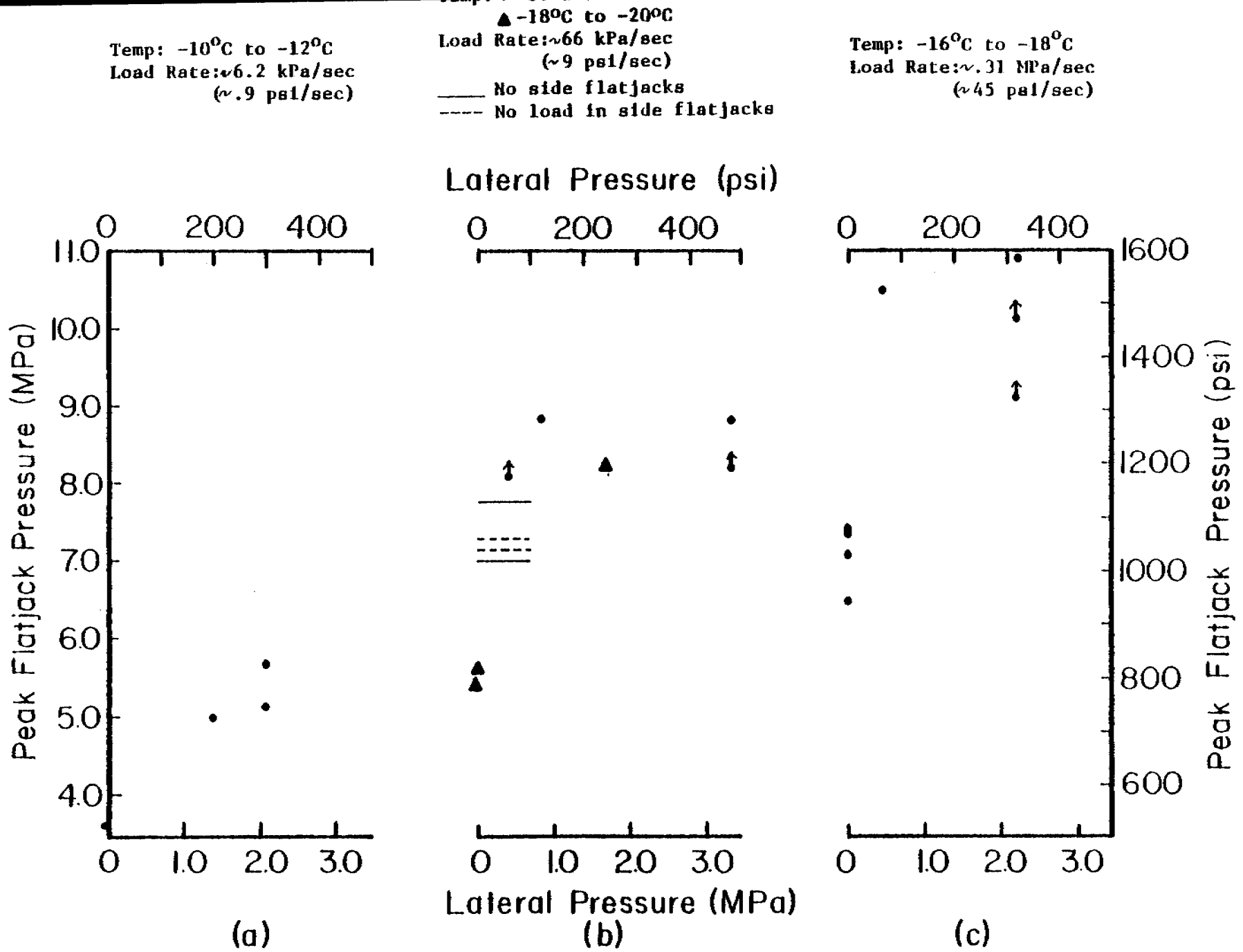
Temp: -10°C to -12°C
Load Rate:~6.2 kPa/sec
(~.9 psi/sec)
▲ -18°C to -20°C
Load Rate:~66 kPa/sec
(~9 psi/sec)
No side flatjacks
No load in side flatjacks
Temp: -16°C to -18°C
Load Rate:~.31 MPa/sec
(~45 psi/sec)
Lateral Pressure (psi)
0 200 400
Peak Flatjack Pressure (MPa)
11.0
10.0
9.0
8.0
7.0
6.0
5.0
4.0
Peak Flatjack Pressure (psi)
1600
1400
1200
1000
800
600
0 1.0 2.0 3.0
Lateral Pressure (MPa)
(a)
(b)
(c)

Figure 4

Historical References to Ice Conditions Along the Beaufort Sea Coast of Alaska

by

Lewis H. Shapiro and Ronald C. Metzner
Geophysical Institute
University of Alaska
Fairbanks, Alaska 99701

Assisted by

Kenneth Toovak Jr.
Barrow, Alaska 99723

I. INTRODUCTION

The existing data base regarding average and extreme ice conditions along the northern coast of Alaska is based primarily on observations made within the last several years. This naturally followed from the interest in the area resulting from the discovery of oil at Prudhoe Bay, and the subsequent recognition that similar deposits may occur in the adjacent continental shelf. Since that time, observations of ice conditions in the region have been intensified, and an understanding of ice motions in the nearshore area has begun to emerge. In the near future, decisions will be made regarding the procedures for exploration and development of these offshore areas. These will be based, in part, upon the available information regarding the potential for major ice motion in the lease areas at different times of the year.

It may be true that the most severe conditions likely to be encountered during the exploration, development and production of oil from the continental shelf along the Beaufort Sea Coast of Alaska have occurred during the years since the observations noted above were begun. However, this cannot be known until the data base of observations is extended in time.

The objective of this project is to attempt to extend the data base backward in time through interviews with local residents of the North Slope who have lived along the coast during past years. These people were primarily engaged in traditional hunting and trapping activities and thus they had both the opportunity and the incentive to carefully observe ice conditions in the area. It may therefore be possible to obtain information regarding extreme or unusual events affecting the ice cover through interviews and discussions with them.

This report covers the initial phase of the study, summarizes the results to date and evaluates the procedures used.

II. PROCEDURES

This project was proposed after we (the Principal Investigators) learned of a planned 'Conference of Elders' to be held at Barrow in May, 1978, under the sponsorship of the North Slope Borough. The purpose of the conference was to bring together some of the older members of the Eskimo community for discussions of local history and culture, so that these could be recorded and saved for the future. Through meetings with some of the conference organizers we arranged for a session to be held regarding ice and weather phenomena, which would involve several members of the various North Slope communities with experience as hunters and trappers on the ice. In addition, we were to name one of the participants of the session who would help guide the discussions to insure that topics of interest to the objectives of this project were included. Translation of the proceedings was to be arranged by the conference organizers. It was anticipated that through the conference we would obtain a sample of the type of information which could be developed through a program of interviews and, in addition, learn of individuals who could be interviewed.

We contacted Mr. Kenneth Toovak Jr. of Barrow to act as our representative at the conference. Mr. Toovak was an employee of the Naval Arctic Research laboratory at Barrow for many years. He is well known to many members of the scientific community who have operated through the laboratory and is respected for this expertise on various aspects of sea ice. He is fluent in English, including much of the technical terminology needed. In addition, as a lifetime resident of the Barrow area he is

acquainted with many of the people who would be likely candidates for interview. We held meetings with Mr. Toovak, explaining the problem and the type of information which we hoped to obtain. In addition, a list of topics for discussion was developed.

Two thirds of the budget of the project was intended to be spent to support the ice and weather session, and approval of the proposal was granted prior to finalization of plans for the conference organization. Subsequently, it became necessary for the conference organizers to restrict active participation to members of the local community so that, while we were present at the conference as observers, we did not take part in the proceedings, nor contribute toward financing the session.

As a result, we decided to move directly to what had previously been considered as the second stage of the project. That is, direct interviews with residents of the area who might be able to supply useful information. With the assistance of Edna MacLean (Head of Iñupiaq Eskimo Research, Alaska Native Language Center, University of Alaska, Fairbanks) we arranged for Mrs. M. Pedersen of the Iñupiaq Language Commission of the North Slope Borough to work with Mr. Toovak in arranging and conducting interviews, and to provide translations.

Without the experience which the Conference of Elders was to provide, there was no means of anticipating what type of information could be obtained. Accordingly, we provided a list of suggested topics for the interviews to Mr. Toovak.

The people interviewed were selected by Mr. Toovak and Mrs. Pederson. Their names and other information are given in Appendix 1. A total of eight interviews were conducted of which four (including Mr. Toovak's)

were narratives into the tape recorder without the presence of an interviewer. The other four interviews were conducted by Mr. Toovak. In one case, one of the Principal Investigators was present during the interview. Most of the translations were done by Mrs. Pederson who provided texts generally paraphrasing or describing what was said. Subsequently, Mr. Toovak listened to the tapes, verbally translating and elaborating on the text material. In one case, the translation was done entirely by Mr. Toovak speaking into a tape recorder while listening to the tape of the interview. The tape of the translation was later transcribed by us.

The resulting transcriptions of the interviews are given in Appendix 2. We emphasize that these are not literal translations but instead include paraphrasings and descriptions by the translators. In addition, some comments by the translators are also included, and in some cases, these could not be clearly identified. If necessary, this can be done in future by going over the tapes again with Mr. Toovak.

III. RESULTS

The points made in the interviews which are considered to be most relevant to the problems of OCS development are summarized below. In this context, it is important to emphasize that the absence of mention of a particular type of event should not be considered as evidence that the event never occurs. As an example, none of the people interviewed mentioned any specific episode of a major winter storm resulting in large ice motions in the landfast ice along the Beaufort Sea coast. However, Samuel Kunaknana, who has lived in the Colville River area for many years, said that a strong wind from the west can cause the ice to break up and go out even in winter, which would clearly constitute an event of this type. Thus, the absence of references to a specific event

may not be significant, and the statement of Mr. Kunaknana may instead be representative of the accumulated experience of the local residents. This, in turn suggests that only a negative response to a specific question can be taken to mean that the type of event referred to is not likely to occur.

The only specific mention of major ice motion in the near shore area during winter came in the interview with Mr. Harold Itta. He described a lead which opened across Harrison Bay from the vicinity of Cape Halkett, extending eastward toward Thetis Island. The event occurred in February, 1928, with the lead opening to a reported width of one mile. From the position of the lead which Mr. Itta indicated on a map of the area, the motion apparently involved a translation about one mile seaward of all of the landfast ice sheet off Harrison Bay outside of the approximately 10 meter depth contour. In this context, it is of interest to note that in the summary of motion of the landfast ice sheet in the Beaufort Sea Synthesis report it was concluded that ice motion of up to a few tens of meters might be anticipated in the floating landfast ice sheet after freeze up was completed. This was based upon observations in the relatively narrow landfast ice area offshore from Narwhal Island. The speculation was offered that significantly greater motions might be possible in areas such as off Harrision Bay, where the landfast ice sheet is wide and the barrier islands are absent. The report also notes that there were no data available to substantiate this, but the results of the interview with Mr. Itta would appear to provide the necessary support.

In the interview with Mr. Elija Kakinya the question of motion in the landfast ice between the barrier islands and the shore after freeze

up, was specifically asked. The response was negative; Mr. Kakinya had no knowledge of any examples of winter ice motion behind the barrier islands in the area around Flaxman Island. In addition, he also noted that he had never seen the ice come over the barrier islands, although it is not certain that he was speaking of islands other than Flaxman Island or seasons other than winter. The question of the ice coming over the barrier islands after freeze up was also asked of Mr. Henry Nashanik who had trapped extensively in the area around the McClure Islands and Stockton and Cross Islands. He reported that he had never seen the ice pushed on top of these islands, but that ice commonly piled all around the islands, including on the inshore side during early winter. The presence of such piles indicates motions of the ice inshore from the barrier islands during freeze up.

In neither of the above interviews was the question of override of the barrier islands during break-up explored. This is a time of year when trappers are not likely to be moving over the ice, but it is still too early for boat travel. However, Mr. Samuel Kunakana mentioned that, during the summer, old ice is occasionally driven or washed up onto the barrier islands by north winds. Specific examples of this, along with the frequency of occurrance would be of interest. In addition Mr. Elija Kakinya notes that west winds tend to keep the ice near shore during the summer, while northeast winds can drive the pack ice out of sight to the north. In addition he noted that times when the ice is near shore during the summer are considered to be good for seal hunting, suggesting an association between the position of the pack ice edge and seal densities. These questions need to be pursued in future interviews.

One episode of spring ice override was described in the interview with Mr. Harold Itta, (note that the same event was described in an informal and untaped discussion with Mr. Herbert Leavitt of Barrow). The event occurred in July of 1928 at Esook on the coast near Cape Halkett. The ice was about 4 feet thick at the time, and the movement formed piles estimated at 20 feet high along the beach. Over part of the movement front, the ice did not pile, but advanced up the beach as a continuous sheet for a distance of up to 200 feet.

Mr. Kenneth Toovak described an episode of overriding of the beach on the Chukchi Sea coast at Barrow, which occurred in late-February or early March of 1935 or 1936. At that time, the ice advanced about 250 feet up the beach, terminating in a pile about 20 feet high. (This may be the same event described by C. Brower in his book "Forty Years at Forty Below," p. 312. Brower noted that a southwest gale drove the ice onshore, forming piles up to 75 feet high. He gives the year as 1937). While not directly related to the Beaufort Sea coast, this episode is of interest for two reasons. First, it indicates that the end of freeze up does not signal the beginning of a period of inherent stability of the ice. Given the appropriate driving conditions, motion of the ice up a beach could conceivably occur at any time of year. Second, this is illustrative of many examples of ice push which have occurred at Barrow during the winter months, suggesting that the ice in nearshore waters of the Chukchi Sea coast is likely to be less stable than that encountered along the Beaufort Sea coast. This is a point which will require study prior to leasing in the Chukchi Sea.

No attempt has been made to summarize the comments made during the interviews regarding summer conditions. These tend to relate primarily

to problems of moving through coastal waters in small boats and are directed towards describing local currents and the effects of weather on travel. However, some information on the relationship between the position of the pack ice edge and local winds was given. It is possible that such observations would provide useful data for studies leading to predictive models of pack ice incursions during the summer months. A series of questions directed toward this should be included in future interviews.

The interviews produced little information regarding synoptic features of the ice cover. This is entirely expected however, because such information requires aircraft or satellite observation platforms. However, one point was raised by several people. That is, that a wind from the west at any time the ice is present, will usually cause a lead to form extending from Cross Island eastward across Camden Bay and towards Barter Island. Apparently this lead forms quite rapidly, and two stories of hunters being trapped on the ice when it moved offshore are included in the transcripts. It was also noted that west winds in summer can cause heavy, polar ice to drift into Prudhoe Bay behind Cross Island and between the Return and Miday islands. However, the size of floes moved in this way will be limited by the depth, state of the tide, and presence and absence of storm surges.

Finally, Mrs. Sarah Kunaknana, who lived on Cross Island and at Prudhoe Bay reported two instances of bowhead whales being taken by crews operating in that area, during the fall migration. Others noted that whales have been sighted between Cross Island and the mainland at that time of year.

IV. DISCUSSION AND EVALUATION

The problem of obtaining data through interviews, as described above, is likely to be new to most physical scientists as it was to us. Further, the fact that the interviews could not be conducted in English compounded the problem. As a result, difficulties arose which limited the amount of information obtained. These resulted both from lack of experience in planning such a program, and from operational problems. However, we believe that these can be overcome and a successful series of interviews conducted.

In general, it proved useful to have the translations done verbally by Mr. Toovak with one of the Principal Investigators present. In this manner it was possible to clarify discrepancies in times and places in the interviews and get the benefits of Mr. Toovaks comments and interpretations. In addition, this type of translation can be obtained rapidly, which would provide opportunities to return to the person interviewed within a short time with additional questions.

Mr. Toovak has also proved to be an effective interviewer and colleague. In the short time available for this project he made significant progress toward understanding the problems which OCSEAP is trying to solve. Continued improvement can be anticipated, and this should enhance the quantity of useful information obtained in future interviews. In addition, in order to make the interviews more uniform and prevent inadvertant oversites, an expanded list of topics for discussion, as well as a list of specific questions to be asked, will be used as a guide. Finally, we would arrange for second interviews with some of the people, in order to have them elaborate on some of the points raised. This was not possible under the present project because of limitations in time and funding.

The procedure of supplying a tape recorder to an individual and suggesting that they supply a narrative on their knowledge of the area is not generally effective, because, while the information gained is useful and interesting, it cannot be expected to address OCSEAP problems unless the person making the tape is familiar with these. However, this method might be acceptable for cases in which an interview in person cannot be arranged.

To date it has not been practical to have one of the Principal Investigators present at the interviews because these have occurred at irregular times in the Barrow area, and the funding level was not sufficient to provide for travel there specifically for the interview. This is likely to be true of future interviews as well unless one of the Principal Investigators is in the area in conjunction with other studies. Thus future work should be planned with this limitation in mind.

The interviews produced useful information regarding specific events. The verification of the occurrence of large motion of the landfast ice sheet during late winter is particularly important, because events of this magnitude have not previously been reported for that time of year. In addition, the description of the ice override at Cape Halkett during break-up is the first report of a break-up override along that part of the coast. However, a reading of the interviews suggests that in general, such information is more likely to be offered in response to specific questions, rather than in a general discussion.

APPENDIX I

List of Persons Interviewed

Itta, Harold; age, 71, Born in Barrow, later lived near Teshepuk Lake and at Esook near Cape Halkett. Interview by Kenneth Toovak; translated by K. Toovak and M. Pederson.

Kakinya, Elija; age 85, presently lives in Anaktuvak Pass. Lived and traveled along much of the coast between Herschell Island and Barrow, but mainly near Flaxman Island, Beechey Point, Gordon Point. Interview by Kenneth Toovak; verbal translation by K. Toovak, transcribed by Teri McClung.

Kunaknana, Samuel; age 64 or 65, Born in Barrow, lived in the Colville River area. Presently resides in Nuiqsit in the Colville Delta. Narrative without interview; translation by M. Pederson and K. Toovak.

Kunaknana, Sarah; age 57, Born in Barrow but grew up on Cross Island and at Prudhoe Bay. Presently resides at Nuiqsit. Narrative without interview; translation by M. Pederson and K. Toovak.

Nageak, Vincent; age 79, Resident of Barrow, but traveled extensively along the coast and mentioned having lived at Barter Island, and at Oliktok. Narrative without interview; translation by M. Pederson.

Nashankvik, Henry; age 73, Resident of Barrow, but has lived at numerous locations along the coast and trapped on many of the larger barrier islands. Interviewed by K. Toovak, translation by M. Pederson and K. Toovak.

Nekapigak, Bruce; age 78, Born in Barrow, later lived at Oliktok, Barter Island, Pt. McIntyre and Beechy Pt. Interview by K. Toovak, translation by M. Pederson and K. Toovak.

Toovak, Kenneth; age 55, Born in Barrow and has always lived in that area. Narrative transcribed by M. Pederson.

APPENDIX II

Transcriptions of Interviews

The following transcriptions include some direct translation which we believe to be verbatum. Parts which are clearly summaries or which represent comments by Mr. Toovak or the Principal Investigators are set off in square brackets.

Harold Itta:

I turned 71 on May 5. I was born in Barrow. In 1914, we moved to Siqulik just 1 mile east of Teshepuk Lake and wintered there 2 years. In 1916 we went to Esook trading post which is along the coast just west of Cape Halkett [before they went inland to trap].*

[The main reason they went to Esook was to hunt seal. That fall he remembers that the ice was extremely flat except for a really flat (?) hunk of ice grounded east of Esook. His father went out hunting when the ice was fairly thin. He was tracking a polar bear and he climbed on top of that big grounded block east of Esook to get a better view. While he was sitting on top of it it split in two right underneath him. He fell down and lost all his gear and his "unapauruk" (ice testing pole) and he was knocked unconscious. He was in the water when he woke up feeling very cold and he couldn't move. He prayed that the Lord would help him move and after praying he finally managed to climb out of the water. Harold Itta worried about him and set the lantern up high over the house so it could be seen from a distance. Finally as Harold was getting the dog team ready to go to look for him his father came home. He took him to Barrow to see Dr. Christ (the minister and doctor in the area at the time). Harold's father stayed in Barrow for a long time (until Christmas) recovering].

I remember in November of 1927, there at Esook, the ice piled up really badly. It was crumpled up from 1 mile out all the way in to the mainland. This was November and there was a strong wind from the northeast.

- -

*see the introduction to Appendix II for the meaning of the square brackets.

Ice ridges were there all winter and lasted into the summer months. When Captain Pederson came they had to stop steaming east because of the ridges. So he dynamited those ridges to make a pass to go through. It took him at least a week. [There also was another ship, the "Bay Chimo", that picked up natives from Barrow as guides and helpers and went all the way to Canada. Kenneth Toovak remembers that when he was a boy they used to take 45 men from Barrow with them. He then told a story about how that ship was coming back from the east and got jammed up by polar ice just in front of Duck Camp. The floating ice opened about 1 mile out from the coast and this ship dynamited a path out and got free. Later that year his father was out driving his dog sled to hunt seals and found a good piece of thick rope out on the ice that was from the ship. He unravelled it and made thinner ropes out of it.]

[Mr. Itta says that after Pederson went through the path he blasted, the "Bay Chimo" came through and followed the same path. Pedersen cut a path through those real high ridges and ran east behind the ridges. They were at least a mile out. In July of 1928, it did the same, (referring to the ice being piled up along the shore) but the wind came from the west. (This was at Esook). The ice was approximately 4 feet thick. It piled as high as Mr. Itta's present house in Barrow (which is 2 stories high or about 20 ft) in places, but at Oliver Morris' boat it moved as a flat sheet and pushed the boat 100 ft to 200 ft up the beach. Harold Itta's father put driftwood under the boat and between the boat and the ice so it wouldn't be damaged. This trick worked and the boat slid sideways up the beach. Oliver Morris' wife started crying when she saw the boat way up the beach. Mr. Itta says Oliver Morris was really lucky because the ice was piling on either side but it just came up as a sheet where Oliver Morris' boat was].

The summer after that the ice was all crumpled up in beach ridges and a large number of ravens nested on the ridges. The ice there is controlled by the winds, not the currents. The west wind also opens leads to take the ice out.

I remember there was quite a lot of huge grounded polar ice in the summer of 1930 in front of Esook, about 3 miles out. It never did melt all summer. It was still there when the ocean froze again. There was also large, grounded polar ice out in the ocean northeast of Cape Halkett. Pieces there never left all summer either. The open leads are usually very far out. In 1932, when I was going out, it would take me all day to get there. The lead is always about 20 to 25 miles out from Esook. This is in winter months where the ice usually opens and closes a little. Sometimes in fall the ice piles up on the shallows a little bit (Pacific Shoal) and also in front of the Colville. In 1928, (February) there was a 1 mile wide open lead in Harrison Bay, almost in a line from Cape Halkett to Thetis Island. The wind was from the west. I never traveled on ice very much after that, but this is what I remember seeing.

[At Barrow in the early 50's Harold had a whaling crew out on the ice in spring. During the day Harold would come in to Barrow for supplies. He knew the current was running north but the wind was calm. His son-in-law and another man borrowed Harold's dog team to go to the whaling camp. Then late in the evening on May 1 (it was the time of year when ducks start arriving) the lead opened between the crews and shore. The wind picked up and came from the southwest. When the drifting started, the hunters headed for shore. They tried pulling a dog team and gear and umiaq. They abandoned Harold's umiaq. They teamed up with another crew that way trying to get back and went with

only the one umiaq. The ice was shearing and piling at the same time. They had to watch themselves and try to get back. (All the crews were doing that). All they saved was a couple of darting guns. They broke the stocks off and just carried the barrels. All crews got back safely but they lost most of their gear. After a day or so, Harold's dogs got loose from the sleds and made it home on their own. They came in one at a time over several days. A day or two later the missionary flew around in his light plane and spotted Harold's umiaq 6 or 7 miles east of Point Barrow on top of a pile of ridges. Something similar happened in 1929 when all the whaling crews were out but it was not as bad as the story above.]

Elija Kakinya - (Verbal translation by K. Toovak)

I've lived around Herschell, some around Flaxman Island and I do know that the ice opened up from westerly winds in winter months and when the wind shift over to east after its opened up from westerly wind the ice always start to crumble up out on the edge of the open lead.

The people that live up around east of Barrow in winter months, they always go out to the open lead to see if they could catch some seals to live on but evidently, the people never had any kayak to retrieve their seal whenever they, when they had a chance to shoot a seal but they use a line with a hook with a floater on the end of it, on the hook.

[There was a good size family, ah, his dad and brothers and sisters and uncles and whatever. They used to live around Flaxman Island back in 1918.]

When my family were living on the coastal area they have to go out to open leads to hunt seals. Some of the families usually move up to the mountains to live. They just go back and forth between the two, ocean and inland searching for the food to live on. I stated in the early part of my talking that westerly wind usually opened the lead and there's a break before it gets real frozen in. When the wind shifts over to northeasterly wind it moves on the shore ice. The ice usually crumbled up and formed some pressure ridges way out on edge of the lead.

In the winter months when the ice is still for quite a number of days or weeks even though the wind is blowing and windy from northeasterly, the ice never opened up. But when the wind is blowing from west the lead opened and thats the time people always go out to seal hunt.

In some years when the ice goes out in spring it isn't visible in summer, and some years the ice goes out and comes back and is visible, and hangs around all summer months.

Sometimes when the ice hangs around in summer months when it gets towards fall some of the polar ice is grounded off shore and thats the time when people are happy to be out hunting for seals; when the polar ice is grounded in fall that means the ice freezes earlier and when there is no ice it freezes little later than usual.

I lived at Flaxman Island till I was just about 20 years old, and my father used to keep us moving -- one year there, another year in different places and finally we got on up to Marchesi(?) [possibly Gordon Point] and lived there for a while when Tom Gordon had a store there as a trading post. Sometimes in the fall, when the wind cames after the ice formed, the westerly wind opened up and then it closes and it piled up ridges close to the barrier islands all the way up to Herschell Island that I could recall.

Right around Flaxman Island, on the lagoon side, that is behind the barrier islands inward to the inland, after the ice formed and freezes it never moved or any disturbance that I could recall in that area.

Before the ice gets any much thicker in fall, the ice usually crumbled up and built kind of bit of ridges along the barrier islands in some places, but not often some years it's flat but some years it's always some piles of ice but I never noticed any ice slide over the barrier islands.

Again when the ice crumbled up right along the ocean side of the barrier islands the highest points that I can figure is approximate 12 to 15 feet high.

That ice crumbled up in the fall, that is before the ice gets thick.

Later part of the years I lived around Beechy Point where Jack Smith had his trading post. I lived in that area and in summer months I used to go with Jack Smith on the way to Barrow to pick up supplies and also return to Beechy Point after we picked up the supplies.

In some years between Beechy and Barrow on a run going towards Barrow and returning, sometimes the ice was always invisible all summer and return in fall.

When the polar ice hang around not far from the barrier islands the people always say that there is a good chance of catching seals when ice is close to shore. In summer months when there is a westerly wind you can see ice from shore but when the wind is blowing from northeasterly, the ice always goes out. I don't know how many miles but you couldn't see any ice from shore when the wind is blowing from the northeast.

When I had family I used to go along with Jack Smith whenever he needed any help when making a run to Barrow.

These days of 1978, the older people who have lived in the general area around Beechy Point and Flaxman Island who are getting to be few, those who understand that general area. [There is a section regarding masses of multi-year ice being grounded or frozen to the bottom and serving as an anchor for the first year ice which freezes in fall. In this case, the ice is safe].

I started to work with Jack Smith in summer to assist him on the boat runs between Barrow and Beechey. In winter I used to move back inland. I lived around Colville, way back just below Umiat and up far as to Anaktuvak in winter and back down to coastline in the spring.

The people that lived at McKenzie River say that the lake ice drifts out through the river and floats out to ocean. That means that they claim the ice, what we call polar ice, is from the lakes of McKenzie. After the ice has drifted out from the river and melted in summer months and when winter comes (on my thinking whether its right or wrong) the ice freezes from the bottom and is still fresh water on top. Then in summer months part of surface melts and I think thats when it gets kind of wavy.

In my early age, when I happened to live and stay a bit around McKenzie area, I used to have dinner with the older people and listen to them tell stories. That's how I learned what the polar ice means.

Samuel Kunaknana

I'll tell what I know about the ice even though we didn't live on the coast all the time -- but I've lived here for many years. The ice in front of Colville piles up and forms pressure ridges when it freezes in the fall, like it does in Barrow. As it thickens it piles up until it completely freezes. There is always some ice on the ocean side of the islands (sandbars) although they are pretty far out, even in August. The ice never sits still and when we check the current from the ice it's always moving. In the winter time the ice goes out when the wind is from the west on the ocean side of the barrier islands. When the weather is bad, the ice piles up in pressure ridges in the ocean. The ice is never smooth. When the wind is strong from the west the ice can break up fast all over the place and go out. No matter how thick the ice is, even in the dead of winter, it will break up and there would appear big bodies of open water.

The ice starts rotting in May, there and it is hard to hunt. [In the spring his parents used to take him out hunting. That's how he knows this.] Sometimes it would be so rough from piling that it would be hard to go out and hunt. The ridges were too rough to get over. No matter how thick the ice may be it can break up and pile up fast. In the summer time, the ocean is deep on the ocean side of the islands. I know it is deep because ships used to travel right alongside the islands, and the ships never let ice stop them. [He doesn't specify which islands]. The ships were built strong so they could push through the summer ice.

[He now refers to the visit the State and OCS people made to Nuiqsit and the maps they brought with them for the Cape Thompson sale hearing.]

I've heard of people who are interested in drilling oil in the ocean and I don't go along with that because of the animals. There are many different kinds of fish down there. Also different kinds of birds. When the old squaw ducks are there there are so many birds in a group on the water they can look like a big piece of land. There are also different kinds of whales.

The first time I learned of whale hunting was when this crew from Barrow caught a whale at Cross Island in the fall. I was just a boy then. [He talks about the boat being built of wood, not a skin umiaq like now and not a big commerical whaler either. He also mentions the first whale that was caught after Nuiqsit was re-established in 1973, and the many types of whale bones from long ago he has seen along the beach there indicating whaling has gone on there before.]

We all know that the ice is especially dangerous, if they are going to drill for oil out there. When the ice starts moving, nothing can hold it. I worked for the navy when they first came up to look for oil. The only thing that worried them was to make the drill stand straight. They never tried to make it safe from moving ice. If they are going to drill it has to be fixed and safe because the moving ice is strong. I don't think a drilling rig can withstand the moving ice. After they strike oil and the ice starts moving there probably won't be any more animals either, they would either die off or they wouldn't be able to come through anymore. We have lived on those animals, and that is why we oppose any offshore

drilling. Nothing stops the ice when it starts moving. Take, for example, that big Canadian ship the ice carried around--a small drill certainly wouldn't stand it. [The reference may be to the Dome oil ship which was forced off site by threatening ice. He says compared to the size of that ship a drilling rig would look like a stick.]

No matter how thick it might be it will break and pile up. No matter how thick it might be it will break and pile up, and no matter how thick it gets it is never guaranteed stable. It just depends on the weather. The ice goes completely out after July 4, around the Colville. That's when the Patterson (Capt. Pederson's ship) used to come up here in July. There is always new ice when it freezes because none of the ocean ice floes come in; the winds blow mostly along the coast. [He is still talking about the Colville area. "Ocean ice" means thick floes of old ice that could ground. Not much of that comes in. This is also why it goes out so easily.]

I'm just talking about what I know about the ocean here. There are different kinds of fish out there, salmon, white fish, flounders, different kinds of birds, seals, polar bears, bearded seals. That is why we oppose the oil drillings around here. This spring the elders talked about how they wouldn't like to see oil rigs in the ocean. Unless that oil rig is put in safe and with strong supports, the moving ice would think nothing of it.

If we agreed to let them drill offshore we would go against the people's wishes who live along the coast, and the elders don't want to see any animals interfered with. They mentioned again and again how the ice can take anything with it, no matter how strong it might be. [There is a long discussion about the Elder's Conference and some reflections that people

live differently in different parts of Alaska].

The Colville River ice goes out the first part of June. It floods badly before it goes out. It usually goes out before June 10, but the flooding can be very bad. Last spring (1977) it flooded so much it was like an ocean there.

We don't have a lot of money like these white people and oil companies. We have to do what they want. If they drill and strike oil they won't give anything to us. They are only doing it for themselves.

[There is now a long discussion of how the people lived in the past in small family groups that were scattered up and down the coast. They would go meet Pederson's supply ship when it came in the spring and they used fox pelts as currency. He also mentions that he was a little boy just school age when his family moved from Barrow to the Colville area but he remembers it well. He says this tape is too long and he's rambling on trying to think of things to say to fill it up. He then talks about going inland to hunt caribou, about how caribou never came down to the coast then as they do now. He describes caribou hunting and what they used the skins for and using dogs with backpacks. They used back packs themselves.]

There is never any ice in between the mainland and the islands once the ice goes out in the spring, because the lagoon ice rots early on the landward side of the islands.

I've never lived near Cape Halkett and Barter Island so I don't know about the ice there. My wife has lived around Cross Island and west

so she can talk about the ice there. As I said before, the ice around here in the Colville area never has old ice coming in when it starts freezing. When it freezes first year ice is all there is because the wind is always parallel with the coast and there is no wind from the north to bring in ice from the ocean to the bays. It is all new first year ice when it freezes. When the wind is from the north, ice comes along with it and gets on the outer islands. In the summertime, this occurs only when the wind is from the north. Sometimes old ice comes in [the old ice is floating pieces surviving from before, he is not talking about new ice ridging on the islands, he's talking about ice pieces driven up or washed up in the summer], but not enough to stay long. The ice is never still when the wind is from the west anytime of the year no matter how thick the ice is it can pile Up.

When the wind is from the west it can go out. When the wind is from the west the ice can also pile up [he's talking about ridging on the ocean in front of the Colville, but does not specify distance from shore]. In the spring, the ice starts rotting before June on the ocean side of the islands. It also rots early in the bays although the ice doesn't go until around July but it's too rotten to travel on between the islands and land. The ocean side of the islands is really deep. The "Patterson used to anchor right alongside the islands.

It's taking a long time to fill up this tape. People around here know about the ice and how it moves. They trapped foxes on the ice and sometimes lost their traps when the leads opened up. [He also talks about how his family moved to the Colville area around 1920, how they travelled inland by Tesheqpuk Lake and came down the river].

Sarah Kunaknana

I am going to talk about ice conditions from Beechy Point to Flaxman Island. I was born in Barrow in 1921. My parents took us with some people to Cross Island, when I was 2 or 3 months old. [She mentions that the mother of Mr. M. Pederson (who did the translation) was on that trip and that her mother is Mrs. Pederson's aunt. She talks about how people in those days were all related and knew it, but nowadays no one knows their relatives]. I grew up around Cross Island and around where Prudhoe Bay is now. I'm the only one left in the family who lived on that island My parents and their crew caught a whale at Cross Island that fall. My father had whaling gear, and that is why he brought the people to Cross Island, to hunt whale. He had not always lived in Barrow, but he settled us at Prudhoe Bay. My earliest memories are of Prudhoe Bay. My father travelled a lot but finally they settled in the Prudhoe area. [She doesn't remember everything she's going to say about ice herself but some of it will be what her parents said].

The ice around here looks sturdy, but the wind doesn't think its sturdy when it blows from the west. The lead opens up right alongside Cross Island on the ocean side because it is very deep there. And when it is an east wind, the ice piles up along the coast. There is nothing to stop the ice seaward of the islands. But the water between the islands and the land is shallow, from Beechy Point to Flaxman Island. There are islands all the way from Beechy Point to Flaxman Island. I have travelled between Barrow and Prudhoe Bay many times by boat and dog team with my parents, so I know the area. There are many kinds of animals here. When we wintered at Cross Island, there were all kinds of animals there. In

the fall we fish in the ocean. In the winter and spring there are seals to hunt. [She says in the spring they hunt seals with nets and there are foxes and polar bears to hunt. Then she talks about how her father caught these animals]. In June and July when the ice is rotting in the little bays along the coast we start seining for fish (iqalukpik). After just seining 1 or 2 times there would be so many fish we would have a hard time putting them all away. And now the white people want to drill for oil out there. We lived on the animals we caught there during the winter, or we traded at the stores at Beechy Point. Besides trading at the store we traded with the ship "Patterson" (Capt. Pederson's ship). [She talks about the food they got from the ship having to last all winter. She then names all the people who had stores but gives no dates. The ship resupplied the chain of trading posts Charlie Brower maintained between Barrow and Canada].

Our houses are still standing at Cross Island and Prudhoe Bay. [She tells where there used to be old houses and how her father fixed one up for them to live in at Cross Island]. If we knew that they were going to strike oil, we would have stayed there and lived high! Our house in Prudhoe is there just standing [its only 30 minutes by plane or 5 hours by snowmachine from Nuiqsit to her house at Prudhoe, but she hasn't been back recently].

I sure hate to see them drill around Cross Island where our winter house is. Another reason I'm against it is that all the animals, fish and seals, come up to Colville River from the ocean and we use them for food. The fish never come from inland they come from the ocean. All kinds of animals do that, even seals. [She notes that "Pani(ng)ona", lived in the Flaxman Island area and his house still stands on Flaxman Island. (Note, this tape was made in July 1978, the first translation was available by the end of

August but was paraphrased and did not include this statement. The verbal translation including the name was made in October. Unfortunately, he died in September so the opportunity to interview him was lost). They used to call Flaxman Island Qikiqtaq in Eskimo. The cost of oil isn't any cheaper even though the oil is from our land. We have a hard time paying for the heating oil to keep us warm even though the oil comes from our land. I mix my words up all right but you'll understand what I mean. We lived in Prudhoe Bay 15 years.

When she lived at Prudhoe Bay she was about 14 and they got another whale (about 1935). They used a wooden boat with an inboard motor. She talks about the whale and how their share which they brought home made two boatloads and they also got bearded seal at that time. That was the first time she'd ever tasted fresh boiled muktuk, and she didn't like it, it tasted too rich. She just tasted it but never ate any although her parents and brothers did. Many people came that winter to get food from them (whale meat and blubber)]. We used to live on all these animals but now we can't hunt at Prudhoe Bay anymore because of oil development. Nobody can hunt there anymore.

Not much more to say, I'm just repeating what my parents said. [Her parents took them to winter just west of Flaxman Island. She doesn't know what things are like east of there]. The map they showed at the hearings (regarding the lease sale in May, 1978 at Nuiqsit) is where all the animals live that they used to live on. When she saw those maps she felt against the leasing because she grew up there and lived off the land there. She followed her brothers when they hunted seals and bearded seals.

She was the youngest and followed. When they hunted bearded seals it never took long to fill their boat. They also got lots of fish whenever they put their nets out in summer time. Because she likes eating animals from the ocean she doesn't agree with drilling in the ocean. She talks about the oil companies always coming back and asking to drill even though they keep telling them no].

[She talks about moving inland up the Shaviovik river in summer and her parents sometimes taking them all the way up to the mountains. She lists the animals they caught when they went inland. They would come back to live at Prudhoe Bay after spending some time inland, probably in the fall].

My parents took us to winter just on this side of Flaxman Island. The map they showed us of the planned oil leases is where I have lived. One winter, in 1934, when the wind was real stormy from the west, my brother was lost out on the ice when the west wind opened the lead. The wind can change real fast and the wind controls the ice. [1934 was a bad year for ice accidents for her family. In November a group of hunters including her brother were caught offshore and drifted east but made it back. In December it happened again to a different party including a different brother who froze to death trying to get back. She skips from brother to brother as she tells the story. The details are clearer in Henry Nashanik's statement although he's not sure of the date. He thought possibly 1932. The best reconstruction is probably her date and his details.]

My brother froze to death out on the ice after the west winds had opened up the leads. He was with several people but they all came back. The ice broke up all around them except where they were. They believe

they were saved because they remembered God and prayed. My brother, Joseph, died in December 1934. The other people with him came towards land through the forming pressure ridges. When the ice starts moving there's nothing you can do about it. [When the wind let up they "came up" (moved landward), but when it got stormy again her brother froze to death]. Henry Nashanik knows about that. I was about 15 years old then. We didn't want to spend another winter alone there. [So in the summer they moved to the Colville (1935?)].

[She then discusses going inland up the Colville hunting caribou and hunting caribou at Umiat before the Navy came. She tells how one of her brothers found an oil seep there].

Just before July 4, we went to hunt for caribou at Umiat. We stayed there and hunted caribou for several days, drying meat. There was just us, the children, up there; our folk were still at "Anaqtuuppaa" [the mouth of the Anaqtu river, one of the tributaries of the Colville?]. While we were up there was when Mark found oil. There weren't any white people at Umiat at that time. He was walking along a little creek when he found it. He put it in a can which he found and brought it home and when we smelled it, it smelled really strong like either gas or fuel oil. When we tried to light it, it burned. He'd dipped it out of a puddle. It was where they drilled and discovered oil later. Another brother, David, put a marker up on a little knoll beside it. He stood up a boulder and wrote his name on it. I don't know if its still there.

[When they left there, they moved to what is now POW 2. The next winter they went back inland. They went to Nirilik tributary of

the Colville). They also moved to Fish Creek and spent the winter there. They traveled so they could live on the fish at that time. They lived wherever they could catch fish. They moved again (not clear where) and built a house which is still used to this day by people who go fishing in that area. Then they moved to "Putuu" (which was on the Colville, upstream from the present village of Nuiqsit) and lived there for 5 winters. They stayed there until the Colville area was empty of people (the last group of people moved away from there sometime in the '40's). They have a cellar there that they still use. They fixed it up when they moved back to the Colville area in 1973 when Nuiqsit was established. When they moved back in 1973 she went to see the place where they had lived and it was like it was someone else's story. There were no houses, only growing grass and it was like people had never lived there. Their house would have still been standing but somebody had torn it apart and moved it somewhere else].

[She says she's traveled by dogsled from Nuiqsit to Anaktuvak Pass and she recognizes places when she flies over that area].

[She says she got the last of the way people lived a long time ago, before there were too many white man things. They lived by following the animals that they used for food. Now things are so easy with all these conveniences even traveling is nothing anymore. Young people just starting to make a living these days, only worry about their jobs. Her father was from Utukak (a village between Point Hope and Wainwright) and her mother was from Nuvuk (Pt. Barrow). Her mother died when she was really young. Her father used to say that the people would go inland just

like wolves. That's how people lived in those days. They followed the caribou living off them. Then they would go back to the mouth of the Utukak River to live off the ocean. They would trade caribou skins for blubber etc., with people who stayed along the coast. She says she's just repeating things her parents told her].

[When she was a girl and they were living at Prudhoe Bay, two men from Greenland came through and stopped and stayed with them. They came on dog sleds and looked like white people but they spoke Eskimo (Inupiaq). When they found out her father was from Utukak it was like finding relatives because some of the people from Greenland are originally from Utukak].

[After taking care of their dogs they would bring out their guitars and play and sing and dance until the kids fell asleep.] "We weren't used to staying up late, unlike kids of today who stay up all hours and never go to sleep". [They stayed quite a while then left for Barrow. She hasn't heard anything more about them after they left]. Even though we don't know each other it must be true that everybody's related somehow or other. Boy, I'm taking a long time to finish this tape. You'll probably laugh at everything I've said not making any sense.

Times have changed so much and we have to move with those changes but we can't do it by ourselves. We must remember we need the help of God. The changes are so many and hard to understand and the forces behind them so powerful and beyond our control that we have to rely on God.

Vincent Nageak

Someone asked that I talk about the currents and ice from Cape Halkett to MacKenzie Bay. I know about the sea in summer around there because I have lived on Barter Island, and at Harrison Bay, a long island called Mitqutaillaqtuuq, islands are in the wrong places on the map that you gave me.

I lived for 4 or 5 years in Ooliktuq (Oliktok). The Bodfish Islands are in front of Ooliktuq. I have travelled by dog team from Ooliktuq to Barrow many times In some years, Harrison Bay ice rots early at the mouth of the Colville River. The shallows go out pretty far at the mouth of the river. The ice there usually moves out to sea when the wind is from the east. It's hard to pass Cape Halkett, especially when the current is strong from the east. The current is so strong it can take you out to sea even though you might think you are going straight. But when the current is not strong you can easily travel where you want, always taking the current into account. You also have to watch the waves in this area, and when the ice starts moving, it all goes, leaving just the ice on the shallow area. They don't travel on it in June because of the danger of moving ice, but I've crossed it in June. We crossed it to go to Beechey Point. It took us 5 days to cross because the way was so bad. The current at Cross Island is about the same as at Harrison Bay but in summer, huge ice chunks can pass the islands into Prudhoe Bay when the wind is from the west. The furthest island out, Cross Island, is dangerous to cross, and when we travel on it we hope that the wind won't change to westerly.

It is very difficult to find a leeward side among any of those three groups of islands. It is difficult to camp out so we usually go to

Foggy Island for protection. The ice at the mouth of MacKenzie River also rots early. Foggy Island is always the place to go when the strong winds start from the west because the water is shallow there. The current is always from the east. [He pointed to the mainland side of Cross Island on a map of the area and says there is supposed to be another island shoreward of it.] There are a lot of islands which are not on this map. There is a string of islands all the way past MacKenzie Bay. The ice all along the coast on the mainland side of these islands rots early from Cape Halkett onward. Travelling by boat you don't run out of open water like you do around Barrow, and the ice does not rush right out. The current is a little different in Brownlow Point but not too bad to travel by boat. When I travel by boat I always steer because I know the currents and can travel in a straight line from Thetis Island to Cape Halkett. I know the weather and currents between Barrow and Barter Island in spring, summer, and fall because I have travelled that way so many times. Once the water muddies the current can take you way out. The sea is dangerous in Harrison Bay because of the spill off of Colville River. The current there also takes the ice out to sea once it starts rotting but sometimes all the ice does not go when there is ice that is stuck fast to the bottom. There are always pressure ridges at Cross Island. The ice takes a little bit longer to go out by Thetis Island.

Sometimes whales travel on the inshore side of Cross Island.

Once the ice goes, you can travel easily by boat on Harrison Bay and Prudhoe Bay. The ice rots early due to the rivers and as long as the wind isn't from the west and you are traveling from the east, boat travel is easy.

When you're traveling from the west you don't want the wind from the east because the water is terrible in Harrison Bay, but once you're past there it's good all the way to Barter Island. The pressure ridges form on the ocean side of these barrier islands.

The only times I've seen ice pushed over the islands is when the flat ice gets pushed on top when it's being pushed from way down in the ocean somewhere.

Henry Nashanknik:

I am 73 years old. I was 15 years old when we first moved to the coast. We began in Canada and travelled toward Barrow, building a house and spending several years at each place we stopped. Sometimes, we stopped for 2 years, sometimes 5 and sometimes just 1 year. We spent about 1 year east of Barter Island at Pokok Bay. Then in the summer we travelled by boat to west of Barter Island.

I got married when I was 25 years old. We lived in different places along the coast and sometimes going inland. I've lived on the Colville River, Canning River, Sagvagniqtuuq, and Shoviovik River, and just east of the mouth of Colville at Kaubik Creek. I would trap on the McClure Islands and Stockton Island, so I travelled in that area by dog team. These Islands have always had ice piled around them. Sometimes in the fall, the ice would pile all around these islands and at times just the ocean side would have pressure ridges. I've seen ice pushed on top of other ice, but I have never seen ice pushed on top of these islands, probably because these islands are high. The same as Cross Island. The ship owned by Captain Pederson would go between Cross Island and the McClure Islands when it headed east in the spring. Seaward of these islands there are usually pressure ridges and at times really high ones. Most of the time you can travel over them. Sometimes there would be huge chunks of polar ice but none of it was grounded and in other years there would be polar ice which was grounded. When the ice opens, when the wind is constantly from the east in summer months, all the ice goes out seaward of these Barrier Islands, The coastal ice also goes out when

the wind is from the west. But even when the wind is strong and constant from the west the ice seaward of the barrier islands is still visible. Only when the wind changes from west to east does it finally go out completely. I don't know about east of Barter Island because the ice can go when the wind is from either direction; land comes to a point there.

Once the ice leaves the mainland coast, it stays out. Below (seaward of) McClure Islands there are often huge pressure ridges. But we can travel through them in the spring, hunting seals. There the open leads are not too far out, so we would be able to hunt for seals in them. From Cross Island it would take us about 4 or 5 hours on dog team to get to open leads. [K. Toovak estimates that on moderately rough ice that is 10 or 12 miles by dog team]. There are always some pressure ridges seaward of the McClure Islands but they're not bad and you can maneuver around them to hunt seals in spring. I know people from Cross Island also hunted on open leads. When the wind is from the west the leads would open.

There was a time in November, 1932, [he is uncertain of the exact time] when five people were out on ice hunting seals from Cross Island. This was when temperatures were mild and the wind direction was from the south and leads opened up. Because the weather was mild and the leads had opened they were out looking for seals. But when the temperatures are mild like that the wind usually changes to the west. This can happen very quickly. The wind started to blow very hard from the west, the ice broke up behind them and they drifted away.

They were out for about five days. They knew they were way out in the ocean because even though they were on a big high ice chunk, the moon would disappear below the horizon when they were in the trough of big waves. When they would wake up there would be water all around and each nightfall they would

look for high ice chunks to sleep on. The waves would break up ice, but when the temperature went down it would freeze up, so they would travel toward shoreline. They made it up to Flaxman Island, on the new formed ice. The ice was so thin that a person couldn't walk on it without breaking through, yet these men drove over it with their dog team and it did not break under them. It was a miracle that they survived. [Mr. Nashanknick and his brother might have been with them but luckily they decided to trap fox that day].

[It happened again that same year just before Christmas time. Pete Sovalik (he had been with the November party that drifted away and later was employed at NARL for many years), his father and four other men were out at the lead. They decided to spend the night. Pete was against it because of his recent close call. He went back and tried to convince his father and another man to go with him. They refused to leave, so Mr. Sovalik went home but his father, "Kingusak", "Kavinga" (Sarah Kanaknana's brother), and "Pilak" plus the other man stayed out on the ice. The wind changed as Mr. Sovalik had feared and the ice broke away behind them. After they were drifting, when daylight came, Kingusak lead the men to where they knew the pack ice was shearing and crumbling against the shorefast ice. He started to walk over it onto the shorefast ice. But the ice opened and closed and caught both of his feet. After he was caught the motion stopped. The others chiseled his feet free and when he was loose they went a good long way onto the shore fast ice. They had to stop because Kingusak couldn't walk. They made a snow house for shelter. The wind shifted to west and it got very cold. They spent the night in the snowhouse. The next day when daylight came two of the younger men, Pilak and Kavinga, decided to walk to shore for help. They walked all day until they were tired and nearly exhausted, then went to sleep on the ice. When Pilak woke up

he tried to wake Kavinga but Kavinga was dead, so Pilak started walking. He missed the island west of Flaxman and walked through the channel onto the lagoon. He also missed the camp of the family that was living just west of Flaxman, probably because of the short daylight. He walked all day until he was exhausted and went to sleep on the ice and died. The details are surmised by the location of the bodies that were found later].

[The other three men in the snow house waited and waited for a dog sled to arrive with help. They had lost their sled and dogs out on the pack ice when they drifted away. However, one dog had gotten loose and followed them to the snow house. When no help came the two uninjured men started for shore. The stray dog followed them and they killed it for food. Each had some food from the dog. They made it to one of the islands and found some driftwood. They found a can and built a driftwood fire to melt snow in the can for drinking water. It was very cold and windy with much blowing snow].

The translation was stopped at this point. However, the remaining members of the party did survive.

[The following story was paraphrased by K. Toovak].

In some years there used to be pieces of polar ice grounded in the bay in front of the Colville. This would happen in the summer. He (Mr. Nashanknik) used to work for Jack Smith who ran the trading post at Beechy Point (Ken Toovak said Smith used to have six or so wooden boats, 20 - 30 feet long, with inboard engines with which he would tow barges. Sometimes he made supply runs to Barrow). He went with Jack Smith on a supply run to Barrow and they had to cross Harrison Bay. The wind was from

the northeast so they stuck close to the line of grounded ice where there was no rough sea. They were running from Thetis Island to Cape Halkett and it took hours and hours. When they thought that they were near Cape Halkett (in fact they had gone past it) they turned south. They got into floating ice again and the wind picked up and they found themselves in a storm. They were towing a boat behind them. The waves got high and the boat being towed smashed into their rudder control so they lost steering. Jack Smith made an emergency repair so they had some control. They made it to a sheltered spot (Pitt Point at the mouth of the Smith River) and waited out the storm. Then they made it to Barrow.

Bruce Nukapigak

I was born here in 1900, April 10, (I'm 78 years old), just at the head of Kuuguq ravine at the southeast corner of what is now Barrow, in a snow house. My parents lived at Ualiqpaa (near the Will Rogers and Wiley Post Monument just south of Barrow,) and they came to Barrow just before I was born. I lived at Ualiqpaa until my grandmother died. We moved to Barrow after our father died. My mother remarried Iaqluk. He had a quayaq that he used for hunting and he never left it. I used to meet him after his hunt. They hunted all the time because that's all they had--not even a penny in their pockets. When I grew up I whaled in Iqasak's crew in the fall. We went out in a whaling boat 20-25 ft with no motor. We used a sail but had no cabin even though the wind was cold.

I would be cold in the boat and we never really slept. When there were grounded ice chunks in the water, they would get over to them and climb up on them to look for whales. When they saw one, they got in the boat to go after it. They never used motors. Once they killed a whale, they would tow it to the Point (Point Barrow) to butcher it, unless they butchered it on the ice. Sometimes grounded ice ridges north of the point never moved in summer or fall and some of them stayed until the next year.

My mother moved to Barter Island when I married and after I had two sons, my mother sent for us to come to Barter Island. That is when I moved there. I had no one to teach me how to hunt on the ice but Uqumailaq's father (his father-in-law). He taught me all the information about ice movement and the proper use of a cod line.

["Cod line" is an English term which K. Toovak thinks approximates the Eskimo term. There are two types of these lines; one type has a float on the end and the other has a sinker. Both have multiple hooks. They are used for retrieving seals that were killed in the water (winter seals float, spring seals sink). However, they have other uses. A cod line with a sinker can be used to test for current and ice motion. It is lowered until it just touches bottom. If it drags along the bottom, the ice is moving. A current may put a bow in the line but it shouldn't drag the weight along. If it is established that the ice is not moving, there are various way to test for current.]

I hunted on Barter Island, and he taught me about the ice. He took me on hunts as far as Cross Island and east of Barter Island to in front of the Jago River. At Barter Island the leads open up when the wind is from the west all the way to Cross and leads close when wind is from the northeast.

The lead in Barter Island is always close. There is never any grounded ice in front of Barter Island. When the wind is from the west the ice goes out at Cross Island and, no matter how big the pieces of polar ice are, the current takes them away. That is when the ice piles up (pressure ridges) along the coast from Barter Island to Jago River. When the ice moves out from Cross Island, it begins to pile up. There is not really much current at Barter Island. When the wind is from the west the ice usually breaks off along the beach all the way to Angun Lagoon.

I've also lived in McIntyre and around Beechy Point for 18 years (from 1932) but I've walked all along the coast. At Beechy Point,

the ice piles along the coast outside of the barrier islands. The pieces of polar ice come in through the bay between Return Islands and Midway Islands. This is in winter, when the strong winds are from the west. When there is little wind, the currents really play with ice along there. This is in summer months and at Pingok, Bodfish and Cottle islands the pieces of ice move in and out through the channels with the tides. The polar ice gets pushed in from the ocean just west of Cross Island to Beechy Point. There is no strong current on the ocean side of the islands, so the ice piles up because of ice movement elsewhere. But the ice in places with "singaq" are controlled [Note: singaq - channel created by either flow from a river or because of the existence of an island or along the shore of a point; isiqsgnaq - during high tide the current flowing in through a channel; anaisagnaq - during low tide the current flowing out through the channel]. [At this point K. Toovak asked the question "Did you ever see ridges off shore in the general area". He answered that off shore in front of Beechy (beyond the islands) there's crumpled ice but he's never seen <u>big</u> piles like you get at Barrow. He personally never saw high ridges from Cross Island to the mouth of the Colville to Cape Halkett].

When I lived in McIntyre from 1932 on there was never any ridges around there because its deep there. When the ice goes there's never any left.

The lead breaks off in somewhat of a straight line from Barter Island to Cross Island so its pretty far out in Camden Bay. That

area has flat ice between the shore and the pressure ridges but its never the same each year. Sometimes you can run into old ice along there but not much. This old ice usually gets stuck to the bottom around Cross Island. Same thing happens in front of the mouth of Colville River because its shallow. The pressure ridges are far out there too. [When he left Cape McIntyre and he headed for Barrow to stay (in 1950) he finally started seeing some ridges out there and some polar ice grounded from Cape Simpson on towards Barrow. These were the kind which usually stay through the summer. They were high but not as high as they get at Barrow. He was traveling by dog team when he saw this].

Out where there are islands when the tide gets high the ice can get pushed up on the islands. This is when the ice first freezes and has thickened a little. I don't know of any permanent (tide) cracks on ice in front of Pt. McIntyre but I know there are always these cracks on the mainland side of Cross Island. When it's high tide these cracks usually widen and close or even jam up when the tide goes down but even after pressure ridging they can open up again. There is this type of crack on both sides of McClure Islands out from the mainland to the ocean.

[When he lived at Pt. McIntyre he used to go out seal hunting in the early fall. He would go to Cross Island and all the way to the McClure Islands. He would make this trip from Pt. McKintire to Cross to McClure by dog team. When the tide comes in ice piles up on the ocean side of the barrier islands. Sometimes it is up to a foot thick].

[When he traveled out to Cross Island and the McClure Islands he would watch the wind carefully. For seal hunting it was good between Cross and McClure because there was usually some open water between those islands in the channel. He also usually saw pieces of polar ice grounded between Cross Island and the mainland. It was not thick but still polar ice (K. Toovak says these are flat pieces of ice probably 6 to 8 ft. thick and on the order of 50 ft. in diameter). They would be driven in during the fall and stay for the winter.

In the early spring Capt. Pederson's ship would usually go through the channel between Cross Island and the Midway Islands and go east in the lagoon behind the islands [K. Toovak says it was a wooden boat of moderate draft. He remembers that when he was a boy it went through behind Pingok Island and out to the ocean through a channel. They stopped various places to trade for fox skins].

But it is early fall when the flat pieces of polar ice drifted in through the channels between Cross Island and Pt. McKintyre. There were always some small ridges formed around the flat pieces of polar ice but they weren't high. Westerly winds usually brought those pieces of ice in when the tide was up. They would stay for the winter.

Then the ice comes in driven by westerly winds in the early fall along with the pieces of polar ice, the ice piles up on the oceanward side of the barrier islands. Also pieces of polar ice can be forced up against the barrier islands and gouge up the sand a bit. But the ice piles aren't high. At the same time these westerly winds cause movements in the ice between the barrier island and the mainland. But this is in the fall before it gets really thick.

But the ice behaves differently from year to year. Some years it can be bad and some years it can be mild. Some winters it's smooth as far as you can see.

Kenneth Toovak:

I'm 55 years old and was born in Barrow. I have lived here all my life, and have never lived any other place. If I was to talk about the ice, I couldn't remember the exact years. The ice here starts freezing in October, sometimes the middle of October, when the temperatures are mild. As soon as there is no wind, it starts to freeze. It has been like this for many years. Some years, when the currents bring stamukhi ice from the east, elders say it freezes early. I'm not that knowledgeable about ice to really talk about it, from the time I can remember, but elders have said when stamukhi ice gets out there in front, the ice usually thickens faster from the shore down to the ice. This is because once the ice is there permanently the ice between it and the shore doesn't move.

I remember one time when I was young coming back from camping on the rivers inland. Even before we could see Barrow, we saw high pressure ridges towering over the hills and banks. This was during one winter -- I really couldn't say what year. Also, when I was a boy, there used to be a wide beach in front of Browers trading post. One year, the ice was piled up, just about reaching the trading post. These pile ups were up to 20 feet tall. This was about 1935 or 1936 in late February or early March. This is one time about the ice that I remember. I came about 250 feet up the beach to the pile.

After I started working out at the camp for arctic contractors in 1949 (either in January or February) there were grounded pressure ridges

on the beach all along the coast, up to 15 feet high. I can't say how far east these ridges went. Then around March, our boss had us bulldoze the ice from the beach so it could melt faster because cargo ships were coming in with equipment for the contractors. We did this over several weeks from March through May. After we finished the wind from the west brought the ice in and it piled up again up to about the same height as before. We started again, but in late May and June the ice can't hold tractors. We had to use water pumps to hose off the ice which had dug into the sand so that it would melt away faster. I can say now the ice piles up along the coast when there isn't too much ice further out which is stuck to the bottom. Usually, this ice is about 3/4 to 1 mile off the coast. But just in front of Pigniq (shooting station) it is usually farther out because it's deeper out there. When the ice packs which come in first don't touch bottom and get stuck, the ice takes longer to freeze. When there's no stuck ice out front, the freezing ice along the coast usually doesn't thicken enough to stay until around December or January.

Once the ice was frozen thick enough to stay fast to the bottom, the people used to start leaving their hunting equipment out on the path. Only then they wouldn't worry that the ice would take them away even though it might get real windy. But they made sure the ice was stuck fast to the bottom before they started leaving their equipment out there. If we had lived then we would probably leave them and lose them, but the elders didn't do that. They made sure it was safe before they did that. The whalers did the same. When the lead closes up they leave their whaling gear where it's safe. Those two are the only instances I remember from years back.

In 1974, around November, when the wind was from the north, the

ice piled up bad about 1/2 mile out until it touched bottom. This was before the ocean completely froze up. That was the year the way was real bad for the hunters to travel on. I've never lived anywhere else so I can't say how the ice behaves nearer to Barter Island. But I can probably say that once there are ice packs stuck to the bottom on the shallow shelf the coastal ice is usually pretty smooth. I have heard that the leads open pretty far out around Beechey Point. In 1963 during our cat train trip to Cape Halkett the pressure ridges were about 1 1/2 miles out. And from these ridges to the coast was smooth. I have also seen the ice smooth in front of the mouth of Kuukpik (Colville) River.

I can also say that the weather here is never the same. The ice usually goes out the middle or last part of July, but the current can bring it back again. During the spring, the current is from the west; in the winter it comes from the east, with the wind. The weather controls the currents during the winter. In the summer, when the wind is from the east for several weeks and the current is from the west, the ice goes so far out you can no longer see it.

The elders used to get together in someone's house or the community house to talk about things. They kept each other informed like this. Some of them would have lean-tos by their houses, and that was where they gathered to discuss weather and hunting. Once the ice is so far out it usually doesn't come back in again until the currents are from the east. It usually stays out until fall. Once the ice thickens and comes from the east and the current isn't strong, it usually freezes and stays.

Once, in September of 1945 or 1946 while I was whaling, we saw an ice berg which was grounded in front of the point; we used it for a marker. You couldn't see the land from it. I don't think it ever left through the summer.

☆ GPO—1979-667-069/1213

MARINE & COASTAL HABITAT MANAGEMENT
ALASKA DEPT. OF FISH & GAME
333 Raspberry Road
Anchorage, Alaska 99502